NEW ORGANIC CATALYSTS FOR THE PHOTOCHEMICAL GENERATION OF RADICALS

Eduardo de Pedro Beato

UNIVERSITAT ROVIRA i VIRGILI

New Organic Catalysts for the Photochemical Generation of Radicals

Eduardo de Pedro Beato

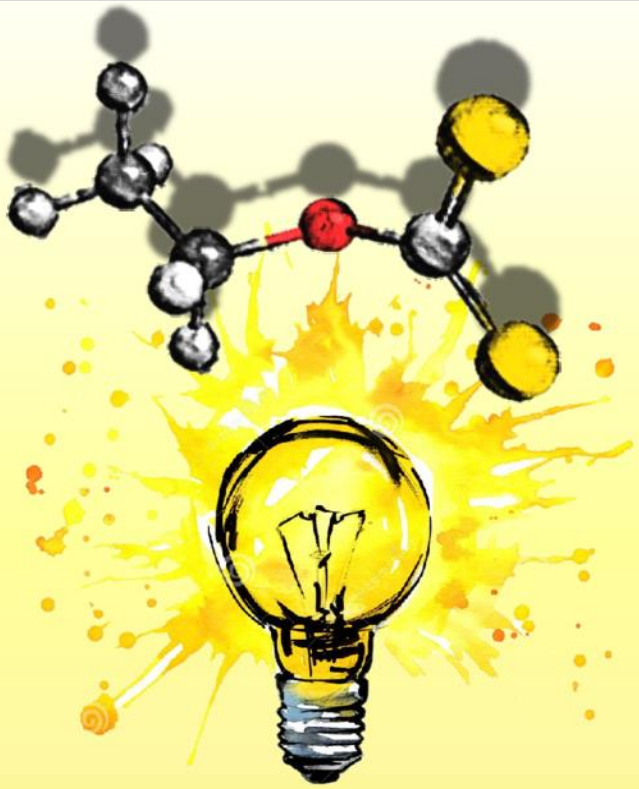

DOCTORAL THESIS
2021

UNIVERSITAT ROVIRA I VIRGILI
NEW ORGANIC CATALYSTS FOR THE PHOTOCHEMICAL GENERATION OF RADICALS
Eduardo de Pedro Beato

UNIVERSITAT ROVIRA I VIRGILI
NEW ORGANIC CATALYSTS FOR THE PHOTOCHEMICAL GENERATION OF RADICALS
Eduardo de Pedro Beato

Eduardo de Pedro Beato

New Organic Catalysts for the Photochemical Generation of Radicals

Doctoral Thesis

Supervised by Prof. Paolo Melchiorre

ICIQ – Institut Català d'Investigació Química

UNIVERSITAT
ROVIRA i VIRGILI

Tarragona
2021

UNIVERSITAT ROVIRA I VIRGILI
NEW ORGANIC CATALYSTS FOR THE PHOTOCHEMICAL GENERATION OF RADICALS
Eduardo de Pedro Beato

Prof. Paolo Melchiorre, ICREA Research Professor & ICIQ Group Leader

I STATE that the present study, entitled "New Organic Catalysts for the Photochemical Generation of Radicals", presented by EDUARDO DE PEDRO BEATO for the award of the degree of Doctor, has been carried out under my supervision at the Institut Català d'Investigació Química (ICIQ).

Tarragona, August 31st, 2021

Doctoral Thesis Supervisor

Prof. Paolo Melchiorre

UNIVERSITAT ROVIRA I VIRGILI
NEW ORGANIC CATALYSTS FOR THE PHOTOCHEMICAL GENERATION OF RADICALS
Eduardo de Pedro Beato

Acknowledgements

During the past 4 years, I had the great pleasure of being a part of the Melchiorre group both inside and outside the lab.

First, I would like to express my deepest gratitude to my supervisor Prof. Paolo Melchiorre for giving me the opportunity of joining his group and for his great support along all these years.

I would also like to acknowledge all former and current members of the Melchiorre group. To everyone I had the pleasure to share lab 2.10 with, specially my fumehood mates Nurty and Eugenio for putting up with my mess with a smile. Thanks to my *Jedi Master* Bertrand, who showed me the power of the sulfur, and to Matthew who learned it with me. To 2.10's *Little Italy*, Giacomo, Adri and Eugenio, for always making me feel like I was in Venice. To Davide for the useful and not so useful, but equally entertaining, discussions. To Daniele for teaching me that an Italian will always prefer anything Italian. To my 1.12 partner Ben for keeping entertained with his "Spanish sentences". To Pablo and Sara from the last Spanish standing. To Emilien and Nurty for making my first months after the lockdown much easier. To Riccardo with two Cs. To everyone I shared a project with: Matteo, Wei, Shuo. To Will for his great help with this, and other manuscripts. To Laura for her efforts to teach me a bit of German. To Laia for all the help in the lab. Many special thanks to YJann^2, Pietro, Davide C. and Elena for sharing lots of their time after the lab with me.

I am also grateful to Núria Planella, Dr. Lorna Piazzi and, Maria Checa for administrative support. I thank the research support units at ICIQ, in particular I am indebted to the NMR-staff, the photophysical unit, the spectroscopy unit and the chromatography unit.

Muchísimas gracias a mi familia y mis amigos, sin su esfuerzo y sin su apoyo, hoy no estaría aquí. En particular a mis padres por siempre creer en mí.

I would also like to acknowledge the financial support from the Ministery of Science for a FPI predoctoral fellowship (BES-2017-080037) and the project PHOTOORGANO CAT supported by MICINN-Agencia Estatal de Investigación (CTQ2016-75520-P).

UNIVERSITAT ROVIRA I VIRGILI
NEW ORGANIC CATALYSTS FOR THE PHOTOCHEMICAL GENERATION OF RADICALS
Eduardo de Pedro Beato

List of Publications

Some of the results presented in this thesis have been published:

- Schweitzer-Chaput, B.; Horwitz, M. A.; de Pedro Beato, E.; Melchiorre, P. Photochemical generation of radicals from alkyl electrophiles using a nucleophilic organic catalyst. *Nat. Chem.* **2019**, *11*, 129–135.

- De Pedro Beato, E.; Mazzarella. D.; Balletti, M.; Melchiorre, P. Photochemical generation of acyl and carbamoyl radicals using a nucleophilic organic catalyst: applications and mechanism thereof. *Chem. Sci.* **2020**, *11*, 6312-6324.

- De Pedro Beato, E.; Spinatto. D.; Zhou, W.; Melchiorre, P. A General Organocatalytic System for Electron Donor–Acceptor Complex Photoactivation and Its Use in Radical Processes*. J. Am. Chem. Soc.* **2021**, *143*, 12304–12314.

UNIVERSITAT ROVIRA I VIRGILI
NEW ORGANIC CATALYSTS FOR THE PHOTOCHEMICAL GENERATION OF RADICALS
Eduardo de Pedro Beato

Table of Contents

Chapter I: General Overview 1

1.1 Photochemistry 1

1.2 Direct excitation of organocatalytic intermediates 7

1.3 General objectives and summary 10

1.3.1 Photochemical generation of radicals from alkyl electrophiles using a nucleophilic organic catalyst 10

1.3.2 Photochemical generation of acyl and carbamoyl radicals using a nucleophilic organic .... catalyst 11

1.3.3 A general organocatalytic system for electron donor–acceptor complex photoactivation and its use in radical processes 11

Chapter II: Photochemical generation of radicals from alkyl electrophiles using a nucleophilic organic catalyst 13

2.1 Photochemistry 13

2.2 Radical generation strategies 16

2.2.1 Strategies based on the redox properties of the substrates 16

2.2.2 Methods based on atom abstraction 18

2.3 Thiocarbonyl compounds 19

2.3.1 Barton esters 20

2.3.2 Xanthate derivatives 21

2.4 Target of the project 23

2.4.1 Design plan 24

2.5 Results and discussion 25

2.5.1 Scope of the radical conjugate addition 29

2.5.2 Other radical processes 30

2.5.3 A dual organocatalytic system for asymmetric radical catalysis 34

2.6 Conclusions 36

2.7 Experimental section 36

2.7.1 General information 36

2.7.2 Substrate synthesis 37

2.7.3 Catalyst synthesis 38

2.7.4 Experimental setup 40

2.7.5 Giese addition 43

2.7.6 Tandem radical addition-cyclization of aromatic acrylamides 53
2.7.7 Alkylation of heteroarenes 59
2.7.8 Asymmetric catalytic α-alkylation of aldehydes 65
2.7.9 Large scale reactions 68
2.7.10 Continous flow reaction 70
2.7.11 Complex substrates 72
2.8 Mechanistic studies 76
2.8.1 Characterization of dithiocarbamate intermediates **3** 76
2.8.2 TEMPO trapping experiment of the benzyl radical 82
2.8.3 Study of the involvement of group transfer mechanism in the catalytic reaction 83

Chapter III: Photochemical generation of acyl and carbamoyl radicals using a nucleophilic organic catalyst 89

3.1 Introduction 89
3.2 Generation of acyl radicals from stoichiometric precursors 91
3.2.1 Acyl radicals from aldehydes 91
3.2.2 Use of stoichiometric oxidants 92
3.2.3 Use of acyl halides 93
3.2.4 Use of acyl chalcogens 94
3.2.5 Use of acylcobalt salophen complexes 96
3.3 Catalytic formation of acyl radicals 97
3.3.1 Photoredox-catalyzed HAT methods 97
3.3.2 Photoredox-catalyzed SET reduction 98
3.3.3 Photoredox-catalyzed SET oxidation 99
3.4 Target of the project 100
3.4.1 Design plan 100
3.5 Results and discussion 101
3.6 Carbamoyl radicals 107
3.6.1 Intermolecular Giese type addition 107
3.6.2 Lactam synthesis through carbamoyl radical-based cyclizations 109
3.7 Mechanistic studies 110
3.7.1 Acyl substitution and photochemical behavior of intermediate **5** 111
3.7.2 Fate and Behavior of the Xanthyl Radical **Ib** 114
3.7.3 Trap of the Acyl Radical and Ensuing Processes 119
3.7.4 Overall catalytic cycle and full mechanistic picture 120

3.8 Conclusions 121

3.9 Experimental section 122

3.9.1 General information 122
3.9.2 Substrate synthesis 124
3.9.3 Reaction with aroyl chlorides 130
3.9.4 Reaction with alkyl acyl chlorides 142
3.9.5 Reaction of carboxylic acids through acyl chloride formation 147
3.9.6 Reaction of carboxylic acids through anhydride formation 151
3.9.7 Scale-up reaction 153
3.9.8 Reaction of Carbamoyl Chlorides 154
3.9.10 Mechanistic studies 163

Chapter IV: A general organocatalytic system for electron donor–acceptor complex photoactivation and its use in radical processes 187

4.1 Introduction 187

4.2 Electron donor-acceptor complexes 190

4.2.1 Synthetic applications of EDA complexes 191
4.2.2 EDA complex with substoichiometric amount of acceptor 195

4.3 EDA complex with redox auxiliaries 196

4.3.1 EDA complex between redox auxiliaries and substrates 197
4.3.2 Catalytic EDA complexes 197

4.4 Target of the Project 201

4.4.1 Design plan 202

4.5 Results and Discussion 204

4.5.1 Developing a Giese-type addition process 205
4.5.2 Redox-neutral process 213
4.5.3 Minisci reaction 216
4.5.4 Further application of the EDA catalytic system 219

4.6 Conclusions 220

4.7 Experiental section 221

4.7.1 General information 221
4.7.2 Substrate synthesis 222
4.7.3 Experimental setups 223

4.7.4 Giese addition 226
4.7.5 Reduction 236
4.7.6 α-Alkylation of silyl enol ethers 240
4.7.7 Minisci reaction 250
4.7.8 Trifluoromethylation 258
4.7.9 Amidyl radical 259
4.7.10 Large scale reactions 260
4.7.11 Unsuccessful substrates 262
4.8 Mechanistic studies 262
4.8.1 Control experiments 262
4.8.2 Catalysts' stability experiments 266
4.8.3 UV-Vis spectroscopy 268
4.8.4 Transient absorption spectroscopy (TAS) 269
4.8.5 Cyclic voltammetry measurements 270
4.8.6 Quantum yield determination 274

Chapter V: General Conclusions 284

UNIVERSITAT ROVIRA I VIRGILI
NEW ORGANIC CATALYSTS FOR THE PHOTOCHEMICAL GENERATION OF RADICALS
Eduardo de Pedro Beato

UNIVERSITAT ROVIRA I VIRGILI
NEW ORGANIC CATALYSTS FOR THE PHOTOCHEMICAL GENERATION OF RADICALS
Eduardo de Pedro Beato

Chapter I

General Overview

1.1 Photochemistry

The International Union of Pure and Applied Chemistry (IUPAC) defines photochemistry as "the branch of chemistry concerned with the chemical effects of light".[1] It was the Swedish chemist Carl W. Scheele in 1777 who first observed darkening of silver chloride when exposed to violet light.[2] This simple observation was the beginning of a journey that ended up establishing a direct relation between light and matter, enunciated in two basic laws of photochemistry:[3]

- *Grotthuss–Draper law*: "only the light absorbed by a substance or substances is effective in bringing about chemical change".

This law highlights the importance of light-absorption in any photochemical process, since only irradiation that can be absorbed by a molecule can induce a chemical reaction. The molecule in question will absorb light at different wavelengths depending on its chemical and physical properties. This qualitative law may seem obvious today, but at the time it represented an important milestone in understanding the relation between light and matter.

- *Stark-Einstein law* or photochemical equivalence law: "in a photochemical process for each quantum of radiation (or photon) absorbed, one molecule of the substance reacts".

The second law is more of a quantitative nature, and represents the ideal scenario where each photon of light absorbed results in a productive photochemical reaction. Max Planck's theory about the discrete nature of light and energy is regarded as the birth of quantum physics.[4] Years later, Einstein proposed that electromagnetic waves consisted of spatially localized discrete wave-packets, which he called "the light quantum".[5] It was not until 1926 that Gilbert N. Lewis used the word *photon* in a letter to *Nature*,[6] and in 1928, Arthur Compton adopted the term and popularized it.

---

[1] Verhoeven, J. *Glossary of terms used in photochemistry* (IUPAC Recommendations 1996). *Pure and App. Chem.*, **1996**, *68*, 2223-2286.
[2] Balzani, V.; Ceroni, P.; Juris, A. *Photochemistry and Photophysics: Concepts, Research, Applications*. John Wiley & Sons, **2014**.
[3] Rennie, R. & Law J. *A Dictionary of Chemistry*. Oxford University Press, **2016**.
[4] Haar, D. ter. *The old quantum theory*. Oxford, New York, Pergamon Press, **1967**.
[5] Einstein, A., Über einen die Erzeugung und Verwandlung des Lichtes betreffenden heuristischen Gesichtspunkt. *Annalen der Physik* **1905**, *322*, 132-148.
[6] Lewis, G. N., The Conservation of Photons. *Nature* **1926**, *118*, 874-875.

The definition of light as a discrete form of energy ultimately opened the door to a quantitative correlation between radiation and matter, between photons and molecules. However, today we know that the second law of photochemistry, as originally enunciated, does not always apply, and there are several processes where the absorption of a photon does not produce any chemical transformation, but rather photophysical changes, such as the emission of light.

When a photon of a suitable energy is absorbed by a given molecule, it promotes an electron of the molecule from the ground state to an excited state.[2] These states are described by the wave functions Ψ, Ψ_f for the excited state and Ψ_i for the ground state. For this transition to take place, there must be a correspondence between the energy gap of the substance's molecular orbitals, and the energy of the incident photon ($h\nu$), where E_f and E_i are the energies of the excited-state Ψ_f and the ground-state Ψ_i, respectively.

$$h\nu = E_f - E_i$$

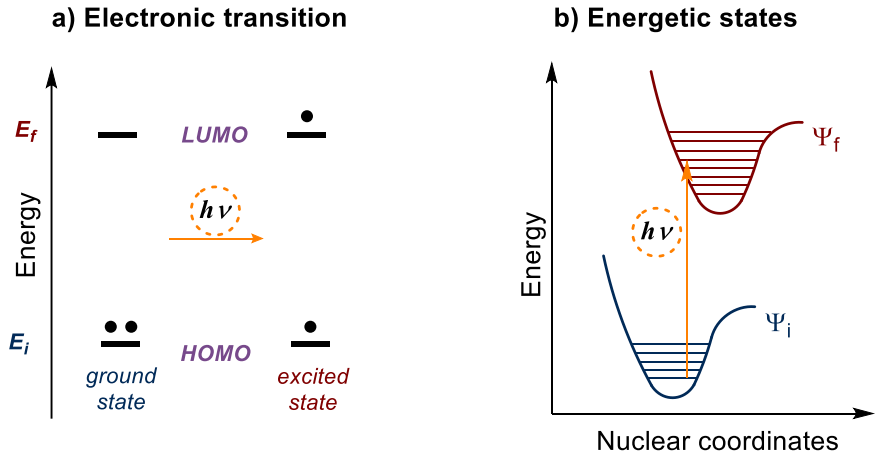

Figure 1.1. a) The energy of the absorbed photon promotes the transition of one electron from the highest occupied orbital (HOMO) to an unoccupied orbital (LUMO) b) Electronic transition from the ground-state Ψi to excited-state Ψ_f.

As a consequence of this electronic transition, the properties of excited-state molecules differ greatly from those of their ground state.[7] This difference could be exploited by organic chemists, who tried to affect the reactivity of a substance by populating its electronically excited state, thus opening new grounds for transformations not available through thermal activation.[8] At the beginning of the last century, pioneering studies by Ciamician and Silber

[7] Turro N. J., Ramamurthy V., Scaiano J. C. *Modern Molecular Photochemistry of Organic Molecules.* University Science Books, **2010**.
[8] Ravelli, D., Protti. S., Fagnoni, M. Carbon-Carbon Bond Forming Reaction via Photogenerated Intermediates. *Chem. Rev.* **2016**, *116*, 9850-9913.

established the field of synthetic photochemistry.[9] Ciamician saw the potential of employing solar energy as an inexpensive, abundant and non-toxic alternative to other energy sources.[10]

The most straightforward approach to photochemistry consists of the *direct excitation* of a molecule. In this unimolecular process, a given substrate absorbs a photon to reach an excited state, which can unlock new transformations unachievable in its ground state. One of the first applications of such approach was developed by Paterno[11] and Büchi.[12] Ultra-violet (UV) light irradiation is absorbed by aldehyde **1**, promoting it to its electronically-excited state **1***, which may then react with olefin **2** to form the oxetane product **3** in a photochemically allowed [2+2]-cycloaddition reaction (Scheme 1.1).

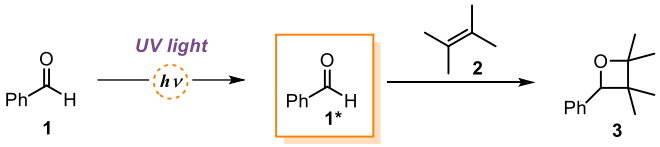

Scheme 1.1. Paterno-Büchi reaction for the synthesis of oxetanes.

In most cases, organic molecules possess a HOMO-LUMO energy gap which requires high energy irradiation (usually UV) to promote the desired transition. An alternative strategy involves the use of *photomediators* or *photocatalysts* (***PC***) to promote reactions under visible-light irradiation.[13] These compounds are often metal complexes or organic dyes with outstanding photophysical properties, which efficiently absorb photons in the visible light region. Once the photocatalyst reaches its excited state, two different bimolecular processes with a given reagent ***R*** can take place: energy transfer,[14] or electron transfer (Figure 1.2).[15] In the first case, an excited-state photocatalyst ***PC**** can transfer energy to a ground-state reagent ***R***, promoting one of its electrons from the HOMO to the LUMO (Figure 1.2a), delivering the excited-state reagent ***R****. On the other hand, in a single-electron transfer (SET) path, an electron is transferred from the ***PC**** to reagent ***R***, affording a radical ion pair (Figure 1.2b).

---

[9] Ciamician, G., Silber, P. Chemische Lichtwirkungen. *Berichte der deutschen chemischen Gesellschaft* **1900**, *33*, 2911-2913.
[10] Ciamician, G. The photochemistry of the future. *Science* **1912**, *36*, 385-394.
[11] Paternò, E.; Cheffi, G.; Sintesi in chimica organica per mezzo della luce. Nota II. Composti degli idrocarburi non saturi con aldeidi e chetoni. *Gazz. Chim. Ital.* **1909**, *39*, 341-361.
[12] Büchi, G.; Inman, C. G.; Lipinsky, E. S. Light-catalyzed Organic Reactions. I. The Reaction of Carbonyl Compounds with 2-Methyl-2-butene in the Presence of Ultraviolet Light. *J. Am. Chem. Soc.* **1954**, *76*, 4327-4331.
[13] Yoon, T. P.; Ischay, M. A.; Du, J. Visible Light Photocatalysis as a Greener Approach to Photochemical Synthesis. *Nature Chem.* **2010**, *2*, 527-532.
[14] Strieth-Kalthoff, F.; James, M. J.; Teders, M.; Pitzer, L.; Glorius, F. Energy transfer catalysis mediated by visible light: principles, applications, directions. *Chem. Soc. Rev.* **2018**, *47*, 7190-7202
[15] Kavarnos, G. J. *Fundamentals of Photoinduced Electron Transfer.* VCH, **1993.**

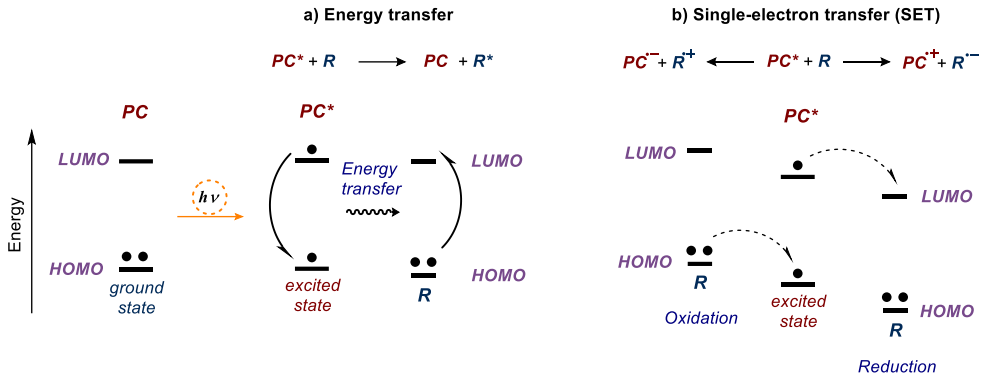

Figure 1.2. Photochemical processes. a) Energy-transfer from the excited-state photocatalyst to a reagent promotes the second to an electronically excited state. c) Electron-tranfer from the photocatalyst to reagent ***R*** gives access to a new radical species. ***R***: reagent. ***PC***: Photocatalyst.

When a molecule is promoted to an excited-state, removing the promoted electron from the half-filled LUMO becomes less endothermic. At the same time, adding one electron to the half-filled HOMO is more exothermic (Figure 1.2b). This phenomenon translates in the increased ability of the molecule (i.e. photocatalyst) to donate or accept electrons, making it a better oxidant and reductant that in its ground state. The field of photoredox catalysis has exploited this feature to activate substrates through an SET event by means of an excited-state photocatalyst (***PC****), allowing the generation of highly reactive open-shell intermediates under mild conditions (Figure 1.3). Upon light absorption, ***PC**** can enter an oxidative quenching cycle, where ***PC**** donates an electron to a suitable electron acceptor (***A***) via SET. This event produces radical anion $\boldsymbol{A}^{\bullet-}$ and the oxidized form to the photocatalyst ($\boldsymbol{PC}^{\bullet+}$). A second SET can take place, this time with an electron donor (***D***), regenerating the ***PC*** and closing the catalytic cycle. Alternatively, the process may proceed through a reductive quenching cycle, where ***PC**** firstly accepts one electron from a donor, affording the radical cation $\boldsymbol{D}^{\bullet+}$ and a reduced form of photocatalyst ($\boldsymbol{PC}^{\bullet-}$). Then, the latter reduces an acceptor (***A***) to regenerate the ground-state ***PC*** to close the cycle. Ultimately, photoredox catalysis exploits the redox properties of the precursor (donor or acceptor) to generate highly reactive open-shell species, which then can undergo subsequent transformations to afford the final reaction products. Unlike other approaches for the generation of reactive radicals, photoredox catalysis can harness visible-light to promote the SET event. This prevents the need for unstable radical precursors or strong reductants/oxidants, making this approach milder.[16]

[16] McAtee, R. C., McClain, E. J., Stephenson, C. R. J. Illuminating Photoredox Catalysis. *Trends in Chemistry* **2019**, *1*, 111-125.

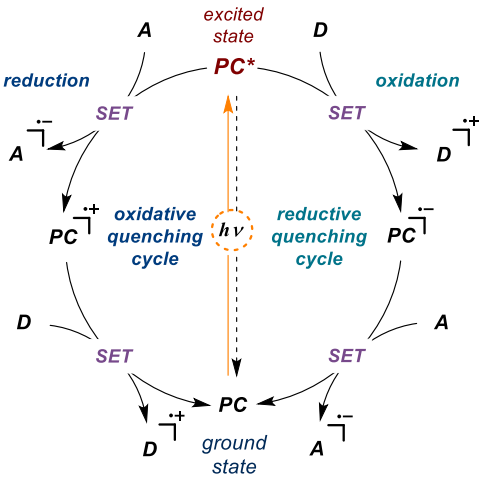

Figure 1.3. Photoredox catalysis.

One of the first examples of modern photoredox catalysis employed the photo-excitation of a Ru(II) complex to achieve the elusive stereoselective α-alkylation of aldehydes with alkyl bromides.[17] Key to this methodology, developed by the group of MacMillan, was to employ a platform for the generation of radicals compatible with an organocatalytic cycle.

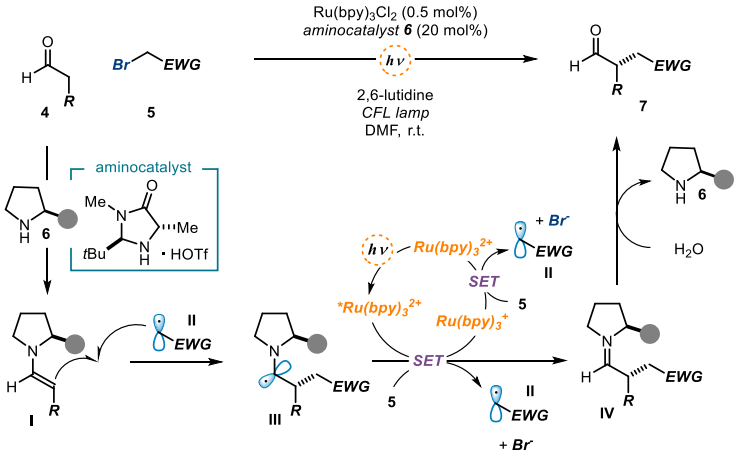

Scheme 1.2. Merging of organocatalysis and photoredox catalysis allowed the enantioselective α-alkylation of aldehydes with activated alkyl bromides.

[17] Nicewicz, D. A., MacMillan, D. W. C. Merging Photoredox Catalysis with Organocatalysis: the Direct Asymmetric Alkylation of Aldehydes. *Science* **2008**, *322*, 77-80.

In this study, MacMillan and coworkers proposed the mechanism depicted in Scheme 1.2. Condensation of aldehyde **4** with the chiral aminocatalyst **6** produces enamine **I**. Photo-excitation of $[Ru(bpy)_3]^{2+}$ generates the excited-state complex, which engages in an SET oxidation event with a sacrificial amount of enamine **I**, delivering the reduced-state $[Ru(bpy)_3]^{+}$. A favorable SET between alkyl bromide **5** by Ru(I) species continues the process, furnishing the target radical **II** and regenerating the $[Ru(bpy)_3]^{2+}$ complex. The electrophilic open-shell species **II** can be trapped by the electron-rich chiral enamine **I**, forging the new C-C bond and a new stereocenter. The ensuing α-amino radical **III** undergoes oxidation by the photo-excited Ru(II) complex forming the iminium **IV**, which is then hydrolysed to afford the enantioenriched product **7** and the organocatalyst **6**.

Further mechanistic studies by the group of Yoon[18] demonstrated that a self-propagating radical chain mechanism was operative in the reaction (Scheme 1.2), where a SET event between intermediate **III** and radical precursor **5**, propagates the chain generating radical **II** and iminium **IV**.

One year later, Stephenson[19] contributed to the field with the tin-free reductive dehalogenation of activated alkyl halides, promoted by the same photo-excited Ru(II) complex (Scheme 1.3). This seminal work achieved the visible-light promoted generation of alkyl radicals **V**, replacing toxic organotin reagents by simple amines as terminal reductants. The proposed mechanism starts with a SET between the protonated amine **9** and excited Ru(II) photocatalyst. Then, a second SET event between Ru(I) complex and alkyl bromide **8** releases radical **V**. The later undergoes hydrogen atom abstraction (HAT) from the radical cation **VI** to afford the dehalogenation product **10**, and the iminium ion **11** as byproduct.

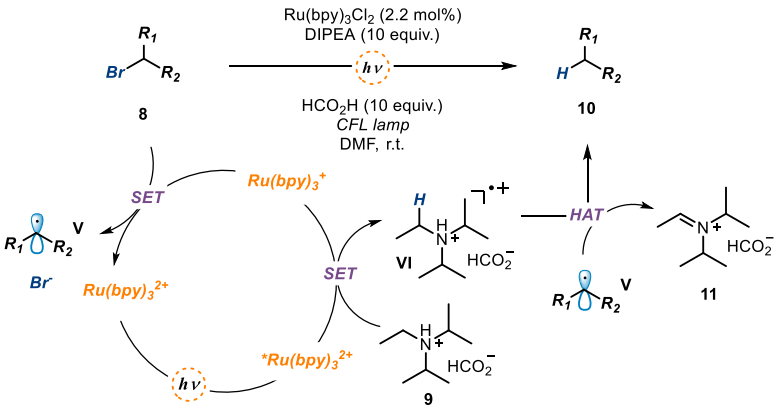

Scheme 1.3. Photocatalysed tin-free dehalogenation of alkyl bromides.

[18] Cismesia, M. A.; Yoon, T. P. Characterizing Chain Processes in Visible Light Photoredox Catalysis. *Chem. Sci.* **2015**, *6*, 5426-5434

[19] Narayanam, J. M., Tucker, J. W., Stephenson, C. R. J. Electron-Transfer Photoredox Catalysis: Development of a Tin-Free Reductive Dehalogenation Reaction. *J. Am. Chem. Soc.* **2009**, *131*, 8756-8757.

These examples marked the start of the renaissance of synthetic photochemistry, demonstrating the great potential of photoredox catalysis as a milder alternative for the generation of radicals. This field has since experienced continuous growth, in both academic and industrial settings.[20]

1.2 Direct excitation of organocatalytic intermediates

The combination of organocatalysis and photoredox catalysis has been one of the many accomplishments of modern photochemistry.[21] However, using an external photocatalyst is not the only way to exploit the potential of radical chemistry in organocatalysis. Our group recently discovered that some organocatalytic intermediates have the ability to absorb visible light to access an electronically excited state. Interestingly, these intermediates showed a bathochromic shift in their UV-vis spectra compared to the parent substrates, which permits the selective irradiation of the chiral intermediate in the presence of the starting materials. This feature allows to develop new stereoselective catalytic transformations previously unavailable by thermal pathways.[22] For example, in 2013 our group found that upon mixing the enamine **VII** with the electron-poor benzyl bromides **13a**, the color of the solution changed from colorless to bright yellow (Scheme 1.4a).[23] This observation was rationalized by a new ground-state association, called an electron donor-acceptor (EDA) complex.[24] These complexes have different physical and chemical properties with respect to the individual components: for example, they can absorb visible light even if their progenitors cannot. Irradiation of the EDA complex promoted an intra-complex SET, ultimately releasing the benzylic radical **VIII**, which is trapped by the ground-state enamine **VII** to give the enantioenriched product **14a.**

[20] Crisenza, G. E. M.; Melchiorre, P., Chemistry glows green with photoredox catalysis. *Nat. Commun.* **2020**, *11*, 803.
[21] Shaw, M. H.; Twilton, J.; MacMillan, D. W. C., Photoredox Catalysis in Organic Chemistry. *J. Org. Chem.* **2016**, *81*, 6898-6926.
[22] Silvi, M.; Melchiorre, P. Enhancing the potential of enantioselective organocatalysis with light. *Nature* **2018**, *554*, 41-49.
[23] Arceo, E.; Jurberg, I. D.; Álvarez-Fernández, A.; Melchiorre, P. Photochemical Activity of a Key Donor–Acceptor Complex Can Drive Stereoselective Catalytic α-alkylation of Aldehydes. *Nature Chem.* **2013**, *5*, 750-756.
[24] Crisenza, G. E. M.; Mazzarella, D.; Melchiorre, P., Synthetic Methods Driven by the Photoactivity of Electron Donor–Acceptor Complexes. *J. Am. Chem. Soc.* **2020**, *142*, 5461-5476.

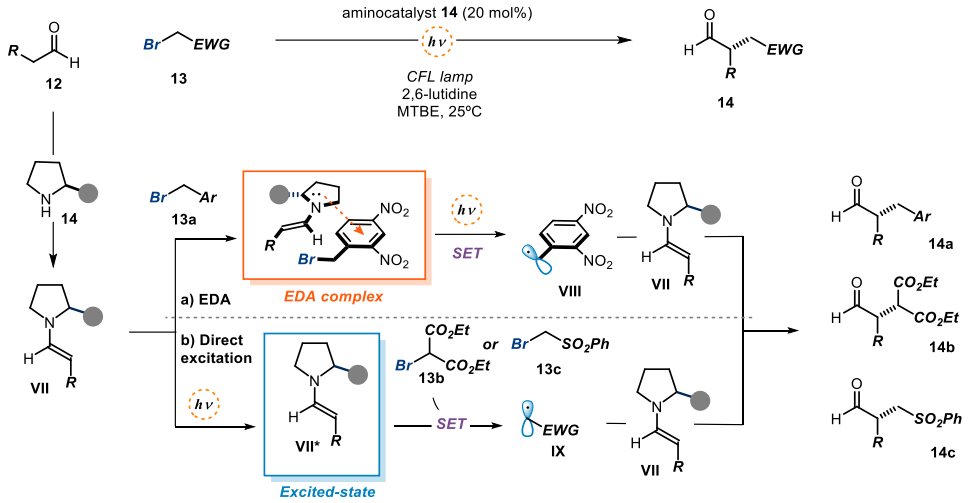

Scheme 1.4. a) Photochemical stereoselective alkylation of aldehydes promoted by EDA complex formation. b) Direct photoexcitation of enamine intermediate **VII** that acts as a strong photoreductant.

The generation of radicals from organocatalytic intermediates is not restricted to EDA complex association. Indeed, when other radical precursors (**13b**, **13c**) are employed, such association is not observed (Scheme 1.4b).[25] Nevertheless, enamine **VII** alone is able to absorb in the near-UV region of the visible spectra, reaching an excited-state **VII*** which behaves as a strong photo-reductant (estimated E_{red}*(**VII**$^{\cdot+}$/**VII***) ~ −2.50 V versus Ag/AgCl, NaCl sat.). This new reactivity acquired in the excited state allows the activation of the otherwise inert substrates **13b-c**. After SET, radical **IX** is formed, which is trapped by the ground-state enamine **VII** following a similar mechanistic pathway as the one proposed for the EDA activation. Mechanistic investigations disclosed that, in analogy to the protocol reported by MacMillan[17] and further studied by Yoon[18] (Scheme 1.2), this transformation relied on a self-propagating radical chain manifold.[26]

The discovery of the photochemistry of organocatalytically-generated enamine intermediates, and how they can unlock new reactivity, encouraged our group to explore the excited-state behavior of other established aminocatalytic intermediates. If electron-rich enamines **VII** can act as strong photo-reductants in their excited state, it follows that an electron-deficient iminium ion **X** may display the opposite behavior and become a strong excited-state photo-

[25] a) Silvi, M., Arceo, E., Jurberg, I. D., Cassani, C., Melchiorre, P. Enantioselective Organocatalytic Alkylation of Aldehydes and Enals Driven by the Direct Photoexcitation of Enamines. *J. Am. Chem. Soc.* **2015**, *137*, 6120-6123. b) Filippini, G., Silvi, M., Melchiorre, P. Enantioselective Formal α-methylation and α-benzylation of Aldehydes by Means of Photo-Organocatalysis. *Angew. Chem. Int. Ed.* **2017**, *56*, 4447-4451.
[26] Bahamonde, A.; Melchiorre, P. Mechanism of the Stereoselective α-Alkylation of Aldehydes Driven by the Photochemical Activity of Enamines. *J. Am. Chem. Soc.* **2016**, *138*, 8019-8030.

oxidant upon irradiation **X*** (Scheme 1.5).[27] Acid-promoted condensation of cinnamaldehyde derivatives **15** and aminocatalyst **17** leads to iminium ions of type **X**. In the excited state, iminium ion **X*** triggers an SET oxidation of benzyl silanes **16**, which upon cleavage of the C-Si bond, release two open-shell species: the benzyl radical **XI** and the chiral allylic radical **XII**. For the next step, a mechanism involving a radical coupling was proposed. Ultimately, hydrolysis will furnish enantioenriched β-alkylation product **18** while closing the catalytic cycle.

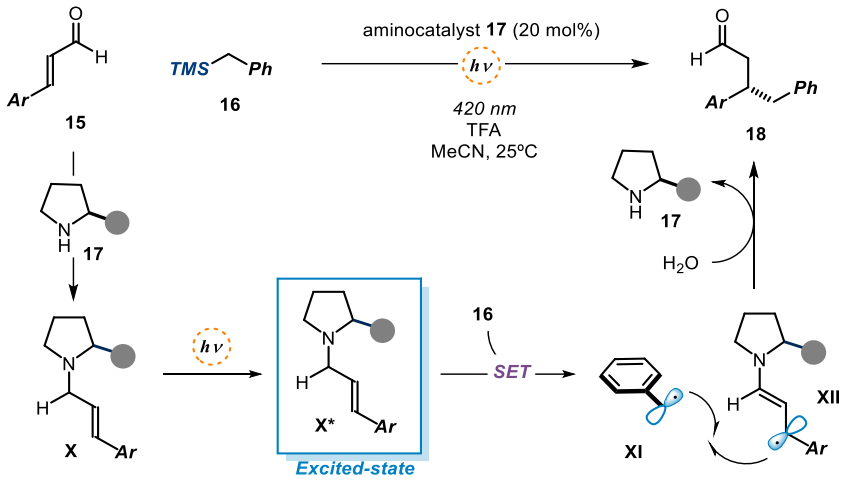

Scheme 1.5. Photochemical β-alkylation of cinnamaldehyde derivatives enabled by the direct excitation of chiral iminium ions.

Our group has applied the direct excitation of iminium ions to activate different radical precursors,[28a,e] and to achieve numerous asymmetric transformations, including cascade processes.[28b,c,d] Overall, the works detailed in this section highlight how direct excitation of organocatalytic intermediates can unlock new reactivity by generating open-shell species.

During my doctoral thesis work, I explored the photochemistry of a new type of in situ formed organocatalytic intermediates. The aim was to activate inert substrates, by using the principle

[27] Silvi, M.; Verrier, C.; Rey, Y. P.; Buzzetti, L.; Melchiorre, P., Visible-Light Excitation of Iminium Ions Enables the Enantioselective Catalytic β-Alkylation of Enals. *Nature Chem.* **2017**, *9*, 868-873.

[28] a) Verrier, C.; Alandini, N.; Pezzetta, C.; Moliterno, M.; Buzzetti, L.; Hepburn, H. B.; Vega-Peñaloza, A.; Silvi, M.; Melchiorre, P. Direct Stereoselective Installation of Alkyl Fragments at the β-Carbon of Enals via Excited Iminium Ion Catalysis. *ACS Catal.* **2018**, *8*, 1062-1066. b) Woźniak, Ł., Magagnano, G., Melchiorre, P. Enantioselective Photochemical Organocascade Catalysis. *Angew. Chem. Int. Ed.* **2018**, *57*, 1080-1084. c) Bonilla, P.; Rey, Y. P.; Holden, C. M.; Melchiorre, P. Photo-Organocatalytic Enantioselective Radical Cascade Reactions of Unactivated Olefins. *Angew. Chem. Int. Ed.* **2018**, *57*, 12819-12823. d) Perego, L. A.; Bonilla, P.; Melchiorre, P., Photo-Organocatalytic Enantioselective Radical Cascade Enabled by Single-Electron Transfer Activation of Allenes. *Adv. Synth. Catal.* **2020**, *362*, 302-307. e) Mazzarella. D.; Crisenza, G. E. M.; Melchiorre, P. Asymmetric Photocatalytic C−H Functionalization of Toluene and Derivatives. *J. Am. Chem. Soc.* **2018**, *140,* 8439-8443.

of covalent organocatalysis, where a new catalytic intermediate can trigger transformations unachievable by the substrate itself. Aims and objectives of the thesis are detailed in the next section.

1.3 General objectives and summary

Traditionally, the generation of radicals requires strategies that exploit either bond dissociation energy or the redox properties of the precursors. The main objective of this doctoral thesis was to study and develop new strategies for the photochemical generation of radicals that exploit the electrophilicity of the substrates rather than their redox properties.
In Chapter II, I will discuss the realization of this radical generation strategy. In the following Chapters (III and IV), I will focus on how we further explored our catalytic design to access different radicals, and achieve a variety of transformations.

1.3.1 Photochemical generation of radicals from alkyl electrophiles using a nucleophilic organic catalyst

In Chapter II, the design of a new class of dithiocarbamate-based organocatalysts **19** and its use in the development of a radical generation platform is discussed. Our goal was to go beyond the redox properties of a potential radical precursor, exploiting a different property rather than its redox potential (Scheme 1.6).

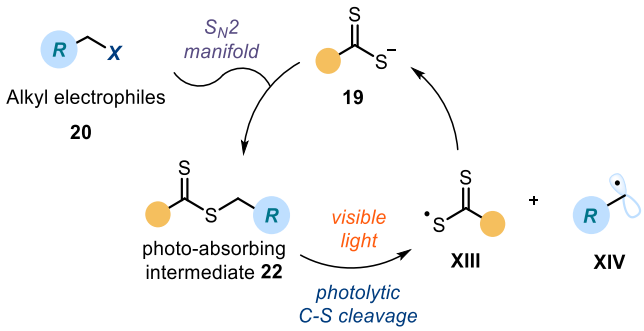

Scheme 1.6. Radical generation platform based on a nucleophilic organic catalyst.

We designed a nucleophilic dithiocarbamate anion catalyst **19**, adorned with a well-tailored chromophoric unit, to activate alkyl electrophiles **20** via an S_N2 pathway. The resulting photon-absorbing intermediate **22** affords radicals upon homolytic cleavage induced by visible light. This catalytic S_N2-based strategy grants access to open-shell intermediates **XIV** from a variety of substrates that would be incompatible with or inert to classical radical-generating strategies, including photoredox catalysis. We also applied the methodology to develop a variety C-C bond-forming reactions, including enantioselective radical catalysis.

1.3.2 Photochemical generation of acyl and carbamoyl radicals using a nucleophilic organic catalyst

In Chapter III, the developed organocatalytic generation strategy was expanded to a new family of radicals, acyl and carbamoyl radicals. By employing electrophilic acyl and carbamoyl chlorides **23**, the corresponding carbon-centered radicals **XV** could be accessed and efficiently trapped (Scheme 1.7).

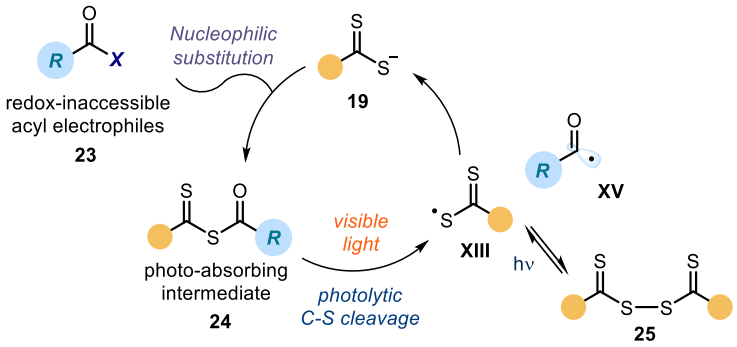

Scheme 1.7. Photochemical generation of acyl radicals activated by a nucleophilic organic catalyst.

This strategy uses a commercially available nucleophilic organic catalyst **19**, which operates via a nucleophilic acyl substitution path. The resulting nucleophilic radicals **XV** were intercepted by a variety of electron-poor olefins in a Giese-type addition process. The chemistry requires low-energy photons (blue LEDs) to activate precursors, which, due to their high reduction potential, are not readily prone to redox-based activation mechanisms. To elucidate the key mechanistic aspects of this catalytic photochemical radical generation strategy, we used a combination of transient absorption spectroscopy investigations, electrochemical studies, quantum yield measurements, and the characterization of key intermediates. We identified a variety of off-cycle intermediates (i.e. **25**) that engage in a light-regulated equilibrium with reactive radicals. These regulated equilibria cooperate to control the overall concentrations of the radicals, contributing to the efficiency of the overall catalytic process and facilitating the turnover of the catalyst.

1.3.3 A general organocatalytic system for electron donor–acceptor complex photoactivation and its use in radical processes

In Chapter IV, we exploited the electronic properties of dithiocarbamate-based anions **19**, rather than its nucleophilicity, developing a new catalytic electron donor-acceptor (EDA) complex platform, where the organocatalyst serves as the catalytic donor. A variety of radical

precursors **26** were suitable acceptors for EDA complex formation, delivering the corresponding radicals **27** upon visible-light excitation with blue light (Scheme 1.8). With this strategy, we could access a plethora of open-shell intermediates under mild conditions, including non-stabilized carbon radicals and nitrogen-centered radicals.

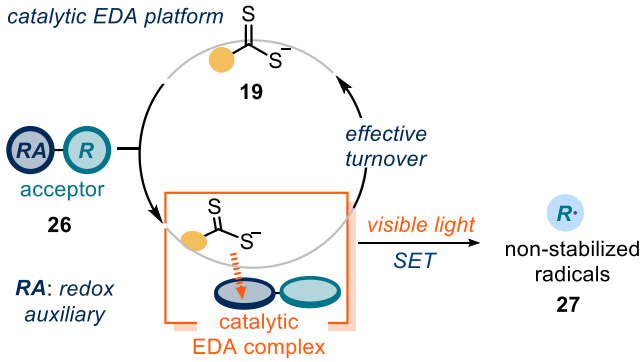

Scheme 1.8. Catalytic EDA platform with dithiocarbamate-based organocatalyst as donor.

The modular nature of the commercially available xanthogenate and dithiocarbamate anion organocatalysts **19** offers a versatile EDA complex catalytic platform for developing mechanistically distinct radical reactions, including redox neutral and net-reductive processes. Mechanistic investigations supported that a closed catalytic cycle is operational, highlighting the ability of the organic catalysts to turnover and iteratively driving every catalytic cycle.

Chapter II

Photochemical generation of radicals from alkyl electrophiles using a nucleophilic organic catalyst

Target

The study and development of a new radical generation strategy that exploits the electrophilicity of the substrates rather than their redox properties. The aim is to form alkyl radicals from difficul-to-activate alkyl electrophiles, including chlorides and mesylates.

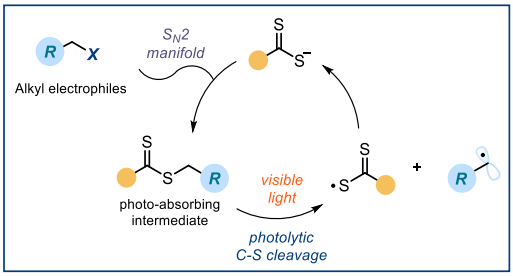

Tool

Using a nucleophilic organic catalyst that, upon S_N2 activation and photolysis of the resulting adduct, can generate a variety of radicals and engage them in different transformations. The reactivity and photophysical properties of the organic catalyst could be modulated to effectively activate radical precursors inert towards classical photoredox methods.[1]

2.1 Photochemistry

Free radical chemistry[2] has found extensive use in numerous applications, ranging from organic synthesis to life science.[3] Radical chemistry offers powerful ways of making molecules that are often complementary to classical methods proceeding via ionic pathways. There are several strategies for generating radicals, which traditionally rely on the redox properties or bond-dissociation energy (BDE) of the precursors (Scheme 2.1). The development of new radical-generating strategies is relevant to further expand the potential of radical transformations. Traditionally, radicals were accessed using initiators, high-energy compounds (e.g. diazo compounds or peroxides) that, upon homolysis induced by heat or high-energy light, generate a reactive radical which can abstract a hydrogen or halogen atom from a substrate **S** (Scheme 2.1, left panel). that undergo homolysis induced by heat or light,

[1] The project discussed in this chapter was conducted in collaboration with Dr. Bertrand Schweitzer-Chaput and Dr. Matthew A. Horwitz. I was involved in the discovery of some of the reactions and explored the scope of the transformations. This work has been published, see: Schweitzer-Chaput, B.; Horwitz, M. A.; de Pedro Beato, E.; Melchiorre, P. Photochemical generation of radicals from alkyl electrophiles using a nucleophilic organic catalyst. *Nature Chem.* **2019**, *11*, 129–135.

[2] Renaud, P.; Sibi, M. P. *Radicals in Organic Synthesis. Eds.*, **2001**, Wiley-VCH: Weinheim, Germany.

[3] Yan, M.; Lo, J. C.; Edwards, J. T.; Baran, P. S., Radicals: Reactive Intermediates with Translational Potential. *J. Am. Chem. Soc.* **2016**, *138*, 12692-12714.

and in the process deliver an open-shell species. Ultimately, this strategy relies on the BDE properties of the precursor **S** to form the target open-shell intermediate ***R*·**.

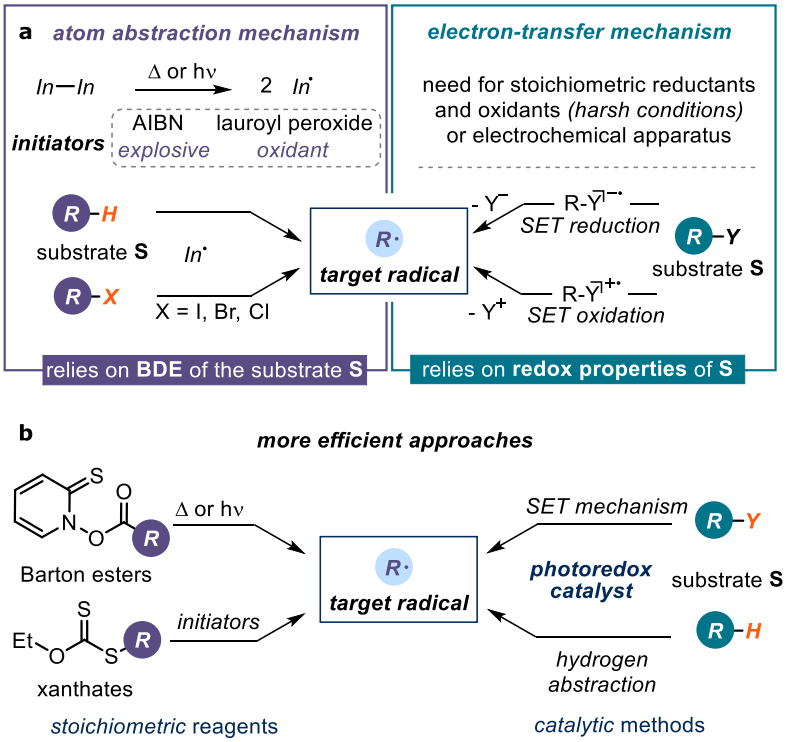

Scheme 2.1. Strategies for generating radicals. a) Established methods based on atom abstraction and electron transfer mechanisms require precursors with suitable bond-dissociation energies (BDE) or redox properties, respectively. b) Practical approaches to generate radicals under milder conditions using stoichiometric precursors and photoredox catalysts. AIBN, azobisisobutyronitrile.

Another extensively studied approach exploits the tendency of a substrate **S** to engage in redox processes, which are triggered by stoichiometric oxidants/reductants,[4] or by electrochemical means[5] (Scheme 2.1, right panel). The radical ions emerging from the single-electron transfer (SET) event can then fragment to yield the target radical ***R*·**. These classical strategies are powerful but generally require relatively harsh conditions, including hazardous and toxic reagents, high temperatures, and/or UV-light irradiation. A crucial step towards milder reaction conditions and, consequently, more selective reactions has been the use of substrates bearing thio functions that can act as both radical initiators and reactants, such as Barton

[4] Lalevée, J.; Fouassier, J. P., Overview of Radical Initiation. In *Encyclopedia of Radicals in Chemistry, Biology and Materials*, **2012**.
[5] Yan, M.; Kawamata, Y.; Baran, P. S., Synthetic Organic Electrochemical Methods Since 2000: On the Verge of a Renaissance. *Chem. Rev.* **2017**, *117*, 13230-13319.

esters[6] and xanthates (Scheme 2.1b, left).[7] The pioneering work of Barton and Zard helped to further expand the synthetic potential of radical chemistry. Although thio-derivatives were easily accessible, these methods still relied on purposely designed stoichiometric reagents.

Recently, radical generation strategies triggered by visible-light have enjoyed an increasing development.[8] This is mainly due to the outburst of photoredox catalysis, which provides an attractive way to access radicals under mild conditions and in a catalytic manner.[9] This approach exploits the ability of light-absorbing metal or organic catalysts to harness photonic energy to repeatedly remove an electron from or donate an electron to simple bench-stable substrates (Scheme 2.1b, right). This SET mechanism is generally used to produce the target radical **I**, but some photoredox catalysts can also adopt a hydrogen abstraction manifold to generate **I**.[10] In analogy to other radical generation strategies, when applying photoredox catalysis a chemist must rely on the redox properties[11] or the BDE to predict the suitability of a given substrate **S** to successfully form the target open-shell species ***R*·**.

We wondered if we could combine the ability of sulfur-containing compounds, including xanthates, to generate radicals with modern photochemistry tools to develop a catalytic strategy that harnesses different physical properties of the substrates to generate carbon radicals under mild conditions (Scheme 2.2). Specifically, we sought to capitalize upon the nucleophilic properties of a dithiocarbamate anion catalyst **2** to form in situ a photoactive dithiocarbamate derivative **3** via S_N2 displacement of simple alkyl electrophiles **1**, bearing different leaving groups (***X*** in Scheme 2.2). The resulting thio-derivative intermediate **3**, whose absorption could be tuned by adorning the progenitor catalyst **2** with a suitable chromophore, would afford radicals **II** and **III** upon excitation by weak visible light (blue light-emitting diodes, LEDs) and homolytic cleavage of the weak C-S bond. The sulfur-

---

[6] (a) Barton, D. H. R.; McCombie, S. W., A new method for the deoxygenation of secondary alcohols. *J. Chem. Soc., Perkin Trans. 1* **1975**, 1574-1585. (b) Barton, D. H. R.; Crich, D.; Motherwell, W. B., New and improved methods for the radical decarboxylation of acids. *J. Chem. Soc., Chem. Commun.* **1983**, 939-941. (c) Barton, D. H. R.; Zard, S. Z., Invention of new reactions useful in the chemistry of natural products. *Pure Appl. Chem.* **1986**, *58*, 675-684. (d) Barton, D. H. R.; Crich, D.; Motherwell, W. B. The Invention of New Radical Chain Reactions. Part VII. Radical Chemistry of Thiohydroxamic Esters: A New Method for the Generation of Carbon Radicals from Carboxylic Acids. *Tetrahedron* **1985**, *41*, 3901–3924.

[7] (a) Delduc, P.; Tailhan, C.; Zard, S. Z., A convenient source of alkyl and acyl radicals. *J. Chem. Soc., Chem. Commun.* **1988**, 308-310. (b) Zard, S. Z., On the Trail of Xanthates: Some New Chemistry from an Old Functional Group. *Angew. Chem., Int. Ed.* **1997**, *36*, 672-685.

[8] Studer, A.; Curran, D. P., Catalysis of Radical Reactions: A Radical Chemistry Perspective. *Angew. Chem. Int. Ed.* **2016**, *55*, 58-102.

[9] (a) Shaw, M. H.; Twilton, J.; MacMillan, D. W. C., Photoredox Catalysis in Organic Chemistry. *J. Org. Chem.* **2016**, *81*, 6898-6926. (b) Matsui, J. K.; Lang, S. B.; Heitz, D. R.; Molander, G. A., Photoredox-Mediated Routes to Radicals: The Value of Catalytic Radical Generation in Synthetic Methods Development. *ACS Catal.* **2017**, *7*, 2563-2575.

[10] Tzirakis, M. D.; Lykakis, I. N.; Orfanopoulos, M., Decatungstate as an efficient photocatalyst in organic chemistry. *Chem. Soc. Rev.* **2009**, *38*, 2609-2621.

[11] Roth, H. G.; Romero, N. A.; Nicewicz, D. A., Experimental and Calculated Electrochemical Potentials of Common Organic Molecules for Applications to Single-Electron Redox Chemistry. *Synlett* **2016**, *27*, 714-723.

centered radical **II** would be reduced through SET to recover the anion catalyst, closing the catalytic cycle. Overall, this S_N2-based manifold would generate open-shell intermediates **III** from a variety of substrates **1** that would be inert to or incompatible with classical radical generating strategies.

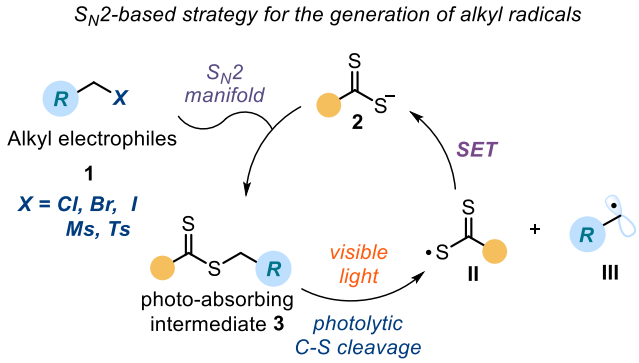

Scheme 2.2. S_N2-based catalytic protocol for photochemically generating radicals from precursors **1** that are redox-inactive or not prone to undergoing atom abstraction activation.

In this chapter, I will detail the successful implementation of this strategy and the development of suitable dithiocarbamate-based organocatalysts.

2.2 Radical generation strategies

Throughout the years, different radical generation strategies have been developed.[2] We can classify these methods in two main families: those relying on the redox properties of the precursors, and those that take advantage of the low BDE of a specific bond in the substrate (Scheme 2.1). In the following section, I will discuss some of those approaches, mainly focusing on thiocarbonyl-based radical strategies which served an inspiration for our developed methodology.

2.2.1 Strategies based on the redox properties of the substrates

The SET reduction or oxidation of a suitable substrate has been largely used to generate radicals and engage them in synthetic chemistry. Earliest examples of this approach used stoichiometric amounts of metal salts (including Fe^{3+}, Ag^{+}, Ce^{4+}, Mn^{3+}, Cu^{+}, Co^{+} or Ti^{3+}, Scheme 2.3).[12] Later, more efficient systems appeared where the metal salts could be used as catalysts or mediators, while an organic compound acted as the terminal oxidant or reductant.[2]

[12] Denisov, E. T.; Denisova, T. G.; Pokidova, T. S. *Handbook of Free Radical Initiators*. John Wiley & Sons, **2005**.

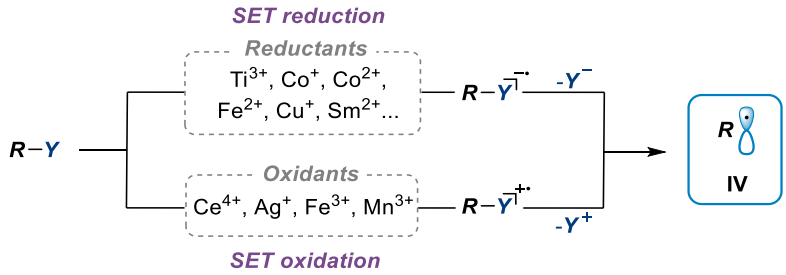

Scheme 2.3. Strategies for the generation of radicals relying on their redox properties.

The advent of modern photoredox catalysis has provided an attractive way to access radicals under mild conditions and in a catalytic manner (Scheme 2.4).[9] The ability of a photocatalyst to absorb visible-light, access a high-energy excited state, and acquire better redox properties unlocked new reactivity manifolds that could not be achieved by classical methods.

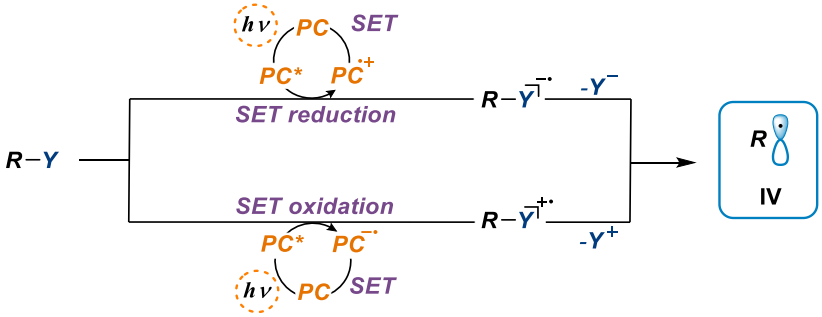

Scheme 2.4. Photoredox catalysis opened new opportunities in radical chemistry replacing traditional oxidant and reductants.

Electrochemistry is another established approach to make radicals that has been extensively revisited during the last few years.[5] In this case, the SET process takes place on the surface of an electrode (cathode or anode) while electricity is the sole energy source (Scheme 2.5). Controlling the applied potential can allow for the selective reduction or oxidation of substrates, but some limitations may arise from incompatibilities between the reagents and the metal electrodes. Moreover, usually external redox mediators are needed to facilitate the SET between the electrode and the radical precursor.

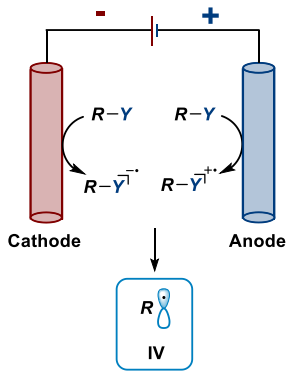

Scheme 2.5. Electrochemistry as an alternative radical formation strategy.

Although powerful, all these methods rely on one specific property of the radical precursors: their redox potential and propensity to accept or donate one electron.

2.2.2 Methods based on atom abstraction

Another classical strategy for the generation of radicals exploits the BDE of a given bond within the substrate. Historically, this approach uses an initiator, a compound which contains one or several weak bonds with a BDEs in the range of 30-50 kcal/mol (Scheme 2.6). Commonly used initiators include peroxides and azo-compounds, which are hazardous and explosive materials.[13] Heat or high-energy light can cleave such weak bonds producing free radicals. This initiating open-shell species (*In*·) can then abstract a hydrogen (via hydrogen atom transfer, HAT) or a halogen (via halogen atom transfer, XAT) from the precursors **S**, leading to the target radical **IV** (Scheme 2.6).[4] Crucial for the activation of the substrate **S** is the difference in BDE between the newly formed bond (*In*-*X*) and the broken one (*R*-*X*).

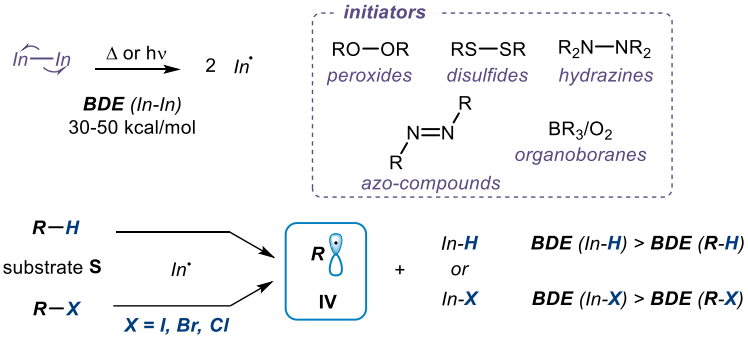

Scheme 2.6. Initiators, upon decomposition and radical formation, abstract an atom from the substrates.

[13] Luo, Y. R. *Handbook of Bond Dissociation Energies in Organic Compounds*. CRC press, **2002**.

The introduction of photoredox catalysis allowed to replace initiators by milder and safer alternatives. Some photocatalysts, such as benzophenone **4**, upon light excitation, can reach a high-energy state **IV** that can abstract atoms from a substrate with a low BDE (Scheme 2.7).[9] Nevertheless, these methods rely on the BDE of a C-H bond of the substrate and selective functionalization can be challenging.

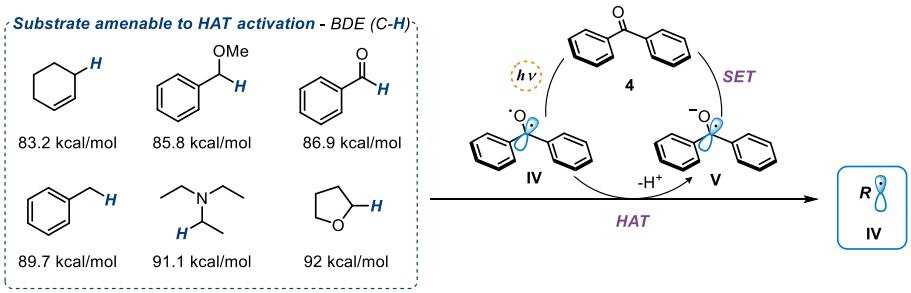

Scheme 2.7. Direct HAT from an excited-state of the photocatalyst.

2.3 Thiocarbonyl compounds

An interesting variation of BDE-based radical strategies was report by Barton in the early 1980's.[6] Thiocarbonyl derivatives can absorb light to then fragment or undergo thermal homolysis, thus removing the need for an external initiator (Scheme 2.8). Specifically, Barton explored *N*-hydroxy-2-thiopyridone acyl derivatives **5** (more commonly known as Barton esters) as precursors of alkyl radicals.[6] This approach was later expanded by Zard with the introduction of other thio functions, acting as both radical precursors and reactants, such as xanthates **6** (and dithiocarbamates).[7]

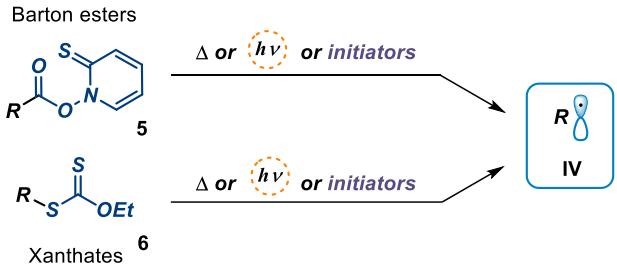

Scheme 2.8. Thiocarbonyl compounds as a more efficient approach to generate radicals.

This section will briefly describe the most relevant applications of thiocarbonyl compounds and the features that made them so useful in radical processes.

2.3.1 Barton esters

Barton esters **5** are thiocarbonyl derivatives that bear a weak N-O bond (~28 Kcal/mol).[14] As a consequence, they have the ability to undergo facile homolysis upon applied energy (Scheme 2.9). Thio-derivatives can also act similarly to other radical precursors in the presence of an initiator (*In*·), for these highly energetic species can react with **5** to form a *In-S* bond in byproduct **8**, eventually releasing radical **VIII**. **VIII** can then undergo fast decarboxylation to afford the target radical **IV** (Scheme 2.9a). On the other hand, thiocarbonyl compounds **5** can also be activated by temperature and heat without any external agent. Indeed, when temperatures higher than 62 ºC are applied, the labile N-O bond within **5** fragments providing radicals **VII** and **VIII**. Decarboxylation of **VIII** leads to radical **IV** (Scheme 2.9b). Activation by UV light is also possible (Scheme 2.9b): compound **5** possesses an absorption maximum at about 365 nm[15] and, when exposed to wavelengths lower or equal to that, a $\Psi_i \rightarrow \Psi_f$ electronic transition is promoted (Ψ = wave-function, associated with ground and excited states). The energy of the excited state is high enough to break the labile N-O bond, leading to homolysis.

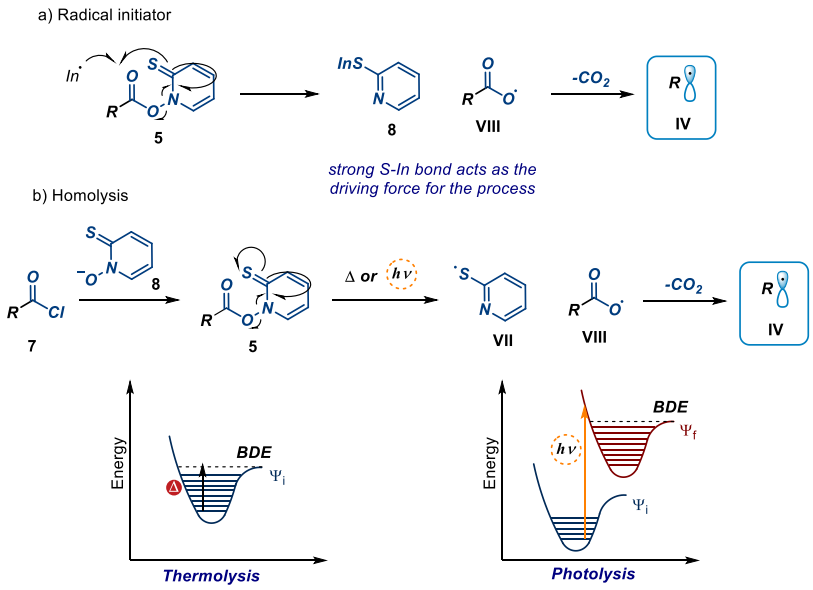

Scheme 2.9. Barton ester decarboxylation mechanism.

[14] For computational details, see: Allonas, X.; Dietlin, C.; Fouassier, J.-P.; Casiraghi, A.; Visconti, M.; Norcini, G.; Bassi, G. Barton Esters as New Radical Photoinitiators for Flat Panel Display Applications *J. Photopolym. Sci. Technol.* **2008**, *21*, 505-509.

[15] (a) Barton, D. H. R.; Blundell, P.; Jaszberenyi, J. C. Quantum Yields in the Photochemically Induced Radical Chemistry of Acyl Derivatives of Thiohydroxamic Acids. *J. Am. Chem. Soc.* **1991**, *113*, 6937–6942. (b) Barton, D. H. R.; Jaszberenyl, J. C.; Tang, D. Photolytic Generation of Carbon Radicals from Barton Esters: Recent Developments. *Tetrahedron Lett.* **1993**, *34*, 3381–3384.

2.3.2 Xanthate derivatives

Xanthate derivatives are other thiocarbonyl compounds broadly explored as radical precursors, mainly by Zard and co-workers.[7] Xanthates (and dithiocarbamates) are readily accessible by nucleophilic substitution from the parent organic salt **2a** and an alkyl electrophile **9** (Scheme 2.10). In analogy to the Barton esters, a key aspect of these radical precursors is the weak C-S bond,[16] which can undergo homolytic cleavage when exposed to an energy source (heat or light).[17] Nevertheless, in most cases an external initiator is required to start the process (Scheme 2.10), where the formation of the new *In-S* bond in byproduct **9** acts as the driving force for the release of the target radical **IV**.

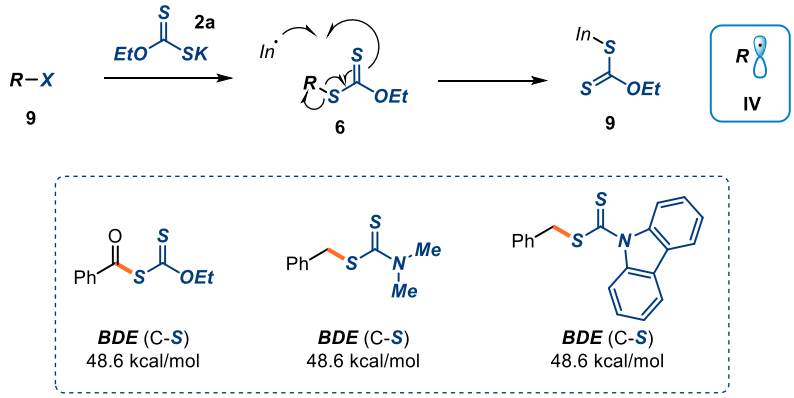

Scheme 2.10. Xanthate radical initiation mechanism.

The mechanism of radical generation and the consequent chain that delivers the group transfer product has been described as *degenerative xanthate transfer*. This xanthate transfer manifold is depicted in Scheme 2.11.[7] The process starts with an initiation, either by an external agent or by homolysis of the xanthate derivative **6**, which releases radical **IV**. The ensuing radical **IV** can carry on two different paths: i) radical **IV** can be intercepted by olefin **10** to forge a new C-C bond (highlighted in orange) and intermediate **IX** (right part of Scheme 2.11). When **IX** encounters the xanthate derivative **6**, the group transfer step can take place delivering the stabilized radical **X**. Finally, radical **X** fragments to provide the transfer product **11** and radical **IV** again, thus propagating the radical chain. ii) A second path available to **IV** is illustrated on the left of Scheme 2.11: when **IV** is captured by xanthate **6**, a more stabilized open-shell species **XI** is formed. This addition-fragmentation equilibrium effectively controls the

[16] Lalevée, J.; Blanchard, N.; El-Roz, M.; Allonas, X.; Fouassier, J. P. New Photoiniferters: Respective Role of the Initiating and Persistent Radicals. *Macromolecules* **2008**, *41*, 2347–2352.
[17] Barton, D. H. R.; George, M. V.; Tomoeda, M. Photochemical Transformations. Part XIII. A New Method for the Production of Acyl Radicals. *J. Chem. Soc.* **1962**, 1967–1974.

concentration of the reactive radical **IV** in solution, avoiding alternative unproductive pathways. The alternative fragmentation of **XI** (Scheme 2.11, in gray) to deliver the high-energy ethyl radical and byproduct **12** does not take place due to energetic requirements to break a strong C-O bond, in comparison with the labile C-S bond.

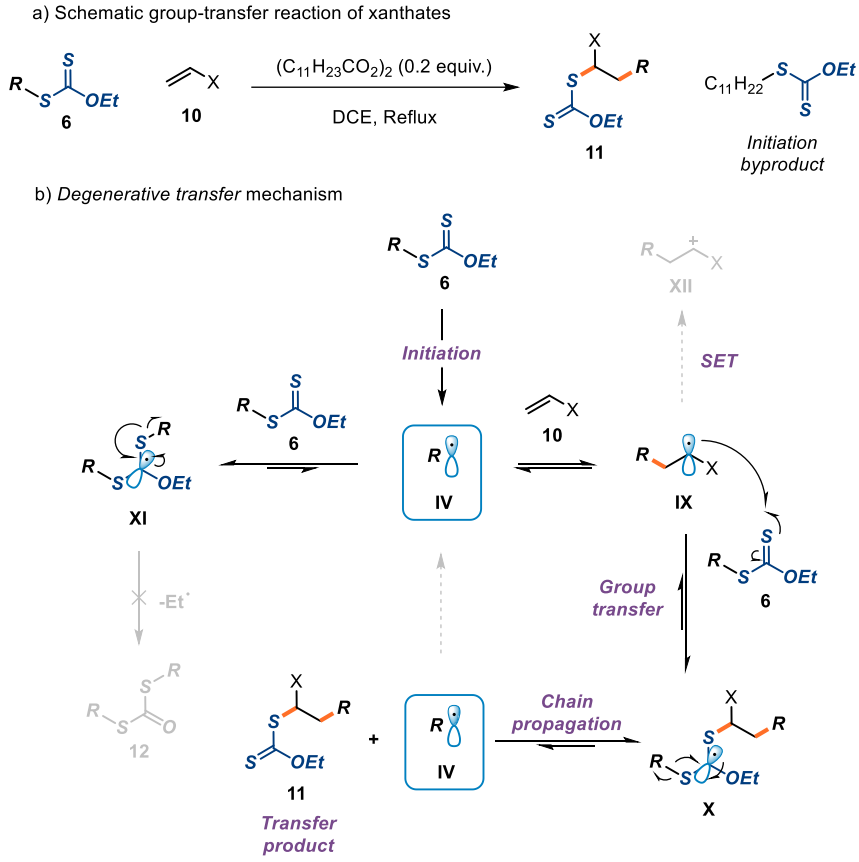

Scheme 2.11. a) Schematic group transfer reaction. b) Degenerative xanthate transfer mechanism.

As detailed in Scheme 2.11, all the steps on this system are equilibria; therefore, the success of the group transfer pathway depends on the relative stability of each of the intermediates. The steps deriving from **X** are particularly crucial for the overall process, determining if the reaction goes further to give product **11** or back to olefin **10**. The newly forged C-S bond in the transfer product **11** has to be stronger (higher BDE) than the one of the xanthate precursor **6**. Overall, the thermodynamic requirement for a successful group-transfer reaction is that radical **IV** has to be more stable than radical **IX**, which ultimately allows to achieve radical addition to non-activated alkenes **10**. A unique feature of this system is the ability to control the concentration of radicals in solution via reversible addition-fragmentation equilibriums

(Scheme 2.11). This constitutes the bases of the so called *reversible addition−fragmentation chain-transfer polymerization* (RAFT).[18] However, the thermodynamic requirements of the *degenerative xanthate transfer* process prevents xanthates to access non-stabilized radicals.

Some xanthates have also the ability to undergo direct homolysis of the C-S bond upon light absorption.[7,16,17] This is because some xanthate and dithiocarbamate derivatives adorned with chromophoric moieties can absorb visible light. This is the case for *S*-acylxanthates **13** (Scheme 2.12), which are bright yellow compounds capable of undergoing photolysis. Moreover, in the field of RAFT polymerization, some dithiocarbamate derivatives **14** have also shown a bathochromic shift in their spectra when the common alkyl substituents at the nitrogen are replaced with heterocycles (i.e. carbazole, Scheme 2.12).[19]

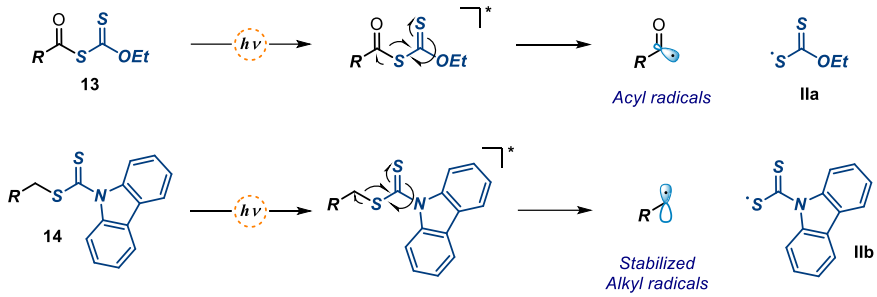

Scheme 2.12. Photolytic cleavage of xanthate/dithiocarbamate derivatives.

Despite the plethora of successful synthetic applications, the use of xanthate derivatives has remained limited to stoichiometric applications, which require the synthesis of large amounts of unstable substrates.

2.4 Target of the project

The aim of this project is to develop a new catalytic radical generation strategy that exploits the electrophilicity of radical precursor **1**, rather than its redox properties (Scheme 2.13). We planned to use a nucleophilic organic catalyst **2** based on a dithiocarbamate salt scaffold, which is nucleophilic enough to undergo substitution reactions on suitable alkyl electrophiles.

[18] For a perspective in RAFT polymerization see: Perrier, S., 50th Anniversary Perspective: RAFT Polymerization—A User Guide. *Macromolecules* **2017**, *50*, 7433-7447.
[19] Cabannes-Boué, B.; Yang, Q.; Lalevée, J.; Morlet-Savary, F.; Poly, J., Investigation into the mechanism of photo-mediated RAFT polymerization involving the reversible photolysis of the chain-transfer agent. *Polym. Chem.* **2017**, *8*, 1760-1770.

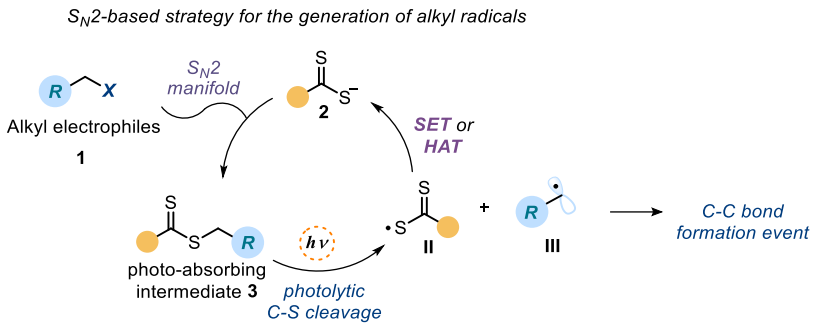

Scheme 2.13. S_N2-based catalytic protocol for generating radicals from precursors that are redox-inactive.

Upon substitution, the ensuing light-absorbing adduct **3** could be photolysed to deliver the target radical **III**, amenable to a variety of transformations. The dithiocarbamate catalyst scaffold offers a high degree of structural tunability, which allowed us to modulate the photophysical and chemical properties of the key intermediate **3**. Applying this system in a catalytic regime required us to close the catalytic cycle by an SET or HAT process that could return the anionic catalyst from the sulfur-centered radical, formed **II** upon photolysis of the intermediate. Synthetically, we aimed at applying this new catalytic radical generation strategy in several organic transformations. Conceptually, success in this endeavor would move the classical xanthate chemistry from a stoichiometric into a catalytic regime.

2.4.1 Design plan

Scheme 2.14 details our proposed strategy to generate radicals by exploiting the electrophilic character of the precursors. We envisioned a catalytic cycle that would start with a S_N2 displacement of the leaving group (*LG*) in the electrophile **1** by the dithiocarbonyl anion catalyst **2** to form adduct **3**. Irradiation of the photoactive intermediate **3** with visible light can promote homolytic cleavage due to the low BDE of the C-S bond,[16] releasing the alkyl radical **III** and the dithiocarbonyl radical **II**. The open-shell species **III** can be captured by the Michael acceptor **15**, forging a new C-C bond and the electrophilic radical **XII**. At this stage of the mechanism, a stabilizing off-cycle equilibrium to give the group transfer product **XIII** can be envisaged. This reversible process could be controlled by irradiation with the same wavelength needed for the photolytic cleavage of intermediate **III**. On the other hand, radical **XII** could abstract a hydrogen atom from 1,4-cyclohexadiene (1,4-CHD), thus delivering the final product **16** and the bis-allylic radical **XIV**. An exergonic SET reduction of the dithiocarbonyl radical **IV** (e.g. ethyl xanthogenate anion, where Z = OEt, has reduction potential E_{red} (**IV**/**1a**) = +0.04 V *vs* SCE)[20] from the cyclohexadienyl radical **XIV** (the parent

[20] Urove, G. A.; Peters, D. G., Electrochemical Reduction of Cyclohexanecarbonyl Chloride at Mercury Cathodes in Acetonitrile. *J. Electrochem. Soc.* **1993**, *140*, 932-935.

hydroxycyclohexadienyl radical has E_{red} = -0.1 V *vs* SCE)[21] would eventually close the catalytic cycle by returning catalyst **2**. This mechanistic plan finds support in (*i*) the high nucleophilicity[22] of dithiocarbonate and dithiocarbamate anions of type **2**; (*ii*) the tendency of thiocarbonyl compounds of type **3** to generate radicals upon photolytic cleavage, as discussed in the introduction of this chapter;[6,7] and (*iii*) the ability of 1,4-CHD to serve as a donor of both hydrogen atoms and electrons.[23]

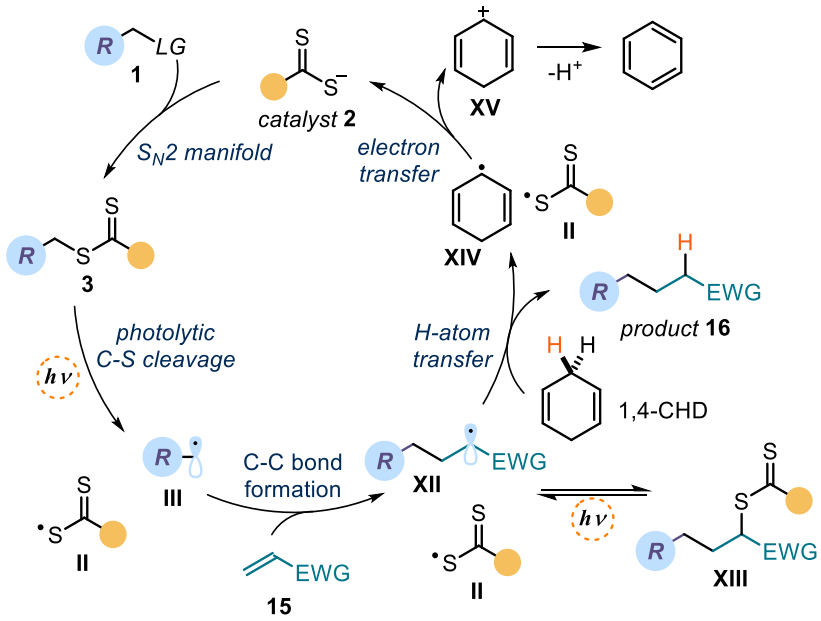

Scheme 2.14. Design plan.

2.5 Results and discussion

To validate our proposal, we studied a Giese-type radical conjugate addition (Table 2.1).[24] We chose dimethyl fumarate **15a** as the model substrate for trapping the radical. We replaced 1,4-CHD for commercially available γ-terpinene as a cheaper and more stable surrogate. Since our overarching goal was to develop a strategy that enables predictable and mild activation of

[21] Bahtia, K.; Schuler, R. H., Oxidation of Hydroxycyclohexadienyl Radical by Metal Ions. *J. Phys. Chem.* **1974**, *78*, 2335-2338.
[22] Duan, X.-H.; Maji, B.; Mayr, H., Characterization of the nucleophilic reactivities of thiocarboxylate, dithiocarbonate and dithiocarbamate anions. *Org. Biomol. Chem.* **2011**, *9*, 8046-8050.
[23] Davies, J.; Svejstrup, T. D.; Fernandez Reina, D.; Sheikh, N. S.; Leonori, D., Visible-Light-Mediated Synthesis of Amidyl Radicals: Transition-Metal-Free Hydroamination and N-Arylation Reactions. *J. Am. Chem. Soc.* **2016**, *138*, 8092-8095.
[24] Giese, B., Formation of CC Bonds by Addition of Free Radicals to Alkenes. *Angew. Chem. Int. Ed. Engl.* **1983**, *22*, 753-764.

electrophiles otherwise inert to redox-based approaches, we chose benzyl chloride **1a** as the model radical precursor. Benzyl chloride shows a reduction potential of (**1**/**1a**$^{\cdot-}$) = -2.13V vs SCE[25] sufficiently negative to remain out of reach of most commonly used photoredox catalysts.[9,26] In contrast, benzyl chloride is an archetypical substrate for S_N2 reactions.[27]

Table 2.1. Optimization studies

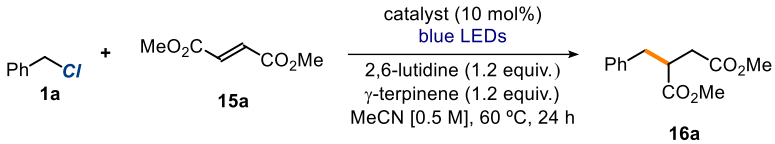

catalysts used in this study

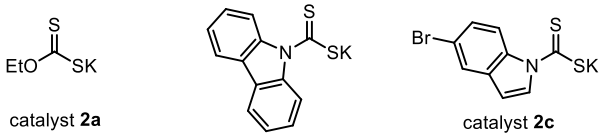

entry	catalyst	deviation	yield **16a** (%)[a]
1	**2a**	20 ºC, 405 nm	19
2	**2a**	20 ºC	0
3	**2b**	20 ºC	22
4	**2c**	20 ºC	43
5	**2c**	none	90
6	**2c**	under air	70
7	**2c**	20 equiv. of water	83
8	**2c**	no light	0
9	none	none	0
10	**2c**	1 equiv. of TEMPO	0
11	**2c**	50 mmol scale	73%[b]

Reactions performed on a 0.5 mmol scale at 60 °C for 24 h using 1 mL of MeCN under illumination by a blue LED strip (λ_{max} = 465 nm, 14 W) and using catalyst (10 mol%), 1.5 equiv. of **1a**, and 1.2 equiv. of 2,6-lutidine. [a] Yield determined by ^{1}H NMR analysis of the crude mixture using trichloroethylene as the internal standard. [b] Yield of the isolated **16a**. LED: Light-emitting diode.

When conducting the model reaction using potassium ethyl xanthogenate **2a** as nucleophilic catalyst (10 mol%) under 405 nm irradiation in acetonitrile (CH_3CN), product **16a** was obtained in 19% yield (entry 1, Table 2.1). This initial result indicated the feasibility to

[25] Isse, A. A.; Falciola, L.; Mussini, P. R.; Gennaro, A., Relevance of electron transfer mechanism in electrocatalysis: the reduction of organic halides at silver electrodes. *Chem. Commun.* **2006**, (3), 344-346.
[26] Brasholz, M., "Super-Reducing" Photocatalysis: Consecutive Energy and Electron Transfers with Polycyclic Aromatic Hydrocarbons. *Angew. Chem. Int. Ed.* **2017**, *56*, 10280-10281.
[27] Clayden, J., Greeves, N., Warren, S. & Wothers, P. Eds. *Organic Chemistry*, **2001**, Oxford University Press.

catalytically generating the benzyl radicals. The reaction was completely inhibited by changing the light source to a blue LED emitting at 465 nm (entry 2). We rationalized this result due to the inhability of intermediate **3a**, emerging from the S_N2 process, to absorb blue light (Figure 2.1). Thanks to the modulability of the catalyst **2** scaffold, we could introduce a chromophoric unit to enhance the absorption properties of the key intermediate **3**. Inspired by previous studies,[19] we introduced a heterocyclic moiety within the catalyst. Specifically, the thiocarbamate catalysts **2b-c**, bearing a carbazole and an indole scaffold, respectively, provided intermediates **3b-c** upon S_N2 reaction with substrate **1a**. These intermediates possess a dramatically increased molar extinction coefficient with respect to **IIa**. When testing our new potential catalysts under the reaction conditions, we were pleased to find restored catalytic activity under blue light irradiation (465 nm, entries 3 and 4).

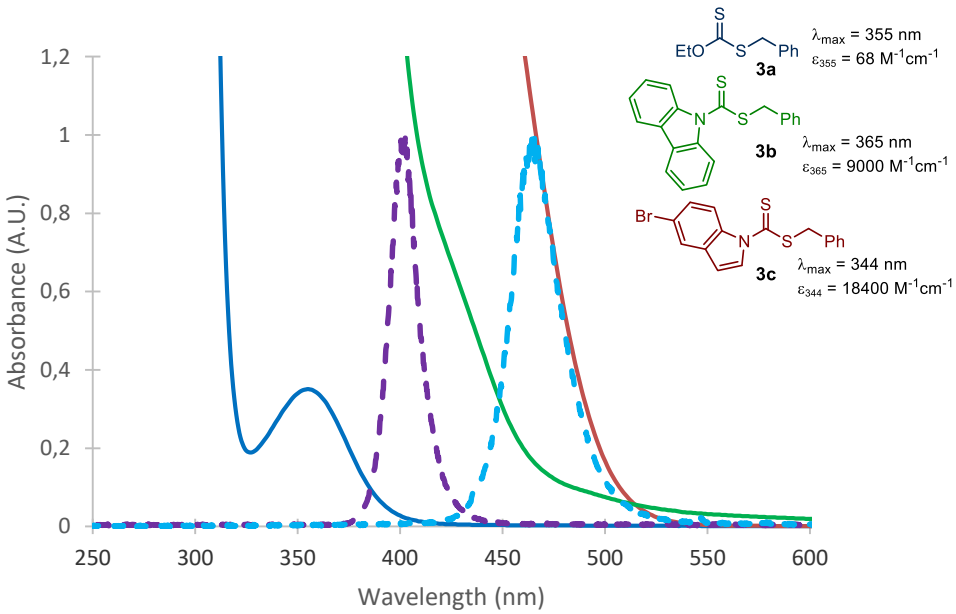

Figure 2.1. UV-Vis spectra of the dithiocarbamate adducts **3**

Finally, when employing indole-containing thiocarbamate catalyst **2c** while raising the temperature to 60 °C, the yield of product **16a** increased to 90% (entry 5). Only a slight decrease in yield was observed when using non-degassed conditions (entry 6) or when water was introduced in the system (entry 7), highlighting the robustness of the methodology. Notably, the solvent can be elected by considering the solubility of different substrates. No significant difference of reactivity was observed when performing the model reaction in a variety of reaction media (e.g. ethyl acetate, dichloroethane, toluene, and tetrahydrofuran all

provided yields in the range of 85-90%). Control experiments showed no product formation in the absence of catalyst **2** or light (entries 8 and 9). The inhibition of the reactivity was also observed in the presence of the radical inhibitor 2,2,6,6-tetramethylpiperidine 1-oxyl, (TEMPO, 1 equivalent, entry 10). To verify the synthetic potential of our newly developed methodology, we challenged the system by performing the reaction in a multigram scale using commonly available glassware (entry 11, Table 2.1, see section 2.7.9 for details of the set-up). Mechanistically, we also considered the possibility that the dithiocarbamate group transfer product **XIII** (Scheme 2.14) could be generated during the reaction. Although we never detected this adduct under catalytic conditions, an authentic sample of intermediate **XIIIc** afforded product **16a** when irradiated with blue LEDs and in the presence of γ-terpinene (Scheme 2.15). This observation suggests that adduct **XIIIc** can be a photoactive species in an off-cycle equilibrium with the progenitor radicals **XII** and **II**.

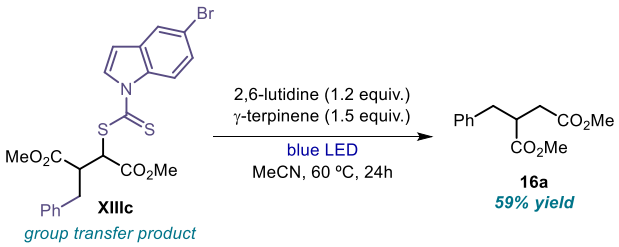

Scheme 2.15. Behavior of the group-transfer product under the reaction conditions.

As the underlying mechanism of our radical generation strategy relies on an S_N2 displacement, other benzylic substrates with different leaving groups should also be amenable to this transformation. Accordingly, when precursors **1b-e** bearing iodide, bromide, mesylate, or trifluoroacetate, were tested, the desired product **16a** was obtained with excellent yields (Scheme 2.16). In contrast, leaving groups with a poor tendency to undergo an S_N2 process, including acetate and phosphate, remained completely unreacted. The choice of one leaving group or another can therefore be dictated by its ease of access or compatibility with other functional groups in a complex synthetic plan.

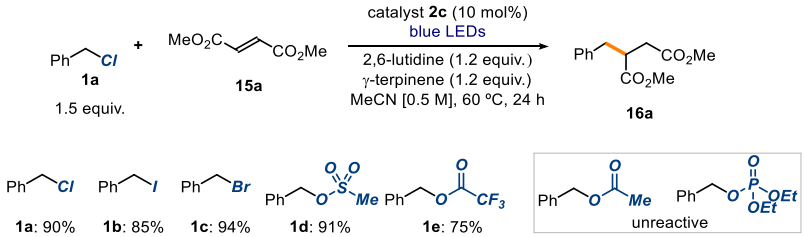

Scheme 2.16. Evaluating the reactivity of different leaving groups of the radical precursor.

2.5.1 Scope of the radical conjugate addition

Our next step was to evaluate the synthetic potential of this photochemical radical generation strategy in the context of different C-C bond-forming transformations. We started by exploring the Giese-type radical conjugated addition (Scheme 2.16). Using fumarate **3a** as the radical trap, a large variety of benzylic electrophiles bearing both electron-rich and electron-poor aryl substituents (**1g-j**) delivered the conjugate addition products in excellent yields. In addition, a secondary benzylic substrate (**1k**) and prenyl chloride (**1l**, an allylic radical precursor) afforded the corresponding products in moderate yields. The strategy can be used to implement a radical α-aminomethylation process, allowing the introduction of a variety of scaffolds (oxazolidinone, a protected secondary amine, or a protected primary amine) from readily available precursors (**1m-o**).

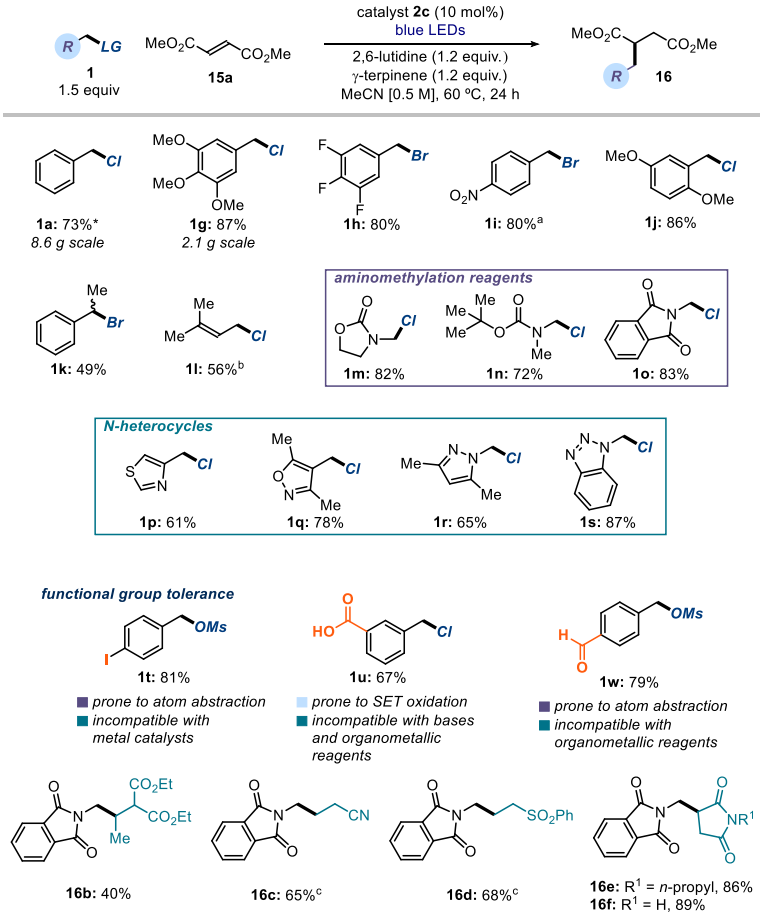

Scheme 2.17. Scope of the Giese-type radical addition. Reactions performed on a 0.5 mmol scale, unless otherwise stated; yields refer to isolated material after purification. Ms, mesylate. *Run over 48 hours using 20 equiv. of H_2O. [a] 2 equivalents of **1**, γ-terpinene, and 2,6-lutidine. [b] 3 equivalents of **1**, γ-terpinene, and 2,6-lutidine. [c] 2 equivalents of γ-terpinene and 2,6-lutidine.

We then assessed the compatibility of the system with unprotected functional groups, an essential criterion for the method's potential applicability to complex molecule synthesis and drug discovery.[28] We confirmed that our approach displayed a high level of tolerance to nitrogen-containing heterocycles, including thiazole (**1p**), isoxazole (**1q**), pyrazole (**1r**), and triazole (**1s**) scaffolds. The unique mechanism of our strategy also allowed the predictable and chemoselective activation of S_N2-prone substrates bearing reactive functional groups, which would be incompatible with other radical generation methods or metal-based strategies. Aryl iodide (**1t**), free carboxylic acid (**1u**), unprotected alcohol (**1v**), and aldehyde (**1w**) motifs were all tolerated and activated exclusively at the desired benzylic position. Finally, we explored the reaction between commercially available *N*-(chloromethyl)phthalimide **1o** and a variety of Michael acceptors (Scheme 2.17). Alkenes bearing distinct electron-withdrawing groups (e.g. esters, nitriles, sulfones, and imides) all reacted in good yields leading to adducts **16a**-**f**. Noteworthy, the choice of the leaving group in the radical precursor used in this scope evaluation was dictated by commercial availability or ease of substrate synthesis.

2.5.2 Other radical processes

We then wondered if our catalytic system could be used to develop other synthetically useful radical C-C bond-forming processes. Based on our mechanistic proposal, we reasoned that a redox-neutral transformation could be possible by accessing a bis-allylic radical of type **XVII** (similar to radical **XIV**, Scheme 2.14). We envisioned a sequential radical addition/cyclization to aromatic acrylamides **17** (Scheme 2.18).[29] The proposed mechanism would go as follows: after addition of the carbon centered radical **III** to alkene **17**, open-shell species **XVI** would be formed. Due to its electrophilic character, **XVI** would react with the electron-rich aromatic ring in a cyclization step delivering **XVII**. Finally, ensuing radical **XVII** could act as a SET reductant of **II**, closing the catalytic cycle to restore catalyst **2** while providing product **18**.

[28] Blakemore, D. C.; Castro, L.; Churcher, I.; Rees, D. C.; Thomas, A. W.; Wilson, D. M.; Wood, A., Organic synthesis provides opportunities to transform drug discovery. *Nature Chem.* **2018**, *10*, 383-394.
[29] Chen, J.-R.; Yu, X.-Y.; Xiao, W.-J., Tandem Radical Cyclization of *N*-Arylacrylamides: An Emerging Platform for the Construction of 3,3-Disubstituted Oxindoles. *Synthesis* **2015**, *47*, 604-629.

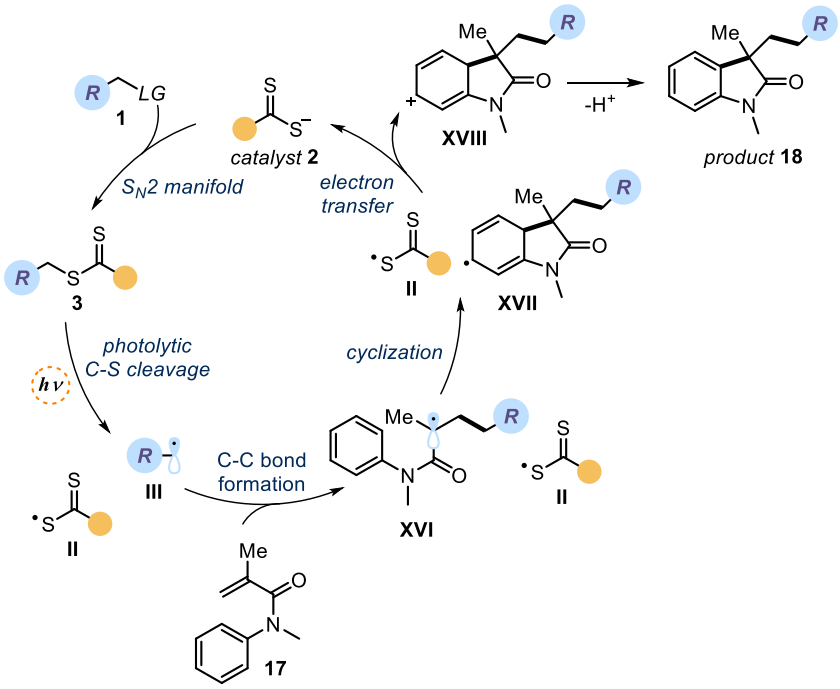

Scheme 2.18. Mechanistic proposal for the redox-neutral process.

This mechanistic variation, which avoids the use of a stoichiometric H atom donor, was successfully implemented to enable the preparation of differently substituted oxindoles **18** using alkyl chlorides **1** as radical precursors (Scheme 2.19). Electron-poor radicals provided good to excellent yields, and several functional groups were introduced, such as nitriles (**18a**, **18i-m**) esters (**18b**, **18f**, **18g**), and ketones (**18c**, **18g**). More nucleophilic radicals, including benzylic (**18d**, **18e**) and α-amino radicals (**18h**), were also efficiently trapped. Several olefins bearing electron-deficient (**18j**) or electron-rich (**18i**) substituents were reactive, as well as those with different alkyl substituents on the nitrogen atom (**18k-m**).

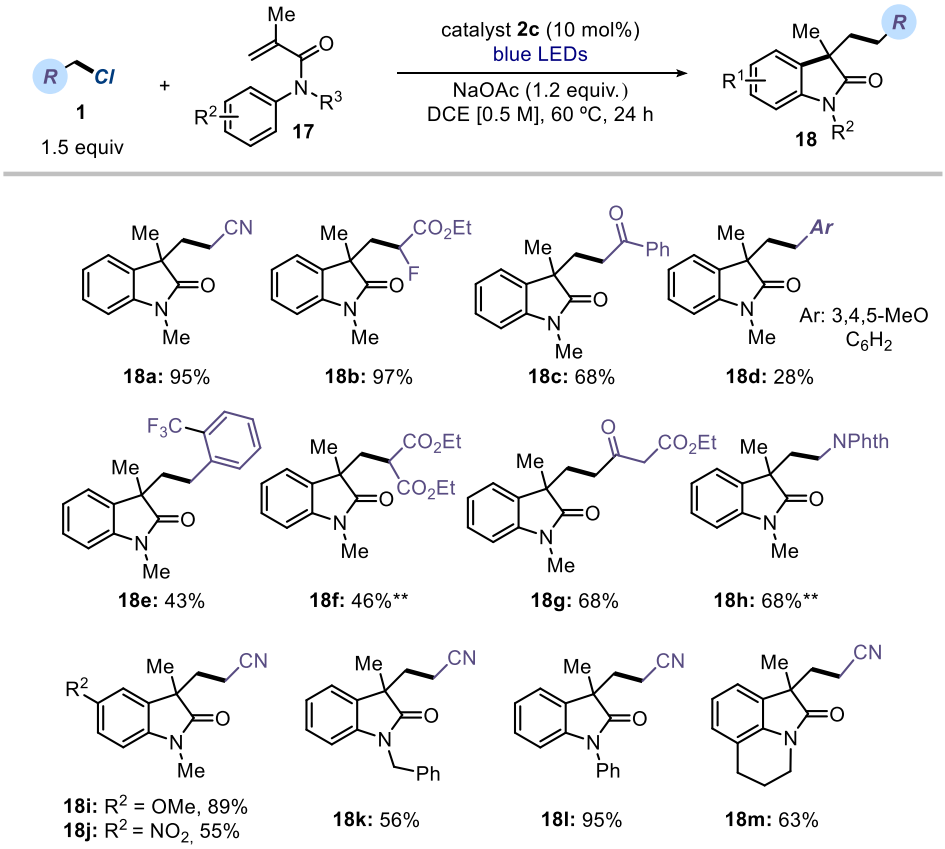

Scheme 2.19. Scope of tandem addition-cyclization. Reactions performed on a 0.5 mmol scale, unless otherwise stated; yields refer to isolated material after purification. DCE, 1,2-dichloroethane; NPhth, phthalimide. **Yield estimated by H NMR analysis.

Similarly, we studied the direct radical alkylation of electron-rich (hetero)arenes starting from easily available alkyl chlorides **1** (Scheme 2.20). Various radical precursors proved reactive allowing the introduction of several functional groups, including ketones (**19a-b**), esters (**19d**, **19f**) and secondary amides (**19e**). A wide variety of heterocycles also reacted under our conditions, affording alkylated indole (**19j**), furanes (**19k-l**), thiophene derivative (**19m**) and even less electron-rich arenes (**19n**) leading to valuable substituted (hetero)aromatic compounds.[30]

[30] Fujiwara, Y. & Baran, P. S. Radical-based late stage C–H functionalization of heteroaromatics in drug discovery in *New Horizons of Process Chemistry*. Springer Nature Singapore Pte Ltd., **2017.**

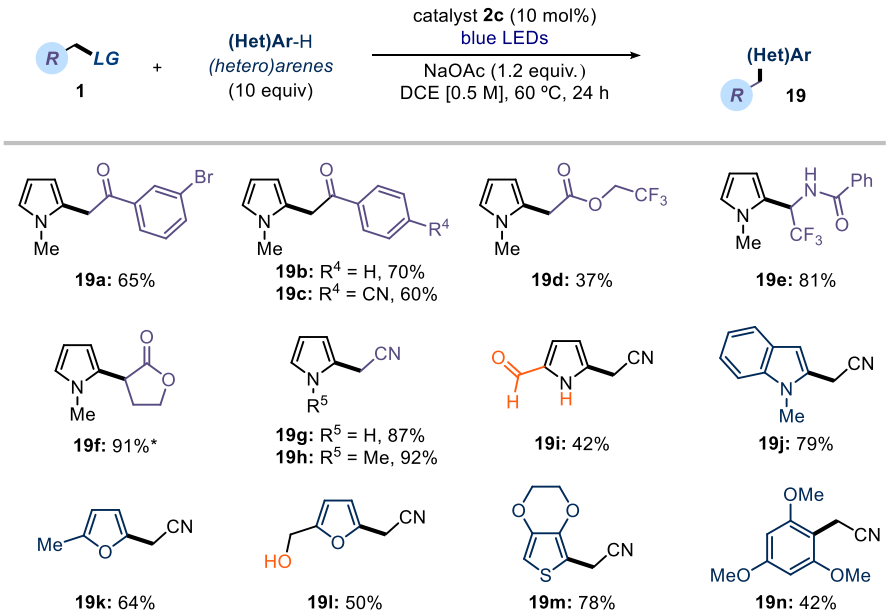

Scheme 2.20. Scope of alkylation of heteroarenes. Reactions performed on a 0.5 mmol scale, unless otherwise stated; yields refer to isolated material after purification. DCE, 1,2-dichloroethane. *Using bromine as leaving group.

To showcase our system's synthetic utility, this strategy was applied to the synthesis of the pyrrole derivative **19h** (Scheme 2.21a). Adduct **19h** is an intermediate *en route* to Tolmetin, a marketed nonsteroidal anti-inflammatory drug.[31,32] Using 5 mol% of catalyst **2c**, we could perform a multigram-scale preparation of **19h** in ethyl acetate, an industrially preferred solvent. The reaction was also amenable to the use of a continuous-flow photoreactor.[33] Further experiments, detailed in Scheme 2.21, demonstrated that this method is compatible with the functionalization of biorelevant compounds bearing unprotected polar functional groups. It allowed the late-stage introduction of a pyrrole (adduct **21**) and an oxindole moiety (**22**) into mesylate derivative **20**, synthesized in a single step from cortisone. The nucleobase analogues **24** and **27** could be readily obtained from commercially available uracyl chloride **23** and adenine **25**, respectively.

[31] Carson, J. R. Uncatalyzed aroylation of 1-alkylpyrrole-2-acetic acid derivatives, **1976**, U.S. Patent US3998844A.
[32] Liu, Z.-Q.; Li, Z., Radical-promoted site-specific cross dehydrogenative coupling of heterocycles with nitriles. *Chem. Commun.* **2016**, *52*, 14278-14281.
[33] Cambié, D.; Bottecchia, C.; Straathof, N. J. W.; Hessel, V.; Noël, T., Applications of Continuous-Flow Photochemistry in Organic Synthesis, Material Science, and Water Treatment. *Chem. Rev.* **2016**, *116*, 10276-10341.

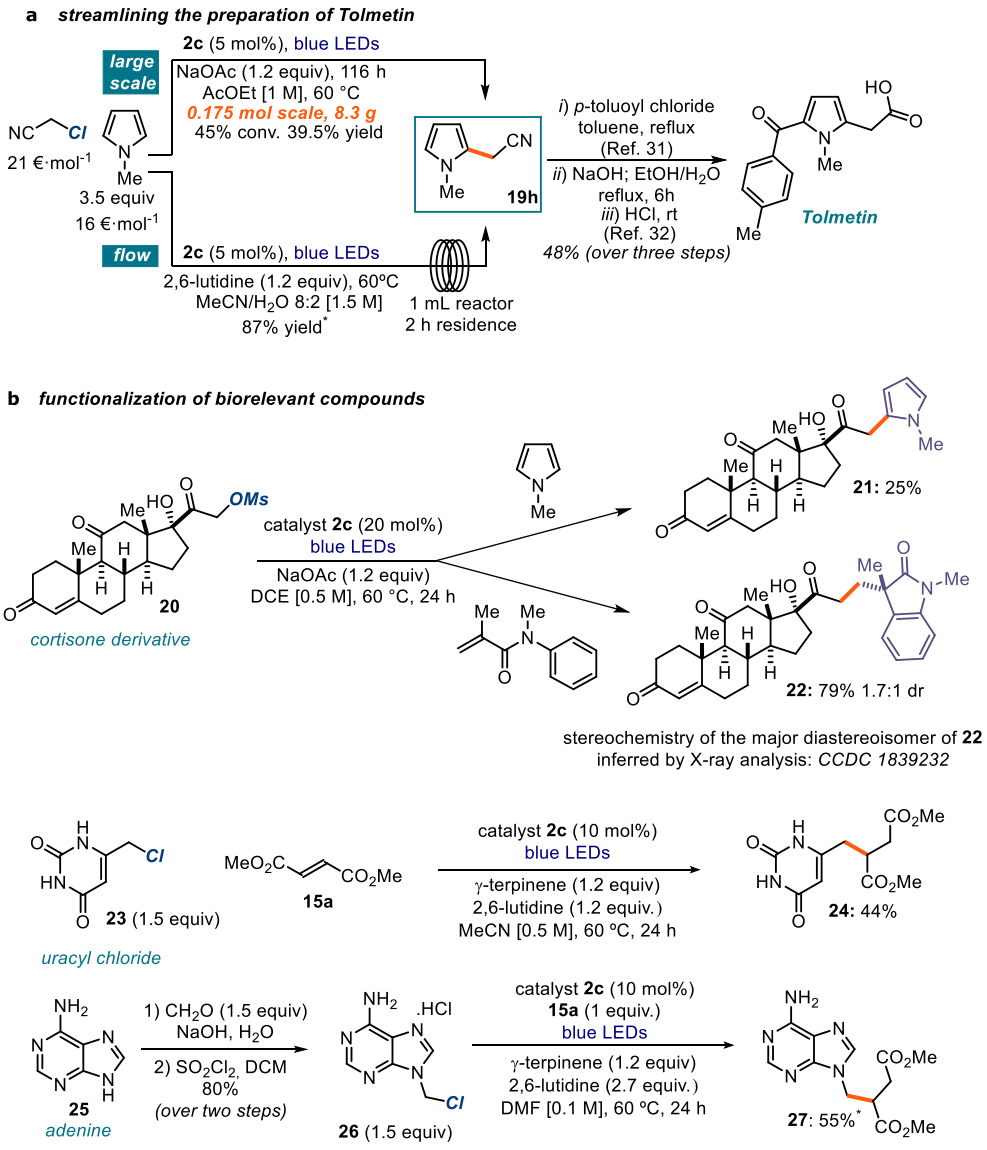

Scheme 2.21. (a) Streamlined preparation of a marketed drug. (b) Late-stage elaboration of biorelevant compounds (b). Prices of reagents determined according to Sigma-Aldrich catalogue at the highest quantity available; *NMR yield.

2.5.3 A dual organocatalytic system for asymmetric radical catalysis

Finally, we applied our strategy to perform an organocatalytic stereoselective intermolecular α-alkylation of aldehydes using alkyl chlorides. This transformation was first reported by MacMillan in 2008[34] using bromomalonate **29a** and the chiral secondary amine catalyst **30a**

[34] Nicewicz, D. A.; MacMillan, D. W. C., Merging Photoredox Catalysis with Organocatalysis: The Direct Asymmetric Alkylation of Aldehydes. *Science* **2008**, *322*, 77-80.

to afford the enantioenriched product **31** (Scheme 2.22a). This process laid the foundations for the development of the modern field of photoredox catalysis.[9,35] Since then, this reaction served as a benchmark to measure the efficiency of new photoredox catalysts.[36,37] All procedures reported so far used alkyl bromides as radical precursors. Nevertheless, the intrinsically different properties of our approach allowed us to achieve the effective activation of easily available alkyl chlorides by the dithiocarbamate anion catalyst **2c** (Scheme 2.21b). Upon formation of the radical, the direct enantioselective α-alkylation of aldehydes **28** was effectively performed at ambient temperature using **2c** in combination with the chiral organocatalysts **30a** or **30b** to afford the corresponding products **32-34**.

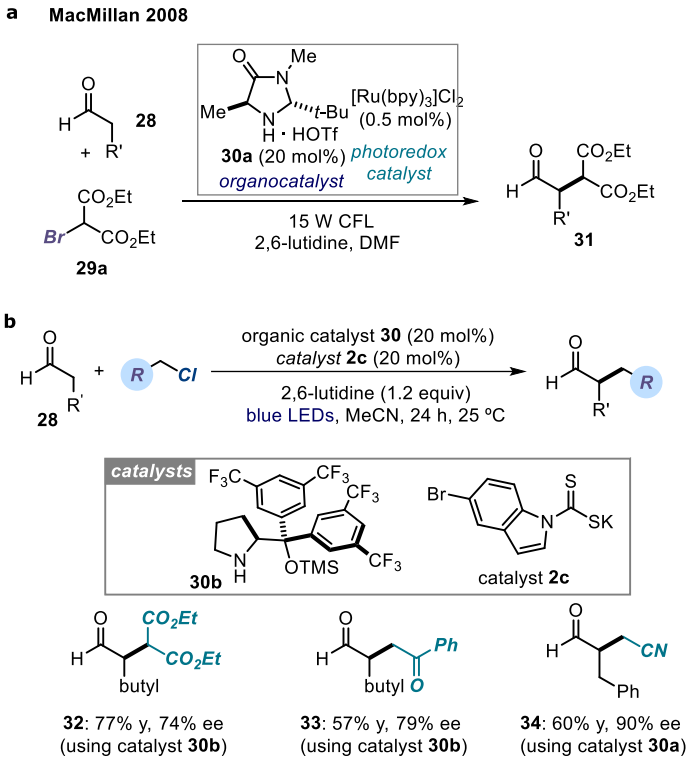

Scheme 2.22. Application in enantioselective radical catalysis. a) The catalytic asymmetric α-alkylation of aldehydes using a visible-light-activated ruthenium catalyst ($Ru(bpy)_3^{2+}$). b) Demonstration that the dithiocarbamate anion catalytic strategy can expand the asymmetric alkylation of aldehydes to include alkyl chlorides. Bpy: 2,2'-bipyridine; TMS: trimethylsilyl.

---

[35] Silvi, M.; Melchiorre, P., Enhancing the potential of enantioselective organocatalysis with light. *Nature* **2018**, *554*, 41-49.

[36] Neumann, M.; Füldner, S.; König, B.; Zeitler, K., Metal-Free, Cooperative Asymmetric Organophotoredox Catalysis with Visible Light. *Angew. Chem. Int. Ed.* **2011**, *50*, 951-954.

[37] Gualandi, A.; Marchini, M.; Mengozzi, L.; Natali, M.; Lucarini, M.; Ceroni, P.; Cozzi, P. G., Organocatalytic Enantioselective Alkylation of Aldehydes with $[Fe(bpy)_3]Br_2$ Catalyst and Visible Light. *ACS Catalysis* **2015**, *5*, 5927-5931.

2.6 Conclusions

In summary, in the course of this project we have developed a photochemical strategy that exploits an S_N2 process (a fundamental path in ionic chemistry) to generate open-shell intermediates from a variety of electrophilic substrates otherwise inert to traditional radical-generating strategies. The method employs a readily available organic catalyst and is promoted by visible-light irradiation. The strategy shows a wide substrate scope and tolerates unprotected polar functional groups and *N*-heterocycles. Preliminary results highlight that this radical-generation strategy can be used in more complex settings, including light-driven enantioselective catalysis. These findings, along with the experimental simplicity and the low cost of the catalyst, suggest that this method can find further synthetic applications and is potentially amenable to medicinal chemistry and process development.

2.7 Experimental section

2.7.1 General information

The NMR spectra are available in the published manuscript[1] and are not reported in the present dissertation.

The NMR spectra were recorded at 400 MHz and 500 MHz for ^{1}H and 100 or 125 MHz for ^{13}C. The chemical shift (δ) for ^{1}H and ^{13}C are given in ppm relative to residual signals of the solvents ($CHCl_3$ @ 7.26 ppm ^{1}H NMR and 77.16 ppm ^{13}C NMR, and tetramethylsilane @ 0 ppm). Coupling constants are given in Hertz. The following abbreviations are used to indicate the multiplicity: s, singlet; d, doublet; q, quartet; m, multiplet; bs, broad signal; app, apparent.

High resolution mass spectra (HRMS) were obtained from the ICIQ HRMS unit on MicroTOF Focus and Maxis Impact (Bruker Daltonics) with electrospray ionization. (ESI). UV-vis measurements were carried out on a Shimadzu UV-2401PC spectrophotometer equipped with photomultiplier detector, double beam optics and D_2 and W light sources or an Agilent Cary60 spectrophotometer. Emission spectra of light sources were recorded on Ocean Optics USB4000 fiber optic spectrometer.

Yields of isolated products refer to materials of >95% purity as determined by ^{1}H NMR.

General Procedures. All reactions were set up under an argon atmosphere in oven-dried glassware. Synthesis grade solvents were used as purchased; anhydrous solvents were taken from a commercial SPS solvent dispenser. Chromatographic purification of products was accomplished using forced-flow chromatography (FC) on silica gel (35-70 mesh). For thin layer chromatography (TLC) analysis throughout this work, Merck pre-coated TLC plates (silica gel 60 GF_{254}, 0.25 mm) were employed, using UV light as the visualizing agent and an acidic mixture of vanillin or basic aqueous potassium permanganate ($KMnO_4$) stain solutions,

and heat as developing agents. Organic solutions were concentrated under reduced pressure on a Büchi rotatory evaporator.

Determination of Enantiomeric Purity. UPC^2 analysis on chiral stationary phase was performed on a Waters Acquity instrument using a Trefoil AMY1 and ID3 chiral column. The exact conditions for the analyses are specified within the characterization section. HPLC analysis on chiral stationary phase was performed on an Agilent 1200-series instrument, employing Daicel Chiralpak IA column.

Materials. Most of the starting materials used in this study are commercial and were purchased in the highest purity available from Sigma-Aldrich, Fluka, Alfa Aesar, Fluorochem, and used as received, without further purifications.

2.7.2 Substrate synthesis

The following substrates were synthesized according to reported procedures (Scheme 2.23).[38]

[38] (a) Loim, N. M.; Kelbyscheva, E. S., Synthesis of dendrimers with terminal formyl groups. *Russ. Chem. Bull.* **2004**, *53*, 2080-2085. (b) Chardin, C.; Rouden, J.; Livi, S.; Baudoux, J., Dimethyldioxirane (DMDO) as a valuable oxidant for the synthesis of polyfunctional aromatic imidazolium monomers bearing epoxides. *Green Chem.* **2017**, *19*, 5054-5059. (c) Wu, G.; Xu, S.; Deng, Y.; Wu, C.; Zhao, X.; Ji, W.; Zhang, Y.; Wang, J., Coupling of arylboronic acids with benzyl halides or mesylates without adding transition metal catalysts. *Tetrahedron* **2016**, *72*, 8022-8030. (d) Hoang, C. T.; Bouillère, F.; Johannesen, S.; Zulauf, A.; Panel, C.; Pouilhès, A.; Gori, D.; Alezra, V.; Kouklovsky, C., Amino Acid Homologation by the Blaise Reaction: A New Entry into Nitrogen Heterocycles. *J. Org. Chem.* **2009**, *74*, 4177-4187. (e) Yang, Z.; Zhou, J., Palladium-Catalyzed, Asymmetric Mizoroki–Heck Reaction of Benzylic Electrophiles Using Phosphoramidites as Chiral Ligands. *J. Am. Chem. Soc.* **2012**, *134*, 11833-11835. (f) Rosowsky, A.; Papoulis, A. T.; Forsch, R. A.; Queener, S. F., Synthesis and Antiparasitic and Antitumor Activity of 2,4-Diamino-6-(arylmethyl)-5,6,7,8-tetrahydroquinazoline Analogues of Piritrexim. *J. Med. Chem.* **1999**, *42*, 1007-1017 (g) Harit, T.; Malek, F.; Bali, B. E.; Khan, A.; Dalvandi, K.; Marasini, B. P.; Noreen, S.; Malik, R.; Khan, S.; Iqbal Choudhary, M., Synthesis and enzyme inhibitory activities of some new pyrazole-based heterocyclic compounds. *Med. Chem. Res.* **2012**, *21*, 2772-2778. (h) Brackemeyer, D.; Schulte to Brinke, C.; Roelfes, F.; Hahn, F. E., Regioselective C8-metalation of N-phosphine tethered adenine derivatives via C8–H activation. *Dalton Trans.* **2017**, *46*, 4510-4513. (i) Song, J.; Yamataka, H.; Rappoport, Z., Dialkoxyphosphinyl-Substituted Enols of Carboxamides. *J. Org. Chem.* **2007**, *72*, 7605-7624. (j) Kiyoshi, T.; Yoshiharu, I.; Keiryo, M., N-Acyl-1-chloro-2,2,2-trifluoroethylamine as a 2,2,2-Trifluoroethylamine-Building Block. *Bull. Chem. Soc. Jpn.* **1993**, *66*, 661-663. (k) Boess, E.; Karanestora, S.; Bosnidou, A.-E.; Schweitzer-Chaput, B.; Hasenbeck, M.; Klussmann, M., Synthesis of Oxindoles by Brønsted Acid Catalyzed Radical Cascade Addition of Ketones. *Synlett* **2015**, *26*, 1973-1976. (l) Li, Y.-L.; Wang, J.-B.; Wang, X.-L.; Cao, Y.; Deng, J., Silver-Catalyzed Decarboxylative Radical Addition/Cyclization of α,α-Difluoroarylacetic Acids with Acrylamides To Synthesize Difluorinated Oxindoles. *Eur. J. Org. Chem.* **2017**, *2017*, 6052-6059.

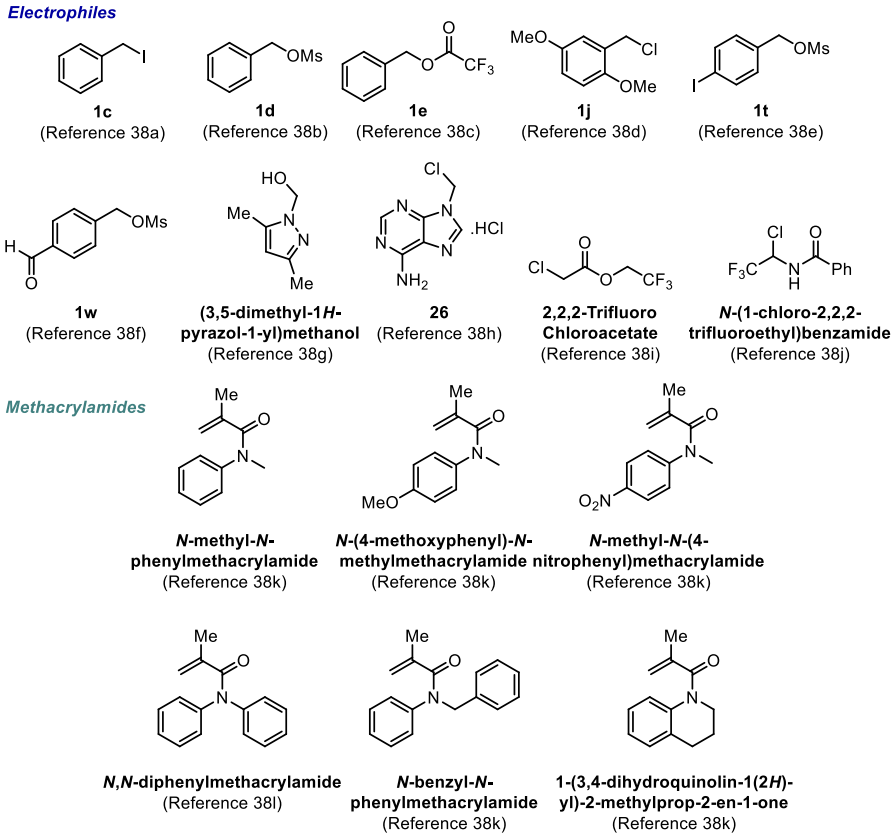

Scheme 2.23. Starting materials synthesised according to known procedures.

2.7.3 Catalyst synthesis

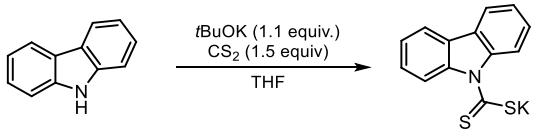

In an oven-dried, round bottom flask under an atmosphere of argon, carbazole (3 g, 17.94 mmol, 1 equiv.) was dissolved in a minimal amount of THF (30 mL, commercial synthesis grade). The flask was cooled to 0 ºC in an ice-water bath and potassium *tert*-butoxide (2.1 g, 1.1 equiv.) was added portionwise. The mixture turned a slight yellow/orange color and was left to stir for 30 minutes. Still at 0 ºC, carbon disulfide (1.6 mL, 1.5 equiv.) was added dropwise *via* syringe addition. The mixture immediately turned a bright orange color and was left to stir for one hour at 0 ºC. After warming up to ambient temperature, THF was evaporated carefully on a rotary evaporator to a thick syrupy consistency. Diethyl ether (50 mL) was added and the resulting suspension stirred vigorously to free the solid. The yellow solid was then filtered under a flow of argon, washed twice with a small amount of ether and further

dried overnight under high vacuum to obtain the desired product as a bright yellow free flowing powder (4.9 g, 97% yield).

Note: Once isolated, **2b** is slightly hygroscopic and should therefore be protected from ambient humidity. It was typically stored in brown glass bottles within a desiccator. Only minor degradation to the parent carbazole was observed over a 3-month period, as indicated by NMR analysis. **2b** could be readily purified again by washing the solid with diethyl ether to remove the carbazole from the yellow solid.

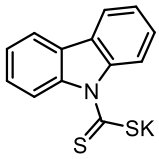

Potassium 9H-carbazole-9-carbodithioate (2b)

^{1}H NMR (400 MHz, d6-DMSO) δ 8.49 (d, *J* = 8.3 Hz, 2H);8.08 (d, *J* = 7.6 Hz, 2H); 7.37 (app t, *J* = 7.9 Hz, 2H); 7.19 (app t, *J* = 7.9 Hz, 2H);

^{13}C NMR (101 MHz, d6-DMSO) δ 221.0 (C), 139.7 (C), 125.3 (CH); 123.1 (C); 120.0 (CH); 119.6 (CH); 115.3 (CH).

HRMS (ESI negative): calculated for $C_{13}H_8NS_2$ (M): 242.0104 found 242.0108.

Potassium 5-bromo-1*H*-indole-1-carbodithioate (2c):

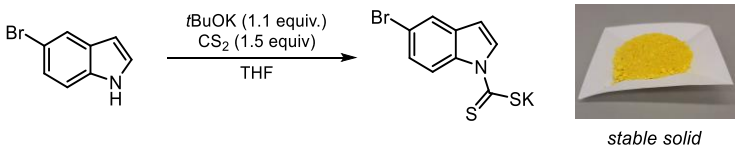

stable solid

In an oven dried round bottom flask under an atmosphere of argon, *5*-bromoindole (1 equiv.) was dissolved in a minimal amount of THF (commercial synthesis grade; 10 mL·g^{-1}). The flask was cooled to 0 ºC in an ice-water bath and potassium *tert*-butoxide (1.1 equiv.) was added portionwise. The mixture turned a slight yellow/orange color and was left to stir for 30 minutes. Still at 0 ºC, carbon disulfide (1.5 equiv.) was added dropwise *via* syringe addition. The mixture immediately turned a bright orange color and was left to stir for one hour at 0 ºC. After warming up to ambient temperature, THF was evaporated carefully on a rotary evaporator to a thick syrupy consistence. Toluene was added and evaporated to obtain a yellow solid residue. The residue was suspended in a 1:1 mixture of pentane and diethyl ether and stirred vigorously to obtain a fine suspension. The yellow solid was then filtered under a flow of argon, washed twice with a small amount of a 1:1 mixture of pentane and diethyl ether and further dried overnight under high vacuum to obtain the desired product as a yellow free flowing powder.

This reaction has been performed on various scales (5 to 55 mmol of starting *5*-bromoindole) with yields of the isolated product ranging from 88 to 95%.

Note: Once isolated, **2c** is slightly hygroscopic and should therefore be protected from ambient humidity. It was typically stored in brown glass bottles in a desiccator. No degradation was detected over a 3-month period, as indicated by NMR analysis.

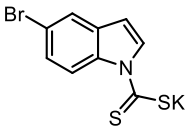

Potassium 5-bromo-1*H*-indole-1-carbodithioate (2c)

^{1}H NMR (400 MHz, d6-DMSO) δ 6.39 (d, *J* = 3.5 Hz, 1H), 7.25 (dd, *J* = 9,2.1 Hz, 1H), 7.68 (d, *J* = 2.1 Hz, 1H), 8,69 (d, *J* = 3.5 Hz, 1H), 9,28 (d, *J* = 9 Hz, 1H)

^{13}C NMR (101 MHz, d6-DMSO) δ 218.7 (C), 134,9 (C), 133.9 (C), 132.2 (CH), 124.9 (CH), 122.7 (CH), 120.0 (CH), 113.5 (C), 102.0 (CH)

IR (thin film) ν 1744, 1438, 1354, 1292, 1204, 1174, 1065, 1000, 829, 724 cm^{-1}.

HRMS (ESI negative): calculated for $C_9H_5{}^{79}BrNS_2$ (M): 269.9052, found 269.9044.

The synthesis of the simple indole-containing dithiocarbamate catalyst (potassium 1*H*-indole-1-carbodithioate) was also possible. However, this compound is highly hygroscopic, which prevented its convenient handling and use under an open atmosphere. After screening of several substitution patterns on the indole scaffold, 5-bromoindole derivative **2c** proved optimal in terms of stability and handling while giving excellent results in the catalytic reactions.

2.7.4 Experimental setup

The photoreactor consisted of a 12.5 cm diameter jar fitted with 4 standard B29 size quickfit-glass joints arranged around a central B29 size joint. A commercial 1-meter LED strip was wrapped around the jar, followed by a layer of aluminium foil and cotton for insulation (Figure 2.2).

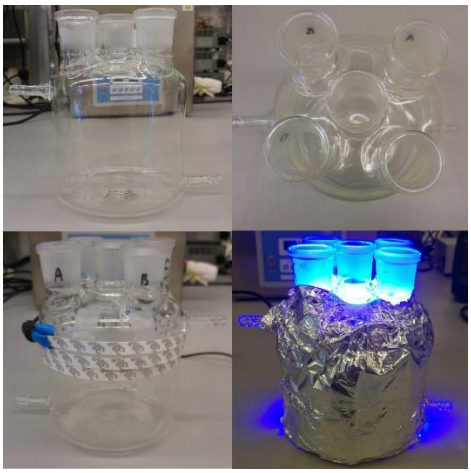

Figure 2.2. Photoreactor used for temperature-controlled reactions - pictures taken at different stages of the set-up assembly.

Each of the joints could be used to fit a standard 16 mm or 25 mm diameter Schlenk tube with a Teflon adaptor (Figure 2.3).

Figure 2.3. Teflon adaptors to use Schlenk tubes in the photoreactor.

An inlet/outlet system provided circulation of liquid (ethylene glycol/water mixture) from a Huber Minichiller 300 inside the jar. This setup allowed the performance of reactions at temperatures ranging from –20 ºC to 80 ºC with accurate control of the reaction temperature (± 1ºC, Figure 2.4).

Figure 2.4. Fully assembled temperature-controlled photoreactor in operation.

In order to maintain consistent illumination between different experiments, only the four external positions were used to perform reactions. The central position was used to monitor the temperature using a thermometer inside another inserted Schlenk tube identical to those used to perform reactions, ensuring that the reaction mixtures were at the desired temperature.

Experiments at *400 nm* were conducted using a 1m strip, 7.2W "Paulmann Function BlackLight LED Strip" purchased from Amazon. The emission spectrum of these LEDs was recorded (Figure 2.5).

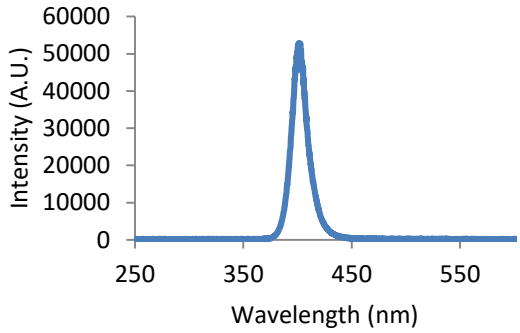

Figure 2.5. Emission spectrum of the 400 nm LED strip used in this study.

The emission maximum was determined as 400 nm with a spectral width of 20 nm (390-410 nm) at half peak intensity and a total spectral width of 80 nm (370-450 nm).

Experiments at *465 nm* were conducted using a 1m strip, 14.4W "LEDXON MODULAR 9009083 LED, SINGLE 5050" purchased from Farnell, catalog number 9009083. The emission spectrum of these LEDs was recorded (Figure 2.6).

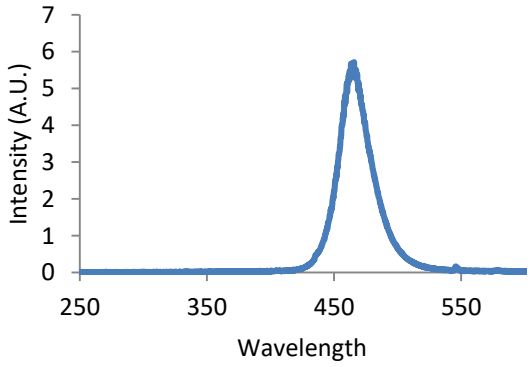

Figure 2.6. Emission spectrum of the 465 nm blue LED strip used in this study.

The emission maximum was determined as 465 nm with a spectral width of 30 nm (450-480 nm) at half peak intensity and a total spectral width of 120 nm (420-540 nm).

2.7.5 Giese addition

2.7.5.1 General procedure A

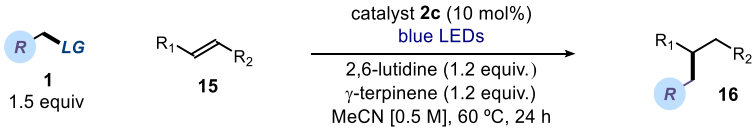

In an oven dried Schlenk tube, catalyst **2c** (15.5 mg, 0.05 mmol, 0.1 equiv.) was dissolved in acetonitrile (1 mL, HPLC grade), then the alkyl electrophile **1** (0.75 mmol, 1.5 equiv.) was added followed by 2,6-lutidine (70 µL, 0.6 mmol, 1.2 equiv.), γ-terpinene (96 µL, 0.6 mmol, 1.2 equiv.), and the Michael acceptor **15** (0.5 mmol, 1 equiv.). The resulting yellow mixture was degassed via three cycles of freeze-pump-thaw. The Schlenk tube was then placed in the irradiation setup (Figure 2.4), maintained at a temperature of 60 ºC (60-61ºC measured in the central well), and the reaction was stirred for 24 hours under continuous irradiation. After cooling to ambient temperature, the solvent was evaporated and the residue purified by column chromatography to afford the corresponding product **16** in the stated yield with >95% purity according to ^{1}H NMR analysis. The exact conditions for chromatography are reported for each compound.

2.7.5.2 Characterization of products with general procedure A

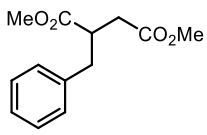

Dimethyl 2-benzylsuccinate (16a): Synthesized according to the general procedure using benzyl chloride **1a** (60 µL, 0.75 mmol, 1.5 equiv.) and dimethyl fumarate **15a** (72 mg, 0.5 mmol, 1 equiv.). Chromatography on silica gel (gradient from pure toluene to 2% AcOEt in toluene as eluent): 92 mg, 78% yield, clear oil.

^{1}H NMR (500 MHz, $CDCl_3$) δ 7.34 – 7.27 (m, 2H), 7.26 – 7.21 (m, 1H), 7.19 – 7.14 (m, 2H), 3.68 (s, 3H), 3.66 (s, 3H), 3.19 – 3.11 (m, 1H), 3.07 (dd, *J* = 13.5, 6.3 Hz, 1H), 2.78 (dd, *J* = 13.5, 8.5 Hz, 1H), 2.70 (dd, *J* = 16.8, 9.2 Hz, 1H), 2.43 (dd, *J* = 16.8, 5 Hz, 1H).

^{13}C NMR (126 MHz, $CDCl_3$) δ 174.6, 172.2, 138.1, 129.0, 128.5, 126.7, 51.9, 51.7, 43.0 (CH), 37.7, 34.9.

Matching reported literature data.[39]

[39] Ueda, M.; Kondoh, E.; Ito, Y.; Shono, H.; Kakiuchi, M.; Ichii, Y.; Kimura, T.; Miyoshi, T.; Naito, T.; Miyata, O., Benzyl radical addition reaction through the homolytic cleavage of a benzylic C–H bond. *Org. Biomol. Chem.* **2011**, *9*, 2062-2064.

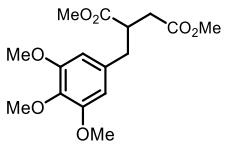

Dimethyl 2-(3,4,5-trimethoxybenzyl)succinate (16g): Synthesized according to the general procedure using 3,4,5-trimethoxybenzyl chloride **1g** (162 mg, 0.75 mmol, 1.5 equiv.) and dimethyl fumarate **15a** (72 mg, 0.5 mmol, 1 equiv.). Chromatography on silica gel (gradient from 20% to 30% AcOEt in hexanes as eluent): 139 mg slowly crystallizing, slightly yellow solid, 85% yield.

^{1}H NMR (500 MHz, $CDCl_3$) δ 6.34 (s, 2H); 3.81 (s, 6H); 3.79 (s, 3H); 366 (S, 3H); 3.63 (s, 3H); 3.14-3.05 (m, 1H); 2.98 (dd, *J* = 13.6, 6.4 Hz, 1H); 2.71-2.61 (m, 2H); 2.41 (dd, *J* = 16.6, 5.1 Hz, 1H).

^{13}C NMR (126 MHz, $CDCl_3$) δ 174.5; 172.2; 153.2; 136.7; 133.8; 105.9; 60.7; 56.0; 51.9; 51.7; 43.0, 38.0; 34.9.

HRMS (ESI pos): calculated for $C_{16}H_{22}NaO_7$ ($M+Na^+$): 349.1258, found 349.1267.

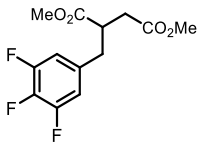

Dimethyl 2-(3,4,5-trifluorobenzyl)succinate (16h): Synthesized according to the general procedure using 5-(bromomethyl)-1,2,3-trifluorobenzene **1h** (169 mg, 0.75 mmol, 1.5 equiv.) and dimethyl fumarate **15a** (72 mg, 0.5 mmol, 1 equiv.). Chromatography on silica gel (gradient from toluene to 2% AcOEt in toluene as eluent): 116 mg slightly yellow oil, 80% yield.

^{1}H NMR (500 MHz, $CDCl_3$) δ 6.86-6.74 (m, 2H); 3.69 (s, 3H); 3.68 (s, 3H); 3.14-3.05 (m, 1H); 2.96 (dd, *J* = 13.7, 7.4 Hz, 1H); 2.77 (dd, *J* = 13.7, 7.2 Hz, 1H); 2.70 (dd, *J* = 16.7, 8.2 Hz, 1H); 2.44 (dd, *J* = 16.7, 5.9 Hz, 1H).

^{13}C NMR (126 MHz, $CDCl_3$) δ 172. (d, *J* = 206.4 Hz), 151.1 (ddd, *J* =250.2, 9.8, 4 Hz), 140.1 (td, *J* =250.2, 15.4 Hz), 134.9-134.4 (m),112.9 (dd, *J* = 15.4, 5.4 Hz), 52.1, 51.9, 42.6, 36.7, 34.9.

^{19}F NMR (376 MHz, $CDCl_3$, proton decoupled) δ -134.03 (d, J = 20.6 Hz, 2F); -162.67 (t, J = 20.6 Hz), 1F).

HRMS (ESI pos): calculated for $C_{13}H_{13}F_3NaO_4$ ($M+Na^+$): 313.0658, found 313.0666.

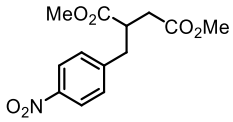

Dimethyl 2-(4-nitrobenzyl)succinate (16i): Synthesized according to a modification of the general procedure: in an oven dried Schlenk tube, catalyst **2c** (15.5 mg, 0.1 equiv.) was dissolved in acetonitrile (1 mL, HPLC grade), then 4-nitrobenzyl bromide **1i** (216 mg, 1 mmol, 2 equiv.) was added followed by 2,6-lutidine (116 μL, 1 mmol, 2 equiv.), γ-terpinene (160 μL, 2 mmol, 2 equiv.), and dimethyl fumarate **15a** (72 mg, 0.5 mmol, 1 equiv.). The resulting yellow mixture was degassed via three cycles of freeze-pump-thaw. The Schlenk tube was then placed in the irradiation setup set at a temperature of 60ºC (60-61ºC measured in the central well) and

irradiated for 24 hours. After cooling to ambient temperature, the solvent was evaporated and the residue purified by column chromatography (gradient from 15% to 30% AcOEt in hexanes as eluent): 112 mg slightly yellow oil, 80% yield.

^{1}H NMR (400 MHz, $CDCl_3$) δ 8.18 (app d, *J* = 8.5 Hz, 2H), 7.37 (app d, *J* = 8.5 Hz, 2H), 3.69 (s, *3*H), 3.67 (s, 3H), 3.24 – 3.06 (m, 2H), 2.95 (dd, *J* = 13.0, 6.6 Hz, 1H), 2.73 (dd, *J* = 16.6, 7.6 Hz, 1H), 2.46 (dd, *J* = 16.6, 5.4 Hz, 1H).

^{13}C NMR (100 MHz, $CDCl_3$) δ 173.8, 171.7, 146.0, 129.8, 123.7, 52.1, 51.9, 42.6, 37.3, 35.1.

HRMS (ESI pos): calculated for $C_{13}H_{15}NaO_6$ ($M+Na^+$): 304.0792, found 304.0805.

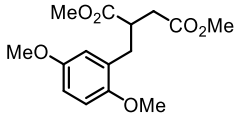

Dimethyl 2-(2,5-dimethoxybenzyl)succinate (16j): Synthesized according to the general procedure using 2-(chloromethyl)-1,4-dimethoxybenzene **1j** (140 mg, 0.75 mmol, 1.5 equiv.) and dimethyl fumarate **15a** (72 mg, 0.5 mmol, 1 equiv.). Chromatography on silica gel (20% AcOEt in hexanes as eluent): 127 mg slightly yellow oil, 86% yield.

^{1}H NMR (400 MHz, $CDCl_3$) δ 6.8-6.71 (m, 2H); 6.67 (d, *J* = 2.8 Hz, 1H); 3.78 (s, 3H); 3.76 (s, 3H); 3.69 (s, 3H); 3.64 (s, 3H); 3.26-3.16 (m, 1H); 3.03 (dd, *J* = 13.2, 6.2 Hz, 1H); 2.78 (dd, *J* = 13.2, 8.6 Hz, 1H); 2.68 (dd, *J* = 16.9, 9.6 Hz, 1H); 2.42 (dd, *J* = 16.9, 4.6 Hz, 1H).

^{13}C NMR (100 MHz, $CDCl_3$) δ 175.0, 172.5, 153.3, 151.9, 127.6, 117.0, 112.2, 111.1, 55.7, 55.7, 51.8, 51.6, 41.3, 34.9, 32.5.

HRMS (ESI pos): calculated for $C_{15}H_{20}NaO_6$ ($M+Na^+$): 31.1152, found 319.1140.

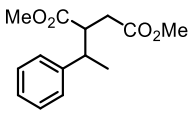

dimethyl 2-(4-fluorobenzyl)succinate (16k): Synthesized according to the general procedure using (1-bromoethyl)benzene **1k** (102 μL, 0.75 mmol, 1.5 equiv.) and dimethyl fumarate **15a** (72 mg, 1 equiv.). The diastereomeric ratio was determined by ^{1}H spectroscopic analysis of the crude reaction mixture by comparison of the resonances at δ 2.34 (minor diastereomer) and δ 2.20 (major diastereomer). Chromatography on silica gel (gradient from pure toluene to 5% AcOEt in toluene as eluent): 61 mg yellow oil, 49% yield and 1:1.2 d.r.

^{1}H NMR for diastereomeric mixture (500 MHz, $CDCl_3$) δ 7.32-7.28 (m, 2H), 7.24-7.15 (m, 3H), 3.74 (s, 3H-major), 3.61 (s, 3H-minor), 3.56 (s, 3H), 3.25-3.20 (m, 1H-minor), 3.14-3.10 (m, 1H-minor), 3.02-2.97 (m, 1H-major), 2.93-2.87 (m, 1H-major), 2.74 (dd, *J* = 16.8, 10.9 Hz, 1H-minor), 2.59 (dd, *J* = 16.9, 11.0 Hz, 1H-major), 2.34 (dd, *J* = 16.8, 3.8 Hz, 1H-minor), 2.20 (dd, *J* = 16.9, 3.8 Hz, 1H-major), 1.28 (d, *J* = 2.3 Hz, 3H-major), 1.27 (d, *J* = 2.1 Hz, 3H-minor).

^{13}C NMR (126 MHz, $CDCl_3$) δ 175.4, 174.6, 173.0, 172.7, 143.9, 143.5, 129.1, 128.8, 127.8, 127.7, 127.3, 127.1, 52.1, 52.1, 52.0, 52.0, 48.7, 48.5, 42.8, 41.1, 35.7, 32.7, 20.6, 16.7.

HRMS (ESI pos): calculated for $C_{14}H_{18}NaO_4^+$ ($M+Na^+$): 273.1097, found 273.1103.

Matching reported data.[39]

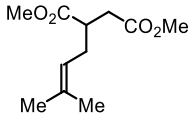

Dimethyl 2-(3-methylbut-2-en-1-yl)succinate (16l): synthesized according to a modification of the general procedure using prenyl chloride **1l** (169 µL, 3 equiv.), 2,6-lutidine (175 µL, 3 equiv.), γ-terpinene (240 µL, 3 equiv.) and dimethyl fumarate **15a** (72 mg, 1 equiv.). Chromatography on silica gel (slow gradient from 1% to 3% AcOEt in hexanes as eluent): 60 mg clear oil, 56% yield.

^{1}H NMR (500 MHz, $CDCl_3$) δ 5.07 (app t; *J* = 7.5 Hz, 1H); 3.71 (s, 3H); 3068 (s, 3H); 2.93-2.85 (m, 1H); 2.70 (dd, *J* = 16.7, 9.2 Hz, 1H); 2.45 (dd, *J* = 16.7, 5.2 Hz, 1H); 2.40-2.32 (m, 1H); 2.31-2.22 (m, 1H); 1.71 (s, 3H); 1.61 (s, 3H).

^{13}C NMR (125 MHz, $CDCl_3$) δ 175.0, 172.6, 134.9, 120.0, 51.8, 51.7, 41.4, 34.9, 30.1, 25.7, 17.7.

HRMS (ESI pos): calculated for $C_{11}H_{18}NaO_4$ ($M+Na^+$): 237.1097, found 237.1092.

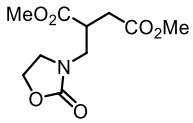

Dimethyl 2-(thiazol-4-ylmethyl)succinate (16m): Synthesized by a two-step one-pot procedure. Following a reported procedure,[40] in an oven dried Schlenk tube, oxazolidin-2-one (65 mg, 0.75 mmol, 1.5 equiv.) and paraformaldehyde (23 mg, 0.75 mmol, 1.5 equiv.) were dissolved in acetonitrile (0.75 mL), TMSCl (479 µL, 3.75 mmol, 7.5 equiv.) was added dropwise and the reaction was refluxed for 16 h. Solvent was removed under vacuum at 25 ºC to obtain the crude 3-(chloromethyl)oxazolidin-2-one **1m** as a white solid that was used without further purification.

In the same Schlenk tube, **2c** (15.5 mg, 0.1 equiv.) was dissolved in acetonitrile (1 mL, HPLC grade), followed by addition of 2,6-lutidine (70 µL, 0.6 mmol, 1.2 equiv.), γ-terpinene (96 µL, 0.6 mmol, 1.2 equiv.) and dimethyl fumarate (72 mg, 0.5 mmol, 1 equiv.). The resulting yellow mixture was degassed via three cycles of freeze-pump-thaw. The Schlenk tube was then placed in the irradiation setup set at a temperature of 60 ºC and irradiated for 24 hours. After cooling to ambient temperature, the solvent was evaporated and the residue purified by column chromatography (50% acetone in hexanes as eluent): 100 mg yellow oil, 82% yield.

^{1}H NMR (500 MHz, $CDCl_3$) δ 4.32-4.22 (m, 2H), 3.68 (s, 3H); 3.64 (s, 3H); 3.59-3.50 (m, 3H), 3.44 (dd, *J* = 6.4, 14.2 Hz, 1H) 3.16-3.06 (m, 1H); 2.75 (dd, *J* = 7.9, 17.1 Hz, 1H); 2.52 (dd, *J* = 5.7, 17.1 Hz, 1H)

^{13}C NMR (125 MHz, $CDCl_3$) δ 173, 171.9, 158.7, 62.0, 52.4, 52.0, 45.7, 45.2, 40.0, 33.4.

---

[40] Fujii, S.; Konishi, T.; Matsumoto, Y.; Yamaoka, Y.; Takasu, K.; Yamada, K.-i., Radical Aminomethylation of Imines. *J. of Org. Chem.* **2014**, *79*, 8128-8133.

HRMS (ESI pos): calculated for $C_{10}H_{15}NNaO_6$ ($M+Na^+$): 268.0792, found 268.0796.

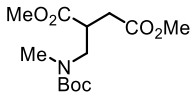

Dimethyl 2-(((*tert*-butoxycarbonyl)(methyl)amino)methyl)succinate (16n): Synthesized by a two-step procedure. Following a reported procedure,[41] in a round bottom flask, *tert*-butyl methylcarbamate (131 mg, 1 mmol, 1 equiv.) and paraformaldehyde (48 mg, 1.6 mmol, 1.6 equiv.) was dissolved in dry DCM (4 mL). TMSCl (383 µL, 3 mmol, 3 equiv.) was added dropwise and the reaction was left stirring at ambient temperature for 2 hours. Solvent was removed under vacuum at 25 ºC to obtain the crude *tert*-butyl (chloromethyl)(methyl)carbamate **1n** as a colorless oil that was used without further purification. The crude product **1n** was dissolved in acetonitrile (HPLC grade) giving a stock solution 0.75 M. The crude *tert*-butyl (chloromethyl)(methyl)carbamate **1n** (0.75 M, 0.75 mmol, 1.5 eq.) was placed in an oven dried Schlenk tube, dissolved in 1 mL of acetonitrile (HPLC grade) followed by the addition of **2c** (15.5 mg, 0.1 equiv.), 2,6-lutidine (70 µL, 0.6 mmol, 1.2 equiv.), γ-terpinene (96 µL, 0.6 mmol, 1.2 equiv.), and dimethyl fumarate (72 mg, 0.5 mmol, 1 equiv.). The resulting yellow mixture was degassed via three cycles of freeze-pump-thaw. The Schlenk tube was then placed in the irradiation setup set at a temperature of 60 ºC and irradiated for 24 hours. After cooling to ambient temperature, the solvent was evaporated and the residue purified by column chromatography (25% AcOEt in hexanes as eluent): 104 mg yellow oil, 72% yield.

^{1}H NMR (500 MHz, $CDCl_3$) δ 3.67 (s, 3H); 3.64 (s, 3H); 3.43 (app d, *J* = 6.9 Hz, 2H) 3.15-3.07 (m, 1H); 3.81 (s, 3H); 2.75-2.63 (m, 1H); 2.45 (dd, *J* = 5.2, 17 Hz, 1H); 1.42 (s, 9H).

^{13}C NMR (125 MHz, $CDCl_3$) δ 173.7 (C); 172.2 (rotamer); 172.0 (C, rotamer); 155.9 (C, rotamer); 155.5 (C, rotamer); 80.1 (C, rotamer); 79.8 (C, rotamers); 52.2 (CH_3); 51.9 (CH_3); 50.4-50.2 (CH_2, rotamers); 40.6 (CH, rotamer); 40.4 (CH, rotamer); 35.2 (CH_3, rotamer); 34.7 (CH_3, rotamer); 33.4 (CH_2); 28.4 (CH_3).

HRMS (ESI pos): calculated for $C_{13}H_{23}NNaO_6$ ($M+Na^+$): 312.1418, found 312.1416.

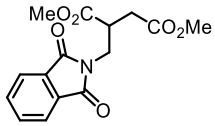

Dimethyl 2-((1,3-dioxoisoindolin-2-yl)methyl)succinate (16o): Synthesized according to the general procedure using 2-(chloromethyl)isoindoline-1,3-dione **1o** (147 mg, 1.5 equiv.) and dimethyl fumarate **15a** (72 mg, 1 equiv.). Chromatography on silica gel (10% AcOEt in toluene as eluent): 127 mg white solid, 83% yield.

[41] Zheng, X.; He, J.; Li, H.-H.; Wang, A.; Dai, X.-J.; Wang, A.-E.; Huang, P.-Q., Titanocene(III)-Catalyzed Three-Component Reaction of Secondary Amides, Aldehydes, and Electrophilic Alkenes. *Angew. Chem. Int. Ed.* **2015**, *54*, 13739-13742.

^{1}H NMR (500 MHz, $CDCl_3$) δ 7.89-7.83 (m, 2H); 7.77-7.71 (m, 2H); 4.05 (dd, *J* = 14; 6.7 Hz, 1H); 3.94 (dd, *J* = 14; 6.4 Hz, 1H); 3.71 (s, 3H); 3.66 (s, 3H); 3.35-3.26 (m, 1H); 2.79 (dd, *J* = 17.2; 8.8 Hz, 1H); 2.59 (dd, *J* = 17.2; 5.2 Hz, 1H).

^{13}C NMR (125 MHz, $CDCl_3$) δ 172.5; 171.6; 168.0; 134.1; 131.8; 123.4; 52.4; 51.9; 40.4; 38.6; 33.3.

HRMS (ESI pos): calculated for $C_{15}H_{15}NaO_6$ ($M+Na^+$): 328.0792, found 328.0801.

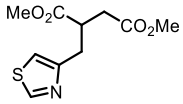

Dimethyl 2-(thiazol-4-ylmethyl)succinate (16p): Synthesized according to a modification of the general procedure: in an oven dried Schlenk tube, 4-(chloromethyl)thiazole hydrochloride **1p** (128 mg, 0.75 mmol, 1.5 equiv.) was dissolved in acetonitrile (1 mL, HPLC grade), then 2,6-lutidine (157 μL, 1.35 mmol, 2.7 equiv.) was added followed by **2c** (15.5 mg, 0.1 equiv.), γ-terpinene (96 μL, 0.6 mmol, 1.2 equiv.), and dimethyl fumarate **15a** (72 mg, 0.5 mmol, 1 equiv.). The resulting yellow mixture was degassed via three cycles of freeze-pump-thaw. The Schlenk tube was then placed in the irradiation setup set at a temperature of 60 ºC and irradiated for 24 hours. After cooling to ambient temperature, the solvent was evaporated and the residue purified by column chromatography (15% acetone in hexanes as eluent): 74 mg yellow oil, 61% yield.

^{1}H NMR (500 MHz, $CDCl_3$) δ 8.72 (d, 1H); 7.01-6.99 (m, 1H); (s, 1H); 3.65 (s, 3H); 3.62 (s, 3H); 3.36-3.28 (m, 1H); 3.22 (dd, *J* = 6.3, 14.4 Hz, 1H); 3.04 (dd, *J* = 7.7, 14.4 Hz, 1H); 2.69 (dd, *J* = 8.7, 16.7 Hz, 1H); 2.50 (dd, *J* = 5.1, 16.7 Hz, 1H).

^{13}C NMR (125 MHz, $CDCl_3$) δ 174.5; 172.2; 154.3; 152.8; 114.9; 52.1; 51.8; 41.3; 35.1; 32.9.

HRMS (ESI pos): calculated for $C_{10}H_{13}NNaO_4S$ ($M+Na^+$): 266.0457, found 266.0457.

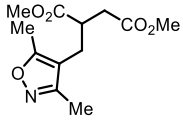

Dimethyl 2-((3,5-dimethylisoxazol-4-yl)methyl)succinate (16q): Synthesized according to the general procedure using 4-(chloromethyl)-3,5-dimethylisoxazole **1q** (93 μL, 0.75 mmol, 1.5 equiv.) and dimethyl fumarate **15a** (72 mg, 0.5 mmol, 1 equiv.). The resulting yellow mixture was degassed via three cycles of freeze-pump-thaw. The Schlenk tube was then placed in the irradiation setup at a temperature of 60 ºC and irradiated for 24 hours. After cooling to ambient temperature, the solvent was evaporated and the residue purified by column chromatography (30% AcOEt in hexanes as eluent): 100 mg yellow oil, 78% yield.

^{1}H NMR (500 MHz, $CDCl_3$) δ 3.62 (s, 3H); 3.62 (s, 3H); 2.97-2.90 (m, 1H); 2.72-2.60 (m, 2H); 2.46 (dd, *J* = 7.7, 14.7 Hz, 1H); 2.39 (dd, *J* = 6.2, 17.7 Hz, 1H); 2.27 (s, 3H); 2.18 (s, 3H).

^{13}C NMR (125 MHz, $CDCl_3$) δ 174.3; 171.8; 166.1; 159.6; 110.4; 52.2; 51.9; 41.3; 35.4; 24.5; 11.0; 10.2.

HRMS: calculated for $C_{12}H_{17}NNaO_5$ ($M+Na^+$): 278.0999, found 278.1009.

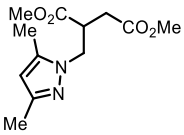

Dimethyl 2-((3,5-dimethyl-1*H*-pyrazol-1-yl)methyl)succinate (16r):

Synthesized by a two-step procedure. Through a variation of a reported procedure,[42] in a round bottom flask, (3,5-dimethyl-1*H*-pyrazol-1-yl)methanol (126 mg, 1 mmol, 1 equiv.) was dissolved in dry chloroform (5 mL) and cooled at 0 ºC. Thionyl chloride (88 µL, 1.2 mmol, 1.2 equiv.) was added dropwise and the reaction was left stirring at ambient temperature for 30 min. Solvent was removed under vacuum at 25 ºC, diethyl ether (5 mL) was added and dried (this was repeated twice) to obtain the crude 1-(chloromethyl)-3,5-dimethyl-1*H*-pyrazole hydrochloride **1r** as a white solid that was used without further purification. The crude product **1r** was dissolved in acetonitrile (HPLC grade) giving a stock solution 0.75 M. 1-(chloromethyl)-3,5-dimethyl-1*H*-pyrazole hydrochloride **1r** (0.75 M, 0.75 mmol, 1.5 equiv.) was added in an oven dried Schlenk tube and diluted with acetonitrile (1 mL, HPLC grade), then catalyst **2c** (15.5 mg, 0.1 equiv.) was added followed by 2,6-lutidine (157 µL, 1.35 mmol, 2.7 equiv.), γ-terpinene (96 µL, 0.6 mmol, 1.2 equiv.), and dimethyl fumarate **15a** (72 mg, 0.5 mmol, 1 equiv.). The resulting yellow mixture was degassed via three cycles of freeze-pump-thaw. The Schlenk tube was then placed in the irradiation setup at a temperature of 60 ºC and irradiated for 24 hours. After cooling to ambient temperature, the solvent was evaporated and the residue purified by column chromatography (30% AcOEt in hexanes as eluent): 105 mg yellow oil: mixture containing product and reported impurity[43] in a proportion of 3:1.

A purity of 78% weight was determined ^{1}H NMR analysis. Corrected yield: 65%.

^{1}H NMR (500 MHz, $CDCl_3$) δ 5.71 (s, 1H); 4.28 (dd, *J* = 6.1, 14.1 Hz, 1H); 4.09 (dd, *J* = 8.2, 14.1z Hz, 1H); 3.65 (s, 3H); 3.60 (s, 3H); 3.40-3.31 (m, 1H); 2.61 (dd, *J* = 7.7, 17.1 Hz, 1H); 2.52 (dd, *J* = 5.3, 17.1 Hz, 1H), 2.16 (s, 3H); 2.13 (s, 3H).

^{13}C NMR (125 MHz, $CDCl_3$) δ 172.7; 171.8; 148; 139.3; 105.2; 52.2; 51.8; 48.4; 42.1; 33.0; 13.4; 10.8.

HRMS (ESI pos): calculated for $C_{12}H_{18}N_2O_4$ ($M+H^+$): 255.1339, found 255.1334.

---

[42] Guerrero, M.; Muñoz, S.; Ros, J.; Calvet, T.; Font-Bardía, M.; Pons, J., New N-pyrazole, P-phosphine hybrid ligands and their reactivity towards Pd(II): X-ray crystal structures of complexes with [PdCl2(N,P)] core. *J. Organomet. Chem.* **2015**, *799-800*, 257-264.

[43] Burns, C. T.; Jordan, R. F., Ethylene Dimerization by Cationic Palladium(II) Alkyl Complexes that Contain Bis(heterocycle)methane Ligands. *Organometallics* **2007**, *26*, 6726-6736.

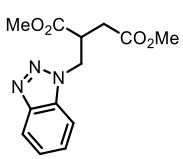

Dimethyl 2-((1*H*-benzo[*d*][1,2,3]triazol-1-yl)methyl)succinate (16s): Synthesized according to the general procedure using 1-(chloromethyl)-1*H*-benzo[*d*][1,2,3]triazole **1s** (120 mg, 0.75 mmol, 1.5 equiv.) and dimethyl fumarate **15a** (72 mg, 0.5 mmol, 1 equiv.). The resulting yellow mixture was degassed via three cycles of freeze-pump-thaw. The Schlenk tube was then placed in the irradiation setup at a temperature of 60 ºC and irradiated for 24 hours. After cooling to ambient temperature, the solvent was evaporated and the residue purified by column chromatography (20% AcOEt in toluene as eluent): 120 mg yellow oil, 87% yield.

^{1}H NMR (500 MHz, $CDCl_3$) δ 8.01 (d, *J* = 8.4 Hz, 1H); 7.53 (d, *J* = 8.4 Hz, 1H); 7.47 (ddd, *J* = 1, 6.8, 8.4 Hz, 1H); 7.34 (ddd, *J* = 1, 6.9, 8.4 Hz, 1H); 4.98 (dd, *J* = 6.3, 14.4 Hz, 1H); 4.90 (dd, *J* = 6.9, 14.4 Hz, 1H); 3.62 (s, 3H); 3.61 (s, 3H); 3.56-3.49 (m, 1H); 2.70 (dd, *J* = 7, 17.3 Hz, 1H); 2.62 (dd, *J* = 6, 17.4 Hz, 1H).

^{13}C NMR (125 MHz, $CDCl_3$) δ 172, 171.5, 145.9, 133.3, 127.7, 124.1, 120.1, 109.3, 52.6, 52.1, 48.0, 41.7, 33.0.

HRMS (ESI pos): calculated for $C_{13}H_{15}N_3NaO_4$ ($M+Na^+$): 300.0955, found 300.0956.

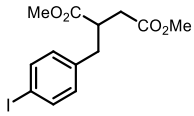

Dimethyl 2-(4-iodobenzyl)succinate (16t): Synthesized according to the general procedure using 4-iodobenzyl methanesulfonate **1t** (234 mg, 0.75 mmol, 1.5 equiv.) and dimethyl fumarate **15a** (72 mg, 0.5 mmol, 1 equiv.). Chromatography on silica gel (gradient from pure toluene to 1% AcOEt in toluene as eluent): 147 mg clear oil, 81% yield.

^{1}H NMR (400 MHz, $CDCl_3$) δ 7.66 – 7.58 (m, 2H), 6.96 – 6.89 (m, 2H), 3.68 (s, *3*H), 3.66 (s, *3*H), 3.16 – 3.06 (m, *1*H), 2.99 (dd, *J* = 13.6, 6.7 Hz, 1H), 2.74 (dd, *J* = 13.6, 8.0 Hz, 1H), 2.68 (dd, *J* = 16.7, 8.8 Hz, 1H), 2.41 (dd, *J* = 16.7, 5.4 Hz, 1H).

^{13}C NMR (100 MHz, $CDCl_3$) δ 174.3, 172.0, 137.8, 137.6, 131.0, 92.0, 51.9, 51.8, 42.7, 37.1, 34.9.

Matching reported data.[39]

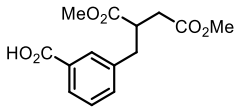

3-(4-Methoxy-2-(methoxycarbonyl)-4-oxobutyl)benzoic acid (16u): Synthesized according to a modification of the general procedure: in an oven dried Schlenk tube, 3-(chloromethyl)benzoic acid **1u** (128 mg, 0.75 mmol, 1.5 equiv.) was dissolved in acetonitrile (1 mL, HPLC grade), then 2,6-lutidine (157 μL, 1.35 mmol, 2.7 equiv.) was added followed by **2c** (15.5 mg, 0.1 equiv.), γ-terpinene (96 μL, 0.6 mmol, 1.2 equiv.) and dimethyl fumarate **15a** (72 mg, 0.5 mmol, 1 equiv.). The resulting yellow mixture was degassed via three cycles of freeze-pump-

thaw. The Schlenk tube was then placed in the irradiation setup at a temperature of 60 ºC and irradiated for 24 hours. After cooling to ambient temperature, the solvent was evaporated and the residue was diluted with AcOEt and NH_4Cl sat. aqueous solution, the layers were separated and extracted with AcOEt (3x15 mL). Organic layer was purified by column chromatography (30% acetone in hexanes with 7% vol. acetic acid as eluent): 94 mg light orange solid, 67% yield.

^{1}H NMR (500 MHz, $CDCl_3$) δ 11.61 (br s, 1H); 7.99-7.95 (m, 1H); 7.90 (s, 1H); 7.41-7.37 (m, 2H); 3.66 (s, 3H); 3.64 (s, 3H); 3.20-3.12 (m, 1H); 3.08 (dd, *J* = 6.8, 13.6 Hz, 1H); 2.86 (dd, *J* = 7.8, 13.6 Hz, 1H); 2.69 (dd, *J* = 8.9, 16.8 Hz, 1H); 2.42 (dd, *J* = 5.2, 16.8 Hz, 1H).

^{13}C NMR (125 MHz, $CDCl_3$) δ 174.5 (C); 172.2 (C); 171.9 (C); 138.8 (C); 134.4 (CH); 130.7 (CH); 130.0 (C); 128.8 (CH); 128.7 (CH); 52.1 (CH_3); 51.9 (CH_3); 43 (CH); 37.5 (CH_2); 35.1 (CH_2).

HRMS (ESI pos): calculated for $C_{14}H_{16}NaO_6$ ($M+Na^+$): 303.0839, found 303.0846.

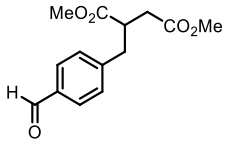

Dimethyl 2-(4-formylbenzyl)succinate (16w): Synthesized according to a modification of the general procedure: in an oven dried Schlenk tube, **2c** (15.5 mg, 0.1 equiv.) was dissolved in acetonitrile (1 mL, HPLC grade), then 4-formylbenzyl methanesulfonate **1w** (214 mg, 1 mmol, 2 equiv.) was added followed by 2,6-lutidine (116 µL, 1 mmol, 2 equiv.), γ-terpinene (160 µL, 2 mmol, 2 equiv.), and dimethyl fumarate **15a** (72 mg, 0.5 mmol, 1 equiv.). The resulting yellow mixture was degassed via three cycles of freeze-pump-thaw. The Schlenk tube was then placed in the irradiation setup at a temperature of 60 ºC and irradiated for 24 hours. After cooling to ambient temperature, the solvent was evaporated and the residue purified by column chromatography (15%AcOEt in hexanes as eluent, two consecutive purifications): 105 mg clear oil, 79% yield.

^{1}H NMR (400 MHz, $CDCl_3$) δ 9.97 (s, 1H); 7.82-7.77 (m, 2H); 7.36-7.29 (m, 2H); 3.64 (app s, 2x3H); 3.21-3.11 (m, 1H); 3.09 (dd, *J* = 7, 13.5 Hz, 1H); 2.87 (dd, *J* = 7.5, 13.5 Hz, 1H); 2.69 (dd, *J* = 8.5, 16.7 Hz, 1H); 2.42 (dd, *J* = 5.4, 16.7 Hz, 1H).

^{13}C NMR (100 MHz, $CDCl_3$) δ 191.7; 174.1; 171.9; 145.5; 135.1; 130.0; 129.7; 52.0; 51.8; 42.6; 37.7; 35.0.

HRMS (ESI pos): calculated for $C_{14}H_{16}NaO_5$ ($M+Na^+$): 287.0890, found 287.0895.

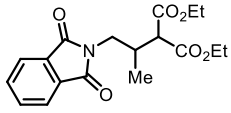

Diethyl 2-(1-(1,3-dioxoisoindolin-2-yl)propan-2-yl)malonate (16b): Synthesized according to the general procedure using 2-(chloromethyl)isoindoline-1,3-dione **1o** (147 mg, 0.75 mmol, 1.5 equiv.), 2,6-lutidine (70 µL, 0.6 mmol, 1.2 equiv.), γ-terpinene (96 µL, 0.6 mmol, 1.2 equiv.)

and diethyl 2-ethylidenemalonate **15b** (91 µL, 0.5 mmol, 1 equiv.). Chromatography on silica gel (gradient from 5% to 25% AcOEt in hexanes as eluent): 69 mg, yellow oil, 40% yield.

^{1}H NMR (500 MHz, $CDCl_3$) δ 7.85-7.81 (m, 2H), 7.72-7.69 (m, 2H), 4.23-4.14 (m, 4H), 3.78 (d, *J* = 6.5 Hz, 2H), 3.34 (d, *J* = 7.5 Hz, 1H), 2.79-2.71 (m, 1H), 1.26 (q, *J* = 7.1 Hz, 6H), 1.03 (d, *J* = 7.0 Hz, 3H).

^{13}C NMR (126 MHz, $CDCl_3$) δ 168.8, 168.6, 168.5, 134.4, 132.3, 123.6, 61.8, 61.8, 55.6, 42.0, 33.3, 15.6, 14.4, 14.4.

HRMS (ESI pos): calculated for $C_{18}H_{21}NNaO_6$ ($M+Na^+$): 370.1261, found 370.1256.

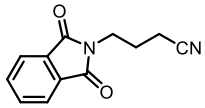

4-(1,3-Dioxoisoindolin-2-yl)butanenitrile (16c): Synthesized according to a modification of the general procedure using 2-(chloromethyl)isoindoline-1,3-dione **1o** (147 mg, 1,5 equiv.), 2,6-lutidine (140 µL, 2 equiv.), γ-terpinene (192 µL, 2 equiv.) and acrylonitrile **15c** (33 µL, 0.5 mmol, 1 equiv.). Chromatography on silica gel (15% AcOEt in hexanes, then a second chromatography with 15% AcOEt in toluene as eluent): 70 mg, slightly yellow solid, 65% yield.

^{1}H NMR (400 MHz, $CDCl_3$) δ 7.87-7.81 (m, 2H); 7.75-7.69 (m, 2H); 3.80 (t, *J* = 6.7 Hz, 2H); 2.42 (t, *J* = 7.3 Hz, 2H); 2.06 (m, *J* = 7.1 Hz, 2H).

^{13}C NMR (100 MHz, $CDCl_3$) δ 168.3; 134.3; 131.9; 123.5; 118.8; 36.7; 24.8; 15.2.

HRMS (ESI pos): calculated for $C_{12}H_{10}N_2NaO_2$ ($M+Na^+$): 327.0634, found 327.0629.

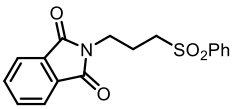

2-(3-(phenylsulfonyl)propyl)isoindoline-1,3-dione (16d): Synthesized according to a modification of the general procedure using 2-(chloromethyl)isoindoline-1,3-dione **1o** (147 mg, 1,5 equiv.), 2,6-lutidine (140 µL, 2 equiv.), γ-terpinene (192 µL, 2 equiv.) and phenyl vinyl sulfone **15d** (84 mg, 0.5 mmol, 1 equiv.). Chromatography on silica gel (10% AcOEt in toluene, then a second chromatography with 40% AcOEt in hexane as eluent): 70 mg, slightly yellow solid, 68% yield.

^{1}H NMR (400 MHz, $CDCl_3$) δ 7.90-7.85 (m, 2H); 7.83-7.76 (m, 2H); 7.73-7.67 (m, 2H); 7.65-7.59 (m, 1H); 7.56-7.50 (m, 2H); 3.74 (t, *J* = 6.7 Hz, 2H); 3.20-3.12 (m, 2H); 2.13-2.03 (m, 2H).

^{13}C NMR (100 MHz, $CDCl_3$) δ 168.2; 138.8; 134.3; 133.9; 131.9; 129.4; 128.2; 123.5; 54.0; 36.3; 22.4.

HRMS (ESI pos): calculated for $C_{17}H_{15}NNaO_4S$ ($M+Na^+$): 352.0614, found 327.0613.

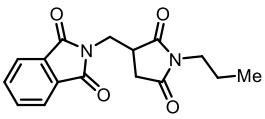

2-((2,5-Dioxo-1-propylpyrrolidin-3-yl)methyl)isoindoline-1,3-dione (16e): Synthesized according to the general procedure using 2-(chloromethyl)isoindoline-1,3-dione **1o** (147 mg, 0.75 mmol, 1.5 equiv.), 2,6-lutidine (70 µL, 0.6 mmol, 1.2 equiv.), γ-terpinene (96 µL, 0.6 mmol, 1.2 equiv.), and *N*-propylmaleimide **15e** (63 µL, 0.5 mmol, 1 equiv.). Chromatography on silica gel (gradient from 5% AcOEt in hexanes to pure AcOEt as eluent): 130 mg, yellow oil, 86% yield.

^{1}H NMR (500 MHz, $CDCl_3$) δ 7.84-7.80 (m, 2H), 7.73-7.69 (m, 2H), 4.08 (dd, *J* = 14.0, 7.3 Hz, 1H), 3.86 (dd, *J* = 14.0, 8.3 Hz, 1H), 3.40 (t, *J* = 7.5 Hz, 2H), 3.35-3.29 (m, 1H), 2.78 (dd, *J* = 18.3, 9.2 Hz, 1H), 2.55 (dd, *J* = 18.3, 4.7 Hz, 1H), 1.57-1.50 (m, 2H), 0.84 (t, *J* = 7.5 Hz, 3H).

^{13}C NMR (126 MHz, $CDCl_3$) δ 177.3, 175.9, 168.4, 134.6, 132.1, 123.9, 40.9, 38.9, 38.8, 33.1, 21.3, 11.6.

HRMS: calculated for $C_{16}H_{16}N_2NaO_4$ ($M+Na^+$): 323.1002, found 323.1014.

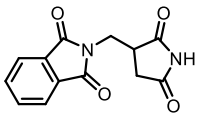

2-((2,5-Dioxopyrrolidin-3-yl)methyl)isoindoline-1,3-dione (16f): Synthesized according to the general procedure using 2-(chloromethyl)isoindoline-1,3-dione **1o** (147 mg, 0.75 mmol, 1.5 equiv.), 2,6-lutidine (70 µL, 0.6 mmol, 1.2 equiv.), γ-terpinene (96 µL, 0.6 mmol, 1.2 equiv.) and maleimide **15f** (49 mg, 0.5 mmol, 1 equiv.). Chromatography on silica gel (gradient from 5% AcOEt in hexanes to pure AcOEt as eluent): 115 mg, light yellow solid, 89% yield. Tautomer observed by ^{1}H NMR.

^{1}H NMR (500 MHz, $CDCl_3$) δ 9.06 (bs, 1H), 7.84-7.82 (m, 2H), 7.72-7.70 (m, 2H), 4.12 (dd, *J* = 14.0, 7.0 Hz, 1H), 3.90 (dd, *J* = 14.0, 8.4 Hz, 1H), 3.40-3.34 (m, 1H), 2.83 (dd, *J* = 18.4, 9.2 Hz, 1H), 2.63 (dd, *J* = 18.4, 5.0 Hz, 1H).

^{13}C NMR (126 MHz, $CDCl_3$) δ 178.1, 176.8, 168.6, 134.7, 132.1, 124.0, 40.4, 38.7, 34.3.

HRMS (ESI pos): calculated for $C_{13}H_{10}N_2NaO_4$ ($M+Na^+$): 281.0553, found 281.0531.

2.7.6 Tandem radical addition-cyclization of aromatic acrylamides

2.7.6.1 General procedure B

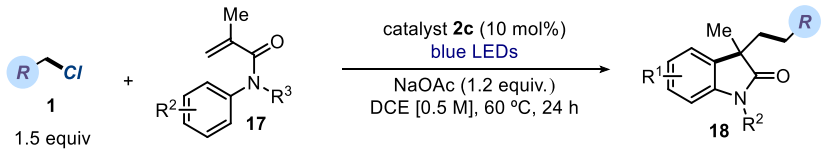

An oven dried Schlenk tube was sequentially charged with the electrophile (0.75 mmol, 1.5 equiv.), dichloroethane (1 mL, reagent grade), and then the catalyst **2c** (15.5 mg, 0.05 mmol,

0.1 equiv.). The aromatic acrylamide **17** (0.50 mmol, 1.0 equiv.) was added, followed by sodium acetate (49.2 mg, 0.60 mmol, 1.2 equiv.). The resulting yellow mixture was degassed via three cycles of freeze-pump-thaw. The Schlenk tube was then placed in the irradiation setup (Figure 2.4) at a temperature of 60 ºC (60-61 ºC measured in the central well) and the reaction mixture was stirred under irradiation for 24 hours. After cooling to ambient temperature, the solvent was evaporated and the residue purified by column chromatography to afford the corresponding product in the stated yield with >95% purity according to 1H NMR analysis. The exact conditions for chromatography are reported for each compound.

2.7.6.2 Characterization of products with general procedure B

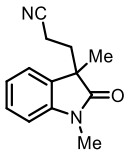

3-(1,3-Dimethyl-2-oxoindolin-3-yl)propanenitrile (18a). Synthesized according to the general procedure using chloroacetonitrile (48 μL, 0.75 mmol, 1.5 equiv.) and *N*-methyl-*N*-phenylmethacrylamide (87.6 mg, 0.5 mmol, 1 equiv.). Chromatography on silica gel (gradient from 10% to 40% AcOEt in hexanes as eluent): 102 mg brown oil, 95% yield.

^{1}H NMR (500 MHz, $CDCl_3$) δ 7.34-7.30 (m, 1H); 7.21-7.19 (m, 1H), 7.13-7.10 (m, 1H), 6.89 (d, *J* = 7.8 Hz, 1H), 3.22 (s, 3H), 2.36-2.30 (m, 1H), 2.13-1.97 (m, 3H), 1.40 (s, 3H).

^{13}C NMR (126 MHz, $CDCl_3$) δ 178.9, 143.2, 131.7, 128.7, 123.0, 122.6, 118.8, 108.5, 47.3, 33.4, 26.3, 23.5, 12.8.

HRMS (ESI pos): calculated for $C_{13}H_{14}N_2NaO^+$ ($M+Na^+$): 237.0998, found 237.0997.

Matching reported data.[44]

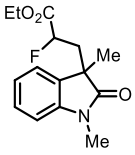

Ethyl 3-(1,3-dimethyl-2-oxoindolin-3-yl)-2-fluoropropanoate (18b) Synthesized according to the general procedure using ethyl bromofluoroacetate (89 μL, 0.75 mmol, 1.5 equiv.) and *N*-methyl-*N*-phenylmethacrylamide (87.6 mg, 0.5 mmol, 1 equiv.). The diastereomeric ratio was determined by ^{1}H NMR analysis of the crude reaction mixture by comparison of the resonances at δ 3.20 (minor diastereomer) and δ 3.17 (major diastereomer). Chromatography on silica gel (gradient from 15% to 35% AcOEt in hexanes as eluent): 135 mg brown oil, 97% yield (1.2:1 dr).

^{1}H NMR for diastereomeric mixture (500 MHz, $CDCl_3$) δ 7.29-7.23 (m, 1H), 7.20-7.17 (m, 1H), 7.06-7.01 (m, 1H), 6.84-6.82 (m, 1H), 4.76 (ddd, *J* = 48.7, 7.4, 4.4 Hz, 1H-minor), 4.61 (ddd, *J* = 49.3, 10.9, 2.6 Hz, 1H-major), 4.16-4.07 (m, 2H), 4.06-3.97 (m, 2H), 3.20 (s, 3H-minor), 3.17 (s, 3H-major), 2.56-2.38 (m, 3H), 2.28 (ddd, *J* = 39.3, 15.0, 2.6 Hz, 1H-major),

[44] Pan, C.; Zhang, H.; Zhu, C., Fe-promoted radical cyanomethylation/arylation of arylacrylamides to access oxindoles via cleavage of the sp3 C–H of acetonitrile and the sp2 C–H of the phenyl group. *Org. Biomol. Chem.* **2015**, *13*, 361-364.

1.39 (s, 3H-major), 1.38 (s, 3H-minor), 1.21 (t, *J* = 7.1 Hz, 3H-major), 1.17 (t, *J* = 7.2 Hz-minor).

^{13}C NMR for diastereomeric mixture (126 MHz, $CDCl_3$) δ 179.6, 179.4, 169.2 (d, *J* = 18.5 Hz), 169.0 (d, *J* = 19.2 Hz), 143.5, 143.2, 132.2, 131.8, 128.5, 128.2, 123.4, 122.9, 122.5, 122.4, 108.4, 108.3, 87.4 (d, *J* = 37.7 Hz), 85.9 (d, *J* = 36.3 Hz), 61.6 (diastereomeric signals overlapping), 46.0, 45.7, 39.9 (d, *J* = 20.3 Hz), 39.3 (d, *J* = 19.8 Hz), 26.3 (diastereomeric signals overlapping), 24.8, 24.2, 14.0, 13.9.

^{19}F NMR for diastereomeric mixture (376 MHz, $CDCl_3$) δ -190.5, -191.0.

HRMS (ESI pos): calculated for $C_{15}H_{19}FNO_3^+$ ($M+H^+$): 280.1343, found 280.1354.

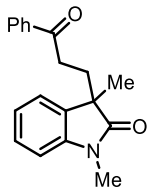

1,3-dimethyl-3-(3-oxo-3-phenylpropyl)indolin-2-one (18c) Synthesized according to the general procedure using 2-chloro-1-phenylethan-1-one (115.9 mg, 0.75 mmol, 1.5 equiv.) and *N*-methyl-*N*-phenylmethacrylamide (87.6 mg, 0.5 mmol, 1 equiv.). Chromatography on silica gel (gradient from 10% to 25% AcOEt in hexanes as eluent): 100 mg orange oil, 68% yield.

^{1}H NMR (500 MHz, $CDCl_3$) δ 7.80-7.78 (m, 2H), 7.51 (t, *J* = 7.4 Hz, 1H), 7.39 (t, *J* = 7.9 Hz, 2H), 7.30-7.26 (m, 1H), 7.22 (d, *J* = 7.3 Hz, 1H), 7.10-7.07 (m, 1H), 6.87 (d, *J* = 7.8 Hz, 1H), 3.26 (s, 3H), 2.84-2.78 (m, 1H), 2.55-2.48 (m, 1H), 2.38-2.33 (m, 1H), 2.28-2.22 (m, 1H), 1.44 (s, 3H).

^{13}C NMR (126 MHz, $CDCl_3$) δ 199.3, 180.2, 143.2, 136.7, 133.4, 133.0, 128.5, 128.1, 128.0, 122.8, 122.7, 108.1, 47.6, 33.6, 32.5, 26.2, 23.8.

HRMS (ESI pos): calculated for $C_{19}H_{20}NO_2^+$ ($M+H^+$): 294.1489, found 294.1498.

Matching reported data.[45]

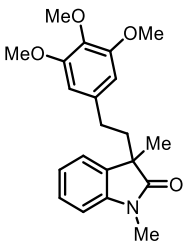

1,3-dimethyl-3-(3,4,5-trimethoxyphenethyl)indolin-2-one (18d) Synthesized according to the general procedure using 5-(chloromethyl)-1,2,3-trimethoxybenzene (162.5 mg, 0.75 mmol, 1.5 equiv.) and *N*-methyl-*N*-phenylmethacrylamide (87.6 mg, 0.5 mmol, 1 equiv.). Chromatography on silica gel (gradient from 20% to 50% AcOEt in hexanes as eluent): 49 mg brown oil, 28% yield.

[45] Fan, J.-H.; Wei, W.-T.; Zhou, M.-B.; Song, R.-J.; Li, J.-H., Palladium-catalyzed oxidative difunctionalization of alkenes with α-carbonyl alkyl bromides initiated through a Heck-type insertion: a route to indolin-2-ones. *Angew. Chem. Int. Ed. Engl.* **2014**, *53*, 6650-6654.

^{1}H NMR (500 MHz, $CDCl_3$) δ 7.34-7.31 (m, 1H), 7.26 (d, *J* = 7.2 Hz, 1H), 7.14 (t, *J* = 7.5 Hz, 1H), 6.88 (d, *J* = 7.7 Hz, 1H), 6.23 (s, 2H), 3.81 (s, 9H), 3.22 (s, 3H), 2.34-2.25 (m, 2H), 2.15-2.00 (m, 2H), 1.42 (s, 3H).

^{13}C NMR (126 MHz, $CDCl_3$) δ 180.4, 153.0, 143.4, 137.0, 136.0, 133.7, 127.9, 122.6, 122.6, 108.0, 105.2, 60.8, 56.0, 48.3, 40.0, 31.5, 26.1, 24.1.

HRMS (ESI pos): calculated for $C_{21}H_{25}NNaO_4^+$ ($M+Na^+$): 378.1676, found 378.1675.

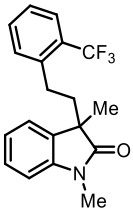

1,3-dimethyl-3-(2-(trifluoromethyl)phenethyl)indolin-2-one (18e)
Synthesized according to the general procedure using 1-(chloromethyl)-2-(trifluoromethyl)benzene (109 μL, 0.75 mmol, 1.5 equiv.) and *N*-methyl-*N*-phenylmethacrylamide (87.6 mg, 0.5 mmol, 1 equiv.). Chromatography on silica gel (gradient from 10% to 30% AcOEt in hexanes as eluent; mixed fractions were re-purified in the same manner): 71 mg yellow oil, 43% yield.

^{1}H NMR (500 MHz, $CDCl_3$) δ 7.53 (d, *J* = 7.7 Hz, 1H), 7.43-7.38 (m, 1H), 7.32-7.29 (m, 1H), 7.25-7.22 (m, 3H9, 7.14-7.11 (m, 1H), 6.88 (d, *J* = 7.8 Hz, 1H), 3.26 (s, 3H), 2.43-2.36 (m, 2H), 2.22-2.15 (m, 1H), 2.07-1.99 (m, 1H), 1.40 (s, 3H).

^{13}C NMR (126 MHz, $CDCl_3$) δ 180.6, 143.7, 140.7, 133.7, 132.1, 131.8, 128.6 (d, *J* = 29.7 Hz), 128.3, 126.4, 126.2 (q, *J* = 5.6 Hz), 125.9, 123.7, 123.1 (d, *J* = 4.7 Hz), 108.4, 48.8, 40.8, 28.3, 26.6, 24.1.

^{19}F NMR (376 MHz, $CDCl_3$) δ -59.8.

HRMS (ESI pos): calculated for $C_{19}H_{18}F_3NNaO^+$ ($M+Na^+$): 356.1233, found 356.1230.

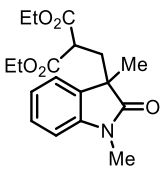

Diethyl 2-((1,3-dimethyl-2-oxoindolin-3-yl)methyl)malonate (18f)
Synthesized according to the general procedure using diethyl 2-chloromalonate (121 μL, 0.75 mmol, 1.5 equiv.) and *N*-methyl-*N*-phenylmethacrylamide (87.6 mg, 0.5 mmol, 1 equiv.). Chromatography on silica gel was not able to remove residual methacrylamide from the reaction mixture, therefore an NMR yield is reported (46%). Semi-preparative HPLC (IA column, 70:30 Hexane/CH_2Cl_2, 1 mL/min) was performed to obtain an analytical amount of the isolated product as a yellow oil.

^{1}H NMR (500 MHz, $CDCl_3$) δ 7.27-7.23 (m, 1H), 7.14 (d, *J* = 6.8 Hz, 1H), 7.04-7.01 (m, 1H), 6.82 (d, *J* = 7.8 Hz, 1H), 4.11 (q, *J* = 7.2 Hz, 2H), 3.85-3.79 (m, 1H), 3.70-3.63 (m, 1H), 3.20 (s, 3H), 3.01 (dd, *J* = 8.1, 5.5 Hz, 1H), 2.55 (dd, *J* = 14.4, 5.5 Hz, 1H), 2.49 (dd, *J* = 14.3, 8.1 Hz, 1H), 1.37 (s, 3H), 1.20 (t, 7.1 Hz, 3H), 1.05 (t, 7.2 Hz, 3H).

^{13}C NMR (126 MHz, $CDCl_3$) δ 179.7, 169.2, 169.1, 143.8, 132.5, 128.6, 123.8, 122.8, 108.5, 61.9, 61.7, 49.0, 47.4, 36.2, 26.6, 24.8, 14.3, 14.1.

HRMS (ESI pos): calculated for $C_{18}H_{24}NO_5^+$ ($M+H^+$): 334.1649, found 334.1648.

Matching reported data.[46]

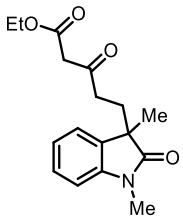

Ethyl 5-(1,3-dimethyl-2-oxoindolin-3-yl)-3-oxopentanoate (18g). Synthesized according to the general procedure using ethyl 4-chloro-3-oxobutanoate (101 μL, 0.75 mmol, 1.5 equiv.) and *N*-methyl-*N*-phenylmethacrylamide (87.6 mg, 0.5 mmol, 1 equiv.). Chromatography on silica gel (gradient from 10% to 40% AcOEt in hexanes as eluent): 103 mg yellow oil, 68% yield. Isolated product sits as ketone:enol mixture (95:5).

^{1}H NMR (500 MHz, $CDCl_3$) δ 7.29-7.26 (m, 1H), 7.15 (d, *J* = 7.3 Hz, 1H), 7.08—7.05 (m, 1H), 6.86 (d, *J* = 7.8 Hz, 1H), 4.11 (q, *J* = 7.2 Hz, 2H), 3.25 (d, *J* = 3.5 Hz, 2H), 3.21 (s, 3H), 2.35-2.28 (m, 1H), 2.20-2.06 (m, 3H), 1.37 (s, 3H), 1.20 (t, *J* = 7.2 Hz, 3H).

^{13}C NMR (126 MHz, $CDCl_3$) δ 201.7, 179.9, 166.9, 143.1, 133.1, 128.1, 122.8, 122.7, 108.1, 61.3, 49.2, 47.2, 38.0, 31.4, 26.2, 23.6, 14.0.

HRMS (ESI pos): calculated for $C_{17}H_{21}NNaO_4^+$ ($M+Na^+$): 326.1363, found 326.1371.

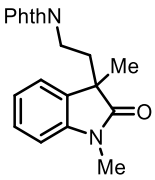

2-(2-(1,3-dimethyl-2-oxoindolin-3-yl)ethyl)isoindoline-1,3-dione (18h). Synthesized according to the general procedure using *N*-(chloromethyl)phthalimide (146.7 mg, 0.75 mmol, 1.5 equiv.) and *N*-methyl-*N*-phenylmethacrylamide (87.6 mg, 0.5 mmol, 1 equiv.). Chromatography on silica gel could not remove a residual byproduct from the reaction mixture, therefore an NMR yield is reported (65%). Semi-preparative HPLC (IA column, 70:30:0.1 hexane/CH_2Cl_2/diethylamine, 1 mL/min) was performed to obtain an analytical amount of the isolated product as a clear oil.

^{1}H NMR (500 MHz, $CDCl_3$) δ 7.66-7.60 (m, 4H), 7.09-7.07 (m, 2H), 6.96-6.93 (m, 1H), 6.74-6.69 (m, 2H), 3.62-3.56 (m, 1H), 3.47-3.42 (m, 1H), 3.19 (s, 3H), 2.48-2.42 (m, 1H), 2.33-2.28 (m, 1H), 1.35 (s, 3H).

^{13}C NMR (126 MHz, $CDCl_3$) δ 179.9, 168.1, 143.5, 133.9, 133.3, 132.3, 127.9, 123.2, 122.7, 122.4, 108.7, 47.3, 35.0, 34.9, 26.6, 25.4.

HRMS (ESI pos): calculated for $C_{20}H_{18}N_2NaO_3^+$ ($M+Na^+$): 357.1210, found 357.1224.

Matching reported data.[46]

[46] Wang, S.; Huang, X.; Li, B.; Ge, Z.; Wang, X.; Li, R., A metal-free synthesis of oxindoles by a radical addition-cyclization onto N-arylacrylamides with xanthates. *Tetrahedron* **2015**, *71*, 1869-1875.

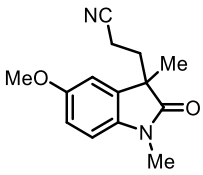

3-(5-Methoxy-1,3-dimethyl-2-oxoindolin-3-yl)propanenitrile (18i). Synthesized according to the general procedure using chloroacetonitrile (48 μL, 0.75 mmol, 1.5 equiv.) and *N*-(4-methoxyphenyl)-*N*-methylmethacrylamide (102.6 mg, 0.5 mmol, 1 equiv.). Chromatography on silica gel (gradient from 10% to 50% AcOEt in hexanes as eluent): 109 mg brown oil, 89% yield.

^{1}H NMR (500 MHz, $CDCl_3$) δ 6.84-6.77 (m, 3H), 3.80 (s, 3H), 3.19 (s, 3H), 2.35-2.27 (m, 1H), 2.12-1.97 (m, 3H), 1.38 (s, 3H).

^{13}C NMR (126 MHz, $CDCl_3$) δ 178.5, 156.4, 136.6, 133.0, 118.9, 112.6, 110.3, 108.9, 55.8, 47.7, 33.5, 26.4, 23.5, 12.8.

HRMS (ESI pos): calculated for $C_{14}H_{17}N_2O_2^+$ ($M+H^+$): 245.1285, found 245.1289.

Matching reported data.[44]

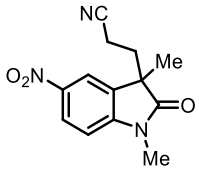

3-(5-Methoxy-1,3-dimethyl-2-oxoindolin-3-yl)propanenitrile (18j). Synthesized according to the general procedure using chloroacetonitrile (48 μL, 0.75 mmol, 1.5 equiv.) and *N*-methyl-*N*-(4-nitrophenyl)methacrylamide (110.1 mg, 0.5 mmol, 1 equiv.). Chromatography on silica gel (gradient from 30% to 50% AcOEt in hexanes as eluent): 71 mg orange oil, 55% yield.

^{1}H NMR (500 MHz, $CDCl_3$) δ 8.33 (dd, *J* = 8.6, 2.2 Hz, 1H), 8.13 (d, *J* = 2.2 Hz, 1H), 7.01 (d, *J* = 8.7 Hz, 1H), 3.32 (s, 3H), 2.44-2.36 (m, 1H), 2.20-2.14 (m, 3H), 1.49 (s, 3H).

^{13}C NMR (126 MHz, $CDCl_3$) δ 179.0, 148.8, 143.7, 132.7, 126.0, 118.7, 118.1, 108.2, 47.3, 32.9, 26.8, 23.4, 12.9.

HRMS (ESI pos): calculated for $C_{13}H_{14}N_3O_3^+$ ($M+H^+$): 260.1030, found 260.1027.

Matching reported data.[44]

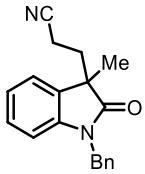

3-(1-benzyl-3-methyl-2-oxoindolin-3-yl)propanenitrile (18k) Synthesized according to the general procedure using chloroacetonitrile (48 μL, 0.75 mmol, 1.5 equiv.) and *N*-benzyl-*N*-phenylmethacrylamide (125.7 mg, 0.5 mmol, 1 equiv.). Chromatography on silica gel (gradient from 20% to 30% AcOEt in hexanes as eluent): 81 mg brown oil, 56% yield.

^{1}H NMR (500 MHz, $CDCl_3$) δ 7.37-7.28 (m, 5H), 7.25-7.22 (m, 2H), 7.12-7.09 (m, 1H), 6.82 (d, *J* = 7.7 Hz, 1H), 4.96 (d, *J* = 15.6 Hz, 1H), 4.91 (d, *J* = 15.6 Hz, 1H), 2.43-2.37 (m, 1H), 2.19-2.11 (m, 2H), 2.07-2.00 (m, 1H), 1.48 (s, 3H).

^{13}C NMR (126 MHz, $CDCl_3$) δ 179.0, 142.3, 135.8, 131.7, 128.9, 128.6, 127.8, 127.3, 123.1, 122.7, 118.9, 109.6, 47.4, 43.9, 33.6, 23.8, 12.9.

HRMS (ESI pos): calculated for $C_{19}H_{18}N_2NaO^+$ ($M+Na^+$): 313.1311, found 313.1297.

Matching reported data.[44]

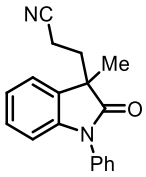

3-(3-Methyl-2-oxo-1-phenylindolin-3-yl)propanenitrile (18l). Synthesized according to the general procedure using chloroacetonitrile (48 μL, 0.75 mmol, 1.5 equiv.) and *N*,*N*-diphenylmethacrylamide (118.7 mg, 0.5 mmol, 1 equiv.). Chromatography on silica gel (gradient from 20% to 40% AcOEt in hexanes as eluent): 131 mg brown oil, 95% yield.

^{1}H NMR (500 MHz, $CDCl_3$) δ 7.57-7.54 (m, 2H), 7.46-7.43 (m, 3H), 7.30-7.26 (m, 2H), 7.19-7.16 (m, 1H), 6.90 (d, *J* = 7.8 Hz, 1H), 2.48-2.42 (m, 1H), 2.30-2.15 (m, 3H), 1.55 (s, 3H).

^{13}C NMR (126 MHz, $CDCl_3$) δ 178.4, 143.1, 134.2, 131.5, 129.7, 128.6, 128.3, 126.5, 123.6, 123.0, 118.8, 109.9, 47.5, 33.7, 24.0, 13.0.

HRMS (ESI pos): calculated for $C_{18}H_{17}N_2O^+$ ($M+H^+$): 277.1335, found 277.1333.

Matching reported data.[44]

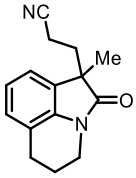

3-(1-Methyl-2-oxo-1,2,5,6-tetrahydro-4*H*-pyrrolo[3,2,1-*ij*]quinolin-1-yl)propanenitrile (18m). Synthesized according to the general procedure using chloroacetonitrile (48 μL, 0.75 mmol, 1.5 equiv.) and 1-(3,4-dihydroquinolin-1(2*H*)-yl)-2-methylprop-2-en-1-one (100.6 mg, 0.5 mmol, 1 equiv.). Chromatography on silica gel (gradient from 20% to 45% AcOEt in hexanes as eluent): 76 mg brown oil, 63% yield.

^{1}H NMR (500 MHz, $CDCl_3$) δ 7.09-6.99 (m, 3H), 3.78-3.69 (m, 2H), 2.81 (t, *J* = 6.0 Hz, 2H), 2.35-2.29 (m, 1H), 2.15-2.01 (m, 5H), 1.42 (s, 3H).

^{13}C NMR (126 MHz, $CDCl_3$) δ 177.7, 138.9, 130.2, 127.4, 122.5, 120.7, 120.4, 118.9, 48.7, 38.9, 33.3, 24.5, 23.2, 21.2, 12.9.

HRMS (ESI pos): calculated for $C_{15}H_{16}N_2NaO^+$ ($M+Na^+$): 263.1155, found 263.1157.

Matching reported data.[47]

2.7.7 Alkylation of heteroarenes

2.7.7.1 General procedure C

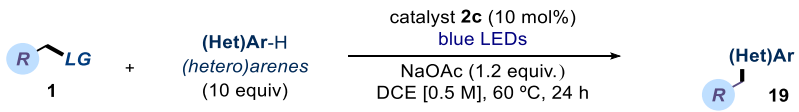

[47] Li, J.; Wang, Z.; Wu, N.; Gao, G.; You, J., Radical cascade cyanomethylation of activated alkenes to construct cyano substituted oxindoles. *Chem. Commun.* **2014**, *50*, 15049-15051.

In an oven dried Schlenk tube, catalyst **2c** (15.5 mg, 0.05 mmol, 0.1 equiv.) and sodium acetate (49 mg, 0.6 mmol, 1.2 equiv.) were suspended in 1,2-dichloroethane (1 mL), then the electrophile (0,5 mmol, 1 equiv.) was added followed by the (hetero)arene (5 mmol, 10 equiv.) substrate. The resulting yellow mixture was degassed via three cycles of freeze-pump-thaw. The Schlenk tube was then placed in the irradiation setup (Figure 2.4) set at a temperature of 60 ºC (60-61ºC measured in the central well) and irradiated for 24 hours. After cooling to ambient temperature, the volatiles were evaporated and the residue purified by column chromatography to afford the corresponding product in the stated yield with >95% purity according to ^{1}H NMR analysis. The exact conditions for chromatography are reported for each compound.

2.7.7.2 Characterization of products with general Procedure C

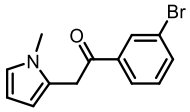

1-(3-Bromophenyl)-2-(1-methyl-1*H*-pyrrol-2-yl)ethan-1-one (19a). Synthesized according to the general procedure using 2-bromo-1-(3-bromophenyl)ethan-1-one (139 mg, 0.5 mmol, 1 equiv.) and N-methylpyrrole (0,444 mL, 5 mmol, 10 equiv.). Chromatography on silica gel (toluene as eluent): 90 mg off white solid, 65% yield.

^{1}H NMR (500 MHz, $CDCl_3$) δ 8.14 (t, *J* = 1.7 Hz, 1H); 7.93 (dt, *J* = 7.8, 1 Hz, 1H); 7.70-7.66 (m, 1H); 7.34 (t, *J* = 7.8 Hz, 1H); 6.61 (t, *J* = 2.3 Hz, 1H); 6.08 (t, *J* = 3 Hz, 1H); 6.02-5.99 (m, 1H); 4.22 (s, 2H); 3.54 (s, 3H).

^{13}C NMR (125 MHz, $CDCl_3$) δ 195.4; 138.4; 136.5; 131.9; 130.6; 127.5; 125.1; 123.4; 123.1; 109.5; 107.6; 37.6; 34.4.

HRMS (ESI pos): calculated for $C_{13}H_{13}{}^{79}BrNO$ (M^+): 278.0175, found 278.0188.

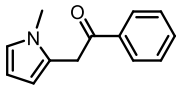

2-(1-Methyl-1*H*-pyrrol-2-yl)-1-phenylethan-1-one (19b). Synthesized according to the general procedure using phenacyl chloride (77 mg, 0.5 mmol, 1 equiv.) and *N*-methylpyrrole (0,444 mL, 5 mmol, 10 equiv.). Chromatography on silica gel (toluene as eluent): 70 mg off white solid, 70% yield.

^{1}H NMR (300 MHz, $CDCl_3$) δ 8.12-8.01 (m, 2H); 7.66-7.56 (m, 1H); 6.65 (t, *J* = 2.2 Hz, 1H); 6.13 (t, *J* = 3 Hz, 1H); 7.56-7.44 (m, 2H); 6.08-6.03 (m, 1H); 4.30 (s, 2H); 3.59 (s, 3H).

^{13}C NMR (75 MHz, $CDCl_3$) δ 196.5; 136.4; 133.3; 128.7; 128.5; 125.4; 122.6; 109.0; 107.1; 37.1; 34.1.

Matching reported data.[48]

[48] Maksymenko, S.; Parida, K. N.; Pathe, G. K.; More, A. A.; Lipisa, Y. B.; Szpilman, A. M., Transition-Metal-Free Intermolecular α-Arylation of Ketones via Enolonium Species. *Org. Lett.* **2017**, *19*, 6312-6315.

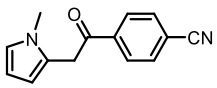

4-(2-(1-methyl-1*H*-pyrrol-2-yl)acetyl)benzonitrile (19c). Synthesized according to the general procedure using 4-(2-bromoacetyl)benzonitrile (112 mg, 0.5 mmol, 1 equiv.) and *N*-methylpyrrole (0,444 mL, 5 mmol, 10 equiv.). Chromatography on silica gel (1% AcOEt in toluene as eluent): 67 mg yellow solid, 60% yield.

^{1}H NMR (500 MHz, $CDCl_3$) δ 8.07 (t, *J* = 8.6 Hz, 2H); 7.74 (t, *J* = 8.6 Hz, 2H); 6.60 (t, *J* = 2.2 Hz, 1H); 6.06 (t, *J* = 3.1 Hz, 1H); 6.0-5.97 (m, 1H), 4.25 (s, 2H); 3.54 (s, 3H).

^{13}C NMR (125 MHz, $CDCl_3$) δ 195.5; 139.6; 132.9; 129.4; 124.6; 123.4; 118.2; 116.8; 109.7; 107.7; 37.9; 34.4.

HRMS (ESI pos): calculated for $C_{14}H_{12}N_2NaO$ ($M+Na^+$): 247.0842, found 247.0840.

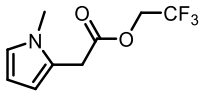

2,2,2-trifluoroethyl 2-(1-methyl-1*H*-pyrrol-2-yl)acetate (19d). Synthesized according to the general procedure using 2,2,2-trifluoroethyl 2-chloroacetate (88 mg, 0.5 mmol, 1 equiv.) and *N*-methylpyrrole (0,444 mL, 5 mmol, 10 equiv.). Chromatography on silica gel (toluene as eluent): 41 mg slightly yellow oil, 37% yield.

^{1}H NMR (500 MHz, $CDCl_3$) δ 6.60 (t, *J* = 2.2 Hz, 1H); 6.09-6.05 (m, 2H); 4.48 (q, *J* = 8.5 Hz, 2H); 3.72 (s, 2H); 3.57 (s, 3H).

^{13}C NMR (125 MHz, $CDCl_3$) δ 169.3; 123.8; 123.3; 123.2 (q, *J* = 277 Hz); 109.5; 107.5 (CH); 61.0 (q, *J* = 36.8 Hz); 34.1; 32.2.

^{19}F NMR (376 MHz, $CDCl_3$, proton decoupled) δ -73.85 (s, 3F).

HRMS (ESI pos): calculated for $C_9H_{11}F_3NO2$ (M^+): 222.0736, found 222.0742.

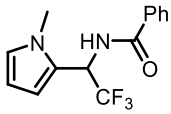

***N*-(2,2,2-trifluoro-1-(1-methyl-1*H*-pyrrol-2-yl)ethyl)benzamide (19e).** Synthesized according to the general procedure using *N*-(1-chloro-2,2,2-trifluoroethyl)benzamide (119 mg, 0.5 mmol, 1 equiv.) and *N*-methylpyrrole (0,444 mL, 5 mmol, 10 equiv.). Chromatography on silica gel (gradient from toluene to 5% AcOEt in toluene as eluent): 113 mg off-white solid, 80% yield.

^{1}H NMR (400 MHz, $CDCl_3$) δ 7.84-7.66 (m, 2H); 7.60-7.53 (m, 1H); 7.51-7.43 (m, 2H); 6.70-6.67 (m, 1H); 6.48 (br d, *J* = 9 Hz, 1H); 6.41-6.36 (m, 1H); 6.16 (dd, *J* = 2.9, 3.7 Hz, 1H); 6.14-6.06 (m, 1H); 3.67 (s, 3H).

^{13}C NMR (100 MHz, $CDCl_3$) δ 166.5; 132.9; 132.3; 128.7; 127.2; 124.5 (q, *J* = 282 Hz); 124.0; 123.8; 108.5 (q, *J* = 1.5 Hz); 107.7; 47.2 (q, *J* = 33.1 Hz); 34.1.

^{19}F NMR (376 MHz, $CDCl_3$, proton decoupled) δ -73.86 (s, 3F).

HRMS: calculated for $C_{14}H_{13}F_3N_2NaO$ ($M+Na^+$): 305.0872, found 305.0876.

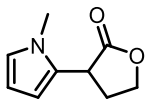

3-(1-Methyl-1*H*-pyrrol-2-yl)dihydrofuran-2(3*H*)-one (19f). Synthesized according to the general procedure using 3-*bromo*dihydrofuran-2(3*H*)-one (41 μL, 0.5 mmol, 1 equiv.) and *N*-methylpyrrole (0,444 mL, 5 mmol, 10 equiv.). Chromatography on silica gel (gradient from 10% AcOEt in hexanes to 40% AcOEt in hexanes as eluent): 76 mg brown oil, 91% yield.

^{1}H NMR (400 MHz, $CDCl_3$) δ 6.63 (app t, *J* = 4.5 Hz, 1H), 6.09 (app t, *J* = 3.6 Hz, 1H), 6.05-6.04 (m, 1H), 4.52-4.47 (m, 1H), 4.39-4.33 (m, 1H), 3.84 (t, *J* = 9.0 Hz, 1H), 3.69 (s, 3H), 2.69-2.61 (m, 1H), 2.57-2.48 (m, 1H).

^{13}C NMR (100 MHz, $CDCl_3$) δ 176.0, 126.8, 123.4, 107.0, 106.4, 66.8, 37.7, 34.2, 29.2.

HRMS: calculated for $C_9H_{11}NNaO_2$ ($M+Na^+$): 188.0682, found 188.0680.

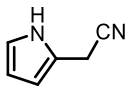

2-(1*H*-pyrrol-2-yl)acetonitrile (19g). Synthesized according to a modification of the general procedure: in an oven dried Schlenk tube, **2c** (31 mg, 0.1 mmol, 0.1 equiv.) and sodium acetate (93 mg, 1.2 mmol, 1.2 equiv.) were suspended in 1,2-dichloroethane (2 mL), then chloroacetonitrile (63 μL, 1 mmol, 1 equiv.) and pyrrole (0,699 mL, 10 mmol, 10 equiv.) were added. The resulting yellow mixture was degassed via three cycles of freeze-pump-thaw. The Schlenk tube was then placed in the irradiation setup at a temperature of 60 ºC and irradiated for 24 hours. After cooling to ambient temperature, the volatiles were evaporated and the residue purified by column chromatography to afford the corresponding product in the stated yield with >95% purity according to ^{1}H NMR analysis. Chromatography on silica gel (gradient from 15% AcOEt in hexanes to 30% AcOEt in hexanes as eluent) followed by a second chromatography (gradient from toluene to 50% AcOEt in toluene as eluent): 91 mg brownish oil, 86% yield.

^{1}H NMR (400 MHz, $CDCl_3$) δ 8.4 (br s, 1H); 6.81-6.79 (m, 1H); 6.22-6.18 (m, 1H); 6.22-6.14 (m, 1H); 3.78 (s, 2H).

^{13}C NMR (100 MHz, $CDCl_3$) δ 118.9; 118.6; 117.2; 109.2; 108.3; 16.9.

HRMS (ESI neg): calculated for $C_6H_5N_2$ (M^-): 105.0458, found 105.0454.

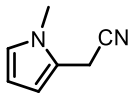

2-(1-Methyl-1*H*-pyrrol-2-yl)acetonitrile (19h). Synthesized according to the general procedure using chloroacetonitrile (32 μL, 0.5 mmol, 1 equiv.) and *N*-methylpyrrole (0.444 mL, 5 mmol, 10 equiv.). Chromatography on silica gel (toluene as eluent): 55 mg yellow oil, 92% yield.

^{1}H NMR (400 MHz, $CDCl_3$) δ 6.66 (app t, *J* = 2.2 Hz, 1H); 6.17-6.12 (m, 1H); 6.10 (app t, *J* = 3.5 Hz, 1H); 3.69 (s, 2H); 3.64 (s, 3H).

^{13}C NMR (100 MHz, $CDCl_3$) δ 123.6; 120.0; 116.6; 109.1; 107.4; 33.8; 15.9.

Matching reported data.[49]

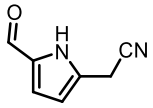

2-(5-Formyl-1*H*-pyrrol-2-yl)acetonitrile (19i). Synthesized according to the general procedure using chloroacetonitrile (32 μL, 0.5 mmol, 1 equiv.) and 1*H*-pyrrole-2-carbaldehyde (476 mg, 5 mmol, 10 equiv.). Chromatography on silica gel (15% acetone in hexanes as eluent): 28 mg slightly brown crystalline solid, 42% yield.

^{1}H NMR (400 MHz, $CDCl_3$) δ 9.40 (s, 1H);7.00-6.95 (m, 1H); 6.39-6.34 (m, 1H); 3.91 (s, 2H); NH proton not detected.

^{13}C NMR (100 MHz, $CDCl_3$) δ 179.7; 133.15; 130.3; 123.4; 115.9; 111.2; 17.0.

HRMS (ESI negative): calculated for $C_7H_5N_2O$ (M^-): 133.0407, found 133.0401.

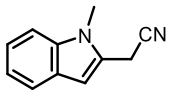

2-(1-Methyl-1*H*-indol-2-yl)acetonitrile (19j). Synthesized according to the general procedure using chloroacetonitrile (32 μL, 0.5 mmol, 1 equiv.) and *N*-methylindole (0.444 mL, 5 mmol, 10 equiv.). Chromatography on silica gel (gradient from 10% AcOEt in hexanes to 15% AcOEt in hexanes as eluent): 67 mg yellow solid, 79% yield.

^{1}H NMR (500 MHz, $CDCl_3$) δ 7.59 (app d, 1H); 7.30-7.23 (m, 2H); 7.15 (dd, J = 6.6, 1.5 Hz, 1H); 6.50 (d, J = 0.7 Hz, 1H); 3.76 (s, 2H); 3.65 (s, 3H).

^{13}C NMR (125 MHz, $CDCl_3$) δ 138.3; 128.2; 127.5; 122.6; 121.0; 120.5; 116.5; 109.6; 102.5; 30.1; 16.9.

Matching reported data.[32]

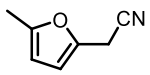

2-(5-Methylfuran-2-yl)acetonitrile (19k). Synthesized according to a modification of the general procedure: in an oven dried Schlenk tube, catalyst **2c** (31 mg, 0.1 mmol, 0.1 equiv.) and sodium acetate (93 mg, 1.2 mmol, 1.2 equiv.) were dissolved in 1.2-dichloroethane (2 mL), then chloroacetonitrile (63 μL, 1 mmol, 1 equiv.) and 2-methylfuran (0.902 mL, 10 mmol, 10 equiv.) were added. The resulting yellow mixture was degassed via three cycles of freeze-pump-thaw. The Schlenk tube was then placed in the irradiation setup at a temperature of 60 ºC and irradiated for 24 hours. After cooling to ambient temperature, the volatiles were evaporated and the residue purified by column chromatography to afford the corresponding product in the stated yield with >95% purity

[49] Cuevas-Yañez, E.; Muchowski, J. M.; Cruz-Almanza, R., Rhodium(II) catalyzed intramolecular insertion of carbenoids derived from 2-pyrrolyl and 3-indolyl α-diazo-β-ketoesters and α-diazoketones. *Tetrahedron* **2004**, *60*, 1505-1511.

according to ^{1}H NMR analysis. Chromatography on silica gel (5% AcOEt in hexanes): 78 mg yellow oil, 64% yield.

Note: the product is volatile and care should be taken during the evaporation steps to avoid losses (no vacuum below 80 mbar was applied).

^{1}H NMR (500 MHz, $CDCl_3$) δ 6.16 (app d, *J* = 3.1 Hz, 1H); 5.90 (dd, *J* = 3.1, 1 Hz, 1H); 3.68 (s, 2H); 2.25 (s, 3H).

^{13}C NMR (125 MHz, $CDCl_3$) δ 153.3; 141.2; 116.1; 109.6; 107.0; 17.9; 13.8.

Matching reported data.[32]

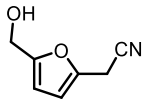

2-(5-(Hydroxymethyl)furan-2-yl)acetonitrile (19l). Synthesized according to the general procedure using chloroacetonitrile (32 μL, 0.5 mmol, 1 equiv.) and furfuryl alcohol (0,434 mL, 5 mmol, 10 equiv.). Chromatography on silica gel (gradient from 20% AcOEt in hexanes to 40% AcOEt in hexanes): 35 mg yellow oil, 50% yield.

^{1}H NMR (500 MHz, $CDCl_3$) δ 6.29-6.27 (m, 1H); 6.27-6.25 (m, 1H); 4.57 (s, 2H); 3.77 (s, 2H); 2.28 (br s, 1H).

^{13}C NMR (125 MHz, $CDCl_3$) δ 154.8; 142.9; 115.5; 109.3; 108.9; 57.1; 17.57.

Matching reported data.[32]

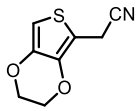

2-(2,3-Dihydrothieno[3,4-b][1,4]dioxin-5-yl)acetonitrile (19m). Synthesized according to the general procedure using chloroacetonitrile (32 μL, 0.5 mmol, 1 equiv.) and 2,3-dihydrothieno[3,4-*b*][1,4]dioxine (0,534 mL, 5 mmol, 10 equiv.). Chromatography on silica gel (gradient from 10% AcOEt in hexanes to 30% AcOEt in hexanes, then a second chromatography with toluene as eluent): 71 mg, slightly yellow oil, 78% yield.

^{1}H NMR (500 MHz, $CDCl_3$) δ 6.24 (s, 1H); 4.21-4.18 (m, 2H); 4.16-4.13 (m, 2H); 3.67 (s, 2H).

^{13}C NMR (125 MHz, $CDCl_3$) δ 141.4; 149.8; 116.7; 103.6; 98.4; 64.8; 64.5; 14.7.

HRMS (ESI pos): calculated for $C_8H_7NNaO_2S$ ($M+Na^+$): 204.0090, found 204.0086.

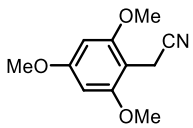

2-(2,4,6-trimethoxyphenyl)acetonitrile (19n). Synthesized according to the general procedure using chloroacetonitrile (32 μL, 0.5 mmol, 1 equiv.) and 1,3,5-trimethoxybenzene (841 mg, 5 mmol, 10 equiv.). Chromatography on silica gel (gradient from toluene to 5% AcOEt in toluene as eluent): 44 mg, off white solid, 42% yield.

^{1}H NMR (400 MHz, $CDCl_3$) δ 6.14 (s, 2H); 3.85 (s, 6H); 3.82 (s, 3H); 3.61 (s, 2H).

^{13}C NMR (100 MHz, $CDCl_3$) δ 161.4; 158.6; 118.8; 99.3; 90.4; 55.8; 55.4; 11.1.

HRMS (ESI pos): calculated for $C_{11}H_{14}NO_3$ ($M+H^+$): 208.0968, found 208.0971.

2.7.8 Asymmetric catalytic α-alkylation of aldehydes

2.7.8.1 General procedure D

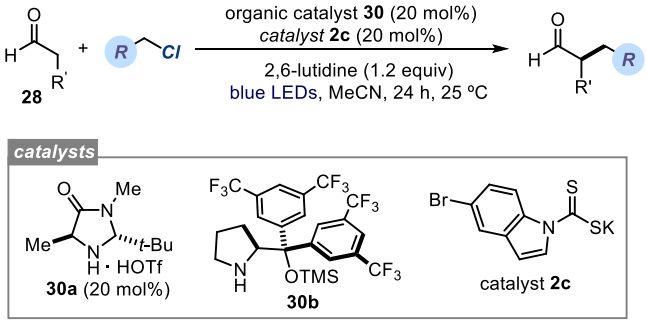

In an oven-dried 10 mL Schlenk tube, the chiral secondary amine catalyst **30** (0.04 mmol, 0.2 equiv.) was dissolved in acetonitrile (0.4 mL, synthesis grade) then freshly distilled aldehyde **28** (0.6 mmol, 3 equiv.) was added followed by freshly distilled 2,6-lutidine (24 μL, 0.24 mmol, 1.2 equiv.), catalyst **2c** (12 mg, 0.04 mmol, 0.2 equiv.) and the alkyl chloride **1** (0.2 mmol, 1 equiv.). The reaction mixture was then degassed via three cycles of Freeze-Pump-Thaw. The Schlenk tube was then placed in the irradiation setup at a temperature of 25 ºC and irradiated for 20 hours. After the end of irradiation, water and ethyl acetate were added and the aqueous layer extracted two more times with ethyl acetate. The combined organic fraction was dried ($MgSO_4$) and concentrated to a yellow oil. Trichloroethylene (18 μL, 0.2 mmol, 1 equiv.) was added and the sample diluted with $CDCl_3$. An aliquot was then analyzed to determine the yield of reaction using ^{1}H NMR analysis.

Note: Since epimerization of the reaction product was commonly observed upon purification on silica gel chromatography (typical loss of 2 to 15 points of e.e. for products that stayed in contact with silica gel for 3 to 30 minutes), the enantiomeric excess of the alkylated aldehyde was determined directly on the crude reaction mixtures or after derivatisation on the crude reaction mixture. Exact conditions are reported for each entry.

An analytical amount of the alkylated aldehyde product was isolated by column chromatography for characterization purposes of unknown products.

2.7.8.2 Characterization of products with general procedure D

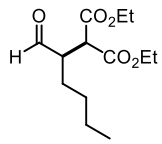

(*R*)-diethyl-2-(1-oxohexan-2-yl)malonate (32)

Prepared according to the general procedure using aminocatalyst **30b** (24 mg, 0.04 mmol, 0.2 equiv.), hexanal (74 μL, 0.6 mmol, 3 equiv.) and diethylchloromalonate (33 μL, 0.2 mmol, 1 equiv.). Yield determined by ^{1}H NMR as 77%. Chromatography on silica gel (gradient from 5% to 10% AcOEt in hexanes as eluent) for characterisation.

^{1}H NMR (400 MHz, $CDCl_3$) δ 9.78 (d, *J* = 0.5 Hz, 1 H), 4.20-4.11 (m, 4 H); 3.75 (d, *J* = 8.6 Hz, 1 H), 3.15-3.07 (m, 1 H), 1.77-1.68 (m, 1 H), 1.65-1.56 (m, 1 H), 1.43-1.25 (m, 10 H), 0.90 (t, *J* = 7.1 Hz, 3 H).

^{13}C NMR (101 MHz, $CDCl_3$) δ 201.5, 168.12, 168.0, 61.8, 61.7, 51.8, 50.2, 28.6, 26.7, 22.6, 14.0, 13.9, 13.7.

HRMS: calculated for $C_{13}H_{22}NaO_5$ ($M+Na^+$): 281.1359, found 281.1363.

The enantiomeric excess was determined as follows: to an aliquot of the $CDCl_3$ solution prepared as described in the general procedure, methanol and *p*-toluenesulfonyl hydrazide were added and the resulting mixture stirred for 15 minutes. The hydrazone was purified via preparative TLC (6:4 hexanes/AcOEt mixture as eluent, R_f = 0.45) and the enantiomeric excess determined by UPC[2] analysis on an Acquity Trefoil AMY1 column: gradient from 100% CO_2 to 60:40 CO_2/EtOH over 5 minutes, curve 6, flow rate 3.00 mL/min, λ = 230 nm; τ_{Major} = 4.38 min, τ_{Minor} = 4.49 min; e.r.= 87.1/12.9; e.e. = 74%

Absolute configuration assigned by correlation with our previously reported data.[50]

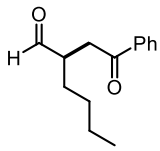

(*R*)-2-(2-oxo-2-phenylethyl)hexanal (33)

Prepared according to the general procedure using aminocatalyst **30b** (24 mg, 0.04 mmol, 0.2 equiv.), hexanal (74 μL, 0.6 mmol, 3 equiv.) and phenacyl chloride (31 mg, 0.2 mmol, 1 equiv.). Yield determined by ^{1}H NMR as 57%. Chromatography on silica gel (gradient from 2% to 5% AcOEt in hexanes as eluent).

^{1}H NMR (400 MHz, $CDCl_3$) δ 9.85 (d, J = 0.9 Hz, 1 H), 8.02-7.97 (m, 2H), 7.62-7.57 (m, 1 H), 7.51-7.46 (m, 2 H), 3.50 (dd, *J* = 7.7, 17.7 Hz, 1 H), 3.16-3.08 (m, 1 H), 3.05 (dd, *J* = 4.8, 17.7 Hz, 1 H), 1.87-1.77 (m, 1 H), 1.62-1.51 (m, 1 H), 1,44-1,31 (m, 4 H), 0.97-0.86 (m, 3 H).

[50] Silvi, M.; Arceo, E.; Jurberg, I. D.; Cassani, C.; Melchiorre, P., Enantioselective Organocatalytic Alkylation of Aldehydes and Enals Driven by the Direct Photoexcitation of Enamines. *J. Am. Chem. Soc.* **2015**, *137*, 6120-6123.

^{13}C NMR (101 MHz, $CDCl_3$) δ 203.6, 198.0, 136.6, 133.2, 128.6, 128.1, 46.7, 37.6, 29.2, 28.5, 22.7, 13.8.

HRMS: calculated for $C_{14}H_{18}NaO_2$ ($M+Na^+$): 241.1199, found 241.1197.

The enantiomeric excess of the alkylated aldehyde was determined directly on the crude reaction mixture after isolation of a few milligrams by a short preparative TLC (toluene as eluent, R_f = 0.2, staining purple with vanillin; typical elution time of 2 to 3 minutes). The aldehyde was then analyzed by HPLC analysis on a Daicel Chiralpak IA: 20 ºC, 98:2 hexane/*i*PrOH, flow rate 0.8 mL/min, λ = 254 nm; τ_{Minor} = 13.4 min, τ_{Major} = 15.9 min; e.r.= 89.8/10.2; e.e.= 79%

Absolute configuration assigned by analogy with our previously reported data.[51]

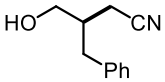

(*R*)-3-benzyl-4-hydroxybutanenitrile (35)

Prepared according to a modification of the general procedure. In an oven-dried 10 mL Schlenk tube, the chiral secondary amine catalyst **30a** (12 mg, 0.04 mmol, 0.2 equiv.) was dissolved in acetonitrile (0.4 mL, synthesis grade) then freshly distilled hydrocinnamaldehyde (79 μL, 0.6 mmol, 3 equiv.) was added followed by freshly distilled 2,6-lutidine (24 μL, 0.24 mmol, 1.2 equiv.), catalyst **2c** (12 mg, 0.04 mmol, 0.2 equiv.) and chloroacetonitrile (13 μL, 0.2 mmol, 1 equiv.). The reaction mixture was then degassed via three cycles of Freeze-Pump-Thaw. The Schlenk tube was then placed in the irradiation setup at a temperature of 25 ºC and irradiated for 20 hours. After the end of irradiation, the reaction mixture was diluted in CH_2Cl_2 and MeOH and an excess of $NaBH_4$ added. After quenching the mixture with a saturated solution of NH_4Cl, the mixture was extracted with AcOEt, three times. The combined organic fractions were dried ($MgSO_4$) and concentrated to a yellow oil. Trichloroethylene (18 μL, 0.2 mmol, 1 equiv.) was added and the sample diluted with $CDCl_3$. An aliquot was then analysed to determine the yield of reaction. Yield determined by ^{1}H NMR as 60%. Product. Chromatography on silica gel (gradient from 20% to 30% AcOEt in hexanes as eluent).

^{1}H NMR (300 MHz, $CDCl_3$) δ 7.38-7.26 (m, 2H); 7.29-7.24 (m, 1H); 7.24-7.17 (m, 2H); 3.77 (dd, *J* = 4.6, 10.7 Hz, 1H); 3.64 (dd, *J* = 6.9, 10.7 Hz, 1H); 2.82 (dd, *J* = 6.9, 13.7 Hz, 1H); 2.69 (dd, *J* = 7.0, 13.7 Hz, 1H); 2.49 (dd, *J* = 5.7, 16.9 Hz, 1H); 2.40 (dd, *J* = 6.0, 16.9 Hz, 1H); 2.29-2.13 (m, 1H)

Matching reported data.[52]

---

[51] Arceo, E.; Jurberg, I. D.; Álvarez-Fernández, A.; Melchiorre, P., Photochemical activity of a key donor–acceptor complex can drive stereoselective catalytic α-alkylation of aldehydes. *Nature Chem.* **2013**, *5*, 750-756.

[52] Welin, E. R.; Warkentin, A. A.; Conrad, J. C.; MacMillan, D. W. C., Enantioselective α-Alkylation of Aldehydes by Photoredox Organocatalysis: Rapid Access to Pharmacophore Fragments from β-Cyanoaldehydes. *Angew. Chem. Int. Ed.* **2015**, *54*, 9668-9672.

The alcohol was analysed by to be 90% by UPC[2] on Acquity Trefoil ID3 column: gradient from 100% CO_2 to 60:40 CO_2/iPrOH over 5 minutes, curve 6, flow rate 3.00 mL/min, $\lambda = 230$ nm; $\tau_{Major} = 3.18$ min, $\tau_{Minor} = 3.31$ min; e.r.= 95.3/4.6; e.e.= 90%.

Absolute configuration assigned according to reported data.[52]

2.7.9 Large scale reactions

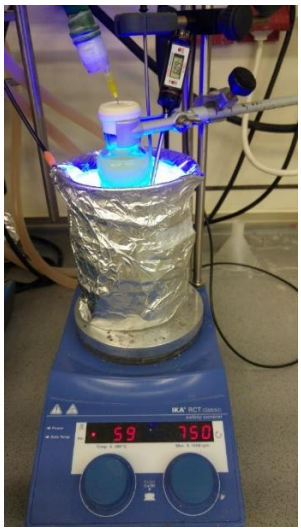

Figure 2.7. Photoreactor employed for the large-scale reactions.

2.7.9.1 Giese addition

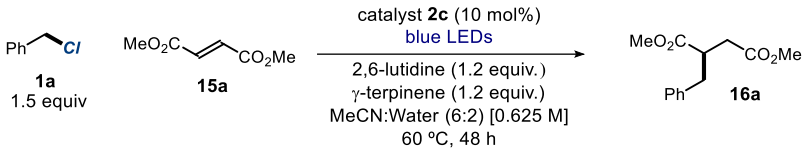

This reaction was performed on *50 mmol scale*: in a 150 mL capacity reaction tube, potassium 5-bromo-1*H*-indole-1-carbodithioate **2c** (1.55 g, 5 mmol, 0.1 equiv.) was dissolved in degassed acetonitrile (20 mL, degassed *via* nitrogen sparging for 30 minutes prior to the reaction), then benzyl chloride **1a** (8.6 mL, 75 mmol, 1.5 equiv.) was added and the mixture stirred for five minutes. 2,6-Lutidine (7 mL, 60 mmol, 1.2 equiv.), γ-terpinene (9.6 mL, 60 mmol, 1.2 equiv.) and dimethyl fumarate **15a** (7.21 g, 50 mmol, 1 equiv.). Acetonitrile (62 mL, degassed *via* nitrogen sparging for 30 minutes prior to the reaction) and distilled water (18 mL) were added. The reaction tube was then immersed in a 1L beaker containing silicon oil heated to 60 ºC and wrapped with a one meter 14W blue LED strip and further wrapped with aluminium foil (Figure 2.7).

The reaction mixture was further degassed via nitrogen sparging for 5 minutes at this temperature then irradiated for 48 hours. After cooling down to ambient temperature, the mixture was transferred to a round bottom flask and acetonitrile evaporated. The yellow oil was transferred to an extraction funnel, diluted with ethyl acetate (100 mL) and washed with 1M HCl (30 mL), saturated $NaHCO_3$ (30 mL), and brine. The organic phase was dried ($MgSO_4$) and concentrated to dryness. Trichloroethylene (0.9 mL, 0.2 equiv.) was added and an aliquot of the resulting mixture analysed by ^1H NMR to determine the yield of the reaction (79% NMR yield, 90% conversion based on dimethyl fumarate **15a**). The product was then distilled under reduced pressure (2 mbar pressure, fraction collected between 129 ºC and 135ºC) to afford 6.924 g of clean product **16a** as a slightly yellow iridescent liquid (29.33 mmol). The distillation apparatus was dismantled and rinsed back into the boiling flask. The orange residue was then purified by chromatography on silica gel to afford an additional 1.706 g of product **16a** as a yellow oil of slightly lower purity (7.22 mmol). The combined yield of the isolated product of the reaction is therefore 8.63 g (36.56 mmol, 73%) of product of >95% purity as determined by ^1H NMR analysis.

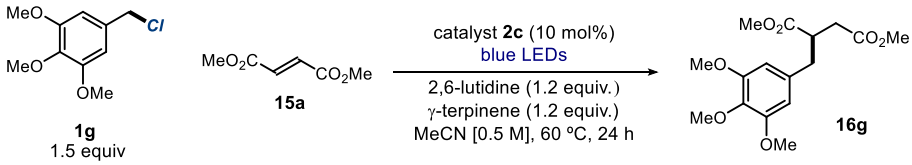

This reaction was performed on *7.5 mmol scale*: to an oven dried 25 mL Schlenk tube, **2c** (233 mg, 0.75 mmol, 0.1 equiv.) was dissolved in acetonitrile (15 mL), then 3,4,5-trimethoxybenzyl chloride **1g** (2.437 g, 11.25 mmol, 1.5 equiv.) was added followed by 2,6-lutidine (1,05 mL, 9 mmol, 1.2 equiv.), γ-terpinene (1.44 mL, 9 mmol, 1.2 equiv.) and dimethyl fumarate **15a** (1.081 g, 7.5 mmol, 1 equiv.). The resulting yellow mixture was degassed via three cycles of freeze-pump-thaw. The Schlenk tube was then placed in the irradiation setup set at a temperature of 60 ºC and irradiated for 24 hours. After cooling to ambient temperature, the reaction mixture was transferred to an extraction funnel containing 25 mL of distilled water and 25 mL of AcOEt. The phases were separated and the aqueous phase extracted twice with AcOEt (25 mL each). The combined organic fractions were combined, washed with brine, dried with $MgSO_4$ and concentrated to dryness. The resulting yellow oil was purified by column chromatography on silica gel (100 g silica, gradient from 20% to 30% AcOEt in hexanes as eluent, R_f = 0,2 @ 20% AcOEt in hexanes, staining red with vanillin stain solution) to afford **16g** as a slowly crystalizing slightly yellow oil: 2.13 g (87% yield).

2.7.9.2 *Alkylation of heteroarenes*

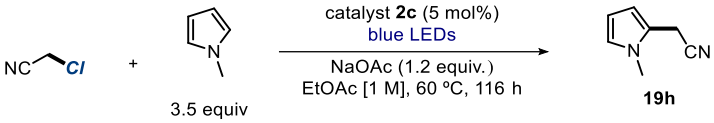

In an oven dried 250 mL capacity Schlenk tube, catalyst **2c** (2.71 g, 8.75 mmol, 0.05 equiv.) and sodium acetate (17.23 g, 0.21 mol, 1.2 equiv.) were suspended in ethyl acetate (175 mL, degassed *via* nitrogen sparging for 30 minutes prior to the reaction), then chloroacetonitrile (11.07 mL, 0.175 mol, 1 equiv.) was added followed by *N*-methylpyrrole (54.4 mL, 0.613 mol, 3.5 equiv.) substrate. The reaction tube was then immersed in a 1L beaker containing silicon oil heated to 60 ºC and wrapped with a one meter 14W blue LED strip and further wrapped with aluminium foil. The reaction mixture was further degassed via nitrogen sparging for 5 minutes at this temperature then irradiated for 116 hours under strong stirring. NMR analysis of an aliquot at this time showed a 45% conversion of chloroacetonitrile.

The mixture was transferred to an extraction funnel and washed with distilled water twice, followed by a saturated solution of $NaHCO_3$. The combined aqueous layers were back extracted with AcOEt and the combined organic layers were dried ($MgSO_4$) and concentrated to a brown oil (14.3 g). A yield of **19h** of 42% was determined by ^1H NMR analysis of the residue after addition of an internal standard. Vacuum distillation (1.4 mbar, 85-91ºC) afforded 7.631g of **19h** as a slightly yellow iridescent liquid (63.525 mmol, 36.3% yield). After rinsing the distillation apparatus back into the boiling flask, an additional 0.67 g of **19h** was obtained after column chromatography as a red oil.

The combined product obtained corresponds to 8.301 g (69.075 mmol, 39.5 % yield)

2.7.10 Continous flow reaction

The flow photoreactor was assembled using a variation of the temperature-controlled photoreactor used for batch reactions. It consisted of a smaller 4 cm diameter jar fitted with a standard 29-sized ground glass joint. A commercial 1-meter LED strip was wrapped around the jar, followed by a layer of aluminium foil and cotton for insulation. The reactor itself consisted of a length of standard HPLC tubing (0.78 mm ID, PTFE) wrapped around a 14 mm diameter test tube to allow an irradiated volume of 1 mL and fitted inside the jar. A syringe pump was used to circulate the reaction mixture at a defined rate (Figure 2.8).

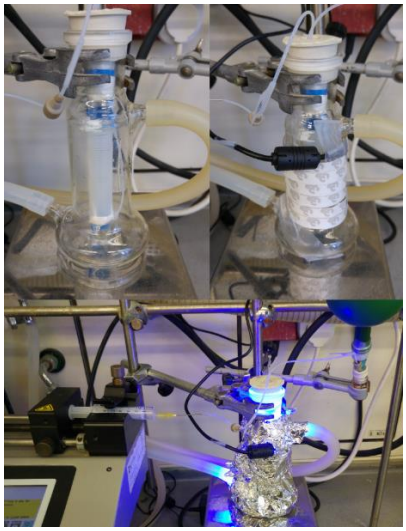

Figure 2.8. Flow photoreactor at different stage of construction and under operation.

To provide homogeneous conditions throughout the progress of the reaction and avoid clogging of the flow reactor, the solvent and base had to be replaced by acetonitrile/water mixtures and 2,6-lutidine, respectively. Using sodium acetate as the base gave phase separation between acetonitrile and water before the start of the reaction without coalescence upon heating to 60 ºC.

Table 2.2. Comparison of alkylation under batch and flow conditions

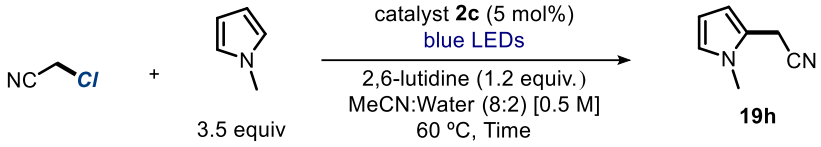

entry	concentration (M)	time	NMR yield (%)
1	[0.5]	6 h (batch)	50
2	[0.5]	16 h (batch)	92
3	[0.5]	20 min (flow)[a]	22
4	[0.5]	40 min (flow)[a]	43
5	[0.5]	2 h (flow)[a]	75
6	[1]	2 h (flow)[a]	82[b]
7	[1.5]	2 h (flow)[a]	87[c]
8	[2]	2 h (flow)[a]	75[d]

Reactions performed on a 0.5 mmol scale, NMR yield determined by comparison with trichloroethylene as internal standard on the crude reaction mixture. [a] Theoretical residence time calculated according to the flow rate programmed. [b] 1 mmol scale. [c] 1.5 mmol scale. [d] 2 mmol scale.

To accurately benchmark the batch and flow systems, we compared similar scales of reaction leading to the adduct **19h**. On a 0.5 mmol scale and under batch conditions, the productivity was 0.028 mmol·h^{-1} (result refers to the formation of product **19h** reported in Table 2.2, entry 2). Under flow conditions, the productivity increased fourteen fold to 0.40 mmol·h^{-1} (calculated under continuous operation, result refers to the formation of product **19h** Table 2.2, entry 7).

2.7.11 Complex substrates

2.7.11.1 Cortisone derivatives

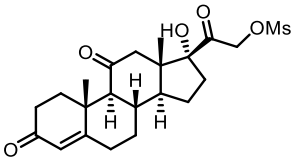

2-((8*S*,9*S*,10*R*,13*S*,14*S*,17*R*)-17-hydroxy-10,13-dimethyl-3,11-dioxo-2,3,6,7,8,9,10,11,12,13,14,15,16,17-tetradecahydro-1*H*-cyclopenta[*a*]phenanthren-17-yl)-2-oxoethyl methanesulfonate (cortisone mesylate) (20). Synthesized according to a procedure adapted from a patent by The Upjohn Company - EP263213, 1988, A1. A round-bottomed flask was charged with cortisone (500 mg, 1.39 mmol, 1.0 equiv.), followed by pyridine (5 mL). The flask was cooled in an ice bath and methanesulfonyl chloride (113 μL, 1.46 mmol, 1.05 equiv.) was added. The reaction was allowed to warm to ambient temperature as the reaction proceeded for a total reaction time of 1 h. The crude reaction was concentrated to remove pyridine, then the residue was dissolved in CH_2Cl_2 and washed with 1M HCl twice. The organic layer was dried with sodium sulfate and concentrated in vacuo. Chromatography on silica gel (gradient from 40% to 70% AcOEt in hexanes as eluent): 307.0 mg, 51% yield.

^{1}H NMR (500 MHz, $CDCl_3$) δ 5.72 (s, 1H), 5.32 (d, *J* = 18.1 Hz, 1H), 4.89 (d, *J* = 18.1 Hz), 3.20 (s, 3H), 2.97 (bs, 1H), 2.89 (d, *J* = 12.4 Hz, 1H), 2.83-2.73 (m, 2H), 2.51-2.27 (m, 5H), 2.17 (d, J = 12.4 Hz, 1H), 2.00-1.91 (m, 4H), 1.75-1.60 (m, 2H), 1.52-1.44 (m, 1H), 1.40 (s, 3H), 1.34-1.25 (m, 1H), 0.67 (s, 3H).

^{13}C NMR (126 MHz, $CDCl_3$) δ 208.6, 203.7, 200.1, 168.9, 124.6, 89.0, 72.1, 62.5, 51.5, 49.9, 49.8, 39.3, 38.2, 36.5, 35.4, 34.7, 33.7, 32.3, 32.2, 23.2, 17.2, 16.0.

HRMS (ESI pos): calculated for $C_{22}H_{30}NaO_7S^+$ (M+Na$^+$): 461.1604, found 461.1604.

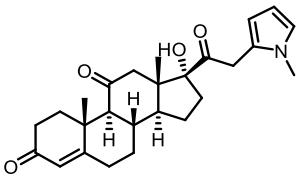

(8*S*,9*S*,10*R*,13*S*,14*S*,17*R*)-17-hydroxy-10,13-dimethyl-17-(2-(1-methyl-1*H*-pyrrol-2-yl)acetyl)-1,6,7,8,9,10,12,13,14,15,16,17-dodecahydro-3*H*-cyclopenta[*a*]phenanthrene-3,11(2*H*)-dione (21). Synthesized according to the general procedure using cortisone mesylate **20** (219 mg, 0.5 mmol, 1 equiv.) and *N*-methylpyrrole (0,444 mL, 5 mmol, 10 equiv.). 20 mol % catalyst was used: **2c** (31.0 mg, 0.10 mmol, 0.2 equiv.). Chromatography

on silica gel (gradient from 40% AcOEt in hexanes to 55% AcOEt in hexanes; three rounds of chromatography were required): 53 mg pink foam, 25% yield.

^{1}H NMR (500 MHz, $CDCl_3$) δ 6.58-6.57 (m, 1H), 6.04-6.03 (m, 1H), 5.91-5.90 (m, 1H), 5.70 (s, 1H), 3.97 (d, *J* = 16.7 Hz, 1H), 3.67 (d, *J* = 16.7 Hz, 1H), 3.50 (s, 3H), 2.95 (br s, 1H), 2.81-2.71 (m, 3H), 2.49-2.24 (m, 5H), 1.98-1.89 (m, 5H), 1.72-1.65 (m, 1H), 1.65-1.58 (m, 1H), 1.47-1.43 (m, 1H), 1.38 (s, 3H), 1.32-1.24 (m, 1H), 0.69 (s, 3H).

^{13}C NMR (126 MHz, $CDCl_3$) δ 209.8, 208.8, 200.2, 169.1, 125.0, 124.9, 123.2, 108.9, 107.6, 89.8, 62.9, 52.0, 50.5, 50.0, 38.6, 38.1, 36.9, 35.2, 35.1, 34.5, 34.1, 32.7, 32.6, 23.8, 17.6, 16.5.

HRMS: calculated for $C_{26}H_{33}NNaO_4$ ($M+Na^+$): 446.2302, found 446.2306.

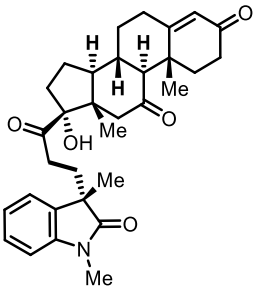

(8*S*,9*S*,10*R*,13*S*,14*S*,17*R*)-17-(3-(1,3-dimethyl-2-oxoindolin-3-yl)propanoyl)-17-hydroxy-10,13-dimethyl-1,6,7,8,9,10,12,13,14,15,16,17-dodecahydro-3*H*-cyclopenta[a]phenanthrene-3,11(2*H*)-dione (22). Synthesized according to the general procedure using cortisone mesylate **20** (219.3 mg, 0.5 mmol, 1.0 equiv.) and *N*-methyl-*N*-phenylmethacrylamide (131.4 mg, 0.75 mmol, 1.5 equiv.). 20 mol % catalyst was used: **2c** (31.0 mg, 0.10 mmol, 0.2 equiv.). The diastereomeric ratio was determined by ^{1}H NMR spectroscopic analysis of the crude reaction mixture by comparison of the resonances at δ 3.17 (minor diastereomer) and δ 3.14 (major diastereomer). Chromatography on silica gel (gradient from 40% to 100% AcOEt in hexanes as eluent): 142 mg major diastereomer as an off-white solid and 62 mg minor diastereomer (isolated as 2.2:1 dr mixture favoring the minor diastereomer, off-white solid), 79% combined yield.

^{1}H NMR for major diastereomer (500 MHz, $CDCl_3$) δ 7.31-7.28 (m, 1H), 7.16 (d, *J* = 6.6 Hz, 1H), 7.10-7.07 (m, 1H), 6.87 (d, *J* = 7.8 Hz, 1H), 5.73 (s, 1H), 3.19 (s, 3H), 2.96-2.91 (m, 1H), 2.88 (d, *J* = 12.1 Hz, 1H), 2.78-2.66 (m, 2H), 2.51-2.38 (m, 3H), 2.32-2.27 (m, 2H), 2.21-2.09 (m, 2H), 2.01 (d, *J* = 12.5 Hz, 1H), 1.99-1.87 (m, 5H), 1.67-1.57 (m, 2H) 1.39 (s, 3H), 1.38 (s, 3H), 1.36-1.25 (m, 2H), 0.49 (s, 3H).

^{13}C NMR (126 MHz, $CDCl_3$) δ 211.1, 209.8, 199.8, 180.6, 168.8, 142.7, 134.2, 128.1, 124.5, 122.9, 122.7, 108.3, 89.1, 62.6, 50.5, 50.3, 49.7, 47.0, 38.2, 36.6, 34.7, 33.7, 33.5, 33.2, 32.5, 32.3, 32.3, 26.3, 23.3, 22.6, 17.2, 15.8.

HRMS (ESI pos): calculated for $C_{32}H_{40}NO_5^+$ ($M+H^+$): 518.2901, found 518.2904.

Stereochemistry of the major diastereomer was determined by synthesis of the brominated derivative below, which was purified (the major diastereomer was isolated) and analyzed by x-ray diffraction.

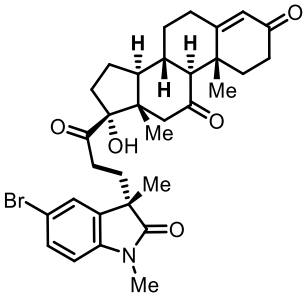

(8*S*,9*S*,10*R*,13*S*,14*S*,17*R*)-17-(3-((*S*)-5-bromo-1,3-dimethyl-2-oxoindolin-3-yl)propanoyl)-17-hydroxy-10,13-dimethyl-1,6,7,8,9,10,12,13,14,15,16,17-dodecahydro-3*H*-cyclopenta[*a*]phenanthrene-3,11(2*H*)-dione (Br-22)

Synthesized according to the general procedure using cortisone mesylate (219.3 mg, 0.5 mmol, 1.0 equiv.) and *N*-(4-bromophenyl)-*N*-methylmethacrylamide (190.6 mg, 0.75 mmol, 1.5 equiv.). 20 mol % catalyst was used: **2c** (31.0 mg, 0.10 mmol, 0.2 equiv.). The diastereomeric ratio was determined by ^{1}H spectroscopic analysis of the crude reaction mixture by comparison of the resonances at δ 3.12 (minor diastereomer) and δ 3.09 (major diastereomer). Chromatography on silica gel (gradient from 40% to 100% AcOEt in hexanes as eluent): 98 mg major diastereomer (33% yield; only collected pure fractions of major diastereomer) as a white solid. Recrystallization from heptane and ethyl acetate provided a crystal, which was analyzed by x-ray diffraction.

^{1}H NMR for major diastereomer (500 MHz, $CDCl_3$) δ 7.41 (dd, *J* = 8.3, 1.9 Hz, 1H), 7.27 (d, *J* = 2.1 Hz, 1H), 6.74 (d, *J* = 8.3 Hz, 1H), 5.72 (s, 1H), 3.71 (bs, 1H), 3.15 (s, 3H), 3.03-2.97 (m, 1H), 2.89 (d, *J* = 12.5 Hz, 1H), 2.77-2.69 (m, 2H), 2.51-2.38 (m, 3H), 2.31-2.27 (m, 2H), 2.17-2.06 (m, 2H), 2.02 (d, *J* = 12.5 Hz, 1H), 1.99-1.86 (m, 5H), 1.67-1.59 (m, 2H), 1.39 (s, 3H), 1.37 (s, 3H), 1.35-1.25 (m, 2H), 0.51 (s, 3H).

^{13}C NMR for major diastereomer (126 MHz, $CDCl_3$) δ 211.1, 210.0, 200.0, 180.4, 168.9, 142.1, 136.8, 131.3, 126.3, 125.0, 116.0, 110.1, 89.5, 63.0, 50.8, 50.7, 50.1, 47.5, 38.5, 37.0, 35.1, 34.1, 33.4, 32.9, 32.7, 32.6, 31.3, 26.7, 23.6, 22.8, 17.6, 16.2.

HRMS (ESI pos): calculated for $C_{32}H_{38}{}^{79}BrNNaO_5^+$ ($M+Na^+$): 618.1826, found 618.1831.

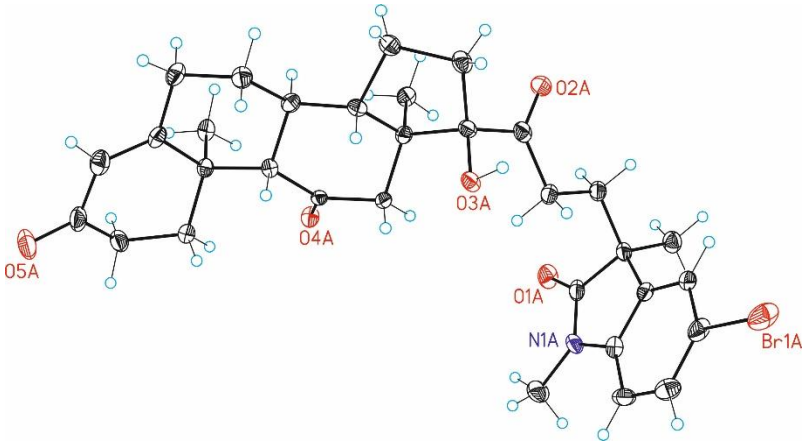

Figure 2.9. ORTEP Diagram of **Br-22** (CCDC 1839232).

2.7.11.2 Nucleobase analogues

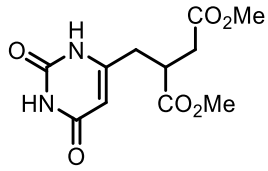

Dimethyl 2-((2,6-dioxo-1,2,3,6-tetrahydropyrimidin-4-yl)methyl)succinate (24): In an oven dried Schlenk tube, 6-(chloromethyl)pyrimidine-2,4(1*H*,3*H*)-dione **23** (126 mg, 0.75 mmol, 1.5 equiv.) was dissolved in DMF (1 mL), then catalyst **2c** (15.5 mg, 0.1 equiv.) was added followed by 2,6-lutidine (70 μL, 0.6 mmol, 1.2 equiv.), γ-terpinene (96 μL, 0.6 mmol, 1.2 equiv.), and dimethyl fumarate **15a** (72 mg, 0.5 mmol, 1 equiv.). The resulting yellow mixture was degassed via three cycles of freeze-pump-thaw. The Schlenk tube was then placed in the irradiation setup at a temperature of 60 ºC and irradiated for 24 hours. After cooling to ambient temperature, the solvent was evaporated and the residue was diluted with AcOEt and water, the layers were separated and extracted with AcOEt (2x15 mL) and DCM (1x15 mL). Organic layer was purified by column chromatography (AcOEt/Acetone/Hexane 1:1:1 as eluent): 60 mg orange oil, 44% yield.

^{1}H NMR (500 MHz, $CDCl_3$) δ 10.52 (s, 1H, NH); 10.15 (s, 1H, NH); 5.53 (s, 1H); 3.70 (s, 3H); 3.67 (s, 3H); 3.25-3.18 (m, 1H); 2.87 (dd, *J* = 7.4, 16.9 Hz, 1H); 2.74 (dd, *J* = 7.4, 16.9 Hz, 1H); 2.68-2.59 (m, 2H).

^{13}C NMR (125 MHz, $CDCl_3$) δ 173.6; 171.8; 164.9; 153.6; 152.6; 101; 52.7; 52.2; 39.5; 35.1; 34.2.

HRMS (ESI pos): calculated for $C_{11}H_{14}N_2NaO_6$ ($M+Na^+$): 293.0744, found 293.0741.

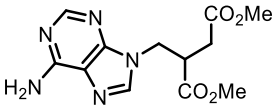

Dimethyl 2-((6-amino-9*H*-purin-9-yl)methyl)succinate (27): In an oven dried Schlenk tube, 9-(chloromethyl)-9*H*-purin-6-amine hydrochloride **26** (83 mg, 0.375 mmol, 1.5 equiv.) was dissolved in DMF (2.5 mL), then catalyst **2c** (7.76 mg, 0.1 equiv.) was added followed by 2,6-lutidine (79 μL, 0.675 mmol, 2.7 equiv.), γ-terpinene (48 μL, 0.3 mmol, 1.2 equiv.), and dimethyl fumarate **15a** (36 mg, 0.25 mmol, 1 equiv.). The resulting yellow mixture was degassed via three cycles of freeze-pump-thaw. The Schlenk tube was then placed in the irradiation setup at a temperature of 60 ºC and irradiated for 24 hours. After cooling to ambient temperature, the solvent was evaporated. Chromatography on silica gel could not remove a residual byproduct from the reaction mixture, therefore an NMR yield is reported (55%) by comparison of the resonance peaks at 4.5 ppm with trichloroethylene (1 equiv.) as internal standard. The residue was purified by column chromatography (AcOEt/Water/MeOH 7:2:1 as eluent) followed by preparative TLC (8% MeOH in DCM as eluent) to obtain an analytical amount of the isolated product **27** as a white solid.

^{1}H NMR (400 MHz, d6-DMSO) δ 8.13 (s, 1H); 8.06 (s, 1H); 7.22 (s, 2H, NH); 4.44 (dd, *J* = 6.9, 14.2 Hz, 1H); 4.37 (dd, *J* = 6.6, 14.2 Hz, 1H); 3.54 (s, 3H); 3.54 (s, 3H); 3.43-3.36 (m, 1H); 2.60 (d, *J* = 6.9 Hz, 2H)

^{13}C NMR (100 MHz, d6-DMSO) δ 172.2; 171.2; 156; 152.5; 149.7; 141; 118.5; 52; 51.6; 43.6; 41.2; 33.

HRMS (ESI pos): calculated for $C_{12}H_{16}N_5O_4$ ($M+H^+$): 294.1197, found 294.1189.

2.8 Mechanistic studies

2.8.1 Characterization of dithiocarbamate intermediates **3**

2.8.1.1 General procedure for the synthesis of benzyl dithiocarbamate intermediates

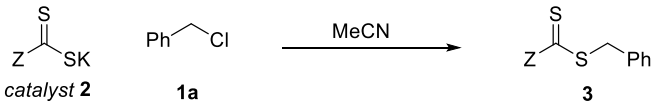

In a round bottom flask, the dithiocarbamate anion salt **2a-c** (1 equiv.) was dissolved in acetonitrile (HPLC grade, 0.1 M). Then benzyl chloride **1a** (1 equiv.) was added and the resulting mixture stirred for one hour at ambient temperature. Solvent was evaporated, then the residue dissolved in ethyl acetate and transferred to an extraction funnel containing water and ethyl acetate, the phases separated and the organic phase washed with distilled water and brine. The combined organic fractions were dried ($MgSO_4$) and concentrated to dryness to obtain the desired product in >95% purity.

*2.8.1.2 Characterization of dithiocarbamate intermediates **3***

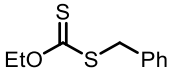

_S_-Benzyl _O_-ethyl carbonodithioate (3a)

Prepared using potassium ethyl xanthogenate **2a** (2 mmol, 321 mg) and benzyl chloride **1a** (2 mmol, 230 μL) in 20mL acetonitrile. After work-up, product **3a** was obtained as a slightly yellow oil (416 mg, 98% yield)

^{1}H NMR (400 MHz, $CDCl_3$) δ 7.40-7.27 (m, 5H); 4.69 (q, *J* = 7 Hz, 2 H); 4.40 (s, 2H); 1.45 (t, *J* = 7 Hz, 3 H).

^{13}C NMR (101 MHz, $CDCl_3$) δ 214.0; 135.7; 129.1; 128.6; 127.5; 70; 40.4; 13.8.

Matching reported data.[53]

[53] Wan, D.; Satoh, K.; Kamigaito, M.; Okamoto, Y., Xanthate-Mediated Radical Polymerization of N-Vinylpyrrolidone in Fluoroalcohols for Simultaneous Control of Molecular Weight and Tacticity. *Macromolecules* **2005**, *38*, 10397-10405.

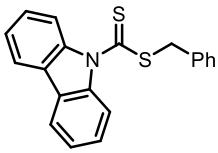

Benzyl 9*H*-carbazole-9-carbodithioate (3b)

Prepared using potassium 9*H*-carbazole-9-carbodithioate **2b** (2 mmol, 563 mg) and benzyl chloride **1a** (2 mmol, 230 μL) in 20mL acetonitrile. After work-up, product **3b** was obtained as a yellow solid (572 mg, 86% yield)

^{1}H NMR (400 MHz, $CDCl_3$) δ 8.50 (td, *J* = 8.4, 0.7 Hz, 2H); 8.03 (app d, *J* = 7.6 Hz, 2H); .7.55-7.33 (m, 9 H); 4.77 (s, 2H).

^{13}C NMR (101 MHz, $CDCl_3$) δ 201.7; 139.8; 134.5; 129.5; 128.8; 127.9; 126.7; 125.8; 123.4; 119.8; 115.2; 42.6.

Matching reported data.[54]

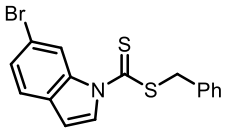

Benzyl 5-bromo-1*H*-indole-1-carbodithioate (3c)

Prepared according to the general procedure using potassium 5-bromo-1*H*-indole-1-carbodithioate **2c** (2 mmol, 621 mg) and benzyl chloride **1a** (2 mmol, 230 μL) in 20mL acetonitrile. After work-up, product **3c** was obtained as a yellow solid (695 mg, 96% yield).

^{1}H NMR (400 MHz, $CDCl_3$) δ 8.88 (d, *J* = 9 Hz, 1H); 8.10 (d, *J* = 3.8 Hz, 1H); 7.70 (d, *J* = 2 Hz, 1H); 7.48-7.42 (m, 3H); 7.41-7.31 (m, 3H); 6.62 (dd, *J* = 3.8, 0.5 Hz, 1H); 4.65 (s, 2H).

^{13}C NMR (101 MHz, $CDCl_3$) δ 197.8; 135.7; 134.2; 133.7; 129.5; 128.8; 128.1; 128.0; 127.9; 123.9; 118.2; 117.3; 108.7; 41.9.

HRMS (APCI pos): calculated for $C_{16}H_{13}{}^{79}BrNS_2$ ($M+H^+$): 361.9667, found 361.9665.

[54] Zhang, J.; Dong, A.; Cao, T.; Guo, R., Carbazyl RAFT agents synthesized by an improved aqueous phase method and their applications in RAFT polymerization. *Eur. Polym. J.* **2008**, *44*, 1071-1080.

2.8.1.3 UV-Vis of dithiocarbamate intermediates ***3***

Dithiocarbamate intermediate	λ_{max} (extinction coefficient)	tail of absorption at 0.05M
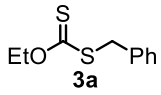 **3a**	355 nm (68)	415 nm
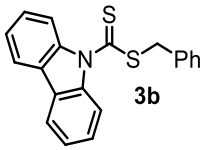 **3b**	365 nm (8.938)	537 nm
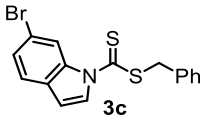 **3c**	344 nm (18.408)	655 nm

After isolation, the UV-Vis spectra of the intermediates **3** were recorded to determine the wavelength of maximal absorption in acetonitrile. Then, the molar absorption coefficient at this wavelength was determined according to Beer-Lambert's law at different concentrations to confirm linearity.

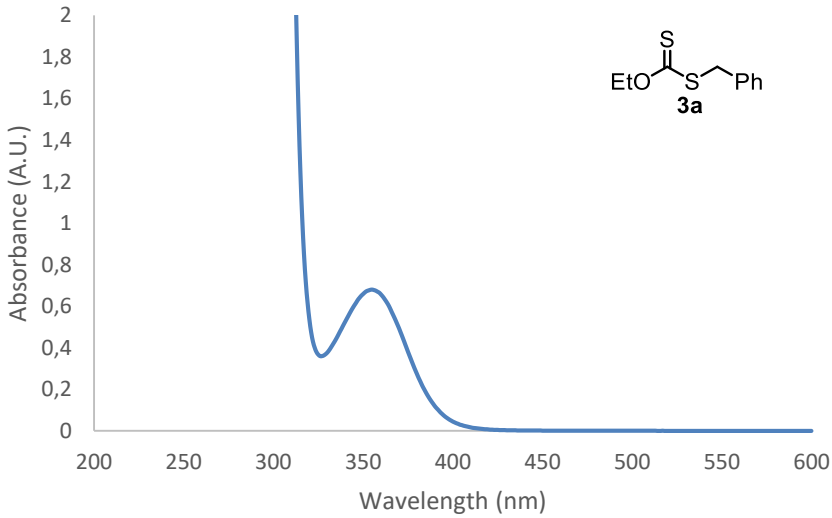

Figure 2.10. UV-Vis absorption spectrum of **3a** recorded at 10^{-2}M concentration in acetonitrile.

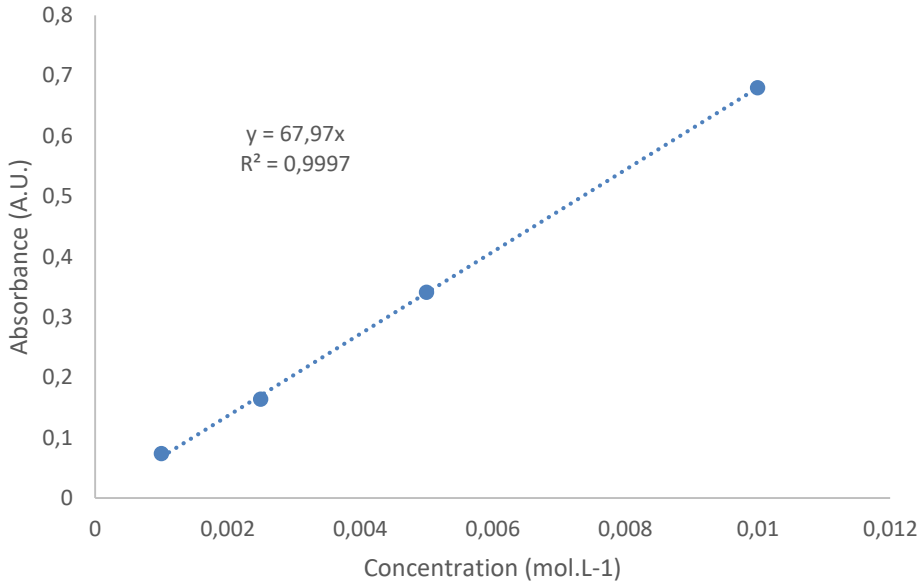

Figure 2.11. Molar absorption coefficient determination of 3**a** at 355 nm.

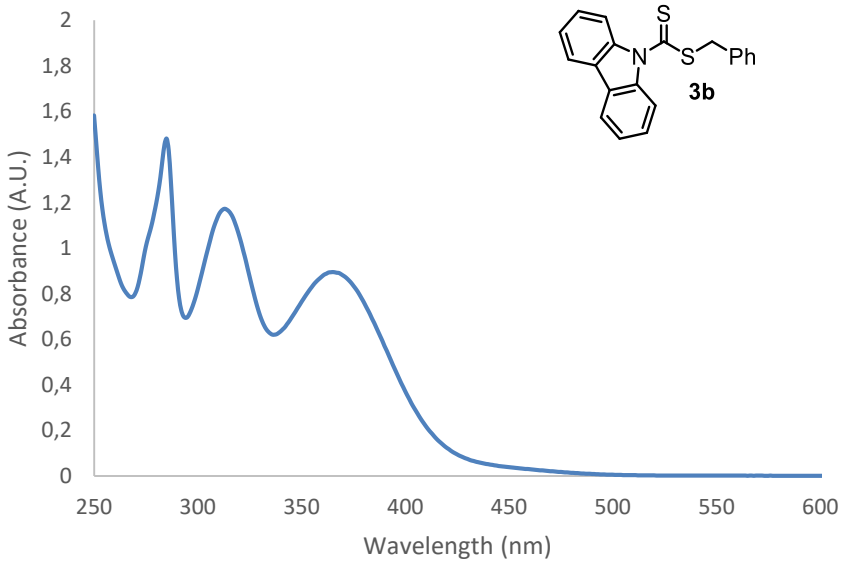

Figure 2.12. UV-Vis absorption spectrum of **3b** recorded at 10^{-4}M concentration in acetonitrile.

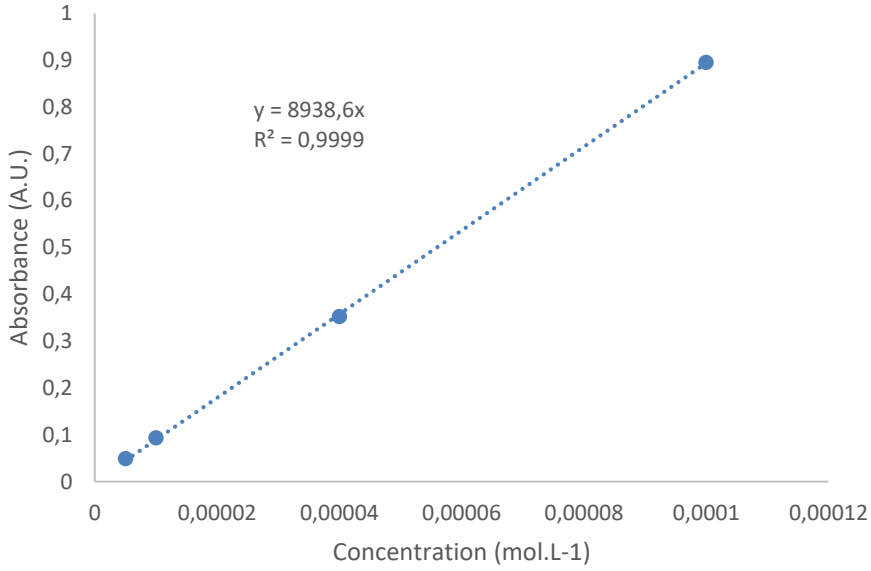

Figure 2.13. Molar absorption coefficient determination of **3b** at 365 nm.

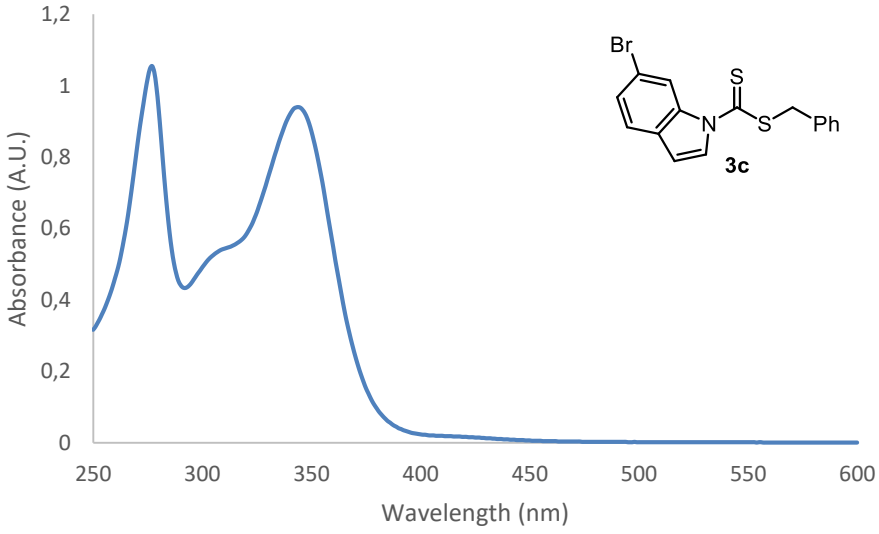

Figure 2.14. UV-Vis absorption spectrum of **3c** recorded at 5.10^{-5} M concentration in acetonitrile.

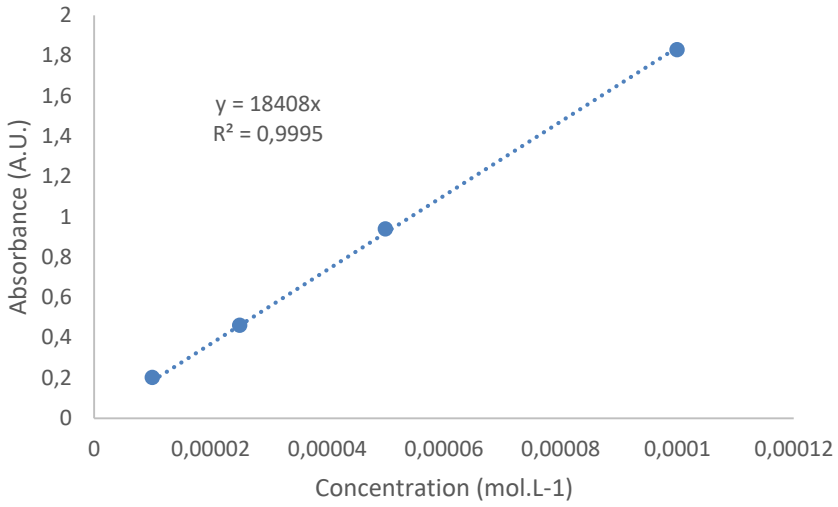

Figure 2.15. Molar absorption coefficient determination of **3c** at 345 nm.

The UV-Vis spectra of the different intermediates were then recorded in a 1mm optical path cuvette at a concentration of 0.05 M, identical to the concentration of the intermediates under the reaction conditions at the beginning of irradiation (10 mol% of catalyst). The maximum wavelength of absorption at this concentration was then determined considering an absorbance of less than 0.01 arbitrary unit.

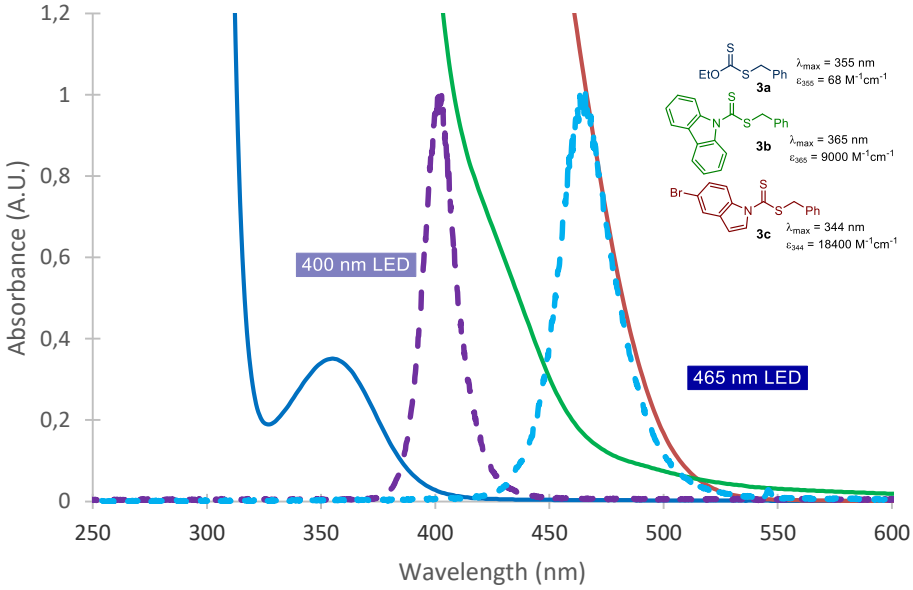

Figure 2.16. Maximum wavelength of absorption of the different benzyl dithiocarbamate intermediates **3**. Spectra recorded at 0.05 M concentration in acetonitrile in a 1mm optical path cuvette. Dashed lines represent the normalized emission spectra of the LED light sources used in this study.

2.8.2 TEMPO trapping experiment of the benzyl radical

*2.8.2.1 Stoichiometric reaction with dithiocarbamate intermediate **3***

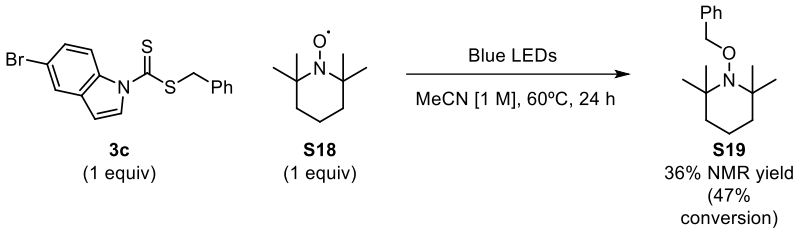

3c (1 equiv) **S18** (1 equiv) **S19** 36% NMR yield (47% conversion)

In an oven-dried Schlenk tube, benzyl 5-bromo-1*H*-indole-1-carbodithioate **3c** (72 mg, 0.2 mmol, 1 equiv.) and 2,2,6,6-tetramethylpiperidine 1-oxyl (TEMPO) **S18** (31 mg, 0.2 mmol, 1 equiv.) were dissolved in acetonitrile (2 mL). The resulting mixture was degassed via three cycles of freeze-pump-thaw. The Schlenk tube was then placed in the irradiation setup at a temperature of 60 ºC and irradiated for 24 hours.

After cooling to ambient temperature, the solvent was evaporated, trichloroethylene (18 µl, 1 equiv.) added as internal standard, the residue diluted with $CDCl_3$ and an aliquot analyzed by ^{1}H NMR spectroscopy to determine conversion and yield of the trapping product **S19** (Figure 2.17).

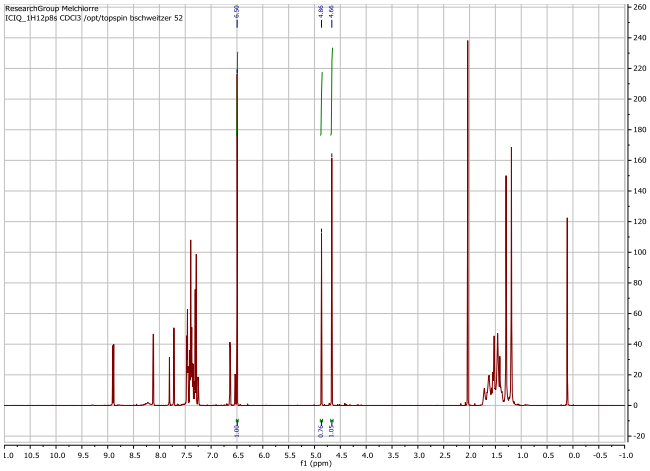

Figure 2.17. ^{1}H NMR of the crude mixture for the trapping of benzyl radical with TEMPO.

Using the peak of trichloroethylene (6.50 ppm, s, 1H) as reference, a conversion of 47% (53% remaining benzyl 5-bromo-1*H*-indole-1-carbodithioate **3c**) was determined (peak at 4.66

ppm, s, 2H). The trapping product **S19** was detected at 4.86 ppm (s, 2H) and a 38% yield determined by integration of this peak.[55]

A control experiment in the absence of light showed no conversion into the trapping product.

2.8.2.2 Catalytic reaction

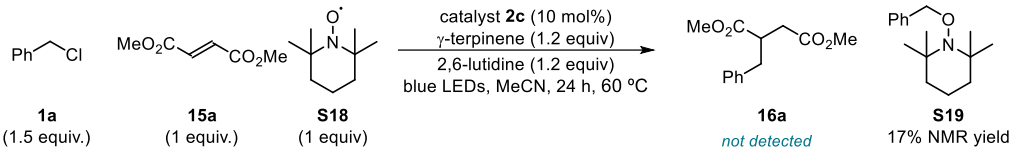

1a (1.5 equiv.) | **15a** (1 equiv.) | **S18** (1 equiv) | **16a** *not detected* | **S19** 17% NMR yield

In an oven dried Schlenk tube, **2c** (15.5 mg, 0.05 mmol, 0,1 equiv.) was dissolved in acetonitrile (1 mL), then benzyl chloride **1a** (60 µL, 0.5 mmol, 1 equiv.) was added followed by 2,6-lutidine (70 µL, 0.6 mmol, 1.2 equiv.), γ-terpinene (96 µL, 0.6 mmol, 1.2 equiv.), dimethyl fumarate **15a** (72 mg, 0.5 mmol, 1 equiv.) and TEMPO **S18** (78 mg, 0.5 mmol, 1 equiv.). The resulting yellow mixture was degassed via three cycles of freeze-pump-thaw. The Schlenk tube was then placed in the irradiation setup at a temperature of 60 ºC and irradiated for 24 hours. After cooling to ambient temperature, the solvent was evaporated, trichloroethylene (45 µl, 1 equiv.) added as internal standard, the residue diluted with $CDCl_3$ and an aliquot analyzed by ^1H NMR spectroscopy to determine conversion and yield.

Product **16a** was not detected by NMR while the trapping product **S19** was formed in 17% yield according to the internal standard.

A control experiment in the absence of light showed no conversion into the trapping product.

2.8.3 Study of the involvement of group transfer mechanism in the catalytic reaction

*2.8.3.1 Synthesis of the group transfer product **XIIIc***

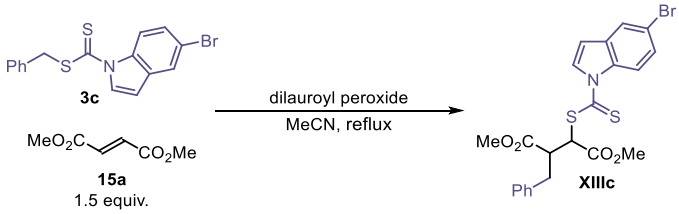

group transfer product

In an oven-dried two necked flask equipped with a reflux condenser and under argon, compound **3c** (362 mg, 1 mmol, 1 equiv.) and dimethyl fumarate **15a** (216 mg, 1.5 mmol, 1.5 equiv.) were dissolved in acetonitrile (10 mL). The mixture was brought to reflux under an argon atmosphere and dilauroyl peroxide was added portionwise (20 mg, 0.05 mmol, 0.05

[55] Yasu, Y.; Koike, T.; Akita, M., Visible Light-Induced Selective Generation of Radicals from Organoborates by Photoredox Catalysis. *Adv. Synth. Catal.* **2012**, *354*, 3414-3420.

equiv. portions; 3 portions in total) every 30 minutes until TLC analysis showed complete conversion of the starting material. The mixture was then transferred to an extraction funnel, diluted with AcOEt and washed with water and brine, dried ($MgSO_4$) and concentrated to a yellow oil. Column chromatography (10% AcOEt in hexanes as eluent) afforded the product as a yellow oil in 36% yield (183 mg) as a mixture of diastereomers (1:1.3 ratio).

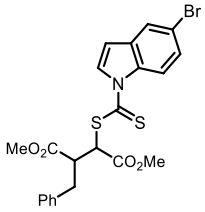

dimethyl 2-benzyl-3-((5-bromo-1H-indole-1-carbonothioyl)thio)succinate (XIIIc):

^{1}H NMR for a 1:1.3 diastereomeric mixture (400 MHz, $CDCl_3$) δ 8.85 (d, *J* = 9.2 Hz, 1H, *major*); 8.82 (d, *J* = 9.2 Hz, 1H, *minor*); 8.17 (d, *J* = 3.8 Hz, 1H, *major*); 8.08 (d, *J* = 3.8 Hz, 1H, *minor)*; 7.72 (d, *J* = 2.0 Hz, 1H, *major*); 7.71 (d, *J* = 2.0 Hz, 1H, *minor*); 7.49-7.43 (m, 2 H, *minor* + *major*); 7.36-7.17 (m, 5H, *minor* + *major*); 6.68 (dd, *J* = 3.8, 0.5 Hz, 1H, *major*); 6.65 (dd, *J* = 3.8, 0.5 Hz, 1H, *minor*); 5.34 (d, *J* = 5.6 Hz, 1H, *minor*); 5.22 (d, *J* = 4.7 Hz, 1H, *major*); 3.83-3.77 (m, 1H, *minor* + *major*); 3.78 (s, 3H, *minor*); 3.76 (s, 3H, *major*); 3.73-3.65 (m, 1H, *major*); 3.72 (s, 3H, *major*); 3.68 (s, 3H, *minor*); 3.51-3.44 (m, 1H; *minor*); 3.31-3.22 (m, 1H, *minor* + *major*); 3.17 (dd, *J* = 13.9, 6.8 Hz, 1H, *minor*); 2.96 (dd, *J* = 14.0, 8.4 Hz, 1H, *major*).

^{13}C NMR (100 MHz, $CDCl_3$) δ 195.72; 194.65; 172.85; 172.40; 169.87; 169.48; 137.88; 137.46; 136.09; 136.05; 133.70; 129.20; 129.01; 128.74; 128.59; 128.22; 128.17; 128.05; 127.97; 126.99; 126.90; 124.05; 124.02; 118.30; 118.28; 117.69; 117.61; 109.30; 109.17; 53.83; 53.81; 53.25; 53.18; 52.41; 52.30; 49.53; 48.56; 36.11; 35.65.

HRMS (ESI pos): calculated for $C_{22}H_{20}{}^{79}BrNNaO_4S_2$ ($M+Na^+$): 527.9909, found 527.9906.

2.8.3.2 *Conjugate addition reaction in the absence of γ-terpinene*

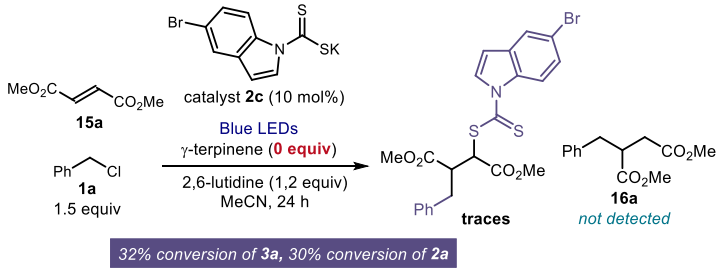

In an oven-dried Schlenk tube, **2c** (16 mg, 0.05 mmol, 0.1 equiv.) was dissolved in acetonitrile (1 mL) and benzyl chloride **1a** (86µL, 0.75 mmol, 1.5 equiv.) was added, followed by 2,6-lutidine (70 µL, 0.6 mmol, 1.2 equiv.) and dimethyl fumarate **15a** (72 mg, 0.5 mmol, 1 equiv.). The mixture was then degassed (freeze-pump-thaw, three cycles) and irradiated at 60 ºC for 24 hours. The majority of volatiles were evaporated under a stream of nitrogen, trichloroethylene (18 µl, 0.2 mmol, 1 equiv.) was added, the residue dissolved in $CDCl_3$ and analyzed by ^{1}H NMR to determine conversion and yield.

Using the peaks at 5.3 ppm (1H) and 5.2 ppm (1H), trace amounts of **XIIIc** were observed. Using the peak at 6.8 ppm (2H), a conversion of dimethyl fumarate **15a** of 32% was inferred (Figure 2.18).

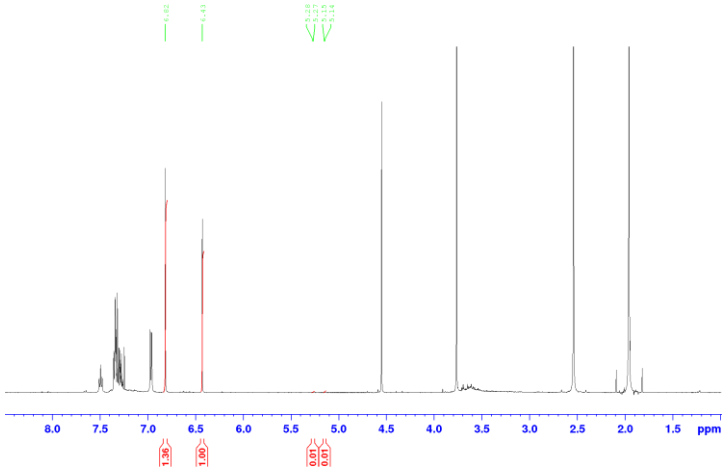

Figure 2.18. ^{1}H NMR of the crude mixture of the Giese-type radical addition in the absence of γ-terpinene.

*2.8.3.3 Formation of **XIIIc** from **3c** under irradiation*

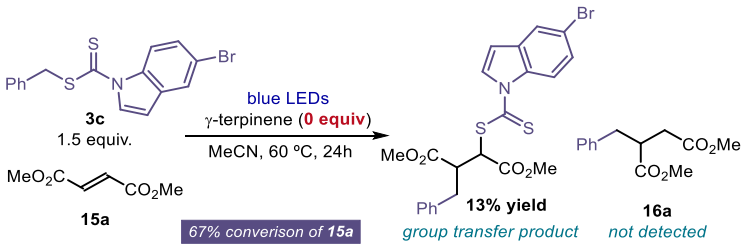

In an oven-dried Schlenk tube, **3c** (109 mg, 0.3 mmol, 1.5 equiv) and dimethyl fumarate **15a** (29 mg, 0.2 mmol, 1 equiv.) were dissolved in acetonitrile (0.4 mL). The mixture was then degassed (freeze-pump-thaw, three cycles) and irradiated at 60 ºC for 24 hours. The majority of volatiles were evaporated under a stream of nitrogen, trichloroethylene (18 µl, 0.2 mmol, 1 equiv.) was added, the residue dissolved in $CDCl_3$ and analyzed by ^{1}H NMR to determine conversion and yield.

Using the peaks at 5.3 ppm (1H) and 5.2 ppm (1H), a yield of **XIIIc** of 13% was determined. Using the peak at 6.8 ppm (2H), a conversion of dimethyl fumarate **3a** of 67% was inferred (Figure 2.19). The appearance of broad signals in the 3.8-3.4 ppm region may suggest the formation of polymers.

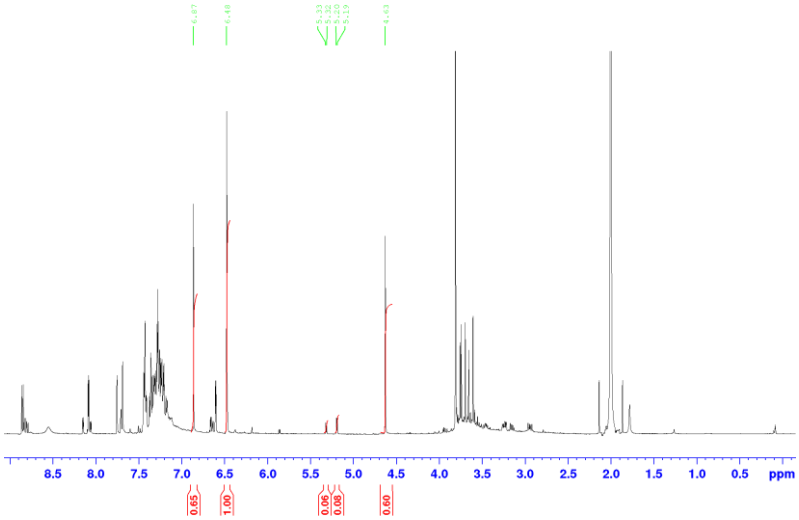

Figure 2.19. ^{1}H NMR of the crude mixture for the formation of **XIIIc** under irradiation at 60 ºC.

*2.8.3.4 Formation of **16a** from **3c** under stoichiometric reaction conditions*

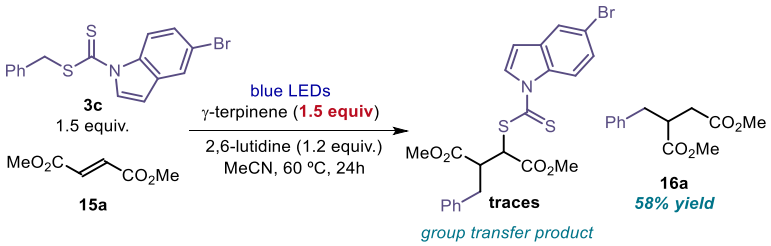

In an oven-dried Schlenk tube, **3c** (109 mg, 0.3 mmol, 1.5 equiv.) and dimethyl fumarate **15a** (29 mg, 0.2 mmol, 1 equiv.) were dissolved in acetonitrile (0.4 mL) and γ-terpinene (948 µL, 0.3 mmol, 1.5 equiv.) and 2,6-lutidine (28 µL, 0.24 mmol, 1.5 equiv.). The mixture was then degassed (freeze-pump-thaw, three cycles) and irradiated at 60 ºC for 24 hours. The majority of volatiles were evaporated under a stream of nitrogen, trichloroethylene (18 µl, 0.2 mmol, 1 equiv.) was added, the residue dissolved in $CDCl_3$ and analysed by ^{1}H NMR to determine conversion and yield.

Using the peaks at 5.3ppm (1H) and 5.2 ppm (1H), traces of **XIIIc** were detected. Using the peak at 3.11 ppm (m, 1H), a 58% yield of **16a** was inferred (Figure 2.20). The presence of γ–terpinene exclusively triggered the Giese-type addition manifold.

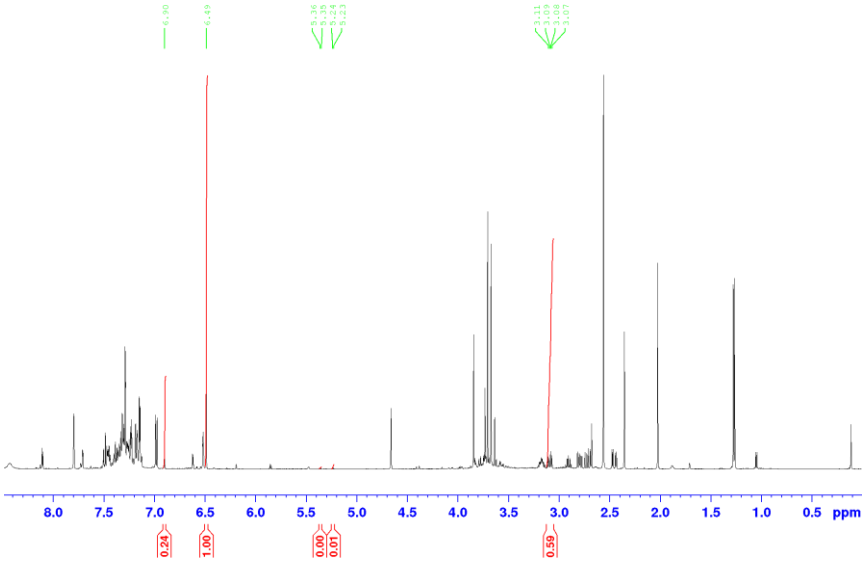

Figure 2.20. ^{1}H NMR of the crude mixture for the formation of **15a** from **XIIIc** under irradiation in the presence of γ-terpinene.

*2.8.3.5 Formation of **16a** upon irradiation of **XIIIc***

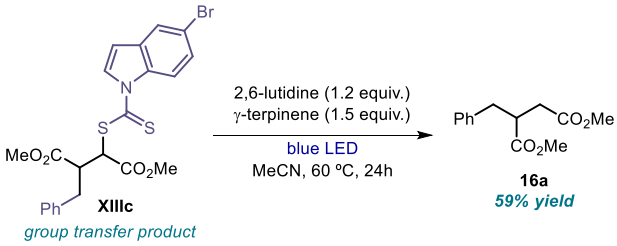

In an oven-dried Schlenk tube, **XIIIc** (20 mg, 0.039 mmol, 1.5 equiv), γ-terpinene (9.5 µL, 0.06 mmol, 1.5 equiv.) and 2,6-lutidine (5.5 µL, 0.06 mmol, 1.5 equiv.) were dissolved in acetonitrile (80 µL). The mixture was then degassed (freeze-pump-thaw, three cycles) and irradiated at 60 ºC for 24 hours. The majority of volatiles were evaporated under a stream of nitrogen, trichloroethylene (9 µl, 0.1 mmol, 2.53 equiv.) was added, the residue dissolved in $CDCl_3$ and analyzed by ^{1}H NMR to determine conversion and yield.

Using the peaks at 5.3ppm (1H) and 5.2 ppm (1H), full conversion of **XIIIc** was determined. Using the peak at 3.14 ppm (m, 1H), a yield of 59% was inferred for the benzylation product **16a** (Figure 2.21).

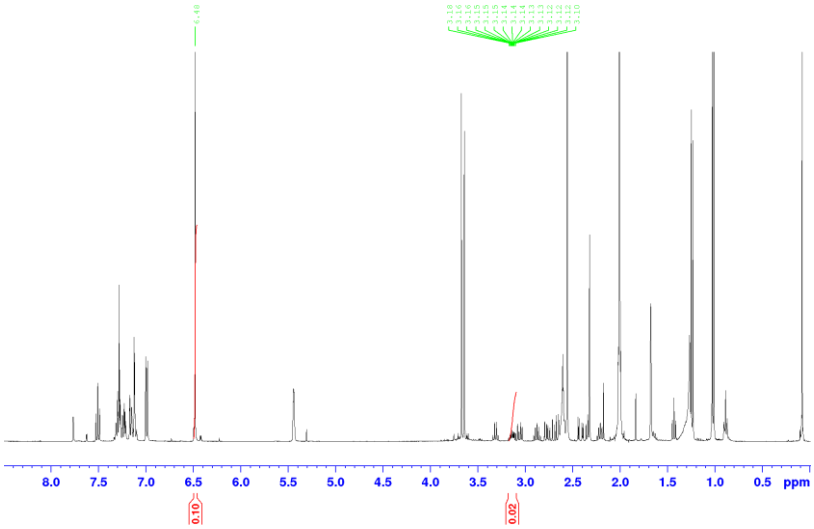

Figure 2.21. ^{1}H NMR of the crude mixture for the conversion of **XIIIc** to **16a** under irradiation.

Based on these experiments, we can draw the following conclusions: *i*) In consonance with the RAFT polymerisation literature, it appears that intermediate **3c** might act as a competent chain transfer agent. The conversion of fumarate in the stoichiometric control experiment conducted in the absence of H-donor and the appearance of broad signals in the NMR analysis may indicate the formation of polymers. *ii*) The presence of γ–terpinene favors the Giese-type addition manifold under catalytic conditions and prevents any efficient polymerisation, as shown by the generally high yields of product **16** obtained in the experiments conducted with a H donor. *iii)* **XIIIc**, if formed under reaction conditions is a competent precursor to radicals **II** and **XII**, that can reenter the catalytic cycle to products **16**.

Chapter III

Photochemical generation of acyl and carbamoyl radicals using a nucleophilic organic catalyst

Target

Developing an organocatalytic photochemical strategy for the generation of acyl and carbamoyl radicals from easily accesible acyl electrophiles.

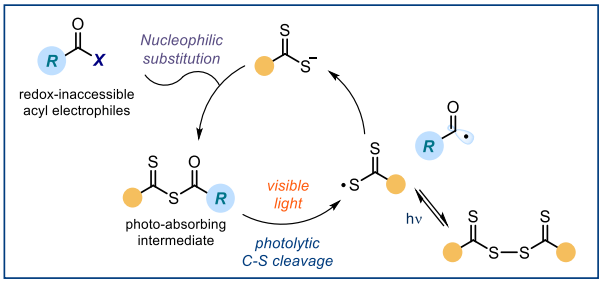

Tool

Exploiting the nucleophilic nature of an organic dithiocarbamate catalyst to activate electrophilic acyl and carbamoyl chlorides and generate reactive acyl and carbamoyl radicals.[1]

3.1 Introduction

The previous chapter detailed the development of a photochemical catalytic strategy that harnesses different physical properties of the substrates to generate radicals (Scheme 3.1).[2] Specifically, our method capitalizes on the electrophilic properties of a given precursor **1** to access a variety of stabilized radicals **II**. We used a nucleophilic organic catalyst **2** to activate alkyl electrophiles through an S_N2 pathway. To further expand the synthetic utility of our nucleophilic catalysts, we envisioned that they could be useful to form acyl and carbamoyl radicals from simple acyl electrophiles **4**, without relying on the redox potential of the substrates. A general mechanistic plan is depicted in Scheme 3.1. Upon acyl nucleophilic substitution of **4** with the nucleophilic catalyst **2**, we sought to exploit the photo-absorbing properties of the ensuing intermediate **5** to induce a photolytic cleavage. This photochemical event would deliver the acyl radical **III** and the sulfur-centered radical **I**. Our previous knowledge of the dithiocarbamate system would then help to identify conditions suitable to

[1] The project discussed in this chapter was conducted in collaboration with Dr. Daniele Mazzarella, who developed the reaction involving carbamoyl radicals and participated in the mechanistic studies, and Matteo Balletti, who performed part of the scope of the carbamoyl derivatives and part of the mechanistic studies. I was involved in the discovery of the reaction with acyl radicals and its optimization, and I investigated the scope of the reaction and performed mechanistic studies. This work has been published, see: De Pedro Beato, E.; Mazzarella. D.; Balletti, M.; Melchiorre, P. Photochemical generation of acyl and carbamoyl radicals using a nucleophilic organic catalyst: applications and mechanism thereof. *Chem. Sci.* **2020**, *11*, 6312-6324.

[2] Schweitzer-Chaput, B.; Horwitz, M. A.; de Pedro Beato, E.; Melchiorre, P., Photochemical generation of radicals from alkyl electrophiles using a nucleophilic organic catalyst. *Nature Chem.* **2019**, *11*, 129-135.

turn-over the nucleophilic catalyst **2**. Overall, this method would offer an organocatalytic photochemical platform for the generation of acyl radicals under mild conditions.

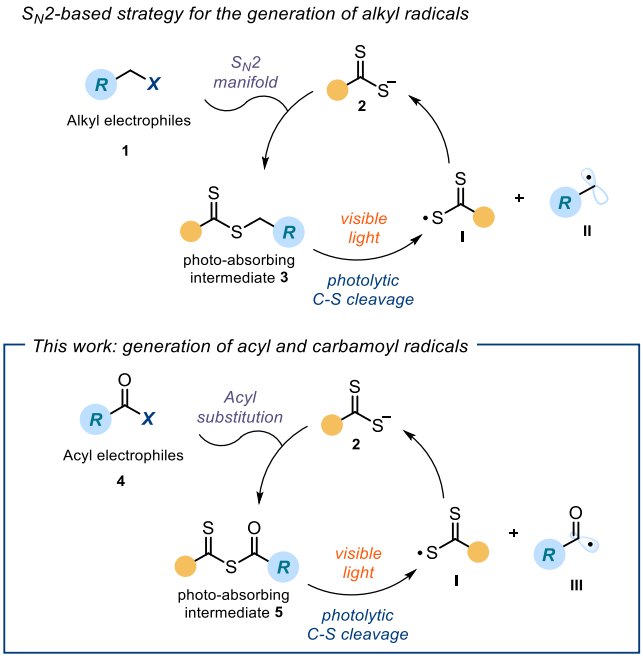

Scheme 3.1. Nucleophilic substitution-based radical generation strategies.

The generation of acyl and carbamoyl radicals is not trivial.[3] Traditional methods rely on the stoichiometric use of oxidants[4] or preformed acyl[5] and carbamoyl[6] chalcogens. These methods use thermal initiators or UV light irradiation to generate radicals. These conditions may hamper the use in complex systems. The advent of photoredox catalysis offered methodologies, based on hydrogen atom transfer (HAT) and single-electron transfer (SET)

[3] Chatgilialoglu, C.; Crich, D.; Komatsu, M.; Ryu, I., Chemistry of Acyl Radicals. *Chem. Rev.* **1999**, *99*, 1991-2070.
[4] Minisci, F.; Gardini, G. P.; Galli, E.; Bertini, F. A New Selective Type of Aromatic Substitution: Homolytic Amidation *Tetrahedron Lett.* **1970**, *11*, 15-16.
[5] (a) Barton, D. H. R.; George, M. V.; Tomoeda, M. Photochemical Transformations. Part XIII. A New Method for the Production of Acyl Radicals. *J. Chem. Soc.* **1962**, 1967-1974. (b) Delduc, P.; Tailhan, C.; Zard, S. Z. A Convenient Source of Alkyl and Acyl Radicals. *J. Chem. Soc., Chem. Comm.* **1988**, 308-310. (c) Chen, C.; Crich, D.; Papadatos, A. The chemistry of acyl tellurides: generation and trapping of acyl radicals, including aryltellurium group transfer. *J. Am. Chem. Soc.* **1992**, *114*, 8313-8314.
[6] (a) Fujiwara, S.; Shimizu, Y.; Shinike, T.; Kambe, N. Photoinduced Group Transfer Radical Addition of Carbamotelluroates to Acetylenes. *Org. Lett.* **2001**, *3*, 2085-2088. (b) Grainger, R. S.; Innocenti, P. Dithiocarbamate Group Transfer Cyclization Reactions of Carbamoyl Radicals under "Tin-Free" Conditions. *Angew. Chem. Int. Ed.* **2004**, *43*, 3445-3448. (c) Millán-Ortiz, A.; Lòpez-Valdez, G.; Cortez-Guzmán, F.; Miranda, L. D. A novel carbamoyl radical based dearomatizing spiroacylation process. *Chem. Commun.* **2015**, *51*, 8345-8348.

mechanisms, to generate radicals under mild conditions (e.g. by means of visible light irradiation and at ambient temperature).[7] While HAT processes provide an elegant and atom-economical strategy to access acyl radicals, these methods depend on the intrinsic properties of the substrates (e.g. bond dissociation energies of different C-H bonds), and they therefore come along with regioselectivity issues in complex molecules.[8] SET methods generally require purposely designed redox-active auxiliaries, which have to be introduced in the substrates adding extra synthetic steps.[9] This explains why developing a general strategy for the generation of acyl and carbamoyl radicals from readily available precursors with high functional group tolerance would be of synthetic interest.

In this chapter, I detail the implementation of our photochemical catalytic plan and the investigations carried out to gain insight into the mechanism. In the following section, I discuss the most relevant strategies for the generation of acyl radicals to put this project into context.

3.2 Generation of acyl radicals from stoichiometric precursors

3.2.1 Acyl radicals from aldehydes

The activation of aldehydes via a HAT mechanism is the most straightforward strategy to access acyl radicals. The first example was reported by Berman,[10] who used thiols as mediators to start a radical chain propagation pathway (Scheme 3.2). This study offered an early example of polarity-reversal catalysis.[11] Upon starting the process by a thermal- or light-induced initiation step, the initial radical can abstract a hydrogen atom from the aldehyde substrate **6**. This process delivers radical **III**. Intermediate **III** can then undergo

---

[7] For reviews on the generation of acyl and carbamoyl radicals via photoredox catalysis: (a) Banerjee, A.; Lei, Z.; Ngai, M.-Y. Acyl Radical Chemistry via Visible-Light Photoredox Catalysis. *Synthesis* **2019**, *51*, 303-333. (b) Raviola, C.; Protti, S.; Ravelli, D.; Fagnoni, M. Photogenerated acyl/alkoxycarbonyl/carbamoyl radicals for sustainable synthesis. *Green Chem.* **2019**, *21*, 748-764.

[8] Ravelli, D.; Fagnoni, M.; Fukuyama, T.; Nishikawa, T.; Ryu, I., Site-Selective C–H Functionalization by Decatungstate Anion Photocatalysis: Synergistic Control by Polar and Steric Effects Expands the Reaction Scope. *ACS Catal.* **2018**, *8*, 701-713.

[9] For selected examples see: (a) Cheng, W.-M.; Shang, R.; Yu, H.-Z.; Fu, Y., Room-Temperature Decarboxylative Couplings of α-Oxocarboxylates with Aryl Halides by Merging Photoredox with Palladium Catalysis. *Chem. Eur. J* **2015**, *21*, 13191-13195. (b) Capaldo, L.; Riccardi, R.; Ravelli, D.; Fagnoni, M. Acyl Radicals from Acylsilanes: Photoredox-Catalyzed Synthesis of Unsymmetrical Ketones *ACS Catal.* **2018**, *8*, 304-309. (c) G. Goti, B. Bieszczad, A. Vega-Peñaloza and P. Melchiorre. Stereocontrolled Synthesis of 1,4-Dicarbonyl Compounds by Photochemical Organocatalytic Acyl Radical Addition to Enals. *Angew. Chem., Int. Ed.* **2019**, 58, 1213–1217. For selected examples on carbamoyl derivatives see: (d) Jouffroy, M.; Kong, J. Direct C-H Carbamoylation of Nitrogen-Containing Heterocycles. *Chem. Eur. J.* **2019**, *25*, 2217-2221. (e) Petersen, W. F.; Taylor, R. J. K.; Donald, J. R. Photoredox-Catalyzed Reductive Carbamoyl Radical Generation: A Redox-Neutral Intermolecular Addition–Cyclization Approach to Functionalized 3,4-Dihydroquinolin-2-ones. *Org. Lett.* **2017**, *19*, 874-877.

[10] Berman, J. D.; Stanley, J. H.; Sherman, W. V.; Cohen, S. G., Sensitization and Catalysis of Light-Induced Decarbonylation of Aldehydes. *J. Am. Chem. Soc.* **1963**, *85*, 4010-4013.

[11] P. Roberts, B., Polarity-reversal catalysis of hydrogen-atom abstraction reactions: concepts and applications in organic chemistry. *Chem. Soc. Rev.* **1999**, *28*, 25-35.

decarbonylation to form the alkyl radical **IV**. Interestingly, the decarbonylation process is an equilibrium that can be controlled to favor acyl radical formation, for example using pressurized conditions.[3] The direct abstraction between radical **IV** and aldehyde **6** is not polarity-matched, since both have a nucleophilic character, making the process slower in comparison to other potential radical pathways. This kinetic conundrum was solved by introducing thiol **7** as a mediator: radical **IV** can now efficiently abstract a hydrogen atom from thiol **7** while the resulting electrophilic thiyl radical **V** can quickly react with aldehyde **6** to form the acyl radical **III**, propagating the radical chain. This regulated sequence of processes is possible because of the large difference in bond-dissociation energy (BDE) between the C-H bonds of aldehyde **6** and the decarbonylation product **8**.[12]

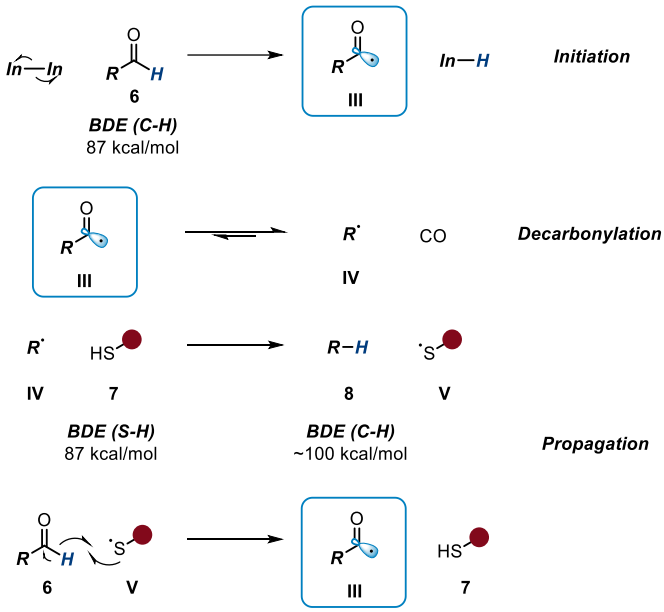

Scheme 3.2. Acyl radical generation from aldehydes and subsequent decarbonylation.

3.2.2 Use of stoichiometric oxidants

The generation of acyl radicals under oxidative conditions was firstly documented by Minisci in 1969 (Scheme 3.3).[13] He explored the formation of acyl radicals from aldehydes by means of HAT. In contrast to the previously mentioned reports, no radical chain was operative and a stoichiometric amount of the oxidant was necessary to ensure the formation of acyl radicals

[12] Bell, J. D.; Murphy, J. A., Recent advances in visible light-activated radical coupling reactions triggered by (i) ruthenium, (ii) iridium and (iii) organic photoredox agents. *Chem. Soc. Rev.* **2021**.
[13] Caronna, T.; Gardini, G. P.; Minisci, F., Nucleophilic character of acyl radicals: a new selective type of aromatic acylation. *J. Chem. Soc. D*, **1969**, 201-201.

III and products **10**. Upon homolytic cleavage of the peroxide (serving as the radical initiator and the oxidant), an alkoxy radical is generated, which undergoes HAT with aldehyde **3** to form the acyl radical **III**. Intermediate **III**, due to its nucleophilic nature, reacts with the activated quinoline H-**7**. The resulting radical cation **VI** is oxidized to yield product **10**.

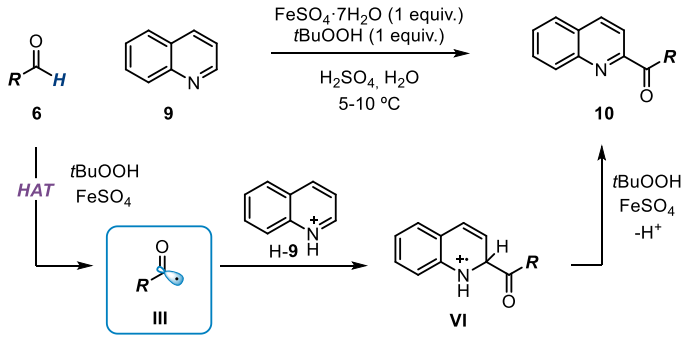

Scheme 3.3. Acyl radical addition to heteroarene under oxidative conditions.

Later studies by Minisci introduced the use of α-ketoacids as alternative acyl radical precursors (Scheme 3.4).[14] Here, the peroxide was replaced by persulfate, while the generation of acyl radicals relied on an SET mechanism followed by decarboxylation.

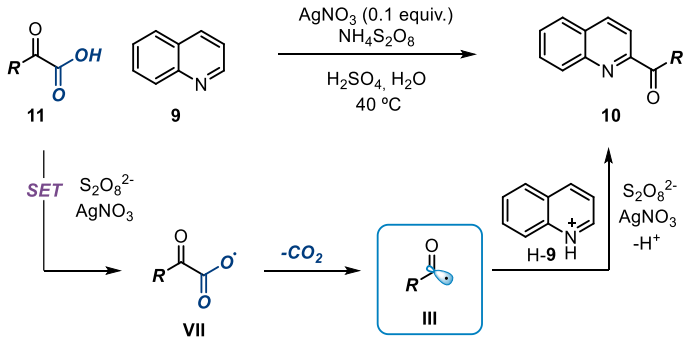

Scheme 3.4. Acyl radical generation by oxidation of α-ketoacids.

3.2.3 Use of acyl halides

The first use of acyl halides as acyl radical precursors was based on a stannane-mediated reduction to aldehydes (Scheme 3.5).[3] This method showed disadvantages because of the

[14] Caronna, T.; Fronza, G.; Minisci, F.; Porta, O., Homolytic acylation of protonated pyridine and pyrazine derivatives. *J. Chem. Soc. Perkin Trans. 2*, **1972**, 2035-2038.

formation of multiple byproducts. Classical activation by organotin reagents (Scheme 3.5) involves the use of alkyl stannanes to form radical **VIII**, which than can undergo chlorine abstraction from acyl halides to deliver the acyl radical **III**. Nevertheless, the need for stoichiometric tin leads to over-reduction pathways that hampered the applicability of this strategy.

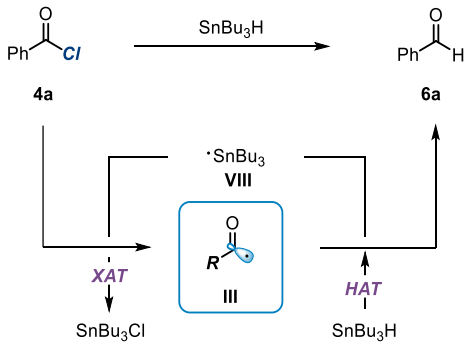

Scheme 3.5. Acyl radical generation by stannane-mediated chloride abstraction.

3.2.4 Use of acyl chalcogens

Acyl chalcogen derivatives have been used to generate acyl radicals too.[3] Different methods of radical formation have been used, including homolytic cleavage of the carbon-chalcogen bond induced by heat or light. Acyl chalcogens are usually easily accessible, but their use generates stoichiometric amount of chalcogen derivatives as waste. Early examples included the photolytic cleavage of thioesters **12** to accomplish the reduction to aldehydes **6b** (Scheme 3.6).[15] This process offered an early demonstration of how the mild conditions of photolytic activation secured access to secondary acyl radicals without decarbonylation taking place.

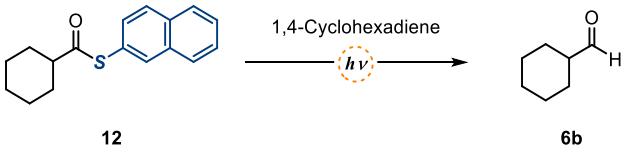

Scheme 3.6. Thioester photolysis.

One of the properties of acyl chalcogens is their capability to undergo group transfer mechanisms. This feature allows to further functionalize the products. As discussed in Chapter II, xanthate derivatives are widely used in radical group transfer processes. In particular, acyl

[15] Grunwell, J. R.; Marron, N. A.; Hanhan, S. I. *J. Org. Chem.* **1973**, *38*, 1559-1562.

xanthates were devised by Barton as acyl radical precursors following homolytic cleavage with light (Scheme 3.7a).[5a] After photolytic cleavage of xanthate **13a**, the acyl radical **IXa** is formed, which rapidly decarbonylates to give the benzylic radical **Xa**. Finally, another molecule of **13a** can act as group transfer reagent, propagating the radical chain while affording product **14a** and the acyl radical **IXa**.

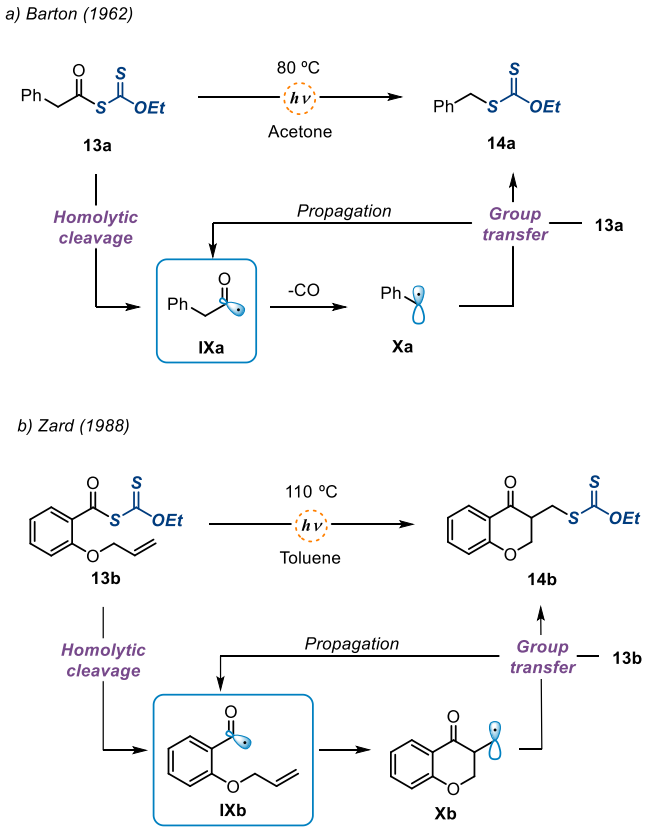

Scheme 3.7. Generation of acyl radicals by photolysis of acyl xanthates.

Acyl xanthates were further explored by Zard, who exploited the formation of aroyl radicals, much less prone to decarbonylation, to trigger C-C bond forming processes via intramolecular addition to olefins (Scheme 3.7b).[5b] Despite these advances, the harsh conditions needed to generate the radicals (far UV irradiation and high temperatures) and the intrinsic group-transfer mechanism hampered the generalization of this strategy. This explains why only a few examples of acyl radical processes using xanthate precursors have been reported so far.[16]

[16] (a) Zard, S. Z., On the Trail of Xanthates: Some New Chemistry from an Old Functional Group. *Angew. Chem. Int. Ed.* **1997**, *36*, 672-685. (b) Heinrich, M. R.; Zard, S. Z., Generation and Intermolecular Capture of Cyclopropylacyl Radicals. *Org. Lett.* **2004**, *6*, 4969-4972.

Aside from sulfur derivatives, tellurides and selenides have also been studied in acyl radical transformations.[3] Compared to thioesters, these substrates have a weaker C-X bond, which are suitable for stannane-based radical chain mechanisms. Nevertheless, applications were limited by the need to synthesize acyl chalcogen derivatives in stoichiometric amounts using potentially harmful and toxic reagents. Interestingly, acyl tellurides can also undergo photolysis by absorbing visible light, thus promoting different transformations, such as radical cyclizations via group transfer mechanism (Scheme 3.8), under mild conditions.[5c] The photolysis of the acyl telluride is achieved under white light irradiation delivering acyl radicals **XI**. This open-shell species undergoes fast 5-*exo-trig* cyclization to form the alkyl radical **XII**, which after group transfer gives product **16** and another molecule of radical **XI**, propagating the chain process.

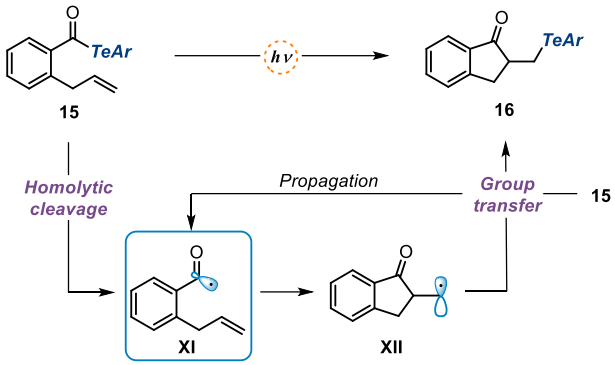

Scheme 3.8. Photoinduced acyl radical cyclization of acyl tellurides.

3.2.5 Use of acylcobalt salophen complexes

Organocobalt Co(III) derivatives have a tendency towards photolytic scission.[17] This prompted Pattenden and co-workers to study the capability of acylcobalt salophen complexes to generate acyl radicals under light excitation.[18,19] Acylcobalt complexes can be easily obtained by nucleophilic substitution of a suitable acyl electrophile. Isolated acylcobalt complex can be activated by white light to cleave the C-Co bond, releasing the fleeting radical **III** which is trapped by a suitable electron deficient olefin to form radical **XIII**. The latter

[17] Schrauzer, G. N.; Sibert, J. W.; Windgassen, R. J., Photochemical and thermal cobalt-carbon bond cleavage in alkylcobalamins and related organometallic compounds. Comparative study. *J. Am. Chem. Soc.* **1968**, *90*, 6681-6688.
[18] Coveney, D. J.; Patel, V. F.; Pattenden, G.; Thompson, D. M., Acylcobalt salophen reagents. Precursors to acyl radical intermediates for use in carbon-to-carbon bond-forming reactions to alkenes. *J. Chem. Soc., Perkin Trans. 1*, **1990**, 2721-2728.
[19] Patel, V. F.; Pattenden, G.; Thompson, D. M., Cobalt-mediated reactions in synthesis. The degradation of carboxylic acids to functionalised noralkanes via acylcobalt salophen intermediates**.** *J. Chem. Soc., Perkin Trans. 1*, **1990**, 2729-2734.

radical undergoes group transfer with another molecule of **17**, propagating the chain. Organocobalt species **19** can then produce a mixture of products **20** and **21**.

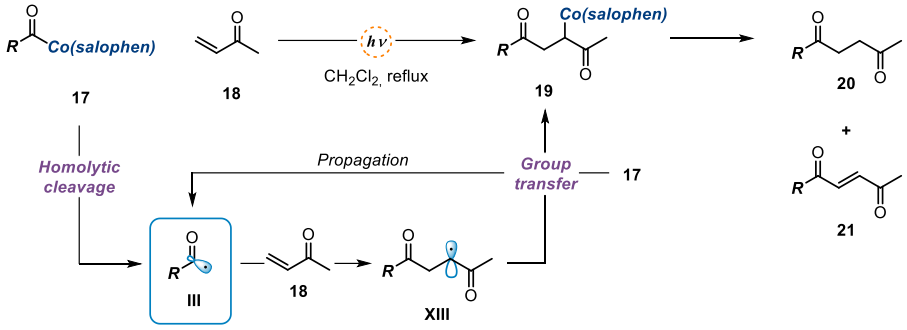

Scheme 3.9. Acylcobalt salophen complexes as an acyl radical source.

Overall, all the discussed methods for acyl radical formation required a stoichiometrically formed radical precursor bearing a purposely designed functional group.

3.3 Catalytic formation of acyl radicals

Recent efforts focused on the development of catalytic strategies to access acyl radicals. In particular, photoredox catalysis provided an effective tool to translate previous stoichiometric approaches into a catalytic regime.[7] We could classify the access to acyl radicals by means of photoredox catalysis in three different categories (Scheme 3.10), which are briefly discussed below.

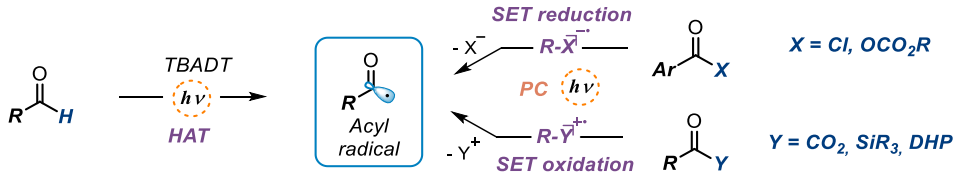

Scheme 3.10. Catalytic formation of acyl radicals by photoredox catalysis.

3.3.1 Photoredox-catalyzed HAT methods

HAT processes represent the most straightforward and atom economical source of acyl radicals. When applying photoredox catalysts, the main advantage, besides the mild reaction conditions offered, relies on the possiblity to avoid the need for a radical chain mechanism. One of the most widely used photocatalysts for HAT is tetrabutylammonium decatungstate (TBADT), which upon light absorption (λ_{max} = 365 nm), acquires the ability to abstract a

hydrogen atom from relatively inert C-H bonds, including alkanes, ethers, and carbonyl derivatives, such as aldehydes.[8,20] In the example in Scheme 3.11, TBADT is excited by light and abstracts a hydrogen from aldehyde **6**. The resulting acyl radical **III** is then trapped by acrylonitrile **22** delivering the radical **XIV**. Finally, the reduced form of TBADT can trigger an SET reduction leading to ketone **23** while closing the photoredox catalytic cycle.

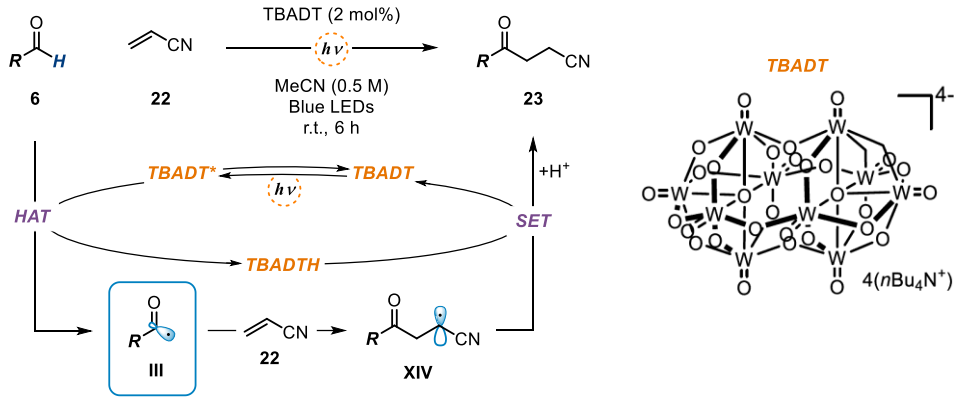

Scheme 3.11. TBADT-catalyzed HAT from aldehydes.

3.3.2 Photoredox-catalyzed SET reduction

Acyl electrophiles are widely exploited as acyl radical precursors. Aromatic acid chlorides and anhydrides can be reduced by a suitable photoredox catalyst and, upon fragmentation, an acyl radical **III** can be released. In an early example of this photoredox strategy, carboxylic acid **24** reacted with dimethyl dicarbonate (DMDC) to form anhydride **26** in situ (Scheme 3.12).[21] An excited iridium photocatalyst could then reduce the anhydride (E_{red} = -1.74 V vs SCE), delivering a radical anion which underwent fragmentation to produce radical **XV**. Then, radical **XV** added to olefin **25**, giving intermediate **XVI** which cyclized to form intermediate **XVII**. Finally, the oxidized photocatalyst Ir(IV) oxidized **XVII**, which after deprotonation delivered product **27** while closing the photoredox cycle. Even though acyl electrophiles are broadly available by one-step activation of carboxylic acids, the main drawback of this strategy remains on the high reduction potential of the alkyl derivatives, which limits the methodology to aryl substituents.

[20] Tzirakis, M. D.; Lykakis, I. N.; Orfanopoulos, M. Decatungstate as an efficient photocatalyst in organic chemistry. *Chem. Soc. Rev.* **2009**, *38*, 2609-2621.
[21] Bergonzini, G.; Cassani, C.; Wallentin, C.-J., Acyl Radicals from Aromatic Carboxylic Acids by Means of Visible-Light Photoredox Catalysis. *Angew. Chem. Int. Ed.* **2015**, *54*, 14066-14069.

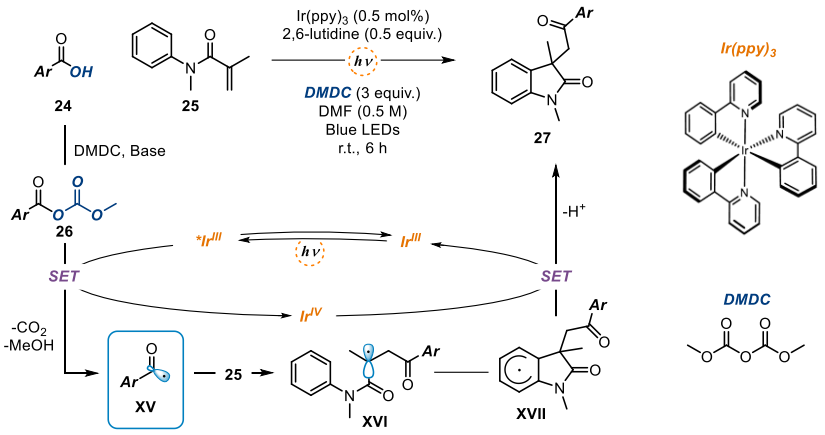

Scheme 3.12. SET reduction of acyl electrophiles to generate acyl radicals with a photoredox catalyst.

3.3.3 Photoredox-catalyzed SET oxidation

Most oxidative methods to access acyl radicals rely on two strategies: the use of a stoichiometric oxidant, where the photocatalyst acts as a mere initiator of a radical chain;[22] or the use of purposely designed precursors bearing a redox active auxiliary, usually needing several synthetic steps to install them.[9] For example, Wang and co-workers[23] reported that, upon light excitation, the Ir photocatalystis can oxidize α-ketoacid **11** via SET (Scheme 3.13).

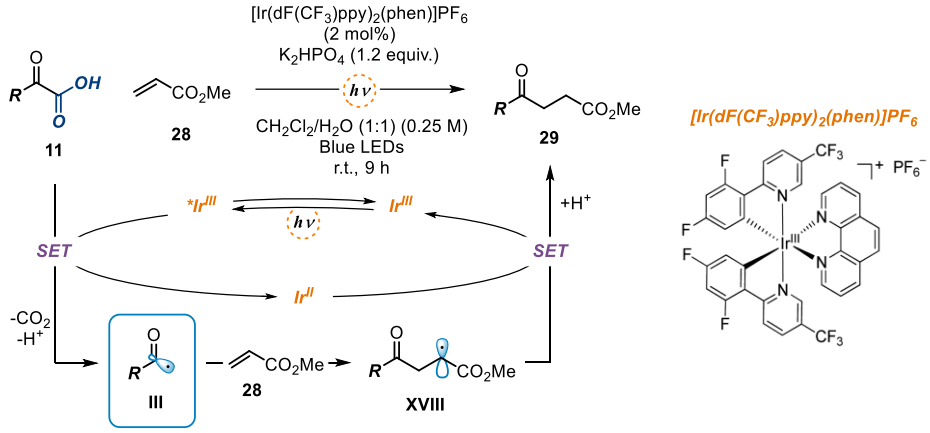

Scheme 3.13. SET oxidation of α-ketoacids with a photoredox catalyst.

[22] For selected examples see: (a) Li, J.; Zhang, J.; Tan, H.; Wang, D. Z., Visible-Light-Promoted Vinylation of Tetrahydrofuran with Alkynes through Direct C–H Bond Functionalization. *Org. Lett.* **2015**, *17*, 2522-2525. (b) Cheng, P.; Qing, Z.; Liu, S.; Liu, W.; Xie, H.; Zeng, J., Regiospecific Minisci acylation of phenanthridine via thermolysis or photolysis. *Tetrahedron Lett.* **2014**, *55*, 6647-6651.

[23] Wang, G.-Z.; Shang, R.; Cheng, W.-M.; Fu, Y., Decarboxylative 1,4-Addition of α-Oxocarboxylic Acids with Michael Acceptors Enabled by Photoredox Catalysis. *Org. Lett.* **2015**, *17*, 4830-4833.

After decarboxylation, the acyl radical **III** is formed, which then reacts with the Michael acceptor **28**. The reduced form of the Ir photocatalyst can then reduce radical **XVIII**, which is ultimately protonated to deliver the Giese addition product **29**.

3.4 Target of the project

The aim of the project discussed in this chapter is to further expand the scope of electrophiles available for the photochemical radical generation strategy based on the use of our newly developed dithiocarbamate (DTC) nucleophilic organic catalysts. To date, our strategy was limited to substrates amenable to an S_N2 substitution. In this project, we envisioned to apply this photochemical catalytic approach to nucleophilic acyl substitution. This substitution manifold would allow us to access acyl and carbamoyl radicals upon activation of simple acyl electrophiles, including chlorides and anhydrides. Since the system does not rely on the reduction potential of the substrates, our strategy could broaden the scope of acyl and carbamoyl radicals to include aliphatic ones.

I will mainly discuss the conception of the strategy, its application for the generation of acyl radicals, and the study of its mechanism, since those are the aspects of the project I was directly involved in.

3.4.1 Design plan

The proposed mechanism for the photochemical catalytic generation of acyl radicals from the corresponding chlorides is depicted in Scheme 3.14. This initial mechanistic picture was based on our previous work dealing with the S_N2 activation of alkyl electrophiles (discussed in Chapter II). By analogy, we envisioned a catalytic cycle where the dithiocarbamate nucleophilic organic catalyst would activate acyl chlorides **4** by means of a nucleophilic acyl substitution path. The resulting acyl adduct **5** possesses a weak C–S bond, which could be cleaved by visible-light irradiation to generate open-shell species **III** and the dithiocarbonyl radical **I**. The feasibility of this crucial step finds support in the pioneering studies by Barton and Zard,[5] who demonstrated the tendency of stoichiometric acyl xanthates to undergo photolysis affording acyl radicals. These previously reported strategies required the use of stoichiometric preformed intermediates **5** and were characterized by a group transfer mechanism.[24] Overall, they found limited application in processes involving acyl radicals, mainly because of the tendency to generate alkyl radicals upon decarbonylation. Our goal was to implement a general and effective catalytic system, which synthetically was not limited within the constraints of a group transfer mechanism, to generate acyl radicals (including aliphatic ones) using blue light irradiation to trigger the photolysis of the catalytic intermediate **5**. Specifically, we surmised that upon photolysis the generated acyl radical **III**

[24] Heinrich, M. R.; Zard, S. Z., Generation and Intermolecular Capture of Cyclopropylacyl Radicals. *Org. Lett.* **2004**, *6*, 4969-4972.

would be intercepted by an electron-poor olefin **31** to forge a new C–C bond. The emerging electrophilic radical **XV** would then abstract a hydrogen atom from γ-terpinene (a H donor), thus forming the final product **32** and the cyclohexadienyl radical **XVI**. Crucial for catalyst turnover would be an SET reduction of the dithiocarbonyl radical **I** from the cyclohexadienyl radical **XVI**, which would eventually close the DTC cycle by restoring the catalyst (for example, ethyl xanthogenate anion has a reduction potential E_{red} of 0.75 V vs SCE) from the cyclohexadienyl radical **XVI** (E_{red} = -0.1 V vs SCE).[2]

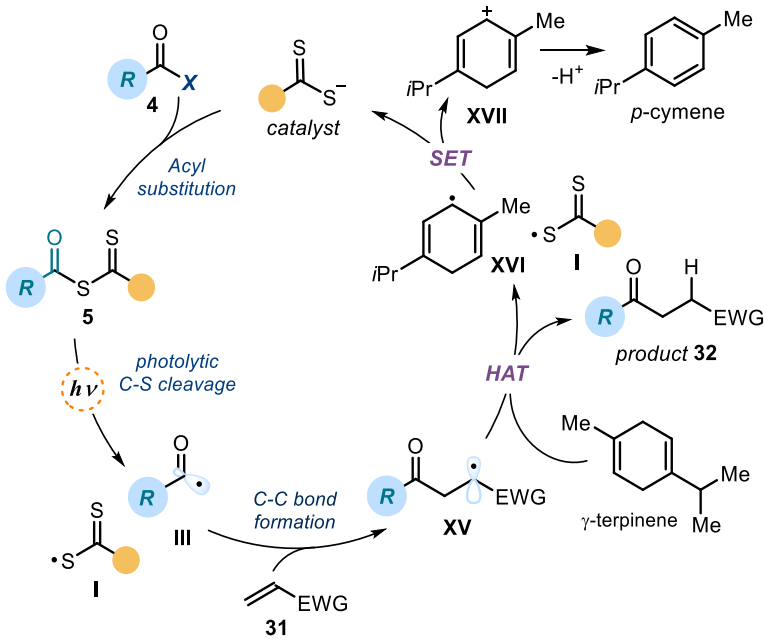

Scheme 3.14. Design plan for a catalytic system that uses acyl electrophiles as radical precursors.

3.5 Results and discussion

To test the feasibility of our strategy, we used the commercially available benzoyl chloride **4a** as the acyl radical precursor and acrylonitrile **31a** as the radical trap (Table 3.1). The experiments were conducted at 60 °C in dichloromethane (DCM) using a blue LED strip emitting at 465 nm, γ-terpinene as the H donor (3 equiv.), and 10 mol% of the nucleophilic DTC organic catalyst. Na_3PO_4 (2 equiv.) was used to neutralize the hydrochloric acid generated during the process. Surprisingly, the indole-based dithiocarbamate anion catalyst

A, which was successful in our previous studies,[2,25,26,27] provided poor results and was not suitable for the generation of acyl radicals (entry 1). We then used the commercially available potassium ethyl xanthate catalyst **B**.

Table 3.1. Optimization studies

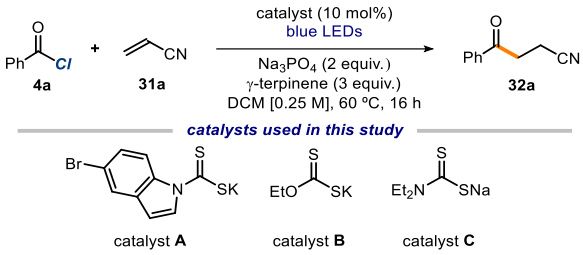

entry	catalyst	deviation	yield **32a** (%)[a]
1	**A**	none	7
2	**B**	none	83 (82)[b]
3	**C**·3H_2O	none	34
4	**C**	none	86
5	**B**	40 °C	40
6	**B**	under air	60
7	**B**	no light	0
8	none	none	0

Reactions performed on a 0.5 mmol scale at 60 °C for 16 h using 2.0 mL of DCM under illumination by a blue LED strip (λ_{max} = 465 nm, 14 W) and using catalyst (10 mol%), 1.5 equiv. of **1a**, and 2 equiv. of Na_3PO_4. [a] Yield determined by ^{1}H NMR analysis of the crude mixture using trichloroethylene as the internal standard. [b] Yield of the isolated product **3a**. LED: Light-emitting diode.

Importantly, the xanthate catalyst **B** provided the target product **32a** in high chemical yield (entry 2). The commercially available sodium diethyldithiocarbamate **C**, in its hydrated form (**C**·3H_2O), was not suitable for this transformation due to the hydrolysis of the acyl chloride to the corresponding acid (entry 3). However, when we synthesized catalyst **C** as an anhydrous salt, it displayed a high catalytic activity (entry 4). Based on these results, we selected the commercially available xanthate catalyst **B** for further investigations. The reaction efficiency was affected by a lower temperature and by the presence of air, but synthetically useful yields were still achieved (entries 5 and 6, respectively). Control experiments showed the need for

[25] Cuadros, S.; Horwitz, M. A.; Schweitzer-Chaput, B.; Melchiorre, P., A visible-light mediated three-component radical process using dithiocarbamate anion catalysis. *Chem. Sci.* **2019**, *10*, 5484-5488.
[26] Mazzarella, D.; Magagnano, G.; Schweitzer-Chaput, B.; Melchiorre, P. Photochemical Organocatalytic Borylation of Alkyl Chlorides, Bromides, and Sulfonates. *ACS Catal.* **2019**, *9*, 5876–5880.
[27] Spinnato, D.; Schweitzer-Chaput, B.; Goti, G.; Ošeka, M.; Melchiorre, P., A Photochemical Organocatalytic Strategy for the α-Alkylation of Ketones by using Radicals. *Angew. Chem. Int. Ed.* **2020**, *59*, 9485-9490.

light and for the nucleophilic catalyst (entries 7 and 8). With the optimized conditions in hand (entry 2, Table 3.1), we tested the possibility of using other acyl electrophiles in addition to acyl chlorides as the radical precursors. We first evaluated benzoic anhydride **4b**, but only moderate yield of the acylation product **32a** could be achieved (Scheme 3.15a). Next, we turned our attention to unsymmetrical anhydride **4c**, which could be conveniently prepared by reaction of benzoic acid and ethyl chloroformate and directly used upon simple filtration. When submitting anhydride **4c** to the reaction conditions, a slight increase of catalyst loading was needed to afford product **32a** in a yield comparable to that using acyl chlorides (Scheme 3.16b). This simple procedure avoids the need for an external base, since the ethoxide anion generated during the process can act as the base. Overall, this sequence allows the direct use of easily available carboxylic acids as acyl radical precursors.

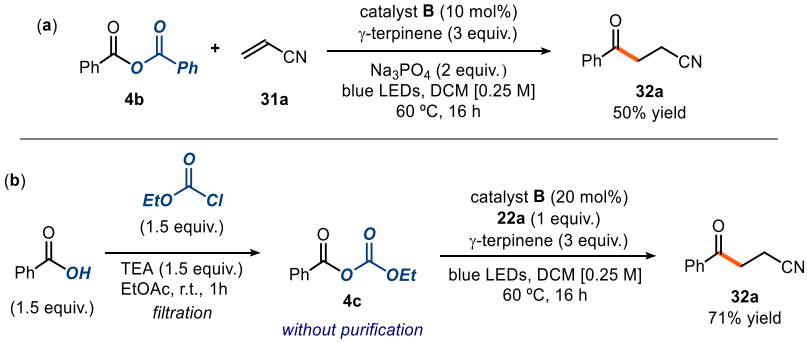

Scheme 3.15. Use of other acyl radical precursors: (a) benzoic anhydride; (b) sequential procedure for the formation of anhydride **4c** from benzoic acid and the ensuing acyl radical chemistry.

We then evaluated the scope of our newly developed catalytic acyl radical generation strategy (Scheme 3.17). In general, the reaction proceeded smoothly leading to the exclusive formation of the desired acylation products. Decarbonylation was exclusively observed when employing particular acyl chlorides, e.g. when a stable radical (benzylic or tertiary) could be formed upon fragmentation. The main by-products formed during the process, which accounted for the moderate yields observed in some examples, arose from the dimerization of the acyl radicals and, sometimes, from the formation of the corresponding aldehydes via an HAT process, presumably from γ-terpinene. We first focused on the scope of the electron-poor olefins as radical traps. We chose *para*-methoxy benzoyl chloride as acyl radical precursor to facilitate purification of the products; however, comparable yields were obtained when using unbiased benzoyl chlorides as substrates (e.g., **32a**, **32b**). A wide variety of olefins, including internal alkenes, delivered the product in synthetically useful yields (products **32a-n**). We then set out to study suitable acyl radical precursors. Aroyl chlorides bearing both electron-poor (products **33b-c**, **33e**) and electron-rich substituents (**32b**, **33f**, **33g**) provided the desired ketone

products in useful yields. Acyl chlorides with highly hindered moieties (**33e**, **33h**) and heterocycles in their structure (**33f**, **33g**, **33h**), which are common scaffolds in medicinal chemistry,[28] were also successfully functionalized through this transformation.

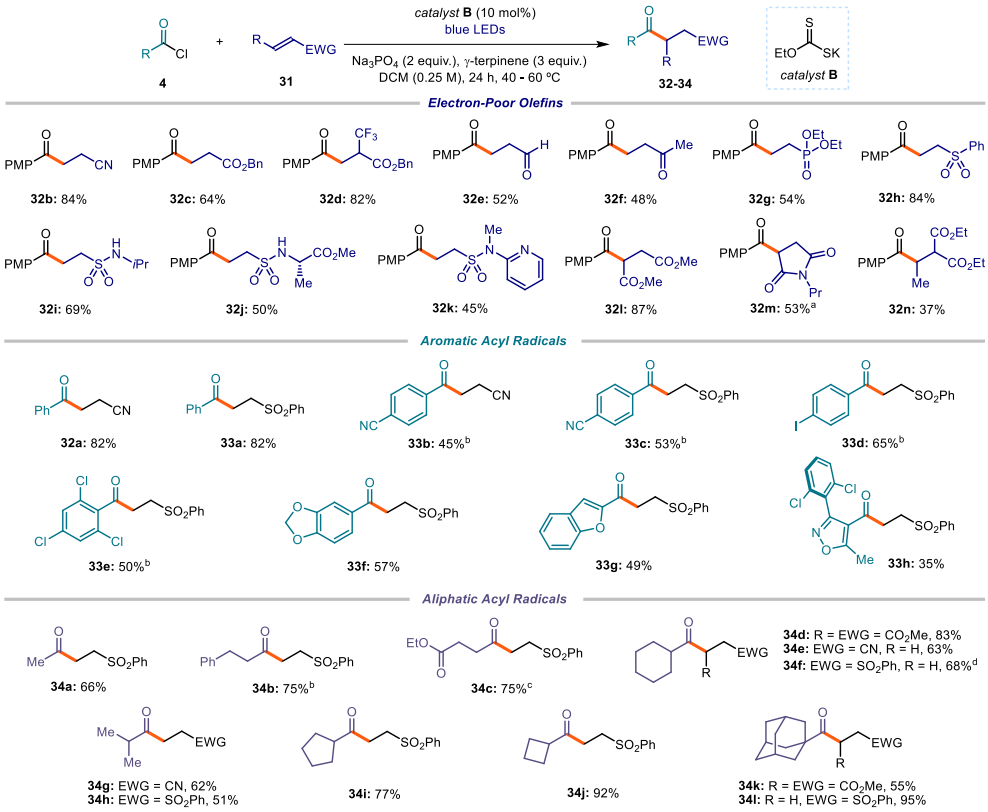

Scheme 3.16. Photochemical catalytic generation of acyl radicals from chloride precursors and their use in Giese addition processes. Reactions performed on a 0.5 mmol scale using 1.5 equiv. of acyl chloride **4** and 2.0 mL of dichloromethane (DCM); yields of products refer to isolated materials after purification; the bold orange bond denotes the newly formed C-C bond. Unless otherwise indicated, reactions with aromatic acyl radical precursors were performed at 60 °C, and with aliphatic acyl radical precursors at 40 °C. [a] Yield measured by ^{1}H NMR analysis using trichloroethylene as the internal standard. [b] Reaction time: 60 h. [c] Reaction temperature: 60 °C. [d] Product isolated as a 6:1 mixture with the olefin substrate; the corrected yield is reported. PMP: *p*-Methoxyphenyl; Pr: propyl; EWG: electron-withdrawing group.

More importantly, due to the unique activation mechanism of this radical generation strategy, aliphatic acyl chlorides, which are recalcitrant to SET activation strategies due to their high redox potential, could also be readily activated by the xanthate catalyst **B** to give the corresponding radicals. Primary (products **34a-c**), secondary (**34d-j**), and bridged tertiary

[28] Blakemore, D. C.; Castro, L.; Churcher, I.; Rees, D. C.; Thomas, A. W.; Wilson, D. M.; Wood, A., Organic synthesis provides opportunities to transform drug discovery. *Nature Chem.* **2018**, *10*, 383-394.

(**34k-l**) acyl electrophiles reacted with Michael acceptors to afford products **34** in moderate to excellent yields. Since our strategy relies on different properties of the substrates compared to previously reported procedures (HAT, SET), it tolerates functionalities that could lead to selectivity issues. For example, aldehydes (product **32e**), iodides (**33d**), and dioxolanes (**33f**) smoothly reacted under the optimized conditions. As a limitation of the system (Scheme 3.18), benzylic, non-bridged tertiary and aminoacid derivative acyl electrophiles were not suitable substrates, undergoing fast decarbonylation and releasing the corresponding alkyl radical. Other hetero(arenes), such as ferrocene, thiophene or pyridine did not deliver the product. Finally, intramolecular trap of the acyl radical was unsuccessful.

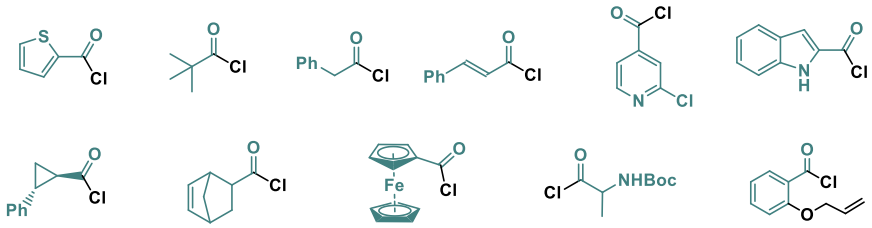

Scheme 3.17. Unsuccessful substrates.

In order to make our catalytic platform as useful and straightforward as possible, we implemented a two-step telescoped sequence to form acyl chlorides **4** in situ and use them without any further purification (Scheme 3.18a). This allowed us to access functionalized acyl radical precursors from commercially available carboxylic acids upon simple treatment with oxalyl chloride. For example, a highly functionalized heteroarene derivative could be used as radical precursors (product **35a**). Alkyl derivatives bearing another electrophilic position selectively reacted at the acyl moiety under the optimized conditions (adduct **35b**). Moreover, acyl radical precursors with rings of different sizes and adorned with several heteroatoms and functionalities (products **35c-h**) successfully delivered the corresponding products upon Giese reaction with electron-poor olefins.

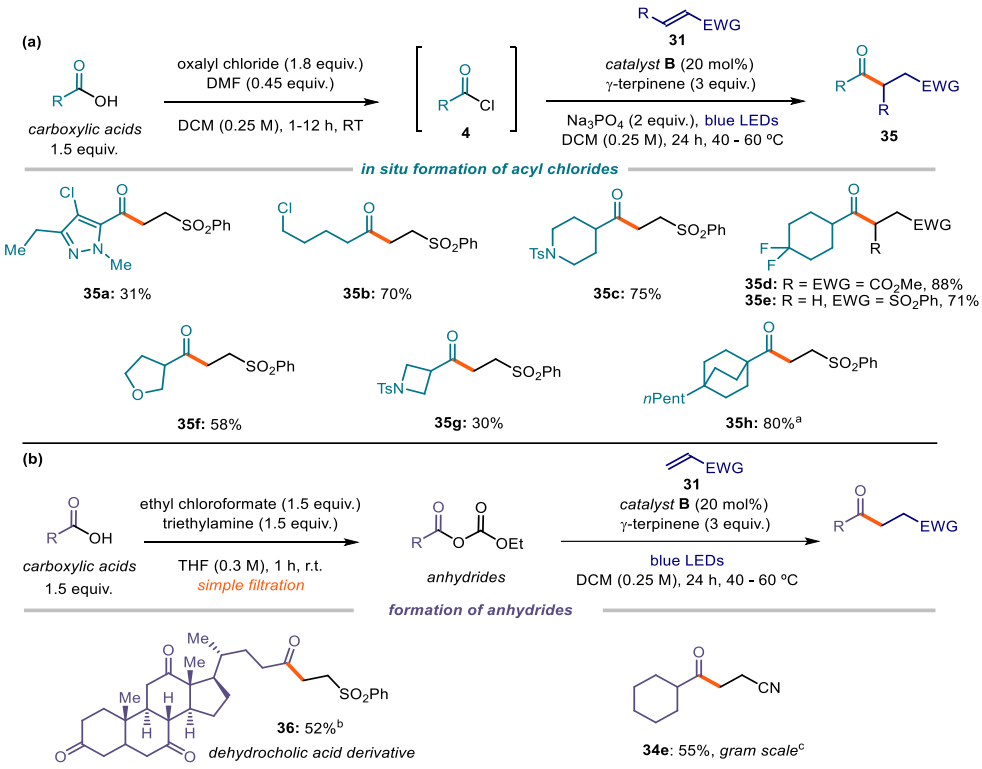

Scheme 3.18. Photochemical catalytic generation of acyl radicals from carboxylic acids upon a) in situ preparation of acyl chlorides. b) sequential formation of anhydrides. Reactions performed on 0.5 mmol scale using 1.5 equiv. of **4** and 2.0 mL of dichloromethane; yields of products refer to isolated material after purification; the bold orange bond denotes the newly formed C-C bond. Unless otherwise indicated, all entries with aromatic acyl radical precursors were performed at 60 °C, and with aliphatic acyl radical at 40 °C. [a] Yield calculated by ^{1}H NMR using trichloroethylene as internal standard. [b] Reaction temperature: 60 °C. [c] 30 mol% of catalyst **B**. Ts: Tosyl, EWG: electron-withdrawing group.

In a different procedure, as discussed above in Scheme 3.15, we showed that unsymmetrical anhydrides could be generated by reaction of carboxylic acids and ethyl chloroformate. Upon simple filtration, and without further purification, they are then activated by catalyst **B** to form an acyl radical. This approach may offer a powerful alternative when using substrates bearing functionalities that are incompatible with the generation of acyl chlorides. For example, the natural product dehydrocholic acid, which did not react under the conditions reported in Scheme 3.18a, could be effectively functionalized to afford product **36** upon treatment with ethyl chloroformate and formation of its mixed anhydride (Scheme 3.18b). This procedure was also suitable for a gram-scale synthesis of adduct **34e** starting from the carboxylic acid substrate: using common laboratory glassware and a simple set-up, 1.13 grams of product **5e** (55% yield) could be obtained.

3.6 Carbamoyl radicals[29]

3.6.1 Intermolecular Giese type addition

We envisioned that the photochemical strategy detailed in the previous section could also be useful to access carbamoyl radicals. Carbamoyl chlorides **37** are not amenable to SET reduction, due to their high reduction potential (see Section 3.9.10.7 for their electrochemical characterisation). Nevertheless, they are good electrophiles that can engage in acyl substitution reactions. In our photochemical strategy, activation of **37** with the nucleophilic catalyst would lead to carbamoyl dithiocarbamate derivatives **5**. These intermediates can undergo homolytic cleavage upon light excitation (Scheme 3.19).

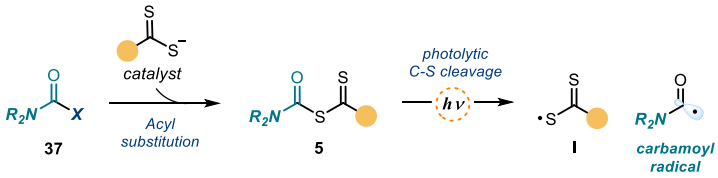

Scheme 3.19. Activation of carbamoyl chlorides

Translating this system into a catalytic manifold required some optimization (Table 3.2).

Table 3.2. Screening of the Catalysts

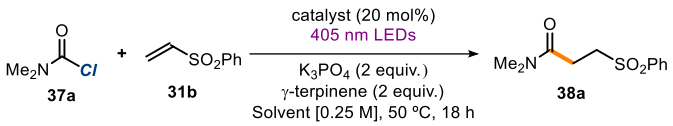

catalysts used in this study

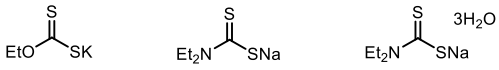

catalyst **B** | catalyst **C** | catalyst **C**·$3H_2O$

entry	catalyst	deviation	Solvent	yield **38a** (%)
1	**C**·$3H_2O$	none	MeCN	60
2	**B**	460 nm, Na_3PO_4	DCM	Traces
3	**B**	Na_3PO_4	DCM	10
4	**C**·$3H_2O$	Na_3PO_4	DCM	11
5	**C**·$3H_2O$	Na_3PO_4	MeCN	20

Reactions performed on a 0.2 mmol scale; yield determined by ^1H NMR analysis of the crude reaction mixture using trichloroethylene as the internal standard.

[29] The experimental work detailed in this section was performed by Daniele Mazzarella and Matteo Balletti.

Due to the reduced electrophilicity of carbamoyl chlorides **37** compared to their acyl counterparts, the more nucleophilic dithiocarbamate catalyst **C**·3H_2O provided the best results (entry 1). Another crucial change was the irradiation wavelength: while acylxanthates efficiently absorb at 460 nm, carbamoyl dithiocarbamate derivatives required a lower wavelength and 405 nm irradiation (entry 3). With the optimized conditions in hand (entry 1), we explored the scope of the reaction.

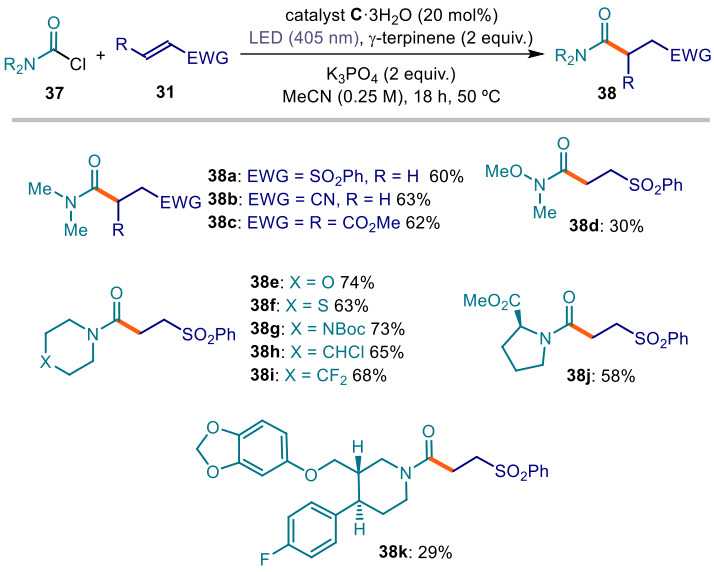

Scheme 3.20. Photochemical catalytic generation of carbamoyl radicals from the chloride precursors and their use in intermolecular Giese addition processes. Reactions performed on a 0.2 mmol scale using 2 equiv. of γ-terpinene and 0.8 mL of acetonitrile; yields of products refer to isolated material after purification; the bold orange bond denotes the newly formed C-C bond.

The results summarized in Scheme 3.20 illustrate the potential of this catalytic method to generate carbamoyl radicals from chloride precursors **37** and their synthetic application in Giese addition processes. Different electron-poor olefins smoothly reacted with dimethylcarbamoyl chloride to furnish the corresponding amides (products **38a**-**39c**). A variety of carbamoyl chlorides could be successfully used, including substrates containing synthetically useful scaffolds such as the Weinreb's amide (**38d**), carbamates, esters, fluorine atoms and rings of different sizes (**38e-i**). Since substrates containing substituted piperidines proved suitable for this transformation, we tested the reactivity of a piperidine-containing pharmaceutically active carbamoyl chloride, smoothly obtaining the paroxetine derivative **38k**. In general, when low yields were obtained, this was due to partial degradation of the catalyst or formation of by-products arising from dimerization or H-abstraction (HAT process) of the carbamoyl radicals.

3.6.2 Lactam synthesis through carbamoyl radical-based cyclizations

We then developed a cyclization triggered by the generated carbamoyl radicals for the straightforward synthesis of β-lactams (Scheme 3.21).[30] Carbamoyl chlorides **39** bearing a double bond in the alkyl chain attached to the nitrogen were prepared. These substrates reacted with the dithiocarbamate catalyst **C** to release the carbamoyl radical upon photolysis and undergo radical cyclization to deliver lactams **40** (Scheme 3.21). By using the optimized conditions and simply adjusting the amount of γ-terpinene (1.5 equivalents) to avoid formation of the correspondent formamide, we could efficiently convert substrates **39** into the corresponding β-lactams fused with a 6-membered ring (**40a**).

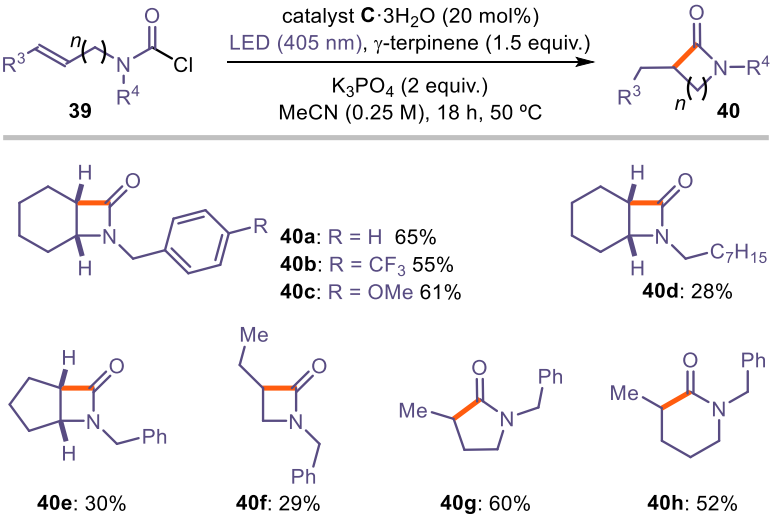

Scheme 3.21. Carbamoyl radical formation and intramolecular processes. Reactions performed on a 0.2 mmol scale using 0.8 mL of acetonitrile; yields of products refer to isolated material after purification; the bold orange bond denotes the newly formed C-C bond.

Since our strategy does not rely on the redox potential of the substrate, both electron-withdrawing (**40b**) and electron-donating (**40c**) substituents at the nitrogen atom performed well. Additionally, a carbamoyl chloride bearing a simple alkyl chain on the nitrogen also delivered the product, albeit with a lower yield compared to the benzyl substituent (**40d**). The method is amenable to the synthesis of a variety of β-lactams, fused to a 6-membered, a 5-membered (**40e**), or without any fused ring (**40f**). Not fused lactams of different sizes could also be obtained in good yields (**40g**, **40h**).

[30] Betou, M.; Male, L.; Steed, J. W.; Grainger, R. S., Carbamoyl Radical-Mediated Synthesis and Semipinacol Rearrangement of β-Lactam Diols. *Chem. Eur. J.* **2014**, *20*, 6505-6517.

3.7 Mechanistic studies

We first approached the mechanistic studies considering our related work for the activation of alkyl halides discussed in Chapter II (Scheme 3.22). In our original mechanistic proposal, we identified three critical features of the system: (i) the ability of the nucleophilic organic catalyst to activate substrates upon nucleophilic attack; (ii) the photoactivity of the ensuing intermediate of type **5**, which can undergo photolytic cleavage upon visible light absorption; and (iii) the ability of the emerging sulfur-centered radical **I** to undergo SET reduction from the cyclohexadienyl radical **XVI**, which represents the turnover event of the proposed catalytic cycle. While evidence in support of points (i) and (ii) were collected in our previous studies, other important mechanistic questions remained unanswered. For example, the proposed catalyst turnover step (point iii) requires an SET event between two fleeting radical intermediates, which is an unlikely scenario. In addition, xanthates and thiocarbamates of type **5** have a great tendency to participate in group transfer manifolds, and it is not clear whether this mechanistic path could play an important role in our catalytic system too.

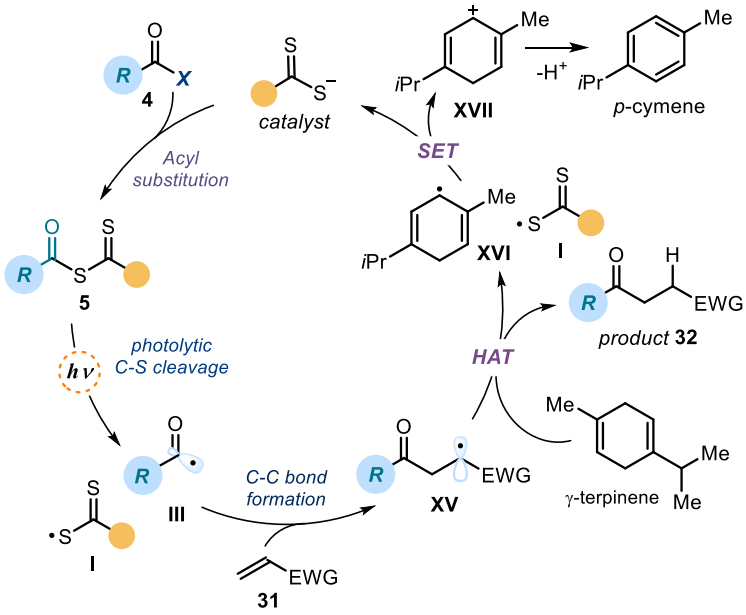

Scheme 3.22. Simplified mechanistic proposal for the generation of acyl radicals.

We therefore performed extensive mechanistic investigations on the catalytic activation of acyl chlorides **4** by the xanthate catalyst **B** and the ensuing Giese addition. Our reasoning was that this process might serve as a suitable probe for testing the mechanism and elucidating unclear aspects, thus providing general information on this radical generation strategy.

In order to shine light on our catalytic platform, we selected the model reaction between benzoyl chloride **4a** and acrylonitrile **31a** promoted by catalyst **B** to perform extensive mechanistic investigations (Scheme 3.23).

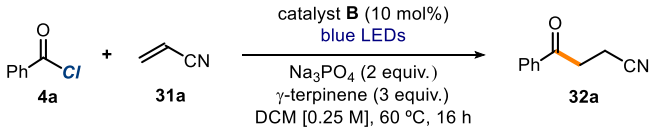

Scheme 3.23. Model reaction for the mechanistic investigation.

In the following sections, I will describe how we carried out a step-by-step study of the catalytic cycle and the characterisation of relevant intermediates, and how we used this knowledge to propose a more complete mechanistic picture of our strategy.

3.7.1 Acyl substitution and photochemical behavior of intermediate **5**

The first step of the proposed mechanism consists of the nucleophilic substitution between potassium ethyl xanthogenate (catalyst **B**) and benzoyl chloride **4a** to form intermediate **5a** (Scheme 3.24a). Catalyst **B** performs a smooth nucleophilic substitution on **4a**, as expected by its high nucleophilicity according to the Mayr's reactivity scale,[31] affording intermediate **5a**. To confirm that intermediate **5a** could absorb light in the visible region, we performed UV/Vis spectroscopic studies of an authentic sample of the compound (Figure 3.1).[5,32]

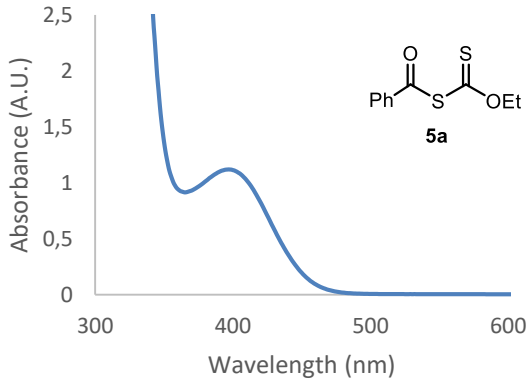

Figure 3.1. UV-Vis absorption spectrum of **5a** recorded at $1 \cdot 10^{-2}$ M concentration in acetonitrile.

[31] Duan, X.-H.; Maji, B.; Mayr, H., Characterization of the nucleophilic reactivities of thiocarboxylate, dithiocarbonate and dithiocarbamate anions. *Org. Biomol. Chem.* **2011**, *9*, 8046-8050.
[32] Lalevée, J.; Blanchard, N.; El-Roz, M.; Allonas, X.; Fouassier, J. P., New Photoiniferters: Respective Role of the Initiating and Persistent Radicals. *Macromolecules* **2008**, *41*, 2347-2352.

Irradiation of intermediate **5a** formed in situ in the presence of 2,2,6,6-tetramethylpiperidine 1-oxyl (TEMPO), a radical trap, delivered the TEMPO adduct **41**, which we could isolate and characterize (Scheme 3.24b). This experiment indicated that intermediate **5a**, which absorbs light in the visible region, could generate the benzoyl radical **IIa** upon illumination by a blue LED. In addition, almost complete inhibition of reactivity was observed when conducting the rectaion in the presence of TEMPO, which acted as radical scavenger (Scheme 3.24c). This experiment indicated the radical nature of the process.

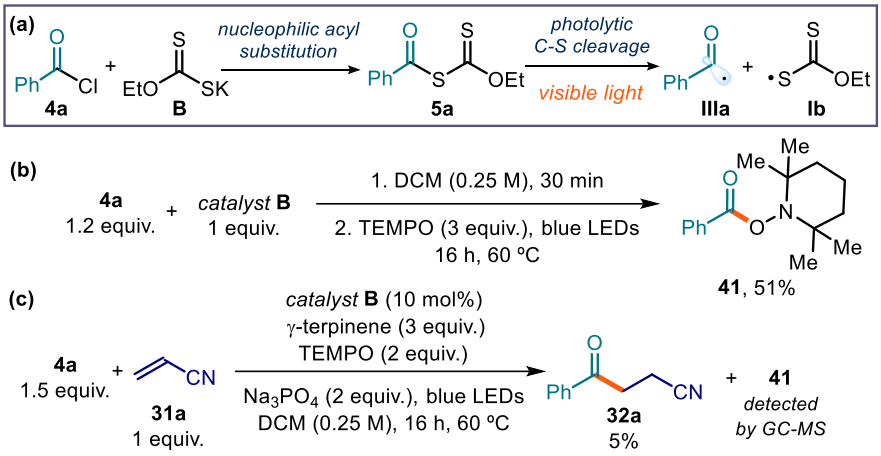

Scheme 3.24. The possible role of the acylxanthate **5a**. Mechanistic experiments to probe that a) **5a** is an active reaction intermediate; b) the benzoyl radical **IIIa** is generated during the process; and c) the model reaction is inhibited by a radical scavenger.

To corroborate that the light-induced homolytic cleavage of **5a** was the key acyl radical generation step (Scheme 3.24a), we used laser flash photolysis to detect the transient formation of the sulfur-centered radical **Ib**. Chiba and coworkers[33] reported that xanthyl radical **I** shows a characteristic absorption peak with maximum at 620 nm. Accordingly, when a freshly prepared authentic sample of intermediate **Ia** was excited with a laser beam centered at 355 nm, we observed the formation of a transient species absorbing at 620 nm (half lifetime = 0.1 ± 0.01 ms), consistent with the characteristic line shape of xanthyl radical **Ib** (Figure 3.2a). Moreover, when the irradiation wavelength was switched to a lower energy (460 nm, more similar to the reaction conditions), formation of the same transient was detected (Figure 3.2b).

[33] Kaga, A.; Wu, X.; Lim, J. Y. J.; Hayashi, H.; Lu, Y.; Yeow, E. K. L.; Chiba, S., Degenerative xanthate transfer to olefins under visible-light photocatalysis. *Beilstein J. Org. Chem.* **2018**, *14*, 3047-3058.

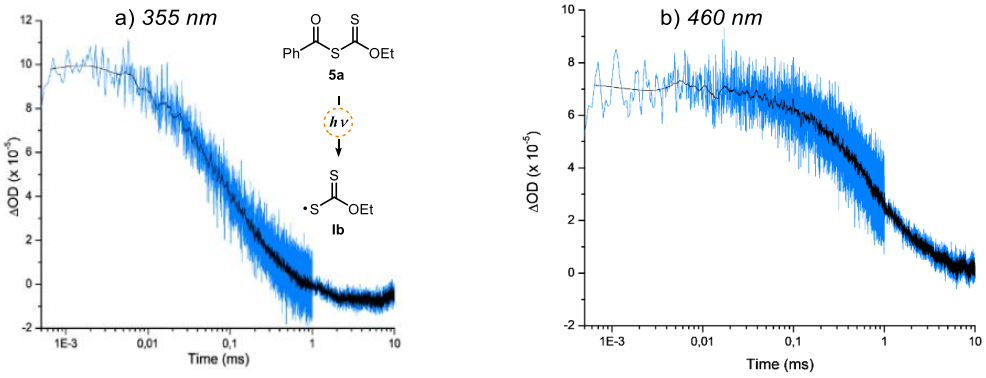

Figure 3.2. Transient absorption spectroscopic studies: absorption at 620 nm of the transient xanthyl radical **Ib** generated upon laser excitation of acylxanthate **5a** ($[\mathbf{5a}]_0$ = 3x10^{-3} M in CH_3CN); absorption decay (black line) processed through Savinsky Golay filter to facilitate lifetime measurement. Note logarithmic scale for time; ΔOD: optical density variation. a) Irradiation wavelength: 355 nm; b) Irradiation wavelength: 460 nm.

We also used electron paramagnetic resonance (EPR) as an analytical technique to directly detect the benzoyl radical **IIIa**, generated upon irradiation of intermediate **5a**. Instead, when a solution of compound **5a** in toluene was irradiated by a mercury lamp, a different radical species was observed (Figure 3.3a). The characteristic signal of the benzoyl radical **IIIa** should be a singlet.[34a] However, the EPR spectrum showed a sharp triplet (centered at 3505 G, g-value = 2.00272, hyperfine splitting value = 2.6 G). This type of signal is consistent with a more stabilized carbon-centered radical of type **XVIII**,[34b] which lies in proximity of two sulfur atoms and an ethoxy moiety (Figure 3.3b).

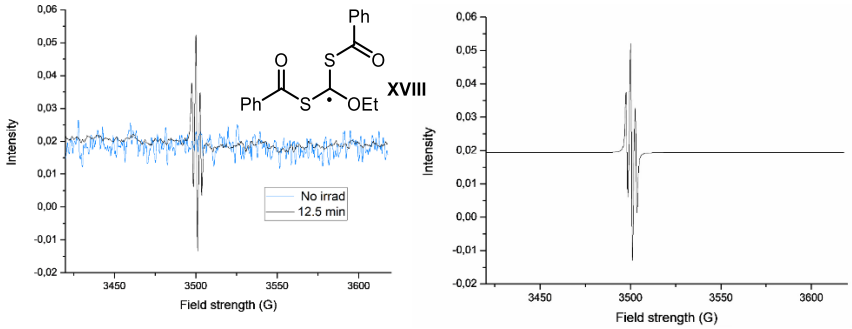

Figure 3.3. a) Comparison between EPR spectra of acylxanthate **5a** (0.1 M in toluene) before irradiation (blue line) and after irradiation with a LSB610 100W mercury lamp during 12.5 min (black line). b) Calculated EPR spectrum for intermediate **XVIII** for a hyperfine coupling with two equivalent nuclei of spin ½.

[34] (a) Bieszczad, B.; Perego, L. A.; Melchiorre, P., Photochemical C−H Hydroxyalkylation of Quinolines and Isoquinolines. *Angew. Chem. Int. Ed.* **2019**, *58*, 16878-16883. (b) Hawthorne, D. G.; Moad, G.; Rizzardo, E.; Thang, S. H., Living Radical Polymerization with Reversible Addition−Fragmentation Chain Transfer (RAFT): Direct ESR Observation of Intermediate Radicals. *Macromolecules* **1999**, *32*, 5457-5459.

The formation of radical **XVIII** is consistent with the high tendency of xanthates, and related thiocarbonylthio congeners, to trap radicals via a group transfer mechanism. This feature is the underlying reason for the xanthates' success as RAFT agents in polymerization.[35] Formation of radical **XVIII** is congruent with the trap of radical **IIIa** by xanthate **5a**. Indeed, this process leads to a reversible addition-fragmentation equilibrium (Scheme 3.24) as supported by the detection of **XVIII**. This equilibrium controls the overall concentration of highly reactive active radicals (such as **III**) by forming the more stabilized radical **XVIII**, which acts as a dynamic reservoir, while increasing their effective lifetime in the medium.

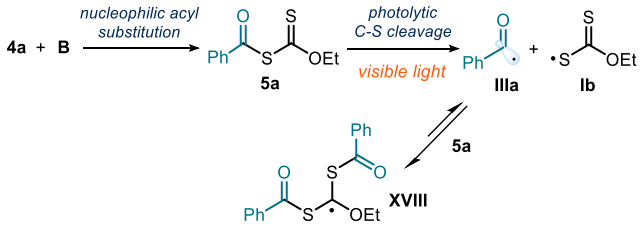

Scheme 3.25. The reaction of the acyl radical **IIIa** with its precursor **5a** is reversible and imparts an increased lifetime to **IIIa**.

3.7.2 Fate and Behavior of the Xanthyl Radical **Ib**

An additional step of the proposed mechanism – the catalyst turn-over event – probably raises some concerns since it requires an SET event to take place between two fleeting species, specifically the xanthyl radical **I** and radical **XVI** (Scheme 3.14). One of the main mechanistic aspects to elucidate therefore concerned the reactivity of the sulfur-centered radical of type **III**, generated upon photolytic cleavage of intermediate **I**. During a previous study of our group involving DTC catalysis,[27] we detected the formation of dimer **42a**, which arised from the self-reaction of the xanthyl radical **Ia** (Scheme 3.26). We wondered if the catalyst dimer could play an important role in the present process too. This off-cycle equilibrium could help prolonging the life-time of the xanthyl radical **I**.

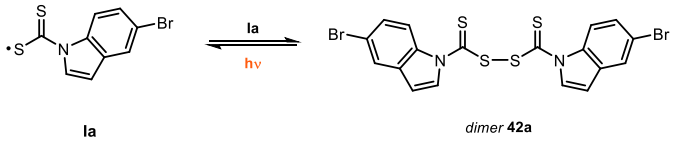

Scheme 3.26. Dimerization of sulfur-centered radical **Ia** and photolysis equilibrium.

[35] Zard, S. Z., Discovery of the RAFT/MADIX Process: Mechanistic Insights and Polymer Chemistry Implications. *Macromolecules* **2020**, *53*, 8144-8159.

To test our hypotheses, we synthesized dimer **42b** and performed UV-Vis studies (Scheme 3.27). Dimer **42b** could absorb within the visible-light region and could be excited by the irradiation set-up employed for the transformation. To verify that this intermediate was catalytically competent, we used an authentic sample of dimer **42b** (5 mol%) to catalyze the model reaction (Scheme 3.27). Irradiation with a blue LED afforded product **3a** in high yield. Importantly, no reaction was observed when the same experiment was performed in the dark. These results are informative of the reaction mechanism, since they imply that dimer **VIIa** is a photoactive species in equilibrium with the progenitor xanthyl radical **IIIa**. This mechanism could indeed confer a persistent radical character to **Ib.** On this basis, the proposed turnover of catalyst **B**, based on the SET reduction of radical **IIIa** from radical **XVI** (see Scheme 3.28), becomes feasible. Indeed, according to the persistent radical effect,[36] processes between two fleeting radicals are feasible when one of them has a relatively longer lifetime.

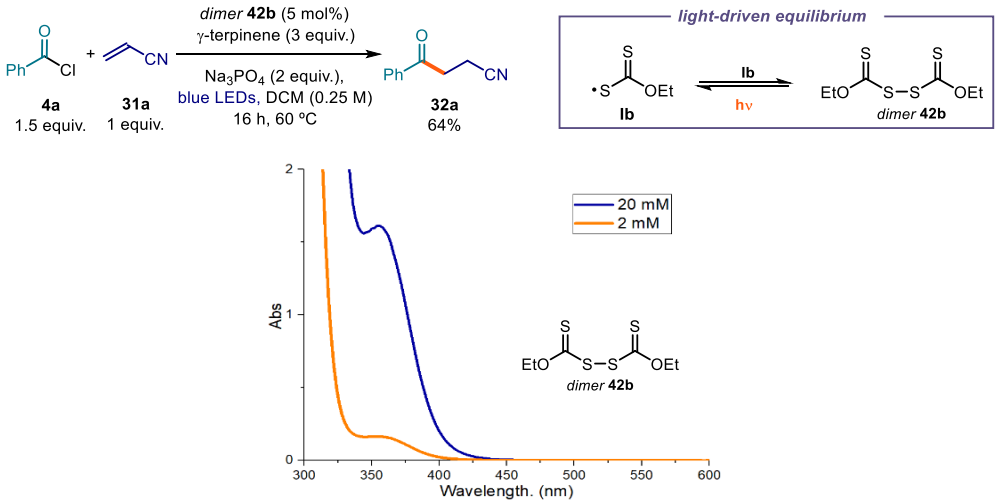

Scheme 3.27. *Top*: Model reaction catalyzed by dimer **42b** and the light-driven equilibrium between the xanthyl radical **Ib** and the dimer. *Bottom*: Absorption of dimer **42b** at different concentration in CH_3CN.

To gain further insights into the light-driven equilibrium between the dimer and its radical progenitor **Ib** shown in Scheme 3.27, we evaluated the behavior of dimer **42b** under the reaction conditions using 1 equivalent of γ-terpinene and under blue light illumination (Scheme 3.28). Dimer **42b** was completely consumed to produce 1.65 equivalents of catalyst **B**. This result provides compelling evidence to rationalize the mechanism of turnover of catalyst **B**. Considering the stoichiometry of the reaction in Scheme 3, it appears that γ-terpinene can provide two different pathways to reduce the xanthyl radical **Ib**, namely an HAT

[36] Leifert, D.; Studer, A., The Persistent Radical Effect in Organic Synthesis. *Angew. Chem. Int. Ed.* **2020**, *59*, 74-108.

process and then an SET reduction from the ensuing cyclohexadienyl-type radical **XVI**. Overall, these experiments support an alternative turn-over event to recover the catalyst.

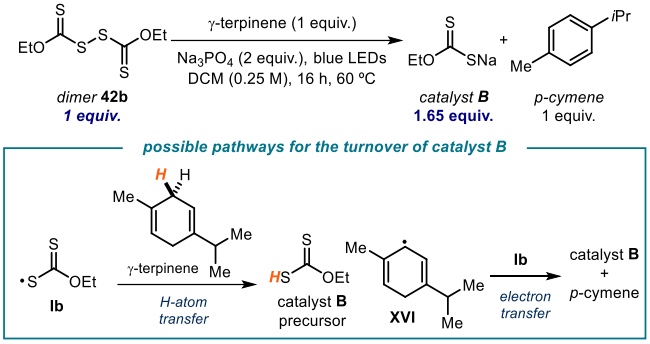

Scheme 3.28. Experiment that probes the ability of γ-terpinene to reduce the xanthyl radical **Ib** via both an HAT and an SET manifold.

We also performed laser flash photolysis studies. When exposed to irradiation, the same transient species observed in the experiment with intermediate **5a** was detected, which is consistent with the formation of the xanthyl radical **Ib**. This observation further confirms the light-driven equilibrium that links dimer **42b** with its radical progenitor **Ib** (shown in Scheme 3.27). Moreover, a quenching experiment of the transient species with γ-terpinene showed that the lifetime of the transient **Ib** decreased (orange, green, and blue lines in Figure 3.4), which corroborates the notion that these two species can readily react.

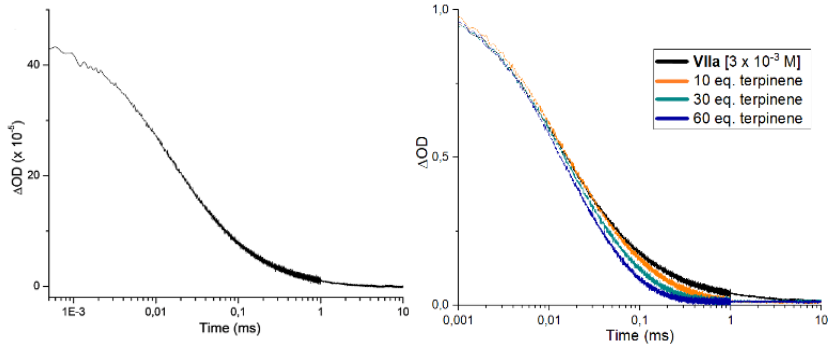

Figure 3.4. a) Absorption at 620 nm of the transient xanthyl radical **Ib** generated upon 355 nm laser excitation of dimer **42b** ($[\mathbf{42b}]_0 = 3x10^{-3}$ M in acetonitrile). b) Decrease of the lifetime of **Ib** upon addition of γ-terpinene. Note logarithmic scale for time; ΔOD: optical density variation. Absorption decays (orange, green, and blue lines) observed in the presence of increasing amounts of γ-terpinene. *Green line*: ratio **42b**/γ-terpinene mimics the reaction conditions. ΔOD: optical density variation.

Collectively, the experiments detailed in Scheme 3.27 and Scheme 3.28, along with the laser flash photolysis studies reported in Figure 3.4, provide compelling evidence that dimer **42b** can form xanthyl radical **Ia** upon photolytic cleavage. To obtain direct evidence of the dimerization tendency of the sulfur-centered radical **Ia**, we performed cyclic voltammetry analysis of both catalyst **B** and dimer **42b** (Figure 3.5 and Figure 3.6). We first focused on catalyst **B**, which was electrochemically analyzed during the initial forward scan applying an increasingly reducing potential (0 to -2.0 V, Figure 3.5, left). No reduction peaks were observed. During the reverse scan towards oxidation (from -2.0 V to +1.5 V), an irreversible peak appeared ($E_p^A = E_{ox}$ = 0.73 V in CH_3CN vs Ag/AgCl), which is ascribable to the oxidation of catalyst **B** to form the xanthyl radical **Ia** (orange dot). We then electrochemically analyzed catalyst **B** in the opposite order (Figure 3.5, right), first applying an increasingly oxidizing potential (0 to +1.5 V). As expected, during oxidation, we observed the same signal as in the previous experiment, which is congruent with the formation of radical **Ia** upon SET oxidation of **B** (orange dot). Interestingly, during the reverse scan towards reduction (from +1.5 V to -2.0 V), an additional peak was observed ($E_p^C = E_{red}$ = -1.40 V in CH_3CN vs Ag/AgCl), which was not detected in the previous experiment (blue dot).

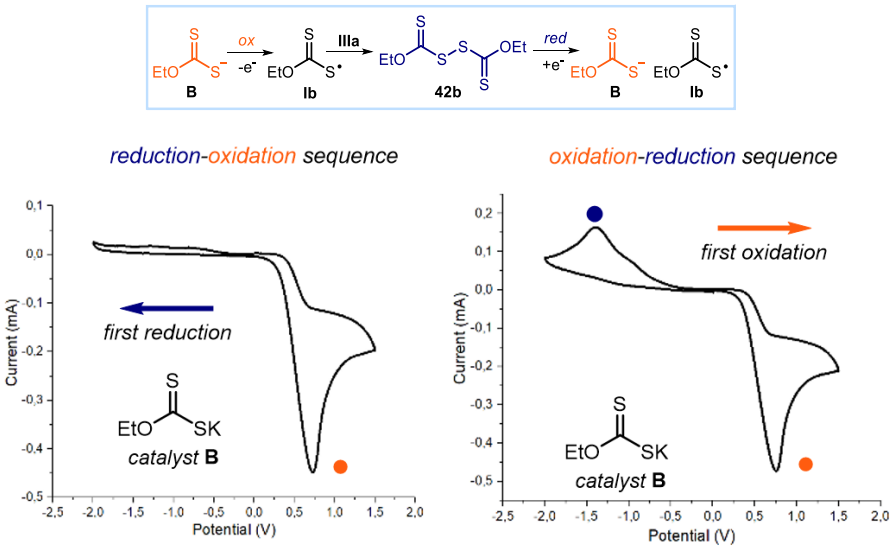

Figure 3.5. Cyclovoltammetric studies of catalyst **B** [0.02 M] in [0.1 M] $TBAPF_6$ in CH_3CN: reduction-oxidation scan sequence; oxidation-reduction scan sequence. The xanthyl radical **Ib**, which can be formed by SET reduction of **42b** and oxidation of **B**, is the link between catalyst **B** and dimer **42b**.

These results can be rationalized based on a fast dimerization of radical **Ia**, generated during the forward oxidation scan, that forms dimer **42b**, which is prone to SET reduction (Figure 3.5, top). This proposal is consonant with the following observation: i) the formation of the

stable dimer makes the oxidation of catalyst **B** irreversible, since **Ia** is rapidly sequestered in the form of its dimer; ii) it is only in the cyclic voltammetric analysis that starts with oxidation (Figure 3.5, top) that a reduction peak appears, which is ascribable to the reduction of dimer **42b**: this is because the dimer first requires the oxidation of catalyst **B** to be generated (Figure 3.5, top). To corroborate this proposal, we repeated the same analysis using dimer **42b**. Applying an initial forward scan towards an increasingly oxidizing potential (0 to +1.5, Figure 3.6), no oxidation was observed. As expected, during the reverse scan (from +1.5 V to -2.0 V), the reduction peak of dimer **42b** (blue dot) was recorded ($E_p^C = E_{red}$ = -1.61 V in CH_3CN vs Ag/AgCl). But when we started the electrochemical analysis towards reduction (0 to -2.0 V and then to +1.5 V, Figure 3.6, right), an additional oxidation peak could be observed ($E_p^A = E_{ox}$ = 0.53 V in CH_3CN vs Ag/AgCl). This is because the reduction of dimer **42b** furnishes the xanthyl radical **Ia** along with the anionic catalyst **B**; the latter species is then oxidized during the reverse scan phase (orange dot), in agreement with the experiments depicted in Figure 3.5. The comparison of the cyclic voltammograms indicates a clear correlation between the new reduction peak observed in the analysis of catalyst **B** in Figure 3.5, with the peak observed upon reduction of dimer **42b** (Figure 3.6, right). A correlation exists also between the new oxidation peak in the analysis of dimer **42b** in Figure 3.6 (left) and the oxidation of catalyst **B** (Figure 3.5). Collectively, these studies indicate that the link between catalyst **B** and dimer **42b** is the xanthyl radical **Ia** (Figure 3.5 and 3.6). They also show the strong tendency of the xanthyl radical **Ia** to dimerize and form **42b**.

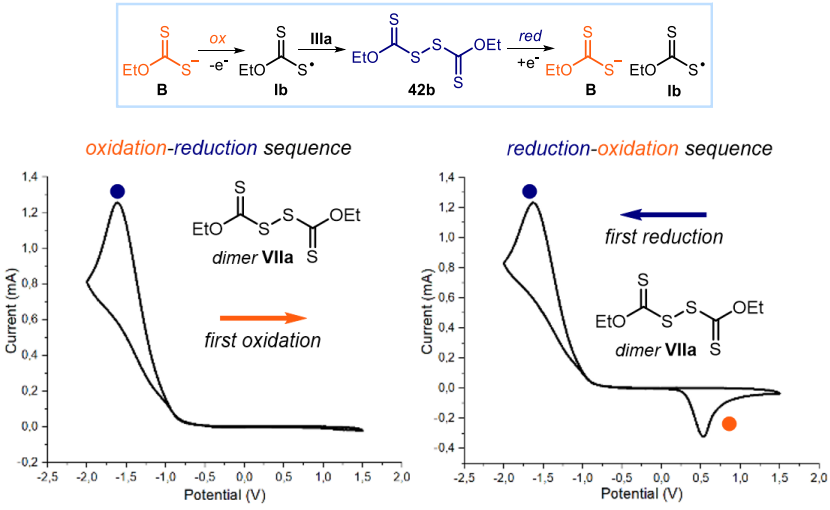

Figure 3.6. Cyclovoltammetric studies of dimer **42b** [0.02 M] in [0.1 M] $TBAPF_6$ in CH_3CN: oxidation-reduction scan sequence; reduction-oxidation scan sequence. Sweep rate: 500 mV/s. Pt electrode working electrode, Ag/AgCl (KCl 3.5 M) reference electrode, Pt wire auxiliary electrode.

3.7.3 Trap of the Acyl Radical and Ensuing Processes

The mechanistic studies conducted so far allowed us to elucidate the photochemical acyl radical generation mechanism while providing a rationale for the turnover of catalyst **B**. Nevertheless, the C-C bond formation process and the involvement of a possible group transfer mechanism are yet to be investigated. We therefore conducted investigations to probe the possible intermediacy of the group transfer product of type **43a** (Scheme 3.29). Intermediate **43a** might be generated via a xanthate transfer manifold between **XVa** and **5a**, which would also generate a benzoyl radical **IIIa** (Scheme 3.29a). **43a** could also arise from a cross-coupling process between radicals **Ia** and **XVa**.

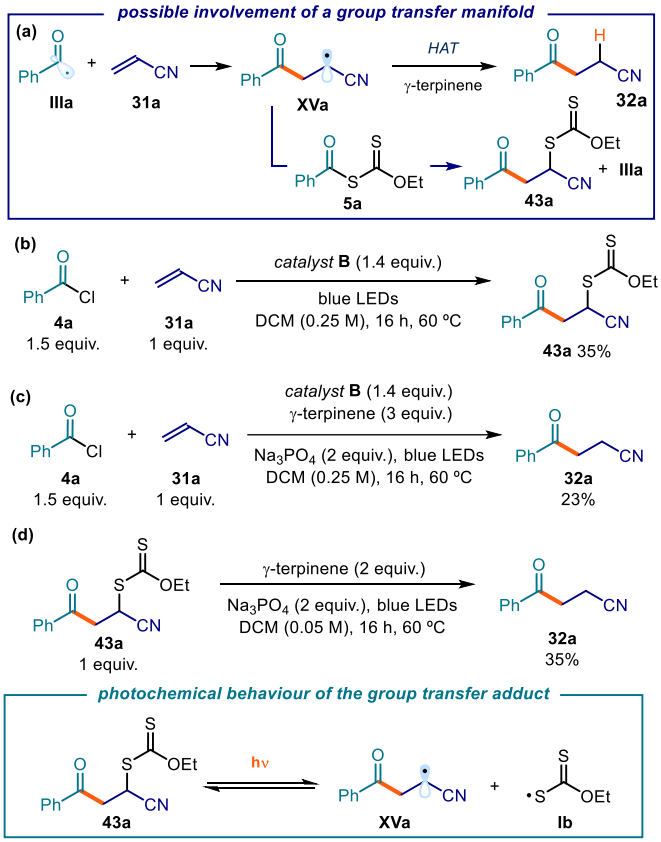

Scheme 3.29. a) Focusing on the acyl radical addition step. The model reaction in the presence of a stoichiometric amount of **B** and b) in the absence or c) in the presence of γ–terpinene (group transfer conditions). d) The behavior of group transfer product **43a** under the reaction conditions and upon blue light irradiation.

To determine the possible intermediacy of a group transfer product of type **43a** (Scheme 3.29b), we performed the model reaction using a stoichiometric amount of catalyst **B** and in

the absence of γ-terpinene, to avoid a competitive HAT pathway leading to product **32a**. The group transfer product **43a** was isolated in 35% yield (Scheme 3.29b). The Giese-type adduct **32a** was not detected, which indicates the importance of γ-terpinene in enabling the radical conjugate addition manifold. By contrast, under identical conditions but in the presence of γ–terpinene, no traces of the group transfer product **43a** could be detected, while the product **32a** was exclusively formed (23% yield, Scheme 3.29c). Interestingly, the yield of **32a** was much lower with respect to the experiment conducted using catalytic amounts of **B** (10 mol%, 82% yield). We suppose that the lower efficiency of the Giese addition path under stoichiometric conditions could be a consequence of the equilibrium showed in Fig. 8, i.e. a higher amount of intermediate **5** inhibits the radical addition to the olefin sequestering the acyl radicals. We also synthesized an authentic sample of the group transfer product **43a** and subjected it to the model reaction conditions (Scheme 3.29d). We confirmed that **43a** under irradiation delivers the correspondent radicals **XVa** and **Ib**, affording the Giese addition product in 35% yield. Laser flash photolysis studies of **43a** showed a transient species that is consonant with the xanthyl radical **Ib**, generated upon photolysis (see the Experimental section 3.9.10.8). Even though we never detected the group transfer adduct of type **43a** under catalytic conditions, we cannot exclude that this pathway is operative in our catalytic system. Intermediate **43a** may serve as a stabilized off-cycle intermediate, which controls the concentration of radicals **Ib** and **XVa** in solution through an additional equilibrium.

3.7.4 Overall catalytic cycle and full mechanistic picture

The mechanistic studies provided important clues to better delineate the mechanism of the photochemical Giese addition process. A more complete mechanistic picture is detailed in Scheme 3.30. During the course of this study, we identified different equilibriums that regulate the overall catalytic cycle and that are essential to stabilizing the radical intermediates and controlling their concentration in solution. For example, the highly reactive acyl radical **IIIa** could be intercepted by xanthates **5** in a reversible addition-fragmentation equilibrium, leading to intermediate **XV**. At the same time, the xanthyl radical **Ib** can both dimerize to form dimer **42b** and engage in a cross-coupling process with radical **XVa** to afford the xanthate transfer product **43a**. These equilibriums, which are regulated by light, confer a persistent radical character to the xanthyl radical **Ib**, facilitating its reduction and the turnover of the catalyst **B**. Importantly, we have demonstrated that γ-terpinene can use two different pathways to reduce the xanthyl radical **Ib**, e.g., a direct HAT process and an SET reduction from the ensuing cyclohexadienyl-type radical **XVI**.

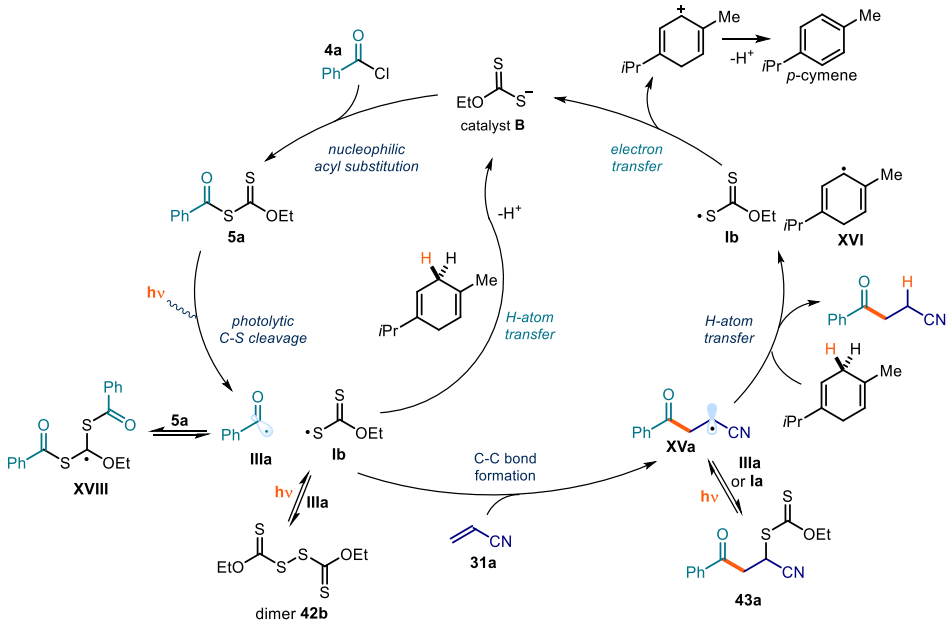

Scheme 3.30. Detailed mechanistic picture, comprehensive of the off-the-cycle equilibriums, based on the mechanistic investigations conducted on the model reaction of acyl chloride **4a** and acceptor **31a** catalyzed by **B**.

The main feature of the proposed mechanism in Scheme 3.30 is that it proceeds through a photocatalytic process, where the photoactivity of intermediate **5** dictates the formation of any molecule of the product. This scenario stands in contrast to a possible alternative radical chain propagation manifold, which would require the photoactivity of intermediate **5** to serve only as an initiation event. A tool to discriminate between these two mechanistic possibilities is to measure the quantum yield (Φ) of the overall reaction.[37] We performed this measurement on the model reaction, and the quantum yield was found to be as low as 0.034 (λ = 460 nm, using potassium ferrioxalate as the actinometer). This result suggests that a radical chain process, based on either a xanthate group transfer manifold or an SET from intermediate **XV** to intermediate **5**, is unlikely. Instead, the low quantum yield is congruent with the proposed photocatalytic mechanism depicted in Scheme 3.30.

3.8 Conclusions

In summary, we developed a catalytic methodology that requires visible light and commercially available organic catalysts to access a wide range of acyl and carbamoyl radicals. These reactive open-shell species were then trapped with a variety of electron-poor

[37] (a) Cismesia, M. A.; Yoon, T. P., Characterizing chain processes in visible light photoredox catalysis. *Chem. Sci.* **2015**, *6*, 5426-5434. (b) Buzzetti, L.; Crisenza, G. E. M.; Melchiorre, P., Mechanistic Studies in Photocatalysis. *Angew. Chem. Int. Ed.* **2019**, *58*, 3730-3747.

olefins in a Giese addition manifold. Our strategy relies on the electrophilicity of the substrates rather than their reduction potential, allowing the use of readily available carboxylic acids/chlorides and carbamoyl chlorides (which would be recalcitrant to other radical generation strategies) as acyl and carbamoyl radical precursors. Extensive mechanistic investigations have been performed, providing a deeper understanding of the whole mechanisctic picture, by means of different analytical techniques such as transient absorption spectroscopy, electrochemical studies, quantum yield measurements, and the characterization of key intermediates. Collectively, these studies identified a variety of off-the-cycle intermediates that are in a light-regulated equilibrium with the reactive radicals. These regulated equilibriums cooperate to control the overall concentrations of the radicals, contributing to the efficiency of the process. The knowledge of the mechanistic details underlying this radical generation strategy may enable the rational development of new reactions. Conceptually, this study allowed us to expand anion dithiocarbamate catalysis to include other types of electrophiles.

3.9 Experimental section

3.9.1 General information

The NMR spectra of the products and previously unreported starting materials are available in the published manuscript[1] and are not reported in the present dissertation.

The NMR spectra were recorded at 400 MHz and 500 MHz for ^{1}H and 100 or 125 MHz for ^{13}C. The chemical shift (δ) for ^{1}H and ^{13}C are given in ppm relative to residual signals of the solvents ($CHCl_3$ @ 7.26 ppm ^{1}H NMR and 77.16 ppm ^{13}C NMR, and tetramethylsilane @ 0 ppm). Coupling constants are given in Hertz. The following abbreviations are used to indicate the multiplicity: s, singlet; d, doublet; q, quartet; m, multiplet; bs, broad signal; app, apparent. High resolution mass spectra (HRMS) were obtained from the ICIQ HRMS unit on MicroTOF Focus and Maxis Impact (Bruker Daltonics) with electrospray ionization. (ESI). UV-vis measurements were carried out on a Shimadzu UV-2401PC spectrophotometer equipped with photomultiplier detector, double beam optics and D_2 and W light sources or an Agilent Cary60 spectrophotometer. Emission spectra of light sources were recorded on Ocean Optics USB4000 fiber optic spectrometer. Yields of isolated compounds refer to materials of >95% purity as determined by ^{1}H NMR analysis.

General Procedures. All reactions were set up under an argon atmosphere in oven-dried glassware. Synthesis grade solvents were used as purchased, anhydrous solvents were taken from a commercial SPS solvent dispenser. Chromatographic purification of products was accomplished using forced-flow chromatography (FC) on silica gel (35-70 mesh). For thin layer chromatography (TLC) analysis throughout this work, Merck pre-coated TLC plates (silica gel 60 GF_{254}, 0.25 mm) were employed, using UV light as the visualizing agent and an

acidic mixture of vanillin or basic aqueous potassium permanganate ($KMnO_4$) stain solutions, and heat as developing agents. Organic solutions were concentrated under reduced pressure on a Büchi rotatory evaporator.

Determination of Enantiomeric Purity. UPC[2] analysis on chiral stationary phase was performed on a Waters Acquity instrument using an ID3 chiral column. The exact conditions for the analyses are specified within the characterization section.

Materials. Most of the starting materials used in this study are commercial and were purchased in the highest purity available from Sigma-Aldrich, Fluka, Alfa Aesar, Fluorochem, and used as received, without further purifications.

The following substrates were synthesized according to reported procedures (Scheme 3.31).[38]

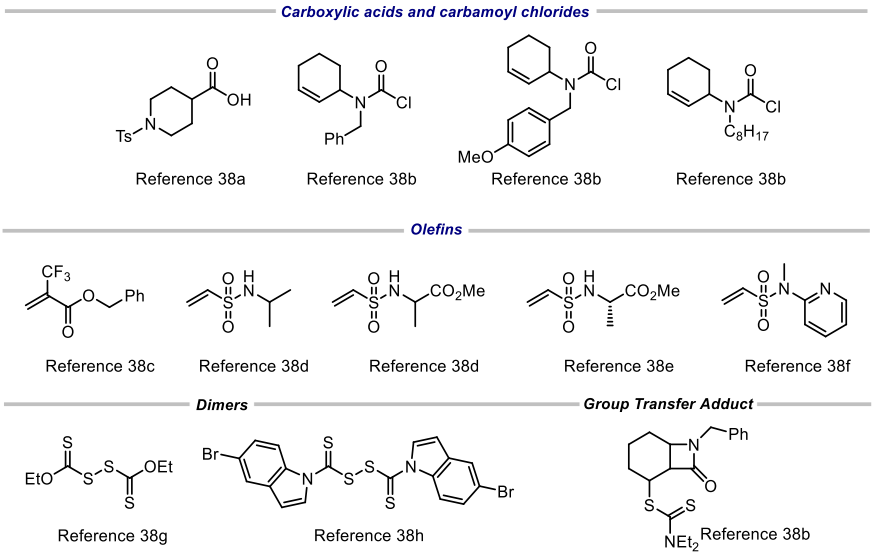

Scheme 3.31. Starting materials synthesized according to known procedures.

[38] (a) Nyfeler, E.; Renaud, P. Decarboxylative Radical Azidation Using MPDOC and MMDOC Esters. *Org. Lett.* **2008**, *10*, 985-988. (b) Grainger, R. S.; Betou, M.; Male, L.; Pitak, M. B.; Coles, S. J. Semipinacol Rearrangement of Cis-Fused β-Lactam Diols into Keto-Bridged Bicyclic Lactams. *Org. Lett.* **2012**, *14*, 2234-2237. (c) Avenoza, A.; Busto, J. H.; Jiménez-Osés, G.; Peregrina, J. M. A Convenient Enantioselective Synthesis of (S)-α- Trifluoromethylisoserine. *J. Org. Chem.* **2005**, *70*, 5721-5724. (d) Wang, M.; Wang, Y.; Qi, X.; Xia, G.; Tong, K.; Tu, J.; Pittman, C. U.; Zhou, A. Selective Synthesis of Seven- and Eight-Membered Ring Sultams via Two Tandem Reaction Protocols from One Starting Material. *Org. Lett.* **2012**, *14*, 3700-3703. (e) Fenster, E.; Long, T. R.; Zang, Q.; Hill, D.; Neuenswander, B.; Lushington, G. H.; Zhou, A.; Santini, C.; Hanson, P. R. Automated Synthesis of a 184-Member Library of Thiadiazepan-1,1-dioxide-4-ones. *ACS Comb. Sci.* **2011**, *13*, 244-250. (f) Huang, R.; Li, Z.; Ren, P.; Chen, W.; Kuang, Y.; Chen, J.; Zhan, Y.; Chen, H.; Jiang, B. *N*-Phenyl-*N*-aceto-vinylsulfonamides as Efficient and Chemoselective Handles for N-Terminal Modification of Peptides and Proteins. *Eur. J. Org. Chem.* **2018**, *2018*, 829-836. (g) Jiang, S.; Li, Y.; Luo, X.; Huang, G.; Shao, Y.; Li, D.; Li, B. $NH_4I/EtOCS_2K$ promoted synthesis of substituted benzils from diphenylacetylene derivatives. *Tetrahedron Lett.* **2018**, *59*, 3249-3252.

3.9.2 Substrate synthesis

Synthesis of *N*-benzylcyclopent-2-en-1-amine:

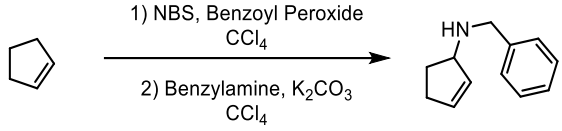

A 2 M solution of cyclopentene (0.973 mL, 11 mmol) in CCl_4 (5.4 mL) was prepared and then *N*-bromosuccinimide (2.26 g, 10 mmol) and benzoic peroxyanhydride (36 mg, 0.15 mmol) were sequentially added. The solution was stirred at *40 °C* for 4 hours, after which the reaction was left at ambient temperature without stirring. After 2 hours, the floating materials were filtered off and washed with CCl_4. The organic phase was then placed in a separatory funnel and washed with distilled water. The organic phase was collected, treated with $MgSO_4$ and subsequently filtered. At this stage, benzylamine (3.28 mL, 30 mmol) and K_2CO_3 (1.38 g, 10 mmol) were directly added to the solution. The reaction was stirred overnight at r.t and the resulting crude mixture was purified by silica gel chromatography (eluent: 9:1 hexane/AcOEt) to afford 234 mg of *N*-benzylcyclopent-2-en-1-amine (14% yield over 2 steps) as a yellow-orange oil.

^{1}H NMR (400 MHz, $CDCl_3$) δ 7.39 – 7.24 (m, 5H), 5.89 (m, 2H), 3.93 (m, 1H), 3.84 (dd, *J* = 16.6, 12.9 Hz, 2H), 2.48 (m, 1H), 2.36 – 2.18 (m, 2H), 1.63 (m, 1H).

^{13}C NMR (101 MHz, $CDCl_3$) δ 140.5, 133, 132.8, 128.4, 128.3, 126.9, 63.9, 51.8, 31.3, 30.8

Synthesis of *N*-(4-(trifluoromethyl)benzyl)cyclohex-2-en-1-amine:

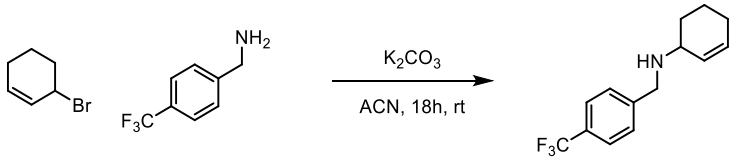

N-(4-(trifluoromethyl)benzyl)cyclohex-2-en-1-amine was prepared according to a reported procedure.[38b] A solution of (4-(trifluoromethyl)phenyl)methanamine (1.314 g, 7.5 mmol) in CH_3CN (1.7 mL) was treated with 3-bromocyclohexene (0.288 mL, 2.5 mmol) and K_2CO_3 (346 mg, 2.5 mmol). After 2 hours at ambient temperature, the reaction mixture was quenched with H_2O (20 mL) and extracted with EtOAc (2 x 25 mL). The combined organic extracts were washed with brine (20 mL), dried over $MgSO_4$, filtered, evaporated under reduced pressure, and purified by column chromatography (eluent: CH_2Cl_2 to CH_2Cl_2/EtOH 9:1) to give the product (607 mg, 95 % yield) as a light-yellow oil.

^{1}H NMR (400 MHz, $CDCl_3$) δ 7.57 (d, *J* = 8.1 Hz, 2H), 7.47 (d, *J* = 8.0 Hz, 2H) 5.82 – 5.76 (m, 1H), 5.75 – 5.62 (m, 1H) 3.90 (dd, *J* = 13.6, 3.3 Hz, 2H), 3.23 – 3.16 (m, 1H), 2.10 – 1.97 (m, 2H), 1.93 – 1.85 (m, 1H), 1.80 – 1.70 (m, 1H), 1.61 – 1.42 (m, 2H).

^{13}C NMR (101 MHz, $CDCl_3$) δ 145.1, 129.8, 129.4, 129.3 (q, *J* = 32.7 Hz) 128.4, 125.4 (q, *J* = 3.7 Hz), 124.4 (q, *J* = 271.9 Hz), 52.6, 50.6, 29.6, 25.4, 20.3.

^{19}F NMR (376 MHz, $CDCl_3$) δ -62.47.

Synthesis of compound 37f:

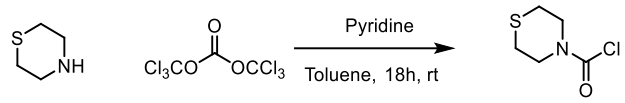

Compound **37f** was prepared according to a modification of a reported procedure.[38b] To a solution of triphosgene (294 mg, 0.99 mmol) in toluene (15 mL) under N_2, pyridine (0.290 mL, 3.60 mmol) and subsequently a solution of thiomorpholine (310 mg, 3 mmol) in toluene (5 mL) were added. The reaction mixture was stirred for 18 hours at ambient temperature, quenched with NH_4Cl (20 mL of a saturated aq. solution) and extracted with Et_2O (2 x 30 mL). The combined organic extracts were washed sequentially with HCl (40 mL of a 0.25 M aq. solution), H_2O (40 mL) and brine (40 mL), dried over $MgSO_4$, filtered and evaporated under reduced pressure to afford carbamoyl chloride **37f** (310 mg, 75% yield) as a colorless oil.

^{1}H NMR (400 MHz, $CDCl_3$) δ 3.94 (dt, *J* = 38.9, 5.1 Hz, 1H), 2.72 – 2.64 (m, 1H).

^{13}C NMR (101 MHz, $CDCl_3$) δ 148.5, 51.7, 49.3, 27.7, 27.3

Synthesis of 37g:

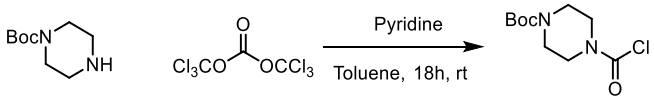

Compound **37g** was prepared according to a modification of a reported procedure.[38b] To a solution of triphosgene (294 mg, 0.99 mmol) in toluene (15 mL) under N_2, pyridine (0.290 mL, 3.60 mmol) and subsequently a solution of *N*-Boc Piperazine (559 mg, 3 mmol) in toluene (5 mL) were sequentially added. The reaction mixture was stirred for 18 hours at ambient temperature, quenched with NH_4Cl (20 mL of a saturated aq. solution) and extracted with Et_2O (2 x 30 mL). The combined organic extracts were washed sequentially with HCl (40 mL of a 0.25 M aq. solution), H_2O (40 mL) and brine (40 mL), dried over $MgSO_4$, filtered and evaporated under reduced pressure to give carbamoyl chloride **37g** (597 mg, 82% yield) as a colorless oil.

^{1}H NMR (300 MHz, $CDCl_3$) δ 3.64 (m, 4H), 3.48 (d, *J* = 4.8 Hz, 4H), 1.46 (s, 9H).
^{13}C NMR (101 MHz, $CDCl_3$) δ 154.3, 148.5, 80.7, 48.5, 46, 28.3.

HRMS (ESI pos): calculated for $C_{10}H_{17}ClNaN_2O_3$ ($M+Na^+$): 271.0800, found: 271.0818.

Synthesis of compound 37h:

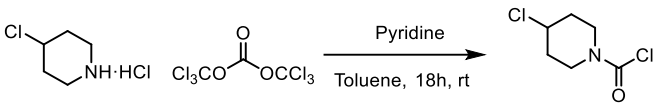

Compound **37h** was prepared according to a modification of a reported procedure.[38b] To a solution of triphosgene (259 mg, 0.872 mmol) in toluene (15 mL) under N_2, pyridine (0.498 mL, 6.15 mmol) and subsequently a solution of 4-chloropiperidine hydrochloride (400 mg, 2.56 mmol) in toluene (5 mL) were sequentially added. The reaction mixture was stirred for 18 hours at ambient temperature, quenched with NH_4Cl (20 mL of a saturated aq. solution) and extracted with Et_2O (2 x 30 mL). The combined organic extracts were washed sequentially with HCl (40 mL of a 0.25 M aq. solution), H_2O (40 mL) and brine (40 mL), dried over $MgSO_4$, filtered and evaporated under reduced pressure to give carbamoyl chloride **37h** (420 mg, 90% yield) as a colorless oil.

^{1}H NMR (400 MHz, $CDCl_3$) δ 4.34 (tt, J = 6.5, 3.6 Hz, 1H), 4.01 – 3.64 (m, 4H), 2.18 – 2.03 (m, 2H), 2.00 – 1.86 (m, 2H).

^{13}C NMR (101 MHz, $CDCl_3$) δ 148.4, 55.6, 45.6, 43.1, 34.7, 34.2.

Synthesis of compound 37j:

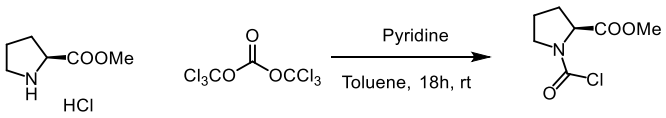

Compound **37j** was prepared according to a modification of a reported procedure.[38b] To a solution of triphosgene (207 mg, 0.68 mmol) in toluene (15 mL) under N_2, pyridine (0.204 mL, 2.54 mmol) and subsequently a solution of L-methyl prolinate hydrochloride (350 mg, 2.13 mmol). The reaction mixture was stirred for 18 hours at ambient temperature, quenched with NH_4Cl (20 mL of a saturated aq. solution), and extracted with Et_2O (2 x 30 mL). The combined organic extracts were washed sequentially with HCl (40 mL of a 0.25 M aq. solution), H_2O (40 mL) and brine (40 mL), dried over $MgSO_4$, filtered and evaporated under reduced pressure to give carbamoyl chloride **37j** (275 mg, 68% yield) as a colorless oil.

^{1}H NMR (400 MHz, $CDCl_3$, 1:1 mixture of rotamers) δ: 4.57 – 4.46 (m, 1H), 3.85 - 3.55 (m, 2H), 3.77 (d, *J* = 12.4 Hz, 3H), 2.35 – 2.25 (m, 1H), 2.17 – 1.93 (m, 3H).

^{13}C NMR (124 MHz, $CDCl_3$, 1:1 mixture of rotamers) δ: 171.8, 171.3, 147.8, 146.9, 62.4, 60.7, 52.9, 50.7, 49.2, 30.4, 30.3, 23.7, 23.6

Synthesis of compound 37k:

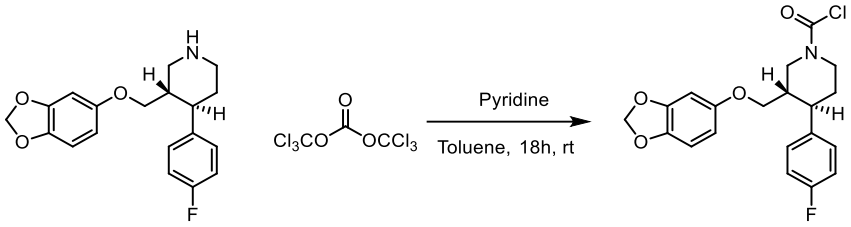

Compound **37k** was prepared according to a modification of a reported procedure.[38b] To a solution of triphosgene (89 mg, 0.30 mmol) in toluene (3 mL) under N_2, pyridine (88 µL, 1 mmol) and subsequently a solution of Paroxetine (300 mg, 0,91 mmol) in toluene (6 mL), were added. The reaction mixture was stirred for 18 hours at ambient temperature, quenched with NH_4Cl (20 mL of a saturated aq. solution) and extracted with Et_2O (2 x 30 mL). The combined organic extracts were washed sequentially with HCl (40 mL of a 0.25 M aq. solution), H_2O (40 mL) and brine (40 mL), dried over $MgSO_4$, filtered and evaporated under reduced pressure to afford carbamoyl chloride **37k** (130 mg, 36% yield) as a white crystal.

^{1}H NMR (500 MHz, $CDCl_3$) δ 7.14 (m, 2H), 7.00 (m, 2H), 6.64 (m, 1H), 6.36 (s, 1H), 6.14 (m, 1H), 5.89 (s, 2H), 4.63 (m, 1H), 4.49 (m, 1H), 3.63 (t, *J* = 8.7 Hz, 1H), 3.48 (dd, *J* = 9.6, 6.0 Hz, 1H), 3.20 (t, *J* = 12.9 Hz, 1H), 3.02 (m, 1H), 2.82 (m, 1H), 2.10 (m, 1H), 1.93 (m, 1H), 1.82 (qd, *J* = 12.9, 4.4 Hz, 1H)

^{13}C NMR (126 MHz, $CDCl_3$) δ 162.9, 160.9, 154.0, 148.4, 142.0, 128.9, 115.8, 108.0, 105.8, 101.3, 98.1, 68.4, 52.2, 49.6, 47.0, 43.8, 42.3, 33.7

^{19}F NMR (376 MHz, $CDCl_3$, proton decoupled) δ -115.51

HRMS (ESI pos): calculated for $C_{20}H_{19}ClFNaNO_4$ ($M+Na^+$): 414.09, found 414.0884

Synthesis of compound 37b:

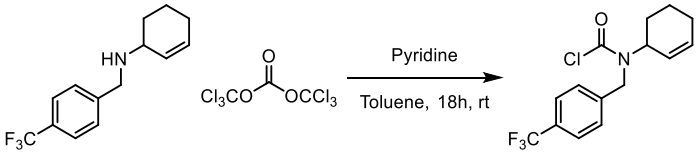

Compound **37b** was prepared according to a modification of a reported procedure.[38b] To a solution of triphosgene (252 mg, 0.848 mmol) in toluene (15 mL) under N_2, pyridine (0.242 mL, 2.99 mmol) and subsequently a solution of *N*-(4-(trifluoromethyl)benzyl)cyclohex-2-en-1-amine (637 mg, 2.5 mmol) in toluene (4 mL), were added. The reaction mixture was stirred for 18 hours at ambient temperature, quenched with NH_4Cl (20 mL of a saturated aq. solution) and extracted with Et_2O (2 x 30 mL). The combined organic extracts were washed sequentially with HCl (40 mL of a 0.25 M aq. solution), H_2O (40 mL) and brine (40 mL), dried over

$MgSO_4$, filtered and evaporated under reduced pressure to give carbamoyl chloride **37b** (722 mg, 91% yield) as a yellow oil.

^{1}H NMR (400 MHz, $CDCl_3$ mixture of rotamers) δ 7.60 (dd, *J* = 16.7, 8.1 Hz, 2H), 7.36 (d, *J* = 7.9 Hz, 2H), 5.85 – 6.00 (m, 1H), 5.55 – 5.41 (m, 1H), 5.10 – 4.90 (m, 1H), 4.82 – 4.49 (m, 2H), 2.08 – 1.94 (m, 3H), 1.85 – 1.40 (m, 3H).

^{13}C NMR (101 MHz, $CDCl_3$ mixture of rotamers) δ 150.4, 150.3, 141.8, 141.4, 133.5, 133.4, 127.3, 126.5, 126.1, 126.1, 125.84 – 125.46 (m), 124.1 (q, *J* = 271.9 Hz) 58.7, 57.0, 50.4, 49.1, 28.5, 27.6, 24.5, 24.4, 21.2, 21.1.

^{19}F NMR (376 MHz, $CDCl_3$ mixture of rotamers) δ -62.59, -62.63.

Synthesis of compound 39e:

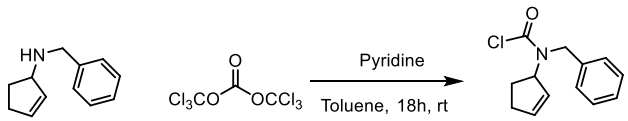

Compound **39e** was prepared according to a modification of a reported procedure.[38b] To a solution of triphosgene (134 mg, 0.44 mmol) in toluene (8 mL) under N_2, pyridine (0.129 mL, 1.6 mmol) and subsequently a solution of *N*-benzylcyclopent-2-en-1-amine (231 mg, 1.33 mmol) in toluene (2 mL). The reaction mixture was stirred for 18 hours at ambient temperature, quenched with NH_4Cl (20 mL of a saturated aq. solution) and extracted with Et_2O (2 x 30 mL). The combined organic extracts were washed sequentially with HCl (40 mL of a 0.25 M aq. solution), H_2O (40 mL) and brine (40 mL), dried over $MgSO_4$, filtered and evaporated under reduced pressure to give carbamoyl chloride **39e** (106 mg, 34% yield) as a yellowish oil.

^{1}H NMR (400 MHz, $CDCl_3$, mixture of rotamers) δ. 7.40 – 7.20 (m, 5H), 6.02 - 5.95 (m, 1H), 5.58 – 5.46 (m, 2H), 4.66 – 4.37 (m, 1H), 2.44 – 2.20 (m, 3H), 1.75 – 1.59 (m, 1H).

^{13}C NMR (101 MHz, $CDCl_3$, mixture of rotamers) δ 150.1, 150, 137.3, 136.9, 136.4, 128.8, 128.7, 128.7, 128.6, 128.5, 127.3, 127.2, 126.2, 67.6, 66, 50.6, 48.9, 31.4, 31.3, 28.9, 28.4.

HRMS (ESI pos): calculated for $C_{13}H_{14}ClNaNO$ ($M+Na^+$) 258.07, found 258.0653.

Synthesis of compound 39f:

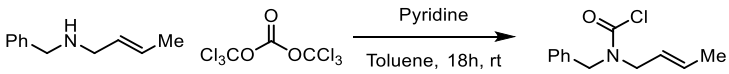

Compound **39f** was prepared according to a modification of a reported procedure.[38b] To a solution of triphosgene (250 mg, 0.843 mmol) in toluene (15 mL) under N_2, pyridine (0.241 mL, 2.98 mmol) and subsequently a solution of *N*-benzylbut-2-en-1-amine (400 mg, 2.48

mmol) in toluene (4 mL), were added. The reaction mixture was stirred for 18 hours at ambient temperature, quenched with NH_4Cl (20 mL of a saturated aq. solution) and extracted with Et_2O (2 x 30 mL). The combined organic extracts were washed sequentially with HCl (40 mL of a 0.25 M aq. solution), H_2O (40 mL) and brine (40 mL), dried over $MgSO_4$, filtered and evaporated under reduced pressure to give carbamoyl chloride **39f** (508 mg, 92% yield) as a yellow oil.

^{1}H NMR (400 MHz, $CDCl_3$, 1:1 mixture of rotamers) 7.42 – 7.30 (m, 3H), 7.29 – 7.24 (m, 2H), 5.75 – 5.54 (m, 1H), 5.53 – 5.34 (m, 1H), 4.68 (s, 1H), 4.55 (s, 1H), 3.90 (dd, *J* = 15.6, 6.3 Hz, 2H), 1.78 – 1.66 (m, 3H).

^{13}C NMR (101 MHz, $CDCl_3$, 1:1 mixture of rotamers) δ 150.2, 149.6, 135.8, 135.6, 131.3, 130.7, 129.0, 128.9, 128.4, 128.3, 128.1, 128.1, 127.3, 124.3, 124.0, 53.2, 51.9, 51.5, 50.5, 17.8.

Synthesis of compound 39g:

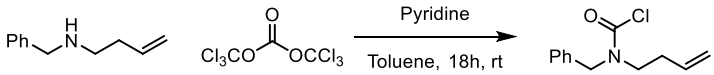

Compound **39g** was prepared according to a modification of a reported procedure.[38b] To a solution of triphosgene (252 mg, 0.85 mmol) in toluene (15 mL) under N_2, pyridine (0.243 mL, 3.0 mmol) and subsequently a solution of *N*-benzylbut-3-en-1-amine (403 mg, 2.5 mmol) in toluene (4 mL), were added. The reaction mixture was stirred for 18 hours at ambient temperature, quenched with NH_4Cl (20 mL of a saturated aq. solution) and extracted with Et_2O (2 x 30 mL). The combined organic extracts were washed sequentially with HCl (40 mL of a 0.25 M aq. solution), H_2O (40 mL) and brine (40 mL), dried over $MgSO_4$, filtered and evaporated under reduced pressure to give carbamoyl chloride **39g** (475 mg, 85% yield) as a yellow oil.

^{1}H NMR (400 MHz, $CDCl_3$, 1:1 mixture of rotamers) δ 7.41 – 7.31 (m, 3H), 7.30 – 7.24 (m, 2H), 5.80 – 5.67 (m, 1H), 5.16 – 5.04 (m, 2H), 4.72 (s, 1H), 4.59 (s, 1H), 3.53 – 3.35 (m, 2H), 2.42 – 2.30 (m, 2H).

^{13}C NMR (101 MHz, $CDCl_3$, 1:1 mixture of rotamers) δ 150.3, 149.6, 135.8, 135.6, 134.3, 134.0, 129.1, 129.0, 128.3, 128.2, 128.2, 127.2, 118.0, 117.8, 54.7, 52.7, 49.8, 48.9, 32.6, 31.7.

Synthesis of compound 39h:

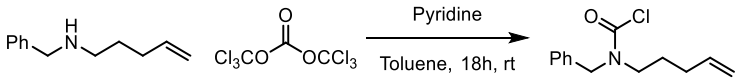

Compound **39h** was prepared according to a modification of a reported procedure.[38b] To a solution of triphosgene (252 mg, 0.85 mmol) in toluene (15 mL) under N_2, pyridine (0.243 mL, 3.0 mmol) and subsequently a solution of *N*-benzylpent-4-en-1-amine (438 mg, 2.5 mmol) in toluene (4 mL), were added. The reaction mixture was stirred for 18 hours at ambient temperature, quenched with NH_4Cl (20 mL of a saturated aq. solution) and extracted with Et_2O (2 x 30 mL). The combined organic extracts were washed sequentially with HCl (40 mL of a 0.25 M aq. solution), H_2O (40 mL) and brine (40 mL), dried over $MgSO_4$, filtered and evaporated under reduced pressure to give carbamoyl chloride **39h** (553 mg, 93% yield) as a yellow oil.

^{1}H NMR (400 MHz, $CDCl_3$, 1:1 mixture of rotamers) δ 7.41 – 7.30 (m, 3H), 7.29 – 7.24 (m, 2H), 5.81 – 5.68 (m, 2H), 5.08 – 4.92 (m, 2H), 4.71 (s, 1H), 4.58 (s, 1H), 3.36 (dt, *J* = 13.6, 7.8 Hz, 2H), 2.05 (q, *J* = 7.5 Hz, 2H), 1.70 (app h, *J* = 7.6 Hz, 2H).

^{13}C NMR (101 MHz, $CDCl_3$, 1:1 mixture of rotamers) δ 150.3, 149.6, 137.3, 137.1, 135.9, 135.7, 129.0, 129.0, 128.2, 127.2, 115.8, 115.6, 54.5, 52.6, 50.0, 49.1, 30.8, 30.8, 27.1, 26.3.

3.9.3 Reaction with aroyl chlorides

3.9.3.1 Experimental Setup

Our photoreactor consisted of a 12.5 cm diameter jar, fitted with 4 standard 29 sized ground glass joints arranged in a square and a central 29 sized joint. A commercial 1-meter LED strip was wrapped around the jar, followed by a layer of aluminium foil and cotton for insulation (Figure 3.7).

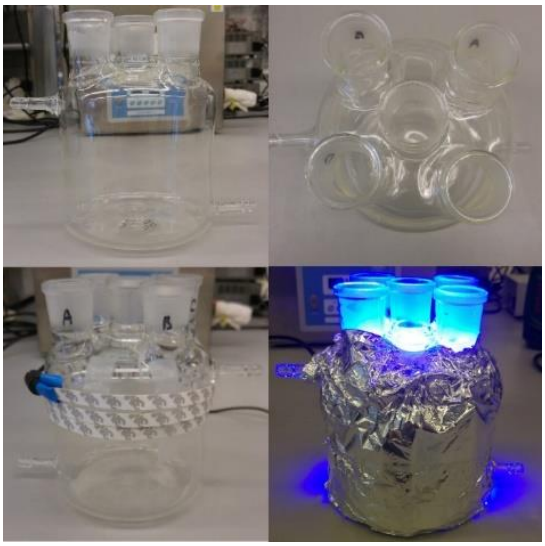

Figure 3.7. Photoreactor used for temperature-controlled reactions - pictures taken at different stages of the set-up assembly.

Each of the joints could be used to fit a standard 16 mm or 25 mm diameter Schlenk tube with a Teflon adaptor (Figure 3.8)

Figure 3.8. Teflon adaptors to use Schlenk tubes in the photoreactor.

An inlet and an outlet allow the circulation of liquid from a Huber Minichiller 300 inside the jar. This setup allows to perform reactions at temperatures ranging from -20 ºC to 80 ºC with accurate control of the reaction temperature (± 1ºC, Figure 3.9).

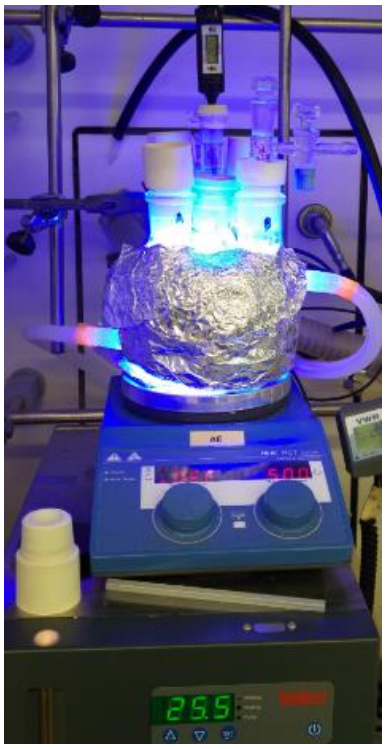

Figure 3.9. Fully assembled controlled temperature photoreactor in operation.

In order to maintain consistent illumination between different experiments, only the four external positions were used to perform reactions. The central position was used to monitor

the temperature inside a Schlenk tube identical to those used to perform reactions, ensuring that the reaction mixtures are at the desired temperature.

3.9.3.2 Optimization studies

Table 3.3. Anhydride method - optimization

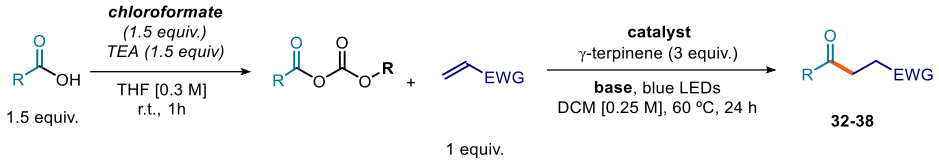

entry	acid	chloroformate	base	catalyst	acceptor	NMR yield (%)
1	Benzoic	Ethyl	Na_3PO_4	10 mol% **B**	Acrylonitrile	50
2	Benzoic	Ethyl	Na_3PO_4	10 mol% **C**	Acrylonitrile	55
3	Benzoic	Ethyl	Na_3PO_4	20 mol% **B**	Acrylonitrile	60
4	Benzoic	Ethyl	Na_3PO_4 (1 equiv.)	20 mol% **B**	Acrylonitrile	69
5	Benzoic	Ethyl	-	20 mol% **B**	Acrylonitrile	71
6	Benzoic	Methyl	-	20 mol% **B**	Acrylonitrile	61
7	Benzoic	Isobutyl	-	20 mol% **B**	Acrylonitrile	15
8	Cyclohexyl	Ethyl	-	20 mol% **B**	Vinyl sulfone	64
9	Cyclohexyl	Ethyl	-	20 mol% **C**	Vinyl sulfone	42
10	Cyclohexyl	Ethyl	-	30 mol% **B**	Vinyl sulfone	83
11	Cyclohexyl	Ethyl	-	50 mol% **B**	Vinyl sulfone	82

All reaction performed on 0.5 mmol scale; yield determined by 1H NMR analysis of the crude reaction mixture using trichloroethylene as the internal standard.

3.9.3.3 General Procedure A

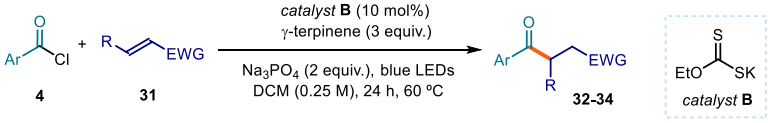

In an oven dried tube of 15 mL (16 mm × 125 mm) with a Teflon septum screw cap, potassium ethyl xanthogenate **B** (8 mg, 0.05 mmol, 0.1 equiv.), sodium phosphate (164 mg, 1.00 mmol, 2 equiv.), acyl chloride **4** (0.75 mmol, 1.5 equiv.) and the electron-poor olefin **31** (0.5 mmol, 1 equiv., *if solid*), were dissolved in DCM (2 mL, HPLC grade). Then, γ-terpinene (240 µL, 1.5 mmol, 3 equiv.) was added. The resulting yellow mixture was degassed with argon sparging for 60 seconds. When the electron-poor olefin **31** is *liquid*, it was added via syringe

after the argon sparging. The reaction vessel was then placed in the temperature-controlled photoreactor (Figure 3.9) set at 60 ºC (60-61 ºC measured in the central well) and irradiated for 16 hours upon stirring, if not otherwise specified. Then, the solvent was evaporated and the residue purified by column chromatography to afford the corresponding product in the stated yield with >95% purity according to ^{1}H NMR analysis.

3.9.3.4 Characterization of Products

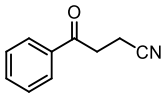

4-Oxo-4-phenylbutanenitrile (32a): Synthesized according to the general procedure A using benzoyl chloride (87 µL, 0.75 mmol, 1.5 equiv.) and acrylonitrile (33 µL, 0.5 mmol, 1 equiv.). The crude mixture was purified by flash column chromatography on silica gel (20% AcOEt in hexanes as eluent) to afford **32a** (65 mg, 82% yield) as a white solid.

^{1}H NMR (500 MHz, $CDCl_3$) δ 7.98 – 7.93 (m, 2H), 7.64 – 7.59 (m, 1H), 7.53 – 7.47 (m, 2H), 3.41 – 3.35 (m, 2H), 2.80 – 2.75 (m, 2H).

^{13}C NMR (126 MHz, $CDCl_3$) δ 195.4, 135.7, 134.0, 129.0, 128.1, 119.3, 34.4, 11.9

Matching reported literature data.[39]

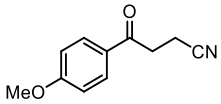

4-(4-methoxyphenyl)-4-oxobutanenitrile (32b): Synthesized according to the general procedure A using 4-methoxybenzoyl chloride (102 µL, 0.75 mmol, 1.5 equiv.) and acrylonitrile (33 µL, 0.5 mmol, 1 equiv.). The crude mixture was purified by flash column chromatography on silica gel (15% AcOEt in hexanes as eluent) to afford **32b** (80 mg, 84% yield) as a white solid.

^{1}H NMR (500 MHz, $CDCl_3$) δ 7.92 (app d, *J* = 8.9 Hz, 2H), 6.95 (app d, *J* = 9.0 Hz, 2H), 3.87 (s, 3H), 3.32 (t, *J* = 7.3 Hz, 2H), 2.75 (t, *J* = 7.3 Hz, 2H).

^{13}C NMR (126 MHz, $CDCl_3$) δ 193.9, 164.2, 130.4, 128.8, 119.5, 114.1, 55.7, 34.0, 12.0

Matching reported literature data.[39]

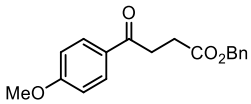

Benzyl 4-(4-methoxyphenyl)-4-oxobutanoate (32c): Synthesized according to the general procedure A using 4-methoxybenzoyl chloride (102 µL, 0.75 mmol, 1.5 equiv.) and benzyl acrylate (77 µL, 0.5 mmol, 1 equiv.). The crude mixture was purified by flash column chromatography on silica gel (15% AcOEt in hexanes as eluent), followed by a second purification (AcOEt/hexanes/toluene 1:6:6 as eluent) to afford **32c** (96 mg, 64% yield) as a yellow solid.

---

[39] Li, Y.; Shang, J.-Q.; Wang, X.-X.; Xia, W.-J.; Yang, T.; Xin, Y.; Li, Y.-M. Copper-Catalyzed Decarboxylative Oxyalkylation of Alkynyl Carboxylic Acids: Synthesis of γ-Diketones and γ-Ketonitriles. *Org. Lett.* **2019**, *21*, 2227- 2230.

^{1}H NMR (500 MHz, $CDCl_3$) δ 7.99 – 7.94 (m, 2H), 7.38 7.29 (m, 5H), 6.96 – 6.91 (m, 2H), 5.15 (s, 2H), 3.87 (s, 3H), 3.28 (t, *J* = 6.7 Hz, 2H), 2.81 (t, *J* = 6.7 Hz, 2H).

^{13}C NMR (126 MHz, $CDCl_3$) δ 196.6, 173.0, 163.7, 136.1, 130.4, 129.8, 128.6, 128.3 (2C overlapping), 113.9, 66.6, 55.6, 33.1, 28.5.

HRMS (ESI pos): calculated for $C_{18}H_{18}NaO_4$ ($M+Na^+$): 321.1097, found: 321.1091.

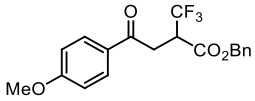

Benzyl 4-(4-methoxyphenyl)-4-oxo-2-(trifluoromethyl)butanoate (32d): Synthesized according to the general procedure A using 4-methoxybenzoyl chloride (102 µL, 0.75 mmol, 1.5 equiv.) and benzyl 2-(trifluoromethyl)acrylate (115 mg, 0.5 mmol, 1 equiv.). The crude mixture was purified by flash column chromatography on silica gel (10% AcOEt in hexanes as eluent). In order to remove traces of *p*-anisaldehyde formed as a byproduct during the reaction, after the chromatographic purification and solvent removal, the mixture was dissolved in 1.5 mL of MeOH, and 7.5 mL of saturated $NaHSO_3$ (aq) were added. Subsequently, the mixture was stirred for 30 s, diluted with 7.5 mL of H_2O, and extracted with 7.5 mL of 10% AcOEt in hexanes. The organic layer was dried with $MgSO_4$, filtered, and concentrated in vacuo[40] to afford **32d** (150 mg, 82% yield) as a colorless oil.

^{1}H NMR (400 MHz, $CDCl_3$) δ 7.99 – 7.91 (m, 2H), 7.42 – 7.29 (m, 5H), 6.99 – 6.91 (m, 2H), 5.24 (dd, *J* = 18.3; 12.3 Hz, 2H), 4.01 – 3.89 (m, 1H), 3.87 (s, 3H), 3.78 (dd, *J* = 17.7, 10.8 Hz, 1H), 3.32 (dd, *J* = 17.7, 3.1 Hz, 1H).

^{13}C NMR (100 MHz, $CDCl_3$) δ 193.8, 166.9 (q, *J* = 2.9 Hz), 164.2, 135.2, 130.6 (2CH overlapping), 128.9, 128.7, 128.5, 128.1, 125.0 (q, *J* = 280.4 Hz), 114.0, 67.9, 55.6, 45.9 (q, *J* = 27.9 Hz), 34.9 (d, *J* = 1.4 Hz).

^{19}F NMR (376 MHz, $CDCl_3$, proton decoupled) δ -67.51 (s, 3F).

HRMS (ESI pos): calculated for $C_{19}H_{17}F_3NaO_4$ ($M+Na^+$): 389.0971, found: 389.0978.

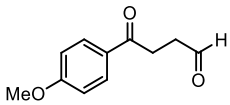

4-(4-Methoxyphenyl)-4-oxobutanal (32e): Synthesized according to the general procedure A using 4-methoxybenzoyl chloride (102 µL, 0.75 mmol, 1.5 equiv.) and acrolein (33 µL, 0.5 mmol, 1 equiv.). The crude mixture was purified by flash column chromatography on silica gel (20% AcOEt in hexanes as eluent), followed by a second purification (5:47:48 of Et_2O/DCM/hexanes as eluent) to afford **32e** (50 mg, 52% yield) as a yellow oil.

[40] Boucher, M. M.; Furigay, M. H.; Quach, P. K.; Brindle, C. S. Liquid–Liquid Extraction Protocol for the Removal of Aldehydes and Highly Reactive Ketones from Mixtures *Org. Process Res. Dev.* **2017**, *21*, 1394-1403.

^{1}H NMR (400 MHz, $CDCl_3$) δ 9.89 (s, 1H), 7.99 – 7.91 (m, 2H), 6.96 – 6.89 (m, 2H), 3.85 (s, 3H), 3.27 (app t, *J* = 6.4 Hz, 2H), 2.89 (app t, *J* = 6.5 Hz, 2H).

^{13}C NMR (100 MHz, $CDCl_3$) δ 201.0, 196.4, 163.7, 130.4, 129.6, 113.9, 55.6, 37.8, 30.8

Matching reported literature data.[41]

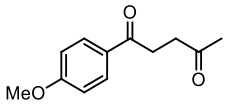

1-(4-Methoxyphenyl)pentane-1,4-dione (32f): Synthesized according to the general procedure A using 4-methoxybenzoyl chloride (102 µL, 0.75 mmol, 1.5 equiv.) and methyl vinyl ketone (41 µL, 0.5 mmol, 1 equiv.). The crude mixture was purified by flash column chromatography on silica gel (20% AcOEt in hexanes as eluent), followed by a second one (10:45:45 of Et_2O/DCM/Hexanes as eluent) to afford **32f** (49 mg, 48% yield) white solid.

^{1}H NMR (400 MHz, $CDCl_3$) δ 7.98 – 7.91 (m, 2H), 6.95-6.89 (m, 2H), 3.85 (s, 3H), 3.25 – 3.18 (m, 2H), 2.88 – 2.82 (m, 2H), 2.24 (s, 3H).

^{13}C NMR (100 MHz, $CDCl_3$) δ 207.6, 197.1, 164.6, 130.4, 129.9, 113.8, 55.6, 37.2, 32.2, 30.2.

Matching reported literature data.[39]

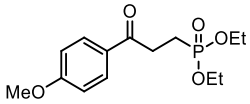

Diethyl (3-(4-methoxyphenyl)-3-oxopropyl)phosphonate (32g): Synthesized according to the general procedure A using 4-methoxybenzoyl chloride (102 µL, 0.75 mmol, 1.5 equiv.) and diethyl vinylphosphonate (77 µL, 0.5 mmol, 1 equiv.). Irradiations time: 24 hours. The crude mixture was purified by flash column chromatography on silica gel (20% AcOEt in hexanes as eluent) to afford **32g** (81 mg, 54% yield) as a white solid.

^{1}H NMR (400 MHz, $CDCl_3$) δ 7.91 (app d, *J* = 8.8 Hz, 2H), 6.89 (app d, *J* = 8.9 Hz, 2H), 4.20 – 3.96 (m, 4H), 3.82 (s, 3H), 3.28 – 3.12 (m, 2H), 2.22 – 2.04 (m, 2H), 1.28 (t, *J* = 7.0 Hz, 6H).

^{13}C NMR (100 MHz, $CDCl_3$) δ 196.0 (d, *J* = 16.2 Hz), 163.7, 130.3, 129.4, 113.8, 61.7 (d, *J* = 6.6 Hz), 55.5, 31.3 (d, *J* = 2.9 Hz), 19.9 (d, *J* = 144.3 Hz), 6.5 (d, *J* = 6.5 Hz).

Matching reported literature data.[42]

---

[41] Wang, J.; Huang, B.; Shi, C.; Yang, C.; Xia, W. Visible-Light-Mediated Ring-Opening Strategy for the Regiospecific Allylation/Formylation of Cycloalkanols *J. Org. Chem.* **2018**, *83*, 9696-9706.
[42] Yu, J.-W.; Huang, S. K. Synthesis of diethyl 3-aryl-3-oxopropylphosphonates. *Org. Prep. Proced. Int.* **1997**, *29*, 214-218.

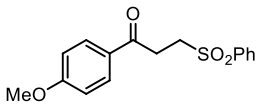

1-(4-Methoxyphenyl)-3-(phenylsulfonyl)propan-1-one (32h): Synthesized according to the general procedure A using 4-methoxybenzoyl chloride (102 μL, 0.75 mmol, 1.5 equiv.) and phenyl vinyl sulfone (84 mg, 0.5 mmol, 1 equiv.). Reaction time: 24 hours. The crude mixture was purified by flash column chromatography on silica gel (25% AcOEt in hexanes as eluent), followed by a second one (20% AcOEt in hexanes as eluent) to afford **32h** (128 mg, 84% yield) as a white solid.

^{1}H NMR (500 MHz, $CDCl_3$) δ 7.96 – 7.93 (m, 2H), 7.91 – 7.87 (m, 2H), 7.69 – 7.63 (m, 1H), 7.60 – 7.54 (m, 2H), 6.95 – 6.90 (m, 2H), 3.86 (s, 3H), 3.57 – 3.51 (m, 2H), 3.46 – 3.40 (m, 2H).

^{13}C NMR (126 MHz, $CDCl_3$) δ 193.9, 164.1, 139.3, 134.0, 130.5, 129.5, 129.0, 128.1 114.1, 55.7, 51.3, 31.0.

Matching reported literature data.[43]

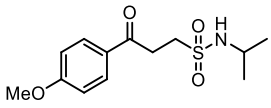

***N*-Isopropyl-3-(4-methoxyphenyl)-3-oxopropane-1-sulfonamide (32i):** Synthesized according to the general procedure A using 4-methoxybenzoyl chloride (102 μL, 0.75 mmol, 1.5 equiv.) and N-isopropylethenesulfonamide (75 mg, 0.5 mmol, 1 equiv.). Reaction time: 24 hours. The crude mixture was purified by flash column chromatography on silica gel (20% AcOEt in hexanes as eluent) to afford **32i** (98 mg, 69% yield) as a white solid.

^{1}H NMR (400 MHz, $CDCl_3$) δ 7.98 – 7.91 (m, 2H), 6.97 – 6.90 (m, 2H), 4.35 (bs, 1H, NH), 3.87 (s, 3H), 3.74 – 3.58 (m, 1H), 3.54 – 3.38 (m, 4H), 1.24 (d, J = 6.4 Hz, 6H).

^{13}C NMR (100 MHz, $CDCl_3$) δ 194.7, 164.1, 130.6, 129.2, 114.1, 55.7, 48.7, 46.5, 32.7, 24.4.

HRMS (ESI neg): calculated for $C_{13}H_{18}NO_4S$ (M^-): 284.0962, found 284.0974.

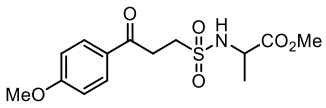

Methyl ((3-(4-methoxyphenyl)-3-oxopropyl)sulfonyl)alaninate (32j): Synthesized according to the general procedure A using 4-methoxybenzoyl chloride (102 μL, 0.75 mmol, 1.5 equiv.) and methyl (vinylsulfonyl)alaninate (97 mg, 0.5 mmol, 1 equiv.). Reaction time: 24 hours. The crude mixture was purified by flash column chromatography on silica gel (35% AcOEt in hexanes as eluent), followed by a second one (20:40:40 of AcOEt/DCM/Hexanes as eluent) to afford **32j** (83 mg, 50% yield) as a colorless oil.

[43] Bhunia, A.; Yetra, S. R.; Bhojgude, S. S.; Biju, A. T. Efficient Synthesis of γ-Keto Sulfones by NHC-Catalyzed Intermolecular Stetter Reaction. *Org. Lett.* **2012**, *14*, 2830-2833.

^{1}H NMR (400 MHz, $CDCl_3$) δ 7.97 – 7.89 (m, 2H), 6.96 – 6.89 (m, 2H), 5.29 (d, *J* = 8.4 Hz, 2H), 4.25 – 4.14 (m, 1H), 3.85 (s, 3H), 3.73 (s, 3H), 3.53 – 3.40 (m, 4H), 1.45 (d, *J* = 7.15 Hz, 3H).

^{13}C NMR (100 MHz, $CDCl_3$) δ 194.5, 173.2, 164.0, 130.5, 129.1, 114.0 55.6, 52.9, 51.7, 48.4, 32.2, 19.9.

HRMS (ESI pos): calculated for $C_{14}H_{19}NNaO_6S$ ($M+Na^+$): 352.0825, found 352.0814.

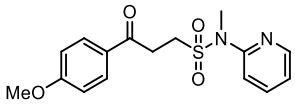

3-(4-Methoxyphenyl)-N-methyl-3-oxo-N-(pyridin-2-yl)propane-1-sulfonamide (32k): Synthesized according to the general procedure A using 4-methoxybenzoyl chloride (102 μL, 0.75 mmol, 1.5 equiv.) and N-methyl-N-(pyridin-2-yl)ethenesulfonamide (99 mg, 0.5 mmol, 1 equiv.). Reaction time: 24 hours. The crude mixture was purified by flash column chromatography on silica gel (20:20:60 of AcOEt/DCM/Hexanes as eluent), followed by a second one (20:20:60 of Et_2O/DCM/Hexanes as eluent) to afford **32k** (75 mg, 45% yield) as a yellowish oil.

^{1}H NMR (400 MHz, $CDCl_3$) δ 8.41 – 8.34 (m, 1H), 7.92 – 7.84 (m, 2H), 7.72 – 7.65 (m, 1H), 7.42 (app d, *J* = 8.3 Hz, 1H), 7.15 – 7.08 (m, 1H), 6.95 – 6.87 (m, 2H), 3.85 (s, 3H), 3.72 – 3.64 (m, 2H), 3.45 (s, 3H), 3.46 – 3.39 (m, 2H).

^{13}C NMR (100 MHz, $CDCl_3$) δ 194.2, 164.0, 154.0, 148.3, 138.2, 130.5, 129.1, 121.0, 118.6, 114.0, 55.6, 46.3, 35.9, 31.8.

HRMS (ESI pos): calculated for $C_{16}H_{19}N_2O_4S$ ($M+H^+$): 335.1060, found 335.1043.

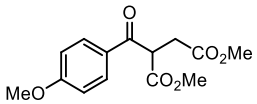

Dimethyl 2-(4-methoxybenzoyl)succinate (32l): Synthesized according to the general procedure A using 4-methoxybenzoyl chloride (102 μL, 0.75 mmol, 1.5 equiv.) and dimethyl fumarate (72 mg, 0.5 mmol, 1 equiv.). The crude mixture was purified by flash column chromatography on silica gel (20% AcOEt in hexanes as eluent) to afford **32l** (122 mg, 87% yield) as a colorless oil.

^{1}H NMR (500 MHz, $CDCl_3$) δ 8.03 – 7.98 (m, 2H), 6.96 – 6.92 (m, 2H), 4.82 (t, *J* = 7.1 Hz, 1H), 3.85 (s, 3H), 3.66 (s, 3H), 3.65 (s, 3H), 3.09 – 2.97 (m, 2H).

^{13}C NMR (126 MHz, $CDCl_3$) δ 192.3, 171.9, 169.5, 164.2, 131.4, 128.8, 114.0, 129.0, 128.1, 114.1, 55.6, 52.8, 52.1, 33.2.

Matching reported literature data.[44]

[44] Bonassi, F.; Ravelli, D.; Protti, S.; Fagnoni, M. Decatungstate Photocatalyzed Acylations and Alkylations in Flow via Hydrogen Atom Transfer. *Adv. Synth. Catal.* **2015**, *357*, 3687-3695.

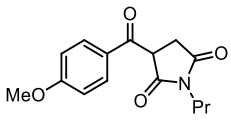

3-(4-Methoxybenzoyl)-1-propylpyrrolidine-2,5-dione (32m): Synthesized according to the general procedure A using 4-methoxybenzoyl chloride (102 μL, 0.75 mmol, 1.5 equiv.) and 1-propyl-1H-pyrrole-2,5-dione (69.6 μL, 0.5 mmol, 1 equiv.). Chromatography on silica gel (20% AcOEt in hexanes as eluent) could not remove byproduct completely. Therefore, a further purification by semipreparative HPLC (Column SunFire C18, 60:40 Methanol/Water 6 min, up to 100% Methanol 1 min, 100% Methanol 4 min, 1 mL/min) was performed to obtain an analytical amount of the isolated product as a white solid. NMR yield (Trichloroethylene was used as internal standard): 53%.

^{1}H NMR (500 MHz, $CDCl_3$) δ 8.12-8.07 (m, 2H), 7.02 – 6.97 (m, 2H), 4.78 (dd, *J* = 8.3, 3.9 Hz, 1H), 3.90 (s, 3H), 3.47 (t, *J* = 7.3 Hz, 2H), 3.37 (dd, *J* = 18.1, 3.8 Hz, 1H), 2.82 (dd, *J* = 18.1, 8.8 Hz, 1H), 1.64 – 1.54 (m, 2H, overlapping with water peak), 0.87 (t, *J* = 7.4 Hz, 3H).

^{13}C NMR (126 MHz, $CDCl_3$) δ 190.9, 176.1, 173.4, 164.7, 132.4, 128.6, 114.2, 55.7, 48.2, 41.0, 31.8, 21.0, 11.3

HRMS (ESI pos): calculated for $C_{15}H_{17}NNaO_4$ ($M+Na^+$): 298.1050, found 298.1056.

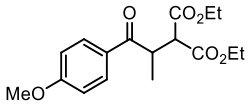

Diethyl 2-(1-(4-methoxyphenyl)-1-oxopropan-2-yl)malonate (32n): Synthesized according to the general procedure A using 4-methoxybenzoyl chloride (102 μL, 0.75 mmol, 1.5 equiv.) and diethyl 2-ethylidenemalonate (93 μL, 0.5 mmol, 1 equiv.). The crude mixture was purified by flash column chromatography on silica gel (10% AcOEt in hexanes as eluent) to afford **32n** (60 mg, 37% yield) as a colorless oil.

^{1}H NMR (400 MHz, $CDCl_3$) δ 8.03 – 7.96 (m, 2H), 6.98 – 6.93 (m, 2H), 4.31 – 4.21 (m, 2H) 4.20 – 4.02 (m, 3H), 3.97 (d, *J* = 10.8 Hz, 1H), 3.87 (s, 3H), 1.31 (t, *J* = 7.0 Hz, 3H), 1.19 (d, *J* = 7.0 Hz, 3H), 1.16 (t, *J* = 7.1 Hz, 3H).

^{13}C NMR (100 MHz, $CDCl_3$) δ 200.2, 169.0, 168.5, 163.8, 131.0, 128.6, 114.0, 61.7, 55.6, 55.1, 40.3, 16.25, 14.3, 14.0.

HRMS (ESI pos): calculated for $C_{17}H_{22}NaO_6$ ($M+Na^+$): 345.1309, found 345.1306.

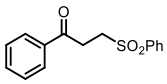

1-Phenyl-3-(phenylsulfonyl)propan-1-one (33a): Synthesized according to the general procedure A using benzoyl chloride (87 μL, 0.75 mmol, 1.5 equiv.) and phenyl vinyl sulfone (84 mg, 0.5 mmol, 1 equiv.). The crude mixture was purified by flash column chromatography on silica gel (20% AcOEt in hexanes as eluent) to afford **33a** (112 mg, 82% yield) as a white solid.

^{1}H NMR (400 MHz, $CDCl_3$) δ 7.99 – 7.88 (m, 4H), 7.70 – 7.63 (m, 1H), 7.63 – 7.54 (m, 3H), 7.51 – 7.43 (m, 2H), 3.60 – 3.53 (m, 2H), 3.53 – 3.46 (m, 2H).

^{13}C NMR (100 MHz, $CDCl_3$) δ 195.5, 139.2, 135.9, 134.1, 133.9, 129.6, 128.9, 128.2, 128.1, 51.1, 31.5.

Matching reported literature data.[43]

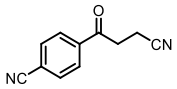

4-(3-Cyanopropanoyl)benzonitrile (33b): Synthesized according to the general procedure A using using 4-cyanobenzoyl chloride (124 mg, 0.75 mmol, 1.5 equiv.) and acrylonitrile (33 µL, 0.5 mmol, 1 equiv.). In this case the reaction was irradiated for 60 hours. The crude mixture was purified by flash column chromatography on silica gel (15% AcOEt in hexanes as eluent) to afford **33b** (92 mg, 45% yield) as a white solid.

^{1}H NMR (500 MHz, $CDCl_3$) δ 8.04 (app d, J = 8.2 Hz, 2H), 7.80 (app d, J = 8.2 Hz, 2H), 3.39 (t, J = 6.9 Hz, 2H), 2.79 (t, J = 7.0 Hz, 2H).

^{13}C NMR (126 MHz, $CDCl_3$) δ 194.3, 138.5, 132.8, 128.6, 118.8, 117.7, 117.3, 34.7, 11.8.

Matching reported literature data.[39]

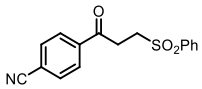

4-(3-(Phenylsulfonyl)propanoyl)benzonitrile (33c): Synthesized according to the general procedure A using 4-cyanobenzoyl chloride (124 mg, 0.75 mmol, 1.5 equiv.) and phenyl vinyl sulfone (84 mg, 0.5 mmol, 1 equiv.). In this case the reaction was irradiated for 60 hours. The crude mixture was purified by flash column chromatography on silica gel (25% AcOEt in hexanes as eluent) to afford **33c** (79 mg, 53% yield) as a white solid.

^{1}H NMR (400 MHz, $CDCl_3$) δ 8.02 (app d, J = 8.5 Hz, 2H), 7.95 (app d, J = 7.3 Hz, 2H), 7.78 (app d, J = 8.4 Hz, 2H), 7.69 (app t, J = 7.4 Hz, 1H), 7.59 (app t, J = 7.7 Hz, 2H), 3.60 – 3.48 (m, 4H).

^{13}C NMR (100 MHz, $CDCl_3$) δ 194.4, 139.1, 138.8, 134.2, 132.8, 129.6, 128.6, 128.1, 117.8, 117.2, 50.9, 31.8.

HRMS (ESI pos): calculated for $C_{16}H_{13}NNaO_3S$ ($M+Na^+$): 322.0508, found 322.0505.

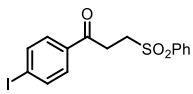

1-(4-Iodophenyl)-3-(phenylsulfonyl)propan-1-one (33d): Synthesized according to the general procedure A using 4-iodobenzoyl chloride (200 mg, 0.75 mmol, 1.5 equiv.) and phenyl vinyl sulfone (84 mg, 0.5 mmol, 1 equiv.). In this case the reaction was irradiated for 60 hours. The crude mixture was purified by flash column chromatography on silica gel (20% AcOEt in hexanes as eluent) to afford **33d** (130 mg, 65% yield) as a white solid.

^{1}H NMR (500 MHz, $CDCl_3$) δ 7.99 – 7.92 (m, 2H), 7.87 – 7.82 (m, 2H), 7.70 – 7.65 (m, 1H), 7.65 – 7.61 (m, 2H), 7.61 – 7.56 (m, 2H), 3.58 – 3.51 (m, 2H) 3.49 – 3.42 (m, 2H).

^{13}C NMR (126 MHz, $CDCl_3$) δ 194.9, 139.2, 138.3, 135.2, 134.1, 129.6, 129.5, 128.1, 102.1, 51.0, 31.4

HRMS (ESI pos): calculated for $C_{15}H_{13}INaO_3S$ ($M+Na^+$): 422.9522, found 422.9519.

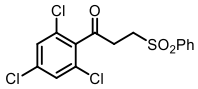

3-(Phenylsulfonyl)-1-(2,4,6-trichlorophenyl)propan-1-one (33e): Synthesized according to the general procedure A using 2,4,6-trichlorobenzoyl chloride (183 mg, 0.75 mmol, 1.5 equiv.) and phenyl vinyl sulfone (84 mg, 0.5 mmol, 1 equiv.). In this case the reaction was irradiated for 60 hours. The crude mixture was purified by flash column chromatography on silica gel (25% AcOEt in hexanes as eluent) followed by a second one (5:25:70 of AcOEt/DCM/Hexanes as eluent) to afford **33e** (95 mg, 50% yield) as a withe solid.

^{1}H NMR (400 MHz, $CDCl_3$) δ 7.98 – 7.92 (m, 2H), 7.72 – 7.65 (m, 1H), 7.63 – 7.56 (m, 2H), 7.36 (s, 2H), 3.58 – 3.50 (m, 2H), 3.33 – 3.25 (m, 2H).

^{13}C NMR (100 MHz, $CDCl_3$) δ 197.2, 138.9, 137.0, 136.6, 134.2, 131.2, 129.6, 128.5, 128.1, 50.1, 36.5

HRMS (ESI pos): calculated for $C_{15}H_{11}Cl_3NaO_3S$ ($M+Na^+$): 398.9387, found 398.9390.

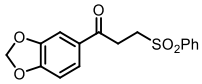

1-(Benzo[d][1,3]dioxol-5-yl)-3-(phenylsulfonyl)propan-1-one (33f): Synthesized according to the general procedure A using benzo[d][1,3]dioxole-5-carbonyl chloride (138 mg, 0.75 mmol, 1.5 equiv.) and phenyl vinyl sulfone (84 mg, 0.5 mmol, 1 equiv.). Reaction time: 24 hours. The crude mixture was purified by flash column chromatography on silica gel (25% AcOEt in hexanes as eluent) to afford **33f** (90 mg, 57% yield) as a white solid.

^{1}H NMR (500 MHz, $CDCl_3$) δ 7.96 – 7.92 (m, 2H), 7.67 (tt, *J* = 7.3, 1.8 Hz, 1H), 7.60 – 7.55 (m, 2H), 7.52 (dd, *J* = 8.1, 1.8 Hz, 1H), 7.36 (d, *J* = 1.7 Hz, 1H), 6.84 (d, *J* = 8.1 Hz, 1H), 6.04 (s, 2H), 3.57 – 3.50 (m, 2H), 3.44 – 3.37 (m, 2H).

^{13}C NMR (126 MHz, $CDCl_3$) δ 193.5, 152.5, 148.5, 139.2, 134.0, 130.8, 129.5, 128.1, 124.7, 108.2, 107.8, 102.2, 51.3, 31.2.

HRMS (ESI pos): calculated for $C_{16}H_{14}NaO_5S$ ($M+Na^+$): 341.0454, found 341.0452.

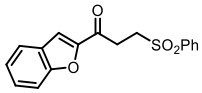

1-(Benzofuran-2-yl)-3-(phenylsulfonyl)propan-1-one (33g): Synthesized according to the general procedure A using benzofuran-2-carbonyl chloride (135 mg, 0.75 mmol, 1.5 equiv.) and phenyl vinyl sulfone (84 mg, 0.5 mmol, 1 equiv.). Reaction time: 24 hours. The crude mixture was purified

by flash column chromatography on silica gel (25% AcOEt in hexanes as eluent) followed by a second one (20% AcOEt in hexanes as eluent) to afford **33g** (77 mg, 49% yield) as a yellowish solid.

^{1}H NMR (500 MHz, $CDCl_3$) δ 7.99 – 7.94 (m, 2H), 7.71 (app d, *J* = 7.8 Hz, 1H), 7.70 – 7.65 (m, 1H), 7.61 – 7.55 (app t, *J* = 8.0 Hz, 3H), 7.55 (s, 1H), 7.53 – 7.48 (m, 1H), 7.35 – 7.30 (m, 1H), 3.61 – 3.55 (m, 2H), 3.53 – 3.47 (m, 2H).

^{13}C NMR (126 MHz, $CDCl_3$) δ 186.6, 155.9, 151.6, 139.0, 134.2, 129.6, 128.9, 128.2, 126.9, 124.3, 123.6, 113.7, 112.6, 50.6, 31.8

HRMS (ESI pos): calculated for $C_{17}H_{14}NaO_4S$ ($M+Na^+$): 337.0505, found 337.0504.

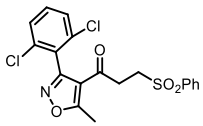

1-(3-(2,6-Dichlorophenyl)-5-methylisoxazol-4-yl)-3-(phenylsulfonyl)propan-1-one (33h): Synthesized according to the general procedure A using 3-(2,6-dichlorophenyl)-5-methylisoxazole-4-carbonyl chloride (218 mg, 0.75 mmol, 1.5 equiv.) and phenyl vinyl sulfone (84 mg, 0.5 mmol, 1 equiv.). Reaction time: 24 hours. The crude mixture was purified by flash column chromatography on silica gel (20% AcOEt in hexanes as eluent) to afford **33h** (75 mg, 35% yield) as a white solid.

^{1}H NMR (400 MHz, $CDCl_3$) δ 7.75 – 7.67 (m, 2H), 7.67 – 7.60 (m, 1H), 7.57 – 7.43 (m, 5H), 3.41 – 3.34 (m, 2H), 2.74 (s, 3H), 3.68 – 3.60 (m, 2H).

^{13}C NMR (126 MHz, $CDCl_3$) δ 189.0, 176.5, 157.2, 138.6, 135.6, 134.0, 132.2, 129.5, 128.6, 128.0, 127.9, 116.1, 50.1, 34.3, 14.2.

HRMS (ESI pos): calculated for $C_{19}H_{15}Cl_2NNaO_4S$ ($M+Na^+$): 445.9991, found 445.9992.

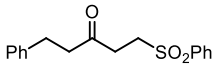

1-Phenyl-5-(phenylsulfonyl)pentan-3-one (34b): Synthesized according to the general procedure A using hydrocinnamoyl chloride (111 μL, 0.75 mmol, 1.5 equiv.) and phenyl vinyl sulfone (84 mg, 0.5 mmol, 1 equiv.). In this case the reaction was irradiated for 60 hours. The crude mixture was purified by two rounds of flash column chromatography on silica gel (25% AcOEt in hexanes as eluent): to afford **34b** (113 mg, 75% yield) as a white solid.

^{1}H NMR (400 MHz, $CDCl_3$) δ 7.92 – 7.87 (m, 2H), 7.71 – 7.63 (m, 1H), 7.61 – 7.53 (m, 2H), 7.31 – 7.23 (m, 2H), 7.22 – 7.16 (m, 1H), 7.16 – 7.10 (m, 2H), 3.42 – 3.33 (m, 2H), 2.92 – 2.82 (m, 4H), 2.81 – 2.72 (m, 2H).

^{13}C NMR (100MHz, CDCl3) δ 205.3, 140.5, 139.1, 134.1, 129.5, 128.7, 128.4, 128.1, 126.5, 50.6, 44.4, 35.3, 29.7.

Matching reported literature data.[45]

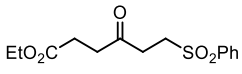

Ethyl 4-oxo-6-(phenylsulfonyl)hexanoate (34c): Synthesized according to the general procedure A using ethyl 4-chloro-4-oxobutanoate (107 μL, 0.75 mmol, 1.5 equiv.) and phenyl vinyl sulfone (84 mg, 0.5 mmol, 1 equiv.). Reaction time: 24 hours. The crude mixture was purified by flash column chromatography on silica gel (33% AcOEt in hexanes as eluent). Product was then dissolved in DCM, washed 3 times with a solution of $CuSO_4$ (5% in water), dried with $MgSO_4$ and evaporated under reduced pressure to afford **34c** (112 mg, 75% yield) as a white solid.

^{1}H NMR (400 MHz, $CDCl_3$) δ 7.92 – 7.87 (m, 2H), 7.69 – 7.63 (m, 1H), 7.61 – 7.53 (m, 2H), 4.09 (q, *J* = 7.1 Hz, 2H), 3.42 – 3.35 (m, 2H), 2.98 – 2.91 (m, 2H), 2.75 – 2.69 (m, 2H), 2.59 – 2.52 (m, 2H), 1.22 (t, *J* = 7.1 Hz, 3H).

^{13}C NMR (126 MHz, $CDCl_3$) δ 204.5, 172.5, 139.1, 134.1, 129.5, 128.1, 60.9, 50.6, 37.2, 35.3, 28.0, 14.2

HRMS (ESI pos): calculated for $C_{14}H_{18}NaO_5S$ ($M+H^+$): 321.0767, found 321.0765.

3.9.4 Reaction with alkyl acyl chlorides

3.9.4.1 Experimental Setup

Figure 3.10. Photoreactor used for the reactions of aliphatic acyl chlorides.

[45] Ravelli, D.; Montanaro, S.; Zema, M.; Fagnoni, M.; Albini, A. A Tin-Free, Radical Photocatalyzed Addition to Vinyl Sulfones. *Adv. Synth. Catal.* **2011**, *353*, 3295-3300.

Our 3D printed photoreactor consisted of a 9 cm diameter crystallizing dish with a 3D printed support of 6 positions, and a hole of 22 mm in the middle to allow ventilation. A commercial 1-meter LED strip was wrapped around the crystallizing dish. In order to control the temperature, a fan was used to cool down the reactor. Reaction temperature was measured, through a vial containing a thermometer, and it stayed between 35-40 ºC (Figure 3.10). Each of the positions could be used to fit a standard 16 mm diameter vial with a Teflon screw cap.

Experiments at 465 nm were conducted using a 1m strip, 14.4W "LEDXON MODULAR 9009083 LED, SINGLE 5050" purchased from Farnell, catalog number 9009083. The emission spectrum of these LEDs was recorded (Figure 3.11).

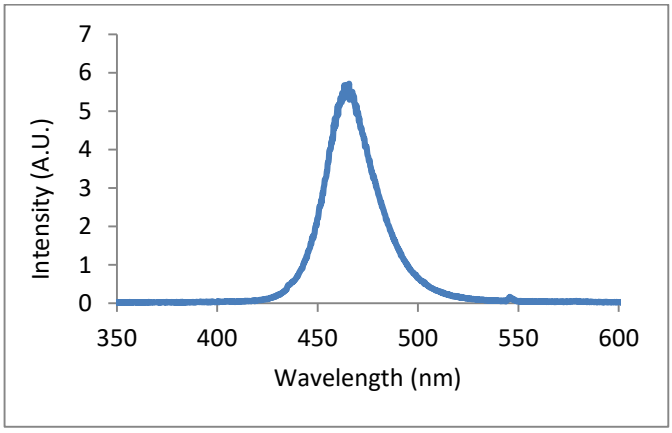

Figure 3.11. Emission spectrum of the 465 nm LED strip used in this study.

The emission maximum was determined as 465 nm with a spectral width of 30 nm (450-480 nm) at half peak intensity and a total spectral width of 120 nm (420-540 nm).

3.9.4.2 General Procedure B

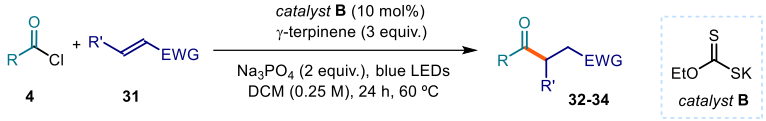

In an oven dried tube of 15 mL (16 mm × 125 mm) with a Teflon septum screw cap, potassium ethyl xanthogenate **B** (8 mg, 0.05 mmol, 0.1 equiv.), sodium phosphate (164 mg, 1.00 mmol, 2 equiv.), acyl chloride **4** (0.75 mmol, 1.5 equiv.) and the electron-poor olefin **31** (0.5 mmol, 1 equiv., *if solid*), were dissolved in DCM (2 mL, HPLC grade). Then, γ-terpinene (240 µL, 1.5 mmol, 3 equiv.) was added. The resulting yellow mixture was degassed with argon sparging for 60 seconds. When the electron-poor olefin **31** is *liquid*, it was added via syringe after the argon sparging. The vial was then placed in the 3D printed support photoreactor

(Figure 3.10) and irradiated under stirring for 24 hours, if not otherwise specified. After this, the solvent was evaporated and the residue purified by column chromatography to afford the corresponding product in the stated yield with >95% purity according to ^{1}H NMR analysis.

3.9.4.3 Characterization of Products

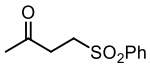

4-(Phenylsulfonyl)butan-2-one (34a): Synthesized according to the general procedure B using acetyl chloride (53 μL, 0.75 mmol, 1.5 equiv.) and phenyl vinyl sulfone (84 mg, 0.5 mmol, 1 equiv.). The crude mixture was purified by flash column chromatography on silica gel (gradient from 25% to 100% AcOEt in hexanes as eluent): to afford product **34a** (70 mg 66% yield) as a colorless oil.

^{1}H NMR (400 MHz, $CDCl_3$) δ 7.94 – 7.86 (m, 2H), 7.70 – 7.62 (m, 1H), 7.61 – 7.53 (m, 2H), 3.40 – 3.33 (m, 2H), 2.96 – 2.88 (m, 2H), 2.17 (s, 3H).

^{13}C NMR (100 MHz, $CDCl_3$) δ 203.8, 139.1, 134.0, 129.6, 128.1, 50.6, 36.0, 30.0

Matching reported literature data.[9b]

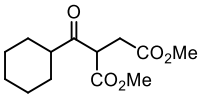

Dimethyl 2-(cyclohexanecarbonyl)succinate (34d): Synthesized according to general procedure B using cyclohexanecarbonyl chloride (100 μL, 0.75 mmol, 1.5 equiv.) and dimethyl fumarate (72 mg, 0.5 mmol, 1 equiv.). The crude mixture was purified by flash column chromatography on silica gel (10% AcOEt in hexanes as eluent) to afford **34d** (107 mg, 83% yield) as a white solid.

^{1}H NMR (500 MHz, $CDCl_3$) δ 4.14 (dd, *J* = 8.1, 6.2 Hz, 1H), 3.72 (s, 3H), 3.66 (s, 3H), 3.82 (s, 3H), 2.93 (dd, *J* = 17.5, 8.1 Hz, 1H), 2.81 (dd, *J* = 17.6, 6.5 Hz, 1H), 2.69 – 2.61 (m, 1H), 2.00 – 1.93 (m, 1H), 1.84 – 1.74 (m, 3H), 1.70 – 1.62 (m, 1H), 1.46 – 1.36 (m, 1H), 1.33 – 1.13 (m, 4H).

^{13}C NMR (126 MHz, $CDCl_3$) δ 206.7, 171.9, 169.2, 52.8, 52.2, 52.1, 50.72, 32.4, 29.0, 28.1, 25.9, 25.8, 25.5.

Matching reported literature data.[46]

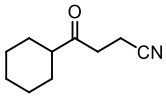

4-Cyclohexyl-4-oxobutanenitrile (34e): Synthesized according to the general procedure B using cyclohexanecarbonyl chloride (100 μL, 0.75 mmol, 1.5 equiv.) and acrylonitrile (33 μL, 0.5 mmol, 1 equiv.). The crude mixture was purified by flash column chromatography on silica gel (20% Et_2O in pentane as eluent) to afford **34e** (52 mg, 63% yield) as a colorless oil.

---

[46] Cartier, A.; Levernier, E.; Corcé, V.; Fukuyama, T.; Dhimane, A.-L.; Ollivier, C.; Ryu, I.; Fensterbank, L. Carbonylation of Alkyl Radicals Derived from Organosilicates through Visible-Light Photoredox Catalysis. *Angew. Chem. Int. Ed.* **2019**, *58*, 1789-1793.

^{1}H NMR (500 MHz, $CDCl_3$) δ 2.85-2.80 (m, 2H); 2.60-2.54 (m, 2H); 2.36 (tt, *J* = 11.3, 3.5 Hz, 1H); 1.89-1.82 (m, 2H); 1.82-1.75 (m, 2H); 1.71-1.64 (m, 1H); 1.40-1.15 (m, 5H).

^{13}C NMR (126 MHz, $CDCl_3$) δ 209.4, 119.3, 50.6, 35.9, 28.5, 25.8, 25.6, 11.6.

Matching reported literature data.[46]

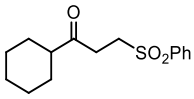

1-Cyclohexyl-3-(phenylsulfonyl)propan-1-one (34f): Synthesized according to the general procedure B using cyclohexanecarbonyl chloride (100 μL, 0.75 mmol, 1.5 equiv.) and phenyl vinyl sulfone (84 mg, 0.5 mmol, 1 equiv.). The crude mixture was purified by flash column chromatography on silica gel (20% AcOEt in hexanes as eluent) to afford **34f** (112 mg, 76% yield) as colorless oil.

A purity of 85% weight was determined ^{1}H NMR analysis (mixture with phenyl vinyl sulfone). Corrected yield: 68%.

^{1}H NMR (400 MHz, $CDCl_3$) δ 7.93 – 7.86 (m, 2H), 7.69 – 7.62 (m, 1H), 7.62 – 7.50 (m, 2H), 3.39 – 3.32 (m, 2H), 2.97 – 2.89 (m, 2H), 2.39 – 2.25 (m, 1H), 1.88 – 1.58 (m, 5H), 1.38 – 1.08 (m, 5H).

^{13}C NMR (100 MHz, $CDCl_3$) δ 193.9, 164.2, 130.4, 128.8, 119.5, 114.1, 55.7, 34.0, 12.0.

Matching reported literature data.[47]

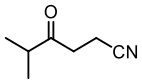

4-Cyclohexyl-4-oxobutanenitrile (34g): Synthesized according to the general procedure B using isobutanoyl chloride (100 μL, 0.75 mmol, 1.5 equiv.) and acrylonitrile (33 μL, 0.5 mmol, 1 equiv.). The crude mixture was purified by flash column chromatography on silica gel (20% Et_2O in pentane as eluent) to afford **34g** (39 mg, 62% yield) as a colorless oil.

^{1}H NMR (500 MHz, $CDCl_3$) δ 2.83 (t, *J* = 7.1 Hz, 2H), 2.66 – 2.56 (m, 1H), 2.57 (t, *J* = 7.2 Hz, 2H), 1.12 (d, *J* = 7.0 Hz, 6H).

^{13}C NMR (126 MHz, $CDCl_3$) δ 210.0, 119.2, 40.7, 35.6, 18.2, 11.6

Matching reported literature data.[48]

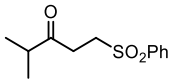

4-Methyl-1-(phenylsulfonyl)pentan-3-one (34h): Synthesized according to the general procedure B using isobutanoyl chloride (100 μL, 0.75 mmol,

[47] Vu, M. D.; Das, M.; Liu, X.-W. Direct Aldehyde Csp2−H Functionalization through Visible-Light-Mediated Photoredox Catalysis. *Chem. Eur. J.* **2017**, *23*, 15899-15902.
[48] Lee, W. Y.; Jang, S. Y.; Chae, W. K.; Park, O. S. A Total Synthesis of Isosolanone. *Synth. Commun.* **1993**, *23*, 3037-3046.

1.5 equiv.) and phenyl vinyl sulfone (84 mg, 0.5 mmol, 1 equiv.). The crude mixture was purified by flash column chromatography on silica gel (20% AcOEt in hexanes as eluent), followed by a second one (15% AcOEt in hexanes as eluent) to afford **34h** (61 mg, 51% yield) as a colorless oil.

^{1}H NMR (500 MHz, $CDCl_3$) δ 7.94 – 7.88 (m, 2H), 7.69 – 7.64 (m, 1H), 7.61 – 7.54 (m, 2H), 3.40 – 3.35 (m, 2H), 3.00 – 2.93 (m, 2H), 2.66 – 2.55 (m, 1H), 1.08 (d, *J* = 7.0 Hz, 6H).

^{13}C NMR (126 MHz, $CDCl_3$) δ 210.0, 139.2, 134.0, 129.5, 128.1, 50.8, 41.1, 32.7, 18.3.

HRMS (ESI pos): calculated for $C_{12}H_{16}NaO_3S$ ($M+Na^+$): 263.0712, found 263.0714.

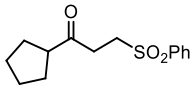

1-Cyclopentyl-3-(phenylsulfonyl)propan-1-one (34i): Synthesized according to the general procedure B using cyclopentanecarbonyl chloride (91 μL, 0.75 mmol, 1.5 equiv.) and phenyl vinyl sulfone (84 mg, 0.5 mmol, 1 equiv.). The crude mixture was purified by flash column chromatography on silica gel (20% AcOEt in hexanes as eluent) to afford **34i** (102 mg, 77% yield) colorless oil.

^{1}H NMR (500 MHz, $CDCl_3$) δ 7.93 – 7.87 (m, 2H), 7.69 – 7.62 (m, 1H), 7.60 – 7.53 (m, 2H), 3.42 – 3.34 (m, 2H), 2.99 – 2.91 (m, 2H), 2.90 – 2.79 (m, 1H), 1.88 – 1.73 (m, 2H), 1.73 – 1.49 (m, 6H).

^{13}C NMR (126 MHz, $CDCl_3$) δ 208.5, 139.2 134.0, 129.5, 128.1, 51.5, 50.8, 34.0, 29.0, 26.0.

HRMS (ESI pos): calculated for C14H18NaO3S ($M+Na^+$): 289.0869, found 289.0873.

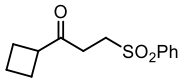

1-Cyclobutyl-3-(phenylsulfonyl)propan-1-one (34j): Synthesized according to the general procedure B using cyclobutanecarbonyl chloride (86 μL, 0.75 mmol, 1.5 equiv.) and phenyl vinyl sulfone (84 mg, 0.5 mmol, 1 equiv.). The crude mixture was purified by flash column chromatography on silica gel (20% AcOEt in hexanes as eluent) to afford **34j** (116 mg, 92% yield) as a colorless oil.

^{1}H NMR (500 MHz, $CDCl_3$) δ 7.92 – 7.88 (m, 2H), 7.68 – 7.63 (m, 1H), 7.60 – 7.54 (m, 2H), 3.40 – 3.35 (m, 2H), 3.29 – 3.20 (m, 1H), 2.87 – 2.81 (m, 2H), 2.24 – 2.08 (m, 4H), 2.02 – 1.90 (m, 1H), 1.84 – 1.75 (m, 1H).

^{13}C NMR (126 MHz, $CDCl_3$) δ 207.1, 139.2, 134.1, 129.5, 128.1, 50.6, 45.4, 32.3, 24.5, 17.9

HRMS (ESI pos): calculated for $C_{13}H_{15}NaO_6$ ($M+Na^+$): 275.0712, found 275.0716.

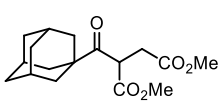

Dimethyl 2-((3r,5r,7r)-adamantane-1-carbonyl)succinate (34k): Synthesized according to the general procedure B using 1-adamantanecarbonyl chloride (149 mg, 0.75 mmol, 1.5 equiv.) and dimethyl fumarate (72 mg, 0.5 mmol, 1 equiv.). The crude mixture was purified by flash

column chromatography on silica gel (5% AcOEt in hexanes as eluent) to afford **34k** (85 mg, 55% yield) as a colorless oil.

^{1}H NMR (500 MHz, $CDCl_3$) δ 4.37 (app t, *J* = 7.2 Hz, 1H), 3.67 (s, 3H), 3.64 (s, 3H), 2.79 (app d, *J* = 7.2 Hz, 2H), 2.03 (bs, 3H), 1.89 – 1.79 (m, 6H), 1.76 – 1.63 (m, 6H).

^{13}C NMR (126 MHz, $CDCl_3$) δ 208.8, 171.7, 169.5, 52.7, 52.1, 47.7, 47.4, 38.0, 36.4, 33.5, 27.9

HRMS (ESI pos): calculated for $C_{17}H_{24}NaO_5$ ($M+Na^+$): 331.1516, found 331.1523.

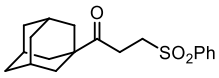

1-((3r,5r,7r)-Adamantan-1-yl)-3-(phenylsulfonyl)propan-1-one (34l): Synthesized according to the general procedure B using 1-adamantanecarbonyl chloride (149 mg, 0.75 mmol, 1.5 equiv.) and phenyl vinyl sulfone (84 mg, 0.5 mmol, 1 equiv.). The crude mixture was purified by flash column chromatography on silica gel (15% AcOEt in hexanes as eluent) to afford **34l** (165 mg, 95% yield) as a colorless oil.

^{1}H NMR (500 MHz, $CDCl_3$) δ 7.93 – 7.88 (m, 2H), 7.68 – 7.63 (m, 1H), 7.60 – 7.54 (m, 2H), 3.37 – 3.29 (m, 2H), 3.00-2.93 (m, 2H), 2.03 (bs, 3H), 1.79 – 1.70 (m, 9H), 1.66 (app d, *J* = 12.2 Hz, 3H).

^{13}C NMR (126 MHz, $CDCl_3$) δ 211.2, 139.3, 133.9, 129.4, 128.0, 50.9, 46.5, 38.3, 36.5, 29.1, 27.9.

HRMS (ESI pos): calculated for $C_{19}H_{25}O_3S$ ($M+H^+$): 333.1519, found 333.1519.

3.9.5 Reaction of carboxylic acids through acyl chloride formation

3.9.5.1 General Procedure C

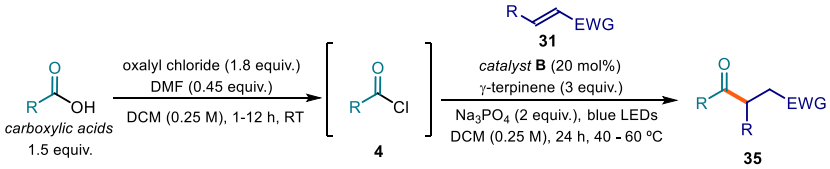

In a round bottom flask, the carboxylic acid (0.75 mmol, 1.5 equiv) was dissolved in DCM (3 mL, HPLC grade). Then, oxalyl chloride (0.79 µL, 0.90 mmol, 1.8 equiv.) and DMF (17 µL, 0.22 mmol, 0.45 equiv.) were added at ambient temperature. The reaction was stirred at ambient temperature until complete consumption of the carboxylic acid was observed by TLC. After that, the solvent was evaporated to dryness under vacuum at ambient temperature to obtain the crude acyl chloride, which was used without further purification in the next step.

In an oven dried vial, with a Teflon septum screw cap, potassium ethyl xanthogenate **B** (16 mg, 0.10 mmol, 0.2 equiv.), sodium phosphate (164 mg, 1.00 mmol, 2 equiv.), and the electron-poor olefin **31** (0.5 mmol, 1 equiv.), were added. The crude acyl chloride was

dissolved in DCM (2 mL, HPLC grade) and the solution was added to the vial, followed by γ-terpinene (240 μL, 1.5 mmol, 3 equiv.). The resulting yellow mixture was degassed via argon sparging for 60 seconds. If the electron-poor olefin **31** was *liquid*, it was added via syringe after the argon sparging. The vial was then placed in the correspondent reactor (depending on the temperature used for the reaction) and irradiated for 24 hours. The solvent was evaporated and the residue purified by column chromatography to afford the corresponding product in the stated yield with >95% purity according to ^{1}H NMR analysis.

3.9.5.2 Characterization of Products

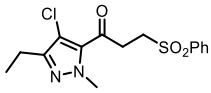

1-(4-Chloro-3-ethyl-1-methyl-1H-pyrazol-5-yl)-3-(phenylsulfonyl)propan-1-one (35a): Synthesized according to the general procedure C using 4-chloro-3-ethyl-1-methyl-1H-pyrazole-5-carboxylic acid (141 mg, 0.75 mmol, 1.5 equiv.) and phenyl vinyl sulfone (84 mg, 0.5 mmol, 1 equiv.). Acyl chloride formation was complete after 2 hours. The crude mixture was purified by flash column chromatography on silica gel (20% AcOEt in hexanes as eluent) to afford **35a** (52 mg, 31% yield) as a white solid.

^{1}H NMR (500 MHz, $CDCl_3$) δ 7.98 – 7.92 (m, 2H), 7.71 – 7.64 (m, 1H), 7.62 – 7.54 (m, 2H), 3.98 (s, 3H), 3.57 – 3.51 (m, 2H), 3.49 – 3.42 (m, 2H), 2.63 (q, *J* = 7.6, 2H), 1.23 (t, *J* = 7.5, 2H).

^{13}C NMR (126 MHz, $CDCl_3$) δ 186.6, 150.4, 139.0, 134.6, 134.1, 129.5, 128.3, 112.7, 50.6, 41.6, 35.5, 19.2, 12.9.

HRMS (ESI pos): calculated for $C_{15}H_{18}ClN_2O_3S$ ($M+H^+$): 341.0721, found 341.0709.

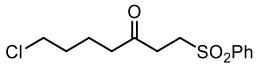

7-chloro-1-(phenylsulfonyl)heptan-3-one (35b): Synthesized according to the general procedure C using 5-chloropentanoic acid (72 μL, 0.75 mmol, 1.5 equiv.) and dimethyl fumarate (72 mg, 0.5 mmol, 1 equiv.). Acyl chloride formation was complete after 3 hours. The crude mixture was purified by flash column chromatography on silica gel (20% AcOEt in hexanes as eluent). The product was then dissolved in DCM, washed 3 times with a solution of $CuSO_4$ (5% in water), dried with $MgSO_4$ and evaporated under reduced pressure to afford **35b** (108 mg, 70% yield) as a white solid.

^{1}H NMR (400 MHz, $CDCl_3$) δ 7.92 – 7.87 (m, 2H), 7.69 – 7.63 (m, 1H), 7.60 – 7.54 (m, 2H), 3.53 – 3.47 (m, 2H), 3.41 – 3.35 (m, 2H), 2.92 – 2.86 (m, 2H), 2.50 – 2.44 (m, 2H), 1.78 – 1.64 (m, 4H).

^{13}C NMR (100 MHz, $CDCl_3$) δ 205.5, 139.1, 134.1, 129.5, 128.1, 50.6, 44.6, 41.9 35.0 31.8 20.9.

HRMS (ESI pos): calculated for $C_{13}H_{17}ClNaO_3S$ ($M+Na^+$): 311.0479, found 311.0477.

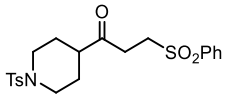

3-(Phenylsulfonyl)-1-(1-tosylpiperidin-4-yl)propan-1-one (35c): Synthesized according to the general procedure C using 1-tosylpiperidine-4-carboxylic acid (213 mg, 0.75 mmol, 1.5 equiv.) and dimethyl fumarate (72 mg, 0.5 mmol, 1 equiv.). Acyl chloride formation was complete after 3 hours. In this case the reaction was irradiated for 36 hours. The crude mixture was purified by flash column chromatography on silica gel (40% AcOEt in hexanes as eluent) to afford **35c** (164 mg, 75% yield) as a white solid.

^{1}H NMR (500 MHz, $CDCl_3$) δ 7.90 – 7.85 (m, 2H), 7.69 – 7.64 (m, 1H), 7.64 – 7.60 (m, 2H), 7.60 – 7.54 (m, 2H), 7.32 (app d, *J*= 7.9 Hz, 2H), 3.71 (dt, *J*= 12.2, 3.5 Hz, 2H), 3.35 (app t, *J*= 7.4 Hz, 2H), 2.91 (app t, *J*= 7.4 Hz, 2H), 2.43 (s, 3H), 2.38 (td, *J*= 11.7, 2.5 Hz, 2H), 2.33 – 2.24 (m, 1H), 1.93 – 1.84 (m, 2H), 1.75 – 1.63 (m, 2H).

^{13}C NMR (126 MHz, $CDCl_3$) δ 206.9, 143.8, 139.1, 134.2, 133.2, 129.9, 129.6, 128.0, 127.8, 50.6, 47.6, 45.5, 33.0, 27.0, 21.7.

HRMS (ESI pos): calculated for $C_{21}H_{26}NO_5S_2$ ($M+H^+$): 436.1247, found 436.1251.

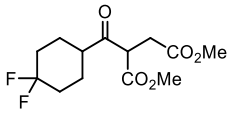

dimethyl 2-(4,4-difluorocyclohexane-1-carbonyl)succinate (35d): Synthesized according to the general procedure C using 4,4-difluorocyclohexane-1-carboxylic acid (123 mg, 0.75 mmol, 1.5 equiv.) and dimethyl fumarate (72 mg, 0.5 mmol, 1 equiv.). Acyl chloride formation was complete after 1 hour. The crude mixture was purified by flash column chromatography on silica gel (20% Et_2O in hexanes as eluent) to afford **35d** (128 mg, 88% yield) as a white solid.

^{1}H NMR (400 MHz, $CDCl_3$) δ 4.16 (dd, *J* = 9.1, 5.3 Hz, 1H), 3.73 (s, 3H), 3.67 (s, 3H), 3.03 (dd, *J* = 17.6, 9.3 Hz, 1H), 2.82 (dd, *J* = 17.5, 5.3 Hz, 1H), 2.83 – 2.74 (m, 1H), 2.22 – 2.02 (m, 3H), 1.98 – 1.65 (m, 5H).

^{13}C NMR (100 MHz, $CDCl_3$) δ 205.6, 171.9, 168.8, 122.7 (dd, *J* = 241.6, 240.9 Hz), 53.0, 52.2, 52.1, 48.0, 32.7 (dd, *J* = 25.0 Hz), 25.2 (d, *J* = 9.0 Hz) 24.4 (d, *J* = 8.6 Hz)

^{19}F NMR (376 MHz, $CDCl_3$, proton decoupled) δ -93.75 (d, *J* = 237.2 Hz, 1F); -100.48 (d, *J* = 238.2 Hz, 1F).

HRMS (ESI pos): calculated for $C_{13}H_{18}F_2NaO_5$ ($M+Na^+$): 315.1015, found 315.1017.

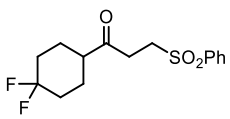

1-(4,4-Difluorocyclohexyl)-3-(phenylsulfonyl)propan-1-one (35e): Synthesized according to the general procedure C using 4,4-difluorocyclohexane-1-carboxylic acid (123 mg, 0.75 mmol, 1.5 equiv.) and dimethyl fumarate (72 mg, 0.5 mmol, 1 equiv.). Acyl chloride formation was

complete after 1 hour. The crude mixture was purified by flash column chromatography on silica gel (30% AcOEt in hexanes as eluent) to afford **35e** (112 mg, 71% yield) as a white solid.

^{1}H NMR (400 MHz, $CDCl_3$) δ 7.93 – 7.88 (m, 2H), 7.70 – 7.64 (m, 1H), 7.61 – 7.55 (m, 2H), 3.41 – 3.35 (m, 2H), 3.01 – 2.94 (m, 2H), 2.52 – 2.39 (m, 1H), 2.18 – 2.04 (m, 2H), 1.99 – 1.86 (m, 2H), 1.85 – 1.64 (m, 4H).

^{13}C NMR (100 MHz, $CDCl_3$) δ 207.4, 139.2, 134.1, 129.6, 128.0, 122.5 (dd, *J* = 241.6, 240.7 Hz) 50.6, 48.1, 33.2, 32.7 (dd, *J* = 24.4, 24.2 Hz), 24.7 (d, *J* = 9.5 Hz).

^{19}F NMR (376 MHz, $CDCl_3$, proton decoupled) δ -93.72 (dd, *J* = 237.6 Hz); -100.82 (d, *J* = 237.7 Hz).

HRMS (ESI pos): calculated for $C_{15}H_{18}F_2NaO_3S$ ($M+Na^+$): 339.0837, found 339.0840.

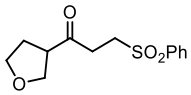

3-(Phenylsulfonyl)-1-(tetrahydrofuran-3-yl)propan-1-one (35f): Synthesized according to the general procedure C using tetrahydrofuran-3-carboxylic acid (72 µL, 0.75 mmol, 1.5 equiv.) and dimethyl fumarate (72 mg, 0.5 mmol, 1 equiv.). Acyl chloride formation was complete after 1 hour. The crude mixture was purified by flash column chromatography on silica gel (50% AcOEt in hexanes as eluent). The product was then dissolved in DCM, washed 3 times with a solution of $CuSO_4$ (5% in water), dried with $MgSO_4$ and evaporated under reduced pressure to afford **35f** (78 mg, 58% yield) as a colorless oil.

^{1}H NMR (500 MHz, $CDCl_3$) δ 7.94 – 7.87 (m, 2H), 7.71 – 7.64 (m, 1H), 7.62 – 7.54 (m, 2H), 3.94 – 3.73 (m, 4H), 3.47 – 3.34 (m, 2H), 3.26 – 3.17 (m, 1H), 3.07 – 2.89 (m, 2H), 3.16 – 2.01 (m, 2H).

^{13}C NMR (126 MHz, $CDCl_3$) δ 205.6, 139.1, 134.1, 129.6, 128.1, 69.3, 68.4, 51.1, 50.6, 34.4, 29.1.

HRMS (ESI pos): calculated for $C_{13}H_{16}NaO_4S$ ($M+Na^+$): 291.0662, found 291.0665.

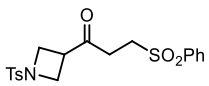

3-(Phenylsulfonyl)-1-(1-tosylazetidin-3-yl)propan-1-one (35g): Synthesized according to the general procedure C using 1-tosylazetidine-3-carboxylic acid (191 mg, 0.75 mmol, 1.5 equiv.) and dimethyl fumarate (72 mg, 0.5 mmol, 1 equiv.). Acyl chloride formation was complete after 2 hours. In this case the reaction was irradiated for 36 hours. The crude mixture was purified by flash column chromatography on silica gel (40% AcOEt in hexanes as eluent) to afford **35g** (63 mg, 31% yield) as a white solid.

^{1}H NMR (400 MHz, $CDCl_3$) δ 7.88 – 7.82 (m, 2H), 7.74 – 7.63 (m, 3H), 7.60 – 7.53 (m, 2H), 7.40 – 7.33 (m, 2H), 3.92 – 3.88 (m, 2H), 3.88 – 3.81 (m, 2H), 3.41 – 3.28 (m, 3H), 2.79 (app t, *J*= 7.3 Hz, 2H), 2.44 (s, 3H).

^{13}C NMR (100 MHz, $CDCl_3$) δ 202.1, 144.6, 138.9, 134.2, 131.3, 130.0, 129.6, 128.5, 128.0, 51.8, 50.3, 38.1, 33.1, 21.7.

HRMS (ESI pos): calculated for $C_{19}H_{21}NNaO_5S_2$ ($M+Na^+$): 430.0753, found 430.0748.

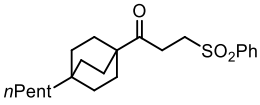

1-(4-Pentylbicyclo[2.2.2]octan-1-yl)-3-(phenylsulfonyl)propan-1-one (35h): Synthesized according to the general procedure C using 4-pentylbicyclo[2.2.2]octane-1-carboxylic acid (168 mg, 0.75 mmol, 1.5 equiv.) and phenyl vinyl sulfone (84 mg, 0.5 mmol, 1 equiv.). Acyl chloride formation was complete after 2 hours. Chromatography on silica gel (10% AcOEt in hexanes as eluent) could not remove byproducts completely. Purification by semipreparative HPLC (IC column, 60:40 Hexane/Ethanol, 1 mL/min) was performed to obtain an analytical amount of product **35h** as a white solid. NMR yield (Trichloroethylene was used as internal standard): 80%.

^{1}H NMR (500 MHz, $CDCl_3$) δ 7.93 – 7.87 (m, 2H), 7.69 – 7.63 (m, 1H), 7.61 – 7.54 (m, 2H), 3.36 – 3.29 (m, 2H), 2.97 – 2.90 (m, 2H), 1.69 – 1.61 (m, 6H), 1.43 – 1.34 (m, 6H), 1.31 – 1.24 (m, 2H), 1.24 – 1.12 (m, 4H), 1.11 – 1.04 (m, 2H), 0.87 (t, *J*= 7.3 Hz, 3H).

^{13}C NMR (126 MHz, $CDCl_3$) δ 211.6, 139.4, 134.0, 129.5, 128.1, 51.0, 45.3, 41.3, 32.9, 30.8, 30.5, 30.1, 28.2, 23.5, 22.8, 14.2.

HRMS (ESI pos): calculated for $C_{22}H_{32}NaO_3S$ ($M+Na^+$): 399.1964, found 399.1951.

3.9.6 Reaction of carboxylic acids through anhydride formation

3.9.6.1 General Procedure D1

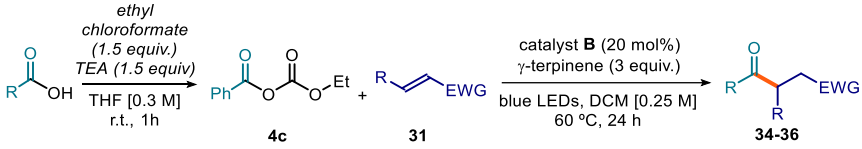

In a round bottom flask or vial, the carboxylic acid (0.75 mmol, 1.5 equiv) was dissolved in THF (2.5 mL, HPLC grade). Then, triethylamine (TEA, 105 µL, 0.75 mmol, 1.5 equiv.) and ethyl chloroformate (72 µL, 0.75 mmol, 1.5 equiv.) were added at ambient temperature. The reaction was stirred at ambient temperature for 1 hour. After that, it was filtered and the remaining solid was washed with diethyl ether. The organic layers were concentrated to dryness under reduced pressure to obtain the crude anhydride, which was used without further purification in the next step. (When the carboxylic acid is not completely soluble in 2.5 mL of THF, follow the general procedure D2 detailed below).

In an oven dried tube or a vial, with a Teflon septum screw cap, potassium ethyl xanthogenate **B** (16 mg, 0.10 mmol, 0.2 equiv.) and the electron-poor olefin **31** (0.5 mmol, 1 equiv., *if solid*), were added. The crude anhydride was dissolved in DCM (2 mL, HPLC grade) and the solution was added to the vial, followed by γ-terpinene (240 μL, 1.5 mmol, 3 equiv.). The resulting yellow mixture was degassed with argon sparging for 60 seconds. If the electron-poor olefin **31** was *liquid*, it was added via syringe after the argon sparging. The vial was then placed in the correspondent photoreactor (depending on the temperature used for the reaction) and irradiated for 24 hours. The solvent was evaporated and the residue purified by column chromatography to afford the corresponding product in the stated yield with >95% purity, according to ^{1}H NMR analysis.

This procedure was employed for the optimization of the catalytic reaction with anhydride as radical precursor and for the scale-up process, as indicated below.

Note: Filtration of the triethylamonium salt is crucial for the reaction to work. Therefore, attempts to perform the reaction one-pot without removal of the ammonium salt were unsuccessful.

3.9.6.2 General Procedure D2

In a round bottom flask or vial, the carboxylic acid (0.75 mmol, 1.5 equiv.) was dissolved in THF (10 mL, HPLC grade). Then, triethylamine (105 μL, 0.75 mmol, 1.5 equiv.) and ethyl chloroformate (72 μL, 0.75 mmol, 1.5 equiv.) were added at ambient temperature. The reaction was stirred for 1 hour. The reaction crude was washed with water and $NaHCO_3$ saturated solution, dried over $MgSO_4$, filtered and the organic layers concentrated to dryness under vacuum. The crude carbonate was used without further purification in the next step.

In an oven dried tube of 15 mL (16 mm × 12.5 mm) or a vial, with a Teflon septum screw cap, potassium ethyl xanthogenate (16.02 mg, 0.10 mmol, 0.2 equiv.) and the electron-poor olefin **31** (0.5 mmol, 1 equiv. *if solid*), were added. The crude carbonate was dissolved in DCM (2 mL, HPLC grade) and the solution was added to the vial, followed by γ-terpinene (240 μL, 1.5 mmol, 3 equiv.). The resulting yellow mixture was degassed with argon sparging for 60 seconds. If the electron-poor olefin **31** was *liquid*, it was added via syringe after the argon sparging. The vial was then placed in the correspondent photoreactor and irradiated for 24 hours. After cooling to ambient temperature, the solvent was evaporated and the residue purified by column chromatography to afford the corresponding product in the stated yield with >95% purity according to ^{1}H NMR analysis.

3.9.6.3 Characterization of Products

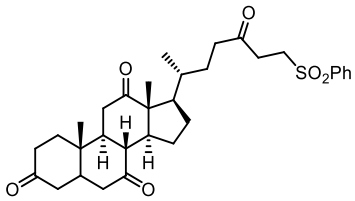

(8R,9S,10S,13R,14S,17R)-10,13-dimethyl-17-((R)-5-oxo-7-(phenylsulfonyl)heptan-2-yl)dodecahydro-3H-cyclopenta[a]phenanthrene-3,7,12(2H,4H)-trione (36): Synthesized according to the general procedure **D2** using dehydrocholic acid (302 µL, 0.75 mmol, 1.5 equiv.) and phenyl vinyl sulfone (84 mg, 0.5 mmol, 1 equiv.). The crude mixture was purified by flash column chromatography on silica gel (33% acetone in hexanes as eluent), followed by a second purification (20% AcOEt in DCM as eluent) to afford **36** (145 mg, 52% yield) as a colorless oil.

^{1}H NMR (500 MHz, $CDCl_3$) δ 7.93 – 7.88 (m, 2H), 7.70 – 7.64 (m, 1H), 7.61 – 7.55 (m, 2H), 3.44 – 3.32 (m, 2H), 2.95 – 2.79 (m, 5H), 2.54 – 2.44 (m, 1H), 2.44 – 2.10 (m, 9H), 2.07 – 1.90 (m, 4H), 1.89 – 1.80 (m, 1H), 1.80 – 1.70 (m, 1H), 1.67 – 1.56 (m, 1H), 1.39 (s, 3H), 1.36 – 1.20 (m, 4H), 1.05 (s, 3H), 0.81 (d, J = 6.5 Hz, 3H).

^{13}C NMR (126 MHz, $CDCl_3$) δ 212.0, 209.1, 208.8, 206.5, 139.2, 134.1, 129.6, 128.1, 57.0, 51.9, 50.6, 49.1, 47.0, 45.7, 45.7, 45.1, 42.9, 40.0, 38.8, 36.6, 36.1, 35.4, 35.4, 35.1, 29.1, 27.8, 25.2, 22.0, 18.9, 12.0.

HRMS (ESI pos): calculated for $C_{32}H_{42}NaO_6S$ ($M+Na^+$): 577.2594, found 577.2607.

3.9.7 Scale-up reaction

3.9.7.1 Experimental Setup and Procedure

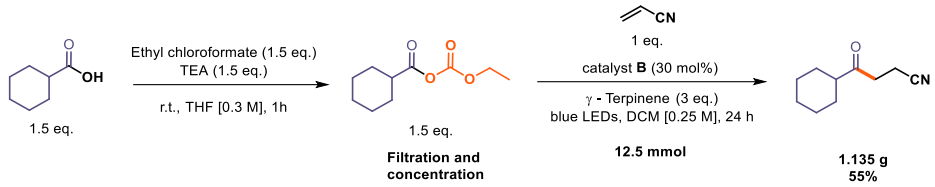

In a 100 mL round bottom flask, cyclohexanecarboxylic acid (2.34 mL, 18.75 mmol, 1.5 equiv.) was dissolved in THF (60 mL, HPLC grade). Then, triethylamine (2.61 mL, 18.75 mmol, 1.5 equiv.) and ethyl chloroformate (1.80 mL, 18.75 mmol, 1.5 equiv.) were added at ambient temperature. The reaction was stirred at ambient temperature for 1 hour. Then, it was filtered into a 100 mL reaction flask that will be used as reaction vessel for the next step (the remaining solid was carefully washed with diethyl ether). The organic phase was concentrated to dryness under vacuum to obtain the crude carbonate, which was used without further purification in the next step.

In the same 100 mL round bottom flask with a Teflon septum, the crude carbonate was dissolved in DCM (50 mL, HPLC grade). Potassium ethyl xanthogenate **B** (601 mg, 3.75 mmol, 0.3 equiv.) and γ-terpinene (6.01 mL, 37.5 mmol, 3 equiv.) were added to the solution.

The resulting yellow mixture was degassed with Nitrogen sparging for 2 minutes. Finally, acrylonitrile (0.819 mL, 12.5 mmol, 1 equiv.) was added via syringe. The round bottom flask was then irradiated for 20 hours with a one meter 14W blue LED strip and cooled with a fan to keep the temperature between 30 and 35 ºC (see Figure 3.12). After 24 hours, complete conversion of acrylonitrile was inferred by ^{1}H NMR analysis. The mixture was transferred to an extraction funnel, water was added and the organic layer was extracted with DCM. The organic layer was dried ($MgSO_4$) and concentrated to dryness. The product was then purified by chromatography on silica gel (10% AcOEt in hexanes) to afford 1.130 g of product **34e** (6.87 mmol, 55% yield) as a yellowish oil. NMR analysis was consistent with product synthesized in the small scale process.

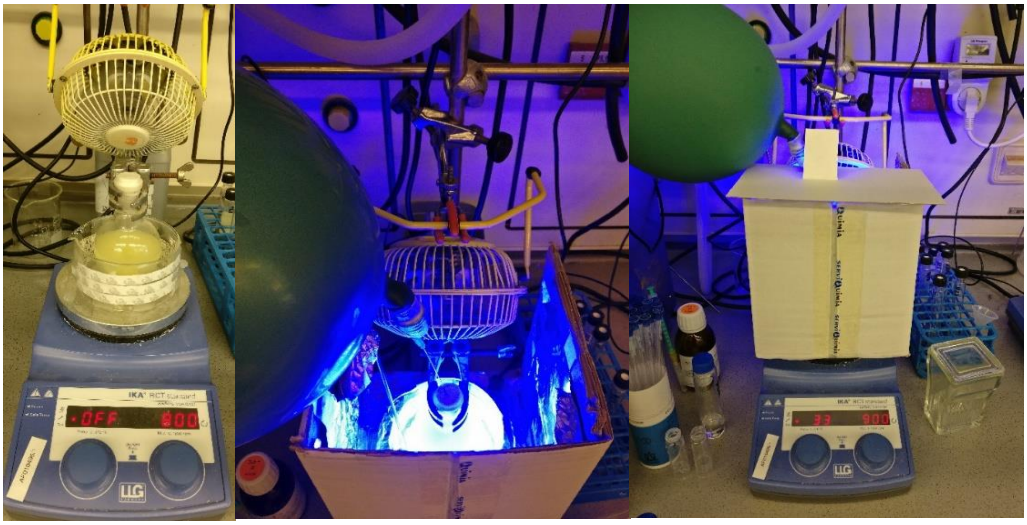

Figure 3.12. Experimental setup used for the large scale set up. (Left) Before irradiation. (Middle) Reaction set up from above. (Right) Reaction set up from the front.

3.9.8 Reaction of Carbamoyl Chlorides

3.9.8.1 Experimental Setup

For the generation of carbamoyl radicals, we used the Hepatochem PhotoRedOx Box equipped with an EvoluChem LED 18 W light source at 405 nm, supplied by Hepatochem.

Figure 3.13. Photoreactor used for the reaction with the carbamoyl chlorides

The reactor was connected to a Huber Minichiller 300 in order to perform reactions at 50 ºC with accurate control of the reaction temperature (± 1ºC, Figure 3.13).

3.9.8.2 Optimization studies

Table 3.4. Screening of the Catalysts

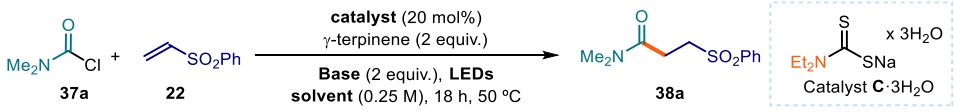

entry	catalyst	wavelenght (nm)	Base	Solvent	NMR yield (%)
1	**B**	460	Na_3PO_4	DCM	<5
2	**B**	405	Na_3PO_4	DCM	10%
3	**C**·$3H_2O$	405	Na_3PO_4	DCM	11%
4	**C**·$3H_2O$	405	Na_3PO_4	MeCN	20%
5	**C**·$3H_2O$	405	K_3PO_4	MeCN	60%

All reaction performed on 0.2 mmol scale, yield determined by ^{1}H NMR analysis of the crude reaction mixture by comparison with trichloroethylene as internal standard.

3.9.8.3 General Procedure for the intermolecular Giese addition (General Procedure E)

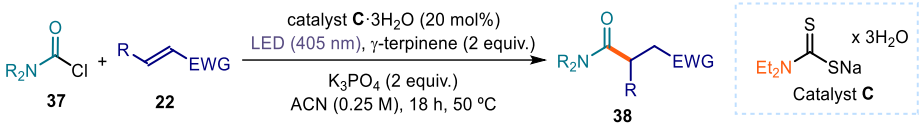

An oven-dried 15 mL Schlenk tube was charged with a mixture of carbamoyl chloride **37** (0.4 mmol, 2 equiv.), catalyst **C** trihydrate (9 mg, 0.04 mmol, 0.2 equiv.), alkene **31** (0.2 mmol, 1 equiv.), γ–terpinene (64 µL, 0.4 mmol, 2 equiv.) and K_3PO_4 (85 mg, 0.4 mmol, 2 equiv.) in acetonitrile (0.8 mL, 0.25 M). The reaction mixture was placed under an atmosphere of argon, cooled to –78 °C, degassed *via* vacuum evacuation (5 minutes), backfilled with argon and, ultimately, warmed to ambient temperature. This freeze-pump-thaw cycle was repeated four times, and then the Schlenk tube was sealed with Parafilm and put into the Hepatochem PhotoRedOx Box equipped with a 405 nm EvoluChem LED 18 W light source at 50 ºC (Figure 3.13). After 18 hours stirring, the reaction was cooled down to ambient temperature, water was added and the mixture was extracted with ethyl acetate (2x15 mL). The combined layers were dried over magnesium sulfate, filtered, and concentrated. The resulting crude mixture was purified by column chromatography on silica gel to give the corresponding product **38** in the stated yield.

3.9.8.4 Characterization of Products

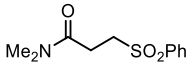

***N,N*-Dimethyl-3-(phenylsulfonyl)propanamide (38a):** Synthesized according to general procedure E using dimethylcarbamic chloride (37 µL, 0.4 mmol, 2.0 equiv.) and phenyl vinyl sulfone (34 mg, 0.2 mmol). The crude mixture was purified by flash column chromatography on silica gel (gradient from hexane 100% to ethyl acetate 100%) to afford product **38a** (29 mg, 60% yield) as a pale-yellow oil.

^{1}H NMR (400 MHz, $CDCl_3$) δ 7.95 – 7.88 (m, 2H), 7.69 – 7.62 (m, 1H), 7.61 – 7.52 (m, 2H), 3.53 – 3.33 (m, 2H), 2.99 (s, 3H), 2.89 (s, 3H), 2.85 – 2.73 (m, 2H).

^{13}C NMR (100 MHz, $CDCl_3$) δ 168.8, 139.2, 134.0, 129.5, 128.1, 52.2, 37.2, 35.7, 26.2.

HRMS (ESI pos): calculated for $C_{11}H_{15}NnaO_3S$ ($M+Na^+$): 264.0665, found 264.0653.

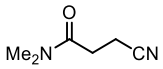

3-Cyano-*N,N*-dimethylpropanamide (38b): Synthesized according to general procedure E using dimethylcarbamic chloride (37 µL, 0.4 mmol, 2.0 equiv.) and acrylonitrile (13 µL, 0.2 mmol). The crude mixture was purified by flash column chromatography on silica gel (gradient from hexane 100% to ethyl acetate 100%) to afford product **38b** (16 mg, 63% yield) as a pale-yellow oil.

^{1}H NMR (400 MHz, $CDCl_3$) δ 3.01 (s, 3H), 2.97 (s, 3H), 2.68 (s, 4H).

^{13}C NMR (100 MHz, $CDCl_3$) δ168.8, 119.6, 37.0, 35.7, 29.5, 13.1.

HRMS (ESI pos): calculated for $C_6H_{11}N_2O$ ($M+H^+$): 127.0866, found: 127.0869.

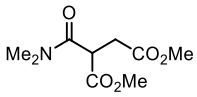

dimethyl 2-(dimethylcarbamoyl)succinate (38c): Synthesized according to general procedure E using dimethylcarbamic chloride (37 μL, 0.4 mmol, 2.0 equiv.) and dimethyl fumarate (29 mg, 0.2 mmol). The crude mixture was purified by flash column chromatography on silica gel (gradient from hexane 100% to ethyl acetate 100%) to afford product **38c** (27 mg, 62% yield) as a pale-yellow oil.

^{1}H NMR (400 MHz, $CDCl_3$) δ 4.14 (dd, *J* = 8.3, 6.0 Hz, 1H), 3.72 (s, 3H), 3.67 (s, 3H), 3.16 (s, 3H), 3.11 – 2.80 (m, 6H).

^{13}C NMR (100 MHz, $CDCl_3$) δ 172.4, 169.5, 167.9, 53.0, 52.2, 44.6, 38.0, 36.4, 33.6.

HRMS (ESI pos): calculated for $C_9H_{15}NNaO_5$ ($M+Na^+$): 240.0842, found: 240.0844.

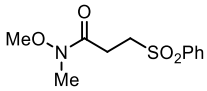

***N*-Methoxy-*N*-methyl-3-(phenylsulfonyl)propanamide (38d):** Synthesized according to general procedure E using methoxy(methyl)carbamic chloride (41 μL, 0.4 mmol, 2.0 equiv.) and phenyl vinyl sulfone (34 mg, 0.2 mmol). The crude mixture was purified by flash column chromatography on silica gel (gradient from hexane 100% to hexane 50% : 50% ethyl acetate) to afford product **38d** (16 mg, 30% yield) as a pale yellow oil.

^{1}H NMR (400 MHz, $CDCl_3$) δ 7.97 – 7.90 (m, 2H), 7.75 – 7.63 (m, 1H), 7.63 – 7.54 (m, 2H), 3.69 (s, 3H), 3.52 – 3.37 (m, 2H), 3.14 (s, 3H), 2.97 – 2.92 (m, 2H).

^{13}C NMR (101 MHz, $CDCl_3$) 170.4, 139.2, 134.0, 129.5, 128.2, 61.6, 51.5, 32.3, 25.4.

HRMS (ESI pos): calculated for $C_9H_{15}NNaO_5$ ($M+Na^+$): 240.0842, found: 240.0844.

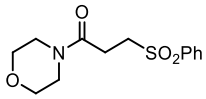

1-Morpholino-3-(phenylsulfonyl)propan-1-one (38e): Synthesized according to general procedure E using morpholine-4-carbonyl chloride (47 μL, 0.4 mmol, 2.0 equiv.) and phenyl vinyl sulfone (34 mg, 0.2 mmol). The crude mixture was purified by flash column chromatography on silica gel (gradient from hexane 100% to ethyl acetate 100%) to afford product **38e** (42 mg, 74% yield) as a pale-yellow oil.

^{1}H NMR (400 MHz, $CDCl_3$) δ 8.00 – 7.85 (m, 2H), 7.71 – 7.62 (m, 1H), 7.62 – 7.51 (m, 1H), 3.76 – 3.58 (m, 5H), 3.55 – 3.49 (m, 2H), 3.47 – 3.42 (m, 3H), 2.94 – 2.74 (m, 2H).

^{13}C NMR (100 MHz, $CDCl_3$) δ 167.5, 139.1, 134.0, 129.5, 128.0, 66.7, 66.5, 52.0, 45.8, 42.3, 25.9.

HRMS (ESI pos): calculated for $C_{13}H_{17}NNaO_4S$ ($M+Na^+$): 306.0770, found: 306.0762.

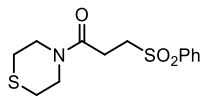

3-(Phenylsulfonyl)-1-thiomorpholinopropan-1-one (38f): synthesized according the general procedure E using thiomorpholine-4-carbonyl chloride **8f** (99 mg, 0.4 mmol, 2 eq.) and phenyl vinyl sulfone (34 mg, 0.2 mmol, 1 eq.). The crude mixture was purified by flash column chromatography on silica gel (5% AcOEt in hexane), followed by a second one (50% AcOEt in Hexane as eluent) to afford **38f** (37.8 mg, 63% yield) as a colorless oil.

^{1}H NMR (400 MHz, $CDCl_3$) δ 7.96 (m, 2H) 7.70 (m, 1H) 7.61 (m, 2H) 3.85 (m, 2H), 3.76 (m, 1H), 3.65 (m, 1H), 3.50 (m, 1H), 2.86, (m, 2H), 2.64 (m, 6H).

^{13}C NMR (126 MHz, $CDCl_3$) δ 167.3, 139.3, 134.1, 129.5, 128.1, 52.2, 48.3, 44.8, 27.9, 27.4, 26.2

HRMS (ESI pos): calculated for $C_{13}H_{17}NaNO_3S_2$ ($M+Na^+$): 322.05, found: 322.0533.

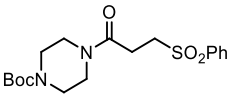

***tert*-Butyl 4-(3-(phenylsulfonyl)propanoyl)piperazine-1-carboxylate (38g):** synthesized according general procedure E using tert-butyl 4-(chlorocarbonyl)piperazine-1-carboxylate **37g** (99 mg, 0.4 mmol, 2 eq.) and phenyl vinyl sulfone (34 mg, 0.2 mmol, 1 eq.). The crude mixture was purified by flash column chromatography on silica gel (5% AcOEt in hexane), followed by a second purification (50% AcOEt in hexane as eluent) to afford **38g** (55 mg, 73% yield) as a white solid.

^{1}H NMR (400 MHz, $CDCl_3$) δ 7.91 (m, 2H), 7.66 (m, 1H), 7.57 (m, 2H), 3.42 (m, 4H) 3.21 (m, 6H), 2.83 (t, *J* = 7.8 Hz, 2H), 1.45 (s, 9H)

^{13}C NMR (126 MHz, $CDCl_3$) δ 167.6, 154.6, 139.3, 134.1, 129.6, 128.1, 80.7, 52.1, 45.4, 41.9, 28.5, 26.1

HRMS (ESI pos): calculated for $C_{18}H_{26}NaN_2O_5S$ ($M+Na^+$): 405.15, found 405.1455.

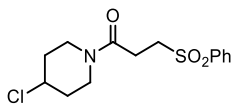

1-(4-Chloropiperidin-1-yl)-3-(phenylsulfonyl)propan-1-one (38h): Synthesized according to general procedure E using 4-chloropiperidine-1-carbonyl chloride (73 mg, 0.4 mmol, 2 equiv.) and phenyl vinyl sulfone (34 mg, 0.2 mmol). The crude mixture was purified by flash column chromatography on silica gel (gradient from hexane 100% to ethyl acetate 100%) to afford product **38h** (41 mg, 65% yield) as a pale-yellow oil.

^{1}H NMR (400 MHz, $CDCl_3$) δ 7.96 – 7.87 (m, 2H), 7.72 – 7.62 (m, 1H), 7.60 – 7.53 (m, 2H), 4.27 (tt, *J* = 7.0, 3.6 Hz, 1H), 3.68 (tdt, *J* = 11.7, 8.2, 3.5 Hz, 2H), 3.58 (ddd, *J* = 13.6, 6.9, 4.0 Hz, 1H), 3.49 – 3.42 (m, 2H), 3.38 (ddd, *J* = 13.9, 7.0, 3.7 Hz, 1H), 2.83 (td, *J* = 7.1, 1.9 Hz, 2H), 2.16 – 1.93 (m, 2H), 1.90 – 1.72 (m, 2H).

^{13}C NMR (100 MHz, $CDCl_3$) δ 167.2, 139.2, 134.0, 129.5, 128.0, 56.1, 52.1, 42.5, 39.1, 35.1, 34.4, 25.9.

HRMS (ESI pos): calculated for $C_{14}H_{19}ClNO_3S$ ($M+H^+$): 316.0769, found: 316.0773.

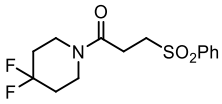

1-(4,4-Difluoropiperidin-1-yl)-3-(phenylsulfonyl)propan-1-one (38i): Synthesized according to general procedure E using 4,4-difluoropiperidine-1-carbonyl chloride (73 mg, 0.4 mmol, 2 equiv.) and phenyl vinyl sulfone (34 mg, 0.2 mmol). The crude mixture was purified by flash column chromatography on silica gel (gradient from hexane 100% to 1:1 hexane/ethyl acetate) to afford product **38i** (43 mg, 68% yield) as an off-white solid.

^{1}H NMR (400 MHz, $CDCl_3$) δ 7.96 – 7.88 (m, 2H), 7.71 – 7.63 (m, 1H), 7.61 – 7.54 (m, 2H), 3.61 (dt, *J* = 43.9, 6.0 Hz, 4H), 3.51 – 3.43 (m, 2H), 2.92 – 2.83 (m, 2H), 2.13 – 1.84 (m, 4H).

^{13}C NMR (100 MHz, $CDCl_3$) δ 167.4, 139.2, 134.1, 129.5, 128.0, 121.3 (t, *J* = 242.4 Hz), 52.1, 40.7 (dt, *J* = 330.8, 5.4 Hz), 34.1 (dt, *J* = 78.0, 23.6 Hz), 25.9.

^{19}F NMR (376 MHz, $CDCl_3$) δ -98.22 (p, *J* = 13.5 Hz).

HRMS (ESI pos): calculated for $C_{18}H_{18}NaO_4$ ($M+Na^+$): 340.0789, found: 340.0785.

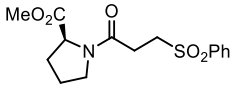

Methyl (3-(phenylsulfonyl)propanoyl)-L-prolinate (38j): synthesized according the general procedure E using methyl (chlorocarbonyl)-L-prolinate (77 mg, 0.4 mmol, 2 eq.) and phenyl vinyl sulfone (34 mg, 0.2 mmol, 1 eq.). The crude mixture was purified by flash column chromatography on silica gel (5% AcOEt in hexane) to afford **38j** (46 mg, 58% yield) as a yellowish oil.

^{1}H NMR (400 MHz, $CDCl_3$) δ 7.95 – 7.89 (m, 2H), 7.69 – 7.64 (m, 1H), 7.61 – 7.53 (m, 2H), 4.42 (dd, *J* = 8.4, 3.5 Hz, 1H), 3.70 (s, 3H), 3.68 – 3.59 (m, 1H), 3.56 – 3.38 (m, 3H), 2.83 (dt, *J* = 9.7, 5.6 Hz, 2H), 2.11 – 1.94 (m, 4H).

^{13}C NMR (126 MHz, $CDCl_3$) δ 172.6, 167.8, 139.2, 134, 129.5, 128.1, 58.9, 52.4, 51.7, 47.1, 29.3, 27.4, 24.8.

HRMS (ESI pos): calculated for $C_{15}H_{19}NaNO_5S$ ($M+Na^+$): 326.10, found: 326.1063.

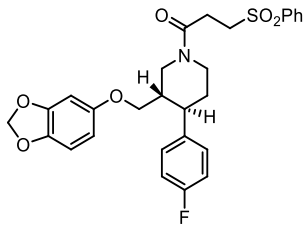

1-(3-((Benzo[d][1,3]dioxol-5-yloxy)methyl)-4-(4-fluorophenyl)piperidin-1-yl)-3-(phenylsulfonyl)propan-1-one (38k): synthesized according the general procedure E using 3-((benzo[d][1,3]dioxol-5-yloxy)methyl)-4-(4-fluorophenyl)piperidine-1-carbonyl chloride **37k** (157 mg, 0.4 mmol, 2 eq.) and phenyl vinyl sulfone (34 mg, 0.2 mmol, 1 eq.). The crude mixture was purified by flash column chromatography on silica gel (gradient from hexane 100% to hexane 50:50 ethyl acetate) to afford product **38k** (46 mg, 29% yield) as a yellowish oil.

^{1}H NMR (400 MHz, $CDCl_3$) δ 7.98 (m, 2H), 7.71 (m, 1H), 7.65 – 7.58 (m, 2H), 7.17 – 7.11 (m, 2H), 7.01 (m, 2H), 6.66 (dd, *J* = 17.8, 8.4 Hz, 1H), 6.38 (dd, *J* = 11.9, 2.5 Hz, 1H), 6.17 (ddd, *J* = 15.1, 8.5, 2.5 Hz, 1H), 5.92 (d, *J* = 13.5 Hz, 2H), 4.79 (dd, *J* = 55.2, 13.1 Hz, 1H), 4.07 (dd, *J* = 69.6, 13.5 Hz, 1H), 3.68 – 3.60 (m, 1H), 3.59 – 3.45 (m, 3H), 3.17 (m, 1H), 3.03 – 2.80 (m, 2H), 2.80 – 2.62 (m, 1H), 1.92 (m, 1H), 1.81 – 1.53 (m, 3H).

^{13}C NMR (126 MHz, $CDCl_3$) δ 167.5, 154.5, 148.7, 142.3, 139.6, 138.4, 134.3, 129.7, 129.1, 128.3, 115.7, 115.8, 108.2, 106.0, 101.5, 98.4, 68.9, 52.5, 49.2, 46.4, 44.5, 42.2, 34.6, 33.8, 30.1, 26.3.

^{19}F NMR (376 MHz, $CDCl_3$, proton decoupled) δ – 115.58

HRMS (ESI pos): calculated for $C_{28}H_{29}FNO_6S$ ($M+H^+$): 526.16, found: 526.1702.

3.9.8.5 General Procedure for the intramolecular cyclization (General Procedure F)

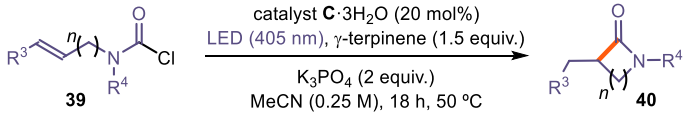

An oven-dried 15 mL Schlenk tube was charged with a mixture of carbamoyl chloride **39** (0.2 mmol, 1 equiv.), catalyst **C** trihydrate (9 mg, 0.04 mmol, 0.2 equiv.), γ–terpinene (48 µL, 0.3 mmol, 1.5 equiv.) and K_3PO_4 (85 mg, 0.4 mmol, 2 equiv.) in acetonitrile (0.8 mL, 0.25 M). The reaction mixture was placed under an atmosphere of argon, cooled to –78 °C, degassed *via* vacuum evacuation (5 minutes), backfilled with argon and, ultimately, warmed to ambient temperature. This freeze-pump-thaw cycle was repeated four times, and then the Schlenk tube was sealed with Parafilm and put into the Hepatochem PhotoRedOx Box equipped with a 405 nm EvoluChem LED 18 W light source at 50 ºC (Figure 3.13). After 18 hours, the reaction vessel was cooled down to ambient temperature, water was added and the mixture was extracted with ethyl acetate (2x15 mL). The combined layers were dried over magnesium sulfate, filtered, and concentrated. The resulting crude mixture was purified by column chromatography on silica gel to give the corresponding product **40** in the stated yield.

3.9.8.6 Characterization of Products

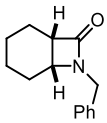

7-Benzyl-7-azabicyclo[4.2.0]octan-8-one (40a): Synthesized according to the general procedure F using benzyl(cyclohex-2-en-1-yl)carbamic chloride (50 mg, 0.2 mmol). The crude mixture was purified by flash column chromatography on silica gel (10% AcOEt in hexanes as eluent) to afford product **40a** (26 mg, 60% yield) as a pale-yellow oil.

^{1}H NMR (500 MHz, $CDCl_3$) δ 7.35 – 7.29 (m, 2H), 7.29 – 7.22 (m, 3H), 4.57 (d, *J* = 15.1 Hz, 1H), 4.08 (d, *J* = 15.1 Hz, 1H), 3.62 (ddd, *J* = 5.4, 4.2, 3.1 Hz, 1H), 3.20 – 3.15 (m, 1H), 1.89 – 1.80 (m, 1H), 1.74 – 1.49 (m, 5H), 1.49 – 1.33 (m, 2H).

^{13}C NMR (126 MHz, $CDCl_3$) δ 171.1, 136.4, 128.9, 128.5, 127.8, 50.3, 47.1, 44.6, 23.0, 19.8, 19.1, 17.0.

HRMS (ESI pos): calculated for $C_{18}H_{18}NaO_4$ ($M+H^+$): 216.1383, found: 216.1374.

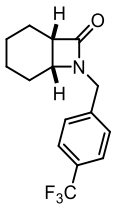

7-(4-(Trifluoromethyl)benzyl)-7-azabicyclo[4.2.0]octan-8-one (40b): Synthesized according to general procedure F using cyclohex-2-en-1-yl(4-(trifluoromethyl)benzyl)carbamic chloride (64 mg, 0.2 mmol). The crude mixture was purified by flash column chromatography on silica gel (5% AcOEt in hexanes as eluent) to afford product **40b** (31 mg, 55% yield) as a yellow oil.

^{1}H NMR (400 MHz, $CDCl_3$) δ 7.59 (d, *J* = 8.0 Hz, 2H), 7.39 (d, *J* = 8.0 Hz, 2H), 4.62 (d, *J* = 15.4 Hz, 1H), 4.16 (d, *J* = 15.4 Hz, 1H), 3.66 (dt, *J* = 5.1, 3.6 Hz, 1H), 3.23 (dt, *J* = 6.8, 4.6 Hz, 1H), 1.92 – 1.83 (m, 1H), 1.77 – 1.55 (m, 5H), 1.50 – 1.34 (m, 2H.

^{13}C NMR (126 MHz, $CDCl_3$) δ 171.1, 140.5, 130.1 (q, *J* = 32.6 Hz), 128.6, 125.9 (q, *J* = 3.8 Hz), 124.2 (q, *J* = 272.1 Hz), 50.5, 47.3, 44.1, 23.0, 19.7, 19.0, 16.9.

HRMS (ESI pos): calculated for $C_{15}H_{17}F_3NO$ ($M+H^+$): 284.1257, found: 284.1258.

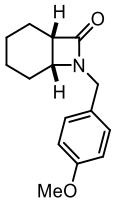

7-(4-Methoxybenzyl)-7-azabicyclo[4.2.0]octan-8-one (40c): Synthesized according to general procedure F using cyclohex-2-en-1-yl(4-methoxybenzyl)carbamic chloride (56 mg, 0.2 mmol). The crude mixture was purified by flash column chromatography on silica gel (15% AcOEt in hexanes as eluent) to afford product **40c** (30 mg, 61% yield) as a yellow oil.

^{1}H NMR (400 MHz, $CDCl_3$) δ 7.23 – 7.14 (m, 2H), 6.91 – 6.80 (m, 2H), 4.51 (d, *J* = 14.9 Hz, 1H), 4.04 (d, *J* = 14.9 Hz, 1H), 3.80 (s, 3H), 3.61 (ddd, *J* = 5.4, 4.1, 3.2 Hz, 1H), 3.17 (dt, *J* = 6.9, 4.6 Hz, 1H), 1.93 – 1.79 (m, 1H), 1.74 – 1.50 (m, 4H), 1.49 – 1.31 (m, 3H).

^{13}C NMR (100 MHz, $CDCl_3$) δ 170.9, 159.2, 129.7, 128.4, 114.2, 55.4, 50.0, 46.9, 43.9, 23.0, 19.7, 19.0, 16.9.

HRMS (ESI pos): calculated for $C_{15}H_{19}NNaO_2$ ($M+Na^+$): 268.1308, found: 268.1304.

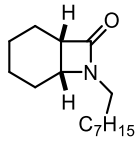

7-Octyl-7-azabicyclo[4.2.0]octan-8-one (40d): synthesized according the general procedure F using cyclohex-1-en-1-yl(octyl)carbamic chloride **39d** (54 mg, 0.2 mmol, 1 eq.). The crude mixture was purified by flash column chromatography on silica gel (5% AcOEt in Hexane) to afford **40d** (13 mg, 28% yield) as a colorless oil.

^{1}H NMR (400 MHz, $CDCl_3$) δ: 3.72 (ddd, *J* = 5.3, 4.2, 3.2 Hz, 1H), 3.33 (dt, *J* = 13.9, 7.6 Hz, 1H), 3.20 – 3.11 (m, 1H), 2.94 (ddd, *J* = 14.0, 7.9, 6.2 Hz, 1H), 1.94 – 1.39 (m, 10H), 1.35 – 1.20 (m, 9H), 1.00 – 0.81 (m, 3H).

^{13}C NMR (101 MHz, $CDCl_3$) δ 171, 50.2, 46.6, 40.3, 31.9, 29.4, 29.3, 28.2, 27.3, 23.3, 22.8, 19.7, 19, 17.1, 14.2.

HRMS (ESI pos): calculated for $C_{15}H_{27}NO$ ($M+H^+$): 238,21 found: 238,2157

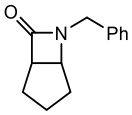

6-Benzyl-6-azabicyclo[3.2.0]heptan-7-one (40e): synthesized according the general procedure F using benzyl(cyclopent-2-en-1-yl)carbamic chloride **39e** (47 mg, 0.2 mmol, 1 eq.). The crude mixture was purified by flash column chromatography on silica gel (5% AcOEt in hexane) to afford **40e** (11 mg, 30% yield) as a yellowish oil.

^{1}H NMR (400 MHz, $CDCl_3$) δ 7.54 – 7.08 (m, 5H), 4.50 (d, *J* = 15.1 Hz, 1H), 4.08 (d, *J* = 15.1 Hz, 1H), 3.91 (t, *J* = 4.1 Hz, 1H), 3.47 (dd, *J* = 8.0, 3.6 Hz, 1H), 2.05 (dd, *J* = 13.2, 6.3 Hz, 1H), 1.83 – 1.70 (m, 2H), 1.58 (m, 1H), 1.47 – 1.30 (m, 1H), 1.18 (m, 1H).

^{13}C NMR (126 MHz, $CDCl_3$) δ 169.6, 136.3, 128.8, 128.4, 127.8, 57.6, 55.1, 44.2, 27, 25.1, 22.8.

HRMS (ESI pos): calculated for $C_{13}H_{15}NaNO$ ($M+Na^+$): 224.11 found: 224.1041

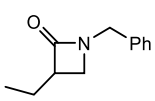

1-Benzyl-3-ethylazetidin-2-one (40f): synthesized according the general procedure F using benzyl(but-2-en-1-yl)carbamic chloride **39f** (47 mg, 0.2 mmol, 1 eq.). The crude mixture was purified by flash column chromatography on silica gel (5% AcOEt in hexane) to afford **40d** (11 mg, 29% yield) as a yellowish oil.

^{1}H NMR (500 MHz, $CDCl_3$) δ 7.37 – 7.26 (m, 5H), 4.46 (s, 2H), 3.60 – 3.52 (m, 2H), 3.18 – 3.10 (m, 1H), 1.72 – 1.65 (m, 2H), 0.93 (t, *J* = 7.3 Hz, 3H)

^{13}C NMR (126 MHz, $CDCl_3$) δ: 171.9 (C), 136.3 (C), 128.9 (CH), 128.3 (CH), 127.9 (CH), 53.6 (CH_2), 48.7 (CH_2), 44 (CH), 29 (CH_2), 11.9 (CH_3).

Matching reported literature data.[49]

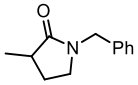

1-Benzyl-3-methylpyrrolidin-2-one (40g): Synthesized according to the general procedure F using benzyl(but-3-en-1-yl)carbamic chloride **39g** (48 mg, 0.2 mmol). The crude mixture was purified by flash column chromatography on silica gel (10% AcOEt in hexanes as eluent) to afford product **40g** (23 mg, 60% yield) as a yellow oil.

^{1}H NMR (500 MHz, $CDCl_3$) δ 7.37 – 7.30 (m, 2H), 7.29 – 7.24 (m, 1H), 7.24 – 7.20 (m, 2H), 4.49 – 4.40 (m, 2H), 3.22 – 3.09 (m, 2H), 2.51 (ddt, *J* = 15.8, 8.7, 7.2 Hz, 1H), 2.21 (dddd, *J* = 12.9, 8.7, 6.5, 4.4 Hz, 1H), 1.59 (dq, *J* = 12.6, 8.5 Hz, 1H), 1.24 (d, *J* = 7.1 Hz, 3H).

^{13}C NMR (126 MHz, $CDCl_3$) δ 177.5, 136.8, 128.8, 128.2, 127.6, 46.9, 44.8, 36.9, 27.2, 16.5.

HRMS (ESI pos): calculated for $C_{12}H_{16}NO$ ($M+H^+$): 190.1226, found: 190.1228.

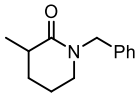

1-Benzyl-3-methylpiperidin-2-one (40h): Synthesized according to the general procedure F using benzyl(pent-4-en-1-yl)carbamic chloride **39h** (48 mg, 0.2 mmol). The crude mixture was purified by flash column chromatography on silica gel (10% AcOEt in hexanes as eluent) to afford product **40h** (21 mg, 52% yield) as a yellow oil.

^{1}H NMR (400 MHz, $CDCl_3$) δ 7.36 – 7.28 (m, 2H), 7.28 – 7.21 (m, 3H), 4.66 (d, *J* = 14.6 Hz, 1H), 4.50 (d, *J* = 14.6 Hz, 1H), 3.20 (dd, J = 7.2, 5.1 Hz, 2H), 2.56 – 2.42 (m, 1H), 1.96 (dtd, *J* = 12.8, 6.2, 3.4 Hz, 1H), 1.84 (dddd, *J* = 13.5, 6.6, 5.0, 3.4 Hz, 1H), 1.78 – 1.66 (m, 1H), 1.53 (dddd, *J* = 12.8, 10.4, 9.1, 3.4 Hz, 1H), 1.30 (d, *J* = 7.2 Hz, 3H).

^{13}C NMR (101 MHz, $CDCl_3$) δ 173.5, 137.7, 128.7, 128.1, 127.4, 50.4, 47.7, 36.8, 29.7, 21.8, 18.2.

HRMS (ESI pos): calculated for $C_{13}H_{18}NO$ ($M+H^+$): 204.1383, found: 204.1376.

3.9.10 Mechanistic studies

3.9.10.1 General procedure for the synthesis of acyl xanthate intermediates (general procedure G)

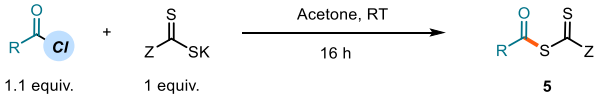

[49] Franco Bella, A.; Jackson, L. V.; Walton, J. C. Preparation of β-and γ-lactams *via* ring closures of unsaturated carbamoyl radicals derived from 1-carbamoyl-1-methylcyclohexa-2,5-dienes. *Org. Biomol. Chem.* **2004**, *2*, 421-428.

In a round bottom flask, acyl chloride (1.1 equiv.) was dissolved in acetone (0.1 M) and cooled to 0 ºC. The dithiocarbamate anion or the xanthate salt **1a-c** (1 equiv.) was then added and the resulting reaction mixture was stirred for 1 hour at 0 ºC. The solvent was removed under reduced pressure at ambient temperature. The residue was then dissolved in DCM and washed with distilled water, $NaHCO_3$ solution and brine. The combined organic fractions were dried over $MgSO_4$ and concentrated to dryness to obtain the desired product.

3.9.10.2 Characterization of the Intermediates

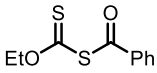

Benzoic (O-ethyl carbonothioic) thioanhydride (5a).

Prepared according to the general procedure G using potassium ethyl xanthogenate **B** (1 mmol, 160 mg) and benzoyl chloride (1.1 mmol, 128 μL) in 10 mL of acetone. After work-up, the product **5a** (226 mg, 99% yield) was obtained as a yellow oil.

^{1}H NMR (300 MHz, $CDCl_3$) δ 7.87 (app d, *J* = 7.7 Hz, 2 H); 7.64-7.54 (m, 1H); 7.49-7.39 (m, 2H); 4.69 (q, *J* = 7.1 Hz, 2H); 1.45 (t, *J* = 7.1 Hz, 3H).

^{13}C NMR (75 MHz, $CDCl_3$) δ 203.4, 185.0, 135.7, 134.4, 129.0, 127.9, 71.1, 13.5.

Matching reported literature data.[50]

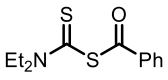

Benzoic diethylcarbamothioic thioanhydride (5b).

Prepared according to the general procedure G using sodium diethylcarbamodithioate trihydrate **C** (1.05 mmol, 237 mg) and benzoyl chloride (1 mmol, 116 μL) in 10 mL of acetone. After work-up, the product **5b** was obtained as a yellow oil (220 mg, 87% yield).

^{1}H NMR (300 MHz, $CDCl_3$) δ 7.95-7.88 (m, 2 H); 7.64-7.56 (m, 1H); 7.52-7.42 (m, 2H); 4.07-3.86 (m, 2H); 1.36 (t, *J* = 7.1 Hz, 3H).

Matching reported literature data.[51]

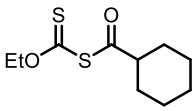

cyclohexanecarboxylic (O-ethyl carbonothioic) thioanhydride (5c).

Prepared according to the general procedure G using potassium ethyl xanthogenate **B** (1 mmol, 160 mg) and cyclohexanecarbonyl chloride (1.1 mmol, 128 μL) in 10 mL of acetone. After work-up, the product **5c** was obtained as a yellow oil (207 mg, 89% yield).

---

[50] Ajayaghosh, A.; Das, S.; George, M. V. S-benzoyl O-ethyl xanthate as a new photoinitiator: Photopolymerization and laser flash photolysis studies. *J. Polym. Sci., Part A: Polym. Chem.* **1993**, *31*, 653-659.
[51] Azizi, N.; Alipour, M. Synthesis of carboxylic dithiocarbamic anhydride and substituted thiourea derivatives in water. *Environ. Chem. Lett.* **2018**, *16*, 1415-1421.

^{1}H NMR (300 MHz, $CDCl_3$) δ 4.65 (q, *J* = 7.1 Hz, 2H); 2.53-2.39 (m, 1H); 1.98-1.85 (m, 2H); 1.83-1.70 (m, 2H); 1.68-1.53 (m, 1H); 1.55-1.35 (m, 5H); 1.34-1.10 (m, 3 H).

^{13}C NMR (75 MHz, $CDCl_3$) δ 204.6; 194.9; 70.8; 52.8; 29.1; 25.5; 25.3; 13.6.

HRMS (ESI pos): calculated for $C_{10}H_{16}NaO_2S_2$ ($M+Na^+$): 255.0484, found: 255.0482.

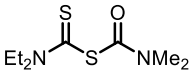

***N*-Diethyl, *N'*-Dimethyl-Thiodicarbonic diamide (5d).** Prepared according to the general procedure G using potassium diethylcarbamodithioate trihydrate **C** (3 mmol, 724 mg) and dimethylcarbamyl chloride (1.1 mmol, 128 μL) in 10 mL of acetone. After work-up and chromatography on silica gel (8:2 hexane/AcOEt), the product **5d** was obtained as a yellow oil (177 mg, 80% yield).

^{1}H NMR (400 MHz, $CDCl_3$) δ 4.02 (q, *J* = 7.1 Hz, 1H), 3.79 (q, *J* = 7.2 Hz, 1H), 3.06 (s, 3H), 1.32 (dt, *J* = 9.7, 7.1 Hz, 3H)

^{13}C NMR (126 MHz, $CDCl_3$) δ 185.2, 162, 50.1, 49, 38.5, 37.3, 13.5, 11.3.

3.9.10.3 UV-Vis Characterization of the Intermediates

Table 3.5. Spectroscopic characteristics of **5a-d**

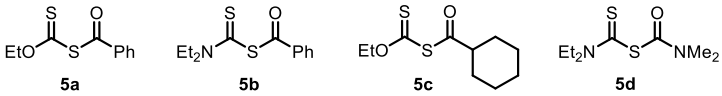

Intermediate	λ max	tail of absorption
5a	397 nm	490 nm
5b	400 nm	490 nm
5c	400 nm	490 nm
5d	343 nm	500 nm

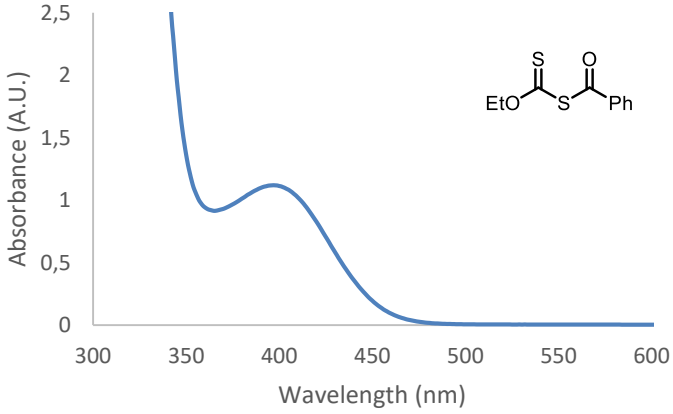

Figure 3.14. UV-Vis absorption spectrum of **5a** recorded at $1 \cdot 10^{-2}$M concentration in acetonitrile.

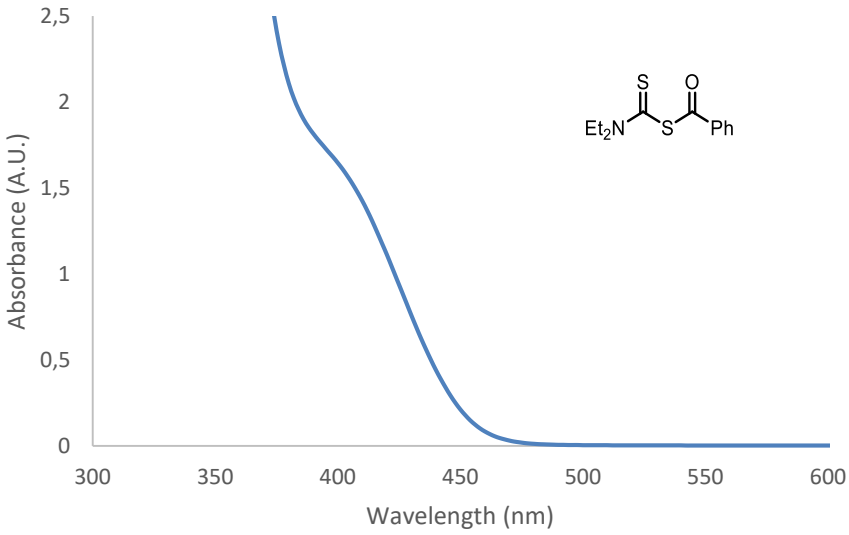

Figure 3.15. UV-Vis absorption spectrum of **5b** recorded at $1 \cdot 10^{-2}$ M concentration in acetonitrile.

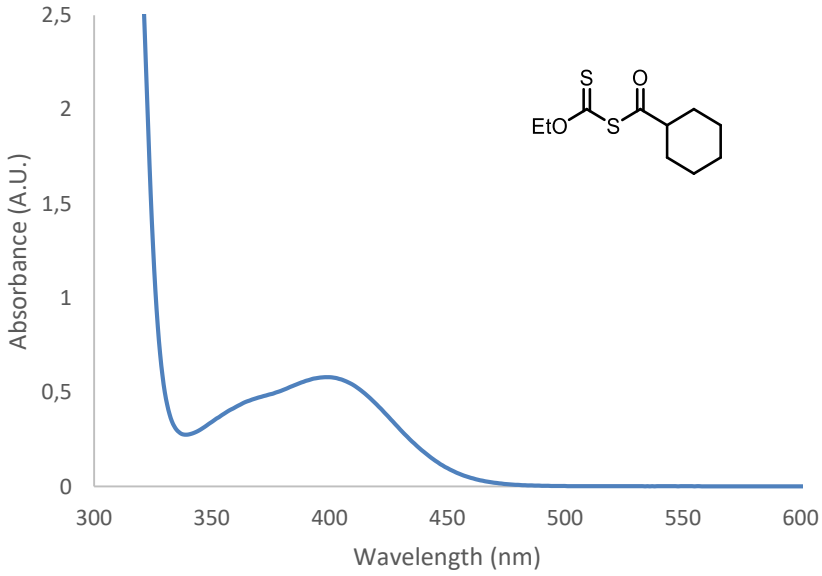

Figure 3.16. UV-Vis absorption spectrum of **5c** recorded at $2 \cdot 10^{-2}$ M concentration in acetonitrile.

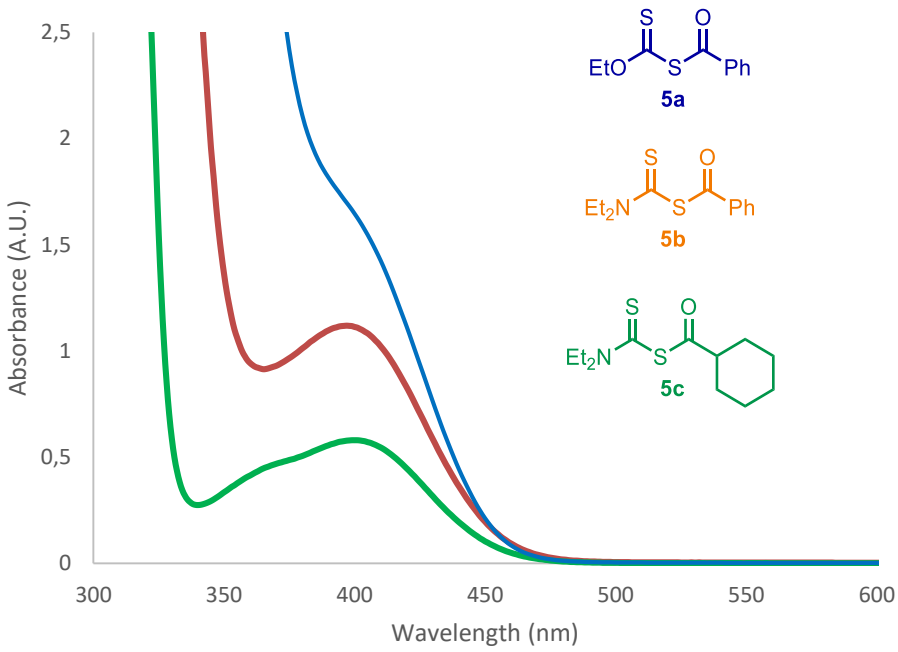

Figure 3.17. Superposition of the absorption spectra of the different acyl xanthates and acyl dithiocarbamate intermediates at the same concentration ($2 \cdot 10^{-2}$ M in acetonitrile).

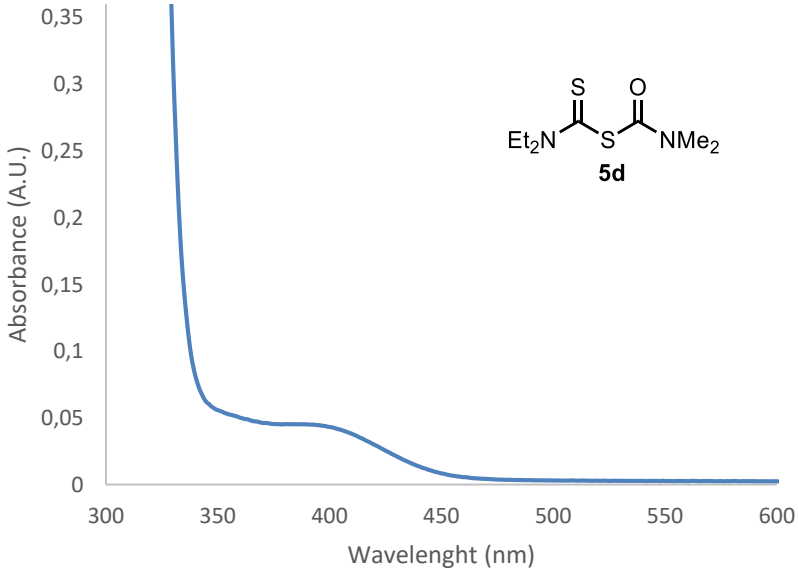

Figure 3.18. UV-Vis absorption spectrum of intermediate **5d** recorded at $2 \cdot 10^{-3}$ M concentration in acetonitrile.

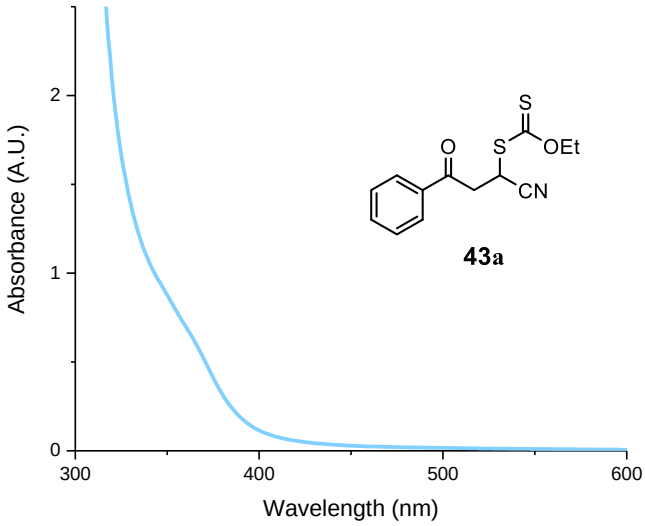

Figure 3.19. UV-Vis absorption spectrum of **43a** recorded at $1 \cdot 10^{-2}$ M in acetonitrile.

3.9.10.4 TEMPO Trapping Experiments

Stoichiometric reaction between TEMPO and in-situ acyl xanthate intermediate

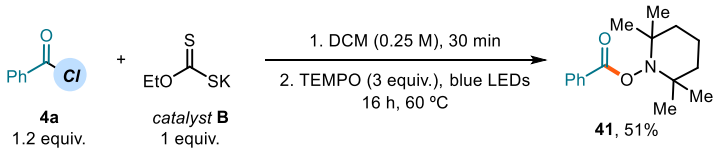

In an oven dried tube of 15 mL (16 mm × 125 mm) with a Teflon septum screw cap, potassium ethyl xanthogenate **B** (80.1 mg, 0.5 mmol, 1 equiv.) was suspended in DCM (2 mL, HPLC grade). Then, benzoyl chloride **4a** (69.6 µL, 0.6 mmol, 1.2 equiv.) was added and the mixture was stirred at ambient temperature for 30 minutes. Then, TEMPO (234.4 mg, 1.5 mmol, 3 equiv.) was added and the resulting yellow solution was degassed with argon sparging for 60 seconds. The tube was then placed in the temperature controlled photoreactor set at a temperature of 60 ºC (60-61ºC measured in the central well) and irradiated for 16 hours. Chromatography on silica gel (5% AcOEt in hexanes as eluent) afforded adduct **41** (66 mg, yellow oil, 51% yield).

^{1}H NMR (500 MHz, $CDCl_3$) δ 8.35 (d, *J* = 6.9 Hz, 2H), 7.83 (m, 1H), 7.74 (m, 2H), 2.12 – 1.70 (m, 6H), 1.55 (s, 6H), 1.40 (s, 6H).

^{13}C NMR (126 MHz, $CDCl_3$) δ 161.45, 128.17, 124.89, 124.74, 123.78, 55.52, 34.28, 27.19, 16.09, 12.26.

Matching reported literature data.[52]

Stoichiometric reaction between TEMPO and dithiocarbamate intermediate Id

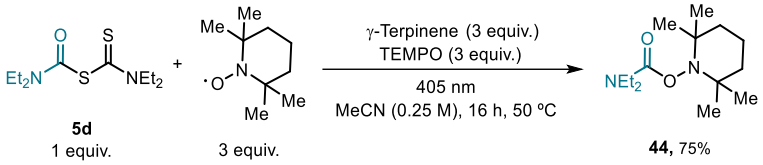

In an oven-dried 15 mL Schlenk tube was added a 0.25 M solution of the dithiocarbamate intermediate **5d** (28 mg, 127 mmol, 1 equiv.) and TEMPO (60 mg, 0.38 mmol, 3 equiv.) in acetonitrile (0.5 mL). The reaction mixture was placed under an atmosphere of argon, cooled to –78 °C, degassed *via* vacuum evacuation (5 minutes), backfilled with argon and, ultimately, warmed to ambient temperature. This freeze-pump-thaw cycle was repeated four times, and then the Schlenk tube was sealed with Parafilm and put into the Hepatochem PhotoRedOx Box equipped with a 405 nm EvoluChem LED 18 W light source at 50 ºC. After 18 hours, the reaction vessel was cooled down to ambient temperature, water was added and the mixture was extracted with ethyl acetate (2x15 mL). The combined layers were dried over $MgSO_4$, filtered, and concentrated. The resulting crude mixture was purified by column chromatography on silica gel (5% to 30% AcOEt in hexane) to give the corresponding product **44** (21 mg, 75% yield).

^{1}H NMR (400 MHz, $CDCl_3$) δ 2.96 (s, 6H), 1.73 – 1.48 (m, 6H), 3.06 (s, 3H), 1.13 (d, *J* = 17.6 Hz, 1H)

^{13}C NMR (101 MHz, $CDCl_3$) δ 157.8, 60.2, 50.1, 39.1, 31.9, 21.1, 17.2.

TEMPO inhibition of the model reactions

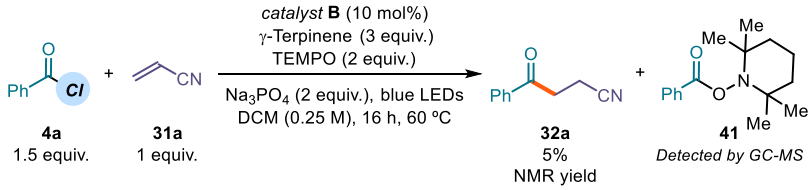

Reaction performed according to the general procedure A using benzoyl chloride (87 µL, 0.75 mmol, 1.5 equiv.) and acrylonitrile (33 µL, 0.5 mmol, 1 equiv.) and adding TEMPO (156.3 mg, 1 mmol, 2 equiv.) before the degassing step. The crude mixture was analyzed by ^{1}H NMR analysis after 16 hours using trichloroethylene (45 µL, 0.5 mmol, 1 equiv.) as internal

[52] He, X.-K.; Cai, B.-G.; Yang, Q.-Q.; Wang, L.; Xuan, J. Visible-Light-Promoted Cascade Radical Cyclization: Synthesis of 1,4-Diketones Containing Chroman-4-One Skeletons. *Chem. Asian J.* **2019**, *14*, 3269-3273.

standard, and by GC-MS. NMR yield: 5%. Traces of the TEMPO adduct **41** were detected by GC-MS analysis.

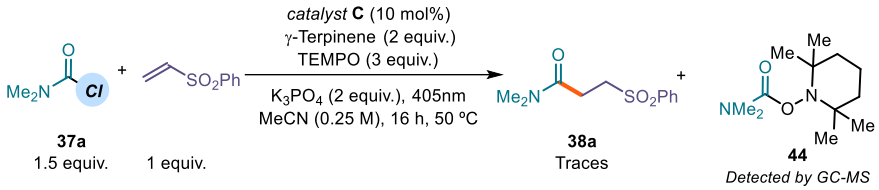

Reaction performed according to the general procedure E using dimethylcarbamyl chloride (37 µL, 0.4 mmol, 2 equiv.) and phenyl vinyl sulfone (34 mg, 0.2 mmol, 1 equiv.) and adding TEMPO (62 mg, 0.4 mmol, 2 equiv.) before the degassing step.

3.9.10.5 Experiments with the Dimer of the Catalyst

Model reaction with catalyst dimer 42b – Acylation

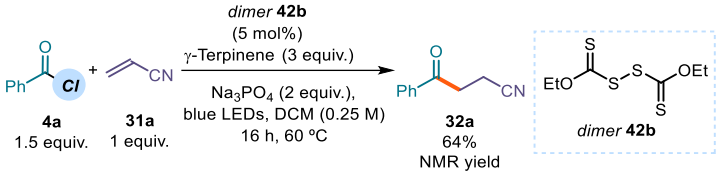

Reaction performed according to the general procedure A using benzoyl chloride (87 µL, 0.75 mmol, 1.5 equiv.) and acrylonitrile (33 µL, 0.5 mmol, 1 equiv.) while replacing *catalyst* **B** with *dimer* **42b** (6 mg, 0.025 mmol, 0.05 equiv.). The crude reaction mixture was analyzed by ^{1}H NMR analysis using trichloroethylene as internal standard. NMR yield: 64%.

Model reaction with dimer catalyst 42c - Carbamoylation

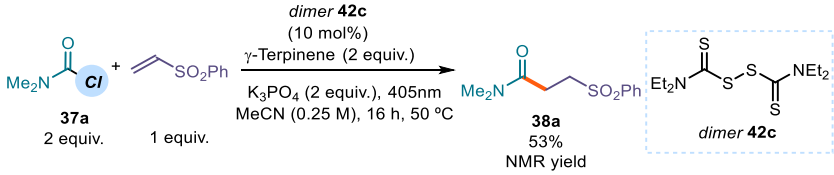

Reaction performed according to general procedure E using dimethylcarbamic chloride (37 µL, 0.4 mmol, 2.0 equiv.) and phenyl vinyl sulfone (34 mg, 0.2 mmol, 1 equiv.) while replacing *catalyst* **C** with *dimer* **42c** (6 mg, 0.02 mmol, 0.1 equiv.). The crude reaction mixture was analyzed by ^{1}H NMR analysis using trichloroethylene as internal standard. NMR yield: 53%.

Turn-over experiment with dimer catalyst B and terpinene

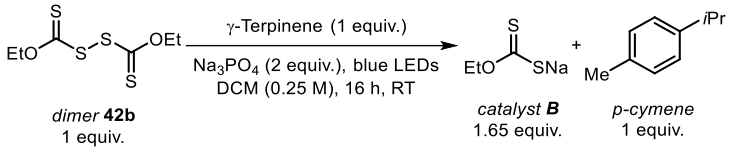

In an oven dried vial (16 mm × 50 mm) with a Teflon septum screw cap, *dimer* **42b** (60.6 mg, 0.25 mmol, 1 equiv.) and sodium phosphate (82 mg, 0.5 mmol, 2 equiv) were dissolved in DCM (2 mL, HPLC grade). Then, γ-terpinene (40 µL, 0.25 mmol, 1 equiv.) was added. The resulting yellow mixture was degassed with argon, sparging for 60 seconds. The vial was then placed in the 3D-printed support photoreactor (Figure S6) and irradiated for 24 hours. Trichloroethylene was added as internal standard and a sample of the crude mixture was diluted in d_6-DMSO to record the NMR yield.

3.9.10.6 Group Transfer Experiments

Stoichiometric group transfer reaction with in-situ acyl xanthate intermediate

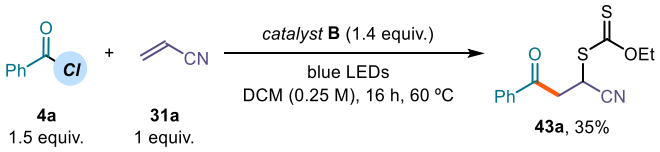

In an oven dried tube of 15 mL (16 mm × 125 mm) with a Teflon septum screw cap, potassium ethyl xanthogenate **B** (112 mg, 0.7 mmol, 1.4 equiv.) was suspended in DCM (2 mL, HPLC grade). Then, benzoyl chloride (87 µL, 0.75 mmol, 1.5 equiv.) was added and the mixture was stirred at ambient temperature for 30 min. The reaction mixture was then degassed with argon, sparging for 60 seconds. Finally, acrylonitrile (33 µL, 0.5 mmol, 1 equiv.) was added via syringe. The tube was then placed in the temperature controlled photoreactor (Figure 3.7) set at a temperature of 60 ºC (60-61ºC measured in the central well) and irradiated for 16 hours. The crude mixture was purified by flash column chromatography on silica gel (5% to 10% AcOEt in hexanes as eluent) to afford **43a** (50 mg, 35% yield) as a yellow oil.

^{1}H NMR (400 MHz, $CDCl_3$) δ 7.97 – 7.89 (m, 2H), 7.69 – 7.58 (m, 1H), 7.50 (app t, *J* = 7.5 Hz, 2H), 5.08 (t, *J* = 6.2 Hz, 1H), 4.72 (q, *J* = 7.1 Hz, 2H), 3.70 (d, *J* = 6.3 Hz, 2H), 1.47 (t, *J* = 7.1 Hz, 3H).

^{13}C NMR (101 MHz, $CDCl_3$) δ 209.05, 193.54, 135.35, 134.39, 129.09, 128.30, 117.96, 71.54, 40.67, 32.49, 13.84.

Stoichiometric group transfer reaction with in-situ acyl xanthate intermediate in the presence of γ-terpinene

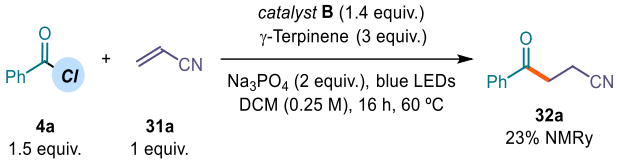

In an oven dried tube of 15 mL (16 mm × 125 mm) with a Teflon septum screw cap, potassium ethyl xanthogenate (112 mg, 0.7 mmol, 1.4 equiv.) and sodium phosphate (164 mg, 1.0 mmol, 2 equiv) were dissolved in DCM (2 mL, HPLC grade). Benzoyl chloride (87 µL, 0.75 mmol, 1.5 equiv.) was added and the mixture was stirred at ambient temperature for 30 min. Then, γ-terpinene (240 µL, 1.5 mmol, 3 equiv.) was added. The mixture was degassed via argon sparging for 60 seconds. Finally, acrylonitrile (33 µL, 0.5 mmol, 1 equiv.) was added via syringe. The tube was then placed in the temperature controlled photoreactor (Figure 3.7) set at a temperature of 60 ºC (60-61 ºC measured in the central well) and irradiated for 16 hours. Trichloroethylene was added as internal standard, and a sample of the crude mixture was diluted in $CDCl_3$ to record the NMR yield. *No group transfer product **43a** was observed.*

Direct photolysis of the group transfer product under reaction conditions

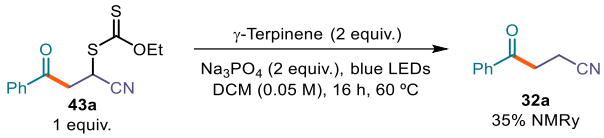

In an oven dried tube of 15 mL (16 mm × 125 mm) with a Teflon septum screw cap, the group transfer product **43a** (28.01 mg, 0.1 mmol, 1 equiv.) and sodium phosphate (33 mg, 0.2 mmol, 2 equiv) were dissolved in DCM (2 mL, HPLC grade). Then, γ-terpinene (33 µL, 0.2 mmol, 2 equiv.) was added. The reaction mixture was degassed with Argon sparging for 60 seconds. The tube was then placed in the temperature controlled photoreactor (Figure 3.7) set at a temperature of 60 ºC (60-61 ºC measured in the central well) and irradiated for 16 hours.

Trichloroethylene was added as internal standard and a sample of the crude mixture was diluted in $CDCl_3$ to record the NMR yield – product **32a** was formed in 35%.

Direct photolysis of the group transfer product for the intramolecular reaction

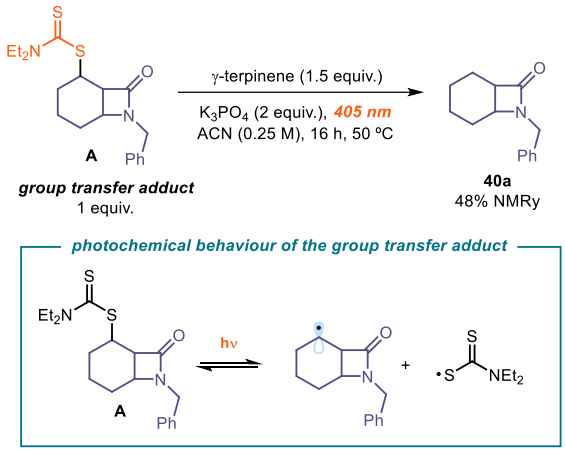

An oven-dried 15 mL Schlenk tube was charged with an authentic sample of the group transfer adduct **A**, prepared according to Ref. 38b, γ–terpinene (48 µL, 0.3 mmol, 1.5 equiv.) and K_3PO_4 (85 mg, 0.4 mmol, 2 equiv.) in acetonitrile (0.8 mL, 0.25 M). The reaction mixture was placed under an atmosphere of argon, cooled to –78 °C, degassed *via* vacuum evacuation (5 minutes), backfilled with argon and, ultimately, warmed to ambient temperature. This freeze-pump-thaw cycle was repeated four times, and then the Schlenk tube was sealed with Parafilm and put into the Hepatochem PhotoRedOx Box equipped with a 405 nm EvoluChem LED 18 W light source at 50 ºC (Figure 3.13). After 18 hours stirring, the reaction was cooled down to ambient temperature, trichloroethylene was added as internal standard and a sample of the crude mixture was diluted in $CDCl_3$ to record the NMR of the crude - product **40a** was formed in 48%.

3.9.10.7 Cyclic Voltammetry Measurements

For the cyclic voltammetry (CV) measurements, a glassy carbon disk electrode (diameter: 3 mm) was used as a working electrode. A silver wire coated with AgCl immersed in a 3.5 M aqueous solution of KCl and separated from the analyte by a fritted glass disk was employed as the reference electrode. A Pt wire counter-electrode completed the electrochemical setup. The scan rate of used in each CV experiment is indicated case by case.

Potentials are quoted with the following notation: E_p^C refers to the cathodic peak potential, E_p^A refers to the anodic peak potential, while the E_{red} value describes the electrochemical properties of the referred compound.

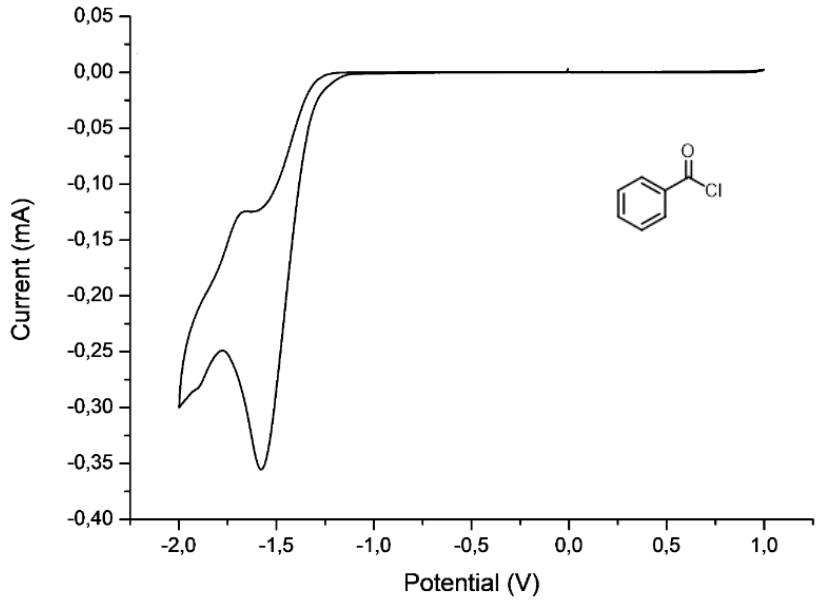

Figure 3.20. Cyclic voltammogram of benzoyl chloride **4a** [0.02 M] in [0.1 M] $TBAPF_6$ in CH_3CN. Sweep rate: 100 mV/s. Glassy carbon electrode working electrode, Ag/AgCl (KCl 3.5 M) reference electrode, Pt wire auxiliary electrode. Irreversible reduction, $E_p^C = E^{red}$ (**4a**/**4a**$^{\bullet-}$) = -1.57 V.

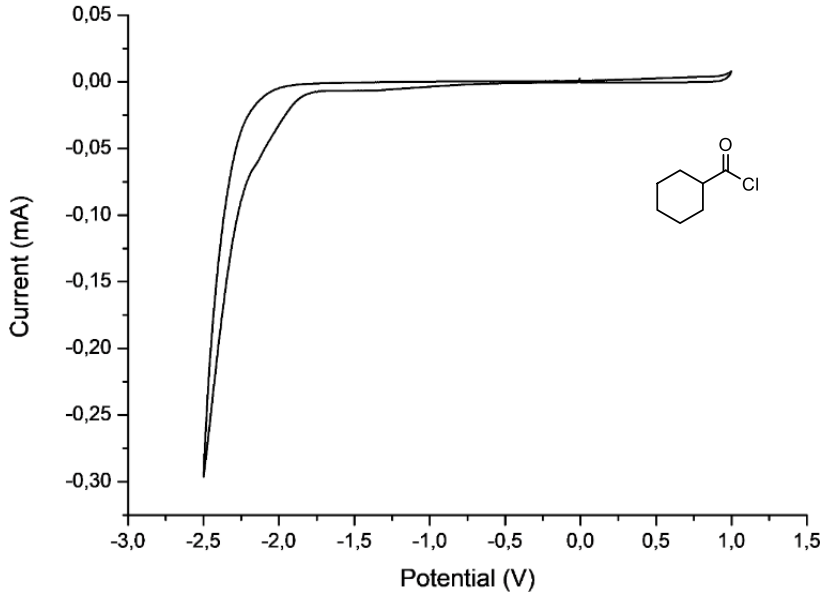

Figure 3.21. Cyclic voltammogram of cyclohexanecarbonyl chloride [0.02 M] in [0.1 M] $TBAPF_6$ in CH_3CN. Sweep rate: 100 mV/s. Glassy carbon electrode working electrode, Ag/AgCl (KCl 3.5 M) reference electrode, Pt wire auxiliary electrode. Reduction of cyclohexanecarbonyl chloride was not observed in the registered potential window (from 0 to -2.50 V).

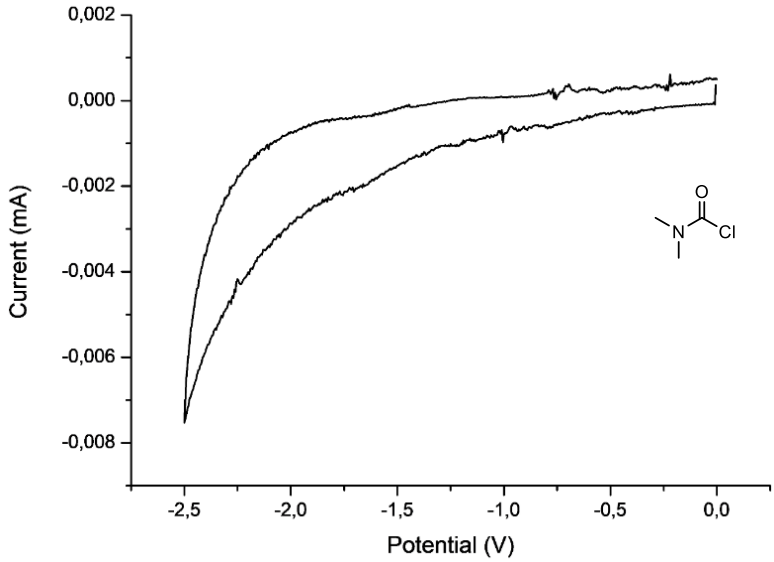

Figure 3.22. Cyclic voltammogram for **37a** [0.02M] in [0.1 M] $TBAPF_6$ in CH_3CN. Sweep rate: 50 mV/s. Glassy carbon electrode working electrode, Ag/AgCl (KCl 3.5 M) reference electrode, Pt wire auxiliary electrode. Reduction of **37a** was not observed in the registered potential window (from 0 to -2.50 V).

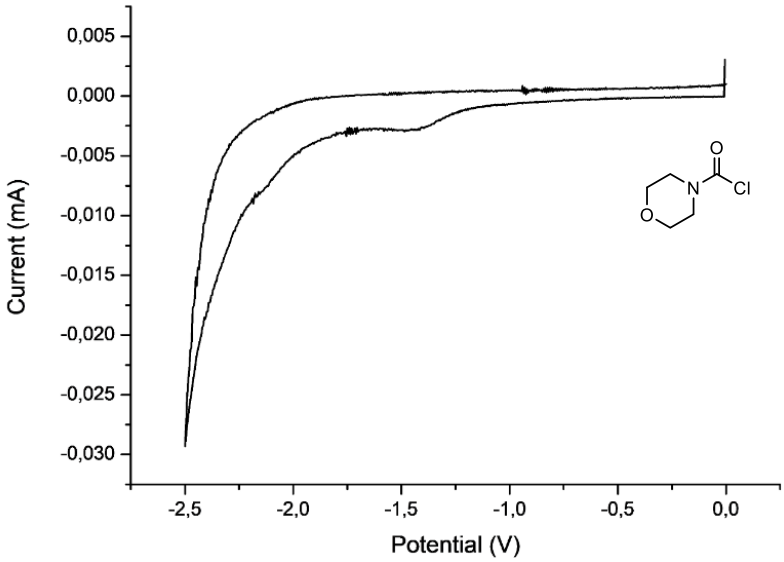

Figure 3.23. Cyclic voltammogram for **37e** [0.02M] in [0.1 M] $TBAPF_6$ in CH_3CN. Sweep rate: 100 mV/s. Glassy carbon electrode working electrode, Ag/AgCl (KCl 3.5 M) reference electrode, Pt wire auxiliary electrode. Reduction of **37e** was not observed in the registered potential window (from 0 to -2.50 V).

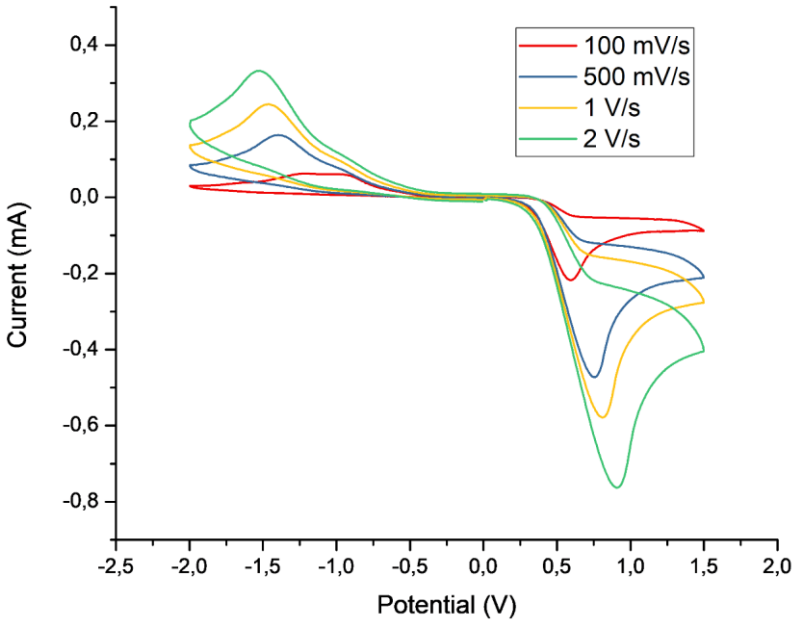

Figure 3.24. Cyclic voltammogram for catalyst **B** [0.02 M] in [0.1 M] $TBAPF_6$ in CH_3CN. Measurement started by oxidation from 0 to +1.5 V, followed by reduction from +1.5 V to -2.0 V, and finishing at 0 V. Glassy carbon electrode working electrode, Ag/AgCl (KCl 3.5 M) reference electrode, Pt wire auxiliary electrode. Two irreversible peaks observed increasing with sweep rate.

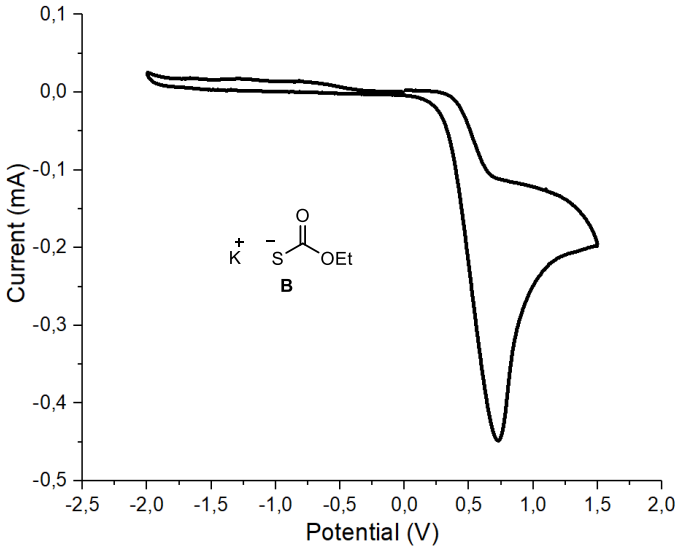

Figure 3.25. Cyclic voltammogram for catalyst **B** [0.02M] in [0.1 M] $TBAPF_6$ in CH_3CN. Measurement started by reduction from 0 to -2.0 V, followed by oxidation from -2.0 V to +1.5 V, and finishing at 0 V. Glassy carbon electrode working electrode, Ag/AgCl (KCl 3.5 M) reference electrode, Pt wire auxiliary electrode. Only one irreversible peak observed. Sweep rate: 500 mV/s.

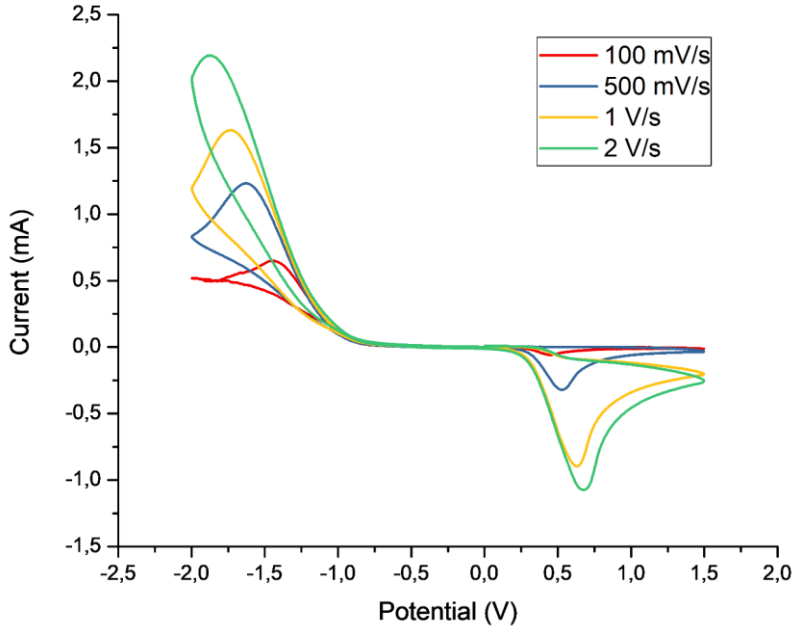

Figure 3.26. Cyclic voltammogram for dimer **42b** [0.02 M] in [0.1 M] $TBAPF_6$ in CH_3CN. Measurement started by reduction from 0 to -2.0 V, followed by oxidation from -2.0 V to +1.5 V, and finishing at 0 V. Glassy carbon electrode working electrode, Ag/AgCl (KCl 3.5 M) reference electrode, Pt wire auxiliary electrode. Two irreversible peaks observed increasing with sweep rate.

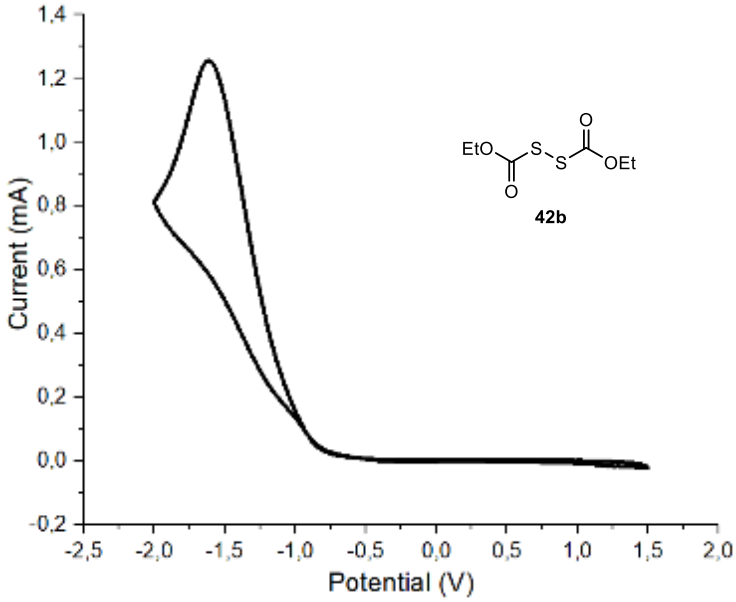

Figure 3.27. Cyclic voltammogram for dimer **42b** [0.02 M] in [0.1 M] $TBAPF_6$ in CH_3CN. Measurement started by oxidation from 0 to +1.5 V, followed by reduction from +1.5 V to -2.0 V, and finishing at 0 V. Glassy carbon electrode working electrode, Ag/AgCl (KCl 3.5 M) reference electrode, Pt wire auxiliary electrode. Two irreversible peaks observed increasing with sweep rate.

3.9.10.8 Transient Absorption Spectroscopy (TAS)

Studies with microsecond transient absorption spectroscopy (TAS) were performed using an excitation source of NdYAG (neodymium-doped yttrium aluminium garnet) Opolette laser with an optical parametric oscillator (OPO) system that allows variable wavelength excitation from 400 -1800 nm, pulse width of 6 ns, up to 2 mJ of energy from OPO output with fiber optic coupled, and high energy output from direct NdYAG harmonics 355 (20 mJ, 5 ns) and 532 (45mJ, 6 ns). The system is completed with 150 W tungsten lamp as probe; 2 monochromators Minuteman MM151; Si amplified photodetector module for VIS; DSPDAU high speed data rate recorder and interface software from RAMDSP. Laser intensities for each wavelength were the following: 355 nm – 1.30 mJ; 420 nm– 1.20 mJ; 460 nm – 1.95 mJ.

Several studies with different wavelengths and laser intensities were carried out, each of the conditions are indicated in a case by case bases. We selected a logarithmic time scale suitable for clearly showing the decay of the transient species in the samples. The characteristics of the detected transient species match literature data.[33]

In a typical transient absorption spectroscopy experiment, solutions in acetonitrile of each of the substrates were prepared under an argon atmosphere and transferred into a screw-top 3.0 mL quartz cuvette for measurement. Upon irradiation with the appropriated wavelength, the decay of absorption at 620 nm of the transient xanthyl radical **Ib** was recorded.

Acylxanthate 5a

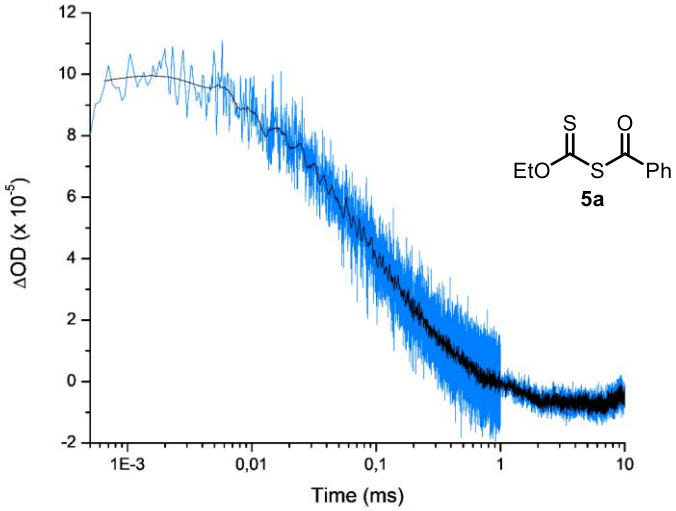

Figure 3.28. Absorption at 620 nm of the transient xanthyl radical **Ib** (blue line) generated upon 355 nm laser excitation of Acylxanthate **5a** ([**5a**] = 3 mM in acetonitrile). Note logarithmic scale for time. Absorption decay (black line) processed through Savinsky Golay filter to facilitate lifetime measurement. ΔOD: optical density variation.

Compound **5a** was also measured upon 460 nm excitation in order to mimic the conditions of photolysis under catalytic conditions. Since photolysis of **5a** is less efficient at longer wavelengths, a higher concentration of **5a** was needed to obtain a comparable scale signal.

Note that changes in concentration of both **5a** and transient **Ib** generated upon photolytic cleavage directly affects the lifetime of the detected species.

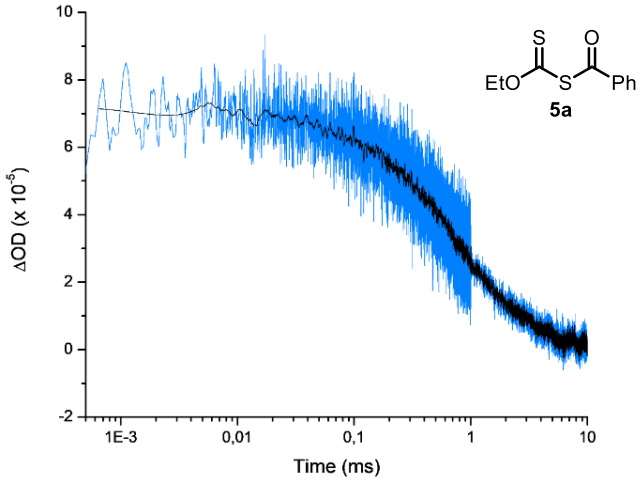

Figure 3.29. Absorption at 620 nm of the transient xanthyl radical **Ib** (blue line) generated upon 460 nm laser excitation of acylxanthate **5a** ([**5a**] = 300 mM in acetonitrile). Note logarithmic scale for time. Absorption decay (black line) processed through Savinsky Golay filter to facilitate lifetime measurement. ΔOD: optical density variation.

Dimer 42b

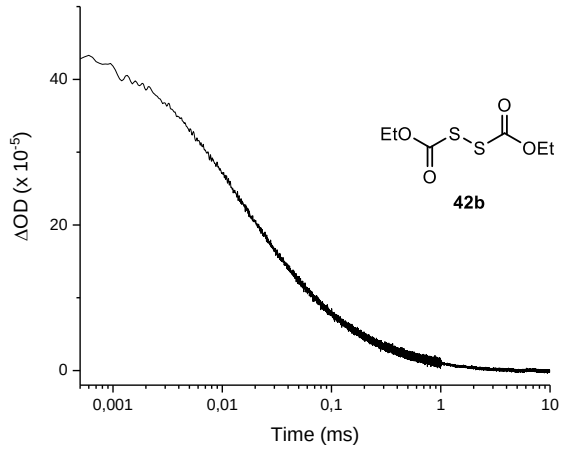

Figure 3.30. Absorption at 620 nm of the transient xanthyl radical **Ib** (black line) generated upon 355 nm laser excitation of dimer **42b** ([**42b**] = 3 mM in acetonitrile). Note logarithmic scale for time. ΔOD: optical density variation.

Dimer **42b** was also measured upon 420 nm and 460 nm irradiation in order to support photolysis under the reaction conditions. A higher concentration of **42b** was used to ensure comparable scale signal.

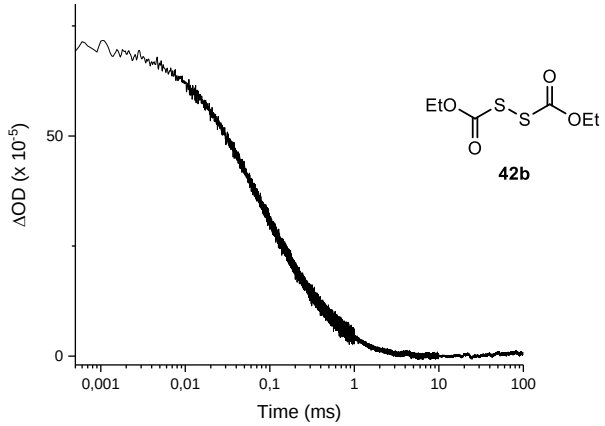

Figure 3.31. Absorption at 620 nm of the transient xanthyl radical **Ib** (black line) generated upon 420 nm laser excitation of dimer **42b** ([**42b**] = 300 mM in acetonitrile). Note logarithmic scale for time. ΔOD: optical density variation.

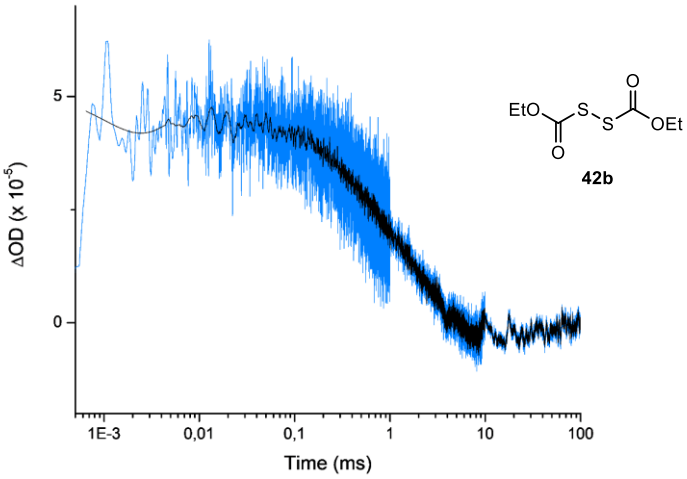

Figure 3.32. Absorption at 620 nm of the transient xanthyl radical **Ib** (blue line) generated upon 460 nm laser excitation of dimer **42b** ([**42b**] = 300 mM in acetonitrile). Note logarithmic scale for time. Absorption decay (black line) processed through Savinsky Golay filter to facilitate lifetime measurement. ΔOD: optical density variation.

In order to perform the quenching experiment, increasing amounts of pure γ-terpinene was added while observing the effect on the absorption at 620 nm of the transient **Ib**, which was recorded after every addition. Increasing amounts of pure γ-terpinene (up to 60 equivalents, 60 μL) were added sequentially to a 2 mL solution of **42b** (3 mM in acetonitrile) in a screw-

top quartz cuvette, providing a final concentration of 2.91 mM. A decay of absorption of the transient xanthyl radical, and therefore a shorter lifetime, was observed upon addition of γ-terpinene (Figure 3.33), which is consonant with a reaction between the two species. Turquoise line: ratio **42b**/γ-terpinene mimics the reaction conditions. Note that precipitation of a solid, associated to ethyl xanthogenate, was observed upon addition and irradiation of the sample.

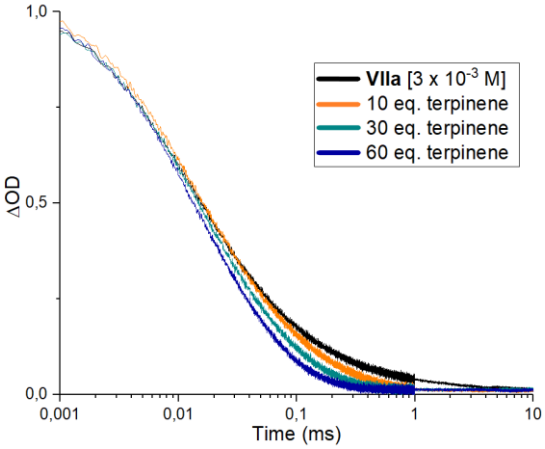

Figure 3.33. Absorption at 620 nm of the transient xanthyl radical **Ib** (black line) generated upon 355 nm laser excitation of dimer **42b** ([**42b**]$_0$ = 3 mM in acetonitrile) and subsequent decay of the absorption upon addition of 10 (orange line), 30 (green line, mimics proportions under reaction conditions) and 60 (blue line) equivalents of γ-terpinene, respectively. Note logarithmic scale for time. Absorption decay was normalized to 1. ΔOD: normalized optical density variation.

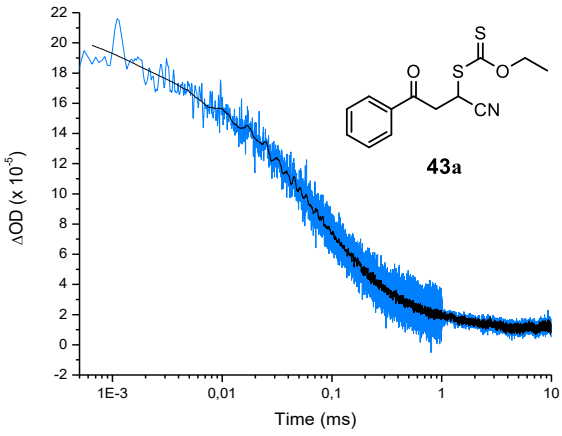

Figure 3.34. Absorption at 620 nm of the transient xanthyl radical **Ib** (blue line) generated upon 355 nm laser excitation of **43a** ([**43a**] = 3 mM in acetonitrile). Note logarithmic scale for time. Absorption decay (black line) processed through Savinsky Golay filter to facilitate lifetime measurement. ΔOD: optical density variation.

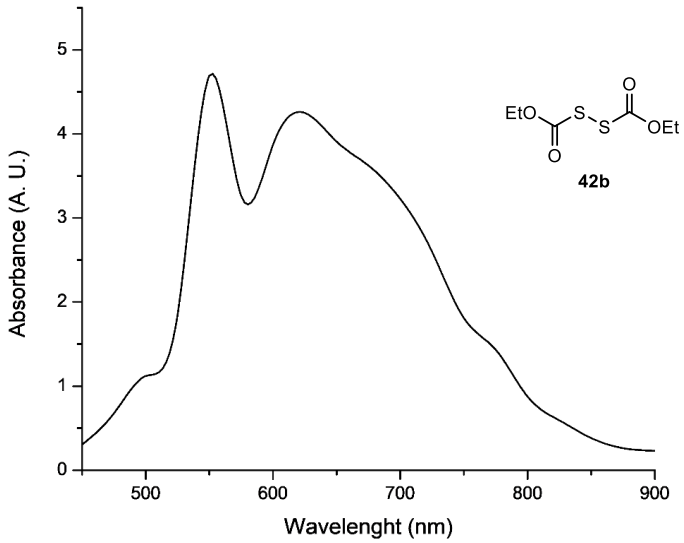

Figure 3.35. Absorption spectra of the transient xanthyl radical **Ib** generated upon 355 nm laser excitation of Dimer **42b** ([**42b**] = 3 mM in acetonitrile) at 1 μS time of irradiation. Maximum characteristic from xanthyl radical can be observed around 625 nm.

3.9.10.9 Electron paramagnetic resonance (EPR)

EPR spectra were acquired on a Bruker EMX X-band EPR spectrometer with an ER 4116 HS cavity (9.86 GHz at room temperature) using 100 kHz field modulation (modulation amplitude: 1 G). Individual EPR tubes were filled with ~0.7 mL of the solution and were placed at the same position of the resonant cavity for EPR spectral acquisition. The spectral data were collected at 298 K with the following spectrometer settings: microwave power = 2.020 mW; center field = 3518 G, sweep width = 200 G, sweep time = 30 s, modulation frequency = 100 KHz, modulation amplitude = 1 G, power attenuation = 20 dB, time constant = 0.01 ms.

A fresh solution of acylxanthate **5a** 0.10 M in Toluene was prepared under air and measured without further precautions to remove oxygen from the solution. As expected, no signal was observed before of irradiation (note that **5a** decomposes rapidly, and a sample older than one day did show signals appearing before irradiation, due to decomposition); on the other hand, upon irradiation of the sample, appearance of a triplet at 3505 G was observed with a g-value of 2.00272 and a hyperfine splitting value α_H (2.6, 2H, γ-H). This signal reaches a maximum of intensity after 12.5 minutes of irradiation. The calculated EPR spectrum for the carbon radical of type **XVIII**, which lies in proximity of two sulfur atoms and an ethoxy moiety, is shown in the Figure below.

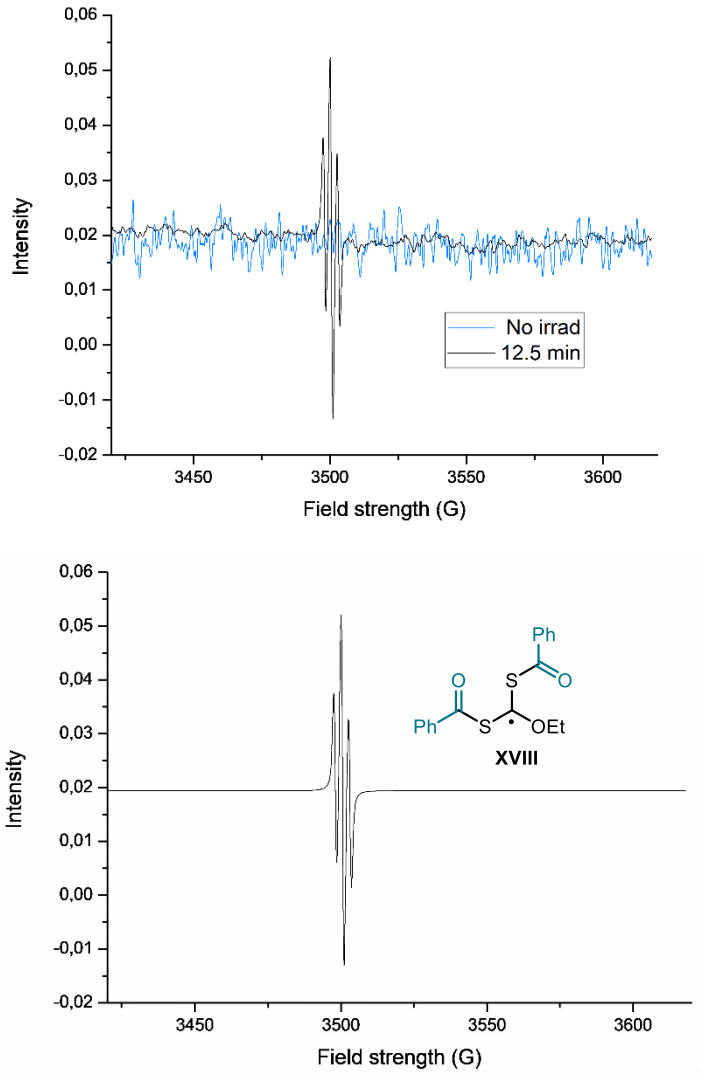

Figure 3.36. Comparison between (top) EPR spectra of acylxanthate **5a** (0.1 M in toluene) before irradiation (blue line) and after irradiation with a LSB610 100W mercury lamp during 12.5 min (black line). Open-shell species was detected by appearance of a new signal centered at 3505 G (triplet); and (bottom) calculated EPR spectrum for intermediate **XVIII** for a hyperfine coupling with two equivalent nuclei of spin ½.

3.9.10.10 Quantum Yield Determination

A ferrioxalate actinometer solution was prepared by following the Hammond variation of the Hatchard and Parker[53] procedure outlined in the Handbook of Photochemistry.[54] The ferrioxalate actinometer solution measures the decomposition of ferric ions to ferrous ions, which are complexed by 1,10-phenanthroline and monitored by UV/Vis absorbance at 510

[53] Hatchard, C. G.; Parker, C. A. A new sensitive chemical actinometer II. Potassium ferrioxalate as a standard chemical actinometer. *Proc. R. Soc. Lond. A* **1956**, 518-536.
[54] Murov, S. L. *Handbook of Photochemistry* **1973**, Marcel Dekker Inc.

nm. The moles of iron-phenanthroline complex formed are related to moles of photons absorbed. The following solutions were prepared and stored in a dark laboratory (red light):

1. Potassium ferrioxalate solution: 294.8 mg of potassium ferrioxalate (commercially available from Alfa Aesar) and 139 µL of sulfuric acid (96%) were added to a 50 mL volumetric flask, and filled to the mark with water (HPLC grade).

2. Phenanthroline solution: 0.2% by weight of 1,10-phenanthroline in water (100 mg in 50 mL volumetric flask).

3. Buffer solution: 2.47 g of NaOAc and 0.5 mL of sulfuric acid (96%) were added to a 50 mL volumetric flask, and filled to the mark with water (HPLC grade).

The actinometry measurements were done as follows:

1. 1 mL of the actinometer solution was added to a screw-cap vial and placed om a single HP LED 1.5 cm away from the light source. The solution was irradiated at 460 nm (irradiance 40 mW/cm^2). This procedure was repeated 4 times, quenching the solutions after different time intervals: 10 s, 15 s, 20 s, and 25 s.

2. After irradiation, the actinometer solutions were removed and placed in a 10 mL volumetric flask containing 0.5 mL of 1,10-phenanthroline solution and 2 mL of buffer solution. These flasks were filled to the mark with water (HPLC grade).

3. The UV-Vis spectra of the complexed actinometer samples were recorded for each time interval. The absorbance of the complexed actinometer solution was monitored at 510 nm.

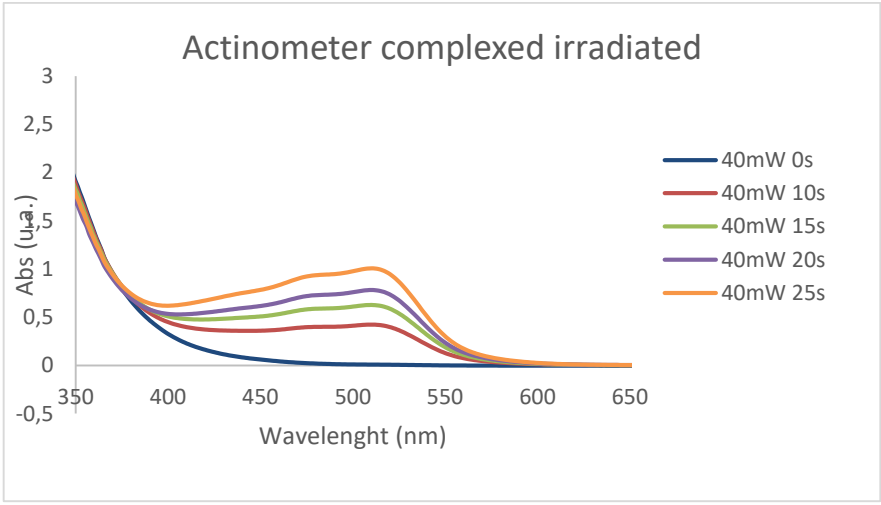

Figure 3.37. Absorbance of the complexed actinometer solutions.

The moles of Fe^{2+} formed for each sample is determined using Beers' Law (Eq. 1):

$$Mols\ of\ Fe(II) = V_1 \times V_3 \times \Delta A(510\ \text{nm})/10^3 \times V_2 \times l \times \varepsilon(510\ nm) \quad \text{(Eq. 1)}$$

where V_1 is the irradiated volume (1 mL), V_2 is the aliquot of the irradiated solution taken for the determination of the ferrous ions (1 mL), V_3 is the final volume after complexation with phenanthroline (10 mL), l is the optical path-length of the irradiation cell (1 cm), ΔA(510 nm) is the optical difference in absorbance between the irradiated solution and the one stored in the dark, ε(510 nm) is the extinction coefficient the complex $Fe(phen)_3^{2+}$ at 510 nm (11100 L mol^{-1} cm^{-1}). The moles of Fe^{2+} formed (x) are plotted as a function of time (t). The slope of this line was correlated to the moles of incident photons by unit of time ($q_{n,}{}^0$) by the use of the following Equation 2:

$$\Phi(\lambda) = dx/dt\ q_{n,p}{}^0\ [1-10^{-A(\lambda)}]\ \text{(Eq. 2)}$$

where dx/dt is the rate of change of a measurable quantity (spectral or any other property), the quantum yield (Φ) for Fe^{2+} at 458 nm is 1.1,[55] $[1\text{-}10^{-A(\lambda)}]$ is the ratio of absorbed photons by the solution, and A(λ) is the absorbance of the actinometer at the wavelength used to carry out the experiments (460 nm). The absorbance at 460 nm A(460) was measured using a Shimadzu 2401PC UV-Vis spectrophotometer in a 1 cm path quartz cuvette, obtaining an absorbance of 0.158.

$q_{n,}{}^0$, which is the photon flux, was determined to be $1.048\text{x}10^{-7}$ einstein s^{-1}.

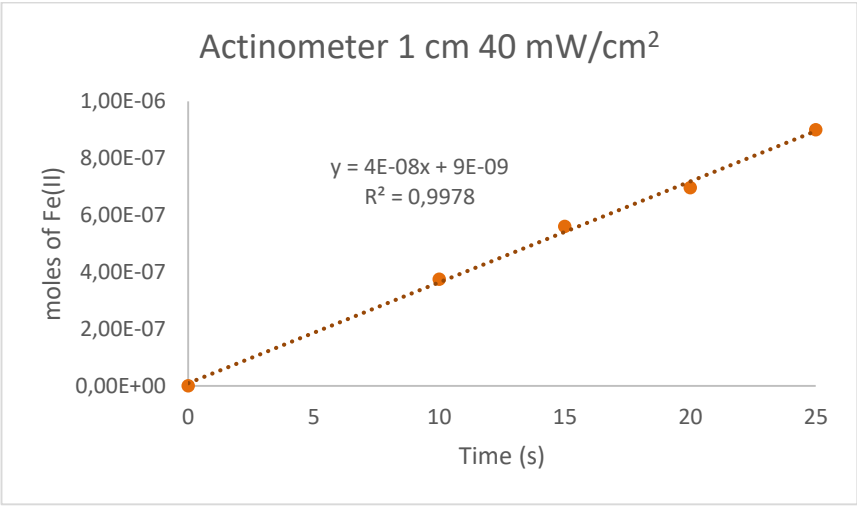

Figure 3.38. Determination of photon flux by linear representation of mols of Fe(II) with respect to irradiation time.

[55] Holubov, C. A.; Langford, C. H. Wavelength and Temperature Dependence in the Photolysis of the Chemical Actinometer, Potassium trisoxalatoferrate(III), at Longer Wavelengths. *Inorganica Chim. Acta* **1981**, *53*, 59-60.

Consequently, the model reactions were performed.

The reactions were prepared on a screw-cap vial with stir bar. Cyclohexanecarbonyl chloride (50 µL, 0.375 mmol, 1.5 equiv.), γ-terpinene (120 µL, 0.75 mmol, 3 equiv.), and lutidine (58 µL, 0.5 mmol, 2 equiv.), were added to a solution of catalyst **B** (4 mg, 0.1 equiv.) in acetonitrile (1 mL). After degassing by bubbling Argon for 30 s, acrylonitrile **31a** (16 µL, 0.25 mmol) was added and the tube was sealed with parafilm and put in the HP-LED 460 nm at 1 cm distance at ambient temperature (reaction reaches around 35 ºC) with irradiance of 40 mW/cm^2. Four different reactions were setup and irradiated for different times: 60 min, 80 min, 100 min and 120 min.

The moles of product **34a** formed for the model reaction were determined by GC measurement (FID detector) using 1,3,5-trimethoxybenzene as internal standard. The moles of product per unit of time are related to the number of photons absorbed. The photons absorbed are correlated to the number of incident photons by the use of Equation 1. According to this, plotting the moles of product (x) versus the moles of incident photons ($q_{n,}{}^{0}\cdot dt$), the slope is equal to: $\Phi\cdot(1\text{-}10^{-A(\lambda)(460\ nm)})$, where Φ is the quantum yield to be determined and A(460 nm) is the absorption of the reaction under study. A(460 nm) was measured using a Shimadzu 2401PC UV-Vis spectrophotometer in 10 mm path quartz. An absorbance of 0.103 was determined for the model reaction mixture. The quantum yield (Φ) of the photochemical transformation was measured to be 0.0338. The procedure was repeated a second time to provide a similar value: quantum yield (Φ) at 460 nm of 0.0332.

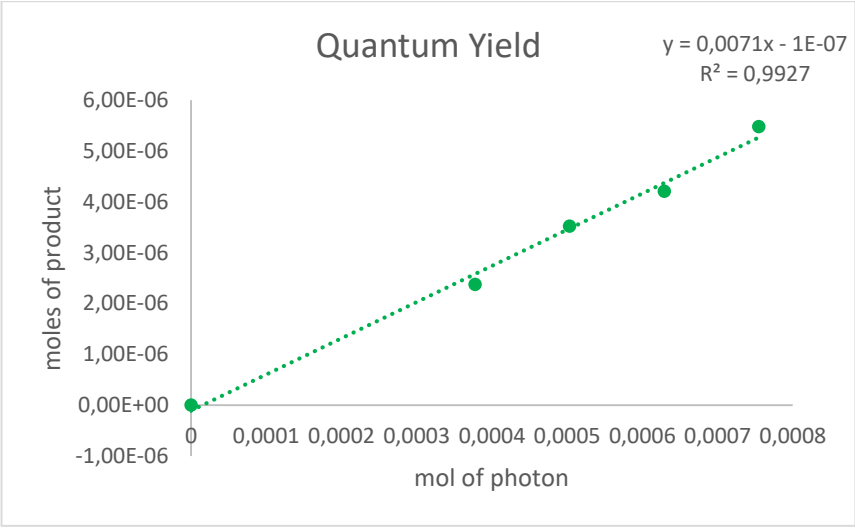

Figure 3.39. Determination of quantum yield by linear representation of mols of product with respect to indicent mol of photons on the reaction.

Chapter IV

A general organocatalytic system for electron donor–acceptor complex photoactivation and its use in radical processes

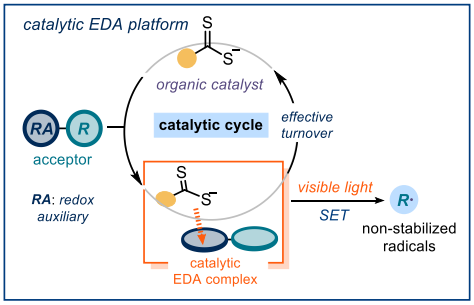

Target

To develop a modular class of organic catalysts that can participate as donors in the formation of photoactive electron donor-acceptor (EDA) complexes with a variety of radical precursors.

Tool

Exploiting the electronic properties of nucleophilic organic dithiocarbamate catalyst developed in the previous studies to demonstrate that they can act as donors in a catalytic EDA manifold. Use the organic catalysts to generate non-stabilized radicals replacing commonly used photoredox catalysts.[1]

4.1 Introduction

Our laboratory recently reported a photochemical catalytic strategy that employs a nucleophilic organic catalyst to generate reactive radicals from simple alkyl(pseudo)halides and trap them in a range of transformations (see Chapters II and III).[2] Our methodology capitalized on the propensity of a given precursor to undergo nucleophilic substitutions (Scheme 4.1a). During the course of our investigation, we undertook a detailed study into the mechanism of the catalytic cycle.[3] Based on this knowledge, we reasoned that, if the

[1] The project discussed in this chapter was conducted in collaboration with Davide Spinnatto and Wei Zhou. I was involved in the discovery and optimization of the reactions and investigated the scope of the conjugated addition and reduction. I also conducted the mechanistic studies. This work has been published: De Pedro Beato, E.; Spinnato. D.; Zhou, W.; Melchiorre, P. A General Organocatalytic System for Electron Donor–Acceptor Complex Photoactivation and Its Use in Radical Processes. *J. Am. Chem. Soc.* **2021**, *143*, 12304–12314.

[2] (a) Schweitzer-Chaput, B.; Horwitz, M. A.; de Pedro Beato, E.; Melchiorre, P. Photochemical generation of radicals from alkyl electrophiles using a nucleophilic organic catalyst. *Nature Chem.* **2019**, *11*, 129–135. (b) Mazzarella, D.; Magagnano, G.; Schweitzer-Chaput, B.; Melchiorre, P. Photochemical Organocatalytic Borylation of Alkyl Chlorides, Bromides, and Sulfonates. *ACS Catal.* **2019**, *9*, 5876–5880. (c) Cuadros, S.; Horwitz, M. A.; Schweitzer-Chaput, B.; Melchiorre, P., A visible-light mediated three-component radical process using dithiocarbamate anion catalysis. *Chem. Sci.* **2019**, *10*, 5484-5488. (d) Spinnato D.; Schweitzer-Chaput B.; Goti G.; M. Ošeka; Melchiorre P., A Photochemical Organocatalytic Strategy for the α-Alkylation of Ketones by using Radicals. *Angew. Chem. Int. Ed.* **2020**, *59*, 9485-9490.

[3] de Pedro Beato, E.; Mazzarella, D.; Balletti, M.; Melchiorre, P., Photochemical generation of acyl and carbamoyl radicals using a nucleophilic organic catalyst: applications and mechanism thereof. *Chem. Sci.* **2020**, *11*, 6312-6324.

dithiocarbamate anion catalyst can undergo nucleophilic substitution, it may also be electron-rich enough to serve as a donor and elicit EDA complex formation with a suitable acceptor partner. In addition, knowing that the sulfur-centered radical, which would arise from a single-electron transfer (SET) event, can be readily converted back to the anion through SET or hydrogen atom transfer (HAT), we could achieve effective catalyst turnover and design an effective EDA complex catalytic system (Scheme 4.1b).

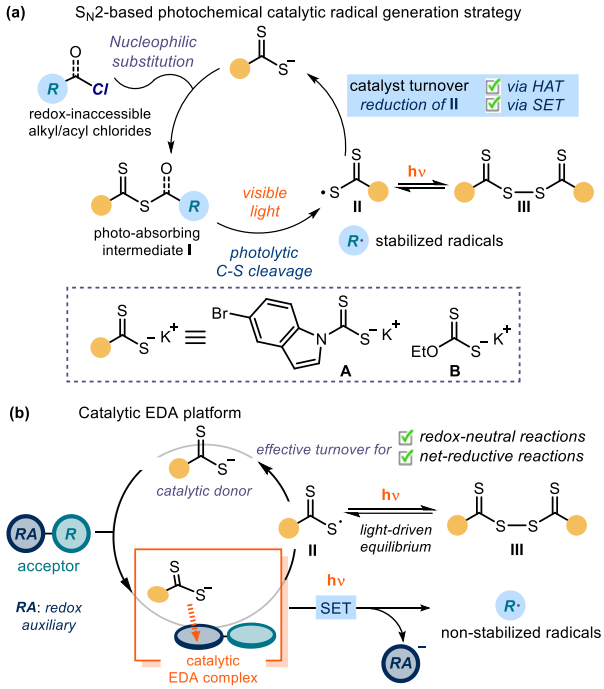

Scheme 4.1. (a) Nucleophilic substitution-based radical generation strategies. (b) Design of a catalytic EDA complex platform.

Over the past decade, numerous advances have been made in the generation of radicals, particularly applying photoredox and electrochemical processes to generate radicals under mild conditions.[4,5] Thanks to these effective methodologies, radical chemistry has become a synthetically established alternative to ionic processes for the production of organic

[4] (a) Shaw, M. H.; Twilton, J.; MacMillan, D. W. C. Photoredox Catalysis in Organic Chemistry. *J. Org. Chem.* **2016**, *81*, 6898–6926. (b) Romero, N.; Nicewicz, D. Organic Photoredox Catalysis. *Chem. Rev.* **2016**, *116*, 10075–10166. (c) Matsui, J. K.; Lang, S. B.; Heitz, D. R.; Molander, G. A. Photoredox-mediated routes to radicals: the value of catalytic radical generation in synthetic methods development, *ACS Catal.* **2017**, *7*, 2563−2575.

[5] Kingston, C.; Palkowitz, M. D.; Takahira, Y.; Vantourout, J. C.; Peters, B. K.; Kawamata, Y.; Baran, P. S. A Survival Guide for the "Electro-curious". *Acc. Chem. Res.* **2020**, 53, 72–83.

compounds.[6] Nevertheless, most current methods generally rely on the employment of either expensive set-ups or low abundant transition metal-based photocatalysts. To address these limitations, several organic photocatalysts have been developed to replace those containing rare metal cores (such as Ir and Ru).[7] Another useful alternative to the use of classical photocatalysts is based on the formation of photoactive EDA complexes. EDA complexes are formed by the association of two (or more) molecules, which generates a set of new molecular orbitals. This is due to re-hybridization of the frontier orbitals of the two associating partners (HOMO for the donor and LUMO for the acceptor).[8] Although the two components, the acceptor (**A**) and the donor (**D**), may not absorb visible light themselves, the resulting EDA complex generally does (Scheme 4.2). In some cases, irradiation of the ground-state EDA complex results in an SET from the electron-rich (donor) to the electron-poor (acceptor) molecule of the complex. This SET delivers a radical pair, which can generate reactive radicals suitable for chemical processes.[9]

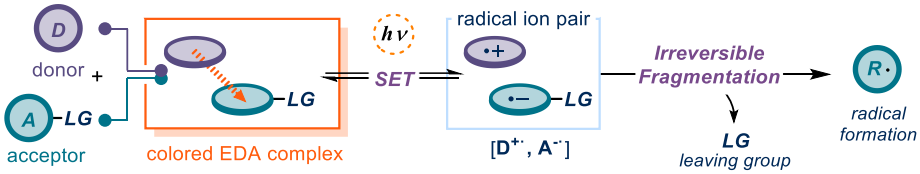

Scheme 4.2. Generation of radicals through EDA complex excitation.

Compared to photocatalyst-based processes, the EDA approach offers the possibility of engaging two reactants without the need of an external catalyst to mediate the transfer of a single electron. However, some aspects lower the generality and versatility of this radical generation strategy. For example, the most straightforward synthetic application of the EDA complex platform is based on the light-driven coupling of two stoichiometric donor and acceptor substrates. The moieties of the substrates (**A** and **D**) will eventually end up in the core of the products, thus restricting their structural diversity. Implementing the EDA complex

---

[6] (a) Blakemore, D. C.; Castro, L.; Churcher, I.; Rees, D. C.; Thomas, A. W.; Wilson, D. M.; Wood, A. Organic synthesis provides opportunities to transform drug discovery. *Nature Chem.* **2018**, *10*, 383–394. (b) Douglas, J. J.; Sevrin, M. J.; Stephenson, C. R. J., Visible Light Photocatalysis: Applications and New Disconnections in the Synthesis of Pharmaceutical Agents. *Organic Process Research & Development* **2016**, *20*, 1134-1147. (c) Sambiagio, C.; Noël, T., Flow Photochemistry: Shine Some Light on Those Tubes! *Trends in Chemistry* **2020**, *2*, 92-106.

[7] Lee, Y.; Kwon, M. S., Emerging Organic Photoredox Catalysts for Organic Transformations. *Eur. J. Org. Chem.* **2020**, *2020*, 6028-6043.

[8] Lima, C. G. S.; de M. Lima, T.; Duarte, M.; Jurberg, I. D.; Paixão, M. W., Organic Synthesis Enabled by Light-Irradiation of EDA Complexes: Theoretical Background and Synthetic Applications. *ACS Catalysis* **2016**, *6*, 1389-1407.

[9] Crisenza, G. E. M.; Mazzarella, D.; Melchiorre, P., Synthetic Methods Driven by the Photoactivity of Electron Donor–Acceptor Complexes. *J. Am. Chem. Soc.* **2020**, *142*, 5461-5476.

activation strategy within a catalytic regime would therefore significantly expand its efficiency and synthetic applicability.[10,11]

In this chapter, the design, development, synthetic implementation and mechanistic study of an EDA complex catalytic strategy, based on the use of readily available dithiocarbamate anion catalysts, is described. In the following section, I will discuss relevant methods based on the photoexcitation of EDA complexes, which served to develop new synthetically useful reactions. I will also discuss the few examples of catalytic EDA complexes reported so far.

4.2 Electron donor-acceptor complexes

Electron Donor-Acceptor (EDA) complexes have been known since last century. In 1949, Benesi and Hildebrand reported the first study of an electron-donor acceptor complex formed between iodine and aromatic hydrocarbons.[12] They concluded that the observed color change was due to a ground-state association. This association is possible due to the donor (Lewis basic) character of the correspondent aromatic molecule and the acceptor (Lewis acidic) character of iodine. Furthermore, they characterized this complex as having a stoichiometry of 1:1. Later, Mulliken,[13] among others,[14] proposed a quantum mechanical theory to

[10] (a) Fu, M.-C.; Shang, R.; Zhao, B.; Wang, B.; Fu, Y, Photocatalytic decarboxylative alkylations mediated by triphenylphosphine and sodium iodide. *Science* **2019**, *363*, 1429–1434. (b) Wang, Y.-T.; Fu, M.-C.; Zhao, B.; Shang, R.; Fu, Y. Photocatalytic decarboxylative alkenylation of α-amino and α-hydroxy acid-derived redox active esters by NaI/PPh3 catalysis. *Chem. Commun.* **2020**, *56*, 2495−2498. (c) Fu, M.-C.; Wang, J. X.; Shang, R. Triphenylphosphine-Catalyzed Alkylative Iododecarboxylation with Lithium Iodide under Visible Light. *Org. Lett.* **2020**, *22*, 8572−8577. (d) Bosque, I.; Bach, T. 3-Acetoxyquinuclidine as Catalyst in Electron Donor-Acceptor Complex-Mediated Reactions Triggered by Visible Light. *ACS Catal.* **2019**, *9*, 9103–9109. (e) McClain, E. J.; Monos, T. M.; Mori, M.; Beatty, J. W.; Stephenson, C. R. J. Design and Implementation of a Catalytic Electron Donor–Acceptor Complex Platform for Radical Trifluoromethylation and Alkylation. *ACS Catalysis* **2020,** *10*, 12636–12641.

[11] (a) Quint, V.; Morlet-Savary, F.; Lohier, J.-F.; Lalevée, J.; Gaumont, A.-C.; Lakhdar, S., Metal-Free, Visible Light-Photocatalyzed Synthesis of Benzo[b]phosphole Oxides: Synthetic and Mechanistic Investigations. *J. Am. Chem. Soc.* **2016**, *138*, 7436-7441. (b) Emmanuel, M. A.; Greenberg, N. R.; Oblinsky, D. G.; Hyster, T. K., Accessing non-natural reactivity by irradiating nicotinamide-dependent enzymes with light. *Nature* **2016**, *540*, 414-417. (c) Biegasiewicz, K. F.; Cooper, S. J.; Gao, X.; Oblinsky, D. G.; Kim, J. H.; Garfinkle, S. E.; Joyce, L. A.; Sandoval, B. A.; Scholes, G. D.; Hyster, T. K., Photoexcitation of flavoenzymes enables a stereoselective radical cyclization. *Science* **2019**, *364*, 1166-1169. (d) Clayman, P. D.; Hyster, T. K., Photoenzymatic Generation of Unstabilized Alkyl Radicals: An Asymmetric Reductive Cyclization. *J. Am. Chem. Soc.* **2020**, *142*, 15673-15677. (e) Page, C. G.; Cooper, S. J.; DeHovitz, J. S.; Oblinsky, D. G.; Biegasiewicz, K. F.; Antropow, A. H.; Armbrust, K. W.; Ellis, J. M.; Hamann, L. G.; Horn, E. J.; Oberg, K. M.; Scholes, G. D.; Hyster, T. K., Quaternary Charge-Transfer Complex Enables Photoenzymatic Intermolecular Hydroalkylation of Olefins. *J. Am. Chem. Soc.* **2021**, *143*, 97-102.

[12] Benesi, H. A.; Hildebrand, J. H., A Spectrophotometric Investigation of the Interaction of Iodine with Aromatic Hydrocarbons. *J. Am. Chem. Soc.* **1949**, 71, 2703-2707.

[13] (a) Mulliken, R. S., Structures of Complexes Formed by Halogen Molecules with Aromatic and with Oxygenated Solvents1. *J. Am. Chem. Soc.* **1950**, *72*, 600-608. (b) Mulliken, R. S. Molecular Compounds and their Spectra. II. *J. Am. Chem. Soc.* **1952**, *74,* 811–824. (c) Mulliken, R. S. Molecular Compounds and their Spectra. III. The Interaction of Electron Donors and Acceptors. *J. Phys. Chem.* **1952**, *56*, 801–822

[14] (a) Lewis, G. N. Acids and Bases. *J. Franklin Inst.* **1938**, *226*, 293–313. (b) Winstein, S.; Lucas, H. J. The Coordination of Silver Ion with Unsaturated Compounds. *J. Am. Chem. Soc.* **1938**, *60*, 836–847. (c) Dewar, M. J. S. Mechanism of the Benzidine and Related Rearrangementes. *Nature* **1945**, *156*, 784.

rationalize the formation of these complexes. According to this theory, the association of a donor **D** (electron-rich substrate with low ionization potential) and an acceptor **A** (electron-poor molecule with high electron affinity) can form a new complex in the ground state (the EDA complex, Scheme 4.3). In this complex, new molecular orbitals are formed, emerging from the frontier orbitals of **D** and **A** (HOMO/LUMO, respectively), which confer different physical properties to the EDA complex with respect to the separated substrates. This new entity is characterized by a new charge-transfer band in the absorption spectrum ($h\nu_{CT}$), associated with an $\Psi_{GS} \rightarrow \Psi_{ES}$ electronic transition (Ψ = wave-function, associated with ground and excited states). Upon excitation of the EDA complex (orange box in **Scheme 4.3**), the Ψ_{ES} is populated, which translates in an intracomplex SET from **D** to **A** to generate a radical ion pair characterized by a net charge separation (light blue box).

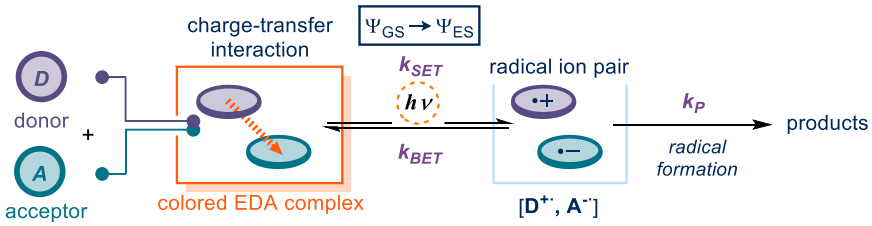

Scheme 4.3. EDA complex formation and intra-complex SET.

4.2.1 Synthetic applications of EDA complexes

Although EDA complexes have been known since the 1940s, it was not until recently that their use in synthetic organic chemistry has become more frequent.[9] This is likely due to the challenges arising from the intrinsic properties of EDA complexes.[15] In particular, the difficulties involving unproductive back-electron transfer (BET) from the radical ion pair, which restores the ground-state EDA complex (Scheme 4.3). When the kinetics of other processes leading to reactive radicals and eventually to the products are not competitive with the kinetics of the BET, the photoactivation of the EDA complex is synthetically unproductive. To overcome this limitation, one strategy relies on the introduction of a suitable leaving group (LG) within the radical anion partner ([$\mathbf{D}^{+\cdot}$, $\mathbf{A}^{-\cdot}$] in Scheme 4.4), which can trigger an irreversible fragmentation event rapid enough to compete with the BET. This can productively render reactive radical intermediates ***R*·**, which can initiate synthetically useful transformations (Scheme 4.4).

[15] Rathore, R.; Kochi, J. K. Donor/Acceptor Organizations and the Electron-Transfer Paradigm for Organic Reactivity. *Adv. Phys. Org. Chem.* **2000**, *35*, 193−318.

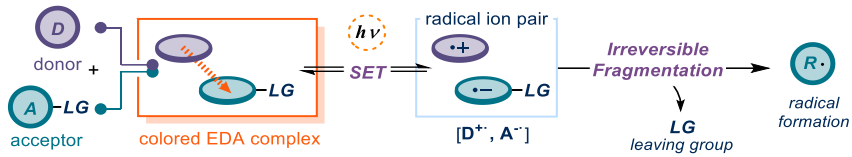

Scheme 4.4. Generation of radicals through EDA complex light excitation.

In an early example, Bunnett extensively studied the application of EDA complexes for radical-nucleophilic aromatic substitution ($S_{RN}1$) reactions (**Scheme 4.5**). This process consists in the addition of an aryl radical (**VII**) to a nucleophile (**3**) to form a new C-C bond. The resulting radical anion (**VIII**) is then oxidized to product **4**. Using this approach,[16] Bennett developed the α-alkylation of acetone **1** with aryl halides **2**, promoted by the association of both substrates (where **3** behaves as the donor). Upon deprotonation, enolate **3** can engage in an EDA complex with aryl halide **2** (Scheme 4.5). The colored EDA complex (Scheme 4.5, orange box) can absorb light to promote an SET between the partners. This SET is reversible and a BET between the radical pair (Scheme 4.5, blue box) can be operative; nevertheless, the irreversible and rapid fragmentation can outcompete the BET, delivering the aryl radical **VII**. Once the open-shell species **VII** can be intercepted by another molecule of enolate **3**, which is present in significantly higher concentration than the oxygen radical **V**, forming the C-C bond and the more stabilized ketyl radical **VIII**. In the last step, **VIII** is reduced by the aryl halide to form the α-alkylation product **4** and propagate the chain process by generating another molecule of aryl radical **VII**. In this process, the EDA complex-promoted SET only act as an initiation for the chain-propagated reaction.[17]

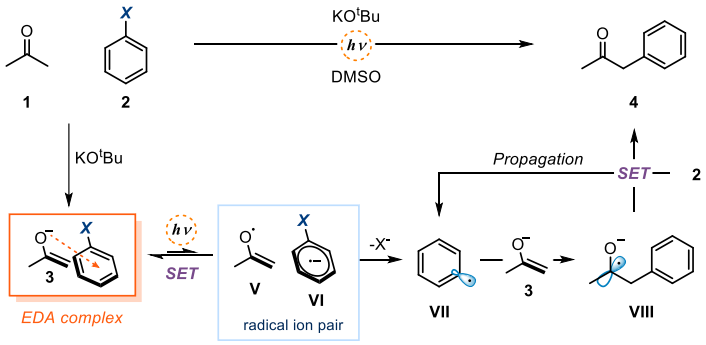

Scheme 4.5. $S_{RN}1$ reaction promoted by light excitation of an EDA complex.

[16] Bunnett, J. F.; Sundberg, J. E., Photostimulated arylation of ketone enolate ions by the SRN1 mechanism. *J. Org. Chem.* **1976**, *41*, 1702-1706.
[17] Radical transformations of type $S_{RN}1$ are inherently characterized by chain mechanisms: after initiation, the chain propagates by itself.

In the following years, only few synthetic methodologies based on the excitation of EDA complexes were reported.[18] It was only in 2013 that a renaissance of EDA complex photochemistry took place. One of the first modern examples was reported by Chatani and coworkers,[19] and consisted on the radical arylation of pyrrole derivatives **5** by aryl iodonium salts **6** (Scheme 4.6). The authors noticed the formation of a yellow-orange complex upon mixing both substrates, which was considered as an indication of a possible EDA aggregation: This was eventually corroborated by spectroscopic studies. Irradiation of the colored EDA complex, followed by irreversible extrusion of aryl iodide, generated the radical intermediates **IX** and **X**, which upon reaction with pyrrole derivative **5**, furnished the C2-arylated product **7**.

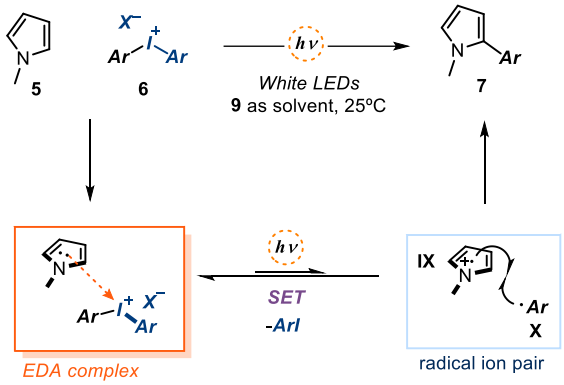

Scheme 4.6. Arylation of pyrrole derivatives promoted by a visible-light absorbing EDA complex.

Up until this point, all methodologies involving EDA complexes relied on the association of two stoichiometric substrates.

---

[18] (a) Cantacuzene, D.; Wakselman, C.; Dorme, R. Condensation of Perfluoroalkyl Iodides with Unsaturated Nitrogen Compounds. *J. Chem. Soc., Perkin Trans. 1* **1977**, 1365−1371. (b) Russell, G. A.; Wang, K. Homolytic Alkylation of Enamines by Electrophilic Radicals. *J. Org. Chem.* **1991**, 56, 3475−3479. (c) Wade, P. A.; Morrison, H. A.; Kornblum, N. The Effect of Light on Electron-Transfer Substitution at a Saturated Carbon Atom. *J. Org. Chem.* **1987**, *52*, 3102−3107. (d) Sankararaman, S.; Haney, W. A.; Kochi, J. K. Annihilation of Aromatic Cation Radicals by Ion-Pair and Radical-Pair Collapse. Unusual Solvent and Salt Effects in the Competition for Aromatic Substitution. *J. Am. Chem. Soc.* **1987**, *109*, 7824−7838. (e) Fukuzumi, S.; Mochida, K.; Kochi, J. K. A Unified Mechanism for Thermal and Photochemical Activation of Charge-Transfer Processes with Organometals. Steric Effects in the Insertion of Tetracyanoethylene. *J. Am. Chem. Soc.* **1979**, *101*, 5961−5972. (f) Gotoh, T.; Padias, A. B.; Hall, J. H. K. An Electron DonorAcceptor Complex and Thermal Triplex as Intermediates in the Cycloaddition Reaction of N-Vinylcarbazole with Dimethyl 2,2-Dicyanoethylene-1,1-dicarboxylate. *J. Am. Chem. Soc.* **1991**, *113*, 1308−1312. (g) Fox, M. A.; Younathan, J.; Fryxell, G. E. Photoinitiation of the SRN1 Reaction by Excitation of Charge-Transfer Complexes. *J. Org. Chem.* **1983**, *48*, 3109−3112.

[19] Tobisu, M.; Furukawa, T.; Chatani, N. Visible Light-mediated Direct Arylation of Arenes and Heteroarenes Using Diaryliodonium Salts in the Presence and Absence of a Photocatalyst. *Chem. Lett.* **2013**, *42*, 1203−1205.

4.2.2 EDA complex with substoichiometric amount of donor

In 2013, our group investigated the enantioselective α-alkylation of aldehydes **8** with electron-deficient alkyl bromides **9** as electrophiles (Scheme 4.7).[20] Previous studies had proven this transformation feasible employing a photocatalyst as the mean to generate the corresponding radicals from substrates **9**.[21] However, during a control experiment, we noticed that for specific halides **9** no photocatalyst was required to promote the stereoselective transformation. Importantly, no product **11** was observed in the absence of light. Mechanistic studies revealed the ability of the enamine intermediate **X**, formed upon condensation of aldehyde **8** and the chiral aminocatalyst **10**, to associate with electron-deficient bromides **9** to form a colored EDA complex in the ground state. Visible-light irradiation promoted an intracomplex SET, delivering a radical ion pair (**XI** and **XII** in Scheme 4.7, light blue box). The irreversible fragmentation of **XII** to afford the benzyl radical **XIII** avoided an unproductive BET. Further mechanistic studies, including quantum yield measurements, established that the reaction proceeded through a self-propagating radical chain mechanism.[22] This implies that the photochemistry of the EDA complex only acted as an initiator to start a radical chain process. The propagation step relies on the ability of α-amino radical **XIV**, which is formed after addition of benzyl radical **XIII** to the ground-state enamine **X**, to reduce a molecule of radical precursor **9** via SET. This last step yields the enantio-enriched product **11**. This study demonstrated the ability of catalytically formed intermediates, such as enamines **X**, to engage in EDA complex formation and promote stereoselective transformations otherwise unavailable via thermal activation, and without the need of any external photocatalyst.[23]

---

[20] Arceo, E.; Jurberg, I. D.; Álvarez-Fernandez, A.; Melchiorre, P. Photochemical activity of a key donor-acceptor complex can drive stereoselective catalytic α-alkylation of aldehydes. *Nature Chem.* **2013**, *5*, 750−756.

[21] Nicewicz, D. A.; MacMillan, D. W. C. Merging Photoredox Catalysis with Organocatalysis: The Direct Asymmetric Alkylation of Aldehydes. *Science* **2008**, *322*, 77–80.

[22] Bahamonde, A.; Melchiorre, P. Mechanism of the Stereoselective α-Alkylation of Aldehydes Driven by the Photochemical Activity of Enamines. *J. Am. Chem. Soc.* **2016**, *138*, 8019–8030.

[23] Silvi, M.; Melchiorre, P. Enhancing the potential of enantioselective organocatalysis with light. *Nature* **2018**, *554*, 41–49.

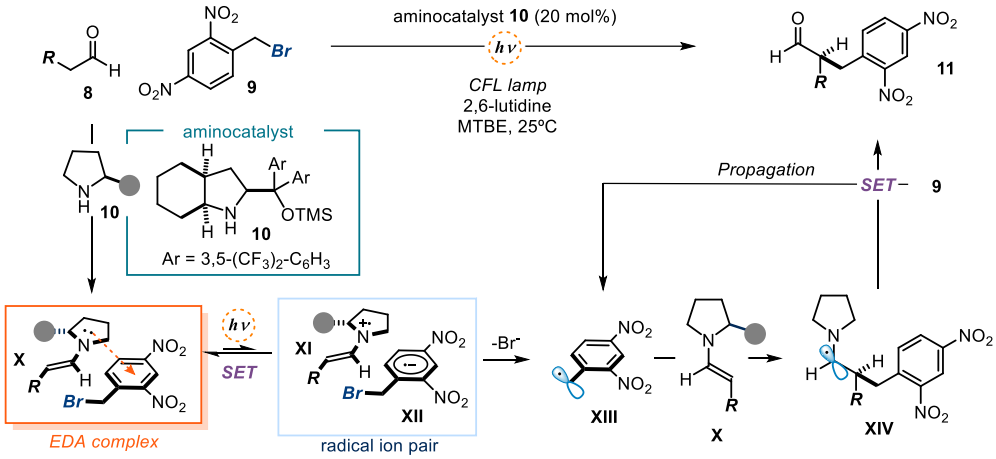

Scheme 4.7. Enantioselective alkylation of aldehydes promoted by a visible-light absorbing enamine-based EDA complex.

This report constituted the first example of an EDA complex where one of the partners was present in catalytic amounts. This approach was then applied to other enantioselective organocatalytic transformations where a chiral intermediate acted as a donor, including in the realm of phase transfer catalysis.[24]

4.2.2 EDA complex with substoichiometric amount of acceptor

In 2019, Gilmour and co-workers reported the first synthetically productive EDA complex formation involving a catalytic amount of an acceptor.[25] Upon condensation of the racemic aminocatalyst **14** with cinnamaldehyde **12**, the catalytic iminium ion intermediate **XV** was formed (Scheme 4.8). The electron-deficient nature of iminium ion **XV** could be exploited as the acceptor moiety for EDA complex formation with a donor substrate (Scheme 4.8). Gilmour used α-ketoacids **9** as the donors. This choice was crucial for several reasons: i) **9** acted as acids, facilitating the condensation of **12** and **14** to form the active iminium ion **XV**; ii) the electron-rich properties of **9** secured the aggregation with **XV** to form an EDA complex (**Scheme 4.8**, orange box), iii) after EDA-promoted SET, radical **XVII** underwent irreversible decarboxylation to deliver the acyl radical **XVIII** that, upon radical coupling, delivered the final product **15**. In contrast to previous examples, this reaction did not rely on the propagation of a radical chain, since the coupling between the stabilized radical **XVI** and the acyl radical **XVIII** was proposed to be the C-C bond forming event. Unfortunately, even though an aminocatalyst **14** bearing a stereogenic center was used as catalyst, a stereoselective version

[24] Woźniak, Ł.; Murphy, J. J.; Melchiorre, P Photo-organocatalytic Enantioselective Perfluoroalkylation of β-Ketoesters. *J. Am. Chem. Soc.* **2015**, *137*, 5678–5681.
[25] Morack, T.; Mück-Lichtenfeld, C.; Gilmour, R. Bioinspired Radical Stetter Reaction: Radical Umpolung.Enabled by Ion-Pair Photocatalysis. *Angew. Chem., Int. Ed.* **2019**, *58*, 1208–1212.

of this reaction could not be developed, highlighting the challenges associated to stereocontrolled radical chemistry.

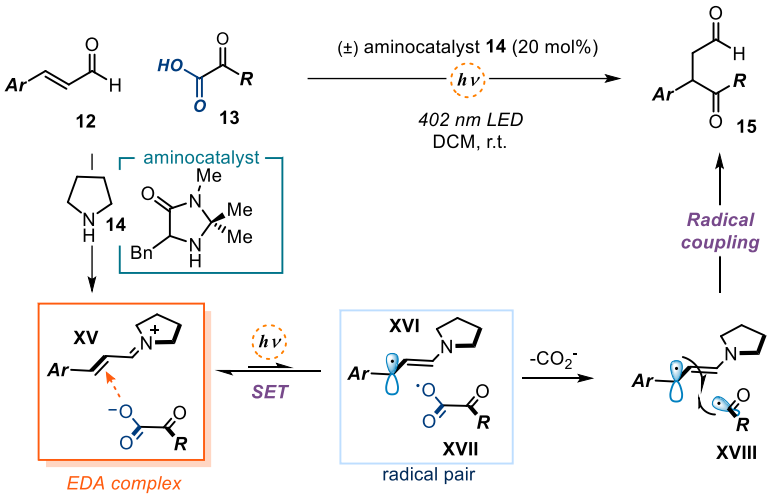

Scheme 4.8. Enantioselective alkylation of aldehydes promoted by a visible-light absorbing EDA complex (Gilmour, 2019).

4.3 EDA complex with redox auxiliaries

The methods highlighted above enabled the coupling of two substrates, which are also involved in the EDA complex formation. Therefore, the diversity of the reaction products is somehow restricted by the need to select highly polarized reagents with donor and acceptor properties, which eventually end up in the product scaffold. One strategy to evade this limitation is to use a reaction partner decorated with a purposely installed activating group, which serves as both redox-auxiliary (RA, blue circle in Scheme 4.9) and leaving group. The substrate's main core does not need to be electronically biased, since the EDA complex formation is facilitated by the electronic properties of the redox-auxiliary/fragmenting group. The radical emerging from the excitation of the EDA complex is therefore electronically unbiased.

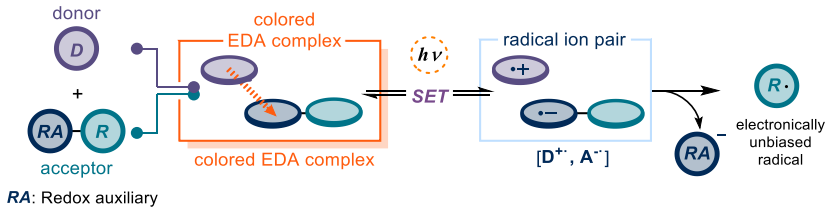

Scheme 4.9. EDA complex activation with redox auxiliaries as radical precursors.

4.3.1 EDA complex between redox auxiliaries and substrates

Recently, several transformations have been developed that take advantage of an EDA association between a substrate and a molecule adorned with a redox auxiliary (**Scheme 4.9**). For example, Aggarwal and coworkers reported photochemical methodologies for the borylation of a wide range of organic molecules (Scheme 4.10).[26] As a general mechanistic proposal, the EDA complex is first formed between the redox auxiliary moiety present in the radical precursor **16** and intermediate **XIX**, arising upon coordination of the solvent and B_2cat_2 **17**. *N*-Hydroxyphthalimide esters **16a** and *N*-alkylpyridium salts **16b** were successfully employed as electron accepting EDA partners. Visible light irradiation promoted the SET and the radical anion **XX** undergoes fast fragmentation to form the target radical **XXII**. The open-shell species **XXII** is then intercepted by another molecule of **XIX** generating the borylated product, which is converted in situ to the correspondent pinacol boronic ester **18**. At the same time, the boron centered radical **XXI** is formed and propagates the radical chain by reducing another molecule of redox-auxiliary-adorned radical precursor **16**.

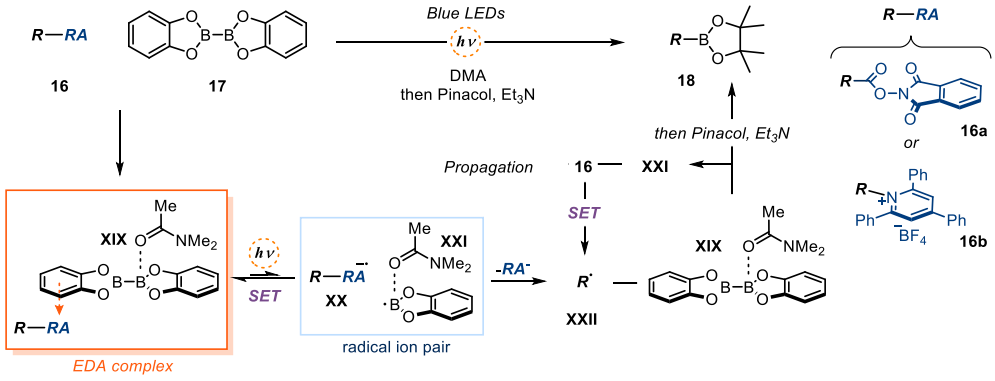

Scheme 4.10. Borylation of alkyl radicals driven by the photochemistry of EDA complexes.

4.3.2 Catalytic EDA complexes

The efficiency and scope of the photochemical processes were considerably improved by adorning substrates with well-tailored activating groups that could participate in EDA interactions and facilitate both the redox processes and radical formation. However, this approach still required the use of stoichiometric substrates for the formation of an EDA

[26] (a) Fawcett, A.; Pradeilles, J.; Wang, Y.; Mutsuga, T.; Myers, E. L.; Aggarwal, V. K. Photoinduced decarboxylative borylation of carboxylic acids. *Science* **2017**, *357*, 283–286. (b) Wu, J.; He, L.; Noble, A.; Aggarwal, V. K. Photoinduced Deaminative Borylation of Alkylamines. *J. Am. Chem. Soc.* **2018**, *140*, 10700–10704. (c) Wu, J.; Bär, R. M.; Guo, L.; Noble, A.; Aggarwal V. K. Photoinduced Deoxygenative Borylations of Aliphatic Alcohols. *Angew. Chem. Int. Ed.* **2019**, *58*, 18830–18834.

complex. An important advance in the field was to implement the EDA complex activation strategy within a catalytic regime.[10] Our group demonstrated that some chiral organocatalytic intermediates, including enamines,[27] iminium ions,[28] and enolates,[24] could serve as catalytic donors in EDA complex formation to trigger photochemical radical formation while stereoselectively trapping the ensuing open-shell intermediates. However, mechanistic studies revealed that a self-propagating radical chain was operative in the system. Therefore, the photoactive EDA complex was only involved in the initiation step, implying that the catalyst involved in the SET could not be regenerated, and a sacrificial amount of the donor was required to start the process. The most challenging yet essential step in the design of a catalytic protocol would be the effective turnover of the catalyst, which requires SET reduction of the catalyst radical cation, arising from the photoactivity of the progenitor EDA complex (Scheme 4.11).

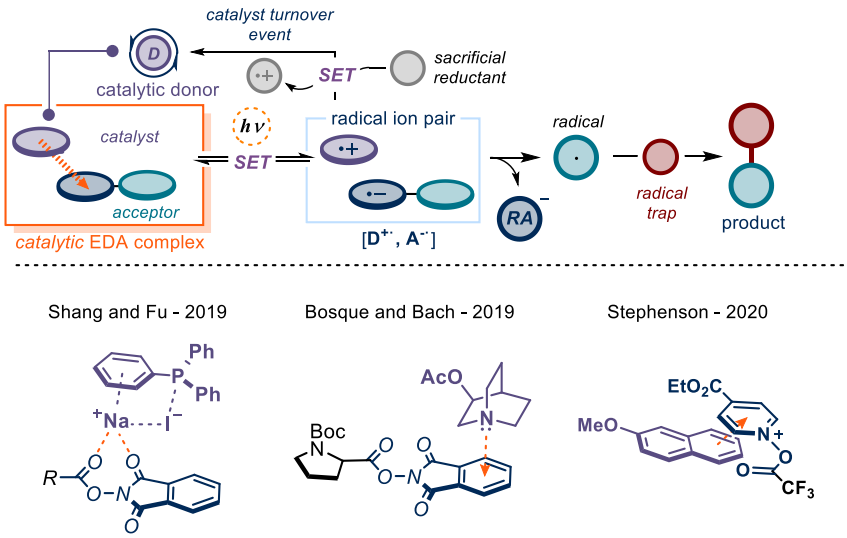

Scheme 4.11. Examples of catalytic EDA complex strategies.

The first report of a light-driven catalytic EDA complex, in which the donor underwent a turnover event to regain its catalytically active form, was reported in 2019 by Shang and Fu.[10a] They described how the combination of sodium iodide (NaI) and triphenyl phosphine (PPh_3) could associate with phthalimide esters **19** to form a colored EDA complex (Scheme 4.12). Irradiation with blue light triggered the formation of the alkyl radical **XXV**, which could be

[27] Arceo, E.; Bahamonde, A; Bergonzini, G.; Melchiorre, P. Enantioselective direct α-alkylation of cyclic ketones by means of photo-organocatalysis. *Chem. Sci.* **2014**, *5*, 2438–2442.
[28] Cao, Z.-Y.; Ghosh, T.; Melchiorre, P. Enantioselective radical conjugate additions driven by a photoactive intramolecular iminium-ion-based EDA complex. *Nat. Commun.* **2018**, *9*, 3274.

efficiently trapped by different substrates. As a model reaction, the α-alkylation of silyl enol ethers was explored (Scheme 4.12). The first step of the reaction is the formation of te EDA complex between ester **19**, PPh_3 and NaI (Scheme 4.12, orange box). This three-component EDA absorbs visible-light and, under irradiation, an intracomplex SET led to the radical ion pair (**Scheme 4.12**, light blue box) composed by the radical anion **XXIII** and the radical **XXIV**. Triphenylphosphine is crucial for the transformation since it stabilized the iodine-centered radical **XXIV**, which was proposed to be persistent, until it can be turnover to the anion via SET. Fragmentation of the radical anion **XXIII** led to the alkyl radical **XXIV**, which was intercepted by silyl enol ether **20** to generate intermediate **XXVI**. Finally, the α-oxoradical **XXVI** reduced the iodine-centered radical **XXIII** to return the catalytically active NaI. Interestingly, this system did not work only with phthalimide esters **19**, but a variety of radical precursors bearing electron-deficient moieties (including pyridinium salts and hypervalent iodine reagents) were also effective EDA acceptors. The same NaI/PPh_3 catalytic system was then used to promote other photo-induced transformations, including a sterocontrolled version of the Minisci reaction, previously reported by Phipps and coworkers with a photoredox catalyst.[29] While demonstrating broad and fairly general applicability, the methodology was only used for redox-neutral transformations since the turnover event relied solely on the SET of the radical intermediate resulting from the trap of radical **XXVI**.

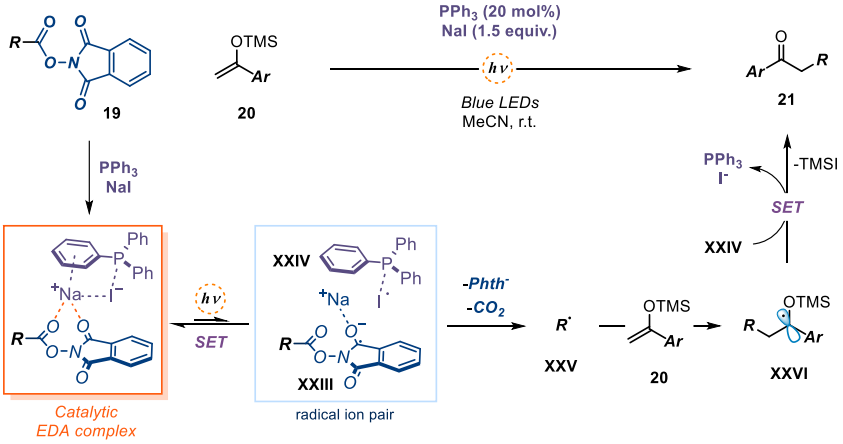

Scheme 4.12. Decarboxylative alkylation of enol ethers catalyzed by PPh_3 and NaI.

The next study to expand the concept of catalytic electron donors in EDA complex activation was reported by Bosque and Bach.[10d] They designed a system where 3-acetoxyquinuclidine **23** could be used in a catalytic regime (Scheme 4.13). Combination with electron-poor

[29] Proctor, R. S. J.; Davis, H. J.; Phipps, R. J., Catalytic enantioselective Minisci-type addition to heteroarenes. *Science* **2018**, *360*, 419-422.

tetrachlorophthalimide ester **22** afforded a photoactive colored EDA complex. Irradiation of the complex triggered an SET from catalyst **23** to the tetrachlorophthalimide moiety, delivering the radical anion **XXVII**. Subsequent fragmentation of anion **XXVIII** followed by decarboxylation provided the α-amino radical **XXIX**. The latter intermediate is then oxidized by the catalyst radical cation **XXVII**: this step turned the catalyst **23** over and afforded the iminium ion **XXX**, which was trapped by the previously liberated tetrachlorophthalimide anion **24** to afford the final product **25**. The low quantum yield value ($\Phi = 0.02$) supported a closed catalytic cycle. Overall, catalyst **23** triggered a redox-neutral pathway, since it acted first as a donor for an intracomplex SET within the EDA complex, and then could get back the electron from intermediate **XXIX**. A crucial aspect for catalysis is the rigid, geometrically-constrained structure of the catalyst's quinuclidine core, which prevented a possible degradation path proceeding through α-deprotonation of the radical cation **XXVIII**.

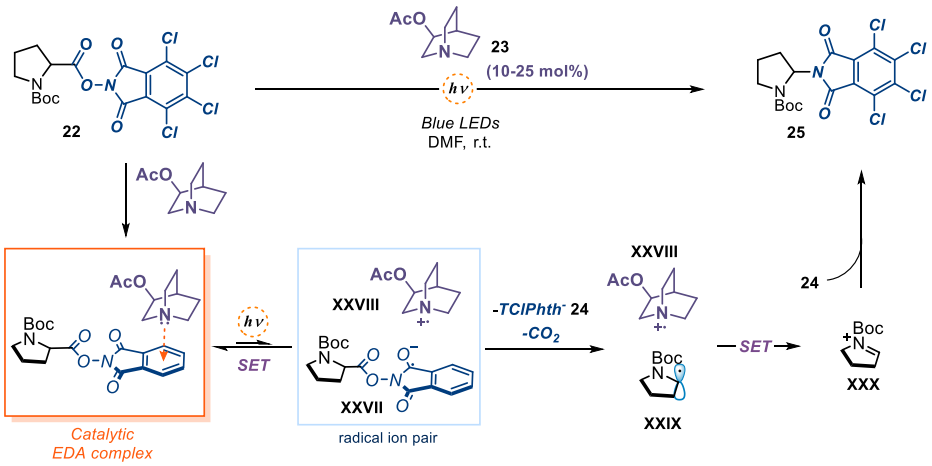

Scheme 4.13. Decarboxylative amination promoted by a catalytic EDA complex.

The latest example of a catalytic EDA system was reported by Stephenson and coworkers.[10e] Previously, the group described the trifluoromethylation of arenes in the presence of a photocatalyst,[30] using pyridinium **XXXI** as radical precursor. Pyridinium salt **XXXI** is readily formed in situ from the reaction between trifluoroacetic acid (TFAA) and *N*-oxide **26** (Scheme 4.14). A control experiment in the absence of the photocatalyst showed formation of product with some of the substrates tested, which was rationalized on the basis of an EDA complex formation between intermediate **XXXI** and the electron-rich (hetero)arene. Based on this observation, Stephenson's group explored replacing the external photocatalyst with a non-

[30] Beatty, J. W.; Douglas, J. J.; Cole, K. P.; Stephenson, C. R. J., A scalable and operationally simple radical trifluoromethylation. *Nat. Comm.* **2015**, *6*, 7919.

photoactive electron-rich organic molecule that could act as a catalytic donor for EDA complex formation.[10e] In the proposed mechanism, the pyridinium intermediate **XXXI** aggregates with a catalytic amount of donor **28** to form the colored EDA complex (Scheme 4.14, orange box), which upon irradiation triggers an intra-complex SET. The resulting radical **XXXII** fragments, breaking the labile N-O bond to release the trifluoromethyl radical **XXXIV** and pyridine **29** as byproduct. Heteroarene **27** traps the ensuing radical **XXXIV**, forging the new C-C bond and leading to adduct **XXXV**. Now the radical cation of catalyst **XXXIII** can oxidize intermediate **XXXV** that, after deprotonation, provides product **30** and regenerates catalyst **28**.

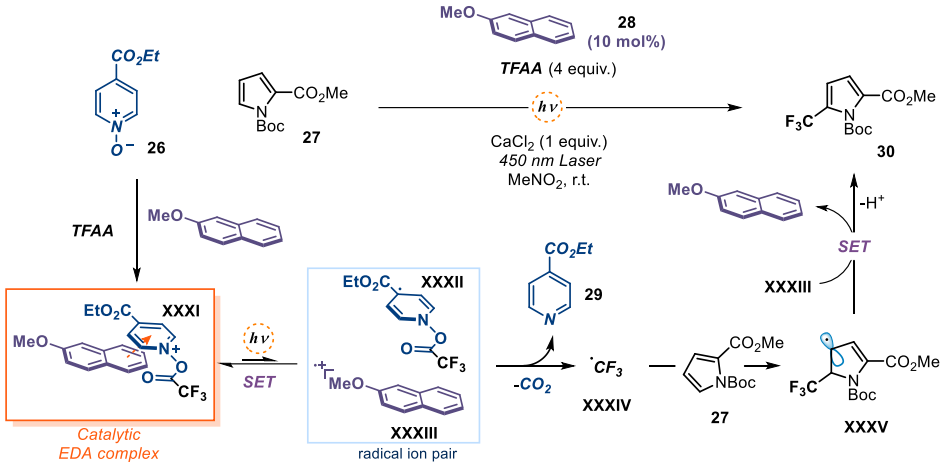

Scheme 4.14. Catalytic EDA-promoted radical trifluoromethylation of heteroarenes.

4.4 Target of the Project

The target of this project was to demonstrate that the dithiocarbamate-based organic catalysts, previously designed for nucleophilic substitution activation, can act as a general and modular class of electron-donor organocatalysts for the formation of photoactive EDA complexes with different radical precursors (Scheme 4.1). Specifically, our target was to employ commercially available dithiocarbamate anion and xanthogenate catalysts **A** and **B** to generate a variety of radicals under blue light irradiation, including non-stabilized primary carbon radicals and nitrogen-centered radicals. The modular nature of these organic catalysts would allow us to tune their properties, including stability towards acidic conditions, thus offering a versatile and robust EDA catalytic strategy. Importantly, we wanted to capitalize upon this flexibility to develop both redox neutral and net-reductive photo-induced radical processes. The latter reactivity could not be achieved with previously reported catalytic EDA strategies. We also wanted to use mechanistic investigations to determine if a closed catalytic cycle was

operational in the developed reactions, thus providing compelling evidence of the catalysts' ability to turn over and iteratively drive every catalytic cycle. Overall, this organocatalytic system could offer a simple general platform to promote a variety of synthetically useful and mechanistically distinct radical processes.

4.4.1 Design plan

In the previous chapters of the thesis, I detailed how the nucleophilic organic catalysts (the dithiocarbamate anion **A**, adorned with an indole chromophoric unit, and potassium ethyl xanthate **B**) could activate alkyl and acyl electrophiles via a nucleophilic substitution pathway (Scheme 4.15a). Visible light excitation of the resulting photon-absorbing intermediates **I** afforded radicals upon homolytic cleavage of the weak C-S bond. A merit of this catalytic platform was that, by relying solely on the electrophilic properties of the precursors, it could grant access to open-shell intermediates from substrates that would be inert to classical radical-generating strategies. Its underlying mechanism, however, also limited the approach, since only substrates amenable to a nucleophilic displacement could be used. In addition, only stabilized radicals (including benzyl, allyl, and radicals bearing either a heteroatom or an electron-withdrawing moiety at the α-position) could be effectively generated and used in a variety of C-C and C-B bond forming processes.[2] Extensive mechanistic studies allowed us to elucidate a crucial aspect of this system, namely the mechanism of catalyst turnover. Specifically, we found that the sulfur radical **II**, which emerges from the photolytic cleavage of intermediate **I**, can dimerize to form **III**. Dimer **III**, which can absorb in the visible region, is in a light-regulated equilibrium with the progenitor sulfur-centered radical **II**. This dimerization manifold, by conferring a longer lifetime to radical **II**,[31] enables an effective catalyst turnover. We demonstrated that the sulfur-centered **II** can be effectively reduced and turned over by an SET event or by a hydrogen atom transfer (HAT) process.[3]

[31] Leifert, D.; Studer, A., The Persistent Radical Effect in Organic Synthesis. *Angew. Chem. Int. Ed.* **2020**, *59*, 74-108.

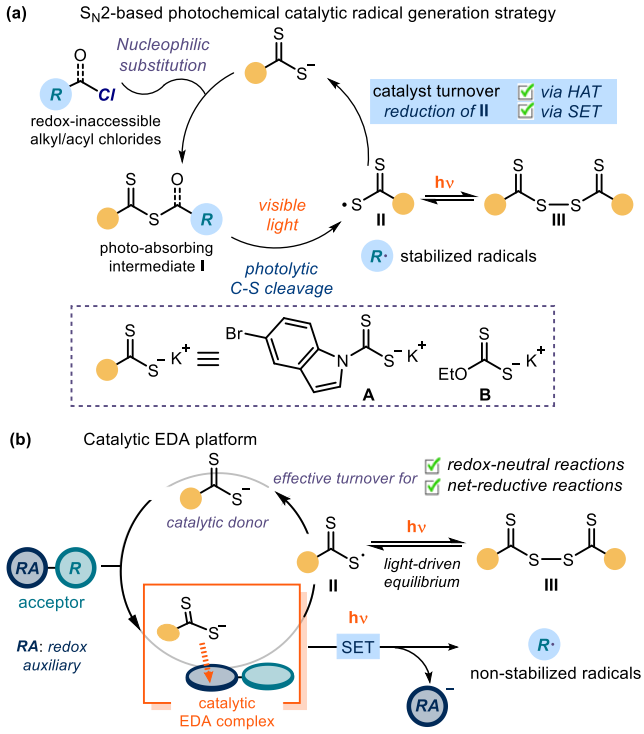

Scheme 4.15. (a) Nucleophilic substitution-based radical generation strategies. (b) Design of a catalytic EDA complex platform.

Based on the versatile mechanism underpinning catalyst turnover and the electron-rich nature of catalysts **A** and **B**, we envisioned that these organic catalysts could be successfully used as catalytic donors for EDA complex photoactivation (**Scheme 4.15**b). We were motivated by the following considerations: *i*) it is synthetically appealing to develop a general EDA complex catalytic strategy based on commercially available organic catalysts and use it to generate a variety of radicals. *ii*) Our understanding of the sulfur-centered radical **II** behavior and its relative kinetic stability could be used to develop mechanistically distinct radical transformations, including *net-reductive processes* that are not accessible via previously reported EDA complex catalytic platforms. Radical **II** would be generated upon EDA complex formation and photoinduced SET with a suitable substrate as acceptor. *iii*) Employing catalysts **A** and **B** as catalytic EDA donors would significantly expand the synthetic potential and applicability of this family of organocatalysts beyond the S_N2-based catalytic platform. For example, using reaction partners decorated with a purposely installed electron-poor activating group, which serves as both redox-auxiliary (RA, blue circle in Figure 4.15b, which triggers EDA complex formation) and leaving group, would allow the generation of previously inaccessible non-stabilized carbon radicals, including primary ones, and nitrogen-centered radicals.

4.5 Results and Discussion

To test the feasibility of our EDA complex catalytic strategy, we investigated *N*-(acyloxy)phthalimide esters as suitable EDA acceptors.[26a] We selected the reaction between cyclohexyl *N*-(acyloxy)phthalimide (NHPI) **31a** and vinyl sulfone **32a** catalyzed by the organic catalysts **A** and **B** as a testbed. This process would require the formation of a non-stabilized cyclohexyl radical **XXXVI**, which was inaccessible through our previous S_N2-based catalytic strategy.[2] Mechanistically, the resulting Giese-type addition of the cyclohexyl radical **XXXVI** to the electron-poor olefin **32a** would require a net-reductive pathway in order to proceed. Scheme 4.16 details the proposed mechanism of the overall process. The ground-state association between the electron-rich donor catalyst (**A** or **B**) and the electron-deficient NHPI substrate **31a** would lead to a visible-light-absorbing EDA complex. The formation of the EDA complex is feasible considering the tendency of stoichiometric thiolates and dithiocarbonyl anions to serve as donor partners for EDA complexes.[32] A photoinduced SET would then generate the cyclohexyl radical **XXXVI** along with the sulfur-centered radical **II**.

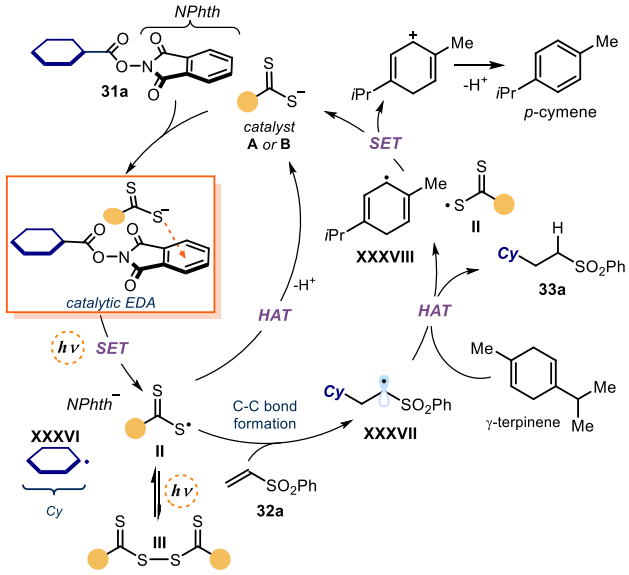

Scheme 4.16. Mechanistic plan for a net-reductive Giese-type addition manifold catalyzed by the excitation of a catalytic EDA complex; NPhth: phthalimide.

[32] (a) Liu, B.; Lim, C.-H.; Miyake, G. M. Visible-Light-Promoted C–S Cross-Coupling via Intermolecular Charge Transfer. *J. Am. Chem. Soc.* **2017**, *139*, 13616–13619. (b) Yang, M.; Cao, T.; Xu, T.; Liao, S., Visible-Light-Induced Deaminative Thioesterification of Amino Acid Derived Katritzky Salts via Electron Donor–Acceptor Complex Formation. *Org. Lett.* **2019**, *21*, 8673–8678. (c) Li, G.; Yan, Q.; Gan, Z.; Li, Q.; Dou, X.; Yang, D., Photocatalyst-Free Visible-Light-Promoted C(sp2)–S Coupling: A Strategy for the Preparation of S-Aryl Dithiocarbamates. *Org. Lett.* **2019**, *21*, 7938–7942. (d) Sundaravelu, N.; Nandy, A.; Sekar, G., Visible Light Mediated Photocatalyst Free C–S Cross Coupling: Domino Synthesis of Thiochromane Derivatives via Photoinduced Electron Transfer. *Org. Lett.* **2021**, *23*, 3115–3119.

Upon interception of radical **XXXVI** by **32a** to forge a new C-C bond, the emerging electrophilic radical **XXXVII** would abstract a hydrogen atom from γ-terpinene (a H donor). This reductive step leads to product **33a** and to the cyclohexadienyl radical **XXXVIII**. Overall, this sequence, which requires reduction of both the radical precursor **31a** (via an SET) and intermediate **XXXVII** (via HAT), characterizes a net-reductive process. Crucial for catalyst turnover would be the reduction of the dithiocarbonyl radical **II** (E_{ox} = 0.45-0.75 V vs. SCE), which our previous studies established could proceed via an SET event from the cyclohexadienyl radical **XXXVIII** (E_{red} = -0.1 V vs. SCE)[12] or via an HAT pathway from γ-terpinene.[13] Both reductive steps would eventually close the catalytic cycle by returning the organic catalysts. Importantly, the fact that *catalyst turnover can be realized by simply using an external reductant* (e.g. γ-terpinene), thus avoiding any specific interaction with a radical intermediate which is progenitor to the reaction product, increases the versatility of this EDA catalytic system.

4.5.1 Developing a Giese-type addition process

Our initial experiments focused on reacting phthalimide ester **31a** and vinyl sulfone **32a** in dimethylacetamide (DMA) as solvent, in the presence of γ-terpinene as the H donor (4 equiv.), and 10 mol% of the anionic donor catalyst (Table 4.1). Irradiation was provided by a blue LED strip (460 nm). All three catalysts tested (the dithiocarbamate **A**, containing a bromoindole moiety, and the more nucleophilic xanthogenate **B** and dithiocarbamate **C**) were all competent to provide the Giese addition product **33a** in good yields (entries 1-3). We selected catalyst **B** for this reaction due to its slightly superior performance, as well as its accessibility. Nevertheless, these results established that dithiocarbamate-based organic catalysts of different properties could act as competent EDA donors and generate non-stabilized alkyl radicals upon SET with phthalimide esters **31**. The modulability of the dithiocarbamate/xanthogenate structure allows to select the best catalyst depending on the required photophysical and chemical properties, providing versatility to the EDA complex catalytic platform. Interestingly, the reaction was also promoted by green light irradiation (λ_{max} = 520 nm, entry 4). Control experiments showed the need for light and for the donor catalyst (entries 6 and 7). The addition of TEMPO as radical scavenger completely shut down reactivity (entry 8), and trapping of the cyclohexyl radical **XXXVI** by TEMPO was observed.

Table 4.1. Optimization studies.

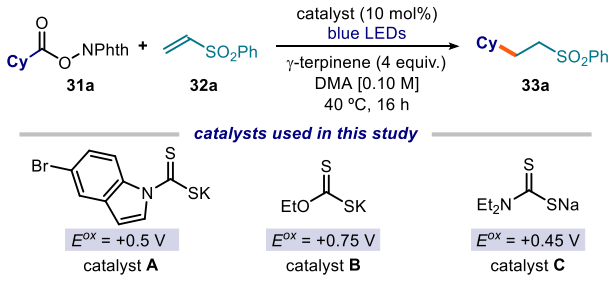

entry	catalyst	deviation	yield (%)[a]
1	**A**	none	81
2	**B**	none	95 (86)[b]
3	**C**	none	85
4	**B**	green LED (520 nm)	95
5	**B**	under air	0
6	**B**	no light	0
7	none	none	0
8	**B**	TEMPO (1.5 equiv.)	0

Reactions performed under inert atmosphere on a 0.1 mmol scale at 40 °C for 16 h under illumination by a blue LED strip (λ_{max} = 465 nm, 14 W) using 1.5 equiv. of **32a** and 4 equiv. of γ-terpinene. Redox potentials of the catalysts measured in CH3CN vs Ag/AgCl, see Experimental section. [a] Yield determined by ^{1}H NMR analysis of the crude mixture using trimethoxybenzene as the internal standard. [b] Yield of the isolated product **33a**. LED: Light-emitting diode. Cy: cyclohexyl, NPhth: phthalimide.

The formation of an EDA complex was confirmed through UV/Vis spectroscopic analysis by mixing catalyst **B** and phthalimide ester **31a** (Figure 4.1). When mixing both compounds, the colorless solution turned to a strong yellow color, while the absorption spectra showed a bathochromic shift diagnostic of a ground-state EDA aggregation.

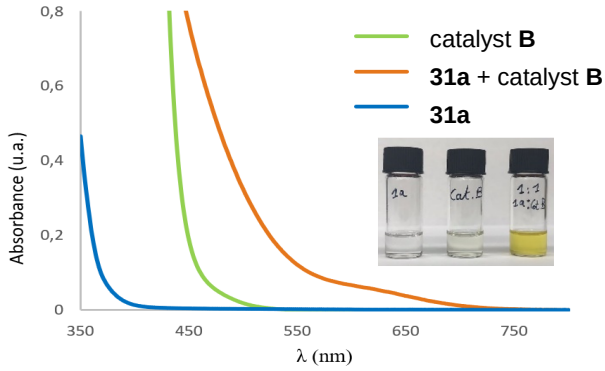

Figure 4.1. Optical absorption spectra, recorded in DMA in 1 mm path quartz cuvettes using a Shimadzu 2401PC UV−vis spectrophotometer, and visual appearance of the separate reaction components and of the colored EDA complex between catalyst **B** and **31a**. [**31a**] = 0.10 M, [catalyst **B**] = 0.01 M.

We also used transient absorption spectroscopy (TAS) to directly detect the formation of the xanthyl radical **IIb** (Figure 4.2). By using laser flash photolysis on a 1:1 mixture of catalyst **B** and ester **31a**, we observed the formation of a transient species absorbing at 620 nm (half lifetime = 0.1 ± 0.01 ms), consistent with the characteristic line shape of xanthyl radical **IIb**.[3,33] This observation corroborates that the key event for radical generation is the photoinduced SET between the compounds forming the EDA complex.

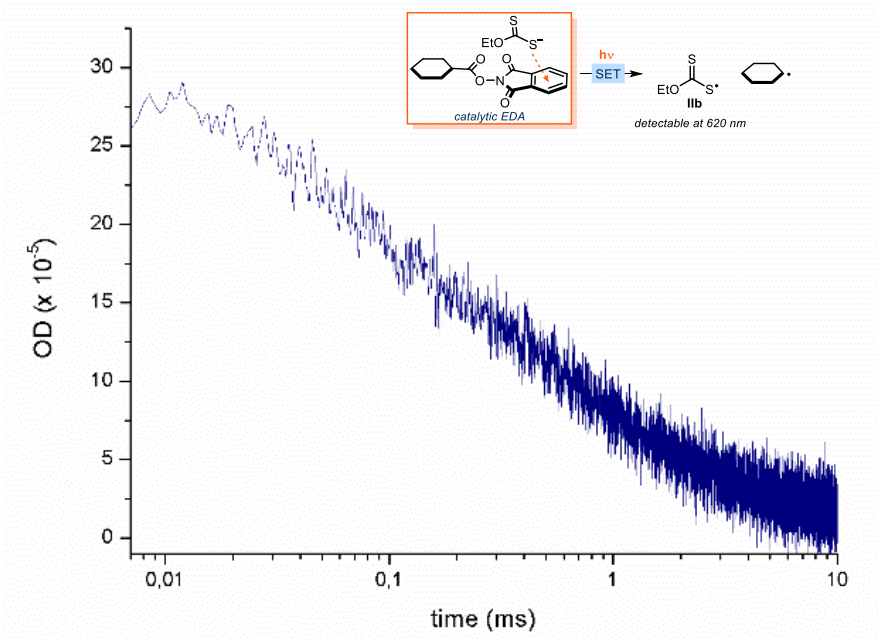

Figure 4.2. Absorption at 620 nm of the transient xanthyl radical **IIb** generated upon 355 nm laser excitation of a 1:1 mixture of **31a** and catalyst **B** 30 mM in DMA.

To gain further insight into the mechanism, we measured the quantum yield (Φ) of the overall model reaction of **31a** and **32a** catalyzed by **B**, which was as low as 0.01 (λ = 460 nm, using potassium ferrioxalate as the actinometer. This information is not consonant with a radical chain propagation manifold and supports a mechanistic scenario depicted in Scheme 4.16: it supports our original plan that the donor **B** serves as an actual EDA catalyst, since it can effectively turn over while iteratively driving the formation of radicals in every catalytic cycle.

To increase the synthetic relevance of this approach, we implemented a two-step telescoped sequence to access the radical precursor **31a** in situ and use it without further purification

[33] Kaga, A.; Wu, X.; Lim, J. Y. J.; Hayashi, H.; Lu, Y.; Yeow, E. K. L.; Chiba, S., Degenerative xanthate transfer to olefins under visible-light photocatalysis. *Beilstein J. Org. Chem.* **2018**, *14*, 3047-3058.

(Scheme 4.17a). This one-pot telescoped procedure delivered product **33a** from a readily available carboxylic acid avoiding the isolation of intermediate **31a** in the process. Moreover, we sought to develop a *domino* protocol, where the reagents of the reaction were added altogether (Scheme 4.17b). add a synthetically useful dimension to the EDA complex catalytic platform, since abundant aliphatic carboxylic acids can be directly functionalized and used as radical precursors without the need to isolate complex phthalimide esters.

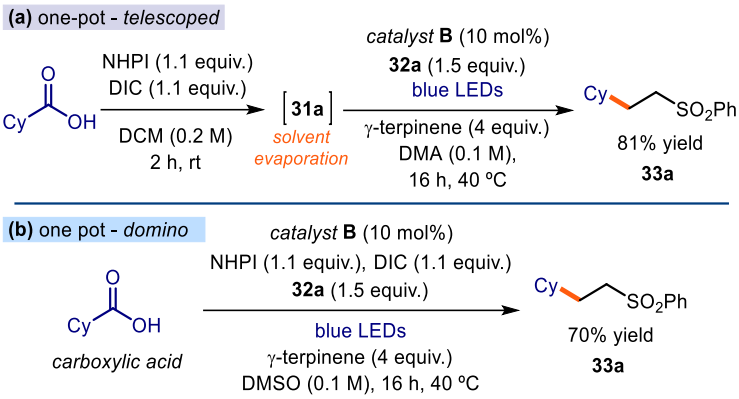

Scheme 4.17. (a) One-pot two-step telescoped procedure to functionalize the carboxylic acid; the solvent was evaporated between the two steps. (b) Domino procedure, where all reagents were added at the same time. Yields refer to the isolated product **33a**. DIC: *N*,*N*'-diisopropylcarbodiimide; NHPI: *N*-(acyloxy)phthalimide; DCM: dichloromethane.

Next, we used the telescoped procedure to study the scope of the decarboxylative Giese-type addition catalyzed by the EDA donor **B** (Scheme 4.18). A variety of carboxylic acids could be directly functionalized. Primary (**33b**, **33e**), secondary (**33c**), and tertiary radicals (**33d**) were generated efficiently and trapped by electron-deficient olefins **32** in good to excellent yields. A variety of functional groups was compatible with the protocol, including free alcohols (**33j**) and carbamates (**33f-i**). The activation of the acids through EDA aggregation was selective in the presence of electrophilic positions, such as alkyl chlorides (**33e**). Access to α-amino radicals was also accomplished (**33f-i)**. We also demonstrated that this method is suitable for the direct functionalization of biorelevant compounds bearing unprotected polar functional groups. Dehydrocholic acid (**33g**), oleanolic acid (**33h**), and biotin (**33l**) could be used without the need for protection of other functional groups on the scaffold. Notably, some of the examples were successful using the one-pot domino procedure directly from the carboxylic acid (products **33g**, **33j**, and **33l**).

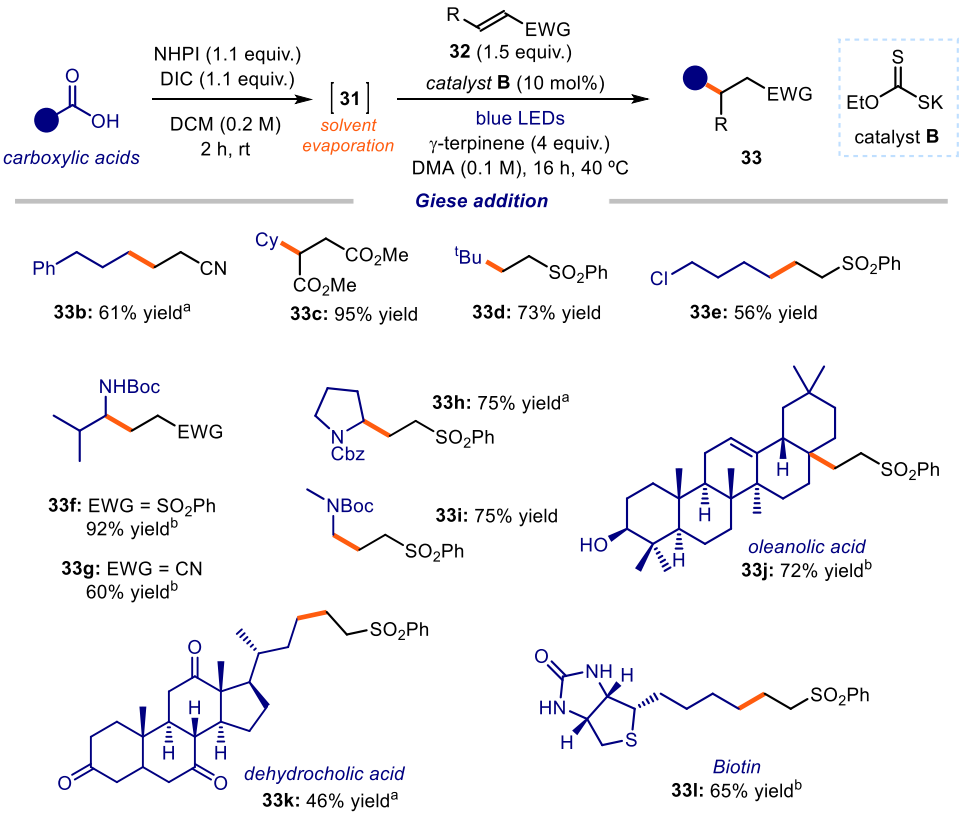

Scheme 4.18. EDA complex catalytic strategy for the generation of alkyl radicals from carboxylic acids and their use in decarboxylative Giese addition processes. Reactions performed on 0.2 mmol scale using 1 equiv. of acid; yields of products refer to isolated products **33** after purification; the bold orange bond denotes the newly formed C-C bonds. Unless otherwise indicated, all entries were performed using a telescoped sequence without isolation of the NHPI adduct **31** by simply evaporating the solvent (DCM) after completion of the first step. [a] Using the preformed NHPI ester **31** as the radical precursor. [b] One-pot domino procedure according to the conditions in Scheme 4.17. NHPI: *N*-Hydroxyphthalimide, DIC: *N,N'*-Diisopropylcarbodiimide, Cy: cyclohexyl, Pr: propyl, Boc: tert-butyloxycarbonyl; Cbz: carboxybenzyl ; Bn: benzyl; Ts: tosyl; EWG: electron-withdrawing group.

Another family of radical precursors that have been reported to engage in EDA complex formation is pyridinium salts **34**.[34] Similarly to phthalimide esters **31**, pyridinium salts **34** are easily accessible by a one-step modification of widely available primary amines. We explored the potential of our photochemical catalytic radical generation method to activate pyridinium salts (Table 4.2). In this case, catalyst **A** (entry 1) proved more effective than catalyst **B** (entry 2). This result was rationalized considering the higher stability of catalyst **A** under relatively acidic conditions,[35] which highlighted how the modular nature of these donor catalysts can be

[34] Wu, J.; Grant, P. S.; Li, X.; Noble, A.; Aggarwal, V. K. Catalyst-Free Deaminative Functionalizations of Primary Amines by Photoinduced Single-Electron Transfer. *Angew. Chem., Int. Ed.* **2019**, *58*, 5697–5701.
[35] As depicted in Scheme 4.16, a proton is released upon aromatization of the resulting carbocation.

leveraged to optimize the activation of electronically different radical precursors. Control experiments proved again the need of catalyst (entry 7) and light (entry 6) for the reaction to take place.

Table 4.2. Giese addition with pyridinium salts as radical precursors

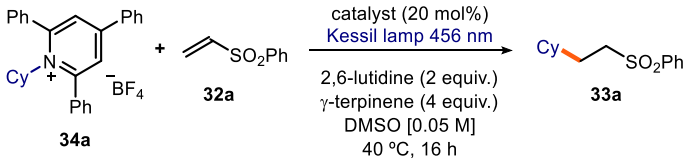

catalysts used in this study

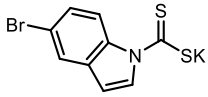

catalyst **A**

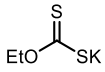

catalyst **B**

entry	catalyst	deviation	yield (%)[a]
1	**A**	none	83 (67)[b]
2	**B**	none	70
3	**A**	Green light	24
4	**B**	Green light	20
5	**A**	under air	0
6	**A**	no light	0
7	-	no catalyst	0

Reactions performed under inert atmosphere on a 0.1 mmol scale. [a] Yield determined by ^{1}H NMR analysis of the crude mixture using trimethoxybenzene as the internal standard. [b] Yield of the isolated product on a 0.2 mmol scale.

Pyridinium salts **34** were successfully reduced by the donor catalyst under blue light irradiation, generating non-stabilized secondary alkyl radicals which were then intercepted by electron-deficient olefins **32** (Scheme 4.19a). The applicability of the method was also showcased by a one-pot telescoped procedure where primary amine **35** was treated with 2,4,6-triphenylpyrylium tetrafluroborate at 85 ºC for 4h; the corresponding pyridinium salt **34** was used without further purification for the photochemical step, by simply adding the reagents sequentially (Scheme 4.19b).

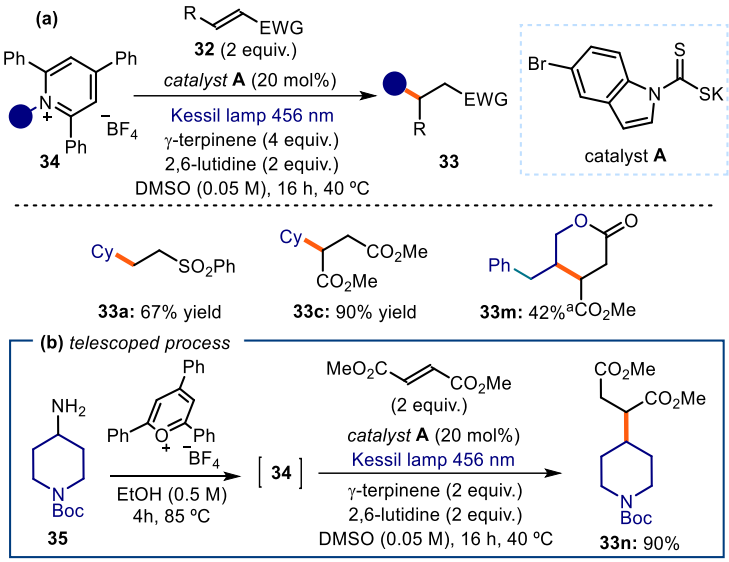

Scheme 4.19. (a) EDA complex catalytic strategy for the deaminative Giese-type addition processes. [a]Product **33m** was formed in a 3.8:1 ratio with the regioisomeric five-member ring adduct, see the Experimental section for details. (b) One-pot telescoped procedure for functionalization of amines. Reactions performed on 0.2 mmol scale.

We envisioned that the same catalytic protocol used for the Giese-type addition could be successfully translated to perform a Barton decarboxylation process.[36] When conducted in the absence of an olefin trap **32**, the EDA complex-based catalytic system would provide an alkyl radical prone to hydrogen atom abstraction (via HAT) from γ-terpinene, delivering the decarboxylation reductive product **36**. We demonstrated the feasibility of this idea by applying a one-pot domino process, which allowed the direct reduction of carboxylic acids (Scheme 4.20). The xanthogenate catalyst **B** (10 mol%) secured the decarboxylation of primary (**36a**), secondary (**36b**) and tertiary (**36c**) carboxylic acids. Due to the extensive use of the Barton decarboxylation in total synthesis, we wanted to test the applicability of our methodology in the reduction of complex biologically relevant carboxylic-acid-containing molecules.[36] The reduction of Gibberellic acid (**36f**) and a baclofen derivative (**36g**) afforded the Barton decarboxylation products in 60% and 74% yield, respectively. A large-scale (4

[36] (a) Barton, D. H. R.; Crich, D.; Motherwell, W. B. New and Improved Methods for the Radical Decarboxylation of Acids. *J. Chem. Soc., Chem. Commun.* **1983**, 939–941. (b) Barton, D. H. R.; Crich, D.; Motherwell, W. B. The invention of new radical chain reactions. Part VIII. Radical chemistry of thiohydroxamic esters; A new method for the generation of carbon radicals from carboxylic acids. *Tetrahedron* **1985**, *41*, 3901–3924. For a recent application: (c) Qin, T.; Malins, L. R.; Edwards, J. T.; Merchant, R. R.; Novak, A. J. E.; Zhong, J. Z.; Mills, R. B.; Yan, M.; Yuan, C.; Eastgate, M. D.; Baran, P. S. Nickel-Catalyzed Barton Decarboxylation and Giese Reactions: A Practical Take on Classic Transforms. *Angew. Chem., Int. Ed.* **2017**, *56*, 260–265.

mmol) functionalization of dehydrocholic acid, which led to product **36d** in 55% yield, demonstrated that this method is amenable to synthetically useful applications.

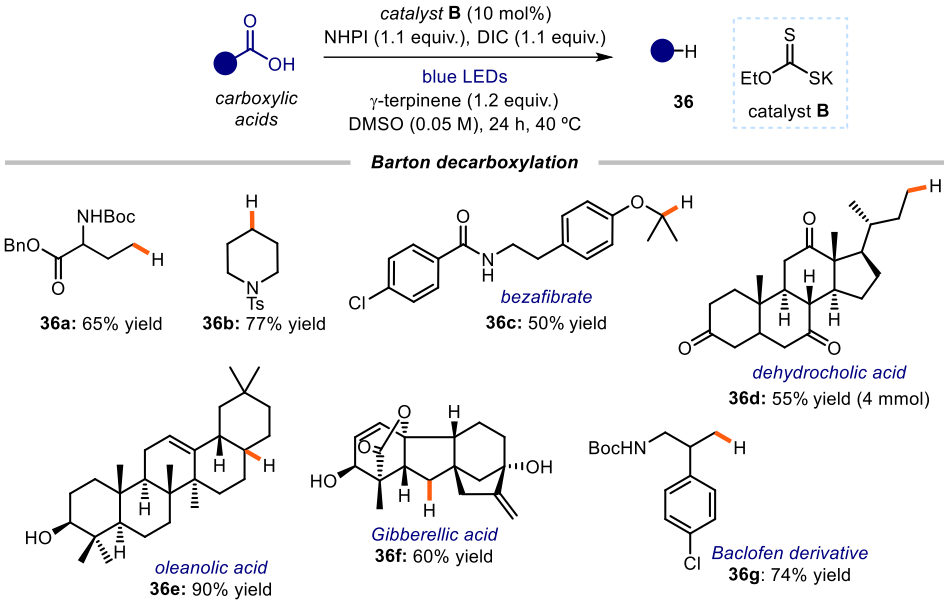

Scheme 4.20. EDA complex catalysis for the Barton decarboxylation. (a) Reactions performed on 0.2 mmol scale using a one-pot domino process; yields refer to isolated products **27** after purification; the bold orange bond denotes the newly formed bonds. NHPI: *N*-Hydroxyphthalimide, DIC: *N,N'*-diisopropylcarbodiimide, , Boc: *tert*-Butyloxycarbonyl; Bn: benzyl.

Finally, this catalytic process could be extended to include a deaminative reduction path, since pyridinium salts **34** were used as radical precursors leading to products **36** in the absence of olefin **32** (Scheme 4.21). As previously observed, the indole-based catalyst **A** performed better when this type of radical precursors was employed.

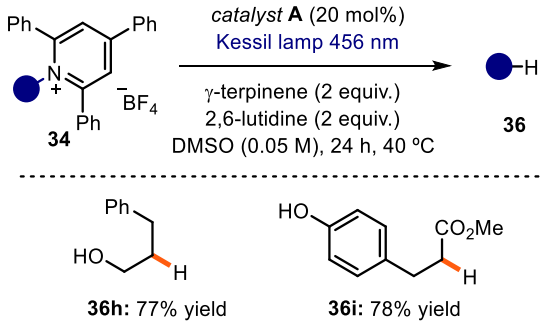

Scheme 4.21. EDA complex catalysis for deaminative reduction.

The mechanism of this reductive defunctionalization is proposed to resemble the net-reductive manifold depicted in Scheme 4.16. In this case, the radical of type **XXXVI** generated after intra-complex SET of the EDA can abstract a H-atom from γ-terpinene to afford product **36**. To close the catalytic cycle, the sulfur-centered radical **II** can then be reduced by cyclohexadienyl radical **XXXXVIII** via an SET, or by a HAT with the H donor (γ-terpinene). We also performed quantum yield measurements of this process. The quantum yield Φ was found to be 0.01 (λ = 460 nm, using potassium ferrioxalate as the actinometer). This supports the scenario where a radical chain process is highly unlikely, confirming the ability of the EDA catalytic donor to turn over and repeatedly trigger radical formation.

4.5.2 Redox-neutral process[37]

One of the target of this project was to find a versatile and general catalytic EDA complex platform. This requires not only the capability of generating radicals from different precursors, but also to apply such radicals in reactions with fundamentally different mechanisms. So far, we have applied our methodology to catalyze net-reductive transformations by using a sacrificial reductant to turn-over the catalyst. We wanted to also develop a redox-neutral process, where one of the intermediates can master the catalyst turn-over with the dithiocarbonyl radical **II** through an SET event. We envisioned the α-alkylation of silyl enol ethers **37** as a suitable reaction to implement this hypothesis. We envisaged the catalytic cycle depicted in Scheme 4.22. The first step involves the EDA aggregation of the pyridinium salt **34** with the organic catalyst, which under irradiation and subsequent SET provides the radical **XXXIX**. This open-shell species is then intercepted by the silyl enol ether **37**, leading to the α-oxo radical **XL**. SET between **XL** and the sulfur-centered radical **II**, which is stabilized by a dimerization mechanism, would regenerate the EDA catalytic donor and form the oxocarbenium ion **XLI**, which can hydrolyze to afford the final α-alkylation ketone product **38**. The overall sequence requires reduction of the radical precursor **34** and oxidation of intermediate **XL**, therefore constituting a redox neutral process. In contrast to previous processes, an effective catalyst turnover would here require an SET between the sulfur radical **II** and a radical intermediate progenitor of the reaction product.

[37] The scope and optimization of the reaction detailed in this section was performed by Davide Spinatto.

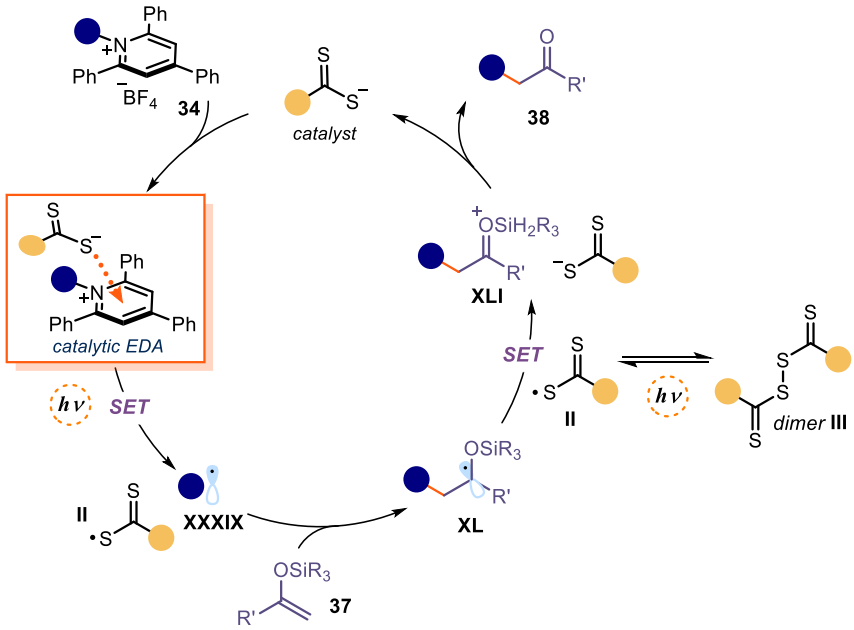

Scheme 4.22. Mechanistic plan for a redox neutral transformation catalyzed by the excitation of a catalytic EDA complex.

We successfully applied our catalytic platform for this reaction. Even though both organic catalyst **A** and **B** were efficient in the photochemical alkylation, we chose the indole-based dithiocarbamate catalyst **A** as it offered more general results. We chose pyridinium salts **34** as radical precursors, since they are readily available from α-amino acid derivatives, and upon SET they generate electrophilic radicals (Scheme 4.23). Silyl enol ethers **37** act as electron-rich olefinic traps, which are polarity matched to react with electrophilic radicals, affording the alkylated ketone **38** after hydrolysis. Pyridinium salts **34** delivering primary (**38a**, **38b**) and secondary (**38c-d**) radicals were competent substrates for the alkylation. Nitrogen-containing heterocycles were well tolerated (**38e-f**). We then demonstrated that silyl enol ethers **37** derived from both aliphatic (product **38g**) and aromatic ketones could intercept an electrophilic α-ester radical. A variety of substitution patterns on the aryl ring, with different electronic or steric profiles (**38h-k**), could be easily accommodated. Last, we tested phthalimide esters as an alternative radical source, this allowed us for the formation of non-stabilized primary (**38o**) and secondary radicals (**38n**) and the construction of the corresponding ketone derivative, albeit in lower yields due to the polarity mismatch of the radicals.

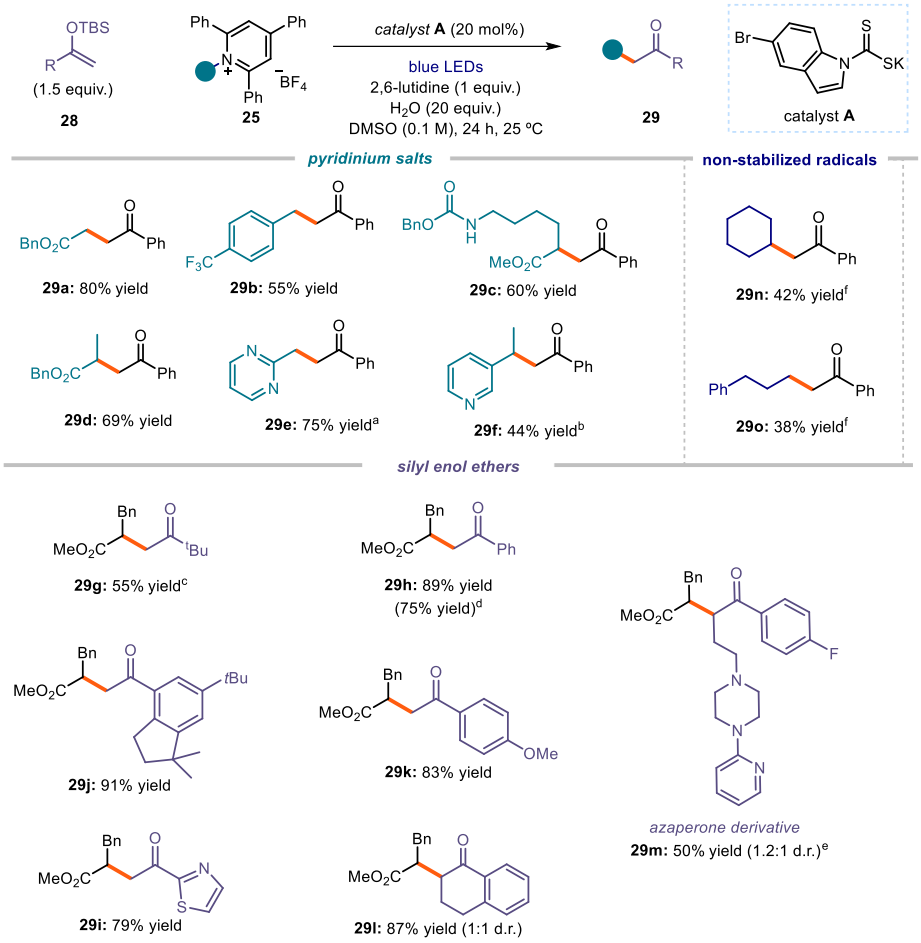

Scheme 4.23. Redox-neutral addition of alkyl radicals to silyl enol ethers under EDA complex catalysis. Reactions performed on 0.2 mmol scale using 2.0 mL of DMSO; yields refer to isolated products **38** after purification; the bold orange bond denotes the newly formed C-C bond. Unless otherwise indicated, all entries were performed at 25 °C. [a] 40 °C; [b] 60 °C; [c] 1:1 mixture of DMSO/DCE used as solvent; [d] with catalyst **B**; [e] in the absence of water; [f] using alkyl *N*-(acyloxy)phthalimides **31** as radical precursors. TBS: *tert*-butyldimethylsilyl.

Given the different underlying mechanism of this redox-neutral process with respect to previously studied net-reductive transformations, we considered it pertinent to determine the quantum yield of the reaction leading to product **38h**. The low quantum yield (Φ = 0.02, λ = 460 nm) supports the mechanism depicted in Scheme 4.22, where catalyst **A** can effectively turn-over by engaging in both a reduction and an oxidation process.

Based on the results involving non-stabilized radicals, we wondered if we could capitalize on the polarity mismatch between the reaction partners to develop a three-component reaction (Scheme 4.24). The protocol would work as follows: upon EDA complex activation, the electrophilic radical **XXIX** would be formed and selectively reacted with the electron-poor

alkene **32**. The emerging secondary electrophilic radical would then be prone to engage in a second bond-forging event with the electron-rich silyl enol ether **37**, affording the complex three-component product **39**. Eventually, the turn-over event of the catalyst would rely on the same SET depicted in Scheme 4.22. This cascade sequence was efficiently catalyzed by the xanthate catalyst **B,** providing rapid access to structurally complex products **39** from readily available substrates and using an experimentally simple protocol.

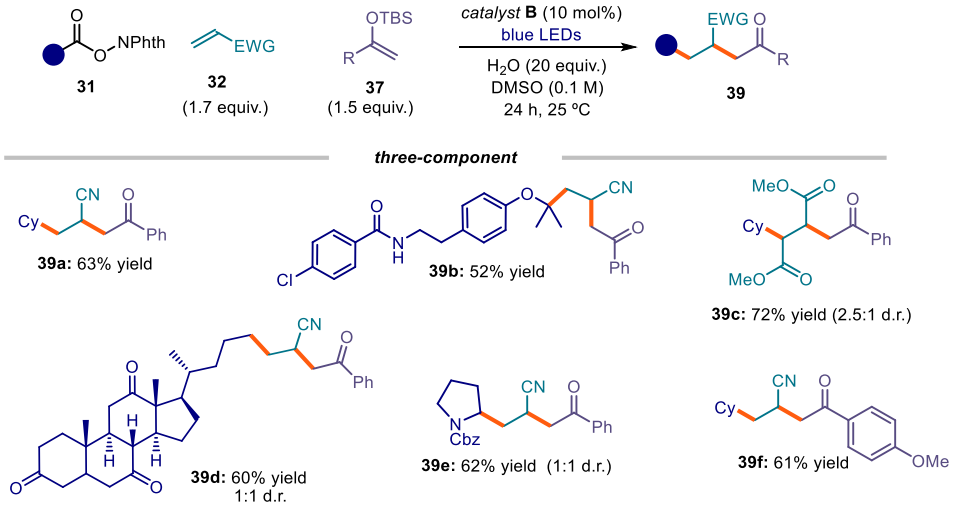

Scheme 4.24. Three-component process under EDA complex catalysis; NPhth: phthalimide.

4.5.3 Minisci reaction[38]

We then wondered if our catalytic EDA platform could be applied to develop another redox-neutral transformation, which could not be previously realized using a nucleophilic substitution activation mechanism, namely the radical C-alkylation of heteroarenes. The Minisci reaction involves the addition of a nucleophilic radical **XLII** to a protonated electron-deficient heteroarene **40** and is widely employed in organic synthesis for the direct functionalization of aza-heterocycles.[39] Mechanistically, the reaction requires a final

[38] The scope and optimization of the reaction detailed in this section has been performed by Wei Zhou.
[39] (a) Minisci, F.; Bernardi, R.; Bertini, F.; Galli, R.; Perchinummo, M. Nucleophilic character of alkyl radicals—VI: A new convenient selective alkylation of heteroaromatic bases. *Tetrahedron* **1971**, *27*, 3575–3580. (b) Minisci, F.; Fontana, F.; Vismara, E. Substitutions by nucleophilic free radicals: A new general reaction of heteroaromatic bases. *J. Heterocycl. Chem* **1990**, *27*, 79. (c) Duncton, M. A. J. Minisci reactions: Versatile CH-functionalizations for medicinal chemists. *Med. Chem. Commun.* **2011**, *2*, 1135–1161. (d) Wang, W. G.; Wang, S. F., Recent Advances in Minisci-type Reactions and Applications in Organic Synthesis. *Cur. Org. Chem.* **2021**, *25*, 894–934.

oxidation to achieve re-aromatization of the ring after radical addition (Scheme 4.25).[40] The catalyst turnover that closes the catalytic cycle would be based on the SET between the sulfur radical **II** (E_{ox} = 0.45 V vs. SCE) and intermediate **XLIV** (E_{red} = -1.01 V vs. SCE),[41] released upon deprotonation of **XLIII**, which should be a thermodynamically favorable process.

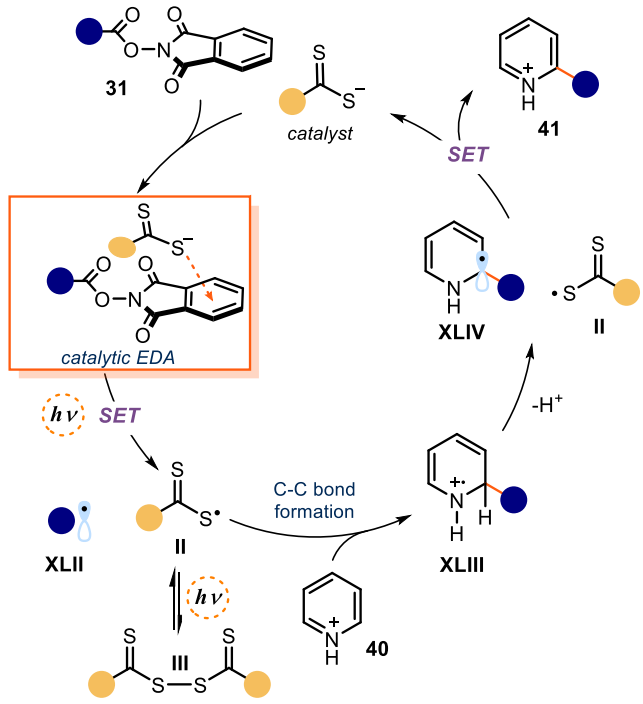

Scheme 4.25. Mechanistic proposal EDA catalyzed Minisci reaction.

This idea was successfully realized using the indole-based catalyst **A** (10 mol%), which offered a better stability than catalyst **B** under the acidic conditions required for the Minisci process. Using phthalimide esters **31** as radical precursors, the functionalization of heterocyclic aromatics **40** was achieved in good yields (Scheme 4.26). We first explored the scope of the heterocycles amenable to this Minisci-type catalytic protocol. The method proved to be fairly general, allowing for the functionalization of quinolines (products **41a-c**), isoquinolines (**41d**), and pyridines (**41e**). The functional group tolerance was also broad since protected amines (**41g**) and unprotected alcohols (**41h-j**) could be tolerated well. In addition, we tested our methodology on complex molecules we successfully performed the alkylation

[40] Proctor, R. S. J.; Phipps, R. J., Recent Advances in Minisci-Type Reactions. *Angew. Chem. Int. Ed.* **2019**, *58*, 13666-13699.
[41] Bieszczad, B.; Perego, L. A.; Melchiorre, P., Photochemical C−H Hydroxyalkylation of Quinolines and Isoquinolines. *Angew. Chem. Int. Ed.* **2019**, *58*, 16878–16883.

of an intermediate used in the synthesis of HIF protyl-hydroxylase inhibitor roxadustat (products **41h-i**), the anti-cancer agent camptothecin (**41j**), and the neuroleptic drug azaperone (**41k**). Last but not least, we wondered if the EDA complex-catalysed Minisci reaction could be used for the methylation of heterocycles using acetic acid derivative as the methyl radical source.[42] The methylation of several heterocycles was successful by a simply changing the solvent for the reaction (adducts **41c**, **41g**, and **41i**). Finally, we demonstrated that a variety of primary, secondary, and tertiary carbon-centered radicals could be generated from NHPI precursors **31** and installed within 2-methylquinoline (products **41l-p**).

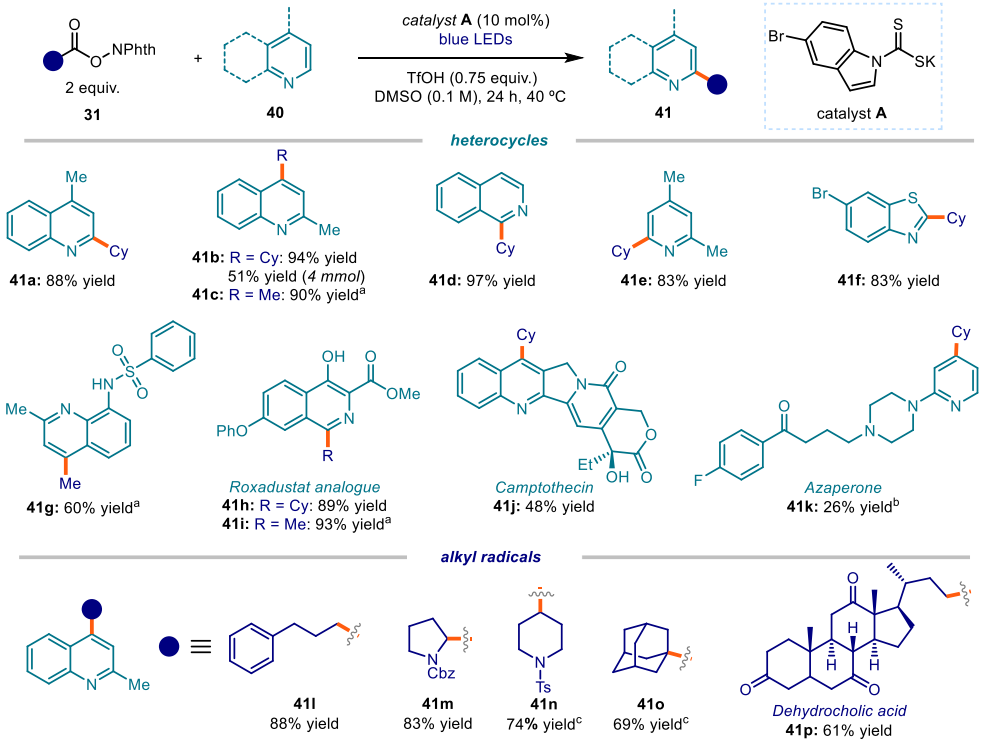

Scheme 4.26. Photochemical catalytic generation of alkyl radicals and their addition to heterocycles. Reactions performed on 0.2 mmol scale using 2.0 mL of DMSO; yields refer to isolated products **41** after purification; the bold orange bond denotes the newly formed C-C bond. [a] Performed in NMP as solvent; [b] 3 equiv. of TfOH; [c] Performed at 60 °C. Cy: cyclohexyl.; Ts: tosyl; NPhth: phthalimide.

We also measured the quantum yield of the Minisci process leading to product **41b**, which was <0.01 (λ = 460 nm, using potassium ferrioxalate as the actinometer, see Experimental section for details). This experiment further supports the ability of donor **A** to catalyze the

[42] For a review in the importance of methylation in medicinal chemistry: Aynetdinova, D.; Callens, M. C.; Hicks, H. B.; Poh, C. Y. X.; Shennan, B. D. A.; Boyd, A. M.; Lim, Z. H.; Leitch, J. A.; Dixon, D. J. Installing the "magic methyl" – C–H methylation in synthesis. *Chem. Soc. Rev.* **2021**, *50*, 5517–5563

photochemical generation of alkyl radicals while triggering the overall Minisci process in the absence of external oxidants.

We finally tested our catalytic EDA system in a more challenging setting, such as asymmetric radical chemistry (Scheme 4.27). Phipps and coworkers recently reported an enantioselective variant of the Minisci reaction based on chiral phosphoric acid catalysis.29 Prochiral radicals were generated from α-amino acid derivatives of type **31** using an external iridium-based photocatalyst, and they were trapped stereoselectively by the heteroarenes **40** activated by the chiral acid ((*R*)-TRIP).[43] When attempting the same transformation by replacing the iridium-based photocatalyst by the EDA donor catalyst **A**, we obtained products (**41q** and **41r**) in high yield and stereocontrol.

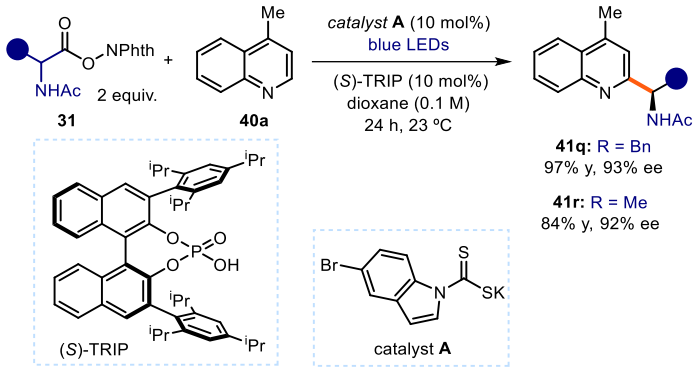

Scheme 4.27. Application in enantioselective radical catalysis; Ac: acetyl; NPhth: phthalimide.

4.5.4 Further application of the EDA catalytic system

We decided to further explore the potential of our EDA catalytic radical generation approach by investigating other radical precursors that can engage in EDA complex formation. Specifically, we targeted the formation of a trifluoromethyl radical (Scheme 4.28). Trifluoromethylation was accomplished using catalyst **A**, the Togni reagent **42** as the EDA complex acceptor, and the silyl enol ether **37a** as an effective trap, affording the α-trifluoromethyl ketone product **43**.[44]

[43] Ermanis, K.; Colgan, A. C.; Proctor, R. S. J.; Hadrys, B. W.; Phipps, R. J.; Goodman, J. M., A Computational and Experimental Investigation of the Origin of Selectivity in the Chiral Phosphoric Acid Catalyzed Enantioselective Minisci Reaction. *J. Am. Chem. Soc.* **2020**, *142*, 21091-21101.

[44] (a) Cheng, Y.; Yu, S. Hydrotrifluoromethylation of Unactivated Alkenes and Alkynes Enabled by an Electron-Donor–Acceptor Complex of Togni's Reagent with a Tertiary Amine. *Org. Lett.* **2016**, *18*, 2962–2965. (b) Tu, H.-Y.; Zhu, S.; Qing, F.-L.; Chu, L. A four-component radical cascade trifluoromethylation reaction of alkenes enabled by an electron-donor–acceptor complex. *Chem. Commun.* **2018**, *54*, 12710–12713.

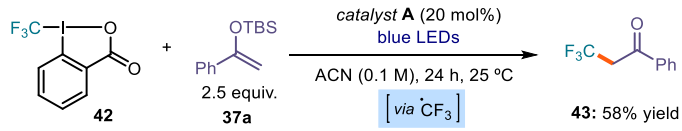

Scheme 4.28. Trifluoromethylation of ketones via EDA complex catalysis.

We also used the xanthate catalyst **B** to generate an amidyl radical upon EDA complex activation of the dinitrophenoxy amide **44** (Scheme 4.29).[45] Radical cyclization afforded the lactam product **45** in high yield.

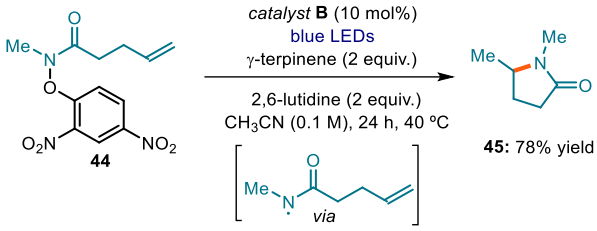

Scheme 4.29. Amidyl radical formation and cyclization.

4.6 Conclusions

In summary, we have developed a catalytic EDA complex system based on our previously developed organic catalyst, which here acted as catalytic donors. This modular class of organic catalysts can readily form photoactive electron donor-acceptor (EDA) complexes with a wide variety of radical precursors. Excitation with weak visible light grants access to stabilized and non-stabilized alkyl radicals under mild experimental conditions. The generated radicals were then leveraged to design synthetically useful transformations. Our previous knowledge of the catalyst behavior informed the design of mechanistically distinct processes, based on photoinduced redox neutral and net-reductive radical transformations. For all the developed processes, we established, by means of quantum yield determination, that a closed catalytic cycle is operational, highlighting the ability of the EDA catalysts to turn over and iteratively drive every catalytic cycle. We also highlighted how the catalysts' stability and the method's high functional group tolerance could be advantageous for the direct radical functionalization of abundant functional groups, including aliphatic carboxylic acids and amines, and for applications in the late-stage elaboration of biorelevant compounds and enantioselective radical catalysis. All these features showcase the versatility of this EDA

[45] Davies, J.; Svejstrup, T. D.; Fernandez Reina, D.; Sheikh, N. S.; Leonori, D., Visible-Light-Mediated Synthesis of Amidyl Radicals: Transition-Metal-Free Hydroamination and N-Arylation Reactions. *J. Am. Chem. Soc.* **2016**, *138*, 8092-8095.

complex catalytic platform, which may be useful for developing further radical processes. This method is complementary to our previously reported methodologies employing these catalysts, since it relies on a different property of the radical precursor (redox properties instead of electrophilicity) and the radical generation event is also different (SET in contrast to C-S bond homolysis). These crucial distinctions granted access to stabilized and non-stabilized alkyl radicals, including heteroatom-centered radicals.

4.7 Experiental section

4.7.1 General information

The NMR spectra are available in the published manuscript[1] and are not reported in the present dissertation.

The NMR spectra were recorded at 400 MHz and 500 MHz for ^{1}H and 100 or 125 MHz for ^{13}C. The chemical shift (δ) for ^{1}H and ^{13}C are given in ppm relative to residual signals of the solvents ($CHCl_3$ @ 7.26 ppm ^{1}H NMR and 77.16 ppm ^{13}C NMR, and tetramethylsilane @ 0 ppm). Coupling constants are given in Hertz. The following abbreviations are used to indicate the multiplicity: s, singlet; d, doublet; q, quartet; m, multiplet; bs, broad signal; app, apparent.

High resolution mass spectra (HRMS) were obtained from the ICIQ HRMS unit on MicroTOF Focus and Maxis Impact (Bruker Daltonics) with electrospray ionization. (ESI). UV-vis measurements were carried out on a Shimadzu UV-2401PC spectrophotometer equipped with photomultiplier detector, double beam optics and D_2 and W light sources or an Agilent Cary60 spectrophotometer. Emission spectra of light sources were recorded on Ocean Optics USB4000 fiber optic spectrometer.

Yields of isolated products refer to materials of >95% purity as determined by ^{1}H NMR.

General Procedures. All reactions were set up under an argon atmosphere in oven-dried glassware. Synthesis grade solvents were used as purchased, anhydrous solvents were taken from a commercial SPS solvent dispenser. Chromatographic purification of products was accomplished using forced-flow chromatography (FC) on silica gel (35-70 mesh). For thin layer chromatography (TLC) analysis throughout this work, Merck pre-coated TLC plates (silica gel 60 GF_{254}, 0.25 mm) were employed, using UV light as the visualizing agent and an acidic mixture of vanillin or basic aqueous potassium permanganate ($KMnO_4$) stain solutions, and heat as developing agents. Organic solutions were concentrated under reduced pressure on a Büchi rotatory evaporator.

Determination of Enantiomeric Purity. HPLC analysis on chiral stationary phase was performed on an Agilent 1200-series instrument, employing Daicel Chiralpak IC column.

Materials. Most of the starting materials used in this study are commercial and were purchased in the highest purity available from Sigma-Aldrich, Fluka, Alfa Aesar, Fluorochem, and used as received, without further purifications.

4.7.2 Substrate synthesis

The following substrates were synthesized according to reported procedures (Scheme 4.30).[46]

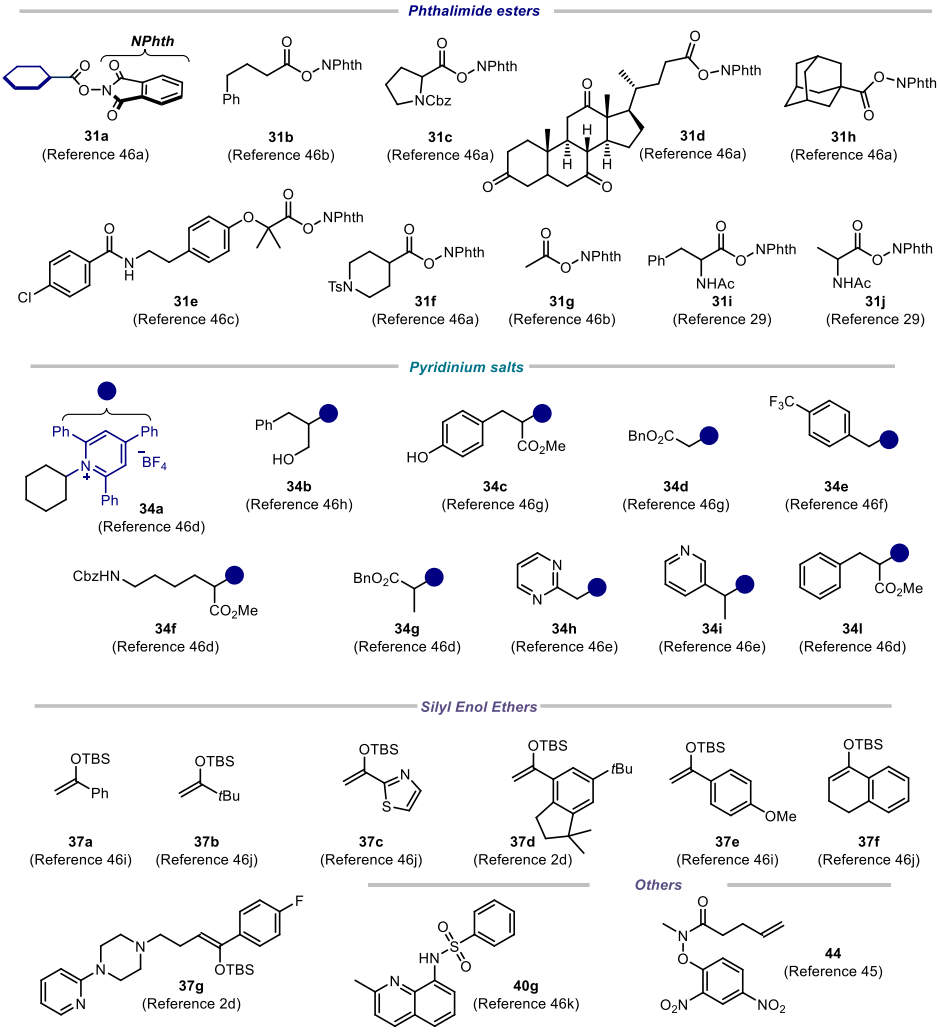

[46] (a) Qin, T.; Malins, L. R.; Edwards, J. T.; Merchant, R. R.; Novak, A. J. E.; Zhong, J. Z.; Mills, R. B.; Yan, M.; Yuan, C.; Eastgate, M. D.; Baran, P. S., Nickel-Catalyzed Barton Decarboxylation and Giese Reactions: A Practical Take on Classic Transforms. *Angew. Chem., Int. Ed.* **2017**, *56*, 260-265. (b) Huihui, K. M. M.; Caputo, J. A.; Melchor, Z.; Olivares, A. M.; Spiewak, A. M.; Johnson, K. A.; DiBenedetto, T. A.; Kim, S.; Ackerman, L. K. G.; Weix, D. J., Decarboxylative Cross-Electrophile Coupling of N-Hydroxyphthalimide Esters with Aryl Iodides. *J. Am. Chem. Soc.* **2016**, *138*, 5016-5019. (c) Ishii, T.; Kakeno, Y.; Nagao, K.; Ohmiya, H., N-Heterocyclic Carbene-Catalyzed Decarboxylative Alkylation of Aldehydes. *J. Am. Chem. Soc.* **2019**, *141*, 3854-3858. (d) Klauck F. J. R.; James M. J.; Glorius F., Deaminative Strategy for the Visible-

Scheme 4.30. Starting materials synthesised according to known procedures.

4.7.3 Experimental setups

4.7.3.1 Set-up 1 - 3D printed reactor with LED strip

For reactions performed using a blue LED strip as the light source, a 3D-printed photoreactor was used, consisting of a 9 cm diameter crystallizing dish with a 3D printed support of 6 positions, and a hole of 22 mm in the middle to allow ventilation (**Figure 4.3**, left). A commercial 1-meter LED strip was wrapped around the crystallizing dish, while a fan was used to cool down the reactor (the reaction temperature was measured to be between 35-40 ºC). Each of the positions could be used to fit a standard 16 mm diameter vial with a Teflon screw cap. Experiments at 465 nm were conducted using a 1m strip, 14.4W "LEDXON MODULAR 9009083 LED, SINGLE 5050" purchased from Farnell, catalog number 9009083. The emission spectrum of these LEDs is shown in **Figure 4.3**, right panel.

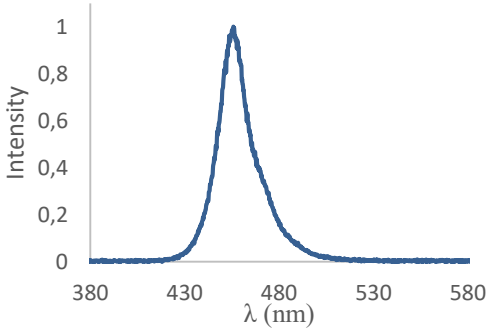

Figure 4.3. Blue LEDs photoreactor used for reactions where temperature control was not needed (*left*). Emission spectrum of the 465 nm LED strip used in this reactor (*right*).

Light-Mediated Generation of Alkyl Radicals. *Angew. Chem., Int. Ed.* **2017**, *56*, 12336-12339. (e) Liao J.; Guan W.; Boscoe B. P.; Tucker J. W.; Tomlin J. W.; Garnsey M. R.; Watson M. P., Transforming Benzylic Amines into Diarylmethanes: Cross-Couplings of Benzylic Pyridinium Salts via C–N Bond Activation. *Org. Lett.* **2018**, *20*, 3030-3033. (f) Xia Q.; Li Y.; Wang X.; Dai P.; Deng H.; Zhang W.-H. Visible Light-Driven α-Alkylation of N-Aryl tetrahydroisoquinolines Initiated by Electron Donor–Acceptor Complexes. *Org. Lett.* **2020**, *22*, 7290-7294. (g) Laroche B.; Tang X.; Archer G.; Di Sanza R.; Melchiorre P., Photochemical Chemoselective Alkylation of Tryptophan-Containing Peptides. *Org. Lett.* **2021**, *23*, 285-289. (h) Lai S.-Z.; Yang Y.-M.; Xu H.; Tang Z.-Y; Luo Z., Photoinduced Deaminative Coupling of Alkylpyridium Salts with Terminal Arylalkynes. *J. Org. Chem.* **2020**, *85*, 15638-15644. (i) Perrotta D.; Racine S.; Vuilleumier J.; de Nanteuil F.; Waser J., [4 + 2]-Annulations of Aminocyclobutanes. *Org. Lett.* **2015**, *17*, 1030-1033. (j) Li Y.; Liu J., Zhao S., Du X.; Guo M.; Zhao W.; Tang X.; Wang G., Copper-Catalyzed Fluoroolefination of Silyl Enol Ethers and Ketones toward the Synthesis of β-Fluoroenones. *Org. Lett.* **2018**, *20*, 917-920. (k) Perez C.; Barkley-Levenson A. M.; Dick B. L.; Glatt P. F.; Martinez Y; Siegel D.; Momper J. D.; Palmer A. A.; Cohen S. M., Metal-Binding Pharmacophore Library Yields the Discovery of a Glyoxalase 1 Inhibitor. *J. Med. Chem.* **2019**, *62*, 1609-1625.

4.7.3.2 Set-up 2 - Kessil lamp setup

For reactions performed with a Kessil lamp, the irradiation set-up consisted of a 50 W Kessil blue LED lamp (PR160L-456, 100% intensity, 2-3 cm away – Figure 4.4).

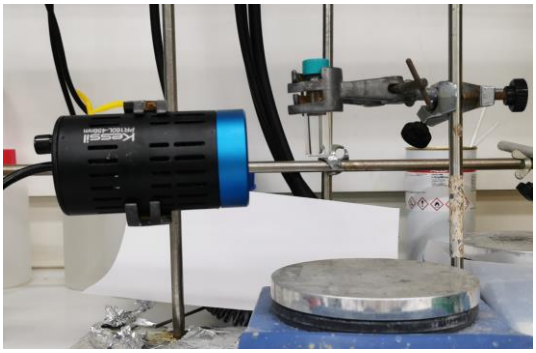

Figure 4.4. Kessil lamp set-up.

4.7.3.3 Set-up 3 - Temperature-controlled 4-position reactor with LED strip

For reactions where temperature control was employed, the photoreactor consisted of a 12.5 cm diameter jar fitted with 4 standard B29 size quickfit-glass joints arranged around a central B29 size joint. A commercial 1-meter LED strip was wrapped around the jar, followed by a layer of aluminium foil and cotton for insulation (Figure 4.5).

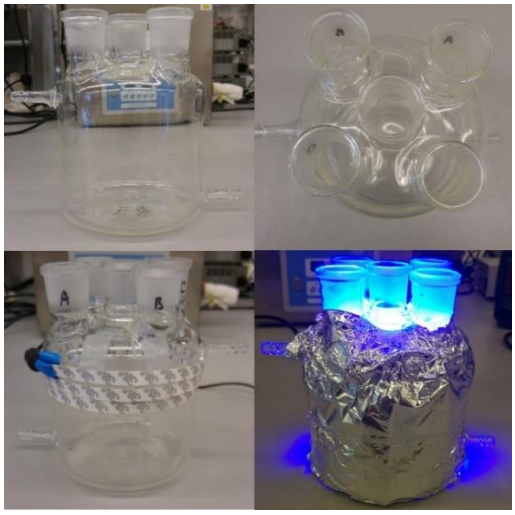

Figure 4.5. Photoreactor used for temperature-controlled reactions - pictures taken at different stages of the set-up assembly.

Each of the joints could be used to fit a standard 16 mm or 25 mm diameter Schlenk tube with a Teflon adaptor (Figure 4.6).

Figure 4.6. Teflon adaptors to use Schlenk tubes in the photoreactor.

An inlet/outlet system provided circulation of liquid (ethylene glycol/water mixture) from a Huber Minichiller 300 inside the jar. This setup allowed the performance of reactions at temperatures ranging from –20 ºC to 80 ºC with accurate control of the reaction temperature (± 1ºC, Figure 4.7).

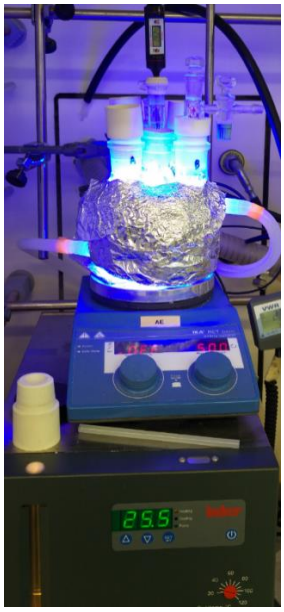

Figure 4.7. Fully assembled temperature-controlled photoreactor in operation.

In order to maintain consistent illumination between different experiments, only the four external positions were used to perform reactions. The central position was used to monitor the temperature using a thermometer inside another inserted Schlenk tube identical to those used to perform reactions, ensuring that the reaction mixtures were at the desired temperature.

4.7.3.4 Set-up 4 - Temperature controlled one-position reactor with LED strip

Our photoreactor for the enantioselective version of the Minisci reaction consisted of a consisted of a 4 cm diameter jar fitted with a standard 29 sized ground glass joint. A commercial 1 meter LED strip was wrapped around the jar, followed by a layer of aluminium foil and cotton for insulation. An inlet and an outlet allow the circulation of liquid from a Huber Minichiller 300 inside the jar. This setup allows to perform reactions at temperatures ranging from -20 ºC to 80 ºC with accurate control of the reaction temperature (± 1 ºC). An inlet and an outlet allow the circulation of liquid from a Huber Minichiller 300 inside the jar. This setup allows to perform reactions at temperatures ranging from -20 ºC to 80 ºC with accurate control of the reaction temperature (± 1ºC, Figure 4.8).

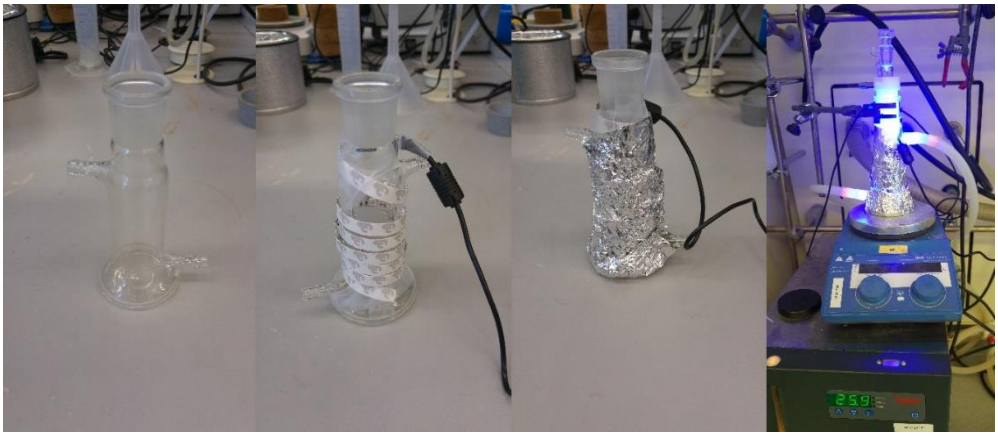

Figure 4.8. Fully assembled controlled temperature photoreactor in operation for enantioselective Minisci reaction.

4.7.4 Giese addition

4.7.4.1 General procedure A

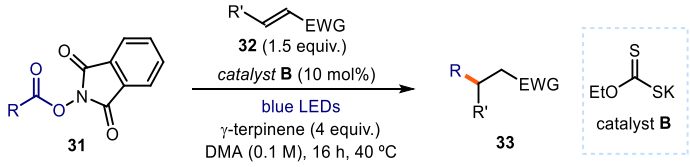

*Reactions performed using **set-up 1** in Figure 4.3*. In an oven dried vial with a Teflon septum screw cap, potassium ethyl xanthogenate **B** (3.2 mg, 0.02 mmol, 0.1 equiv.), *N*-hydroxyphthalimide ester **31** (0.2 mmol, 1 equiv.) and the electron-poor olefin **32** (0.3 mmol, 1.5 equiv., *if solid*), were dissolved in DMA (2 mL, synthesis grade solvent). Then, γ-terpinene (128 μL, 0.8 mmol, 4 equiv.) was added. The resulting orange mixture was degassed with

argon sparging for 60 seconds. If the electron-poor olefin **32** was *liquid*, it was added via syringe after the argon sparging. The vial was then placed in the 3D printed support photoreactor and irradiated under stirring for 16 hours, unless otherwise specified. The mixture was transferred to an extraction funnel, NaOH 1M solution was added, and the organic layer was extracted with DCM. The organic layer was washed with brine twice. The combined organic layers were dried over anhydrous $MgSO_4$, filtered, and concentrated to dryness. The crude residue was purified by column chromatography to afford the corresponding product **33** in the stated yield with >95% purity according to ^{1}H NMR analysis.

4.7.4.2 Characterization of products with general procedure A

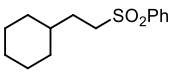

2-cyclohexylethyl)sulfonyl)benzene (33a): Synthesized according to General Procedure A using 1,3-dioxoisoindolin-2-yl cyclohexanecarboxylate **31a** (54.5 mg, 0.2 mmol, 1 equiv.) and phenyl vinyl sulfone **32a** (50.4 mg, 0.3 mmol, 1.5 equiv.). The crude mixture was purified by flash column chromatography on silica gel (5% AcOEt in hexanes as eluent) to afford **33a** (43.5 mg, 86% yield) as a white solid.

^{1}H NMR (500 MHz, $CDCl_3$) δ 7.94 – 7.85 (m, 2H), 7.69 – 7.61 (m, 1H), 7.61 – 7.52 (m, 2H), 3.13 – 3.05 (m, 2H), 1.71 – 1.54 (m, 7H), 1.28 (ddt, *J* = 14.6, 7.5, 3.8 Hz, 1H), 1.23 – 1.06 (m, 3H), 0.92 – 0.76 (m, 2H).

^{13}C NMR (126 MHz, $CDCl_3$) δ 139.4, 133.7, 129.4, 128.2, 54.5, 36.8, 32.9, 29.7, 26.4, 26.1.

Matching reported literature data.[47]

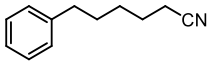

6-phenylhexanenitrile (33b): Synthesized according to General Procedure A using 5 equiv. of γ-terpinene, 1,3-dioxoisoindolin-2-yl 4-phenylbutanoate **31b** (62 mg, 0.2 mmol, 1 equiv.) and acrylonitrile **32b** (26.3 µL, 0.4 mmol, 2 equiv.). The crude mixture was purified by flash column chromatography on silica gel (5% AcOEt in hexanes as eluent) to afford **33b** (21 mg, 61% yield) as a yellow oil.

^{1}H NMR (400 MHz, $CDCl_3$) δ 7.33 – 7.24 (m, 2H), 7.23 – 7.14 (m, 3H), 2.64 (t, *J* = 7.6 Hz, 2H), 2.33 (t, *J* = 7.1 Hz, 2H), 1.75 – 1.62 (m, 4H), 1.54 – 1.42 (m, 2H).

^{13}C NMR (101 MHz, $CDCl_3$) δ 142.1, 128.5, 128.5, 126.0, 119.9, 35.7, 30.7, 28.4, 25.4, 17.2.

Matching reported literature data.[48]

---

[47] Chen, X.; Luo, X.; Peng, X.; Guo, J.; Zai, J.; Wang, P., Catalyst-Free Decarboxylation of Carboxylic Acids and Deoxygenation of Alcohols by Electro-Induced Radical Formation. *Chem. Eur. J.* **2020**, *26*, 3226-3230.
[48] Bhunia, A.; Bergander, K.; Studer, A., Cooperative Palladium/Lewis Acid-Catalyzed Transfer Hydrocyanation of Alkenes and Alkynes Using 1-Methylcyclohexa-2,5-diene-1-carbonitrile. *J. Am. Chem. Soc.* **2018**, *140*, 16353-16359.

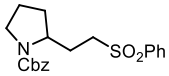

Benzyl 2-(2-(phenylsulfonyl)ethyl)pyrrolidine-1-carboxylate (33h): Synthesized according to General Procedure A using 1-benzyl 2-(1,3-dioxoisoindolin-2-yl) pyrrolidine-1,2-dicarboxylate **31c** (54.5 mg, 0.2 mmol, 1 equiv.) and phenyl vinyl sulfone **32a** (50.4 mg, 0.3 mmol, 1.5 equiv.). The crude mixture was purified by flash column chromatography on silica gel (20% AcOEt in hexanes as eluent) to afford **33h** (56 mg, 75% yield) as a white solid.

^{1}H NMR (400 MHz, $CDCl_3$) mixture of rotamers: δ 7.96 – 7.77 (m, 2H), 7.68 – 7.60 (m, 1H), 7.54 (d, *J* = 7.5 Hz, 2H), 7.40 – 7.20 (m, 5H), 5.05 (d, *J* = 7.6 Hz, 2H), 3.94 (d, *J* = 9.9 Hz, 1H), 3.58 – 3.28 (m, 2H), 3.27 – 2.91 (m, 2H), 2.23 – 1.74 (m, 5H), 1.63 (ddd, *J* = 11.3, 5.5, 3.0 Hz, 1H).

^{13}C NMR (101 MHz, $CDCl_3$) mixture of rotamers: δ 155.5, 139.3, 136.9, 133.8, 129.4, 128.6, 128.1, 127.9, 67.2, 66.9, 56.5, 55.9, 54.0, 53.7, 46.9, 46.5, 31.2, 30.7, 27.9, 23.8, 23.1.

Matching reported literature data.[49]

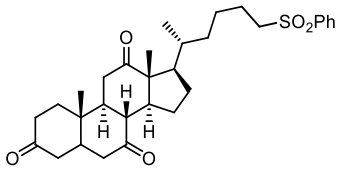

(5*S*,8*R*,9*S*,10*S*,13*R*,14*S*,17*R*)-10,13-dimethyl-17-(6-(phenylsulfonyl)hexan-2-yl)dodecahydro-3H-cyclopenta[a]phenanthrene-3,7,12(2H,4H)-trione (33k): Synthesized according to General Procedure A using 1,3-dioxoisoindolin-2-yl 4-((5*S*,8*R*,9*S*,10*S*,13*R*,14*S*,17*R*)-10,13-dimethyl-3,7,12-trioxohexadecahydro-1H-cyclopenta[a] phenanthren-17-yl)pentanoate **31d** (54.5 mg, 0.2 mmol, 1 equiv.) and phenyl vinyl sulfone **32a** (50.4 mg, 0.3 mmol, 1.5 equiv.). The crude mixture was purified by flash column chromatography on silica gel (50% AcOEt in hexanes as eluent) to afford **33k** (48.0 mg, 46% yield) as a white solid.

^{1}H NMR (400 MHz, $CDCl_3$) δ 7.95 – 7.85 (m, 2H), 7.70 – 7.61 (m, 1H), 7.61 – 7.53 (m, 2H), 3.16 – 3.00 (m, 2H), 2.95 – 2.78 (m, 3H), 2.38 – 2.17 (m, 6H), 2.16 – 2.06 (m, 2H), 2.02 – 1.90 (m, 4H), 1.88 – 1.52 (m, 5H), 1.47 – 1.30 (m, 1H), 1.39 (s, 3H), 1.32 – 1.12 (m, 5H), 1.04 (s, 3H), 0.78 (d, *J* = 6.6 Hz, 3H).

^{13}C NMR (101 MHz, $CDCl_3$) δ 212.1, 209.1, 208.9, 139.4, 133.8, 129.4, 128.2, 57.0, 56.5, 51.9, 49.1, 47.0, 45.8, 45.7, 45.1, 42.9, 38.8, 36.6, 36.2, 35.9, 35.4, 34.9, 28.0, 25.4, 25.3, 23.1, 22.0, 19.0, 12.0.

Matching reported literature data.[47]

[49] Chu, L.; Ohta, C.; Zuo, Z.; MacMillan, D. W. C., Carboxylic Acids as A Traceless Activation Group for Conjugate Additions: A Three-Step Synthesis of (±)-Pregabalin. *J. Am. Chem. Soc.* **2014**, *136*, 10886-10889.

4.7.4.3 General procedure B (one-pot telescoped from carboxylic acids)

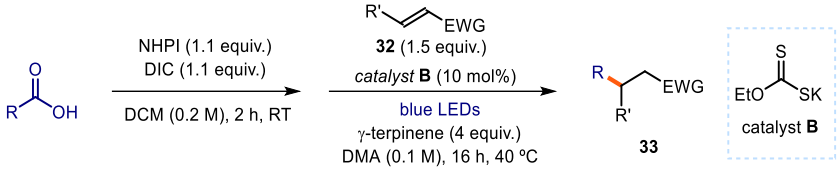

*Reactions performed using **set-up 1** in Figure 4.3*. In an oven dried vial with a Teflon septum screw cap, carboxylic acid (0.2 mmol, 1 equiv.) and *N*-hydroxyphthalimide (NHPI, 35.8 mg, 0.22 mmol, 1.1 equiv.) were dissolved in CH_2Cl_2 (1 mL, HPLC grade) and *N,N'*-diisopropylcarbodiimide (DIC, 34 µL, 0.22 mmol, 1.1 equiv.) was added via syringe. The reaction was stirred at ambient temperature until complete consumption of the carboxylic acid was observed by TLC (usually 1-2 hours). The crude reaction mixture was concentrated under vacuum to obtain the crude phthalimide ester, which was used without further purification in the next step.

In the same vial containing the crude phthalimide ester, xanthogenate **B** (3.2 mg, 0.02 mmol, 0.1 equiv.) and the electron-poor olefin **32** (0.3 mmol, 1.5 equiv., *if solid*) were dissolved in DMA (2 mL, synthesis grade). Next, γ-terpinene (128 µL, 0.8 mmol, 4 equiv.) was added and the resulting orange mixture was degassed with argon sparging for 60 seconds. If the electron-poor olefin **32** was *liquid*, it was added via syringe after the argon sparging. The vial was then placed in the 3D printed support photoreactor and irradiated under stirring for 16 hours, if not otherwise specified. The mixture was transferred to an extraction funnel, NaOH 1M solution was added and the organic layer was extracted with CH_2Cl_2. The organic layer was washed with brine twice. The combined organic layers were dried over anhydrous $MgSO_4$, filtered, and concentrated to dryness. The crude residue was purified by column chromatography to afford the corresponding product in the stated yield with >95% purity according to ^{1}H NMR analysis.

4.7.4.4 Characterization of products with general procedure B

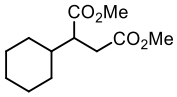

dimethyl 2-cyclohexylsuccinate (33c): Synthesized according to General Procedure B using 2 equiv. of γ-terpinene, cyclohexanecarboxylic acid (25.6 mg, 0.2 mmol, 1 equiv.) and dimethyl fumarate **32c** (43 mg, 0.3 mmol, 1.5 equiv.). The crude mixture was purified by flash column chromatography on silica gel (5% AcOEt in hexanes as eluent) to afford **33c** (44 mg, 95% yield) as a yellow oil.

^{1}H NMR (500 MHz, $CDCl_3$) δ 3.69 (s, 3H), 3.66 (s, 3H), 2.78 – 2.66 (m, 2H), 2.45 (dt, *J* = 13.1, 8.9 Hz, 1H), 1.78 – 1.69 (m, 2H), 1.69 – 1.52 (m, 4H), 1.31 – 1.15 (m, 2H), 1.15 – 1.07 (m, 1H), 1.06 – 0.92 (m, 2H).

^{13}C NMR (126 MHz, $CDCl_3$) δ 175.1, 173.1, 51.9, 51.7, 47.2, 40.1, 33.4, 30.8, 30.3, 26.4, 26.3.

Matching reported literature data.[47]

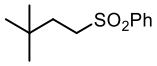

((3,3-dimethylbutyl)sulfonyl)benzene (33d): Synthesized according to General Procedure B using pivalic acid (20.4 mg, 0.2 mmol, 1 equiv.) and phenyl vinyl sulfone **32a** (50.4 mg, 0.3 mmol, 1.5 equiv.). The crude mixture was purified by flash column chromatography on silica gel (7% AcOEt in hexanes as eluent) to afford **33d** (33.0 mg, 73% yield) as a yellow oil.

^{1}H NMR (400 MHz, $CDCl_3$) δ 7.98 – 7.85 (m, 2H), 7.71 – 7.62 (m, 1H), 7.65 – 7.53 (m, 2H), 3.10 – 3.01 (m, 2H), 1.64 – 1.55 (m, 2H), 0.86 (s, 9H).

^{13}C NMR (101 MHz, $CDCl_3$) δ 142.1, 128.5, 128.5, 126.0, 119.9, 35.7, 30.7, 28.4, 25.4, 17.2.

Matching reported literature data.[47]

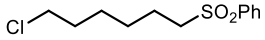

((7-chloroheptyl)sulfonyl)benzene (33e): Synthesized according to General Procedure B using 5-Chlorovaleric acid (27.3 mg, 0.2 mmol, 1 equiv.) and phenyl vinyl sulfone **32a** (50.4 mg, 0.3 mmol, 1.5 equiv.). The crude mixture was purified by flash column chromatography on silica gel (20% DCM in hexanes as eluent) to afford **33e** (29.1 mg, 56% yield) as a white solid.

^{1}H NMR (400 MHz, $CDCl_3$) δ 7.95 – 7.88 (m, 2H), 7.69 – 7.64 (m, 1H), 7.61 – 7.55 (m, 2H), 3.50 (t, *J* = 6.5 Hz, 2H), 3.12 – 3.05 (m, 2H), 1.77 – 1.71 (m, 4H), 1.44 – 1.39 (m, 4H).

^{13}C NMR (101 MHz, $CDCl_3$) δ 139.3, 133.8, 129.4, 128.2, 56.3, 44.9, 32.2, 29.8, 27.7, 26.4, 22.7.

Matching reported literature data.[50]

4.7.4.5 General procedure C (one-pot domino from carboxylic acids)

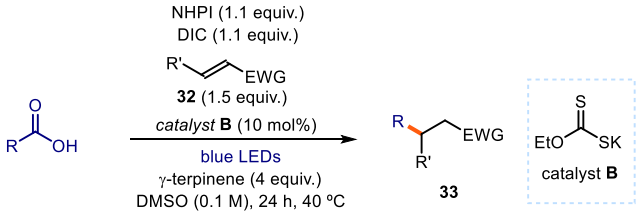

*Reactions performed using **set-up 1** in Figure 4.3*. In an oven dried vial with a Teflon septum screw cap, carboxylic acid (0.2 mmol, 1 equiv.), *N*-hydroxyphthalimide (NHPI, 35.8 mg, 0.22 mmol, 1.1 equiv.), xanthogenate catalyst **B** (3.2 mg, 0.02 mmol, 0.1 equiv.), and the electron-poor olefin **32** (0.3 mmol, 1.5 equiv., *if solid*) were dissolved in DMSO (2 mL) and *N,N'*-diisopropylcarbodiimide (DIC, 34 μL, 0.22 mmol, 1.1 equiv.) was added via syringe. Next,

[50] Li, D.; Ma, T.-K.; Scott, R. J.; Wilden, J. D. Electrochemical radical reactions of alkyl iodides: a highly efficient, clean, green alternative to tin reagents, *Chem. Sci.* **2020**, *11*, 5333-5338.

γ-terpinene (128 μL, 0.8 mmol, 4 equiv.) was added and the resulting orange mixture was degassed with argon sparging for 60 seconds. If the electron-poor olefin **32** were *liquid*, it was added via syringe after the argon sparging. The vial was then placed in the 3D printed support photoreactor and irradiated under stirring for 24 hours, unless otherwise specified. The mixture was transferred to an extraction funnel, NaOH 1M solution was added and the organic layer was extracted with CH_2Cl_2. The organic layer was washed with brine twice. The combined organic layers were dried over anhydrous $MgSO_4$, filtered, and concentrated to dryness. The crude residue was purified by column chromatography to afford the corresponding product in the stated yield with >95% purity according to ^{1}H NMR analysis.

4.7.4.6 Characterization of products with general procedure C

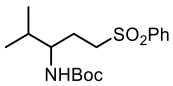

***tert*-butyl (4-methyl-1-(phenylsulfonyl)pentan-3-yl)carbamate (33f):** Synthesized according to General Procedure C using NMP as solvent, L-valine (43.5 mg, 0.2 mmol, 1 equiv.) and phenyl vinyl sulfone **32a** (50.4 mg, 0.3 mmol, 1.5 equiv.). The crude mixture was purified by flash column chromatography on silica gel (25% AcOEt in hexanes as eluent) to afford **33f** (63 mg, 92% yield) as a white solid.

^{1}H NMR (500 MHz, $CDCl_3$) δ 7.93 – 7.88 (m, 2H), 7.69 – 7.63 (m, 1H), 7.57 (dd, *J* = 8.4, 7.1 Hz, 2H), 4.32 (d, *J* = 10.1 Hz, 1H), 3.42 (td, *J* = 10.4, 4.8 Hz, 1H), 3.15 (ddd, *J* = 9.1, 6.1, 1.7 Hz, 2H), 1.93 (tdd, *J* = 12.1, 7.4, 3.4 Hz, 1H), 1.82 – 1.61 (m, 2H), 1.40 (s, 9H), 0.87 (dd, *J* = 10.0, 6.8 Hz, 6H).

^{13}C NMR (126 MHz, $CDCl_3$) δ 156.1, 139.4, 133.9, 129.5, 128.1, 79.7, 54.7, 54.1, 32.8, 28.5, 25.9, 19.2, 17.8.

Matching reported literature data.[51]

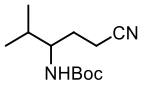

***tert*-butyl (1-cyano-4-methylpentan-3-yl)carbamate (33g):** Synthesized according to General Procedure C using 5 equiv. of γ-terpinene, L-valine (43.5 mg, 0.2 mmol, 1 equiv.) and acrylonitrile **32b** (26.3 μL, 0.4 mmol, 2 equiv.). The crude mixture was purified by flash column chromatography on silica gel (15% AcOEt in hexanes as eluent) to afford **33g** (27 mg, 60% yield) as a yellow oil.

^{1}H NMR (400 MHz, $CDCl_3$) δ 4.34 (d, *J* = 9.9 Hz, 1H), 3.45 (tdd, *J* = 10.4, 5.5, 3.4 Hz, 1H), 2.49 – 2.30 (m, 2H), 1.90 (td, *J* = 11.7, 9.8, 5.5 Hz, 1H), 1.72 (dt, *J* = 13.0, 6.5 Hz, 1H), 1.62 (td, *J* = 15.0, 14.5, 9.7 Hz, 1H), 1.44 (s, 9H), 0.91 (dd, *J* = 10.4, 6.8 Hz, 6H).

^{13}C NMR (101 MHz, $CDCl_3$) δ 156.1, 119.9, 79.7, 55.4, 32.5, 29.4, 28.5, 19.2, 17.9, 14.7.

---

[51] Yoshimi, Y.; Masuda, M.; Mizunashi, T.; Nishikawa, K.; Maeda, K.; Koshida, N.; Itou, T.; Morita, T.; Hatanaka, M., Inter- and Intramolecular Addition Reactions of Electron-Deficient Alkenes with Alkyl Radicals, Generated by SET-Photochemical Decarboxylation of Carboxylic Acids, Serve as a Mild and Efficient Method for the Preparation of γ-Amino Acids and Macrocyclic Lactones. *Org. Lett.* **2009**, *11*, 4652-4655.

Matching reported literature data.[51]

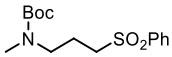

***tert*-butyl methyl(3-(phenylsulfonyl)propyl)carbamate (33i):** Synthesized according to General Procedure C using *N*-(tert-butoxycarbonyl)-N-methylglycine (38 mg, 0.2 mmol, 1 equiv.) and phenyl vinyl sulfone **32a** (50.4 mg, 0.3 mmol, 1.5 equiv.). The crude mixture was purified by flash column chromatography on silica gel (20% AcOEt in hexanes as eluent) to afford **33i** (47 mg, 75% yield) as a yellow oil.

^{1}H NMR (400 MHz, $CDCl_3$) mixture of rotamers: δ 7.94 – 7.86 (m, 2H), 7.70 – 7.62 (m, 1H), 7.57 (dd, *J* = 8.3, 6.8 Hz, 2H), 3.29 (t, *J* = 6.8 Hz, 2H), 3.11 – 2.99 (m, 2H), 2.79 (s, 3H), 1.99 – 1.87 (m, 2H), 1.40 (s, 9H).

^{13}C NMR (101 MHz, $CDCl_3$) mixture of rotamers: δ 155.9, 139.2, 133.9, 129.5, 128.1, 79.9, 53.9, 47.4, 34.3, 28.5, 21.0.

HRMS: calculated for $C_{15}H_{23}NNaO_4S$ ($M+Na^+$): 336.1240, found 336.1236.

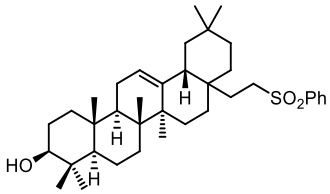

(3*S*,4a*R*,6a*R*,6b*S*,12a*R*,14a*R*,14b*R*)-4,4,6a,6b,11,11,14b-heptamethyl-8a-(2-(phenylsulfonyl)ethyl)-1,2,3,4,4a,5,6,6a,6b,7,8,8a,9,10,11,12,12a,14,14a,14b-icosahydropicen-3-ol (33j): Synthesized according to General Procedure C using NMP as solvent, oleanolic acid (91 mg, 0.2 mmol, 1 equiv) and phenyl vinyl sulfone **32a** (50.4 mg, 0.3 mmol, 1.5 equiv.). The crude mixture was purified by flash column chromatography on silica gel (40% AcOEt in hexanes as eluent) to afford **33j** (84 mg, 72% yield) as light-yellow solid.

^{1}H NMR (400 MHz, $CDCl_3$) δ 7.90 – 7.84 (m, 2H), 7.67 – 7.59 (m, 1H), 7.58 – 7.50 (m, 2H), 5.15 (t, *J* = 3.6 Hz, 1H), 3.19 (dd, *J* = 10.7, 4.8 Hz, 1H), 3.01 (dtd, *J* = 37.9, 13.5, 4.3 Hz, 2H), 2.01 – 1.76 (m, 7H), 1.66 (t, *J* = 13.5 Hz, 1H), 1.62 –z 1.36 (m, 7H), 1.37 – 1.26 (m, 3H), 1.23 – 1.11 (m, 4H), 1.09 (s, 3H), 1.02 (dd, *J* = 13.7, 2.1 Hz, 1H), 0.97 (s, 3H), 0.94 – 0.90 (m, 1H), 0.88 (s, 3H), 0.85 (s, 3H), 0.82 (s, 3H), 0.77 (s, 3H), 0.68 (dd, *J* = 11.5, 1.9 Hz, 1H), 0.60 (s, 3H).

^{13}C NMR (101 MHz, $CDCl_3$) δ 143.6, 139.3, 133.6, 129.4, 128.1, 123.1, 79.0, 55.2, 51.6, 47.6, 46.9, 46.5, 41.6, 39.7, 38.9, 38.7, 37.0, 34.7, 34.3, 33.2, 32.9, 32.5, 31.9, 31.0, 29.8, 28.2, 27.3, 26.1, 25.5, 23.6, 23.3, 18.4, 16.5, 15.7, 15.6.

Matching reported literature data.[47]

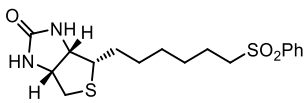

(3a*S*,4*S*,6a*R*)-4-(6-(phenylsulfonyl)hexyl)tetrahydro-1H-thieno[3,4-d]imidazol-2(3H)-one (33l): Synthesized

according to General Procedure C using 4 mL of DMSO, biotin (49 mg, 0.2 mmol, 1 equiv.) and phenyl vinyl sulfone **32a** (50.4 mg, 0.3 mmol, 1.5 equiv.). The crude mixture was purified by flash column chromatography on silica gel (2-5% MeOH in DCM as eluent) to afford **33j** (48 mg, 65% yield) as a yellow oil.

^{1}H NMR (500 MHz, Methanol-d_4) δ 7.99 – 7.89 (m, 2H), 7.77 – 7.70 (m, 1H), 7.72 – 7.58 (m, 2H), 4.53 – 4.46 (m, 1H), 4.29 (ddd, *J* = 12.2, 7.9, 4.5 Hz, 1H), 3.24 – 3.19 (m, 2H), 3.19 – 3.14 (m, 1H), 2.92 (dt, *J* = 12.7, 5.1 Hz, 1H), 2.70 (dd, *J* = 12.7, 4.4 Hz, 1H), 1.66 (tdd, *J* = 15.3, 8.3, 4.4 Hz, 3H), 1.53 (ddd, *J* = 16.8, 8.8, 5.5 Hz, 1H), 1.45 – 1.27 (m, 6H).

^{13}C NMR (101 MHz, $CDCl_3$) δ 164.5, 139.2, 133.8, 129.4, 128.1, 62.4, 60.8, 56.1, 55.8, 40.6, 31.4, 31.0, 28.8, 28.7, 28.4, 27.9, 22.7, 22.5, 14.1.

HRMS: calculated for $C_{17}H_{24}N_2NaO_3S_2$ ($M+Na^+$): 391.1120, found 391.1121.

4.7.4.7 General procedure D (using pyridinium salts)

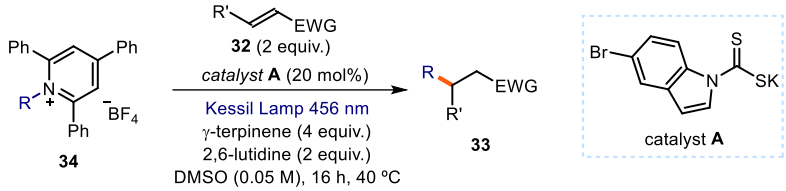

*Reactions performed using **set-up 2** in Figure 4.4.* In an oven dried vial, with a Teflon septum screw cap, dithiocarbamate **A** (12.4 mg, 0.04 mmol, 0.2 equiv.), pyridinium salt **34** (0.2 mmol, 1 equiv.) and the electron-poor olefin **32** (0.4 mmol, 2 equiv.), were dissolved in DMSO (4 mL). Then, γ-terpinene (128 μL, 0.8 mmol, 4 equiv.) and 2,6-lutidine (46 μL, 0.4 mmol, 2 equiv.) were added. The resulting orange mixture was degassed with argon sparging for 60 seconds. The vial was then placed at 2-3 cm of a 50 W Kessil blue LED lamp and irradiated under stirring for 16 hours. The mixture was transferred to an extraction funnel, $NaHCO_3$ sat. solution was added and the organic layer was extracted with EtOAc. The organic layer was washed with brine twice. The combined organic layers were dried over anhydrous $MgSO_4$, filtered, and concentrated to dryness. The crude residue was purified by column chromatography to afford the corresponding product in the stated yield with >95% purity according to ^{1}H NMR analysis.

4.7.4.8 Characterization of products with general procedure D

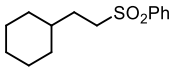

((2-cyclohexylethyl)sulfonyl)benzene (33a): Synthesized according to General Procedure D using 1-cyclohexyl-2,4,6-triphenylpyridin-1-ium tetrafluoroborate **34a** (95 mg, 0.2 mmol, 1 equiv.) and phenyl vinyl sulfone **32a** (67 mg, 0.4 mmol, 2 equiv.). The crude mixture was purified by flash column chromatography on silica gel (10% AcOEt in hexanes as eluent) to afford **33a** (34 mg, 67% yield) as a white solid.

^{1}H NMR (500 MHz, $CDCl_3$) δ 7.94 – 7.85 (m, 2H), 7.69 – 7.61 (m, 1H), 7.61 – 7.52 (m, 2H), 3.13 – 3.05 (m, 2H), 1.71 – 1.54 (m, 7H), 1.28 (ddt, *J* = 14.6, 7.5, 3.8 Hz, 1H), 1.23 – 1.06 (m, 3H), 0.92 – 0.76 (m, 2H).

^{13}C NMR (126 MHz, $CDCl_3$) δ 139.4, 133.7, 129.4, 128.2, 54.5, 36.8, 32.9, 29.7, 26.4, 26.1.

Matching reported literature data.[47]

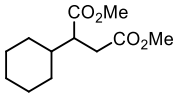

dimethyl 2-cyclohexylsuccinate (33c): Synthesized according to General Procedure D using 2 equiv. of γ-terpinene, 1-cyclohexyl-2,4,6-triphenylpyridin-1-ium tetrafluoroborate **34a** (95 mg, 0.2 mmol, 1 equiv.) and dimethyl fumarate **32c** (57 mg, 0.4 mmol, 2 equiv.). The crude mixture was purified by flash column chromatography on silica gel (5% AcOEt in hexanes as eluent) to afford **33c** (41 mg, 90% yield) as a yellow oil.

^{1}H NMR (400 MHz, $CDCl_3$) δ 3.69 (s, 3H), 3.66 (s, 3H), 2.78 – 2.66 (m, 2H), 2.45 (dt, *J* = 13.1, 8.9 Hz, 1H), 1.78 – 1.69 (m, 2H), 1.69 – 1.52 (m, 4H), 1.31 – 1.15 (m, 2H), 1.15 – 1.07 (m, 1H), 1.06 – 0.92 (m, 2H).

^{13}C NMR (126 MHz, $CDCl_3$) δ 175.1, 173.1, 51.9, 51.7, 47.2, 40.1, 33.4, 30.8, 30.3, 26.4, 26.3.

Matching reported literature data.[47]

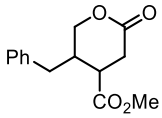

33m

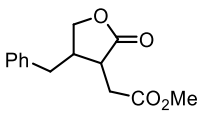

33m'

methyl 5-benzyl-2-oxotetrahydro-2H-pyran-4-carboxylate (33m): Synthesized according to General Procedure D using 2 equiv. of γ-terpinene, 1-(1-hydroxy-3-phenylpropan-2-yl)-2,4,6-triphenylpyridin-1-ium tetrafluoroborate **34b** (106 mg, 0.2 mmol, 1 equiv.) and dimethyl fumarate **32c** (57 mg, 0.4 mmol, 2 equiv.). The crude mixture was purified by flash column chromatography on silica gel (10% AcOEt in hexanes as eluent) to afford an unseparable mixture of regiosiomers **33m**/**33m'** ***(3.8:1)*** (27 mg, 54% yield) as a yellow oil. Corrected yield for **33m** (42% yield)

Products formed upon intramolecular esterification promoted by the acidic conditions delivered by the silica during purification.

^{1}H NMR (400 MHz, $CDCl_3$) mixture of regiosiomers δ 7.35 – 7.28 (m, 2.5H), 7.28 – 7.21 (m, 1.25H), 7.19 – 7.10 (m, 2.5H), 4.35 – 4.28 (m, 1H), 4.14 – 4.06 (m, 0.5H), 3.96 – 3.88 (m, 1H), 3.74 (s, 0.75H), 3.69 (s, 3H), 3.31 – 3.23 (m, 0.25H), 3.05 – 2.85 (m, 1.5H), 2.85 – 2.66 (m, 3.25H), 2.63 (d, *J* = 10.2 Hz, 0.25H), 2.61 – 2.55 (m, 2H), 2.34 (dd, *J* = 13.7, 11.9 Hz, 0.25H).

^{13}C NMR (101 MHz, $CDCl_3$) mixture of regiosiomers: δ 177.8, 171.6, 137.8, 129.1, 129.0, 129.0, 128.7, 127.1, 126.9, 71.4, 70.1, 52.3, 52.2, 42.4, 42.0, 40.8, 39.7, 38.4, 33.6, 33.3, 30.2, 29.8.

HRMS: calculated for $C_{14}H_{16}NaO_4$ ($M+Na^+$): 271.0941, found 271.0939.

4.7.4.9 General procedure E (telescoped reaction from amine)

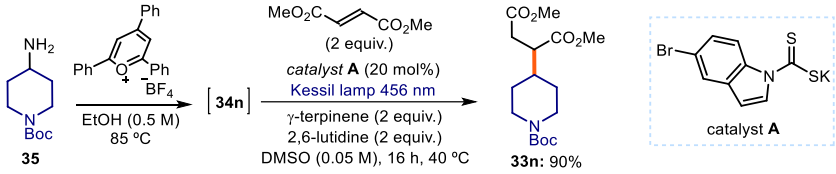

*Reactions performed using **set-up 2** in Figure 4.4.* In an oven dried vial, with a Teflon septum screw cap, primary amine (0.22 mmol, 1.1 equiv.) and 2,4,6-triphenylpyrylium tetrafluoroborate (79.2 mg, 0.2 mmol, 1 equiv.) were dissolved in ethanol (0.4 mL, HPLC grade). The reaction was stirred at 80 ºC for 4 hours. In the same vial without evaporating the solvent, dithiocarbamate **A** (12.4 mg, 0.04 mmol, 0.2 equiv.), electron-poor olefin **32** (0.4 mmol, 2 equiv.), DMSO (4 mL), γ-terpinene (64 µL, 0.4 mmol, 2 equiv.) and 2,6-lutidine (46 µL, 0.4 mmol, 2 equiv.) were added sequentially. The resulting orange mixture was degassed with argon sparging for 60 seconds. The vial was then placed at 2-3 cm of a 50 W Kessil blue LED lamp and irradiated under stirring for 16 hours. The mixture was transferred to an extraction funnel, saturated aqueous $NaHCO_3$ was added, and the organic layer extracted with EtOAc. The organic layer was washed with brine twice. The combined organic layers were dried over anhydrous $MgSO_4$, filtered, and concentrated to dryness. The crude residue was purified by column chromatography to afford the corresponding product in the stated yield with >95% purity according to ^{1}H NMR analysis.

A control experiment without catalyst **A** delivered no conversion of the pyridinium salt upon irradiation.

4.7.4.10 Characterization of products with general procedure E

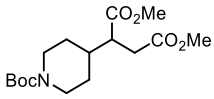

dimethyl 2-(1-(tert-butoxycarbonyl)piperidin-4-yl)succinate (33n): Synthesized according to General Procedure E using 2 equiv. of γ-terpinene, *tert*-butyl 4-aminopiperidine-1-carboxylate (40 mg, 0.2 mmol, 1 equiv.) and dimethyl fumarate **32c** (57 mg, 0.4 mmol, 2 equiv.). The crude mixture was purified by flash column chromatography on silica gel (0-40% AcOEt in hexanes as eluent) to afford **33n** (59 mg, 90% yield) as a yellow oil.

^{1}H NMR (400 MHz, $CDCl_3$) δ 4.12 (d, *J* = 13.3 Hz, 2H), 3.70 (s, 3H), 3.66 (s, 3H), 2.81 – 2.68 (m, 2H), 2.63 (tt, *J* = 13.0, 3.0 Hz, 2H), 2.52 – 2.41 (m, 1H), 1.73 (tdd, *J* = 12.3, 6.1, 3.6 Hz, 1H), 1.57 (ddt, *J* = 23.3, 13.0, 3.0 Hz, 2H), 1.44 (s, 9H), 1.34 – 1.15 (m, 2H).

^{13}C NMR (126 MHz, $CDCl_3$) δ 174.7, 172.9, 155.1, 79.9, 52.2, 46.6, 44.2, 38.7, 33.6, 33.6, 29.9, 29.7, 28.8, 28.8.

HRMS: calculated for $C_{16}H_{27}NNaO_6$ ($M+Na^+$): 352.1731, found 352.1726.

4.7.5 Reduction

4.7.5.1 General procedure F (Barton decarboxylation)

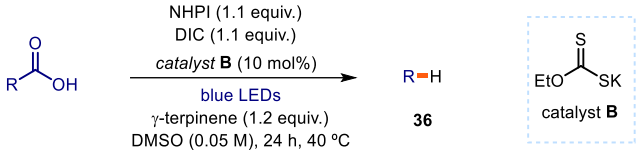

*Reactions performed using **set-up 1** in Figure 4.3.* In an oven dried vial, with a Teflon septum screw cap, carboxylic acid (0.2 mmol, 1 equiv.), *N*-hydroxyphthalimide (NHPI, 35.8 mg, 0.22 mmol, 1.1 equiv.) and xanthogenate **B** (3.2 mg, 0.02 mmol, 0.1 equiv.) were dissolved in DMSO (4 mL) and *N,N'*-diisopropylcarbodiimide (DIC, 34 μL, 0.22 mmol, 1.1 equiv.) was added via syringe. Then, γ-terpinene (38 μL, 0.24 mmol, 1.2 equiv.) was added. The resulting orange mixture was degassed with argon sparging for 60 seconds. The vial was then placed in the 3D printed support photoreactor and irradiated under stirring for 24 hours, unless otherwise specified. The mixture was transferred to an extraction funnel, NaOH 1M solution was added and the organic layer was extracted with CH_2Cl_2. The organic layer was washed with brine twice. The combined organic layers were dried over anhydrous $MgSO_4$, filtered, and concentrated to dryness. The crude residue was purified by column chromatography to afford the corresponding product in the stated yield with >95% purity according to ^{1}H NMR analysis.

4.7.5.2 Characterization of products with general procedure F

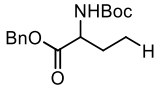

benzyl (*S*)-2-((tert-butoxycarbonyl)amino)butanoate (36a): Synthesized according to General Procedure F using (*S*)-5-(benzyloxy)-4-((*tert*-butoxycarbonyl)amino)-5-oxopentanoic acid (67 mg, 0.2 mmol, 1 equiv.). The crude mixture was purified by flash column chromatography on silica gel (25% AcOEt in hexanes as eluent) to afford **36a** (38 mg, 65% yield) as a yellow oil.

^{1}H NMR (400 MHz, $CDCl_3$) δ 7.41 – 7.28 (m, 5H), 5.24 – 5.10 (m, 2H), 5.04 (d, *J* = 8.3 Hz, 1H), 4.30 (t, *J* = 7.1 Hz, 1H), 1.93 – 1.80 (m, 1H), 1.69 (dt, *J* = 14.2, 7.2 Hz, 1H), 1.44 (s, 9H), 0.90 (t, *J* = 7.5 Hz, 3H).

^{13}C NMR (101 MHz, $CDCl_3$) δ 172.8, 155.5, 135.6, 128.7, 128.5, 128.4, 79.9, 67.1, 54.8, 28.5, 26.1, 9.7.

Matching reported literature data.[38a]

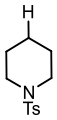

1-tosylpiperidine (36b): Synthesized according to General Procedure F using 1-tosylpiperidine-4-carboxylic acid (57 mg, 0.2 mmol, 1 equiv.). The crude mixture was purified by flash column chromatography on silica gel (10% AcOEt in hexanes as eluent) to afford **36b** (37 mg, 77% yield) as a white solid.

^{1}H NMR (500 MHz, $CDCl_3$) δ 7.66 – 7.60 (m, 2H), 7.34 – 7.28 (m, 2H), 2.99 – 2.93 (m, 4H), 2.42 (s, 3H), 1.63 (p, *J* = 5.9 Hz, 4H), 1.40 (tt, *J* = 8.2, 4.7 Hz, 2H).

^{13}C NMR (126 MHz, $CDCl_3$) δ 143.4, 133.5, 129.7, 127.8, 47.1, 25.3, 23.7, 21.6.

Matching reported literature data. [38a]

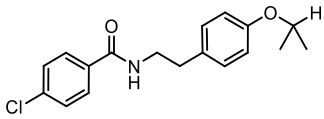

4-chloro-N-(4-isopropoxyphenethyl)benzamide (36c): Synthesized according to General Procedure F using Bezafibrate (72 mg, 0.2 mmol, 1 equiv.). The crude mixture was purified by flash column chromatography on silica gel (25% AcOEt in hexanes as eluent) to afford **36c** (32 mg, 50% yield) as a white solid.

^{1}H NMR (400 MHz, $CDCl_3$) mixture of rotamers: δ 7.65 – 7.59 (m, 2H), 7.37 (dd, *J* = 8.6, 2.0 Hz, 2H), 7.15 – 7.04 (m, 2H), 6.89 – 6.79 (m, 2H), 6.13 (s, 1H), 4.52 (p, *J* = 6.1 Hz, 1H), 3.67 (qd, *J* = 6.7, 6.3, 3.7 Hz, 2H), 2.85 (t, *J* = 6.9 Hz, 2H), 1.33 (d, *J* = 6.1 Hz, 6H).

^{13}C NMR (101 MHz, $CDCl_3$) mixture of rotamers: δ 166.6, 156.8, 137.8, 133.1, 130.6, 130.0, 129.9, 129.0, 128.4, 116.3, 115.8, 70.1, 41.5, 34.8, 22.2.

HRMS: calculated for $C_{16}H_{18}ClN_4NaO$ ($M+Na^+$): 340.1061, found 340.1075 (+4.1 ppm).

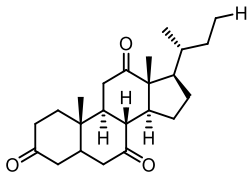

(5*S*,8*R*,9*S*,10*S*,13*R*,14*S*,17*R*)-17-(sec-butyl)-10,13-dimethyldodecahydro-3H-cyclopenta[a]phenanthrene-3,7,12(2H,4H)-trione (36d): Synthesized according to General Procedure F using dehydrocholic acid (81 mg, 0.2 mmol, 1 equiv.). The crude mixture was purified by flash column chromatography on silica gel (30% AcOEt in hexanes as eluent) to afford **36d** (37 mg, 51% yield) as a light-yellow solid.

^{1}H NMR (400 MHz, $CDCl_3$) δ 2.96 – 2.80 (m, 3H), 2.39 – 2.17 (m, 6H), 2.13 (dd, *J* = 12.5, 4.8 Hz, 2H), 2.09 – 1.90 (m, 4H), 1.85 (td, *J* = 11.2, 7.0 Hz, 1H), 1.68 – 1.56 (m, 2H), 1.52 – 1.44 (m, 1H), 1.40 (s, 3H), 1.35 – 1.20 (m, 3H), 1.20 – 1.10 (m, 1H), 1.07 (s, 3H), 0.85 (dd, *J* = 15.9, 6.9 Hz, 6H).

^{13}C NMR (101 MHz, $CDCl_3$) δ 212.2, 209.2, 208.9, 57.0, 52.0, 49.2, 47.0, 45.7, 45.6, 45.1, 42.9, 38.8, 37.6, 36.6, 36.2, 35.4, 28.0, 27.8, 25.4, 22.1, 18.6, 12.0, 11.0.

Matching reported literature data.[38a]

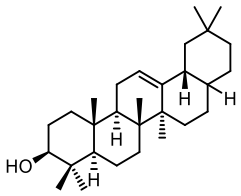

(3*S*,4a*R*,6a*R*,6b*S*,12a*R*,14a*R*,14b*R*)-4,4,6a,6b,11,11,14b-heptamethyl-1,2,3,4,4a,5,6,6a,6b,7,8,8a,9,10,11,12,12a,14,14a,14b-icosahydropicen-3-ol (36e): Synthesized according to General Procedure F using oleanolic acid (91 mg, 0.2 mmol, 1 equiv). The crude mixture was purified by flash column chromatography on silica gel (15% AcOEt in hexanes as eluent) to afford **36e** (74 mg, 90% yield) as white solid.

^{1}H NMR (400 MHz, $CDCl_3$) δ 5.19 (t, *J* = 3.7 Hz, 1H), 3.22 (ddz, *J* = 11.0, 5.0 Hz, 1H), 2.34 (dt, *J* = 13.7, 4.8 Hz, 1H), 1.91 – 1.83 (m, 2H), 1.83 – 1.75 (m, 1H), 1.74 – 1.65 (m, 2H), 1.65 – 1.58 (m, 4H), 1.5 – 1.54 (m, 2H), 1.50 – 1.31 (m, 6H), 1.29 – 1.17 (m, 4H), 1.11 (d, *J* = 0.9 Hz, 3H), 1.08 – 1.04 (m, 1H), 1.02 – 0.96 (m, 4H), 0.93 (s, 3H), 0.89 (s, 3H), 0.87 (s, 6H), 0.79 (s, 3H), 0.77 – 0.70 (m, 1H).

^{13}C NMR (101 MHz, $CDCl_3$) δ 146.1, 121.2, 79.2, 55.4, 47.9, 45.1, 42.6, 41.1, 39.3, 38.9, 38.6, 37.3, 35.9, 33.8, 33.8, 33.2, 31.3, 31.2, 29.9, 28.3, 28.1, 27.4, 25.2, 24.0, 23.5, 22.4, 18.6, 17.6, 15.8, 15.5.

Matching reported literature data.[38a]

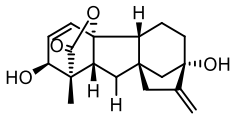

(1*S*,2*S*,4a*R*,4b*R*,7*S*,9a*R*,10a*R*)-2,7-dihydroxy-1-methyl-8-methylene-1,2,4b,5,6,7,8,9,10,10a-decahydro-4a,1-(epoxymethano)-7,9a-methanobenzo[a]azulen-13-one (36f): Synthesized according to General Procedure F using gibberellic acid (69 mg, 0.2 mmol, 1 equiv.). The crude mixture was purified by flash column chromatography on silica gel (40% AcOEt in hexanes as eluent) to afford **36f** (36 mg, 60% yield) as a white solid.

^{1}H NMR (400 MHz, Acetone-d_6) δ 6.34 (dd, *J* = 9.3, 0.9 Hz, 1H), 5.85 (dd, *J* = 9.3, 3.7 Hz, 1H), 5.16 (td, *J* = 2.5, 1.1 Hz, 1H), 4.81 (tt, *J* = 2.1, 1.0 Hz, 1H), 4.56 – 4.50 (m, 1H), 4.01 (dd, *J* = 6.4, 3.6 Hz, 1H), 3.71 (s, 1H), 2.85 – 2.74 (m, 1H), 2.40 (q, *J* = 2.0 Hz, 2H), 2.03 – 2.00 (m, 1H), 1.91 (dd, *J* = 13.6, 8.2 Hz, 1H), 1.87 – 1.80 (m, 2H), 1.79 – 1.65 (m, 3H), 1.61 (dd, *J* = 13.6, 11.0 Hz, 1H), 1.53 – 1.47 (m, 1H), 1.21 (s, 3H).

^{13}C NMR (101 MHz, Acetone-d_6) δ 179.6, 160.6, 134.0, 133.3, 105.7, 92.8, 78.9, 70.2, 54.5, 52.3, 50.2, 48.2, 45.9, 40.1, 36.4, 30.2, 17.6, 15.2.

HRMS: calculated for $C_{18}H_{22}NaO_4$ ($M+Na^+$): 325.1410, found 325.1400.

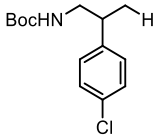

***tert*-butyl (2-(4-chlorophenyl)propyl)carbamate (36g):** Synthesized according to General Procedure F using 4-((*tert*-butoxycarbonyl)amino)-3-(4-chlorophenyl)butanoic acid (63 mg, 0.2 mmol, 1 equiv.). The crude mixture was purified by flash column chromatography on silica gel (10% AcOEt in hexanes as eluent) to afford **36g** (40 mg, 74% yield) as colorless oil.

^{1}H NMR (400 MHz, $CDCl_3$) δ 7.34 – 7.20 (m, 2H), 7.17 – 7.07 (m, 2H), 4.41 (s, 1H), 3.35 (s, 1H), 3.15 (dd, *J* = 13.6, 8.3 Hz, 1H), 2.91 (q, *J* = 7.1 Hz, 1H), 1.41 (s, 9H), 1.24 (d, *J* = 7.0 Hz, 3H).

^{13}C NMR (101 MHz, $CDCl_3$) δ 156.0, 142.9, 132.4, 129.8, 128.8, 128.8, 128.6, 47.4, 39.8, 28.5, 28.5, 19.2, 1.2.

Matching reported literature data.[52]

4.7.5.3 General procedure G (deaminative reduction)

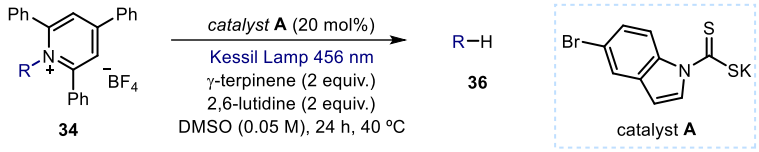

*Reactions performed using **set-up 2** in Figure 4.4.* In an oven dried vial, with a Teflon septum screw cap, dithiocarbamate **A** (12.4 mg, 0.04 mmol, 0.2 equiv.) and pyridinium salt **34** (0.2 mmol, 1 equiv.) were dissolved in DMSO (4 mL). Then, γ-terpinene (64 μL, 0.4 mmol, 2 equiv.) and 2,6-lutidine (46 μL, 0.4 mmol, 2 equiv.) were added. The resulting orange mixture was degassed with argon sparging for 60 seconds. The vial was then placed at 2-3 cm of a 50 W Kessil blue LED lamp and irradiated under stirring for 16 hours. The mixture was transferred to an extraction funnel, $NaHCO_3$ sat. solution was added and the organic layer was extracted with EtOAc. The organic layer was washed with brine twice. The combined organic layers were dried over anhydrous $MgSO_4$, filtered, and concentrated to dryness. The crude residue was purified by column chromatography to afford the corresponding product in the stated yield with >95% purity according to ^{1}H NMR analysis.

4.7.5.4 Characterization of products with general procedure G

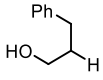

3-phenylpropan-1-ol (36h): Synthesized according to General Procedure G using 1-(1-hydroxy-3-phenylpropan-2-yl)-2,4,6-triphenylpyridin-1-ium tetrafluoroborate **34b** (106 mg, 0.2 mmol, 1 equiv.). The crude mixture was purified by flash column chromatography on silica gel (15% AcOEt in pentane as eluent) to afford **36h** (21 mg, 77% yield) as a colorless oil.

^{1}H NMR (400 MHz, $CDCl_3$) δ 7.33 – 7.26 (m, 2H), 7.23 – 7.17 (m, 3H), 3.68 (t, *J* = 6.4 Hz, 2H), 2.72 (dd, *J* = 8.7, 6.8 Hz, 2H), 1.96 – 1.85 (m, 2H).

^{13}C NMR (101 MHz, $CDCl_3$) δ 141.9, 128.6, 128.5, 126.0, 62.4, 34.4, 32.2.

[52] Steiman, T. J.; Liu, J.; Mengiste, A.; Doyle, A. G., Synthesis of β-Phenethylamines via Ni/Photoredox Cross-Electrophile Coupling of Aliphatic Aziridines and Aryl Iodides. *J. Am. Chem. Soc.* **2020**, *142*, 7598-7605.

Matching reported literature data.[53]

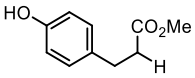

methyl 3-(4-hydroxyphenyl)propanoate (36i): Synthesized according to General Procedure G using 1-(3-(4-hydroxyphenyl)-1-methoxy-1-oxopropan-2-yl)-2,4,6-triphenylpyridin-1-ium tetrafluoroborate **34c** (115 mg, 0.2 mmol, 1 equiv.). The crude mixture was purified by flash column chromatography on silica gel (0-40% AcOEt in hexanes as eluent) to afford **36i** (28 mg, 78% yield) as a colorless oil.

^{1}H NMR (400 MHz, $CDCl_3$) δ 7.04 (d, *J* = 8.4 Hz, 2H), 6.79 – 6.71 (m, 2H), 5.74 (s, 1H), 3.67 (s, 3H), 2.88 (t, *J* = 7.7 Hz, 2H), 2.61 (dd, *J* = 9.0, 6.5 Hz, 2H).

^{13}C NMR (101 MHz, $CDCl_3$) δ 174.1, 154.4, 132.4, 129.5, 115.5, 51.9, 36.2, 30.2.

Matching reported literature data.[54]

4.7.6 α-Alkylation of silyl enol ethers

4.7.6.1 General procedure H

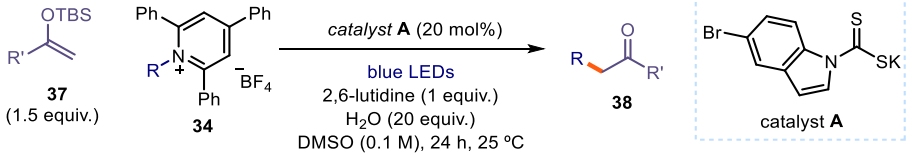

Reactions performed using ***set-up 3*** *in Figure 4.7*. In an oven dried vial with a Teflon septum screw cap, silyl enol ether **37** (0.3 mmol, 1.5 equiv.) was dissolved in DMSO (2 mL), followed by addition of 2,6-lutidine (23 μL, 0.2 mmol, 1.0 equiv.), pyridinium salt **34** (0.2 mmol, 1.0 equiv.), catalyst **A** (12.4 mg, 0.04 mmol, 0.2 equiv.) and water (4.0 mmol, 20 equiv.). The resulting orange mixture was degassed by bubbling argon for 60 seconds. The vial was then placed in the irradiation setup, maintained at a temperature of 25 ºC (25-26 ºC measured in the central well), and the reaction was stirred for 24 hours under continuous irradiation from a blue LED strip, unless otherwise stated. The crude mixture was diluted with EtOAc and brine was added. The layers were separated, and the aqueous layer extracted with EtOAc (×3). The combined organic fractions were dried over anhydrous $MgSO_4$, filtered, and concentrated to dryness. The crude residue was purified by column chromatography on silica gel to afford the corresponding product in the stated yield with >95% purity according to ^{1}H NMR analysis.

---

[53] Vechorkin, O.; Proust, V.; Hu, X., Functional Group Tolerant Kumada−Corriu−Tamao Coupling of Nonactivated Alkyl Halides with Aryl and Heteroaryl Nucleophiles: Catalysis by a Nickel Pincer Complex Permits the Coupling of Functionalized Grignard Reagents. *J. Am. Chem. Soc.* **2009**, *131*, 9756-9766.

[54] Percec, V.; Peterca, M.; Sienkowska, M. J.; Ilies, M. A.; Aqad, E.; Smidrkal, J.; Heiney, P. A., Synthesis and Retrostructural Analysis of Libraries of AB3 and Constitutional Isomeric AB2 Phenylpropyl Ether-Based Supramolecular Dendrimers. *J. Am. Chem. Soc.* **2006**, *128*, 3324-3334.

4.7.6.2 Characterization of products with general procedure H

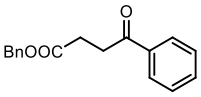

Benzyl 4-oxo-4-phenylbutanoate (38a): Prepared according to General Procedure H using ***set-up 2*** (75% intensity). 2,6-lutidine (46 μL, 0.4 mmol, 2 equiv.), *tert*-butyldimethyl((1-phenylvinyl)oxy)silane **37a** (70 mg, 0.4 mmol, 2 equiv.) and 1-(2-(benzyloxy)-2-oxoethyl)-2,4,6-triphenylpyridin-1-ium tetrafluoroborate **34d** (109 mg, 0.2 mmol, 1 equiv.). Flash column chromatography (hexanes/EtOAc 95:5) to afford product **38a** as an off-white oil (43 mg, 80% yield).

^{1}H NMR (300 MHz, $CDCl_3$) δ 8.03 – 7.94 (m, 2H), 7.56 (m, 1H), 7.46 (m, 2H), 7.40 – 7.23 (m, 5H), 5.15 (s, 3H), 3.34 (t, *J* = 6.6 Hz, 2H), 2.83 (t, *J* = 6.6 Hz, 2H).

^{13}C NMR (75 MHz, $CDCl_3$) δ 198.2, 172.9, 136.7, 136.0, 133.4, 128.8, 128.7, 128.4, 128.2, 66.7, 33.5, 28.43.

Matching reported literature data.[55]

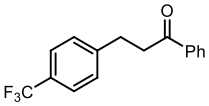

1-phenyl-3-(4-(trifluoromethyl)phenyl)propan-1-one (38b): Prepared according to General Procedure H using *tert*-butyldimethyl((1-phenylvinyl)oxy)silane **37a** (70 mg, 0.3 mmol,) and 2,4,6-triphenyl-1-(4-(trifluoromethyl)benzyl)pyridin-1-ium tetrafluoroborate **34e** (111 mg, 0.2 mmol). Time of irradiation: 24 hours at 25 °C. Flash column chromatography (Toluene) to afford product **38b** as a white solid (35 mg, 55% yield).

^{1}H NMR (300 MHz, $CDCl_3$) δ 7.97 – 7.90 (m, 2H), 7.59 – 7.50 (m, 3H), 7.48 – 7.44 (m, 2H), 7.41 – 7.35 (m, 2H), 3.33 (t, *J* = 7.5 Hz, 2H), 3.15 (t, *J* = 7.5 Hz, 2H).

^{13}C NMR (75 MHz, $CDCl_3$) δ 198.2, 145.5, 136.8, 136.8, 133.4, 129.1, 128.8, 128.7, 128.1, 125.4 (q, *J* = 3.9 Hz), 124.5 (q, *J* = 270 Hz), 39.9, 29.9.

^{19}F NMR (376 MHz, $CDCl_3$) δ –62.49.

Matching reported literature data.[56]

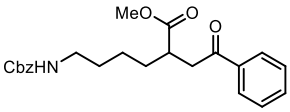

Methyl 6-(((benzyloxy)carbonyl)amino)-2-(2-oxo-2-phenylethyl)hexanoate (38c): Prepared according to General Procedure H using *tert*-butyldimethyl((1-phenylvinyl)oxy)silane **37a** (70 mg, 0.3 mmol) and (±)-1-(6-(((benzyloxy)carbonyl)amino)-1-methoxy-1-oxohexan-2-yl)-2,4,6-triphenylpyridin-1-ium tetrafluoroborate **34f** (135 mg,

[55] Dong S.; Wu G.; Yuan X.; Zou C.; Ye J., Visible-light photoredox catalyzed hydroacylation of electron-deficient alkenes: carboxylic anhydride as an acyl radical source. *Org. Chem. Front.* **2017**, *4*, 2230-2234.
[56] Ding B.; Zhang Z.; Liu Y.; Sugiya M.; Imamoto T.; Zhang W., Chemoselective Transfer Hydrogenation of α,β-Unsaturated Ketones Catalyzed by Pincer-Pd Complexes Using Alcohol as a Hydrogen Source. *Org. Lett.* **2013**, *15*, 3690-3693.

0.2 mmol). Flash column chromatography (hexanes/EtOAc 7:3 to 1:1) to afford product **38e** as a yellowish oil (53 mg, 67% yield).

^{1}H NMR (400 MHz, $CDCl_3$) δ 7.99 – 7.93 (m, 2H), 7.60 – 7.54 (m, 1H), 7.49 – 7.44 (m, 2H), 7.36 – 7.30 (m, 5H), 5.09 (s, 2H), 4.76 (s, 1H), 3.69 (s, 3H), 3.56 – 3.34 (m, 1H), 3.20 (q, *J* = 6.7 Hz, 2H), 3.15 – 2.99 (m, 2H), 1.77 – 1.50 (m, 5H), 1.39 (m, 1H).

^{13}C NMR (101 MHz, $CDCl_3$) δ 198.2, 176.1, 156.5, 136.8, 136.7, 133.4, 128.8, 128.7, 128.3, 128.2, 66.8, 52.0, 40.9, 40.6, 40.3, 31.9, 29.9, 24.5.

HRMS: calculated for $C_{23}H_{27}NNaO_5$ ($M+Na^+$): 420.1781, found 420.1771.

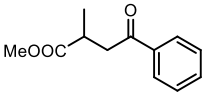

Benzyl 2-methyl-4-oxo-4-phenylbutanoate (38d): Prepared according to General Procedure H using *tert*-butyldimethyl((1-phenylvinyl)oxy)silane **37a** (70 mg, 0.3 mmol) and (±)-1-(1-(benzyloxy)-1-oxopropan-2-yl)-2,4,6-triphenylpyridin-1-ium tetrafluoroborate **34g** (111 mg, 0.2 mmol). Time of irradiation: 24 hours at 25 °C. Flash column chromatography (hexanes/EtOAc 98:2 to 90:10) to afford product **38d** as a yellowish oil (39 mg, 69% yield).

^{1}H NMR (300 MHz, $CDCl_3$) δ 8.07 – 7.88 (m, 2H), 7.72 – 7.53 (m, 1H), 7.53 – 7.42 (m, 2H), 7.35 (m, 5H), 5.22 – 5.09 (dd, *J* = 16.5 Hz, 12.4 Hz, 2H), 3.52 (dd, *J* = 17.5 Hz, 7.8 Hz, 1H), 3.22 (m, 1H), 3.06 (dd, *J* = 17.5 Hz, 5.5 Hz, 1H), 1.32 (d, *J* = 7.1 Hz, 3H).

^{13}C NMR (75 MHz, $CDCl_3$) δ 198.1, 175.9, 136.8, 136.2, 133.3, 128.7, 128., 128.2, 128.2, 128.2, 66.5, 42.0, 35.2, 17.4.

Matching reported literature data.[55]

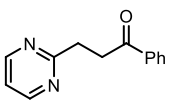

1-phenyl-3-(pyrimidin-2-yl)propan-1-one (38e): Prepared according to General Procedure H at 40 ºC using *tert*-butyldimethyl((1-phenylvinyl)oxy)silane **37a** (70 mg, 0.3 mmol) and 2,4,6-triphenyl-1-(pyrimidin-2-ylmethyl)pyridin-1-ium tetrafluoroborate **34h** (98 mg, 0.2 mmol). Flash column chromatography (hexanes/EtOAc 7:3) to afford product **38e** as a yellowish oil (32 mg, 75% yield).

^{1}H NMR (300 MHz, $CDCl_3$) δ 8.66 (d, *J* = 4.9 Hz, 2H), 8.25 – 7.88 (m, 2H), 7.61 – 7.52 (m, 1H), 7.51 – 7.39 (m, 2H), 7.13 (t, *J* = 4.9 Hz, 1H), 3.66 – 3.55 (m, 2H), 3.46 (m, 2H).

^{13}C NMR (75 MHz, $CDCl_3$) δ 199.0, 170., 157.1, 137.1, 133.2, 128.7, 128.3, 118.8, 36.2, 33.1.

HRMS: calculated for $C_{13}H_{13}N_2O$ ($M+H^+$): 213.1022, found 213.1020.

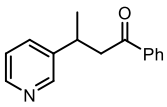

1-phenyl-3-(pyridin-3-yl)butan-1-one (38f): Prepared according to General Procedure H at 60 ºC using *tert*-butyldimethyl((1-phenylvinyl)oxy)silane **37a** (70 mg, 0.3 mmol) and (±)-2,4,6-triphenyl-1-(1-(pyridin-3-yl)ethyl)pyridin-1-ium tetrafluoroborate **34i** (100 mg, 0.2 mmol). Flash column chromatography (hexanes/EtOAc 8:2) to afford product **38f** as a yellowish oil (20 mg, 44% yield).

^{1}H NMR (400 MHz, $CDCl_3$) δ 8.52 (d, *J* = 4.9, 1H), 8.04 – 7.91 (m, 2H), 7.64 (td, *J* = 7.7 Hz, 1.9 Hz, 1H), 7.58 – 7.49 (m, 1H), 7.48 – 7.37 (m, 2H), 7.30 (d, *J* = 7.8 Hz, 1H), 7.13 (m, 1H), 3.82 – 3.60 (m, 2H), 3.25 (dd, *J* = 16.4 Hz, 5.6 Hz, 1H), 1.40 (d, *J* = 6.8 Hz, 3H).

^{13}C NMR (101 MHz, $CDCl_3$) δ 199.3, 164.9, 148.7, 137.3, 133.1, 128.6, 128.3, 123.0, 121.7, 45.0, 37.2, 21.2.

HRMS: calculated for $C_{15}H_{16}NO$ ($M+H^+$): 226.1226, found 226.1222.

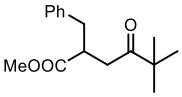

Methyl 2-benzyl-5,5-dimethyl-4-oxohexanoate (38g): Prepared according to General Procedure H with ***set-up 2*** (75% intensity) and solvent system DMSO/DCE (1:1). 2,6-Lutidine (47 µL, 0.4 mmol, 2.0 equiv.), methyl 2-benzyl-5,5-dimethyl-4-oxohexanoate **37b** (119 mg, 0.5 mmol) and (±)-1-(1-methoxy-1-oxo-3-phenylpropan-2-yl)-2,4,6-triphenylpyridin-1-ium tetrafluoroborate **34l** (111 mg, 0.2 mmol). Flash column chromatography (Hexanes/EtOAc from 98:2 to 96:4) to afford product **38g** as a yellow oil (33 mg, 63% yield).

^{1}H NMR (400 MHz, $CDCl_3$) δ 7.31 – 7.26 (m, 2H), 7.24 – 7.19 (m, 1H), 7.17 – 7.10 (m, 2H), 3.63 (s, 3H), 3.21 – 3.09 (m, 1H), 3.01 (dd, *J* = 13.6 Hz, 6.6 Hz, 1H), 2.93 (dd, *J* = 18.1, 8.9 Hz, 1H), 2.73 (dd, *J* = 13.6 Hz, 8.3 Hz, 1H), 2.52 (dd, *J* = 18.1 Hz, 4.6 Hz, 1H), 1.10 (s, 9H).

^{13}C NMR (101 MHz, $CDCl_3$) δ 214.2, 175.6, 138.8, 129.1, 128.6, 126.7, 51.9, 44.1, 42.1, 37.93, 37.9, 26.5.

HRMS: calculated for $C_{18}H_{21}O_3$ ($M+H^+$): 285.1485, found 285.1475.

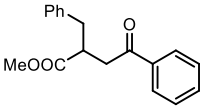

Methyl 2-benzyl-4-oxo-4-phenylbutanoate (38h): Prepared according to General Procedure H using *tert*-butyldimethyl((1-phenylvinyl)oxy)silane **37a** (70 mg, 0.3 mmol) and (±)-1-(1-methoxy-1-oxo-3-phenylpropan-2-yl)-2,4,6-triphenylpyridin-1-ium tetrafluoroborate **34l** (111 mg, 0.2 mmol). Flash column chromatography (hexanes/EtOAc 92:8) to afford product **38h** as a yellowish oil (50 mg, 89% yield).

^{1}H NMR (400 MHz, $CDCl_3$) δ 7.93 – 7.87 (m, 2H), 7.59 – 7.50 (m, 1H), 7.43 (dd, *J* = 8.4 Hz, 7.0 Hz, 2H), 7.34 – 7.16 (m, 5H), 3.67 (s, 3H), 3.47 – 3.32 (m, 2H), 3.12 (dd, *J* = 13.6 Hz, 6.0 Hz, 1H), 3.05 – 2.99 (m, 1H), 2.85 (dd, *J* = 13.6, 8.1 Hz, 1H).
^{13}C NMR (101 MHz, $CDCl_3$) δ 198.2, 175.4, 133.4, 129.2, 128.7, 128.7, 128.2, 126.8, 52.1, 42.4, 39.5, 38.0.

HRMS: calculated for $C_{18}H_{18}NaO_3$ ($M+Na^+$): 305.1148, found 305.1142 (+2.0 ppm).

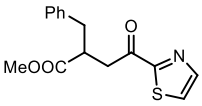

Methyl 2-benzyl-4-oxo-4-(thiazol-2-yl)butanoate (38i): Prepared according to General Procedure H using 2-(1-((tert-butyldimethylsilyl)oxy)vinyl)thiazole **37c** (73 mg, 0.3 mmol) and (±)-1-(1-methoxy-1-oxo-3-phenylpropan-2-yl)-2,4,6-triphenylpyridin-1-ium tetrafluoroborate **34l** (111 mg, 0.2 mmol). Flash column chromatography (Hexanes/Acetone 95:5) to afford product **38i** as a yellowish solid (46 mg, 79% yield).

^{1}H NMR (300 MHz, $CDCl_3$) δ 7.98 (d, *J* = 3.0 Hz, 1H), 7.65 (d, *J* = 3.0 Hz, 1H), 7.33 – 7.26 (m, 2H), 7.23 – 7.18 (m, 3H), 3.76 – 3.58 (m, 4H), 3.40 – 3.30 (m, 1H), 3.26 – 3.10 (m, 2H), 2.84 (dd, *J* = 13.6, 8.6 Hz, 1H).

^{13}C NMR (75 MHz, $CDCl_3$) δ 192.0 (C), 174.9 (C), 166.7 (C), 144.9 (CH), 138.5 (C), 129.2 (CH), 128.7 (CH), 126.8 (CH), 126.4 (CH), 52.1 (CH_3), 42.3 (CH), 39.5 (CH_2), 38.0 (CH_2).

HRMS: calculated for $C_{15}H_{15}NNaO_3S$ ($M+Na^+$): 312.0665, found 312.0665.

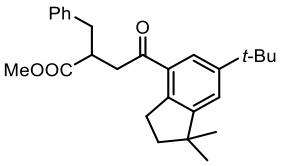

Methyl 2-benzyl-4-(6-(tert-butyl)-1,1-dimethyl-2,3-dihydro-1H-inden-4-yl)-4-oxobutanoate (38j): Prepared according to General Procedure H using tert-butyl((1-(6-(tert-butyl)-1,1-dimethyl-2,3-dihydro-1H-inden-4-yl)vinyl)oxy)dimethylsilane **37d** (108 mg, 0.3 mmol) and (±)-1-(1-methoxy-1-oxo-3-phenylpropan-2-yl)-2,4,6-triphenylpyridin-1-ium tetrafluoroborate **34l** (111 mg, 0.2 mmol). Flash column chromatography (Hexanes/EtOAc 98:2) to afford product **38j** as a yellowish oil (74 mg, 91% yield).

^{1}H NMR (400 MHz, $CDCl_3$) δ 7.62 (d, *J* = 1.8 Hz, 1H), 7.33 – 7.26 (m, 3H), 7.24 – 7.17 (m, 3H), 3.66 (s, 3H), 3.47 – 3.22 (m, 2H), 3.14 – 3.07 (m, 3H), 3.05 – 2.97 (m, 1H), 2.84 (dd, *J* = 13.5, 7.9 Hz, 1H), 1.94 – 1.87 (m, 2H), 1.33 (s, 9H), 1.24 (d, *J* = 2.6 Hz, 6H).

^{13}C NMR (101 MHz, $CDCl_3$) δ 200.2, 175.6, 154.5, 150.1, 141.2, 138.9, 133.3, 129.2, 128.6, 126.7, 124.0, 123.5, 52.0, 43.6, 42.6, 41.6, 41.5, 38.1, 34.9, 31.6, 30.88, 28.9.

HRMS: calculated for $C_{27}H_{34}NaO_3$ ($M+Na^+$): 429.2400, found 429.2409.

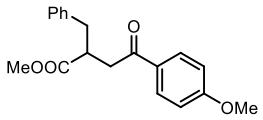

Methyl 2-benzyl-4-(4-methoxyphenyl)-4-oxobutanoate (38k): Prepared according to General Procedure H using tert-butyl((1-(4-methoxyphenyl)vinyl)oxy)dimethylsilane **37e** (80 mg, 0.3 mmol) and (±)-1-(1-methoxy-1-oxo-3-phenylpropan-2-yl)-2,4,6-triphenylpyridin-1-ium tetrafluoroborate **34l** (111 mg, 0.2 mmol). Flash column chromatography (Hexanes/EtOAc 93:7) to afford product **38k** as an off-white solid (52 mg, 83% yield).

^{1}H NMR (400 MHz, $CDCl_3$) δ 7.88 (d, *J* = 9.0 Hz, 2H), 7.32 – 7.27 (m, 2H), 7.24 – 7.17 (m, 3H), 6.90 (d, *J* = 9.0 Hz, 2H), 3.86 (s, 3H), 3.66 (s, 3H), 3.44 – 3.26 (m, 2H), 3.10 (dd, *J* = 13.6, 5.9 Hz, 1H), 2.97 (d, *J* = 12.9 Hz, 1H), 2.84 (dd, *J* = 13.6, 7.9 Hz, 1H).

^{13}C NMR (101 MHz, $CDCl_3$) δ 196.7, 175.6, 163.7, 138.7, 130.4, 129.9, 129.2, 128.7, 126.8, 113.8, 55.6, 52.0, 42.4, 39.2, 38.0.

HRMS: calculated for $C_{27}H_{34}NaO_3$ ($M+Na^+$): 429.2400, found 429.2409.

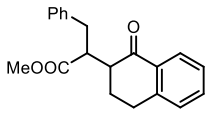

Methyl 2-benzyl-4-(6-(tert-butyl)-1,1-dimethyl-2,3-dihydro-1H-inden-4-yl)-4-oxobutanoate (38l): Prepared according to General Procedure H using tert-butyl((3,4-dihydronaphthalen-1-yl)oxy)dimethylsilane **37f** (104 mg, 0.4 mmol) and (±)-1-(1-methoxy-1-oxo-3-phenylpropan-2-yl)-2,4,6-triphenylpyridin-1-ium tetrafluoroborate **34l** (111 mg, 0.2 mmol). Flash column chromatography (Hexanes/EtOAc from 95:5 to 85:15) to afford product **38l** as an off-green solid (50 mg, 81% yield, 1:1 dr).

^{1}H NMR (300 MHz, $CDCl_3$) (1:1 mixture of diasteroisomers) δ 8.02 (ddd, *J* = 9.7, 7.8, 1.5 Hz, 1H), 7.54 – 7.39 (m, 1H), 7.35 – 7.26 (m, 3H), 7.26 – 7.14 (m, 4H), 3.66 – 3.60 (m, 0.4 H), 3.59 (s, 1.1 H), 3.57 (s, 1.8 H), 3.47 – 3.38 (m, 0.6 H), 3.26 – 3.17 (m, 0.5H), 3.05 – 2.75 (m, 4H), 2.66 – 2.58 (m, 0.7H), 2.19 – 2.32 (m, 1H), 1.94 – 1.87 (m, 1H).

^{13}C NMR (75 MHz, $CDCl_3$) (1:1 mixture of diasteroisomers) δ 197.8, 175.3, 174.3, 143.9, 143.7, 139.9, 139.3, 133.7, 133.5, 132.6, 129.2, 129.0, 128.8, 128.8, 128.7, 128.5, 127.7, 127.7, 126.9, 126.8, 126.6, 126.5, 51.80, 50.3, 48.7, 47.3, 46.1, 35.4, 34.7, 29.6, 29.2, 26.1, 25.4.

HRMS: calculated for $C_{20}H_{20}NaO_3$ ($M+Na^+$): 331.1305, found 331.1289.

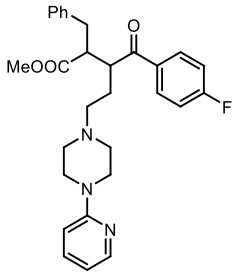

Methyl 2-benzyl-3-(4-fluorobenzoyl)-5-(4-(pyridin-2-yl)piperazin-1-yl)pentanoate (38m): Prepared according to General Procedure H using (*Z*)-1-(4-((tert-butyldimethylsilyl)oxy)-4-(4-fluorophenyl)but-3-en-1-yl)-4-(pyridin-2-yl)piperazine **37g** (133 mg, 0.3 mmol) and (±)-1-(1-methoxy-1-oxo-3-phenylpropan-2-yl)-2,4,6-triphenylpyridin-1-ium tetrafluoroborate **34l** (111 mg, 0.2 mmol), no water is added into the reaction mixture. Flash column

chromatography (Hexanes/Acetone from 7:3 to 1:1) to afford product **38m** as an off-white solid (49 mg, 50% yield, 1.2:1 dr).

^{1}H NMR (500 MHz, $CDCl_3$) δ 8.14 (m, 1H), 8.05 – 7.97 (m, 2H), 7.47 – 7.39 (m, 1H), 7.25 – 7.14 (m, 4H), 7.13 – 7.04 (m, 5H), 6.62 – 6.51 (m, 2H), 3.95 – 3.82 (m, 1H), 3.49 (s, 1H), 3.44 (s, 2H), 3.28 (t, *J* = 44.1 Hz, 4H), 3.12 – 3.04 (m, 1H), 2.80 – 2.61 (m, 1H), 2.34 (d, *J* = 37.0 Hz, 6H), 2.13 (ddd, *J* = 13.9, 10.4, 6.4 Hz, 1H), 1.99 (s, 1H), 1.70 (s, 1H)

^{13}C NMR (126 MHz, $CDCl_3$) 1:1 mixture of diasteroisomer δ 200.5, 200.1, 174.5, 174.4, 159.5, 148.1, 148.1, 138.8, 138.6, 137.6, 137.6 135.1, 134.0, 131.2, 131.2, 131.1, 131.0, 129.0, 128.9, 128.6, 128.5, 126.7, 126.7, 115.9, 115.9, 115.8, 115.7, 113.5, 113.4, 107.2, 107.1, 56.1, 55.9, 52.8, 52.6, 51.8, 51.6, 51.4, 49.2, 45.9, 45.6, 44.9, 44.8, 37.2, 34.7.

^{19}F NMR (376 MHz, $CDCl_3$) 1:1 mixture of diasteroisomer δ –105.4 (s, 1F), –105.6 (s, 1F).

HRMS: calculated for $C_{29}H_{33}FN_3O_3$ ($M+H^+$): 490.2500, found 490.2500.

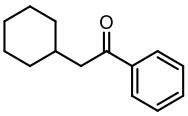

Methyl 2-benzyl-5,5-dimethyl-4-oxohexanoate (38n): Prepared according to General Procedure H with ***set-up 1*** and no 2,6-Lutidine. *tert*-butyldimethyl((1-phenylvinyl)oxy)silane **37a** (70 mg, 0.3 mmol) and 1,3-dioxoisoindolin-2-yl cyclohexanecarboxylate **31a** (54.5 mg, 0.2 mmol, 1 equiv.). Flash column chromatography (Hexanes/EtOAc from 100:0 to 98:2) to afford product **38n** as a yellow oil (17 mg, 42% yield).

^{1}H NMR (400 MHz, $CDCl_3$) δ 7.98 – 7.92 (m, 2H), 7.58 – 7.51 (m, 1H), 7.49 – 7.42 (m, 2H), 2.82 (d, *J* = 6.8 Hz, 2H), 2.04 – 1.93 (m, 1H), 1.80 – 1.73 (m, 2H), 1.73 – 1.61 (m, 2H), 1.34 – 1.23 (m, 3H), 1.22 – 1.14 (m, 1H), 1.07 – 0.96 (m, 2H).

^{13}C NMR (101 MHz, $CDCl_3$) δ 200.5, 137.6, 133.0, 128.7, 128.3, 46.4, 34.7, 33.6, 26.4, 26.3.

Matching reported literature data.[57]

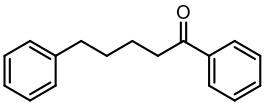

Methyl 2-benzyl-5,5-dimethyl-4-oxohexanoate (38o): Prepared according to General Procedure H with ***set-up 1*** and no 2,6-Lutidine. *tert*-butyldimethyl((1-phenylvinyl)oxy)silane **37a** (70 mg, 0.3 mmol) and 1,3-dioxoisoindolin-2-yl 4-phenylbutanoate **31b** (62 mg, 0.2 mmol, 1 equiv.). Flash column chromatography (Hexanes/EtOAc from 100:0 to 98:2) to afford product **38o** as a yellow oil (18 mg, 38% yield).

[57] Kong, W.; Yu, C.; An, H.; Song, Q., Photoredox-Catalyzed Decarboxylative Alkylation of Silyl Enol Ethers To Synthesize Functionalized Aryl Alkyl Ketones. *Org. Lett.* **2018**, *20*, 349-352.

^{1}H NMR (400 MHz, $CDCl_3$) δ 7.97 – 7.92 (m, 2H), 7.59 – 7.52 (m, 1H), 7.49 – 7.42 (m, 2H), 7.31 – 7.21 (m, 2H), 7.19 (dt, *J* = 8.0, 1.8 Hz, 3H), 2.99 (t, *J* = 7.2 Hz, 2H), 2.67 (t, *J* = 7.5 Hz, 2H), 1.83 – 1.76 (m, 2H), 1.76 – 1.68 (m, 2H).

^{13}C NMR (101 MHz, $CDCl_3$) δ 200.4, 142.4, 137.2, 133.1, 128.7, 128.5, 128.5, 128.2, 125.9, 38.5, 35.9, 31.2, 29.8, 24.1.

Matching reported literature data.[58]

4.7.6.3 General procedure I (three-component reaction)

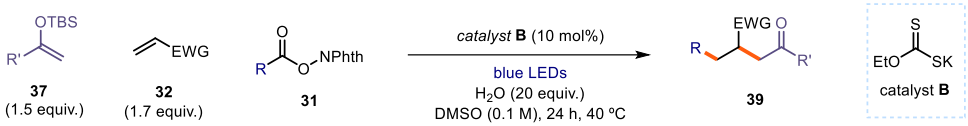

*Reactions performed using **set-up 1** in Figure 4.3.* In an oven dried vial, with a Teflon septum screw cap, silyl enol ether **37** (0.3 mmol, 1.5 equiv.) was dissolved in DMSO (2 mL), then phthalimide ester **31** (0.2 mmol, 1.0 equiv.) was added, followed by catalyst **B** (3.2 mg, 0.02 mmol, 0.1 equiv.), electron-poor olefin **32** (0.34 mmol, 1.7 equiv.) and water (4.0 mmol, 20 equiv.). The resulting orange mixture was degassed by bubbling argon for 60 seconds. The vial was then placed in the 3D printed support photoreactor and irradiated under stirring for 24 hours, unless otherwise specified. The crude mixture was diluted with EtOAc and brine was added. The combined organic fractions were dried over anhydrous $MgSO_4$ and concentrated to dryness. The crude residue was purified by column chromatography on silica gel to afford the corresponding product in the stated yield with >95% purity according to ^{1}H NMR analysis.

4.7.6.4 Characterization of products with general procedure I

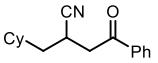

2-(cyclohexylmethyl)-4-oxo-4-phenylbutanenitrile (39a): Prepared according to General Procedure I using *tert*-butyldimethyl((1-phenylvinyl)oxy)silane **37a** (63 mg, 0.24 mmol), 1,3-dioxoisoindolin-2-yl cyclohexanecarboxylate **31a** (55 mg, 0.2 mmol), and acrylonitrile **32b** (22 µL 0.34 mmol). Flash column chromatography (hexanes/EtOAc 94:6) to afford product **39a** as an off-white solid (31 mg, 61% yield).

^{1}H NMR (300 MHz, $CDCl_3$) δ 8.04 – 7.86 (m, 2H), 7.72 – 7.59 (m, 1H), 7.52 – 7.45 (m, 2H), 3.52 – 3.30 (m, 2H), 3.30 – 3.13 (m, 1H), 1.89 (d, *J* = 12.9 Hz, 1H), 1.83 – 1.57 (m, 6H), 1.49 – 1.40 (m, 1H), 1.24 – 1.08 (m, 2H), 1.06 – 0.83 (m, 3H).

^{13}C NMR (75 MHz, $CDCl_3$) δ 195.5, 136.1, 134.0, 129.0, 128.2, 122.3, 41.5, 39.9, 35.7, 33.8, 32.2, 26.5, 26.2, 26.0, 24.0.

---

[58] Zheng, Y.-L.; Xie, P.-P.; Daneshfar, O.; Houk, K. N.; Hong, X.; Newman, S. G., Direct Synthesis of Ketones from Methyl Esters by Nickel-Catalyzed Suzuki–Miyaura Coupling. *Angew. Chem. Int. Ed.* **2021,** *60*, 13476-13483.

HRMS: calculated for $C_{17}H_{21}NNaO$ ($M+Na^+$): 278.1515, found 278.1511.

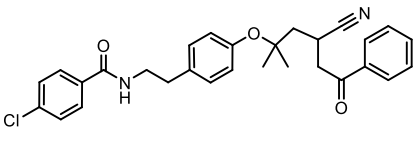

4-chloro-N-(4-((4-cyano-2-methyl-6-oxo-6-phenylhexan-2-yl)oxy)phenethyl)benzamide (39b): Prepared according to General Procedure I using *tert*-butyldimethyl((1-phenylvinyl)oxy)silane **37a** (63 mg, 0.24 mmol), 1,3-dioxoisoindolin-2-yl 2-(4-(2-(4-chlorobenzamido)ethyl)phenoxy)-2-methylpropanoate **31e** (101 mg, 0.2 mmol), and acrylonitrile **32b** (22 µL, 0.34 mmol). Flash column chromatography (hexanes/EtOAc from 7:3 to 1:1) to afford product **39b** as a yellowish fluffy solid (51 mg, 52% yield).

^{1}H NMR (300 MHz, $CDCl_3$) δ 8.05 – 7.86 (m, 2H), 7.64 (d, *J* = 8.4 Hz, 3H), 7.57 – 7.46 (m, 2H), 7.42 – 7.38 (m, 2H), 7.14 (d, *J* = 8.4 Hz, 2H), 6.98 (d, *J* = 8.4 Hz, 2H), 6.09 (s, 1H), 3.74 – 3.61 (m, 3H), 3.57 – 3.37 (m, 2H), 2.90 (t, *J* = 6.9 Hz, 2H), 2.23 (dd, *J* = 14.2, 9.2 Hz, 1H), 1.99 (dd, *J* = 14.2, 3.8 Hz, 1H), 1.44 (s, 3H), 1.40 (s, 3H).

^{13}C NMR (75 MHz, $CDCl_3$) δ 195.8, 166.5, 153.4, 136.1, 134.2, 134.0, 133.5, 129.6, 129.0, 128.4, 128.2, 124.3, 79.2, 44.8, 42.3, 35.0, 27.1, 26.2, 21.9.
HRMS: calculated for $C_{29}H_{29}ClN_2NaO_3$ ($M+Na^+$): 511.1759, found 511.1759.

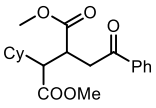

Dimethyl 2-cyclohexyl-3-(2-oxo-2-phenylethyl)succinate (39c): Prepared according to General Procedure I using *tert*-butyldimethyl((1-phenylvinyl)oxy)silane **37a** (63 mg, 0.24 mmol), 1,3-dioxoisoindolin-2-yl cyclohexanecarboxylate **31a** (55 mg, 0.2 mmol), and dimethylfumarate **32c** (43 mg, 0.3 mmol). Flash column chromatography (hexanes/EtOAc 88:12) to afford the two separable diastereoisomeric products **39c** (major diastereoisomer) and **39c'** (minor diastereoisomer) as off-white solids (d.r. 1:2.5, 50 mg, 72% yield).

*Spectroscopic data for **39c***:

^{1}H NMR (300 MHz, $CDCl_3$) δ 8.05 – 7.86 (m, 2H), 7.63 – 7.52 (m, 1H), 7.52 – 7.45 (m, 2H), 3.69 (s, 3H), 3.67 (s, 3H), 3.67 – 3.59 (m, 1H), 3.46– 2.94 (m, 2H), 2.71 (dd, *J* = 8.7, 5.6 Hz, 1H), 1.81 – 1.59 (m, 6H), 1.22 – 1.17 (m, 2H), 1.09 – 0.77 (m, 3H).

^{13}C NMR (75 MHz, $CDCl_3$) δ 198.3, 174.7, 173.8, 136.7, 133.4, 128.7, 128.3, 52.6, 52.3, 51.7, 39.8, 37.4, 36.6, 31.1, 30.4, 26.3, 26.3, 26.2.
HRMS: calculated for $C_{20}H_{26}NaO_5$ ($M+Na^+$): 369.1677, found 369.1672.

*Spectroscopic data for **39c'***:

^{1}H NMR (300 MHz, $CDCl_3$) δ 8.01 – 7.94 (m, 2H), 7.61 – 7.54 (m, 1H), 7.50 – 7.42 (m, 2H), 3.68 (s, 3H), 3.68 (s, 3H), 3.58 – 3.47 (m, 2H), 3.24 – 3.10 (m, 1H), 2.66 – 2.55 (m, 1H), 1.96 (m, 1H), 1.80 – 1.64 (m, 6H), 1.07 – 0.85 (m, 5H).

^{13}C NMR (75 MHz, $CDCl_3$) δ 197.9, 174.2, 173.9, 136.8, 133.4, 128.8, 128.2, 53.4, 52.2, 51.7, 39.3, 38.1, 37.4, 31.1, 30.9, 26.4, 26.4.
HRMS: calculated for $C_{20}H_{26}NaO_5$ ($M+Na^+$): 369.1677, found 369.1672 (+1.4 ppm).

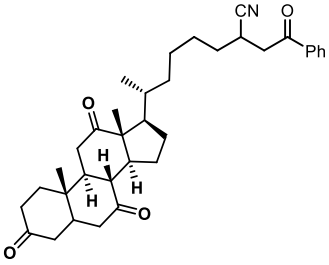

6-((5S,8R,9S,10S,13R,14S,17R)-10,13-dimethyl3,7,12-trioxohexadecahydro-1H-cyclopenta[a]phenanthren-17-yl)-2-(2-oxo-2-phenylethyl)heptanenitrile (39d): Prepared according to General Procedure I using *tert*-butyldimethyl((1-phenylvinyl)oxy)silane **37a** (63 mg, 0.24 mmol), 1,3-dioxoisoindolin-2-yl 4-((5S,8R,9S,10S,13R,14S,17R)-10,13-dimethyl-3,7,12-trioxohexadecahydro-1H-cyclopenta[a]phenanthren-17-yl)pentanoate **31d** (110 mg, 0.2 mmol), and acrylonitrile **32b** (22 µL, 0.340 mmol). Flash column chromatography (hexanes/EtOAc 1:1) to afford product **39d** as a white solid (64 mg, 60% yield).

^{1}H NMR (300 MHz, $CDCl_3$) δ 8.03 – 7.89 (m, 2H), 7.72 – 7.57 (m, 1H), 7.53 – 7.45 (m, 2H), 3.63 – 3.15 (m, 3H), 2.99 – 2.75 (m, 3H), 2.39 – 1.80 (m, 14H), 1.77 – 1.43 (m, 6H), 1.40 (s, 3H), 1.35 – 1.16 (m, 3H), 1.07 (s, 3H), 0.86 (dd, *J* = 6.4, 2.0 Hz, 3H).

^{13}C NMR (75 MHz, $CDCl_3$) δ 212.0, 209.1, 208.8, 195.3, 135.9, 133.9, 128.9, 128.1, 121.9, 56.9, 51.8, 49.0, 46.9, 45.8, 45.6, 45.0, 42.8, 40.9, 40.8, 38.7, 36.5, 36.0, 36.0, 35.3, 34.8, 32.4, 29.7, 27.9, 26.4, 26.3, 25.2, 24.5, 24.4, 21.9, 19.0, 18.9, 11.9.
HRMS: calculated for $C_{34}H_{43}NNaO_4$ ($M+Na^+$): 552.3081, found 552.3084.

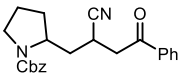

Benzyl 2-(2-cyano-4-oxo-4-phenylbutyl)pyrrolidine-1-carboxylate (39e): Prepared according to General Procedure I using *tert*-butyldimethyl((1-phenylvinyl)oxy)silane **37a** (63 mg, 0.240 mmol), 1-benzyl 2-(1,3-dioxoisoindolin-2-yl) pyrrolidine-1,2-dicarboxylate **31c** (55 mg, 0.2 mmol), and acrylonitrile **32b** (22 µL, 0.34 mmol). Flash column chromatography (hexanes/acetone 7:3) to afford product **39e** as a reddish oil (47 mg, 62% yield, 1:1 dr).

^{1}H NMR (400 MHz, $CDCl_3$) (1:1 mixture of diastereoisomers) δ 8.01 – 7.79 (m, 2H), 7.68 – 7.59 (m, 1H), 7.50 (t, *J* = 7.6 Hz, 2H), 7.46 – 7.30 (m, 5H), 5.26 – 5.10 (m, 2H), 4.24 – 3.96 (m, 1H), 3.57 – 3.19 (m, 5H), 2.15 – 2.04 (m, 1H), 2.02 – 1.65 (m, 5H).

^{13}C NMR (101 MHz, $CDCl_3$) (1:1 mixture of diastereoisomers) δ 195.3, 194.8, 155.3, 136.8, 136.8, 133.8, 128.8, 128.5, 128.1, 127.8, 123.7, 122.0, 121.1 66.9, 66.8, 56.2, 55.6, 55.3 46.4, 41.0, 40.7, 36.9, 36.5, 36.0, 32.5, 30.6, 30.3, 29.7, 24.3, 23.9, 23.4, 23.0.
HRMS: calculated for $C_{23}H_{24}N_2NaO_3$ ($M+Na^+$): 399.1679, found 399.1682.

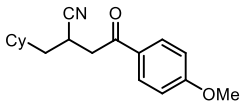

2-(cyclohexylmethyl)-4-(4-methoxyphenyl)-4-oxobutanenitrile (39f): Prepared according to General Procedure I using tert-butyl((1-(4-methoxyphenyl)vinyl)oxy)dimethylsilane **37e** (65 mg, 0.24 mmol), 1,3-dioxoisoindolin-2-yl cyclohexanecarboxylate **31a** (55 mg, 0.2 mmol), and acrylonitrile **32b** (22 µL, 0.34 mmol). Flash column chromatography (hexanes/acetone 88:12) to afford product **39f** as an off-white solid (31 mg, 61% yield).

^{1}H NMR (300 MHz, $CDCl_3$) δ 7.93 (d, *J* = 8.9 Hz, 2H), 6.95 (d, *J* = 8.9 Hz, 2H), 3.88 (s, 3H), 3.42 – 3.29 (m, 2H), 3.21 – 3.10 (m, 1H), 1.88 (d, *J* = 12.8 Hz, 1H), 1.77 – 1.58 (m, 7H), 1.23 – 1.10 (m, 2H), 1.00 – 0.79 (m, 3H).

^{13}C NMR (75 MHz, $CDCl_3$) δ 193.9, 164.2, 130.5.0, 129.2, 122.4, 114.1, 55.7, 41.1, 39.9, 35.7, 33.8, 32.2, 26.5, 26.2, 26.0, 24.0.

HRMS: calculated for $C_{18}H_{23}NNaO_2$ ($M+Na^+$): 308.1630, found 308.1621.

4.7.7 Minisci reaction

4.7.7.1 General procedure J

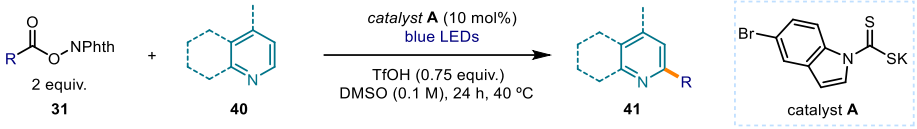

*Reactions performed using **set-up 1** in Figure 4.3.* In an oven dried vial, with a Teflon septum screw cap, heteroarene **40** (0.2 mmol, 1.0 equiv.) and trifluoromethanesulfonic acid (13.3 µL, 0.15 mmol, 0.75 equiv.) were dissolved in DMSO (2 ml). Then, phthalimide ester **31** (0.4 mmol, 2 equiv.) and catalyst **A** (6.2 mg, 0.02 mmol, 0.1 equiv.) were added. The resulting yellow mixture was degassed with argon sparging for 60 seconds. The vial was placed in the 3D printed photoreactor and irradiated under stirring for 24 hours, unless otherwise specified. The mixture was transferred to an extraction funnel, $NaHCO_3$ sat. solution was added and the organic layer was extracted with EtOAc. The organic layer was washed with brine twice. The combined organic layers were dried over anhydrous $MgSO_4$, filtered, and concentrated to dryness. The crude residue was purified by column chromatography to afford the corresponding product in the stated yield with >95% purity according to ^{1}H NMR analysis.

4.7.7.2 Characterization of products with general procedure J

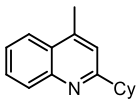

2-Cyclohexyl-4-methylquinoline (41a): Synthesized according to General Procedure J using 1,3-dioxoisoindolin-2-yl cyclohexanecarboxylate **31a** (109 mg, 0.4 mmol, 2 equiv.) and 4-methylquinoline **40a** (26.4 µL, 0.2 mmol, 1 equiv.). The crude mixture was purified by flash column chromatography on silica gel (10% EtOAc in hexane as eluent) to afford **41a** (39.6 mg, 88% yield) as a yellow oil.

^{1}H NMR (400 MHz, $CDCl_3$) δ 8.28 (s, 1H), 7.98 – 7.96 (m, 1H), 7.74 – 7.70 (m, 1H), 7.57 – 7.53 (m, 1H), 7.23 (s, 1H), 3.15 – 3.10 (m, 1H), 2.73 (s, 3H), 2.06 – 2.01 (m, 2H), 1.89 (dt, *J* = 13.0, 3.3 Hz, 2H), 1.83 – 1.76 (m, 1H), 1.63 (qd, *J* = 12.3, 3.0 Hz, 2H), 1.49 (qt, *J* = 12.8, 3.0 Hz, 2H), 1.38 – 1.30 (m, 1H).

^{13}C NMR (101 MHz, $CDCl_3$) δ 166.0, 130.2, 128.1, 127.1, 126.3, 123.8, 120.3, 46.5, 32.9, 26.5, 26.1, 19.3.

Matching reported literature data.[59]

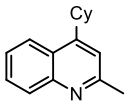

4-Cyclohexyl-2-methylquinoline (41b): Synthesized according to General Procedure J using 1,3-dioxoisoindolin-2-yl cyclohexanecarboxylate **31a** (109 mg, 0.4 mmol, 2 equiv.) and 2-methylquinoline **40b** (27.1 µL, 0.2 mmol, 1.0 equiv.). The crude mixture was purified by flash column chromatography on silica gel (10% EtOAc in hexane as eluent) to afford **41b** (42.3 mg, 94% yield) as a yellow oil.

^{1}H NMR (400 MHz, $CDCl_3$) δ 8.05 (t, *J* = 9.8 Hz, 2H), 7.67 - 7.63 (m, 1H), 7.51 – 7.47 (m, 1H), 7.17 (s, 1H), 3.32 – 3.27 (ddd, *J* = 11.4, 8.3, 3.4 Hz, 1H), 2.73 (s, 3H), 2.05 – 1.90 (m, 4H), 1.88 - 1.83 (m, 1H), 1.61 – 1.48 (m, 4H), 1.40 – 1.31(m, 4H).

^{13}C NMR (101 MHz, $CDCl_3$) δ 158.8, 153.8, 147.9, 129.4, 129.1, 125.5, 125.3, 123.0, 118.5, 39.0, 33.7, 27.1, 26.5, 25.5.

Matching reported literature data.[59]

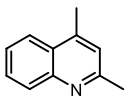

2,4-Dimethylquinoline (41c): Synthesized according to General Procedure J using 1,3-dioxoisoindolin-2-yl acetate **31g** (82.1 mg, 0.4 mmol, 2 equiv.) and 2-methylquinoline **40b** (27.1 µL ,0.2 mmol, 1.0 equiv.) in NMP (2 ml) for 48 hours. The crude mixture was purified by flash column chromatography on silica gel (20% CH_2Cl_2 in MeOH as eluent) to afford **41c** (28.3 mg, 90% yield) as a colorless oil.

^{1}H NMR (400 MHz, $CDCl_3$) δ 8.09 (dt, *J* = 8.5, 0.9 Hz, 1H), 7.89 – 7.85 (m, 1H), 7.72 (ddd, *J* = 8.4, 6.9, 1.4 Hz, 1H), 7.54 (ddd, *J* = 8.3, 6.9, 1.3 Hz, 1H), 6.98 (s, 1H), 2.86 (s, 3H), 2.73 (s, 3H).

^{13}C NMR (101 MHz, $CDCl_3$) δ 159.2, 148.6, 129.9, 129.7, 126.4, 124.1, 123.4, 122.1, 29.8, 25.6.

Matching reported literature data.[60]

---

[59] McCallum, T.; Barriault, L., Direct alkylation of heteroarenes with unactivated bromoalkanes using photoredox gold catalysis. *Chem. Sci.* **2016**, *7*, 4754-4758.
[60] Zidan, M.; Morris, A. O.; McCallum, T.; Barriault, L., The Alkylation and Reduction of Heteroarenes with Alcohols Using Photoredox Catalyzed Hydrogen Atom Transfer via Chlorine Atom Generation. *Eur. J. Org. Chem.* **2020**, 1453-1458.

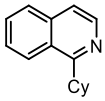

1-Cyclohexylisoquinoline (41d): Synthesized according to General Procedure J using 1,3-dioxoisoindolin-2-yl cyclohexanecarboxylate **31a** (109 mg, 0.4 mmol, 2 equiv.) and isoquinoline **40c** (25.8 mg, 0.2 mmol, 1.0 equiv.). The crude mixture was purified by flash column chromatography on silica gel (10% EtOAc in hexane as eluent) to afford **41d** (40.9 mg, 97% yield) as a colorless oil.

^{1}H NMR (400 MHz, $CDCl_3$) δ 8.50 (d, *J* = 5.8 Hz, 1H), 8.25 (d, *J* = 8.5 Hz, 1H), 7.83 (d, *J* = 8.3 Hz, 1H), 7.72 – 7.66 (m, 1H), 7.63 – 7.59 (ddd, *J* = 8.3, 6.9, 1.4 Hz, 1H), 7.53 (d, *J* = 5.8 Hz, 1H), 3.58 (tt, *J* = 11.6, 3.2 Hz, 1H), 2.05 – 1.78 (m, 7H), 1.61 – 1.37 (m, 3H).

^{13}C NMR (101 MHz, $CDCl_3$) δ 165.7, 141.1, 136.8, 130.3, 127.8, 127.3, 126.4, 125.1, 119.4, 41.6, 32.7, 27.0, 26.3.

Matching reported literature data.[59]

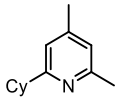

2-Cyclohexyl-4,6-dimethylpyridine (41e): Synthesized according to General Procedure J using 1,3-dioxoisoindolin-2-yl acetate **31a** (109 mg, 0.4 mmol, 2 equiv) and 2,4-dimethylpyridine **40d** (23.1µL, 0.2 mmol, 1.0 equiv.). The crude mixture was purified by flash column chromatography on silica gel (10% EtOAc in hexane as eluent) to afford **41e** (31.3 mg, 83% yield) as a colorless oil.

^{1}H NMR (400 MHz, $CDCl_3$) δ 6.80 (s, 2H), 2.71 (dd, *J* = 8.5, 4.8 Hz, 1H), 2.50 (s, 3H), 2.29 (s, 3H), 1.95 (dd, *J* = 13.4, 3.0 Hz, 2H), 1.86 – 1.79 (m, 2H), 1.78 – 1.70 (m, 1H), 1.51 – 1.36 (m, 4H), 1.33 – 1.25 (m, 1H).

^{13}C NMR (101 MHz, $CDCl_3$) δ 165.8, 157.0, 122.0, 118.6, 44.1, 33.3, 26.7, 26.3, 23.1, 21.2.

Matching reported literature data.[59]

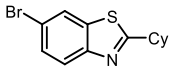

6-Bromo-2-cyclohexylbenzo[d]thiazole (41f): Synthesized according to General Procedure J using 1,3-dioxoisoindolin-2-yl cyclohexanecarboxylate **31a** (109 mg, 0.4 mmol, 2 equiv.) and 6-bromo-1,3-benzothiazole **40e** (42.8 mg, 0.2 mmol, 1.0 equiv.). The crude mixture was purified by flash column chromatography on silica gel (10% AcOEt in hexane as eluent) to afford **41f** (49.1 mg, 83% yield) as a white solid.

^{1}H NMR (500 MHz, $CDCl_3$) δ 7.96 (d, *J* = 2.0 Hz, 1H), 7.81 (d, *J* = 8.7 Hz, 1H), 7.53 (dd, *J* = 8.7, 2.0 Hz, 1H), 3.07 (tt, *J* = 11.6, 3.6 Hz, 1H), 2.22 – 2.15 (m, 2H), 1.88 (dp, *J* = 10.6, 3.5 Hz, 2H), 1.76 (dtt, *J* = 13.1, 3.4, 1.5 Hz, 1H), 1.69 – 1.57 (m, 2H), 1.50 – 1.37 (m, 2H), 1.32 (tt, *J* = 12.5, 3.5 Hz, 1H).

^{13}C NMR (126 MHz, $CDCl_3$) δ 178.3, 152.1, 136.4, 129.4, 124.2, 123.8, 118.2, 43.5, 33.5, 26.1, 25.9.

Matching reported literature data.[60]

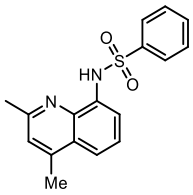

***N*-(2,4-Dimethylquinolin-8-yl) benzenesulfonamide (41g)**: Synthesized according to General Procedure J using 1,3-dioxoisoindolin-2-yl acetate **31g** (82.1 mg, 0.4 mmol, 2.0 equiv.) and 2-((4-((7-chloro-2-methylquinolin-4-yl) amino) pentyl) (ethyl) amino) ethan-1-ol **40f** (59.7 mg, 0.2 mmol, 1.0 equiv.) in NMP (2 ml, 0.1 M) for 48 hours. The crude mixture was purified by flash column chromatography on silica gel (20% CH_2Cl_2 in MeOH as eluent) to afford **41g** (37.5 mg, 60% yield) as a white solid.

^{1}H NMR (300 MHz, $CDCl_3$) δ 9.48 (s, 1H), 8.01 – 7.91 (m, 2H), 7.80 (dd, *J* = 7.3, 1.5 Hz, 1H), 7.53 – 7.36 (m, 5H), 6.98 (s, 1H), 2.82 (s, 3H), 2.70 (s, 4H).

^{13}C NMR (101 MHz, $CDCl_3$) δ 176.0, 158.0, 139.6, 138.2, 134.0, 133.0, 129.1, 127.4, 126.7, 124.2, 116.7, 115.4, 29.1, 25.3.

HRMS: calculated for $C_{17}H_{16}N_2NaO_2S$ ($M+Na^+$): 335.3762, found: 335.3768.

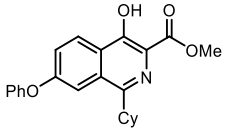

Methyl 1-cyclohexyl-4-hydroxy-7-phenoxyisoquinoline-3-carboxylate (41h): Synthesized according to General Procedure J using 1,3-dioxoisoindolin-2-yl cyclohexanecarboxylate **31a** (109 mg, 0.4 mmol, 2.0 equiv.,) and Roxadustat analogue **40g** (59.1 mg, 0.2 mmol, 1.0 equiv.). The crude mixture was purified by flash column chromatography on silica gel (50% EtOAc in hexane as eluent) to afford **41h** (67.1 mg, 89% yield) as a white solid.

^{1}H NMR (400 MHz, $CDCl_3$) δ 8.41 (d, *J* = 9.1 Hz, 1H), 7.62 (d, *J* = 2.4 Hz, 1H), 7.49 – 7.41 (m, 3H), 7.27 – 7.21 (m, 1H), 7.17 – 7.10 (m, 2H), 4.08 (s, 3H), 3.18 (tt, *J* = 11.6, 3.3 Hz, 1H), 1.99 – 1.85 (m, 4H), 1.86 – 1.71 (m, 3H), 1.51 – 1.31 (m, 3H).

^{13}C NMR (101 MHz, $CDCl_3$) δ 171.8, 159.0, 156.1, 155.4, 155.4, 131.4, 130.3, 126.2, 124.6, 124.2, 121.9, 119.8, 119.0, 111.4, 53.0, 41.9, 32.2, 26.8, 26.2.

HRMS: calculated for $C_{23}H_{24}NO_4$ ($M+H^+$): 378.1700, found: 378.1702.

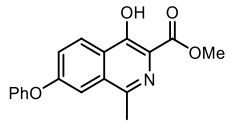

Methyl 4-hydroxy-1-methyl-7-phenoxyisoquinoline-3-carboxylate (41i): Synthesized according to General Procedure J using 1,3-dioxoisoindolin-2-yl acetate **31g** (82.1 mg, 0.4 mmol, 2.0 equiv.) and Roxadustat analogue **40g** (59.1 mg, 0.2 mmol, 1.0 equiv.) in NMP (2 ml) for 48 hours. The crude mixture was purified by flash column chromatography on silica gel (50% EtOAc in hexane as eluent) to afford **41i** (57.5 mg, 93% yield) as a white solid.

^{1}H NMR (300 MHz, $CDCl_3$) δ 11.83 (s, 1H), 8.44 (d, *J* = 9.1 Hz, 1H), 7.53 – 7.43 (m, 3H), 7.38 (m, 1H), 7.29 (tt, *J* = 6.4, 1.2 Hz, 1H), 7.16 – 7.09 (m, 2H), 4.04 (s, 3H), 2.71 (s, 3H).

^{13}C NMR (101 MHz, $CDCl_3$) δ 175.4, 160.1, 156.4, 155.2, 147.5, 130.7, 130.5, 126.7, 125.4, 124.2, 122.4, 120.4, 119.1, 108.6, 53.0, 30.0.

Matching reported literature data.[61]

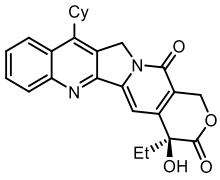

(*S*)-11-Cyclohexyl-4-ethyl-4-hydroxy-1,12-dihydro-14H-pyrano [3',4':6,7] indolizino [1,2-b] quinoline-3,14(4H)-dione (41j): Synthesized according to General Procedure using J 1,3-dioxoisoindolin-2-yl cyclohexanecarboxylate **31a** (109 mg, 0.4 mmol, 2 equiv.) and Camptothecin **40h** (69.7 mg, 0.2 mmol, 1.0 equiv.). The crude mixture was purified by flash column chromatography on silica gel (5% CH_2Cl_2 in MeOH as eluent) to afford **41j** (41,3 mg, 48% yield) as a white solid.

^{1}H NMR (400 MHz, $CDCl_3$) δ 8.27 – 8.15 (d, *J* = 8.4 Hz, 2H), δ 7.76 (t, *J* = 7.5 Hz, 1H), 7.66 - 7.61 (m, 2H), 5.74 (d, *J* = 16.3 Hz, 1H), 5.39 (s, 2H), 5.29 (d, *J* = 16.3 Hz, 1H), 3.95 (s, 1H), 3.61 (s, 1H), 2.06 – 1.82 (m, 8H), 1.66 – 1.53 (m, 3H), 1.46 (t, *J* = 12.7 Hz, 1H), 1.03 (t, *J* = 7.4 Hz, 3H).

^{13}C NMR (101 MHz, $CDCl_3$) δ 174.1, 157.7, 150.4, 148.8, 130.9, 130.0, 127.8, 127.1, 118.5, 97.9, 72.9, 66.5, 50.8, 31.9, 31.8, 29.8, 27.1, 26.1, 8.0.

Matching reported literature data.[62]

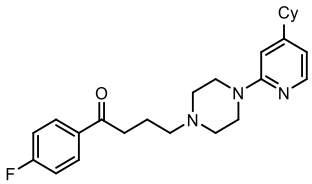

4-(4-(4-Cyclohexylpyridin-2-yl) piperazin-1-yl)-1-(4-fluorophenyl) butan-1-one (41k): Synthesized according to General Procedure J using 1,3-dioxoisoindolin-2-yl cyclohexanecarboxylate **31a** (109 mg, 0.4 mmol, 2.0 equiv.) and Azaperone **40i** (65.5 mg, 0.2 mmol, 1.0 equiv.). The crude mixture was purified by flash column chromatography on silica gel (50% EtOAc in hexane as eluent) to afford **41k** (21.3 mg, 26% yield) as a white solid.

^{1}H NMR (400 MHz, Acetone-d_6) δ 8.15 – 8.07 (m, 2H), 7.46 (dd, *J* = 8.4, 7.3 Hz, 1H), 7.30 – 7.24 (m, 2H), 6.63 (d, *J* = 8.4 Hz, 1H), 6.54 (d, *J* = 7.4 Hz, 1H), 3.65 – 3.53 (m, 4H), 3.19

[61] Wei, W.; Wang, L.; Bao, P.; Shao, Y.; Yue, H.; Yang, D.; Yang, X.; Zhao, X.; Wang, H., Metal-Free C(sp2)–H/N–H Cross-Dehydrogenative Coupling of Quinoxalinones with Aliphatic Amines under Visible-Light Photoredox Catalysis. *Org. Lett.* **2018**, *20*, 7125-7130.

[62] Li, G.-X.; Morales-Rivera, C. A.; Wang, Y.; Gao, F.; He, G.; Liu, P.; Chen, G., Photoredox-mediated Minisci C–H alkylation of N-heteroarenes using boronic acids and hypervalent iodine. *Chem. Sci.* **2016**, *7*, 6407-6412.

(t, *J* = 6.9 Hz, 2H), 3.00 – 2.90 (m, 5H), 2.52 (tt, *J* = 11.8, 3.4 Hz, 1H), 2.15 – 2.07 (m, 2H), 1.83 – 1.28 (m, 10H).

^{13}C NMR (101 MHz, Acetone-d_6) δ 198.7, 165.1, 159.5, 138.7, 131.8, 131.7, 116.4, 116.2, 111.1, 105.1, 58.1, 53.5, 47.1, 45.1, 36.4, 33.5, 30.6, 27.3, 26.9.

^{19}F NMR (376 MHz, Acetone-d_6) δ –108.12.

HRMS: calculated for $C_{25}H_{33}FN_3O$ ($M+H^+$): 410.2602, found 410.2595.

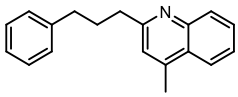

4-Methyl-2-(3-phenylpropyl)quinoline (41l): Synthesized according to General Procedure J using 1,3-dioxoisoindolin-2-yl 4-phenylbutanoate **31b** (123 mg, 0.4 mmol, 2.0 equiv.) and 4-methylquinoline **40a** (26.4 µL, 0.2 mmol, 1.0 equiv.). The crude mixture was purified by flash column chromatography on silica gel (10% EtOAc in hexane as eluent) to afford **41l** (46.0 mg, 88% yield) as a white solid.

^{1}H NMR (400 MHz, $CDCl_3$) δ 8.11 – 8.03 (m, 1H), 7.95 (dd, *J* = 8.3, 1.4 Hz, 1H), 7.68 (ddd, *J* = 8.4, 6.9, 1.4 Hz, 1H), 7.51 (ddd, *J* = 8.2, 6.9, 1.3 Hz, 1H), 7.33 – 7.26 (m, 2H), 7.26 – 7.15 (m, 3H), 7.13 (d, *J* = 1.1 Hz, 1H), 3.03 – 2.95 (m, 2H), 2.79 – 2.71 (m, 2H), 2.67 (d, *J* = 1.0 Hz, 3H), 2.21 – 2.10 (m, 2H).

^{13}C NMR (101 MHz, $CDCl_3$) δ 162.3, 147.7, 144.6, 142.3, 129.4, 129.3, 128.6, 128.4, 126.9, 125.9, 125.7, 123.7, 122.2, 38.8, 35.9, 31.7, 18.8.

HRMS: calculated for $C_{19}H_{20}N$ ($M+H^+$): 262.1586, found 262.1590.

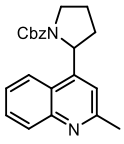

Benzyl 2-(2-methylquinolin-4-yl)pyrrolidine-1-carboxylate (41m): Synthesized according to General Procedure J using 1-benzyl 2-(1,3-dioxoisoindolin-2-yl) pyrrolidine-1,2-dicarboxylate **31c** (157 mg, 0.4 mmol, 2 equiv.) and 2-methylquinoline **40b** (27.1 µL ,0.2 mmol, 1.0 equiv.). The crude mixture was purified by flash column chromatography on silica gel (30% EtOAc in hexane as eluent) to afford **41m** (57.3 mg, 83% yield) as a yellow oil.

^{1}H NMR (400 MHz, $CDCl_3$) mixture of rotamers: δ 8.08 (t, *J* = 9.5 Hz, 1H), 7.92 (dd, *J* = 8.8, 4.0 Hz, 1H), 7.67 (dt, *J* = 12.4, 7.6 Hz, 1H), 7.50 (t, *J* = 7.5 Hz, 1H), 7.44 – 7.28 (m, 2H), 7.11 (dt, *J* = 14.7, 7.2 Hz, 2H), 6.98 (d, *J* = 3.3 Hz, 1H), 6.85 (d, *J* = 7.4 Hz, 1H), 5.76 – 5.61 (m, 1H), 5.18 (s, 1H), 5.10 – 4.83 (m, 1H), 3.82 (td, *J* = 9.5, 8.2, 3.1 Hz, 1H), 3.77 – 3.62 (m, 1H), 2.67 (d, *J* = 26.7 Hz, 3H), 2.59 – 2.40 (m, 1H), 2.00 – 1.79 (m, 3H).

^{13}C NMR (101 MHz, $CDCl_3$) mixture of rotamers: δ 158.8, 158.6, 154.9, 149.3, 148.6, 148.0, 136.9, 136.5, 129.5, 129.3, 128.6, 128.3, 128.2, 128.1, 127.8, 127.4, 125.8, 124.1, 124.0, 123.0, 122.8, 117.6, 117.3, 67.2, 66.7, 58.1, 57.5, 47.6, 47.3, 34.2, 33.2, 25.5, 23.7, 23.0.

HRMS: calculated for $C_{22}H_{23}N_2O_2$ ($M+H^+$): 347.1754, found 347.1760.

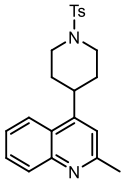

2-Methyl-4-(1-tosylpiperidin-4-yl)quinoline (41n): Synthesized according to General Procedure J using 1,3-dioxoisoindolin-2-yl 1-tosylpiperidine-4-carboxylate **31f** (171 mg, 0.4 mmol, 2.0 equiv.) and 2-methylquinoline **40b** (27.1 µL ,0.2 mmol, 1.0 equiv.) using *set-up 4* at 60 °C. The crude mixture was purified by flash column chromatography on silica gel (30% EtOAc in hexane as eluent) to afford **41n** (56.2 mg, 74% yield) as a white solid.

^{1}H NMR (400 MHz, $CDCl_3$) δ 8.04 (dd, *J* = 8.5, 1.3 Hz, 1H), 7.85 (dd, *J* = 8.5, 1.4 Hz, 1H), 7.74 – 7.67 (m, 2H), 7.63 (ddd, *J* = 8.3, 6.8, 1.4 Hz, 1H), 7.43 (ddd, *J* = 8.3, 6.8, 1.3 Hz, 1H), 7.36 (d, *J* = 2.0 Hz, 2H), 7.12 (s, 1H), 4.08 – 3.96 (m, 2H), 3.20 (tt, *J* = 11.5, 3.8 Hz, 1H), 2.71 (s, 3H), 2.47 (m, 5H), 2.07 – 1.85 (m, 4H).

^{13}C NMR (101 MHz, $CDCl_3$) δ 159.0, 150.3, 148.2, 143.8, 133.1, 129.9, 129.8, 129.2, 127.9, 125.8, 124.8, 122.2, 118.6, 47.0, 36.4, 31.8, 25.5, 21.7.

HRMS: calculated for $C_{22}H_{25}N_2O_2S$ ($M+H^+$): 381.1627, found 381.1631.

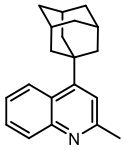

4-((3s)-Adamantan-1-yl)-2-methylquinoline (41o): Synthesized according to General Procedure J using 1,3-dioxoisoindolin-2-yl (3r,5r,7r)-adamantane-1-carboxylate **31h** (130 mg, 0.4 mmol, 2 equiv.) and 2-methylquinoline **40b** (27.1 µL ,0.2 mmol, 1.0 equiv.) using *set-up 4* at 60 °C. The crude mixture was purified by flash column chromatography on silica gel (10% EtOAc in hexane as eluent) to afford **41n** (38.2 mg, 69% yield) as a white solid.

^{1}H NMR (400 MHz, $CDCl_3$) δ 8.62 (d, *J* = 8.8 Hz, 1H), 8.35 (s, 1H), 7.69 (ddd, *J* = 8.3, 6.8, 1.3 Hz, 1H), 7.52 (ddd, *J* = 8.5, 6.8, 1.5 Hz, 1H), 7.28 (s, 1H), 2.85 (s, 3H), 2.29 – 2.28 (m, 6H), 2.23 - 2.22 (m, 3H), 1.89 (t, *J* = 3.1 Hz, 6H).

^{13}C NMR (101 MHz, $CDCl_3$) δ 159.5, 130.1, 126.3, 125.4, 125.3, 119.7, 42.3, 39.3, 36.9, 29.1.

HRMS: calculated for $C_{20}H_{24}N$ ($M+H^+$): 278.1897, found 278.1903.

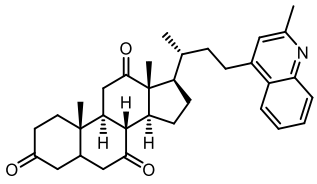

(8*R*,9*S*,10*S*,13*R*,14*S*,17*R*)-10,13-dimethyl-17-((*R*)-4-(2-methylquinolin-4-yl)butan-2-yl)dodecahydro-3H-cyclopenta[a]phenanthrene-3,7,12(2H,4H)-trione (41p): Synthesized according to General Procedure J using Dehydrocholic acid phthalimide ester **31d** (219 mg, 0.4 mmol, 2.0 equiv.) and 2-methylquinoline **40b** (27.1 µL ,0.2 mmol, 1.0 equiv.). The crude mixture was purified by flash column chromatography on silica gel (30% EtOAc in hexane as eluent) to afford **41p** (70.0 mg, 61% yield) as a white solid.

^{1}H NMR (400 MHz, $CDCl_3$) δ 8.12 (d, *J* = 8.4 Hz, 1H), 7.96 (dd, *J* = 8.5, 1.4 Hz, 1H), 7.67 (ddd, *J* = 8.4, 6.9, 1.4 Hz, 1H), 7.51 (ddd, *J* = 8.2, 6.9, 1.3 Hz, 1H), 7.14 (s, 1H), 3.15 (ddd, *J* = 13.7, 11.7, 5.0 Hz, 1H), 2.96 – 2.85 (m, 4H), 2.74 (s, 3H), 2.41 –1.22 (m, 19H), 1.39 (s, 3H), 1.08 (s, 3H), 1.05 (d, *J* = 6.6 Hz, 3H).

^{13}C NMR (101 MHz, $CDCl_3$) δ 212.1, 209.1, 208.8, 158.4, 150.6, 146.9, 129.7, 128.6, 126.0, 125.9, 123.4, 121.8, 57.0, 51.9, 49.1, 46.9, 45.7, 45.6, 45.1, 42.9, 38.7, 36.6, 36.5, 36.3, 36.1, 35.4, 29.5, 27.9, 25.2, 24.8, 22.0, 19.2, 12.0.

HRMS: calculated for $C_{33}H_{42}NO_3$ ($M+H^+$): 500.3157, found: 500.3159.

4.7.7.3 General procedure K (enantioselective variant)

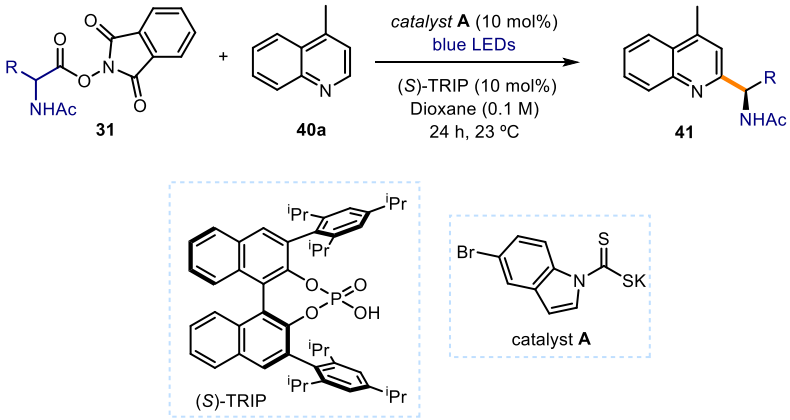

*Reactions performed using **set-up 4** in Figure 4.8.* In an oven dried vial, with a Teflon septum screw cap, 4-methylquinoline (26.4 µL ,0.2 mmol, 1.0 equiv.) and chiral phosphoric acid (*S*)-TRIP (7.5 mg, 0.01 mmol, 5 mol%) were dissolved in dioxane (2 ml). Then, phthalimide ester **31** (0.4 mmol, 2 equiv.) and catalyst **A** (6.2 mg, 0.02 mmol, 0.1 equiv.) were added. The resulting yellow mixture was degassed with argon sparging for 60 seconds. The vial was placed in the one-position photoreactor with temperature control and irradiated under stirring for 24 hours, unless otherwise specified. The solvent was evaporated, and the residue purified by column chromatography to afford the corresponding product in the stated yield with >95% purity according to ^{1}H NMR analysis.

4.7.7.4 Characterization of products with general procedure K (enantioselective variant)

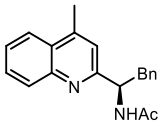

(*R*)-*N*-(1-(4-methylquinolin-2-yl)-2-phenylethyl) acetamide (41q): Synthesized according to General Procedure K using 1,3-dioxoisoindolin-2-yl acetylphenylalaninate **31i** (140 mg, 0.4 mmol) and 4-methylquinoline **40a** (26.4 μL, 0.2 mmol). The crude mixture was purified by flash column chromatography on silica gel (40% EtOAc in hexane as eluent) to afford **41q** (60.0 mg, 97% yield) as a white solid.

^{1}H NMR (400 MHz, $CDCl_3$) δ 8.05 (dt, *J* = 8.5, 0.9 Hz, 1H), 7.96 (ddd, *J* = 8.3, 1.5, 0.6 Hz, 1H), 7.70 (ddd, *J* = 8.4, 6.9, 1.5 Hz, 1H), 7.59 – 7.51 (m, 1H), 7.27 (s, 1H), 7.18 – 7.13 (m, 3H), 6.99 – 6.92 (m, 2H), 6.82 (d, *J* = 1.2 Hz, 1H), 5.39 (td, *J* = 7.7, 5.4 Hz, 1H), 3.35 (dd, *J* = 13.3, 5.4 Hz, 1H), 3.17 (dd, *J* = 13.3, 7.9 Hz, 1H), 2.59 (d, *J* = 0.9 Hz, 3H), 2.07 (s, 3H).

^{13}C NMR (101 MHz, $CDCl_3$) δ 169.6, 158.9, 147.1, 144.9, 137.3, 129.8, 129.5, 129.4, 128.2, 127.6, 126.6, 126.3, 124.00, 121.7, 55.6, 42.3, 23.7, 18.9.
Matching reported literature data.[29]

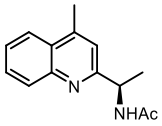

(*R*)-*N*-(1-(4-methylquinolin-2-yl) ethyl) acetamide (41r): Synthesized according to General Procedure K using 1,3-dioxoisoindolin-2-yl acetylalaninate **31j** (110 mg, 0.4 mmol) and 4-methylquinoline **40a** (26.4 μL ,0.2 mmol). The crude mixture was purified by flash column chromatography on silica gel (40% AcOEt in hexane as eluent) to afford **41r** (38.3 mg, 84% yield) as a white solid.

^{1}H NMR (400 MHz, $CDCl_3$) δ 8.08 (dt, *J* = 8.1, 1.0 Hz, 1H), 7.98 (ddd, *J* = 8.3, 1.5, 0.7 Hz, 1H), 7.71 (ddd, *J* = 8.4, 6.9, 1.4 Hz, 1H), 7.56 (ddd, *J* = 8.3, 6.9, 1.3 Hz, 1H), 7.51 (s, 1H), 7.17 (d, *J* = 1.1 Hz, 1H), 5.21 (p, *J* = 6.8 Hz, 1H), 2.70 (d, *J* = 1.0 Hz, 3H), 2.11 (s, 3H), 1.54 (d, *J* = 6.8 Hz, 3H).

^{13}C NMR (101 MHz, $CDCl_3$) δ 169.6, 160.7, 146.9, 145.8, 129.6, 129.3, 127.6, 126.4, 123.9, 120.5, 50.1, 23.74, 22.8, 19.0.
Matching reported literature data.[29]

4.7.8 Trifluoromethylation

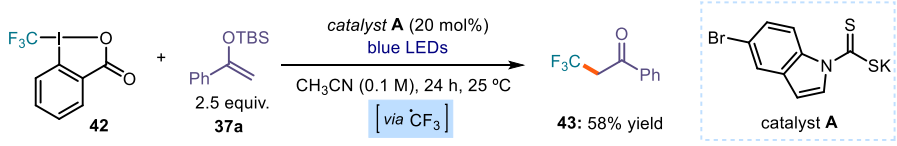

*Reactions performed using **set-up 3** in Figure 4.7*. In an oven dried vial with a Teflon septum screw cap, silyl enol ether **37a** (117 mg, 0.5 mmol, 2.5 equiv.) was dissolved in MeCN (2 mL), then the Togni reagent **42** (105 mg (60% Wt) 0.2 mmol, 1.0 equiv.), catalyst **A** (6.2 mg, 0.02 mmol, 0.1 equiv.). The resulting orange mixture was degassed bubbling argon for 60

seconds. The vial was then placed in the irradiation setup, maintained at a temperature of 25 ºC (25-26 ºC measured in the central well), and the reaction, unless otherwise stated, was stirred for 24 hours under continuous irradiation from a blue LED strip. The crude mixture was diluted with AcOEt and brine was added. The combined organic fractions were dried over anhydrous $MgSO_4$, filtered, and concentrated to dryness. The crude mixture was purified by flash column chromatography on silica gel (Hexane/AcOEt) to afford **43** (22 mg, 58% yield) as a yellow oil.

^{1}H NMR (300 MHz, $CDCl_3$) δ 8.01 – 7.91 (m, 2H), 7.69 – 7.61 (m, 1H), 7.60 – 7.46 (m, 3H), 3.82 (q, *J* = 10.0 Hz, 2H).

^{19}F NMR (376 MHz, $CDCl_3$) δ –62.11.

^{13}C NMR (126 MHz, CDCl3) δ 135.7, 134.2, 128.9, 128.4, 124.7, 42.2.
Matching reported literature data.[63]

4.7.9 Amidyl radical

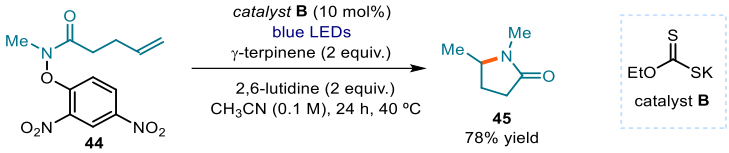

*Reactions performed using **set-up 1** in Figure 4.3.* In an oven dried vial, with a Teflon septum screw cap, **44** (29 mg, 0.1 mmol, 1 equiv.) and catalyst **B** (1.6 mg, 0.01 mmol, 0.1 equiv.) were dissolved in CH_3CN (1 mL), then 2,6-lutidine (23 µL, 0.2 mmol, 2.0 equiv.) was added, followed by γ-terpinene (32 µL, 0.2 mmol, 2 equiv.). The resulting orange mixture was degassed with argon sparging for 60 seconds. The vial was then placed in the 3D printed support photoreactor and irradiated under stirring for 16 hours. The crude mixture was concentrated to dryness. Trichloroethylene was added as internal standard (9 µL, 0.1 mmol, 1.0 equiv) and NMR yield was determined by ^{1}H NMR in $CDCl_3$ matching reported literature data.[45]

[63] Jacquet J.; Cheaib K.; Ren Y.; Vezin H.; Orio M.; Blanchard S.; Fensterbank L.; Desage El Murr M., Circumventing Intrinsic Metal Reactivity: Radical Generation with Redox-Active Ligands. *Chem. Eur. J.* **2017**, *23*, 15030-15034.

4.7.10 Large scale reactions

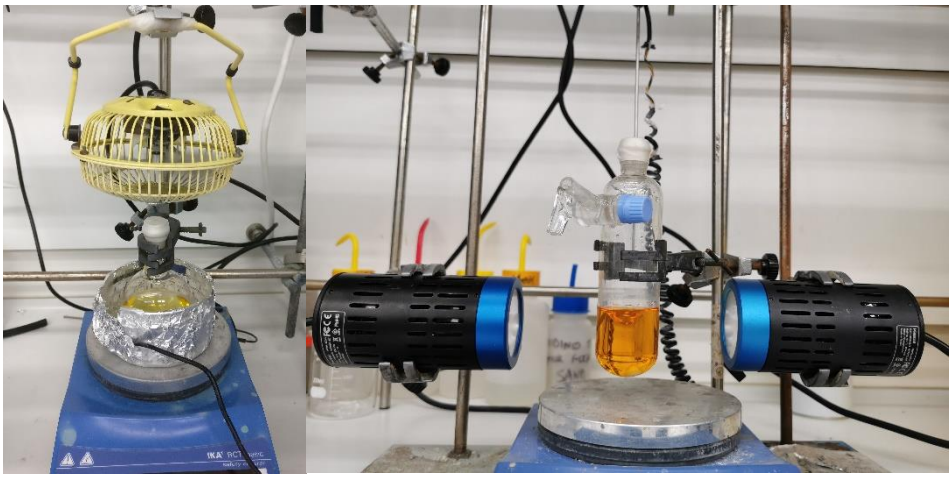

Figure 4.9. Scale-up set-ups. Barton decarboxylation (left). Minisci reaction (right).

4.7.10.1 Barton decarboxylation

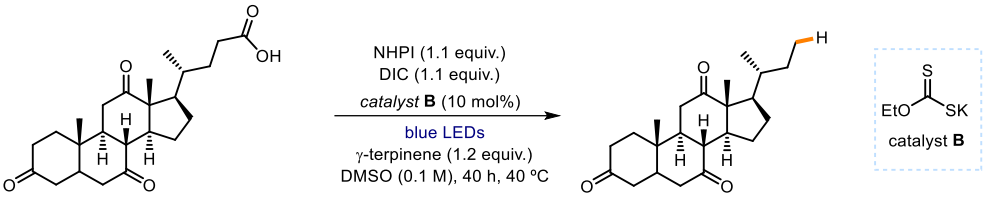

dehydrocholic acid

36d: 55% yield (4 mmol)

Using set-up in Figure 4.9 (left). In a 100 mL round bottom flask with a Teflon cap, dehydrocholic acid (1,62 g, 4 mmol, 1 equiv.), *N*-hydroxyphthalimide (NHPI, 716 mg, 4.4 mmol, 1.1 equiv.), and xanthogenate catalyst **A** (64 mg, 0.4 mmol, 0.1 equiv.) were dissolved in DMSO (40 mL), and *N,N'*-diisopropylcarbodiimide (DIC, 760 µL, 4.4 mmol, 1.1 equiv.) was added via syringe. Then, γ-terpinene (760 µL, 4.8 mmol, 1.2 equiv.) was added. The resulting orange mixture was degassed with nitrogen sparging for 5 min. The round bottom flask was then irradiated for 40 hours with a 1-meter 14W blue LED strip and cooled with a fan to keep the temperature between 30 and 35 ºC (see Figure 4.9, left). The mixture was transferred to an extraction funnel, NaOH 1M solution was added and the organic layer was extracted with CH_2Cl_2. The organic layer was dried over anhydrous $MgSO_4$, filtered, and concentrated to dryness. The crude residue was purified by chromatography on silica gel (10% AcOEt in hexanes) to afford 800 mg of product **36d** (2.2 mmol, 55% yield) as an off white solid. NMR analysis was consistent with product synthesized in the small scale process.

4.7.10.2 Minisci reaction

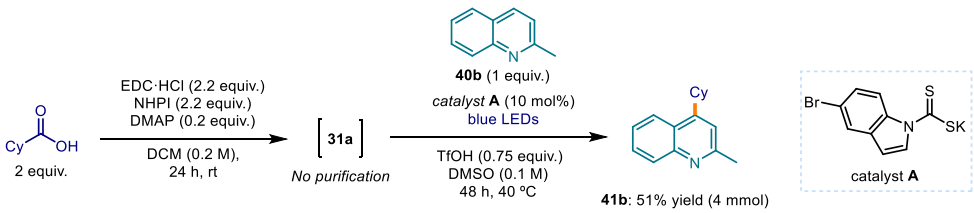

Using set-up in Figure 4.9 (right). In a 100 mL round bottom flask, cyclohexanecarboxylic acid (1.03 g, 8 mmol, 2 equiv.), EDC·HCl (1.69 g, 8.8 mmol, 2.2 equiv.), DMAP (97.7 mg, 0.8 mmol, 0.2 equiv.), and *N*-hydroxyphthalimide (1.44 g, 8.8 mmol, 2.2 equiv.) were dissolved in CH_2Cl_2 (20 mL). The reaction was stirred at ambient temperature for 24 hours. The mixture was transferred to an extraction funnel, $NaHCO_3$ sat. solution was added and the organic layer was extracted with CH_2Cl_2. The organic phase was concentrated to dryness under vacuum to obtain the crude phthalimide ester, which was used without further purification in the next step.

In a 100 mL Schlenk flask with a Teflon septum, the crude phthalimide ester was dissolved in DMSO (40 mL). Then, 2-methylquinoline (540 µL, 4.00 mmol, 1.0 equiv.), trifluoromethanesulfonic acid (265 µL, 3.00 mmol, 0.75 equiv.) and catalyst **A** (124 mg, 0.40 mmol, 0.1 equiv.) were added. The resulting orange mixture was degassed with nitrogen sparging for 5 minutes. The Schlenk flask was irradiated with stirring for 48 hours using two 50 W Kessil blue LED lamp (one PR160L-456 and one PR160L-427, 100% intensity, 4-5 cm away) (see Figure 4.9, right). The mixture was transferred to an extraction funnel, $NaHCO_3$ sat. solution was added and the organic layer was extracted with CH_2Cl_2. The organic layer was dried over anhydrous $MgSO_4$, filtered, and concentrated to dryness. The crude residue was purified by chromatography on silica gel (10% AcOEt in hexanes) to afford 459 mg of product **41b** (2.04 mmol, 51% yield) as a yellowish oil. NMR analysis was consistent with product synthesized in the small scale process.

4.7.11 Unsuccessful substrates

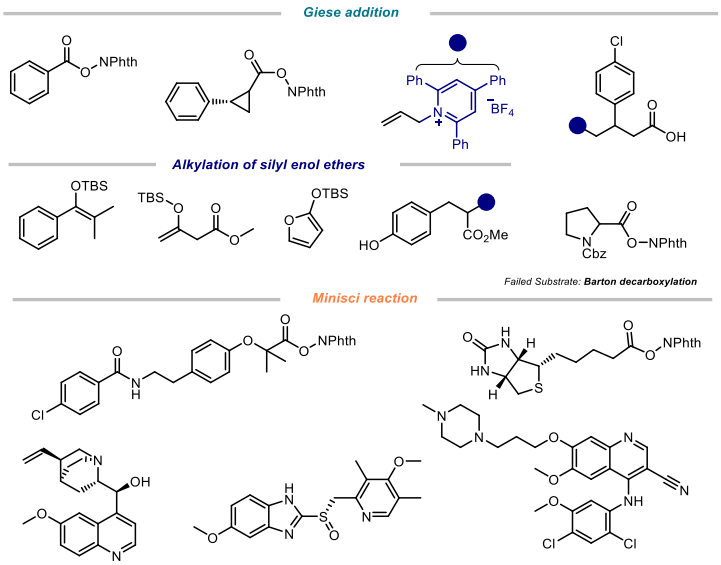

Scheme 4.31. Unsuccessful substrates that offered poor yields (ranging from 0 to <20%).

4.8 Mechanistic studies

4.8.1 Control experiments

4.8.1.1 Experiments with green light

For the reactions performed under green light irradiation, an EvoluChem™ P303-30-1 LEDs (18 W, λ_{max}= 520 nm) was used. The reaction temperature was measured to be between 25 °C and 30 °C using the setup depicted in Figure 4.10).

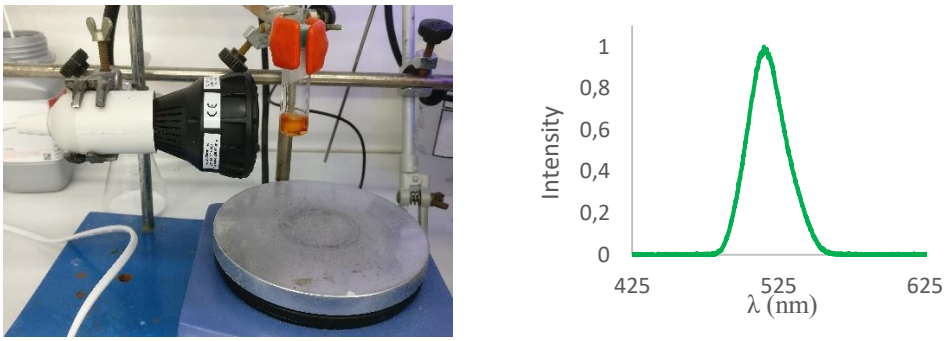

Figure 4.10. Reaction set-up for green light irradiation (*left*). Emission spectrum of the 520 nm EvoluChem™ P303-30-1 LEDs used in this reactor (*right*).

4.8.1.2 Optimization studies

Table 4.3. Barton decarboxylation.

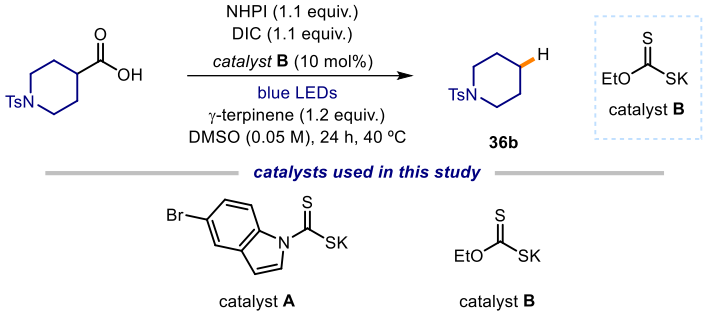

entry	catalyst	deviation	yield (%)[a]
1	**B**	none	80 (77)[b]
2	**B**	isolated RAE	80
3	**A**	none	traces
4	**B**	under air	0
5	**B**	no light	0
6	none	none	0

Reactions performed using ***set-up 1*** *in Figure 4.3.*

Table 4.4. Deamination with pyridinium salts as radical precursors.

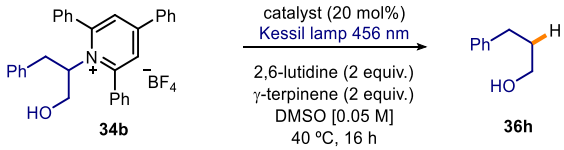

entry	catalyst	deviation	yield (%)[a]
1	**A**	none	95 (78)[b]
2	**A**	under air	0
3	**A**	no light	0
4	none	none	0

Reactions performed using ***set-up 2*** in Figure 4.4.

Table 4.5. α-alkylation of silyl enol ethers.

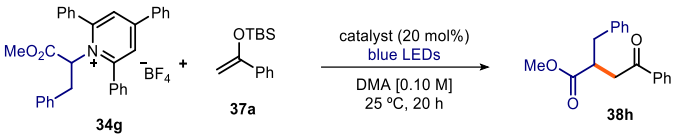

catalysts used in this study

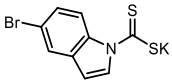

catalyst **A**

catalyst **B**

entry	catalyst	Base	deviation	yield (%)[a]
1	**A**	-	none	16
2	**A**	2,6-lutidine (1 equiv.)	none	95 (89%)[b]
3	**B**	2,6-lutidine (1 equiv.)	none	80
4	**B**	2,6-lutidine (1 equiv.)	Green light	45
5	**A**	2,6-lutidine (1 equiv.)	cat. 10 mol%	62
6	**A**	2,6-lutidine (1 equiv.)	under air	0
7	**A**	2,6-lutidine (1 equiv.)	no light	0
8	none	2,6-lutidine (1 equiv.)	none	0

Reactions performed using ***set-up 3*** *in Figure 4.7.*

Table 4.6. Minisci reaction.

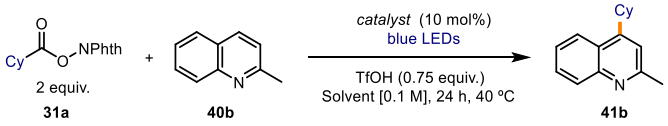

catalysts used in this study

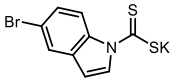

catalyst **A**

catalyst **B**

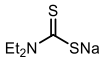

catalyst **C**

entry	catalyst	Solvents	deviation	yield (%)[a]
1	**A**	DMSO	TFA	82
2	**B**	DMSO	TFA	0
3	**C**	DMSO	TFA	0
6	**A**	DMSO	none	97(95)[b]
8	**A**	DMSO	Green light	8
9	**A**	DMSO	No acid	0
10	**A**	DMSO	No light	0
11	**A**	DMSO	under air	0
12	none	DMSO	none	0

Reactions performed using ***set-up 2*** *in* Figure 4.4.

Table 4.7. Trifluoromethylation of silyl enol ethers.

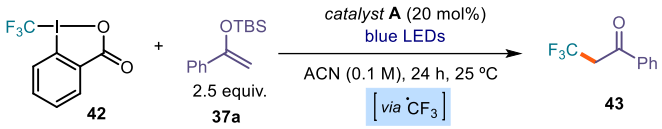

entry	catalyst	Base	deviation	yield (%)[a]
1	**A**	-	Acetone	21
2	**A**	-	none	63(58%)[b]
3	**A**	2,6-lutidine (1 equiv.)	none	62
4	**B**	-	none	22
5	**C**	-	none	27
6	-	-	No catalyst	0

*Reactions performed using **set-up 3** in Figure 4.7.*

Table 4.8. Amidyl radical cyclization

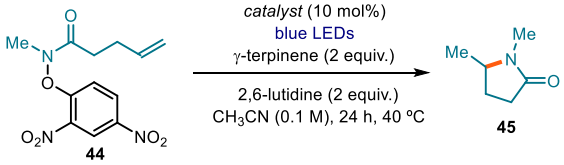

catalysts used in this study

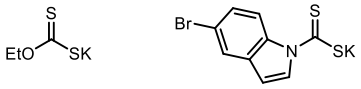

catalyst **A** catalyst **B**

entry	catalyst	deviation	yield (%)[a]
1	**A**	None	86
2	**B**	None	78
3	**A**	No base	60
4	**B**	No base	50
5	**A**	Under air	0
6	**A**	No light	0
7	none	None	0

*Reactions performed using **set-up 1** in Figure 4.3.*

4.8.1.3 TEMPO trapping experiment

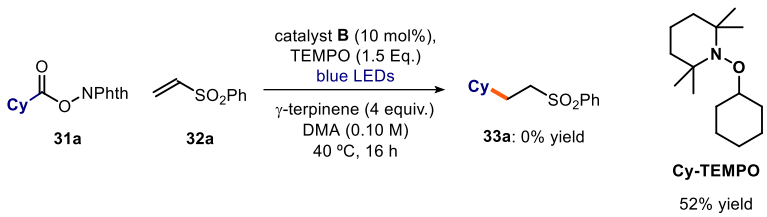

*Reactions performed using **set-up 1** in Figure 4.3.* In an oven dried vial with a Teflon septum screw cap, potassium ethyl xanthogenate **B** (1.6 mg, 0.01 mmol, 0.1 equiv.), phthalimide ester **31a** (0.1 mmol, 27.3 mg, 1 equiv.), 2,2,6,6-tetramethylpiperidine 1-oxyl (TEMPO, 0.15 mmol, 23.5 mg, 1.5 equiv.) and **32a** (0.15 mmol, 25.2 mg, 1.5 equiv.) were dissolved in DMA (1 mL). Then, γ-terpinene (64 μL, 0.4 mmol, 4 equiv.) was added. The resulting orange mixture was degassed by argon sparging for 60 seconds. The vial was then placed in the 3D printed support photoreactor (**Figure 4.3**) and irradiated under stirring for 16 hours. The mixture was transferred to an extraction funnel, brine was added and the organic layer was extracted with EtOAc. The organic layer was dried over anhydrous $MgSO_4$, filtered, and concentrated to dryness. The crude residue was then purified by column chromatography (2% EtOAc in hexanes) to afford the corresponding **Cy-TEMPO** adduct in 52% yield. No product corresponding with giese addition was detected in the crude NMR or during the purification.

^{1}H NMR (500 MHz, $CDCl_3$) δ 3.68 – 3.64 (m, 1H), 2.07 (brs, 2H), 1.76 (brs, 2H), 1.57 – 1.54 (m, 2H), 1.48 – 1.45 (m, 4H), 1.31 – 1.06 (m, 19H).

^{13}C NMR (126 MHz, $CDCl_3$) δ 81.7, 59.6, 40.3, 32.9, 26.0, 25.1, 17.3.

Characterization data matching data reported in the literature.[64]

4.8.2 Catalysts' stability experiments

During the course of our investigation into the EDA complex system, we realized stability of the catalyst under reaction conditions was often the reason one of the catalyst greatly out-performed the other in some transformations.

In general, the potassium ethyl xanthate catalyst **B** is a suitable EDA donor catalyst when no protonated organic based is present in the mixture, we believed this is due to decomposition of the catalyst promoted by the pyridinium salt. On the other hand, indole-based dithiocarbamate anion catalyst **A** seems to be more stable to acidic media, and it does not undergo decomposition when faced with the same pyridinium salts. In order to test this hypothesis, we conducted the follwing experiments. These experiments provide an explanation on why the Minisci reaction is completely shut down when employing catalyst **B**.

[64] Tobisu M.; Koh K.; Furukawa T.; Chatani N., Modular Synthesis of Phenanthridine Derivatives by Oxidative Cyclization of 2-Isocyanobiphenyls with Organoboron Reagents. *Angew. Chem., Int. Ed.* **2012**, *51*, 11363-11366.

- *Catalyst **A***:

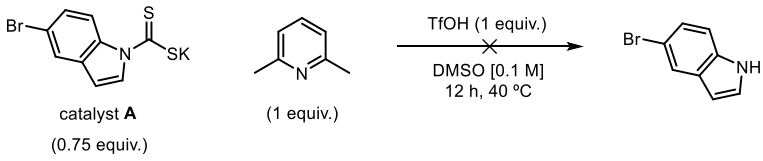

In an oven dried vial with a Teflon septum screw cap, 2,6-lutidine (0.1 mmol, 12 μL) was added followed by triflic acid (0.1 mmol, 8.9 μL). The resulting pyridinium salt was then dissolved in 1 mL of d^6-DMSO, followed by the addition of catalyst **A** (23.3 mg, 0.075 mmol). The mixture was stirred overnight and the crude mixture was analyzed by ^{1}H NMR. Catalyst A showed no degradation to the corresponding indole (see Figure 4.11).

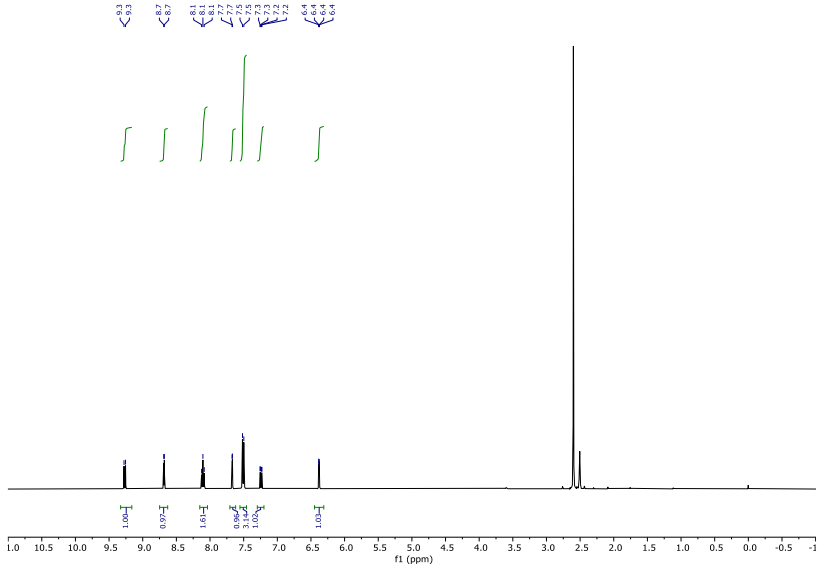

Figure 4.11. ^{1}H NMR analysis to evaluate catalyst A stability.

- *Catalyst **B***:
-

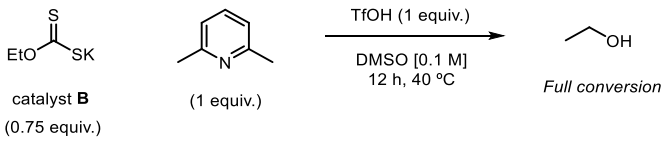

In an oven dried vial with a Teflon septum screw cap, 2,6-lutidine (0.1 mmol, 12 μL) was added followed by triflic acid (0.1 mmol, 8.9 μL). The resulting pyridinium salt was then

dissolved in 1 mL of d^6-DMSO, followed by the addition of catalyst **B** (12 mg, 0.075 mmol). The mixture was left stirring overnight and the crude mixture is analyzed by ^{1}H NMR. Catalyst **B** showed complete degradation to ethanol (Figure 4.12).

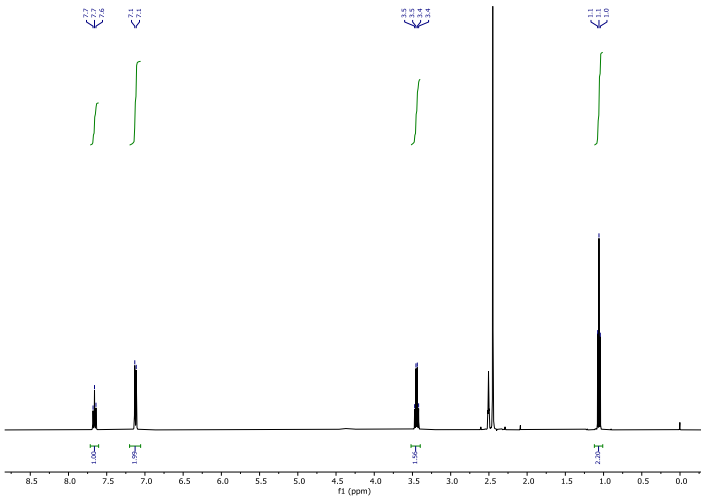

Figure 4.12. ^{1}H NMR analysis to evaluate catalyst B stability.

4.8.3 UV-Vis spectroscopy

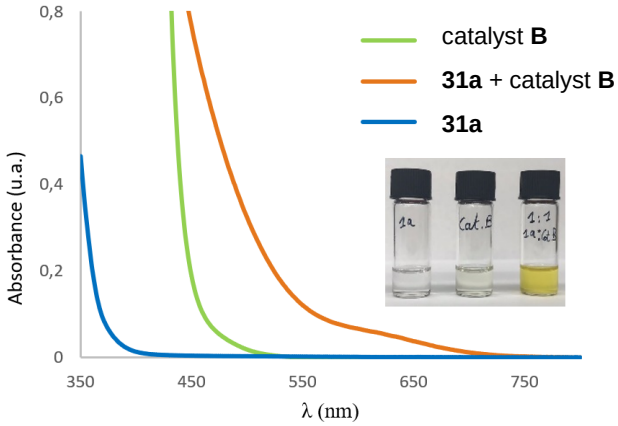

Figure 4.13. Optical absorption spectra, recorded in DMA in 1 mm path quartz cuvettes using a Shimadzu 2401PC UV−vis spectrophotometer, and visual appearance of the separate reaction components and of the colored EDA complex between catalyst **B** and **31a**. [**31a**] = 0.10 M, [catalyst **B**] = 0.01 M.

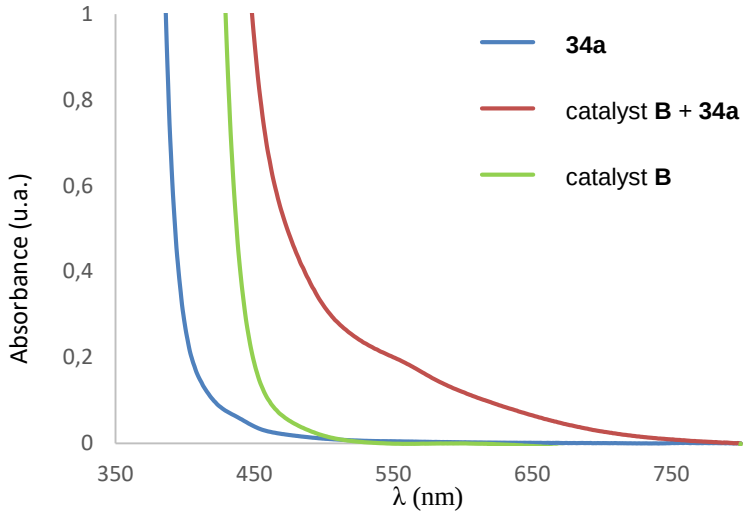

Figure 4.14. Optical absorption spectra, recorded in DMA in 1 mm path quartz cuvettes using a Shimadzu 2401PC UV−vis spectrophotometer of the separate reaction components and of the colored EDA complex between catalyst **B** and **34a.** [**34a**] = 0.10 M, [catalyst **B**] = 0.01 M.

4.8.4 Transient absorption spectroscopy (TAS)

Studies with microsecond transient absorption spectroscopy (TAS) were performed using an excitation source of NdYAG (neodymium-doped yttrium aluminium garnet) Opolette laser with an optical parametric oscillator (OPO) system that allows variable wavelength excitation from 400 -1800 nm, pulse width of 6 ns, up to 2 mJ of energy from OPO output with fiber optic coupled, and high energy output from direct NdYAG harmonics 355 (20 mJ, 5 ns) and 532 (45mJ, 6 ns). The system is completed with 150 W tungsten lamp as probe; 2 monochromators Minuteman MM151; Si amplified photodetector module for VIS; DSPDAU high speed data rate recorder and interface software from RAMDSP. Laser intensity for the chosen wavelength was 355 nm – 1.30 mJ.

We selected a logarithmic time scale suitable for clearly showing the decay of the transient species in the samples. The characteristics of the detected transient species match literature data.[3,33]

In a typical transient absorption spectroscopy experiment, solutions in DMA of a mixture of **31a** and catalyst **B** was prepared under an argon atmosphere and transferred into a screw-top 3.0 mL quartz cuvette for measurement. Upon irradiation with the appropriated wavelength, the decay of absorption at 620 nm of the transient xanthyl radical **IIb** was recorded. Irradiation at 420 nm and 460 nm of the sample also provided signal absorbing at 620 nm, but in a much lower intensity and higher noise.

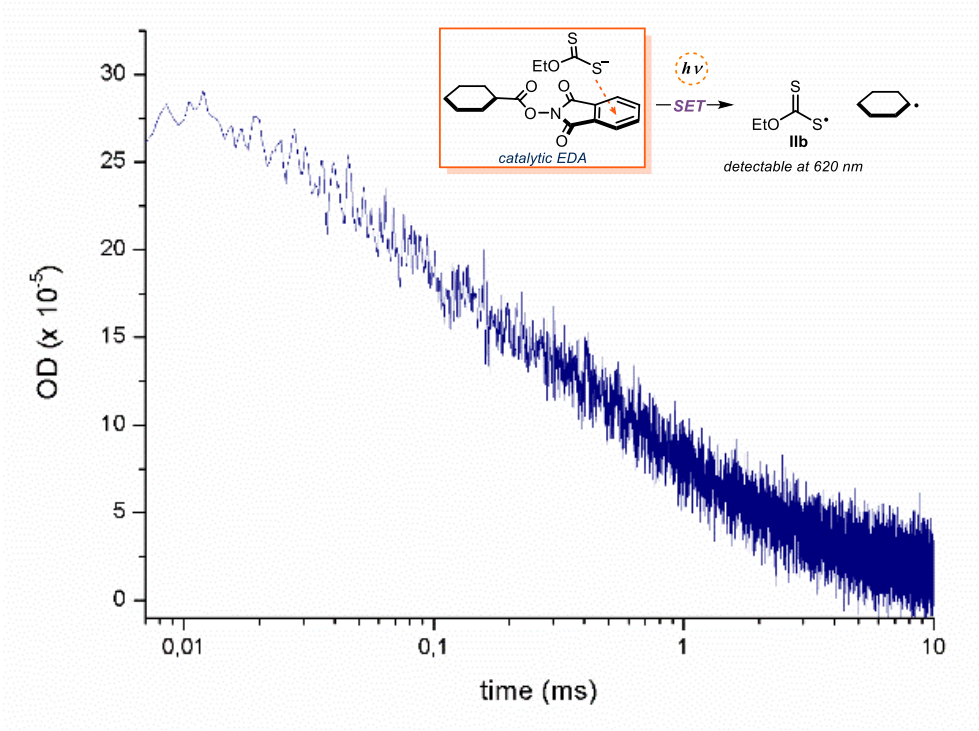

Figure 4.15. Absorption at 620 nm of the transient xanthyl radical **IIb** (blue line) generated upon 355 nm laser excitation of of a 1:1 mixture of **31a** and catalyst **B** 30 mM in DMA. Note logarithmic scale for time. ΔOD: optical density variation.

4.8.5 Cyclic voltammetry measurements

For all cyclic voltammetry (CV) measurements, a glassy carbon disk electrode (diameter 3 mm) was used as the working electrode. A silver wire coated with AgCl immersed in a 3.5 M aqueous solution of KCl and separated from the analyte by a fritted glass disk was employed as the reference electrode. A Pt wire counter-electrode completed the electrochemical setup. The scan rate used in each CV experiment is indicated case by case.

Potentials are quoted with the following notation: E_p^C refers to the cathodic peak potential, E_p^A refers to the anodic peak potential, while the E_{red} value describes the electrochemical properties of the referred compound.

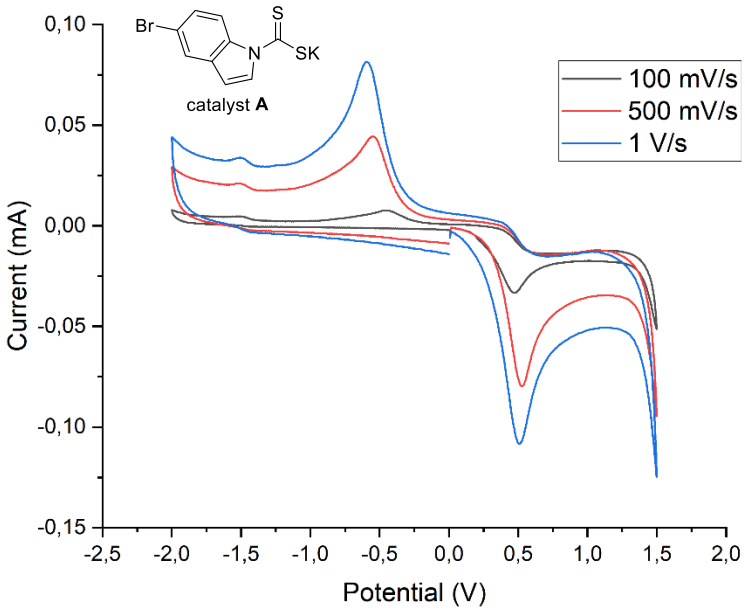

Figure 4.16. Cyclic voltammogram for catalyst **A** [0.02 M] in [0.1 M] $TBAPF_6$ in CH_3CN. Measurement started by oxidation from 0 to +1.5 V, followed by reduction from +1.5 V to -2.0 V, and finishing at 0 V. Glassy carbon electrode working electrode, Ag/AgCl (KCl 3.5 M) reference electrode, Pt wire auxiliary electrode. Two irreversible peaks observed increasing with sweep rate.

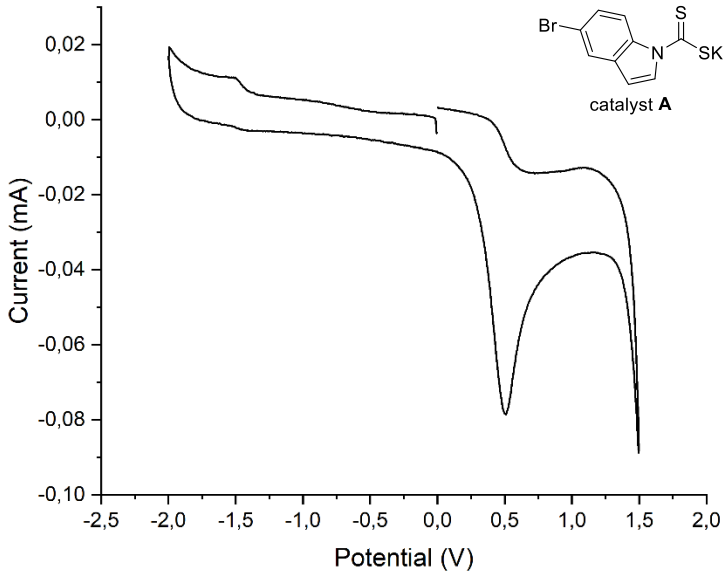

Figure 4.17. Cyclic voltammogram for catalyst **A** [0.02M] in [0.1 M] $TBAPF_6$ in CH_3CN. Measurement started by reduction from 0 to -2.0 V, followed by oxidation from -2.0 V to +1.5 V, and finishing at 0 V. Glassy carbon electrode working electrode, Ag/AgCl (KCl 3.5 M) reference electrode, Pt wire auxiliary electrode. Only one irreversible peak observed. Sweep rate: 500 mV/s.

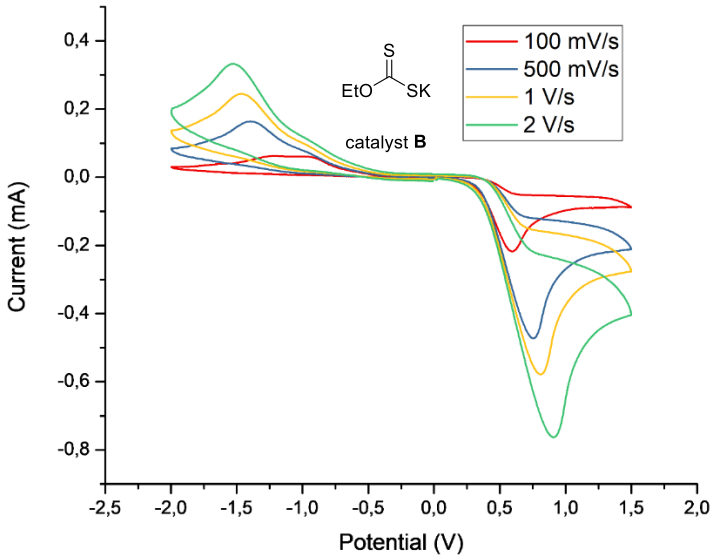

Figure 4.18. Cyclic voltammogram for catalyst **B** [0.02 M] in [0.1 M] $TBAPF_6$ in CH_3CN. Measurement started by oxidation from 0 to +1.5 V, followed by reduction from +1.5 V to -2.0 V, and finishing at 0 V. Glassy carbon electrode working electrode, Ag/AgCl (KCl 3.5 M) reference electrode, Pt wire auxiliary electrode. Two irreversible peaks observed increasing with sweep rate.

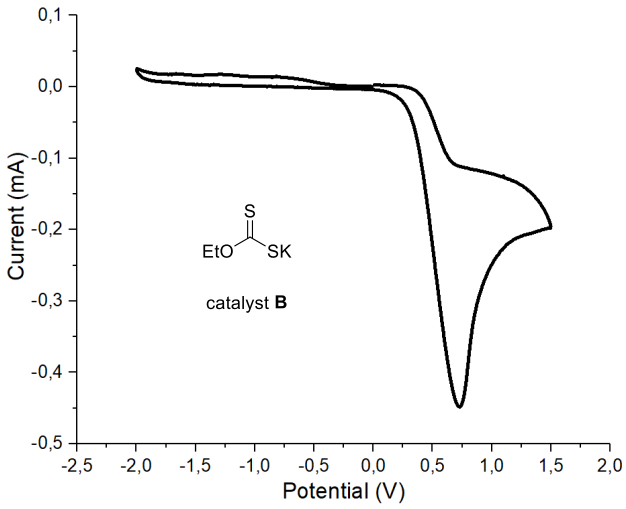

Figure 4.19. Cyclic voltammogram for catalyst **B** [0.02M] in [0.1 M] $TBAPF_6$ in CH_3CN. Measurement started by reduction from 0 to -2.0 V, followed by oxidation from -2.0 V to +1.5 V, and finishing at 0 V. Glassy carbon electrode working electrode, Ag/AgCl (KCl 3.5 M) reference electrode, Pt wire auxiliary electrode. Only one irreversible peak observed. Sweep rate: 500 mV/s.

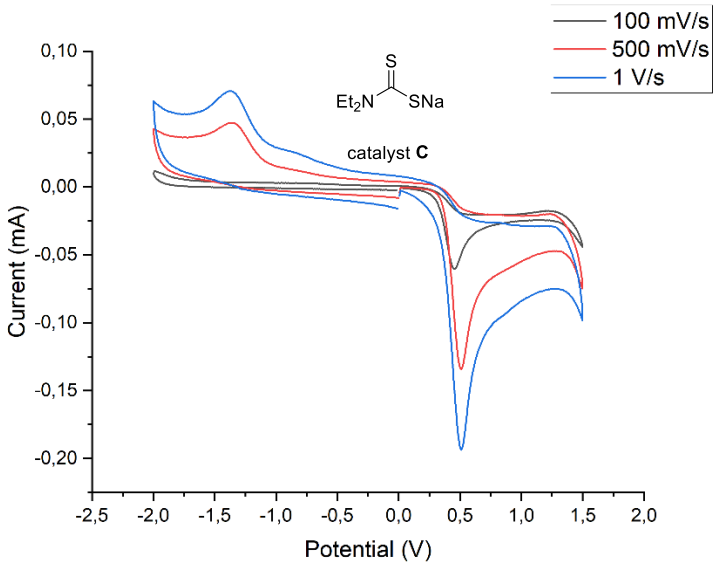

Figure 4.20. Cyclic voltammogram for catalyst **C** [0.02 M] in [0.1 M] $TBAPF_6$ in CH_3CN. Measurement started by oxidation from 0 to +1.5 V, followed by reduction from +1.5 V to -2.0 V, and finishing at 0 V. Glassy carbon electrode working electrode, Ag/AgCl (KCl 3.5 M) reference electrode, Pt wire auxiliary electrode. Two irreversible peaks observed increasing with sweep rate.

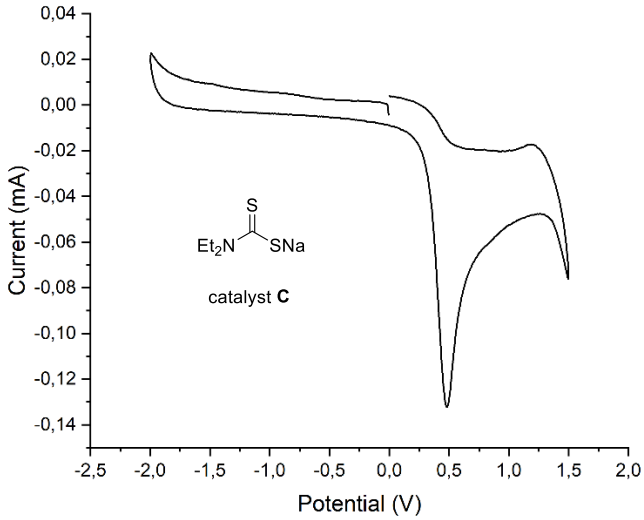

Figure 4.21. Cyclic voltammogram for catalyst **C** [0.02M] in [0.1 M] $TBAPF_6$ in CH_3CN. Measurement started by reduction from 0 to -2.0 V, followed by oxidation from -2.0 V to +1.5 V, and finishing at 0 V. Glassy carbon electrode working electrode, Ag/AgCl (KCl 3.5 M) reference electrode, Pt wire auxiliary electrode. Only one irreversible peak observed. Sweep rate: 500 mV/s.

4.8.6 Quantum yield determination

4.8.6.1 Giese addition

A ferrioxalate actinometer solution was prepared by following the Hammond variation of the Hatchard and Parker procedure outlined in the Handbook of Photochemistry.[65] The ferrioxalate actinometer solution measures the decomposition of ferric ions to ferrous ions, which are complexed by 1,10-phenanthroline and monitored by UV/Vis absorbance at 510 nm. The moles of iron-phenanthroline complex formed are related to moles of photons absorbed. The following solutions were prepared and stored in a dark laboratory (red light):

1. Potassium ferrioxalate solution: 294.8 mg of potassium ferrioxalate (commercially available from Alfa Aesar) and 139 μL of sulfuric acid (96%) were added to a 50 mL volumetric flask, and filled to the mark with water (HPLC grade).

2. Phenanthroline solution: 0.2% by weight of 1,10-phenanthroline in water (100 mg in 50 mL volumetric flask).

3. Buffer solution: 2.47 g of NaOAc and 0.5 mL of sulfuric acid (96%) were added to a 50 mL volumetric flask and filled to the mark with water (HPLC grade).

The actinometry measurements were done as follows:

1. 1 mL of the actinometer solution was added to a Schlenk tube (diameter = 12 mm). The Schlenk tube was placed in one of the positions of the 3D printed reactor (Figure 4.3). The solution was irradiated at 460 nm. This procedure was repeated 4 times, quenching the solutions after different time intervals: 1 s, 2 s, 4 s, and 8 s.
2. Then 1 mL of the model reaction following general procedure A with **31a** (0.10 mmol) and **32a** as substrates was placed in a Schlenk tube, degassed via argon bubbling, placed in the irradiation set up and irradiated for 15 minutes. This procedure was performed a total of four times with different irradiation times (30 min, 45 min, 60 min).
3. After irradiation, the actinometer solutions were removed and placed in a 10 mL volumetric flask containing 0.5 mL of 1,10-phenanthroline solution and 2 mL of buffer solution. These flasks were filled to the mark with water (HPLC grade).
4. The UV-Vis spectra of the complexed actinometer samples were recorded for each time interval. The absorbance of the complexed actinometer solution was monitored at 510 nm.

The moles of Fe^{2+} formed for each sample is determined using Beers' Law (Eq. 1):

$$\text{Mols of Fe(II)} = V_1 \times V_3 \times \Delta A(510\text{ nm})/10^3 \times V_2 \times l \times \varepsilon(510\ nm) \quad \text{(Eq. 1)}$$

where V_1 is the irradiated volume (1 mL), V_2 is the aliquot of the irradiated solution taken for the determination of the ferrous ions (1 mL), V_3 is the final volume after complexation with phenanthroline (10 mL), l is the optical path-length of the irradiation cell (1 cm), ΔA(510 nm) is the optical difference in absorbance between the irradiated solution and the one stored in the dark, ε(510 nm) is the extinction coefficient the complex $Fe(phen)_3^{2+}$ at 510 nm (11100 L mol-1 cm1). The moles of Fe2+ formed (x) are plotted as a function of time (t). The slope of

[65] Murov, S. L. Ed. *Handbook of Photochemistry* (Marcel Dekker, New York, 1973).

this line was correlated to the moles of incident photons by unit of time (q0 n,p) by the use of the following Equation 2:

$$\Phi(\lambda) = dx/dt\ qn,p\ 0\ [1-10-A(\lambda)\ ] \text{ (Eq. 2)}$$

where dx/dt is the rate of change of a measurable quantity (spectral or any other property), the quantum yield (Φ) for Fe^{2+} at 458 nm is 1.1,[66] $[1\text{-}10^{-A(\lambda)}]$ is the ratio of absorbed photons by the solution, and A(λ) is the absorbance of the actinometer at the wavelength used to carry out the experiments (460 nm). The absorbance at 460 nm A(460) was measured using a Shimadzu 2401PC UV-Vis spectrophotometer in a 10 mm path quartz cuvette, obtaining an absorbance of 0.183. $q^0_{n,p}$, which is the photon flux, was determined to be $5.3x10^{-7}$.

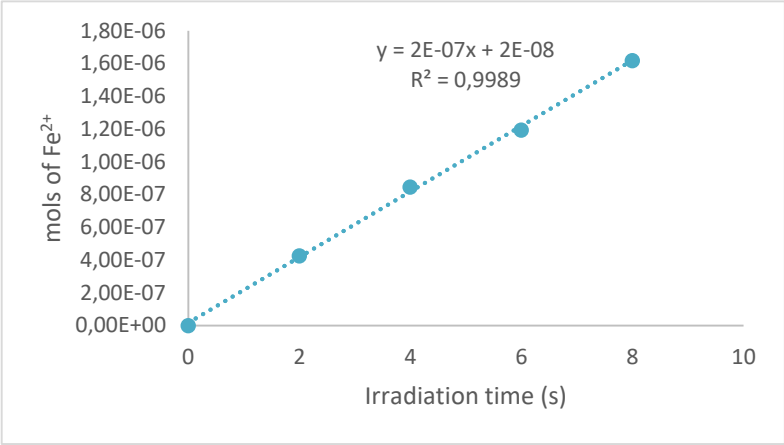

Figure 4.22. Plot of mols of Fe^{2+} formed vs irradiation time. Slope of the line correlates to the moles of incident photons by unit of time.

The moles of product **33a** formed for the model reaction were determined by GC measurement (FID detector) using 1,3,5-trimethoxybenzene as internal standard. The moles of product per unit of time are related to the number of photons absorbed.

The photons absorbed are correlated to the number of incident photons by the use of Equation 1. According to this, if we plot the moles of product (y) versus the moles of incident photons (q0 n,p·dt), the slope is equal to: $\Phi\cdot(1\text{-}10^{-A(460\ nm)})$, where Φ is the quantum yield to be determined and A(460 nm) is the absorption of the reaction under study. A(460 nm) was measured using a Shimadzu 2401PC UV-Vis spectrophotometer in 10 mm path quartz. An absorbance of 0.049 was determined for the model reaction mixture (1:4 dilution). The quantum yield $(\Phi)_{cat.}$ of the photochemical transformation was measured to be 0.01.

[66] Holubov C. A.; Langford C. H., Wavelength and temperature dependence in the photolysis of the chemical actinometer, potassium trisoxalatoferrate(III), at longer wavelengths. *Inorg. Chim. Acta.* **1981**, *53*, 59-60.

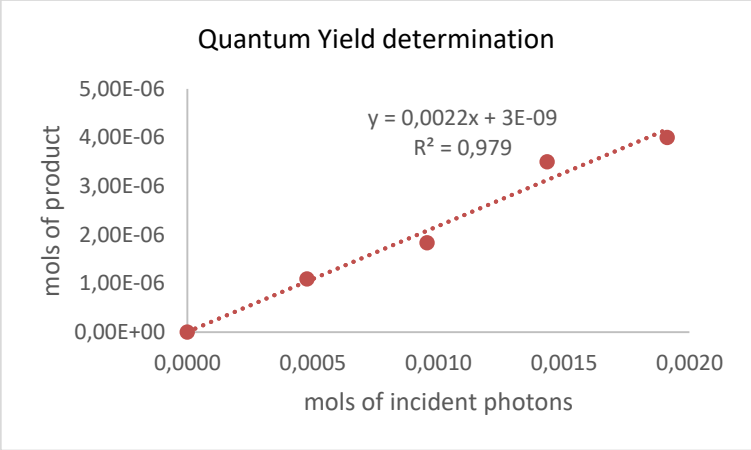

Figure 4.23. Plot of mols of incident photons vs mols of product formed. Slope of the line correlates to quantum yield of the photochemical transformation.

4.8.6.2 Barton decarboxylation

A ferrioxalate actinometer solution was prepared by following the Hammond variation of the Hatchard and Parker procedure outlined in the Handbook of Photochemistry.[65] The ferrioxalate actinometer solution measures the decomposition of ferric ions to ferrous ions, which are complexed by 1,10-phenanthroline and monitored by UV/Vis absorbance at 510 nm. The moles of iron-phenanthroline complex formed are related to moles of photons absorbed. The following solutions were prepared and stored in a dark laboratory (red light):

1. Potassium ferrioxalate solution: 294.8 mg of potassium ferrioxalate (commercially available from Alfa Aesar) and 139 μL of sulfuric acid (96%) were added to a 50 mL volumetric flask and filled to the mark with water (HPLC grade).

2. Phenanthroline solution: 0.2% by weight of 1,10-phenanthroline in water (100 mg in 50 mL volumetric flask).

3. Buffer solution: 2.47 g of NaOAc and 0.5 mL of sulfuric acid (96%) were added to a 50 mL volumetric flask and filled to the mark with water (HPLC grade).

The actinometry measurements were done as follows:

1. 1 mL of the actinometer solution was added to a Schlenk tube (diameter = 12 mm). The Schlenk tube was placed in one of the positions of the 3D printed reactor (Figure 4.3). The solution was irradiated at 460 nm. This procedure was repeated 4 times, quenching the solutions after different time intervals: 1 s, 2 s, 4 s, and 8 s.
2. Then 1 mL of the model reaction following general procedure F starting from isolated **31f** (0.10 mmol) as substrate was placed in a Schlenk tube, degassed via argon bubbling, placed in the irradiation set up and irradiated for 15 minutes. This procedure was performed a total of four times with different irradiation times (30 min, 60 min, 120 min).

3. After irradiation, the actinometer solutions were removed and placed in a 10 mL volumetric flask containing 0.5 mL of 1,10-phenanthroline solution and 2 mL of buffer solution. These flasks were filled to the mark with water (HPLC grade).
4. The UV-Vis spectra of the complexed actinometer samples were recorded for each time interval. The absorbance of the complexed actinometer solution was monitored at 510 nm.

The moles of Fe^{2+} formed for each sample is determined using Beers' Law (Eq. 1):

$$\text{Mols of Fe(II)} = V_1 \times V_3 \times \Delta A(510\text{ nm})/10^3 \times V_2 \times l \times \varepsilon(510\ nm) \text{ (Eq. 1)}$$

where V_1 is the irradiated volume (1 mL), V_2 is the aliquot of the irradiated solution taken for the determination of the ferrous ions (1 mL), V_3 is the final volume after complexation with phenanthroline (10 mL), l is the optical path-length of the irradiation cell (1 cm), ΔA(510 nm) is the optical difference in absorbance between the irradiated solution and the one stored in the dark, ε(510 nm) is the extinction coefficient the complex $Fe(phen)_3^{2+}$ at 510 nm (11100 L mol-1 cm1). The moles of Fe2+ formed (x) are plotted as a function of time (t). The slope of this line was correlated to the moles of incident photons by unit of time (q0 n,p) by the use of the following Equation 2:

$$\Phi(\lambda) = dx/dt\ qn,p\ 0\ [1-10-A(\lambda)\ ] \text{ (Eq. 2)}$$

where dx/dt is the rate of change of a measurable quantity (spectral or any other property), the quantum yield (Φ) for Fe^{2+} at 458 nm is 1.1,[66] $[1\text{-}10^{-A(\lambda)}]$ is the ratio of absorbed photons by the solution, and A(λ) is the absorbance of the actinometer at the wavelength used to carry out the experiments (460 nm). The absorbance at 460 nm A(460) was measured using a Shimadzu 2401PC UV-Vis spectrophotometer in a 10 mm path quartz cuvette, obtaining an absorbance of 0.183. $q^0_{n,p}$, which is the photon flux, was determined to be 5.2×10^{-7}.

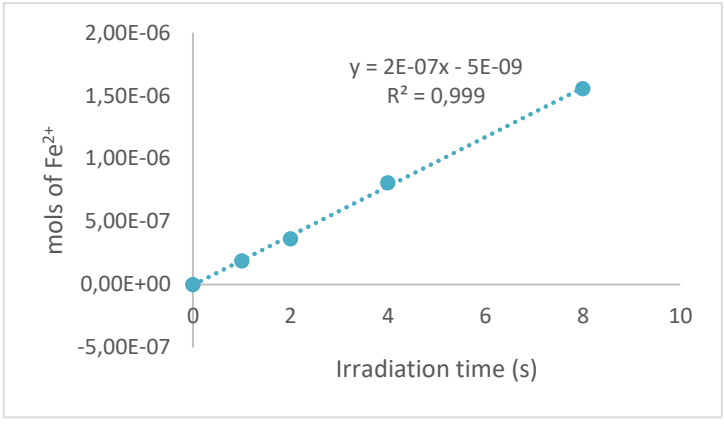

Figure 4.24. Plot of mols of Fe^{2+} formed vs irradiation time. Slope of the line correlates to the moles of incident photons by unit of time.

The moles of product **36b** formed for the model reaction were determined by GC measurement (FID detector) using 1,3,5-trimethoxybenzene as internal standard. The moles of product per unit of time are related to the number of photons absorbed.

The photons absorbed are correlated to the number of incident photons by the use of Equation 1. According to this, if we plot the moles of product (y) versus the moles of incident photons (q0 n,p·dt), the slope is equal to: $\Phi \cdot (1\text{-}10^{-A(460\ nm)})$, where Φ is the quantum yield to be determined and A(460 nm) is the absorption of the reaction under study. A(460 nm) was measured using a Shimadzu 2401PC UV-Vis spectrophotometer in 10 mm path quartz. An absorbance of 0.052 was determined for the model reaction mixture. The quantum yield $(\Phi)_{cat.}$ of the photochemical transformation was measured to be 0.01.

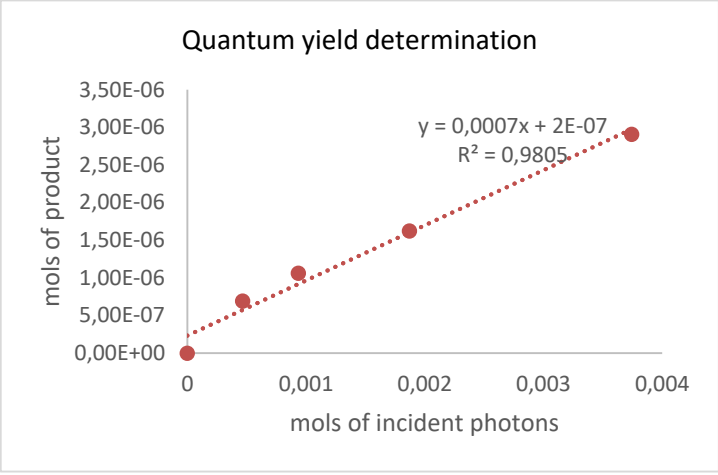

Figure 4.25. Plot of mols of incident photons vs mols of product formed. Slope of the line correlates to quantum yield of the photochemical transformation.

4.8.6.3 Alkylation enol ethers

A ferrioxalate actinometer solution was prepared by following the Hammond variation of the Hatchard and Parker procedure outlined in the Handbook of Photochemistry.[65] The ferrioxalate actinometer solution measures the decomposition of ferric ions to ferrous ions, which are complexed by 1,10-phenanthroline and monitored by UV/Vis absorbance at 510 nm. The moles of iron-phenanthroline complex formed are related to moles of photons absorbed. The following solutions were prepared and stored in a dark laboratory (red light):

1. Potassium ferrioxalate solution: 294.8 mg of potassium ferrioxalate (commercially available from Alfa Aesar) and 139 µL of sulfuric acid (96%) were added to a 50 mL volumetric flask and filled to the mark with water (HPLC grade).

2. Phenanthroline solution: 0.2% by weight of 1,10-phenanthroline in water (100 mg in 50 mL volumetric flask).

3. Buffer solution: 2.47 g of NaOAc and 0.5 mL of sulfuric acid (96%) were added to a 50 mL volumetric flask, and filled to the mark with water (HPLC grade).

The actinometry measurements were done as follows:

1. 1 mL of the actinometer solution was added to a Schlenk tube (diameter = 12 mm). The Schlenk tube was placed in a single HP LED 1.5 cm away from the light source (irradiance 10 mW/cm^2).[12] The solution was irradiated at 460 nm. This procedure was repeated 4 times, quenching the solutions after different time intervals: 5 s, 10 s, 20 s, and 40 s.
2. Then 1 mL of the model reaction following general procedure H with **37a** (0.10 mmol) and **34l** as substrates was placed in a Schlenk tube, degassed via argon bubbling, placed in the irradiation set up and irradiated for 15 minutes. This procedure was performed a total of four times with different irradiation times (30 min, 50 min, 70 min).
3. After irradiation, the actinometer solutions were removed and placed in a 10 mL volumetric flask containing 0.5 mL of 1,10-phenanthroline solution and 2 mL of buffer solution. These flasks were filled to the mark with water (HPLC grade).
4. The UV-Vis spectra of the complexed actinometer samples were recorded for each time interval. The absorbance of the complexed actinometer solution was monitored at 510 nm.

The moles of Fe^{2+} formed for each sample is determined using Beers' Law (Eq. 1):

$$\text{Mols of Fe(II)} = V_1 \times V_3 \times \Delta A(510\text{ nm})/10^3 \times V_2 \times l \times \varepsilon(510\ nm) \quad \text{(Eq. 1)}$$

where V_1 is the irradiated volume (1 mL), V_2 is the aliquot of the irradiated solution taken for the determination of the ferrous ions (1 mL), V_3 is the final volume after complexation with phenanthroline (10 mL), l is the optical path-length of the irradiation cell (1 cm), ΔA(510 nm) is the optical difference in absorbance between the irradiated solution and the one stored in the dark, ε(510 nm) is the extinction coefficient the complex $Fe(phen)_3^{2+}$ at 510 nm (11100 L mol-1 cm1). The moles of Fe^{2+} formed (x) are plotted as a function of time (t). The slope of this line was correlated to the moles of incident photons by unit of time (q0 n,p) by the use of the following Equation 2:

$$\Phi(\lambda) = dx/dt\ qn,p\ 0\ [1-10-A(\lambda)\ ] \quad \text{(Eq. 2)}$$

where dx/dt is the rate of change of a measurable quantity (spectral or any other property), the quantum yield (Φ) for Fe^{2+} at 458 nm is 1.1,[66] $[1\text{-}10^{-A(\lambda)}]$ is the ratio of absorbed photons by the solution, and A(λ) is the absorbance of the actinometer at the wavelength used to carry out the experiments (460 nm). The absorbance at 460 nm A(460) was measured using a Shimadzu 2401PC UV-Vis spectrophotometer in a 10 mm path quartz cuvette, obtaining an absorbance of 0.148. $q^0_{n,p}$, which is the photon flux, was determined to be 1.18×10^{-7}.

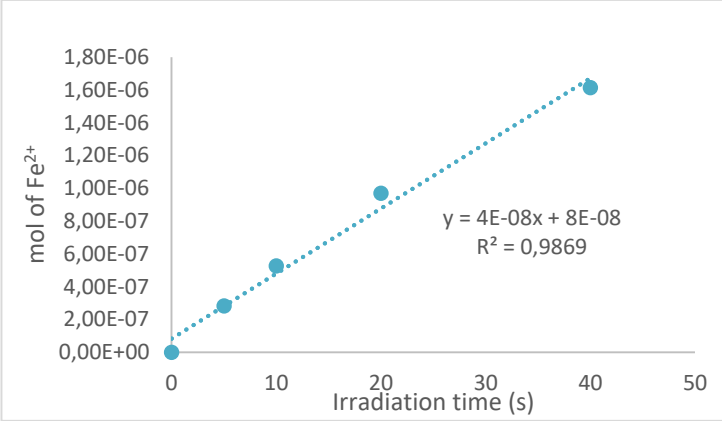

Figure 4.26. Plot of mols of Fe^{2+} formed vs irradiation time. Slope of the line correlates to the moles of incident photons by unit of time.

The moles of product **38h** formed for the model reaction were determined by GC measurement (FID detector) using 1,3,5-trimethoxybenzene as internal standard. The moles of product per unit of time are related to the number of photons absorbed.

The photons absorbed are correlated to the number of incident photons by the use of Equation 1. According to this, if we plot the moles of product (y) versus the moles of incident photons (q0 n,p·dt), the slope is equal to: $\Phi \cdot (1\text{-}10^{-A(460\ nm)})$, where Φ is the quantum yield to be determined and A(460 nm) is the absorption of the reaction under study. A(460 nm) was measured using a Shimadzu 2401PC UV-Vis spectrophotometer in 10 mm path quartz. An absorbance of 0.018 was determined for the model reaction mixture (1:100 dilution). The quantum yield $(\Phi)_{cat.}$ of the photochemical transformation was measured to be 0.02.

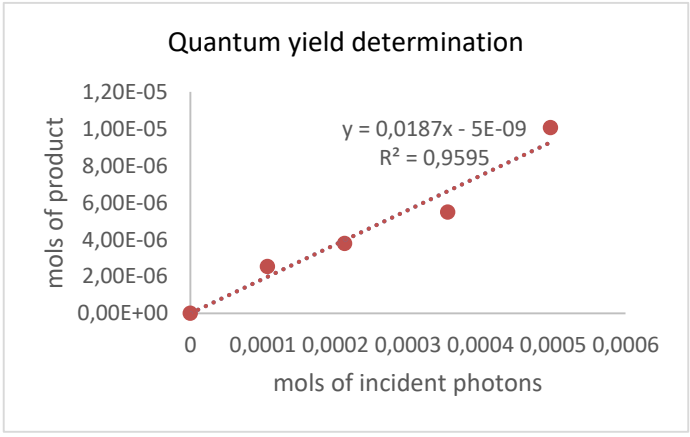

Figure 4.27. Plot of mols of incident photons vs mols of product formed. Slope of the line correlates to quantum yield of the photochemical transformation.

4.8.6.4 Minisci reaction

A ferrioxalate actinometer solution was prepared by following the Hammond variation of the Hatchard and Parker procedure outlined in the Handbook of Photochemistry.[65] The ferrioxalate actinometer solution measures the decomposition of ferric ions to ferrous ions, which are complexed by 1,10-phenanthroline and monitored by UV/Vis absorbance at 510 nm. The moles of iron-phenanthroline complex formed are related to moles of photons absorbed. The following solutions were prepared and stored in a dark laboratory (red light):

1. Potassium ferrioxalate solution: 294.8 mg of potassium ferrioxalate (commercially available from Alfa Aesar) and 139 μL of sulfuric acid (96%) were added to a 50 mL volumetric flask, and filled to the mark with water (HPLC grade).

2. Phenanthroline solution: 0.2% by weight of 1,10-phenanthroline in water (100 mg in 50 mL volumetric flask).

3. Buffer solution: 2.47 g of NaOAc and 0.5 mL of sulfuric acid (96%) were added to a 50 mL volumetric flask, and filled to the mark with water (HPLC grade).

The actinometry measurements were done as follows:

1. 1 mL of the actinometer solution was added to a Schlenk tube (diameter = 12 mm). The Schlenk tube was placed in one of the position of the 3D printed reactor (Figure 4.3). The solution was irradiated at 460 nm. This procedure was repeated 4 times, quenching the solutions after different time intervals: 1 s, 2 s, 4 s, and 8 s.
2. Then 1 mL of the model reaction following general procedure J with **31a** (0.10 mmol) and 2-methylquinoline **40b** as substrates was placed in a Schlenk tube, degassed via argon bubbling, placed in the irradiation set up and irradiated for 60 minutes. This procedure was performed a total of four times with different irradiation times (90 min, 120 min, 150 min).
3. After irradiation, the actinometer solutions were removed and placed in a 10 mL volumetric flask containing 0.5 mL of 1,10-phenanthroline solution and 2 mL of buffer solution. These flasks were filled to the mark with water (HPLC grade).
4. The UV-Vis spectra of the complexed actinometer samples were recorded for each time interval. The absorbance of the complexed actinometer solution was monitored at 510 nm.

The moles of Fe^{2+} formed for each sample is determined using Beers' Law (Eq. 1):

$$\text{Mols of Fe(II)} = V_1 \times V_3 \times \Delta A(510\ \text{nm}) / 10^3 \times V_2 \times l \times \varepsilon(510\ nm) \quad \text{(Eq. 1)}$$

where V_1 is the irradiated volume (1 mL), V_2 is the aliquot of the irradiated solution taken for the determination of the ferrous ions (1 mL), V_3 is the final volume after complexation with phenanthroline (10 mL), l is the optical path-length of the irradiation cell (1 cm), ΔA(510 nm) is the optical difference in absorbance between the irradiated solution and the one stored in the dark, ε(510 nm) is the extinction coefficient the complex $Fe(phen)_3^{2+}$ at 510 nm (11100 L mol-1 cm1). The moles of Fe2+ formed (x) are plotted as a function of time (t). The slope of this line was correlated to the moles of incident photons by unit of time (q0 n,p) by the use of the following Equation 2:

$$\Phi(\lambda) = dx/dt\ qn,p\ 0\ [1-10-A(\lambda)\ ] \quad \text{(Eq. 2)}$$

where dx/dt is the rate of change of a measurable quantity (spectral or any other property), the quantum yield (Φ) for Fe^{2+} at 458 nm is 1.1,[66] $[1-10^{-A(\lambda)}]$ is the ratio of absorbed photons by the solution, and A(λ) is the absorbance of the actinometer at the wavelength used to carry out the experiments (460 nm). The absorbance at 460 nm A(460) was measured using a Shimadzu 2401PC UV-Vis spectrophotometer in a 10 mm path quartz cuvette, obtaining an absorbance of 0.183. $q^0_{n,p}$, which is the photon flux, was determined to be $4.68x10^{-7}$.

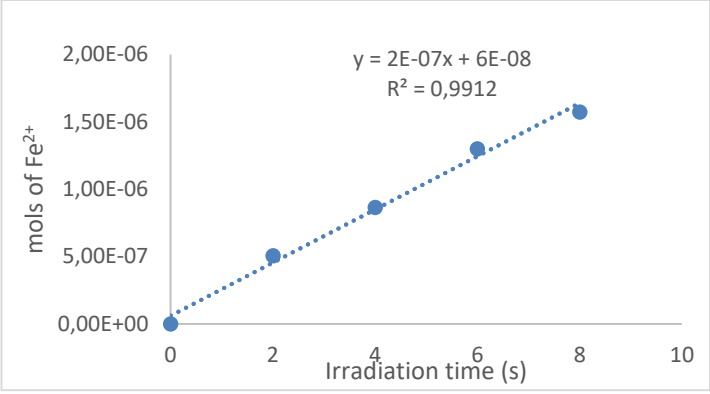

Figure 4.28. Plot of mols of Fe^{2+} formed vs irradiation time. Slope of the line correlates to the moles of incident photons by unit of time.

The moles of product **41b** formed for the model reaction were determined by GC measurement (FID detector) using 1,3,5-trimethoxybenzene as internal standard. The moles of product per unit of time are related to the number of photons absorbed.

The photons absorbed are correlated to the number of incident photons by the use of Equation 1. According to this, if we plot the moles of product (y) versus the moles of incident photons (q0 n,p·dt), the slope is equal to: $\Phi\cdot(1-10^{-A(460\ nm)})$, where Φ is the quantum yield to be determined and A(460 nm) is the absorption of the reaction under study. A(460 nm) was measured using a Shimadzu 2401PC UV-Vis spectrophotometer in 10 mm path quartz. An absorbance of 0.174 was determined for the model reaction mixture (1:10 dilution). The quantum yield $(\Phi)_{cat.}$ of the photochemical transformation was measured to be 0.0003.

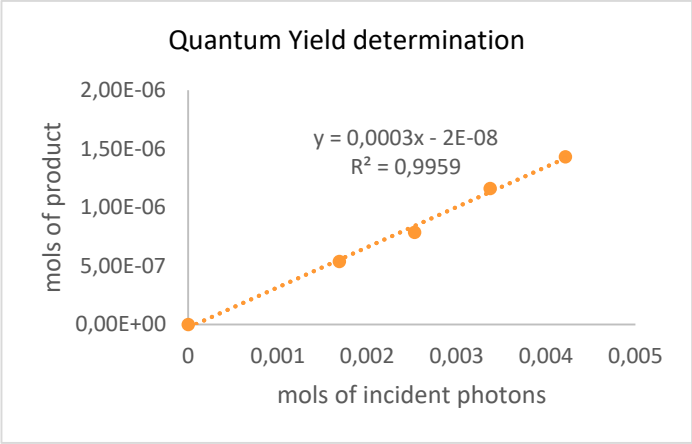

Figure 4.29. Plot of mols of incident photons vs mols of product formed. Slope of the line correlates to quantum yield of the photochemical transformation.

Chapter V

General Conclusions

During my doctoral studies, I have developed a new class of dithiocarbamate and xanthate organic catalysts that can generate radicals via photochemical processes. I have used the new catalysts to develop a variety of different C-C bond forming radical processes under mild conditions. Chapter II describes the design of these nucleophilic catalysts and their ability to activate alkyl electrophiles via an S_N2 pathway. The catalytic S_N2-based strategy granted access to open-shell intermediates from a variety of substrates that would be incompatible with or inert to classical radical-generating strategies, including photoredox catalysis. We also applied the methodology to develop a variety C-C bond-forming reactions, including enantioselective radical catalysis.

In Chapter III, I demonstrated that this radical generation strategy could be expanded to activate acyl electrophiles, so to access acyl and carbamoyl radicals via an acylative nucleophilic substitution pathway. The corresponding intermediates underwent photolytic cleavage to provide the open-shell species, subsequently trapped by olefins in a Giese-type radical addition. Extensive mechanistic studies, based on transient absorption spectroscopy, cyclic voltammetry, and electron paramagnetic resonance (EPR), among others, provided insight into the catalytic cycle of the organic catalysts, highlighting the relevance of several off-cycle equilibria.

In Chapter IV, I explored the use of dithiocarbamates and xanthogenates as catalytic donors in the formation of photoactive electron donor-acceptor (EDA) complexes with a variety of radical precursors. Excitation with visible light granted access to open-shell intermediates under mild conditions, including non-stabilized carbon radicals and nitrogen-centered radicals. The modular nature of the organocatalysts offered a versatile EDA complex catalytic platform for developing mechanistically distinct radical reactions, including redox neutral and net-reductive processes. Mechanistic investigations supported the hypothesis that a closed catalytic cycle is operational, highlighting the ability of the organic catalysts to turnover and iteratively drive each catalytic cycle.

UNIVERSITAT ROVIRA I VIRGILI
NEW ORGANIC CATALYSTS FOR THE PHOTOCHEMICAL GENERATION OF RADICALS
Eduardo de Pedro Beato

UNIVERSITAT ROVIRA I VIRGILI
NEW ORGANIC CATALYSTS FOR THE PHOTOCHEMICAL GENERATION OF RADICALS
Eduardo de Pedro Beato

UNIVERSITAT ROVIRA I VIRGILI
NEW ORGANIC CATALYSTS FOR THE PHOTOCHEMICAL GENERATION OF RADICALS
Eduardo de Pedro Beato

UNIVERSITAT
ROVIRA i VIRGILI